An annually resolved climate record for MIS 11 from Marks Tey, eastern England: Investigating landscape response to abrupt events during the closest climatic analogue to the Holocene

Gareth Jonathan Tye

Thesis submitted for the degree of Doctor of Philosophy,
Royal Holloway, University of London

March 2015

Institution of study:
Centre for Quaternary Research
Department of Geography
Royal Holloway
University of London

Declaration of Authorship

I, Gareth Jonathan Tye, hereby declare that this thesis and the work presented in it is entirely my own. Where I have consulted the work of others, this is always clearly stated.

Signed:

Abstract

Climatic and environmental reconstructions from previous interglacial episodes of the Quaternary Period are of significant interest, as previous interglacials may have the potential to act as analogues for the Holocene. Based on the similarity in long-term insolation patterns during both interglacials, Marine Isotope Stage 11 (MIS 11, ca. 410,000 yrs BP.) is widely considered to offer the best orbital analogue for the Holocene. The palaeo-lake sequence at Marks Tey, eastern England, represents one of the key MIS 11 sites in the UK and Europe because not only does it record a full vegetation succession for the interglacial at a single site, the sediments are also purportedly annually-laminated (varved) in parts of the sequence (Turner, 1970). Furthermore, the vegetation succession is interrupted during full interglacial conditions by an abrupt event (the Non-Arboreal Pollen (NAP) phase), which may be analogues to the 8.2 ka event that punctuated the early Holocene (Koutsodendris et al., 2012).

This thesis presents a re-examination of the early Hoxnian (MIS 11) sequence from a new core drilled at Marks Tey in 2010, providing discussion of: 1) Micro-facies analysis of the laminated sediments preserved during the early part of MIS 11; to demonstrate the annual nature of sedimentation and produce a varve chronology; 2) Results of stable oxygen and carbon isotopic analysis from authigenic carbonate laminations that occur throughout the core section studied and their environmental significance; and 3) Combining the varve chronology and stable isotope results with other proxy evidence to investigate the timing and forcing mechanism for, as well as the rate of proxy response during the NAP phase.

Acknowledgements

First and foremost, I wish to thank my supervisors Dr I. Candy and Dr A. Palmer for their endless encouragement, support and patience over the last four years. Thank you to all of the staff of the CQR for their discussions and useful insights, and for making the department such a great place to be.

I would like to thank Prof. Pete Coxon (TCD) for his work on producing the pollen record for the new core, as well as Dr Mark Hardiman (Portsmouth) for providing the charcoal counts and Dr Dave Ryves and Katie Loakes for undertaking the diatom analysis. I would also like to thank Prof. Anson Mackay (UCL) for supervising the diatom work that I undertook as part of this project. Dr Ian Matthews is thanked for useful discussions about statistics and Dr Dave Lowry is thanked for running the isotope samples. I would also like to thank Maurice Page (W.H. Collier Ltd) for allowing us to core the site, and Ecologia Ltd. for undertaking the coring. A huge thanks is due to the RHUL geography laboratory and support staff Iñaki Valcarcel, Robyn Christie, Jenny Kynaston and Elaine Turton for all of their assistance over the last four years.

Thanks to all of the CQR PhD students for making my time at RHUL so enjoyable; and a special thanks to Jenni Sherriff, Paul Lincoln, Chris Satow and Mark Hardiman for all of their support and making the past four years so enjoyable! This thesis is dedicated to my family and to Claire Gallant for their endless support and for always believing in me. Thank you.

List of contents

List of Figures

List of Tables

Chapter 1. Introduction

1.1 Scientific rationale

It is becoming increasingly apparent that the Holocene climate system is being modified by human practices (e.g. see review by Rahmstorf, 2008), with the IPCC highlighting the possibility of this anthropogenic forcing leading to abrupt climatic events in the future (IPCC, 2007; Vellinga and Wood, 2002, 2008). Abrupt (sub-Milankovitch on centennial to decadal timescales) climatic events also occurred in the early Holocene (the 9.3 and 8.2 ka events) and are primarily considered to result from changes in ocean circulation patterns in the North Atlantic due to large influxes of freshwater (e.g. Barber et al., 1999; Alley and Ágústdóttir, 2005; Fleitmann et al., 2008; Daley et al., 2011), which is significant, given that this region is currently undergoing rapid freshening due to ice sheet melting (Dickson et al., 2002; Velling and Wood, 2002, 2008). Determining the mechanisms behind abrupt climatic events that have occurred in the past, and the impact that they have on the terrestrial environment is, therefore, important for our understanding of the possible impact of abrupt climatic events in the future.

Due to its location, the British Isles represents an ideal site to study terrestrial records of abrupt climatic events. Although some sites do provide clear evidence for abrupt climatic events (e.g. Marshall et al., 2007), one of the limitations of reconstructing such events from Holocene archives is that landscape and ecosystem response to climate events is frequently masked and complicated by human influence (Edwards et al., 2007). The study of past interglacials is therefore important, as they have the ability to provide records of natural environmental and climatic variability, but without the issue of anthropogenic modification.

In this context, Marine Isotope Stage 11 (MIS 11), an interglacial period that occurred ca 410,000 yrs BP, is highly significant for two reasons: 1) due to the similarity between variations in insolation that have occurred during the Holocene (and predicted to occur in the future) and those that occurred during MIS 11, the interglacial is widely considered to represent one of the most suitable climatic analogues for the Holocene

(Fig. 1.1) (Howard, 1997; Droxler and Farrel, 2000; Loutre and Berger, 2003; Droxler et al., 2003; Raynaud et al., 2005), and 2) this interglacial contains evidence for abrupt environmental events (e.g. Turner, 1970; Koutsodendris et al., 2012, also see review by Candy et al., 2014) that may be climatically driven (Kelly, 1964; Muller, 1974; Kukla, 2003; Koutsodendris et al., 2012).

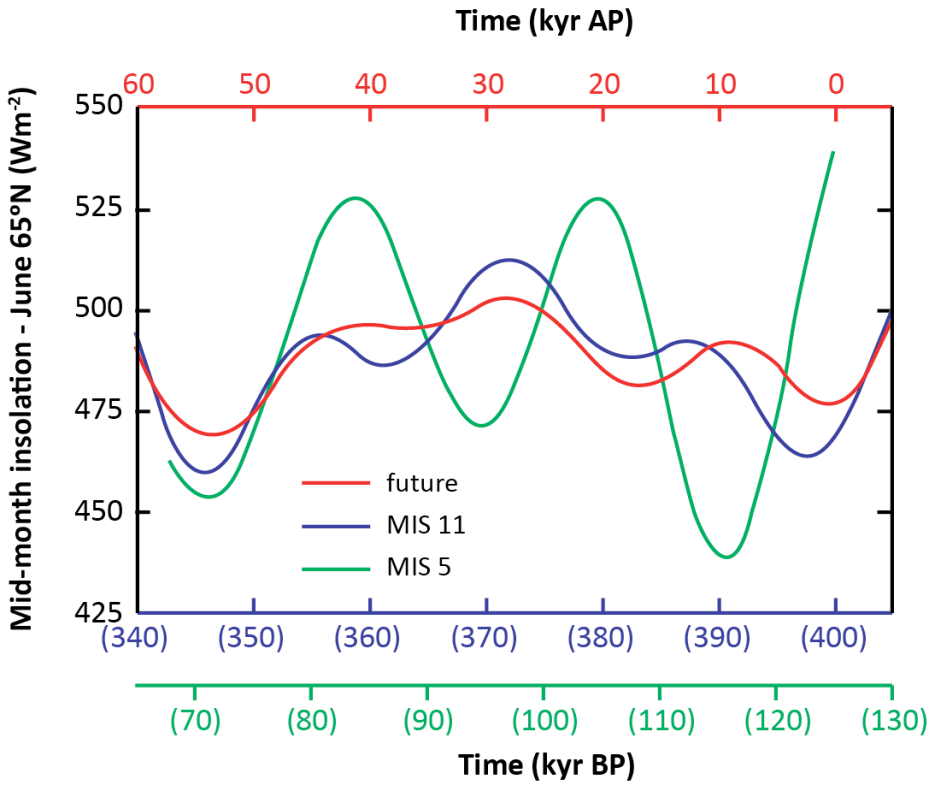

Figure 1.1. *Insolation patterns during MIS 11 and MIS 5 compared with modelled insolation changes from 0 to 60 ka BP (target period). The linear correlation between insolation changes during MIS 5 and the target period is 0.17, whereas for MIS 11 and the correlation period it is 0.87. Redrawn and modified from Loutre and Berger (2003).*

At present, however, there is a lack of understanding about abrupt events that occurred during MIS 11, as much of our understanding is based on the occurrence of short-term vegetation regressive phases identified in a number of European pollen sequences (e.g. Kelly, 1964; West, 1956; Turner, 1970; Meyer, 1974; Muller, 1974; Coxon, 1985), which have been suggested to reflect vegetation response to wildfires, volcanic eruptions and cooling events (Kelly, 1964; Turner, 1970; Muller, 1974; Koutsodendris et al., 2012).

It is only possible to use such events as analogues for comparable oscillations in the Holocene if records are available that fulfil the following criteria. Firstly, they need to be securely correlated to MIS 11, to ensure that these events are being investigated in an interglacial that is analogous to the Holocene. Secondly, as well as containing pollen evidence for these short-term regressive events, they need to contain the potential for the application of other proxies that can be used to infer temperature variations. Without such independent evidence, establishing whether the vegetation is responding to climatic or non-climatic factors is almost impossible. Finally, the sequence needs to contain high-resolution, ideally annually-resolved records of these events, so that high-resolution reconstructions of environmental and landscape changes can be undertaken and their duration quantified. This thesis will seek to overcome these issues by investigating the Hoxnian (the British correlative of MIS 11) lacustrine sequence at Marks Tey, eastern England. This site contains evidence for an abrupt event and is suggested, but not proven, to be annually-laminated (varved) (Tuner, 1970), allowing for a detailed reconstruction of the event. Furthermore, as these sediments contain laminations of authigenic carbonate throughout the record of this event, high-resolution $\delta^{18}O$ and $\delta^{13}C$ analysis can be applied to the sequence, a technique which has been widely used to reconstructed abrupt climatic events in the Holocene (Marshall et al., 2007; Daley et al., 2011). Marks Tey is crucial to the development of our understanding of abrupt events in pre-Holocene interglacials as it is the only site in western Europe that meets all of these criteria. Although sites in eastern Europe may also fulfil some or all of these criteria, the occurrence of Marks Tey in the maritime margin of western Europe makes it more suited to recording abrupt events, as they are routinely suggested to be driven by oceanic forcing. Marks Tey is the closet appropriate site to the Atlantic margin and occurs at a latitude that is highly sensitive to fluctuations in ocean current strength (Vellinga and Wood , 2002, 2008)

1.1.1.Varved lake sequences

Annually-laminated (varved) lake sediment sequences have the potential to provide high-precision records of environmental change. Due to the resolution attainable, varved lacustrine records have a number of important applications within palaeoclimatic reconstruction. Varve counting provides an independent fixed or

floating chronology for sedimentary archives (Zolitschka, 1991; Lotter et al., 1997; Brauer et al., 1999a; Lamoureux, 2001). Because varves often contain other proxies within their sub-annual structure (e.g. diatoms, pollen, calcite), varve chronologies can be used to determine the timing, structure and duration of proxy response to climatic events (Lotter, 1991; Brauer et al., 1999b, 2007; Prasad et al., 2009; Palmer et al., 2010; Koutsodendris et al., 2012). This is particularly significant for time periods such as MIS 11, where the development of high-resolution site chronologies is precluded because of the upper limits and high uncertainties of traditional radiometric dating techniques (e.g. Rowe et al., 1999; Karner and Marra, 2003). If it can be demonstrated that the sequence at Marks Tey is varved, then the abrupt event can be reconstructed at an annual resolution.

1.1.2. Lacustrine stable isotopic records

Lacustrine stable isotope records have the potential to provide important records of terrestrial environmental change during the Quaternary. This reasoning is based on the following principles: 1) the $\delta^{18}O$ value of authigenic calcite is related to the $\delta^{18}O$ of the water that it precipitated from and the temperature at which mineralisation occurred (e.g. Urey, 1947; Kim and O'Neil, 1997), 2) the $\delta^{18}O$ of lake water is primarily controlled by the $\delta^{18}O$ of recharge water, which is primarily controlled by the $\delta^{18}O$ of rainfall (e.g. Rozanski et al., 1997; Darling et al., 2003), and 3) in temperate regions like Northwest Europe, a positive linear relationship exists between the $\delta^{18}O$ of meteoric waters and air local air temperature (e.g. Craig, 1961; Dansgaard, 1964). If it can be demonstrated that the $\delta^{18}O$ value of lake water has not been significantly altered after falling as rain, then lacustrine carbonates have the potential to act as qualitative proxies for past temperature shifts (Leng and Marshall, 2004; Andrews, 2006; Marshall et al., 2007; Candy et al., 2011). Furthermore, the fact that changes in prevailing air temperature and subsequent response of the $\delta^{18}O$ value of rainfall is effectively instantaneous, on geological timescales, makes lacustrine carbonates an ideal proxy for the reconstruction of abrupt climate change (see Marshall et al., 2007).

1.2. Site introduction and previous work

Marks Tey, located in southeastern England (Fig. 1a), is a para-stratotype for the Hoxnian interglacial, a temperate episode defined by West (1956) on the basis of pollen stratigraphy at the stratotype site of Hoxne (Mitchell et al., 1973). The Hoxnian-aged sediments at Marks Tey were formed within palaeo-lake basins generated as either kettle holes or sub-glacial scour features during the Anglian (MIS 12) glaciation (West, 1956; Turner, 1970), and have been Uranium-series dated to MIS 11 (Rowe et al., 1999). It could be argued that Marks Tey contains the most important Hoxnian sequence as, unlike other sites from the same interglacial, it records the full interglacial vegetation succession from the end of the Anglian through the entire Hoxnian interglacial into the subsequent cold interval (Turner, 1970) (Fig. 1b).

A key characteristic of the pollen record of Marks Tey, as well as many Hoxnian sequences in Britain, is the occurrence of a short-lived increase in non-arboreal pollen (NAP) relative to arboreal pollen (AP) during the early-Temperate zone (Ho IIc), i.e. under fully interglacial conditions (West, 1956; Turner, 1970; Candy et al., 2014). This event is commonly referred to as the NAP phase (Fig. 1b) (see Turner, 1970 and Candy et al., 2014 for discussion). A feature that is potentially unique to the Marks Tey sequence, however, is that varved sediments are thought to occur during Ho I to Ho IIIa (Turner, 1970). Based on this assumption, the NAP Phase at Marks Tey is thought to have lasted ca 300 years (Turner, 1970). The sequence has also been used to provide estimates of the duration of the Hoxnian Interglacial. Based on the assumption that varved sediments occur from Ho I to early Ho IIIa, and that these sedimentation rates can be applied to non-varved sections of the sequence, Shackleton and Turner (1967), and Turner (1970, 1975) estimated that the Hoxnian Interglacial had a duration of between 30,000-50,000 years for MIS 11 (Shackleton and Turner, 1967; Turner, 1970), although this figure was subsequently reduced to 25,000 years (Turner, 1975).

There are uncertainties associated with this previous work, however, which will be the focus of this thesis. The first is that the forcing mechanism for the NAP Phase is uncertain, due to the occurrence of charcoal fragments in association with this event at Marks Tey, and other Hoxnian sites, which led Turner (1970) to suggest that that the pollen event was caused by a wildfire, not a climatic event.

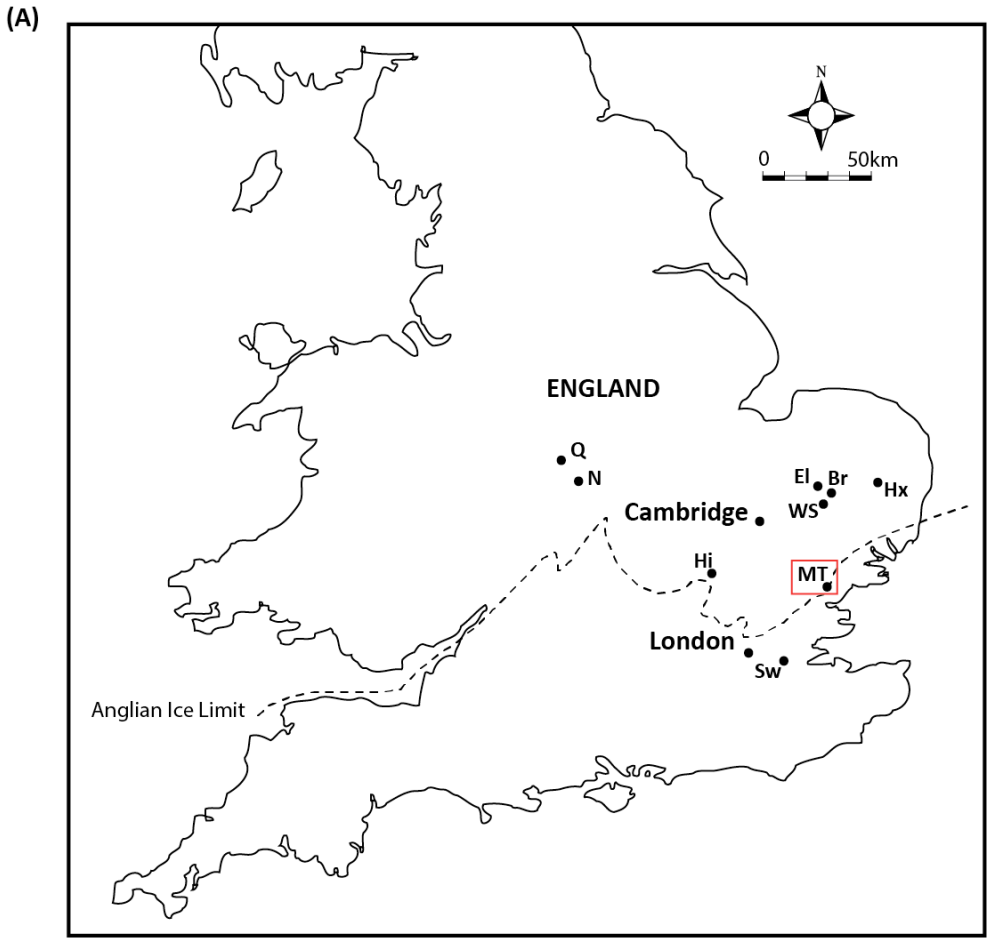

Q = Quinton, N = Nechells, Hi = Hitchen, Sw = Swanscombe, MT = Marks Tey, Hx = Hoxne, Br = Barnham, WS = West Stow, El = Elveden (Adapted from Candy, 2009).

Figure 1.2. *A) Map showing the location of Marks Tey, as well as some other key British Hoxnian sites. B) Summary pollen diagram of the sequence, showing a vegetation succession covering the late Anglian (LA), entire Hoxnian interglacial (Ho I to Ho IV) and the early part of the proceeding cold stage (eWo). The location of the NAP-Phase is highlighted in red. Re-drawn from Turner (1970).*

This is in contrast with other researchers, who have suggested that on the continent (in sequences relating to the Holsteinian interglacial, the continental correlative of the Hoxnian), the event could be climatically forced (Kelly, 1964; Muller, 1974; Kukla, 2003; Koutsodendris et al., 2012) or even a response to volcanism (see Diehl and Sirocko, 2007). The second is that estimating the duration of the Hoxnian at the site is based on the assumption that 1) all of the laminated sediments contained within Ho I to Ho IIIa are varved, and 2) these sedimentation rates provide accurate estimates of non-varved sediments that occur in the sequence. The varved nature of the Marks Tey sediment is entirely assumed, with no published work validating the origin of these laminations, meaning that all suggestions about the duration of the interglacial, and the events that occurred with in it, are highly speculative.

1.3. Aims and objectives

1.3.1. Aims

This thesis will determine the duration, structure, nature of landscape and limnological response during the NAP Phase at Marks Tey with the aim of establishing whether; 1) it is a climatically forced event, and 2) it is analogous to abrupt events seen in the Holocene (i.e. the 8.2 ka event). This aim will be established through high precision sediment and stable isotopic analysis of the Marks Tey sequence coupled with a compilation of all other proxy data currently available for the Marks Tey record and the interval of the NAP phase in particular. To achieve this the work undertaken will, therefore, address these subsidiary aims:

1. To establish whether the laminated sediments within the Marks Tey sequence are varved and, therefore, whether or not they can be used to produce an annually-resolved framework for the Hoxnian interglacial.
2. To use the sections of the Marks Tye sequence that have a true “varved” signal to calculate the duration of the section of the Hoxnian interglacial that they cover.
3. To use varve counting to calculate the duration of the NAP phase and use the sedimentary characteristics of the varves to reconstruct changing sedimentation patterns across this interval.

4. To use the $\delta^{18}O$ and $\delta^{13}C$ analysis of the carbonate laminations within the Marks Tey sequence to provide a qualitative reconstruction of climate variations across the Hoxnian and, in particular, across the NAP phase.
5. To combine this with other proxy data (pollen, diatoms and charcoal) to produce a model for the climatic change and landscape response that occurred during the NAP phase.
6. To compare this model with reconstructions of climatic and landscape response to that of the 8.2 ka event and short-lived oscillations in continental Holsteinian sequences to establish whether the NAP phase is; 1) analogues to abrupt events that occurred in the Holocene, and 2) the same event that is seen in other MIS 11 records in Europe.

1.3.2. Objectives

To achieve the aims stated above, a number of objectives need to be achieved:

1. A new sediment sequence will be extruded from the site, comprising two overlapping boreholes to cover breaks introduced between drilling runs. These core sections will then be correlated and macro-scale sediment descriptions undertaken, to produce a composite record for the site. Macro-scale sediment characterisation will also involve determining bulk sedimentary characteristics for calcium carbonate and total organic carbon content.
2. The sedimentology of the sequence will also be determined at the micro-scale. This will involve cutting overlapping blocks of sediment from the sequence using specially made Kubiena tins, which will then be processed to make sediment thin sections.
3. To provide an environmental framework, as well as identify the location of the NAP Phase in the new sequence, the cores will be sub-sampled for pollen analysis (Prof. P Coxon).
4. Once the location of the NAP Phase has been established, further sub-sampling will be undertaken for the high-resolution reconstruction of the NAP Phase. This will involve taking samples for the following analyses:
    a. Pollen (Prof. P Coxon)
    b. Diatoms (Dr D Ryves and K Loakes)

c. Macro-charcoal (Dr M Hardiman, Portsmouth)

5. The micro-scale sediment descriptions will also determine the location in the sequence where varve-like lamination structures occur. To investigate the suggestion that the laminations are varves, individual laminations will be subsampled for pollen (Prof. P Coxon), diatom and stable isotopic analysis. Assuming that within-lake production and water chemistry varies seasonally, as does pollen sedimentation, the laminations should contain seasonal variations in these proxies.
6. Assuming that a seasonal signal can be determined from this analysis, the thin sections will be used to count the number of varves preserved in the sequence to produce a varve chorology.
7. The core will also be sub-sampled for carbonate samples. These samples will be analysed for their stable oxygen and carbon isotopic composition. This analysis will produce a stable isotope stratigraphy for the sequence, giving a proxy for environmental structure of the early Hoxnian.
8. By combining the varve chronology and stable isotope stratigraphy with the pollen, diatom and macro-charcoal results, an annually-resolved model for the NAP Phase can be constructed. The pollen results will provide a detailed framework of floristic changes during the event and the diatoms will record the limnological response. The sedimentological response during the event will be characterised by varve mico-facies characteristics (varve thickness, sub-annual varve structure) and the charcoal results. The stable isotope results, combined with the charcoal results, will allow for a discussion about the underlying forcing mechanism. Furthermore, the duration of the event will be determined using varve chronology, as well as the timing of proxy response.

1.4. Thesis structure

This thesis is divided into thirteen chapters. Chapter 2 provides a review of MIS 11 in terms of why it is considered a suitable climatic analogue for the Holocene, the climatic structure of the interglacial, as well as the evidence for the occurrence of abrupt climatic events within it, therefore, placing this study into a wider climatic context. Chapter 3 provides a review of how the stable isotopic composition of

lacustrine carbonates can be used in environmental reconstruction and the potential for these records to reconstruct abrupt events. Chapter 4 will highlight how varves form, the methods that are applied to determine a depositional model for their formation, as well as the value of varve chronologies in palaeoenvironmental reconstruction. Chapter 5 outlines the methods used in this study. Chapter 6 is the first of five results chapters, and presents results of the correlation and description (macro- and micro-scale) of the new sediment cores extruded from the site. This chapter also presents the results of the pollen analysis. Chapter 7 focuses on developing a depositional model for varve formation at Marks Tey. Micro-facies descriptions of the sediments are presented, as well as the results from the high-resolution pollen, diatom and stable isotopic analyses. Chapter 8 presents the results of varve counts undertaken on the sequence to produce a varve chronology for the site. Chapter 9 presents results of the stable isotopic analysis of the authigenic carbonate laminations contained within the sequence and interprets this signal in terms of our current understanding surrounding the controls over the $\delta^{18}O$ and $\delta^{13}C$ of rainfall and lake water with the aim of identifying palaeoclimatic variability within this record. Chapter 10 brings together the results generated in this thesis with those from secondary sources to produce an annually-resolved reconstruction of the NAP Phase. Chapter 11 then interprets this model in terms of landscape and limnological changes that occur during the pollen event. The underlying forcing mechanism is also discussed and the NAP Phase is then compared to similar events in Europe during MIS 11, as well as the Holocene. Chapter 12 uses the varve record and isotopic data produced in this study to provide a discussion about the Hoxnian and MIS 11, primarily focussing on; 1) how robust previous estimates of interglacial duration based on the Marks Tey sequence are, and 2) how the data from this study regarding the climatic structure of the Hoxnian compares to the structure of the interglacial as preserved in other European lacustrine records and North Atlantic marine records of MIS 11. The main conclusions of this study are presented in chapter 13.

2. Marine Isotope Stage 11

Overview of chapter

Marine Isotope Stage 11 (MIS 11) is a potentially important analogue for current and future climate variability because it occurs during a period of time (ca. 410,000 yrs BP) when orbital parameters, which control the latitudinal distribution of insolation that reaches the Earth's surface, had a similar configuration to those that occurred during the Holocene (Loutre and Berger, 2000, 2003). As the pattern of insolation distribution across the surface of the Earth will, to some degree, control the duration, climatic structure and degree of warmth that occurs during interglacial periods, climate proxy records from MIS 11 therefore allow the study of natural climate variability within a Holocene-like interglacial.

It has becoming increasing apparent that the climate of the early Holocene was punctuated by a number of abrupt cooling events (e.g. 9.3 ka and 8.2 ka events), which are considered to be forced by freshwater inputs into the North Atlantic Ocean (e.g. Barber et al., 1999; Fleitmann et al., 2008). Given that the North Atlantic is currently undergoing rapid freshening (Dickson et al., 2002), understanding the mechanisms behind abrupt climate events and their impact on the terrestrial environment is an important area of research. One of the limitations of studying such events in the Holocene is that landscape and ecosystem response to climate events is frequently masked and complicated by human influence (Edwards et al., 2007). Like the Holocene, some terrestrial records from MIS 11 indicate the presence of at least one abrupt event that occurred during fully interglacial conditions, which may provide analogues for Holocene events (Kukla, 2003; Koutsodendris et al., 2012). It has been noted, however, that there are distinct regional differences in the expression of, and the environmental response to, the 8.2 ka event (Alley and Ágústdóttir, 2005; Rohling and Palike, 2005; Daley et al., 2011).

The British Isles represents an excellent location to study the palaeoclimates and palaeoenvironments of MIS 11 because this region contains a large number of sediment records that are rich in a diverse range of environmental proxies that date to

this interval. A key research theme in this thesis focusses on an event that occurs early on in many British Hoxnian (MIS 11) pollen records that may represent a period of climatic instability (see Candy et al., 2014 for a review). Given the climatic similarities between MIS 1 and MIS 11, this event might be analogous to the climatic events that punctuate the early Holocene (Koutsodendris et al., 2012; Candy et al., 2014). The lacustrine sediments at Marks Tey present a unique opportunity to investigate this event in the British terrestrial record because, not only is the abrupt event clearly expressed in the pollen sequence at the site, but it is also the only Hoxnian site where annually-laminated sediments are thought to be preserved (Turner, 1970). As climatic variability during MIS 11 is the focus of this study, the aim of this chapter is to review the following topics; 1) Why MIS 11 is considered to be a suitable climatic analogue for the current Interglacial; 2) How the climatic structure of the interglacial is expressed on a global scale and in the North Atlantic region; 3) The magnitude of warmth that occurred during MIS 11 in the British Isles; and 4) The evidence is for abrupt climatic events. Many of the ideas presented in this chapter are based on topics covered in the recently published paper by Candy et al. (2014). This chapter will, however, go into more detail when covering abrupt climatic events during MIS 11, the main focus of this thesis.

2.1. Introduction

The Quaternary Period covers the last 2.58 million years (Gibbard and Head, 2010) and is characterised in long marine records (e.g. Lisiecki and Raymo, 2004) (and ice core records for the last 800 ka, e.g. EPICA, 2004) by a repetitive trend between relatively warmer (interglacial) and colder (glacial) episodes that are primarily driven by long-term changes in orbital forcing patterns (Milankovitch, 1941; Hays et al., 1976). Interglacial episodes have received a great deal of attention over the past twenty years because they have the potential to provide analogues for the current interglacial. Marine Isotope Stage 11 (MIS 11), ca 410,000 yrs BP, is one of the most significant interglacial episodes that occurred during the Quaternary because it is widely considered to represent one of the most appropriate climate analogue for the Holocene (Howard, 1997; Droxler and Farrell, 2000; Loutre and Berger, 2003; Droxler et al., 2003; Raynaud et al., 2005). This idea is based on the observation that long-term

insolation patterns (i.e. a low peak in eccentricity and its modulation of precession) that occurred during MIS 11 and the Holocene were very similar (Berger and Loutre, 2002, 2003; Loutre and Berger, 2003, but also see Ruddiman, 2003; Tzedakis, 2010, as well as Candy et al., 2014 for a recent review). As temporal variations in insolation patterns will partially control the duration, climatic structure and degree of warmth that occurs during an interglacial episode, detailed palaeoclimatic records from MIS 11 can allow the climate variability that would occur naturally during a Holocene-like interglacial, in the absence of anthropogenic modification, to be understood (Candy et al., 2014).

A number of sites located from eastern England to the midlands contain sediment sequences that are correlated to the Hoxnian Interglacial (the British equivalent to the Holsteinian Interglacial in continental Europe), a period widely considered to represent the British terrestrial equivalent to MIS 11c (Fig. 2.1) (Jones and Keen, 1993; Bridgland, 1994; Bowen et al., 1999; Rowe et al., 1999; Grun and Schwarcz, 2000; Schreve, 2001a,b; Thomas, 2001; Penkman et al., 2011, also see Geyh and Muller, 2005, 2006; Scourse, 2006; Preece et al., 2007). Due to a number of palaeogeographical features, the British Isles preserves an excellent terrestrial record of MIS 11. A number of basins formed close to the margin of the ice sheet that covered large parts of the region during the Anglian glaciation (MIS 12, Pawley et al., 2008), which then accumulated sediments during the subsequent interglacial (e.g. West, 1956; Turner, 1970). The record of MIS 11 is well preserved because mapped ice limits of the MIS 12 ice sheet indicate that it was the most extensive glaciation to have occurred in the British Isles (Perrin et al., 1979; Rose, 1987, 2001; Ehlers and Gibbard, 2001; Clark et al., 2004; Gibbard and Clark, 2011). Subsequent glacial limits in the British Isles are far less extensive than MIS 12, with many MIS 11 sites located beyond these limits (e.g. Clark et al., 2004), resulting in increased preservation potential.

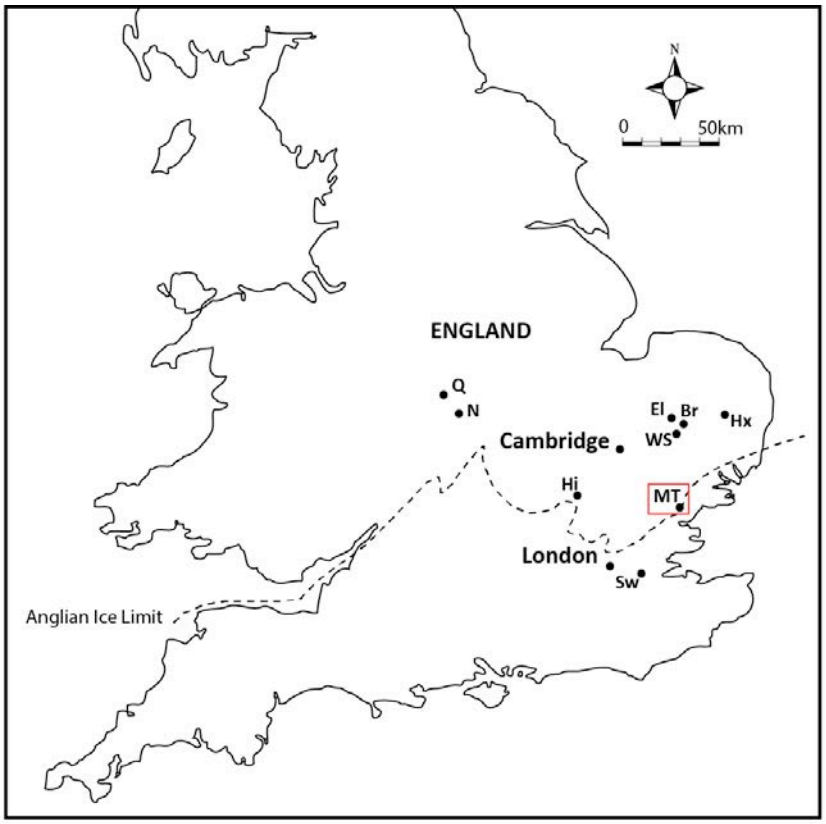

Q = Quinton, N = Nechells, Hi = Hitchen, Sw = Swanscombe, MT = Marks Tey, Hx = Hoxne, Br = Barnham, WS = West Stow, El = Elveden

Figure 2.1. *Map of some key Hoxnian sites in Britain. The red box highlights the location of Marks Tey. Adapted from Candy (2009).*

Marks Tey, located in eastern England (Fig. 2.1), is one such site. It is a parastratotype site for the Hoxnian Interglacial as defined by West (1956). The palaeolake basin contains arguably the most important Hoxnian palaeoclimatic sequence as, unlike other sites from the same time period, it records a full (albeit fragmented) interglacial vegetational succession. A key characteristic of the pollen record at Marks Tey is the occurrence of a short-lived (~300 year) increase in Non-Arboreal Pollen relative to Arboreal Pollen (AP) during the early temperate zone (Ho IIc), known as the Non-Arboreal Pollen (NAP) Phase (Turner, 1970). The NAP Phase is also present in a number of other MIS 11 sequences in Britain, as well as MIS 11 sites in Western and Central Europe, where it is referred to as the Older Holsteinian Oscillation (OHO) (see Thomas, 2001; Koutsodendris et al., 2012 and Candy et al., 2014 for reviews). The forcing mechanism for this event is unclear, however, as the occurrence of charcoal fragments at the start of the NAP Phase led Turner (1970) to suggest a wildfire caused the rapid decline in arboreal pollen, while others have suggested that it was climatically driven (Kelly, 1964; Turner, 1975; Koutsodendris et al., 2012).

2.2. MIS 11 as an analogue for the Holocene

The suggestion that MIS 11 may be an appropriate analogue for the Holocene is based on long-term climate change during the Quaternary Period between glacial/interglacial cycles is primarily driven by variations in the shape of the Earth's orbit around the sun (eccentricity), combined with changes in the tilt (obliquity) and wobble (precession) of the Earth's axis (Milankovitch, 1941; Hays et al., 1976; Imbrie et al., 1984, 1992; Berger and Yin, 2012). The changes in these three orbital parameters occur on predictable cycles, with the eccentricity component having a 96,000 year cycle, the obliquity component a 41,000 year cycle, and changes in the precession component occurring on a 23,000 year cycle (Fig. 2.2, 2.3) (Milankovitch, 1941).

These three parameters combine to determine how incoming solar radiation (insolation) is distributed across the Earth's surface (Fig. 2.2) and provide the timescale to which ice core and marine records are "tuned" (Hays et al., 1976; Imbrie et al, 1984; EPICA, 2004; Lisiecki and Raymo, 2005). Although other methods have been used to tune climate records (Ruddiman, 2007), the most commonly used method is to tune changes in a record to insolation at a latitude of 65°N on June 21st (Hays et al., 1976; Martinson et al., 1987), because it is the critical latitude for the development of northern hemisphere ice sheets (Laurentide and Fennoscandian) (Imbrie et al., 1984; Martinson et al., 1987; Ruddiman et al., 2005; Berger and Yin, 2012). As the Antarctic ice sheet has been relatively stable over the past 1 million years, and does not contribute to the benthic $\delta^{18}O$ record this, therefore, is predominantly a record of northern Hemisphere ice volume (Raymo et al., 2006). The 21st June marks the summer solstice and because summer insolation will control whether snow preserves or melts over the season, it is a critical factor in the development of ice sheets, so insolation on 21st June at 65°N should therefore be the main control on the benthic $\delta^{18}O$ record (Hays et al., 1976; Imbrie et al., 1984, 1992, 1993).

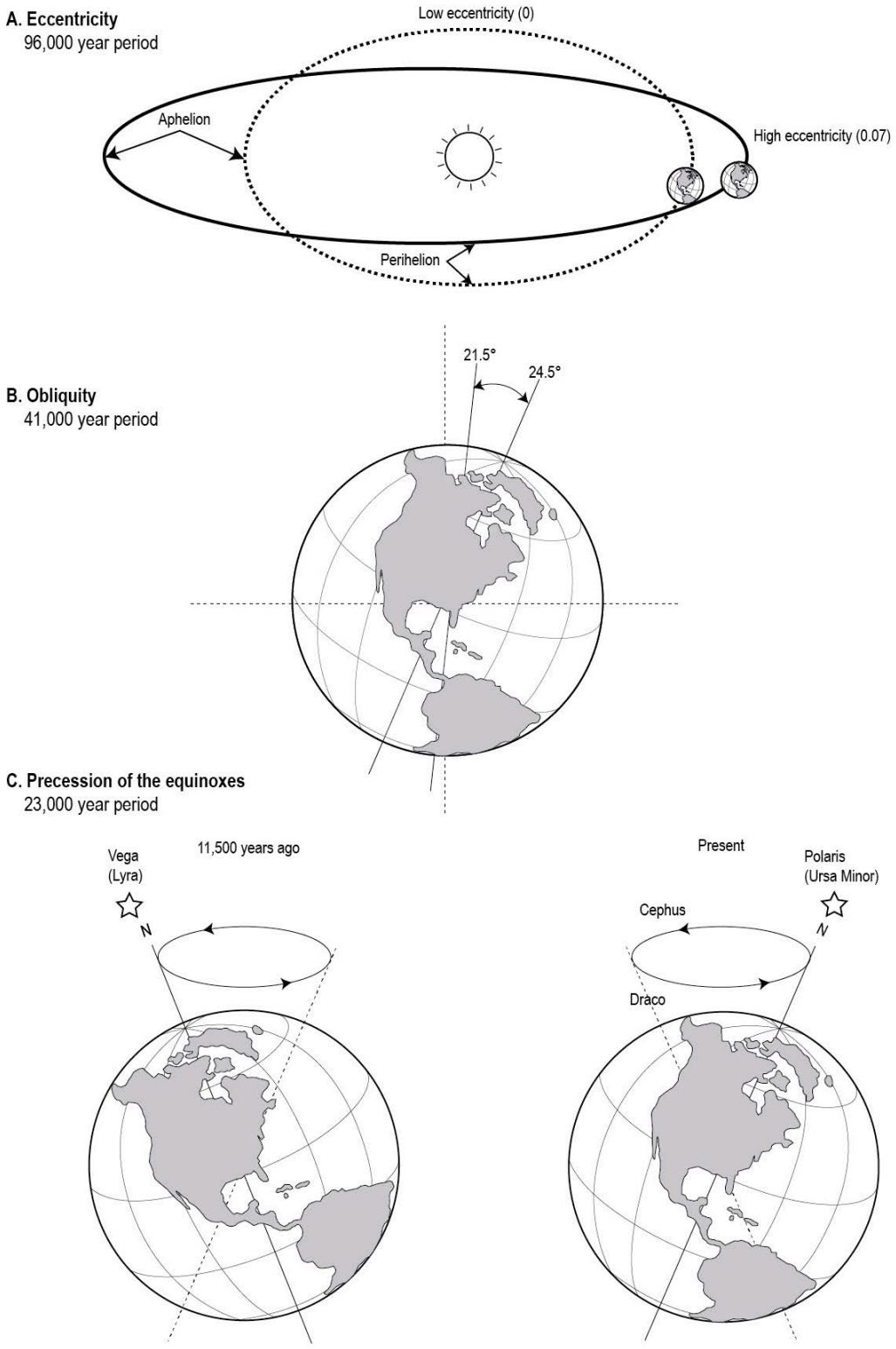

Figure 2.2. *Schematic diagram of the three orbital parameters responsible for Milankovitch cycles. A) Eccentricity (96,000 years), which controls the distance between the Earth and the Sun, B) Obliquity (41,000 years), which relates to the tilt of Earth's axis away from the sun between 21.5 and 24.5°, and C) Precession (23,000 years), which relates to the wobble of the Earth's axis, exposing more or less of each hemisphere to the sun, controlling in which seasons the earth is closest to the Sun. 11,500 years ago, the Earth was closest to the Sun during the boreal summer, whereas today it is closest to the sun during the boreal winter. Re-drawn and adapted from Hardy (2003).*

Based on this reasoning, Loutre and Berger (2000, 2003) identified a number of time intervals over the last three million years that showed a high linear correlation to the insolation patterns in their target period of the Holocene and the near future; between 5 kyr before present (BP) and 60 kyr after present (AP). Of these time intervals, MIS 11 and MIS 19 show the highest correlation over the last 800 kyr (shaded areas in Fig. 2.3). All three cases (MIS 1, 11 and 19) are periods of common insolation variations, dominated by the 413 kyr eccentricity cycle and its modulation of precession, i.e. low values of eccentricity (more circular orbit) which lead to a subdued precessional signal and therefore low-amplitude insolation variations (Loutre and Berger, 2000, 2003). The low eccentricity peak that occurs on this 413 kyr cycle and the muted insolation variations that accompany it are therefore key reasons that MIS 11 (Howard, 1997; Berger and Loutre, 2002; Droxler et al., 2003; Loutre and Berger, 2000, 2003) and MIS 19 (Tzedakis et al., 2009, 2012; Tzedakis, 2010) have been cited as Holocene analogues.

Although both MIS 11 and MIS 19 represent possible analogues for Holocene climate change based on their insolation characteristics, there are differing views on which one provides the best analogue for the Holocene. Despite the volume of literature dedicated to the suitability of MIS 11 as a climatic analogue (Droxler et al., 2003; EPICA, 2004; Masson-Delmotte et al., 2006; Pol et al., 2011), some have suggested that it may only provide a partial analogue for the Holocene (e.g. Dickson et al., 2009), while others prefer comparisons with MIS 19 (Tzedakis et al., 2009, 2012; Tzedakis, 2010), or MIS 9e (Ruddiman, 2007). A detailed discussion of the merits and limitations of these interglacials as potential Holocene analogues is, however, beyond the scope of this review.

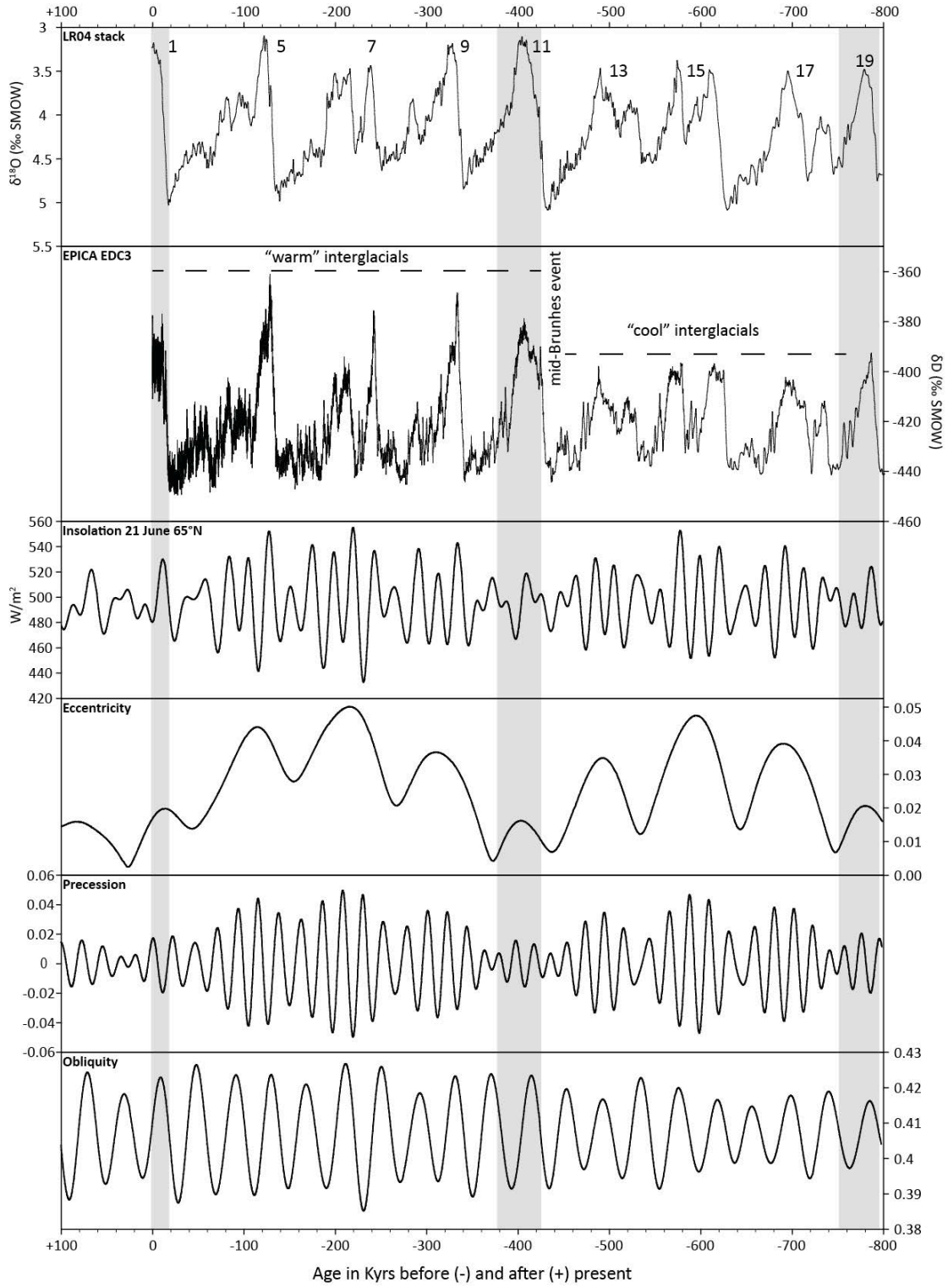

Figure 2.3. *Changes in the orbital parameters over the last 800 kyr and expected changes 100kyr into the future (Laskar et al., 2004). They are compared with the high resolution EPICA ice core record with EDC3 age model of Parrenin et al., 2007 (Jouzel et al., 2007) and the stacked benthic* $\delta^{18}O$ *record of Lisiecki and Raymo (2005). The most suitable Holocene analogues during the last 800 ka are MIS 11 and MIS 19. Taken from Candy et al., 2014.*

2.3. Climatic structure of MIS 11

A number of records are now available that provide the opportunity to examine the climatic structure of MIS 11, the majority of these being from ocean sediments and Antarctic ice core records. In this section, the climatic structure of MIS 11 will be described from the most widely used records; the stacked marine records of Imbrie et al. (1984) and Lisiecki and Raymo (2005), as well as the EPICA Dome C ice core record (EPICA, 2004). A more regional view from the North Atlantic will also be described, using a number of marine sea surface temperature (SST) records that now exist (Martrat et al., 2007; Lawrence et al., 2009; Stein et al., 2009; Voelker et al., 2010; Kandiano et al., 2012). The reliance on SST records in the North Atlantic region is related to the Greenland ice cores not extending beyond the last interglacial (MIS 5e) (e.g. Dahl-Jensen et al., 2013).

2.3.1. Ice core and stacked marine records

Figure 2.3 shows the structure of MIS 11 from LR04 (Lisiecki and Raymo, 2005) and the EPICA Dome C ice core (EPICA, 2004) compared to the structure of other interglacial periods over the last 800,000 years. The benthic $\delta^{18}O$ record of MIS 11 shows that it was an interglacial period characterised by an extended period of reduced global ice volume, with maximum ice volume reduction occurring at approximately 405,000 yrs BP (Imbrie et al., 1984; Lisiecki and Raymo, 2005). It is clear from the benthic $\delta^{18}O$ record that, unlike may of the other warm periods of the Middle and Late Pleistocene, which reach their interglacial peak within ~12,000 years of the preceding glacial maximum, rates of global ice volume reduction after MIS 12 are relatively slow, with a ~30,000 year interval occurring between the glacial-interglacial transition (Termination V) and the interglacial peak (Fig. 2.3). The EPICA Dome C deuterium (δD) record (Fig 2.3) shows a similar trend to the benthic $\delta^{18}O$ record (long duration and peak interglacial conditions late in the interval), but provides a much higher resolution record of MIS 11. This is more evident in figure 2.4, where MIS 11 is considered in isolation.

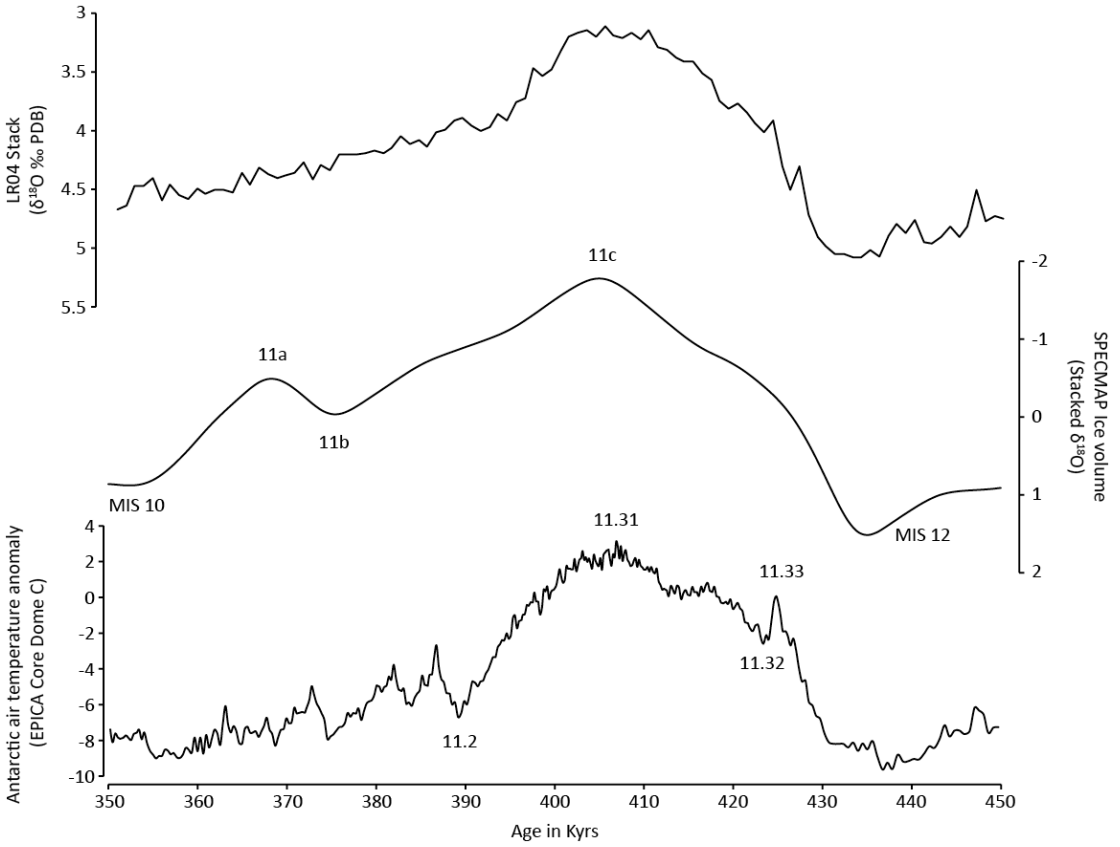

Figure 2.4. *The climatic structure of MIS 11 in a) SPECMAP (Imbrie et al., 1984), b) the LR04 stack of 57 benthic marine records (Lisiecki and Raymo, 2005) and c) EPICA Dome C deuterium record (Jouzel et al., 2007). The numbers from 11.33 to 11.2 on the EPICA record correspond to the isotope events identified by Spahni et al. (2005).*

In terms of sub-stage variability, the extended interglacial conditions of MIS 11 (~30,000 years) are then followed in the SPECMAP record by a stadial (MIS 11b) and interstadial (MIS 11a), before the next glacial cycle begins (Imbrie et al., 1984). This variability is not seen in the LR04 benthic $\delta^{18}O$ record, presumably because during the process of stacking multiple (57) records, the detail has been lost. The higher resolution in the EPICA Dome C (EDC) record shows that much greater variability exists (Fig. 2.4). While the general trend in the data is comparable to the marine records, the EPICA sequence indicates a much more dynamic and complex climate, with an early temperature rise (ca 425,000 yrs BP), followed by a cooling event centred on ca 423,000 years, before temperatures increase and recover. The main peak of interglacial conditions is characterised by relatively stable conditions persisting until approximately 412,000 yrs BP, followed by a rapid warming (Fig 2.4). Peak interglacial conditions are reached at ca 407,000 yrs BP, before conditions gradually start to deteriorate. Unlike SPECMAP, the EDC record highlights a more complex transition into

the subsequent glacial period, with a number of stadial/interstadial like events (Fig. 2.4).

2.3.2. North Atlantic marine records

Numerous palaeoclimate records now exist from the North Atlantic that enable the detailed structure of MIS 11 in the region to be characterised in terms of sea-surface temperature (SST) variations (Fig 2.5). Figure 2.6 displays a selection of SST records from the mid-latitude North Atlantic, arranged on a northward transect (Martrat et al., 2007; Stein et al., 2009; Voelker et al, 2010; Lawrence et al., 2009; Rodrigues et al., 2011; Kandiano et al., 2012), as well as one record from the high-latitude North Atlantic (Nordic Sea) (Kandiano et al., 2012). The main characteristics of the SST records from the North Atlantic region have recently been summarised by Voelker et al. (2010) and Kandiano et al. (2012), with the SST records from MD01-2443, MD03-2699 and U1313 (37.5-41°N) indicating that the picture in the mid-latitude North Atlantic is a fairly consistent one. Where present, these records show rapid warming of SST's at the onset of MIS 11, in accordance with insolation and Greenhouse Gas (GHG) changes during the glacial-interglacial transition from MIS 12 (Termination V) (Kandiano et al., 2012). Subsequent to this rapid warming, the next ~30,000 years are characterised by two relatively stable temperature "plateaus", with the older one showing slightly cooler SST's (~18°C) compared to the later one (~19°C) (Stein et al., 2009; Voelker et al., 2010; Rodrigues et al., 2011; Kandiano et al., 2012). These two plateaus are separated by a short cold phase that occurred ~413,000 yrs (Stein et al., 2009; Voelker et al., 2010; Rodrigues et al., 2011). In terms of comparison to average Holocene SST's, the first plateau (~18°C) shows good agreement with modern day values while the second peak (~19°C) shows slightly elevated SST's compared to the Holocene (Martrat et al., 2007; Rodrigues et al., 2011).

Figure 2.5. *Map of Europe showing some of the marine and terrestrial records referred to in this chapter.*

Although the same general trend is evident at the more northerly latitude of M23414 (53°N) (Fig. 2.6c), it appears more subdued, with the two "plateaus" not easily distinguishable (Kandiano et al., 2012). Moving north further still (57°N), MIS 11 is characterised in OPD 982 by a series of clear and discrete temperature peaks, although this record is constructed at a much lower resolution (Fig. 2.6b). The record in figure 2.6a is from MD992277 (69°N) (Kandiano et al., 2012) and shows very different conditions occurred in the high-latitude North Atlantic during MIS 11. This record shows that peak interglacial values in the Nordic Seas were only attained in the latter stages of MIS 11, during the second insolation peak, and that the first part of MIS 11 in this region was characterised by cold conditions and possibly extended winter sea-ice coverage (Kandiano et al., 2012), a situation very different to the early Holocene record of the same region, where an early SST optimum is evident (Bauch et al., 2001).

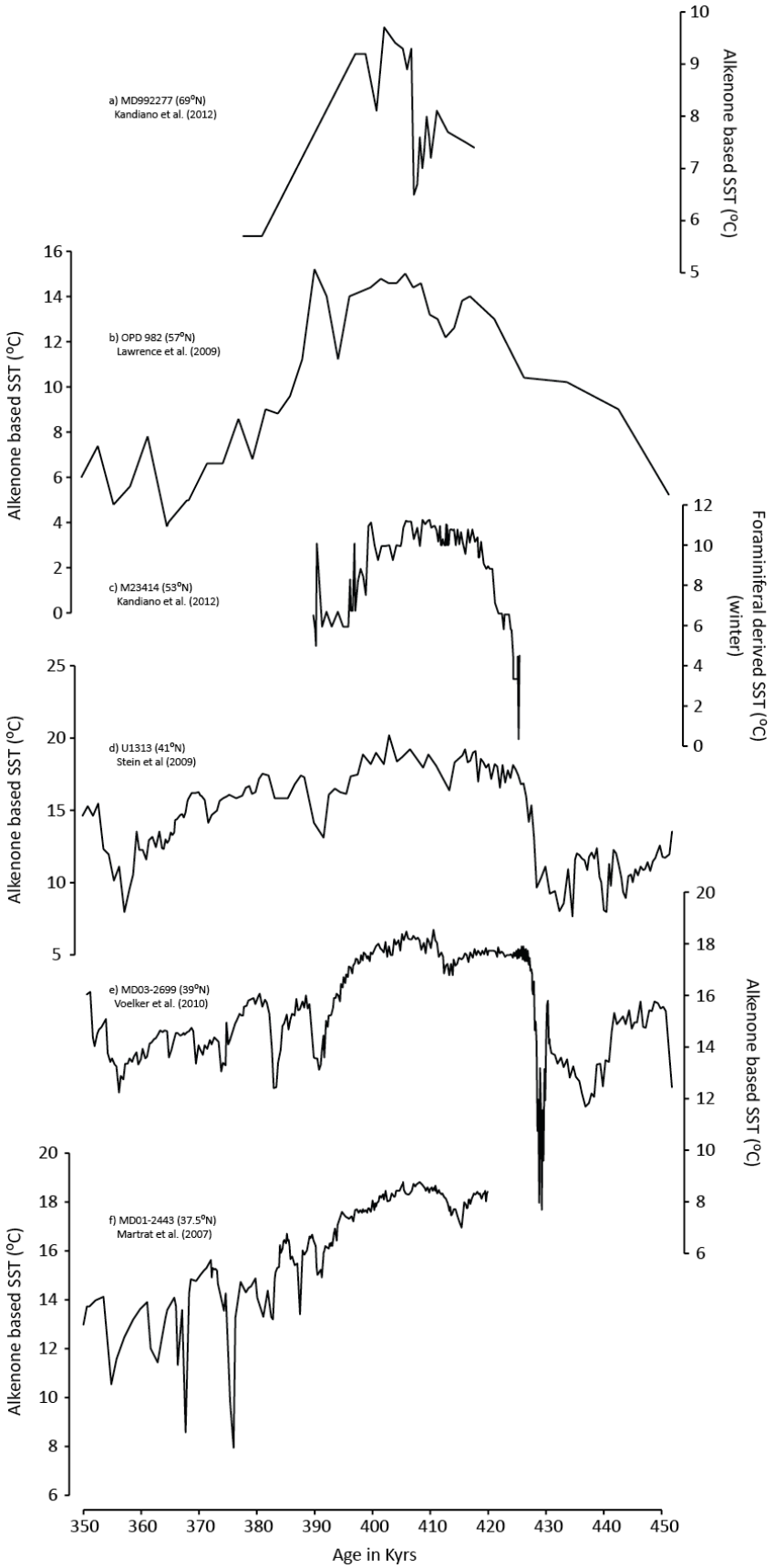

Figure 2.6. *The climatic structure of MIS 11 as expressed in SST records from the North Atlantic on a northward transect. All SST records are alkenone based with the exception of M23414, which is based on a foraminifera transfer function. Modified from Candy et al. (2014).*

This apparent difference in the SST gradient between the Nordic Seas and the Mediterranean for MIS 11 and the Holocene led Kandiano et al (2012) to suggest that the first part of MIS 11 was characterised by a predominantly negative North Atlantic Oscillation (NAO) mode (decreased pressure gradient between Iceland low and Azores high) compared to a more positive NAO mode during the later part of MIS 11 (increased pressure gradients, stronger westerlies and northward advection of warm water). Furthermore, Kandiano et al. (2012) state that prolonged de-glacial conditions and extended ice cover in the Nordic Seas would deflect the warm waters of the Norwegian Atlantic current westward, therefore causing warm conditions over Greenland, which appears to be corroborated by the work of de Vernal and Hillaire-Marcel (2008) and Reyes et al. (2014), where increased forest cover in Greenland during MIS 11, combined with a reduction in sediment delivery to the continental shelf, indicates melting of the southern sector of the ice sheet during MIS 11.

2.3.3. Climatic structure of MIS 11 in the British Isles

The British Isles contains a more detailed terrestrial record of MIS 11 than for any other interglacial period during the Quaternary (Fig. 2.1) (e.g. Jones and Keen, 1993; Thomas, 2001). In British stratigraphical nomenclature, the Hoxnian Interglacial is routinely correlated with MIS 11, based on a number of lines of evidence; pollen (e.g. West, 1956; Turner and West, 1968, but also see Thomas, 2001 for a summary of issues with this technique), faunal biostratigraphy (Keen, 2001; Schreve, 2001), radiometric dating (Rowe et al., 1999; Preece et al., 2007, but also see Geyh and Muller, 2005, 2006; Scourse, 2006), relative dating by river terrace stratigraphy (Bridgland, 1994, 2000) and amino acid racemisation (Penkman et al., 2007, 2011), as well as optically stimulated luminescence dating (Pawley et al., 2010) .

The most complete record of the Hoxnian (MIS 11) in the British Isles is provided by the pollen records from Marks Tey (Turner, 1970) and Quinton (Horton, 1974, 1979; Thomas, 2001). The sequence at Marks Tey is slightly longer than that of Quinton, as it also contains pollen relating to the subsequent cold stage (Turner, 1970). The Marks Tey record is therefore unique as it records a full interglacial vegetational succession, which is sub-divided into four major pollen zones (Fig. 2.7a) (Turner and West, 1968;

Turner, 1970); 1) the pre-temperate zone (Hoxnian I, Ho I), where total arboreal pollen (AP) first exceeds total non-arboreal pollen (NAP), is characterised by the closed boreal forest species *Betula* and *Pinus*, 2) the early-temperate zone (Ho II), which sees the expansion of mixed oak forest and a succession from *Quercus* (Ho IIa), to *Alnus* (Ho IIb) and *Corylus* (Ho IIc), 3) the subsequent late-temperate zone (Ho III), which is characterised by the progressive decline of mixed oak forest and increase in late-migrating temperate trees like *Carpinus* (Ho IIIa) and then *Abies* (Ho IIIb), and 4) the post-temperate zone, with a return to boreal and heathland species like *Pinus* and *Empetrum* (Ho IVa) as well as *Betula* and *Gramineae* (Ho IVb). Although Marks Tey provides a full interglacial vegetation succession for the Hoxnian, it should be noted that that no single borehole extracted from the site contains an *in situ* and continuous sediment sequence. Borehole GG contains sediments that have undergone brecciation, as well as a major hiatus where sediments from pollen zone Ho IV should occur (Turner, 1970). The pollen diagram of Turner (1970) is, therefore, made up of multiple cores. The sequence also contains cold-climate pollen assemblages either side of this succession that have a greater NAP:AP ratio, which Turner (1970) attributes to the late Anglian (late-glacial zone, MIS 12) and the proceeding cold stage. A key characteristic of the pollen record at Marks Tey is the occurrence of a short-lived (~300 year) increase in NAP relative to AP during the early temperate zone (Ho IIc), known as the NAP Phase (Turner, 1970), which will be discussed in more detail in section 2.4 below.

The ability to estimate the duration of MIS 11 in the British terrestrial record is made possible by the fact that laminated sediments are preserved in the Marks Tey sequence from pollen zones Ho I to Ho IIIa (Fig. 2.7a), which Turner (1970) suggests are varves (see chapter 4 for more detail). Based on the observation that Ho I to Ho IIIa contain between 9,500 and 14,500 laminations, extrapolation through the rest of the sequence based on sediment thickness, gave a figure for the duration of MIS 11 of between 30,000 to 50,000 years (Shackleton and Turner, 1967; Turner, 1970), although this was subsequently reduced to 25,000 years (Turner, 1975).

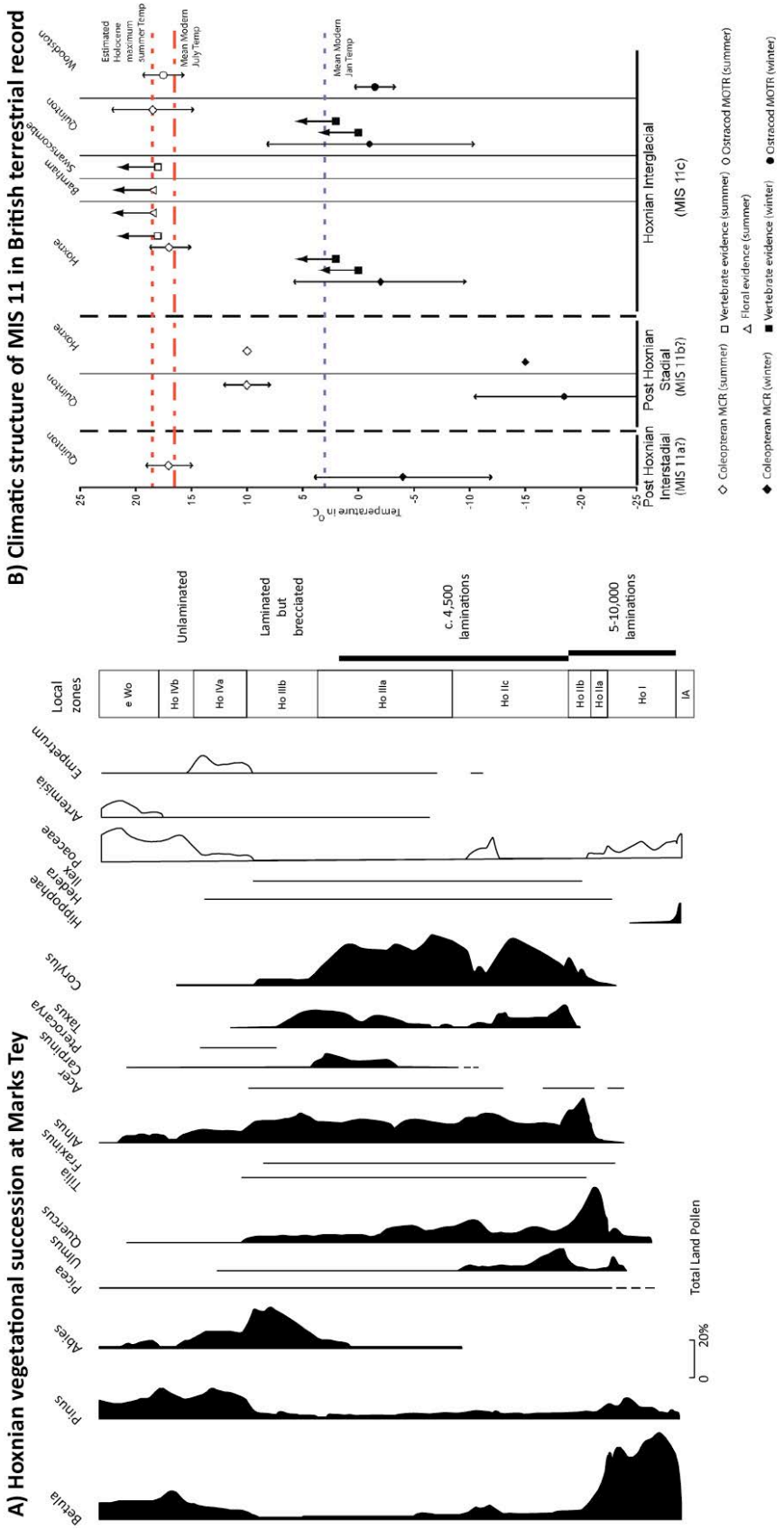

Figure 2.7. *A) Summary pollen diagram from Marks Tey along with pollen zones and estimated number of laminations preserved, re-drawn from Turner (1970). B) The* climatic *structure of MIS 11 in Britain from terrestrial proxies at a number of sites. From Candy et al. (2014).*

While the range in possible durations is very large, they point to an extended duration of MIS 11 relative to other interglacials, which is consistent with the marine and ice core records described above. This estimation is based on the assumption that the laminations are varved, an assumption that has never been proven. Consequently, the estimates for the duration of the Hoxnian that are based on varve estimation must be considered highly speculative. More detailed work needs to be carried out, however, in order to investigate whether or not the lamination structures at Marks Tey can be considered varves, which would allow a more quantitative estimate of the number persevered in the sequence.

Despite the fact that most British Hoxnian sequences are fragmentary in nature, restricting any high-precision stratigraphic correlation to climatic variations in marine and ice core records of MIS 11, snap-shots of temperatures are available from these terrestrial deposits via a number of different proxies. Figure 2.7b shows a diagram compiled by Candy et al. (2014), in which temperature reconstructions from coleopteran Mutual Climatic Ranges (MCR), vertebrates, floral and Mutual Ostracod Temperature Ranges (MOTR) from a range of sites suggest that during peak interglacial conditions (MIS 11c), temperature conditions were not dissimilar from the present day. The figure also shows coleopteran MCR evidence from Hoxne and Quinton, which indicates the possibility that post-MIS 11c sub-stages (possibly MIS 11b and a) are also present in the British record (Fig. 2.7b) (Candy et al., 2014). Although such records provide valuable evidence for the general temperature regime in the British Isles during MIS 11, in order to investigate short-term temperature variability more complete and higher resolution records are required. With the potential of sediment preservation at an annual resolution, Marks Tey provides an excellent site to undertake this, which will be described in the next section.

2.4. Abrupt events during MIS 11

As well as the potential significance of using MIS 11 as an analogue for long-term climate variability in the current interglacial, it also provides the possibility of studying the occurrence and nature of abrupt climate events in a Holocene-like interglacial. Superimposed on the long-term climate trends of the Quaternary are abrupt climatic

events that occur on sub-orbital (millennial to centennial) timescales (Allen et al., 1999; Maslin et al., 2001; Alley et al., 2003; Overpeck and Cole, 2006; Holmes et al., 2011). The most striking evidence for such events is found within archives of the last glacial cycle (Heinrich et al., 1988; Dansgaard et al., 1989; 1993) and the last glacial/interglacial transition (Dansgaard et al., 1989; Walker et al., 1999), although they are not thought to be limited to this period (Broecker et al., 2010; Siddall et al., 2010). There is also an increasing body of evidence that suggests rapid climatic events occurred during the Holocene under fully interglacial conditions, with the discovery of abrupt events (at 9.2 and 8.2 ka) in the Greenland ice core records (Alley et al., 1997; Thomas et al., 2007), and in a number of terrestrial sequences (Alley and Ágústdóttir, 2005; Rohling and Palike, 2005; Thomas et al., 2007; Daley et al., 2011). Furthermore, a number of studies have shown that such events may be common features in pre-Holocene interglacials, such as the Mid-Eemian cooling event (e.g. Maslin and Tzedakis, 1996) and, with particular relevance to this study, an event seen in many MIS 11 pollen records that may be analogous to the 8.2 ka event (Koutsodendris et al., 2012).

2.4.1. Identification of abrupt events in MIS 11 sequences

Long climate records from ice and marine cores do show climatic variability during peak interglacial conditions of MIS 11c (e.g. EPICA, 2004; Desprat et al., 2005; Lisiecki and Raymo, 2005; Jouzel et al., 2007; Stein et al., 2009). Such variability is not seen in the benthic stack of Lisiecki and Raymo (2005) (Fig. 2.8a), but the higher resolution record from EPICA Dome C does indicate a number of oscillations (Fig. 2.8b). As well as the isotope events identified by Spahni et al. (2005), sub-millennial variability has been detected in the EPICA record by Pol et al. (2011). By increasing the resolution of the δD record to approximately 50 years, Pol et al. (2011) identified significant periodicities ranging between ~180 to ~500 years. Sub-orbital events have also been noted in individual marine records (e.g. Desprat et al., 2005; Stein et al., 2009). A prominent drop in SST's is noted in some North Atlantic marine records at around 413 ka (Fig. 2.8c and 2.4) (Stein et al., 2009; Voelker et al., 2010; Rodrigues et al., 2011), and two cooling phases at 417 ka and 402 ka have been noted from the pollen assemblage in marine core MD01-2447 (Desprat et al., 2005).

While these records indicate the existence of cooling events and climatic variability on sub-orbital time-scales, when considering the duration of abrupt climatic events like the 8.2 ka event (~160 years, Thomas et al., 2007), the ability of such records to preserve any such perturbation is limited, due to their relatively coarse resolution. By way of example, if an 8.2 ka-like event occurred during MIS 11c, this would only equate to three data points in the highest resolution records of the EDC sequence. As a result, while such events may be recognised in these records, it is not possible to determine their duration and detailed climatic structure. Evidence for such events in MIS 11 is therefore best preserved in high-resolution terrestrial records, as the next sections of this chapter will demonstrate.

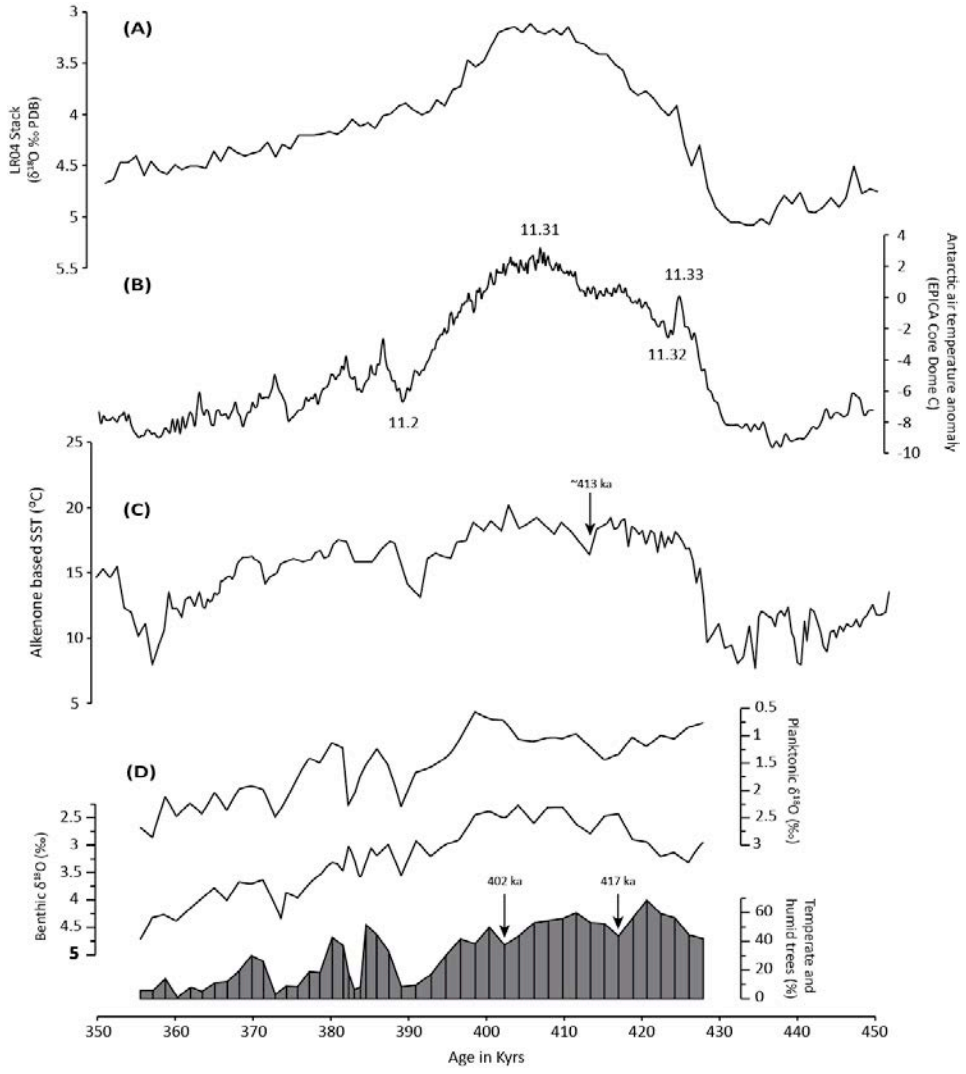

Figure 2.8. *The identification of abrupt events in MIS 11 from a selection of long climate records. a) The LR04 stack of 57 benthic marine records (Lisiecki and Raymo, 2005), b) EPICA Dome C deuterium record (Jouzel et al., 2007) with the isotope events of Spahni et al. (2005), c) North Atlantic SST record from site U1313 (Stein et al., 2009), and d) planktonic $\delta^{18}O$, benthic $\delta^{18}O$ and temperate and humid forest taxa from MD01-2447 (Desprat et al., 2005).*

2.4.1.1. The British Isles

The presence of an abrupt event in MIS 11c (possibly of climatic origin) has long been recognised in Hoxnian pollen records from the British Isles (West, 1956; Turner, 1970; Thomas, 2001). Of the number of sites in the British Isles considered to be MIS 11 in age, it is only the higher-resolution lacustrine records from Athelington (Coxon, 1985), Barford (Phillips, 1976), Hoxne (West, 1956), Marks Tey (Turner, 1970), Quinton (Horton, 1974, 1989; Thomas, 2001), Nechells (Duigan, 1956; Kelly, 1964) and St Cross South Elmham (West, 1961; Coxon, 1979) that contain such evidence (Table 2.1) (Coxon, 1993; Thomas, 2001).

Table 2.1. *Summary of Hoxnian lacustrine sites that contain evidence for the OHO/NAP phase (dots). Lines indicate the pollen zones present at each site. Modified from Thomas (2001).*

Site	GL	Ho I	Ho II	Ho III	Ho IV	GL
Athelington (Coxon, 1985)			●			
Barford (Philips, 1976)			●			
Hoxne (West, 1956)			●			
Marks Tey (Turner, 1970)			●			
Nechells (Duigan, 1956; Kelly, 1964)			●			
Quinton (Horton, 1974, 1989)			●			
St Cross South Elmham (West, 1956; Coxon, 1979)			●			

In these pollen diagrams, the natural interglacial floristic succession is interrupted during pollen zone Ho IIc (also referred to as the early temperate phase by Turner and West, 1968), where non-arboreal pollen (NAP) briefly expanded at the expense of arboreal pollen (AP), known as the NAP phase (Turner, 1970). Although the response of taxa during the NAP phase varies regionally (see Koutsodendris et al., 2012 for a summary), the event occurs during the same pollen zone at each site. In the case of Marks Tey, the clearest expression of this event is seen in the reduction of *Corylus* and a corresponding increase in *Betula* and *Poaceae* (Fig. 2.7a) (Turner, 1970).

2.4.1.2. Continental Europe

Land-sea correlations for continental Europe also correlate the Holsteinian Interglacial with MIS 11 (e.g. Nitychoruk et al., 2005, 2006; Geyh and Muller, 2005, 2006; Turner, 1998). Like the records of the British Isles, Holsteinian/MIS 11 pollen records from sites in continental Europe like Munster Breloh (Muller, 1974; Kukla, 2003), Hetendorf (Meyer, 1974), Dottingen (Diehl and Sirocko, 2007) and Dethlingen (Koutsodendris et al., 2010, 2012) in Germany, and Ossowka in Poland (Nitychoruk et al., 2005), also show evidence for the occurrence of an abrupt event occurring at a similar stage of the interglacial vegetation succession to the NAP phase, although the pollen response is different; *Pinus* woodland (rather than *Poaceae*) expands at the expense of deciduous woodland. In Holsteinian records, the correlative of NAP phase is referred to as the Older Holsteinian Oscillation (OHO) (Koutsodendris et al., 2010).

Some of the continental European pollen records also contain a second, younger event where boreal tree taxa increase at the expense of temperate tree taxa (Muller, 1974; Kukla, 2003; Koutsodendris et al., 2012 and possibly Nitychoruk et al., 2005). Koutsodendris et al. (2012) refer to this event as the Younger Holsteinian Oscillation (YHO). Interestingly, there is no evidence for a YHO-type event in the British pollen records. This may be due to the fact that many of the Hoxnian basins infill before the middle/later part of the interglacial (e.g. West, 1956; Coxon, 1979) and/or contain complex reworking/brecciation patterns in the second half of the interglacial (e.g. Turner, 1970).

2.4.1.3. The Mediterranean

In their review of Holsteinian/MIS 11 sites, Koutsodendris et al. (2012) suggest that, based on available data (some of which lacks the resolution to detect abrupt events), the OHO/NAP phase is restricted to a latitudinal zone between approximately 50° and 55°N and is not present in the Mediterranean. The one exception is the site of Praclaux in the Velay region of France, which they suggest may contain evidence for the OHO/NAP phase. This is based on the pollen diagrams of Reille et al. (2000) that contain evidence for two abrupt events (the Chaconac and Coucouron stadials), which Kukla (2003) suggested could be analogous to pollen zones VIII and XI of the Holsteinian record (Muller, 1974), redefined as the OHO and YHO by Koutsodendris et

al. (2010). Rather than occurring during fully interglacial conditions, Reille et al. (2000) suggest that these events occur during the transition into the proceeding glacial cycle. While it is true that the sites presented by Koutsodendris et al. (2012) that occur below this latitudinal zone do not contain evidence for the OHO, they do not discuss the Piánico-Sèllere record from northern Italy, which has been correlated with MIS 11 on the basis of tephrostratigraphy (Brauer et al., 2007c). This sequence shows evidence for an abrupt decrease in woodland taxa 10,000 years after the establishment of temperate broad-leaved trees. This is based on visual matching of the varve (Mangili et al., 2007) and pollen records (Moscariello et al., 2000). The decrease of temperate broad-leaved taxa coincides with an increase in *Pinus* and NAP (Moscariello et al., 2000). There are a number of reasons why including the Piánico-Sèllere record in a review of the OHO may not be appropriate. These will be discussed in section 2.4.2.6.

2.4.2. The OHO/NAP phase: an analogue for early Holocene abrupt climate events?

This section of the chapter is based on a recent suggestion by Koutsodendris et al. (2012) that the OHO/NAP phase could represent an analogue for the 8.2 ka event. The first section will give a summary of the duration, impact and forcing mechanisms behind the 8.2 ka event. The next section will summarise potential forcing mechanisms that have been proposed for the OHO/NAP phase, before discussing the rationale behind identifying it as an analogue for the 8.2 ka event. Potential issues surrounding the suggested comparison will then be highlighted, as well as potential strategies for resolving this issue.

2.4.2.1. The 8.2 ka event

The 8.2 ka event was a centennial-scale climate anomaly that has been identified in the Greenland ice cores, as well as a number of records from the North Atlantic region and further afield (Alley and Ágústdóttir, 2005; Rohling and Palike, 2005; Wiersma and Renssen, 2006; and Daley et al., 2011 provide reviews of this data). Studies of ice core records indicate the event was associated with cold, dry conditions over Greenland (Johnsen et al., 1992; Alley et al., 1997; Leunberger et al., 1999; Thomas et al., 2007), but the magnitude of the cooling over Greenland is uncertain, with estimates ranging from 7.4°C (Leuenberger et al., 1999) to around 3.3°C (Kobashi et al., 2007). The duration and structure of this cooling event in Greenland has most recently been

constrained by Thomas et al. (2007), who analysed the event by stacking the $\delta^{18}O$ signal of four Greenland ice core records (Fig. 2.9). The results show that the event lasted for 160.5 years and is asymmetrical; the lowest $\delta^{18}O$ values were reached ~60 years after the onset of this event, with the recovery from this low point taking ~100 years (Thomas et al., 2007). The 160.5 year period also contains a central event (lasting for 70 years) where $\delta^{18}O$ values are consistently below 1 standard deviation of the long-term mean. This event is preceded and proceeded by sharp warming peaks that punctuate the deterioration and recovery phases (Thomas et al., 2007). Using a number of proxies from the GISP2 record (one of the records in the Thomas et al., 2007 stack), Kobashi et al. (2007) also report similar estimates for event duration, with the coldest phase of the event occurring early on, followed by a longer period of cool conditions.

The 8.2 ka event is thought to have been caused by freshwater input into the North Atlantic from lake Agassiz during the final stages of deglaciation of the Laurentide ice sheet (possibly due to multiple drainage events; Teller and Leverington, 2004; Hillaire-Marcel et al., 2007), which has been dated to 8,470±300 cal yr. BP (Barber et al., 1999). This routing of fresh water into the ocean disrupted North Atlantic Deep Water (NADW) formation, resulting in the reduction of heat transport by the disruption of Atlantic Meridional Overturning Circulation (AMOC) (Barber et al., 1999; Clark et al., 2001; Clarke et al., 2004). A number of published records now provide evidence in support of this idea including, for example, sedimentological evidence from iceberg scour marks in Hudson Bay (Lajeunesse and St-Onge, 2008), a distinctive reddish-pink sediment layer in the Hudson Strait (Kerwin, 1996) and two layers of carbonate-rich turbidites in the Labrador Sea (Hillaire-Marcel et al., 2007). Proxy evidence for ocean water freshening includes stable isotope records from the Labrador Sea (Kleiven et al., 2008; Hoffman et al., 2012) and the wider North Atlantic ocean (Risebrobakken et al., 2003; Ellison et al., 2006), as well results from climate modelling studies (Renssen et al., 2001; Clark et al., 2004; Wiersma and Renssen, 2006).

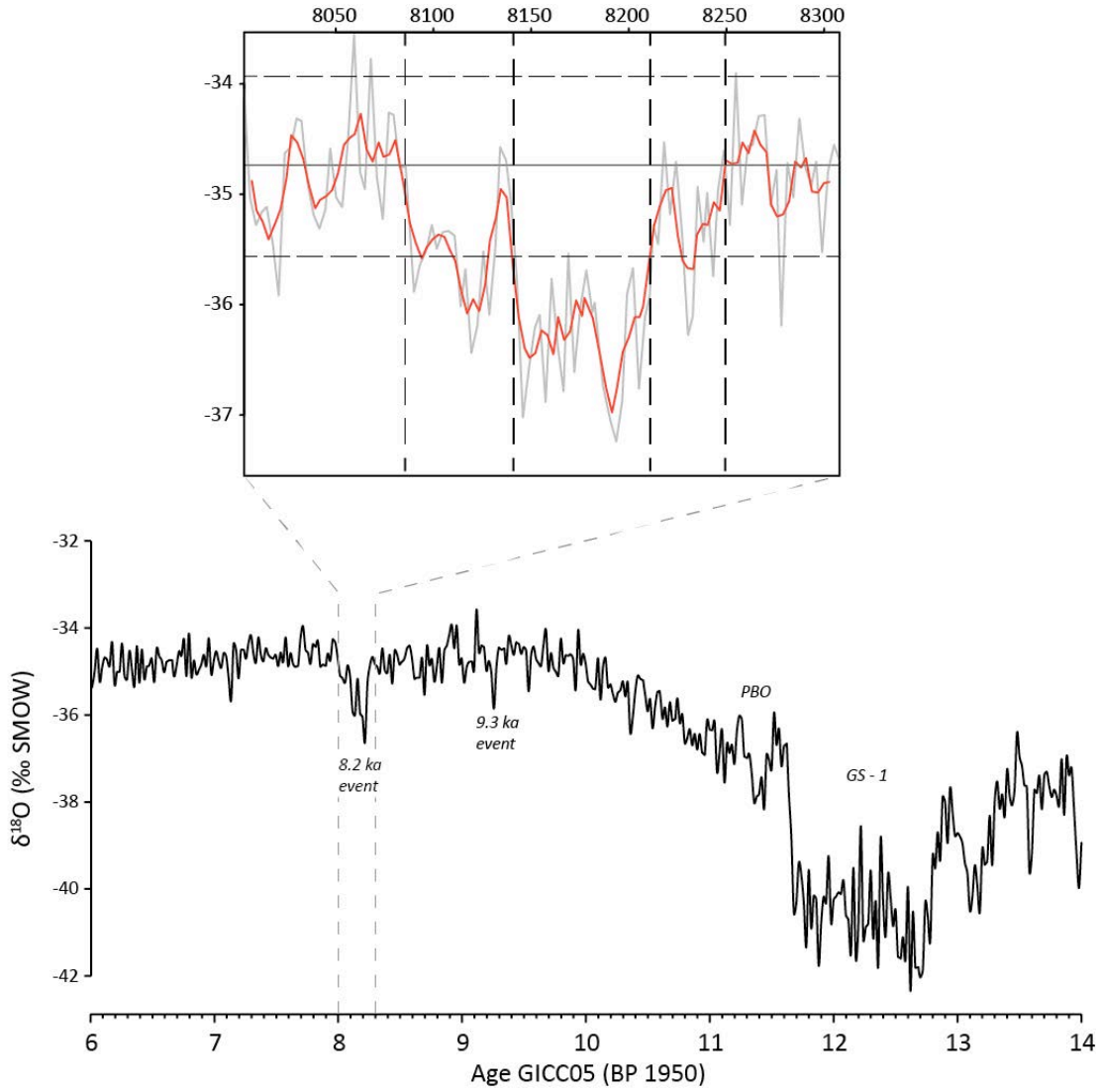

Figure 2.9. *Composite record of the 8.2 ka event from four Greenland ice cores (Dye 3, GRIP, GISP2 and NGRIP). The grey line represents a sample resolution of ~2.5 years and the red line decadal variability. The horizontal lines represent the mean and ±1 standard deviation of the data set. Dashed vertical lines (outside) represent the beginning and end of the entire event (when the signal crosses the mean) and the inside lines represent the central event (when signal consistently below 1 SD) (modified from Thomas et al., 2007).*

Although the abrupt event in the $\delta^{18}O$ record from Greenland corresponds well with the timing of melt water input into the North Atlantic from lake Agassiz, other contributing factors have also been proposed. Evidence for increased magnetic susceptibility values from a series of cores studied around the Greenland shelf provide evidence for melt water outflow from the Greenland ice sheet ~8,200 cal yr BP, which may have also contributed to freshening of the North Atlantic (Ebbeson et al., 2008). While Ebbeson et al. (2008) do not favour melting of the Greenland Ice Sheet (GIS) over the drainage of North American glacial lakes as a forcing mechanism, they suggest

that it could provide an important contributing factor in the driving mechanism behind the 8.2 ka event.

It is also important to note that the 8.2 ka event is just one of a number of abrupt cooling events, that occurred during the early Holocene. Figure 2.9 highlights the 9.3 ka event, which is also thought to be forced by meltwater (e.g. Fleitmann et al., 2008), as are other shorter-lived $\delta^{18}O$ oscillations that are not named. The 8.2 ka event is not, therefore, an isolated cooling event, but rather one of a number of early Holocene abrupt shifts that occur during the ~1,000 year interval between the 9.3 and 8.2 ka events (e.g. von Grafenstein et al., 1999; Marshall et al., 2007; Rasmussen et al., 2007; Fletimann et al., 2008). When focusing on abrupt cooling events in previous interglacials that might be analogues to the 8.2 ka event, it may be reasonable to assume that such events occur during multiple phases of instability.

2.4.2.2. Rationale of the comparison of the OHO/NAP phase and 8.2 ka event

By combining the high-resolution pollen record, varve counts and $\delta^{18}O_{silica}$ record from the site of Dethlingen, Germany, Koutsodendris et al. (2012) suggest that the OHO/NAP phase provides an analogue for 8.2 ka-like events during MIS 11c. The detailed reconstruction of this event is shown in figure 2.10 and can be summarised as follows:

1) The duration of the pollen event was 220 years, there is a 90 year regression phase where boreal trees (*Pinus* and to a lesser extent *Betula*) expanded at the expense of temperate trees (e.g. *Taxus, Corylus, Quercus, Alnus*), suggesting colder climate conditions. A 130 year recovery phase followed, where temperate tree populations are re-established;
2) There is also an impact on the aquatic environment, with the regression of vegetation coinciding with an increase in the abundance of *Stephanodiscus medius* and a more gradual increase in *Fragilaria* spp. (indicative of increased nutrients, may be the result of cooling-induced stratification break-up, as well as longer ice-cover, respectively) at the expense of *Ulnaria ulna* and *Aulacoseira subarctica*. The recovery phase is also characterised by a domination of *S. medius*, as well as a recovery of *A. subarctica* abundances,

while *U. ulna* and *Fragilaria* spp. do not recover to pre-OHO levels and remain low;

3) Although there is a lot of scatter in the $\delta^{18}O_{silica}$ record for this interval, it shows a trend consistently lower (~0.6‰) than the calculated background average (~34.6‰), which equates to an approximate maximum temperature decline of ~1.5°C, which calculated from the net effect of the temperature/diatom silica relationship (-0.2‰/°C) and the temperature/precipitation relationship (+0.6‰/°C), which results in +0.4‰/°C.

When the OHO is compared to selected records of the 8.2 ka event (Table 2.2), good agreement is found when comparing the timing and duration of floristic changes, as well as the duration of the $\delta^{18}O_{silica}$ anomaly (90 years), which shows good agreement with the central event documented in Greenland (Thomas et al., 2007; Kobashi et al., 2007) (Table 2.2). Furthermore, comparison of the sea level records and general climate patterns in Europe also appear to show good agreement (Table 2.2) (Koutsodendris et al., 2012).

Table 2.2. Comparison between the OHO and the 8.2 ka event with regard to timing, boundary conditions, characteristics and impact. Table redrawn from Koutsodendris et al. (2012).

Criterion	**8.2 ka event**	**OHO (~408 ± 0.5 ka)**
Timing after establishment of temperate forestation	~3500 yrs[a,b]	3100 ± 500 yrs
Sea level below present	~15-20m[c]	~15-20 or ~40m[c]
Duration of climate regression	~80 yrs[d]	90 yrs
Duration of vegetation regression and recovery	~300 yrs[e,f]	220 yrs
Climate pattern in Europe	Northern Europe: cold and dry Mountainous central Europe: cold and wet[g,h]	Northern Europe: cold and increasingly drier towards East Mountainous central Europe: possibly wetter

[a]Litt et al. (2001); [b]Lowe et al. (2008); [c]Rohling et al. (2010); [d]Kobashi et al. (2007); [e]Tinner and Lotter (2001); [f]Veski et al. (2004); [g]Magny et al. (2003); [h]Wiersma and Renssen (2006).

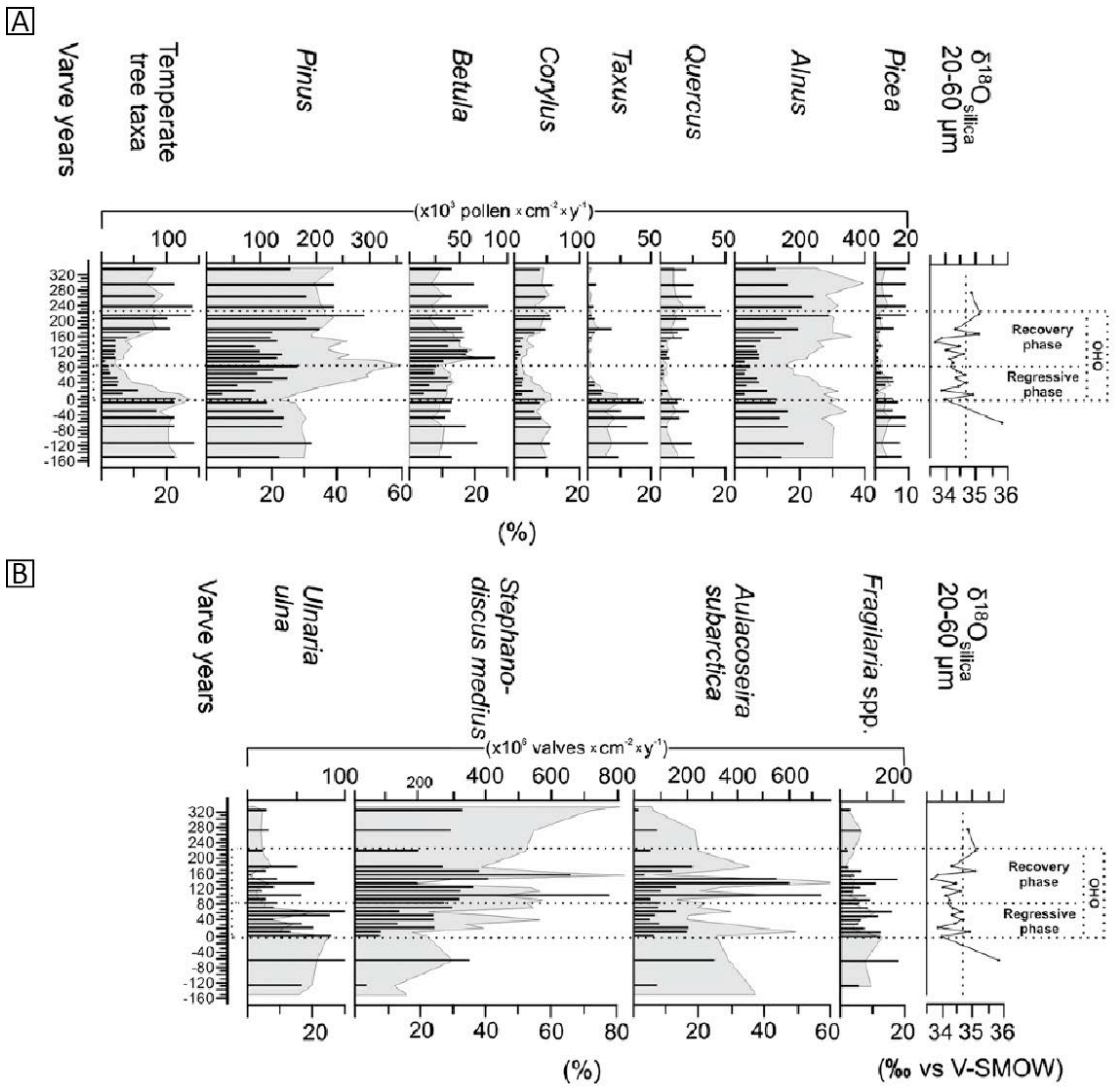

Figure 2.10. *Reconstruction of the OHO at Dethlingen, Germany. A) Selected pollen taxa and the* $\delta^{18}O_{diatom\ silica}$ *data are plotted against varve years. B) Selected diatom taxa and the* $\delta^{18}O_{diatom\ silica}$ *data are plotted against varve years. The filled grey silhouettes show relative taxa abundance, while the black lines represent accumulation rates. Varve year one indicates the onset of the OHO, which has been split into two phases: a regressive and recovery phase. Modified from Koutsodendris et al., 2012).*

While the data presented by Koutsodendris et al. (2012) provides a compelling argument for a similarity in nature between the OHO/NAP phase and the 8.2 ka event, some important questions still remain about the suitability of the OHO/NAP phase as an analogue for the 8.2 ka event, despite the apparent consistency between the two (Table 2.2). These issues will be discussed individually over the next three sections.

2.4.2.3. Structure and duration of the OHO/NAP pollen event

Researchers have been aware for some time of the presence of at least one abrupt event in Hoxnian/Holsteinian pollen records (e.g. West, 1956; Turner, 1970; Muller, 1974). This event has not been studied using detailed multi-proxy analysis until

recently (Koutsodendris et al., 2011, 2012). In terms of the British record, the only site that has the resolution to investigate the OHO/NAP phase at a comparable resolution to the work of Koutsodendris et al. (2011; 2012) is Marks Tey (Turner, 1970). The structure of the NAP Phase differs from that of the OHO in terms of pollen variations. The OHO is characterised by the expansion of *Pinus* forest at the expense temperate tree taxa (Koutsodendris et al., 2010; 2012), whereas the NAP Phase is characterised by the expansion of *Poaceae* at the expense of *Corylus* (Turner, 1970).

Based on averaged sedimentation rates from sediments considered to be varved, Turner (1970) suggested that at Marks Tey the loss and recovery of arboreal pollen lasted for approximately 350 years. This is almost 100 years longer than the duration of the event at Dethlingen, at 220 years (90 year regressive phase, 130 year recovery phase) (Koutsodendris et al. (2012). The duration of the MIS 11 pollen events in the Piánico-Sèllere and Ossowka sequences is unknown. While there is some discrepancy in terms of their duration, the estimates from Marks Tey and Dethlingen mark them out as centennial scale events, like the 8.2 ka event (Table 2.2). As is seen in the difference between the British NAP and the continental OHO the vegetation response to this event is regionally variable (Table 2.2), which is also the case for the 8.2 ka event. Again, it needs to be stressed that all of the estimates presented from Marks Tey assume that the laminations are varves and are based on estimates rather than actual counts

2.4.2.4. Timing of the OHO/NAP phase

While similarities exist between the floristic response that occurred during the OHO/NAP phase and the 8.2 ka event, a recent suggestion by Koutsodendris et al. (2011, 2012) about the timing of the event is controversial. Considering the British sequences in isolation, the simplest way to compare the relative positions of the OHO/NAP phase and the 8.2 ka event is to determine their locations in the pollen successions of both Interglacials from the same region (undertaken by Koutsodendris et al., 2012, Table 2.2) (Fig. 2.11).

Table 2.3. *Selected records showing the complexity of regional terrestrial response to the 8.2 ka event.*

Site	Location	Chronology	Duration of pollen event	Climate poxy used	Climatic signal	Lag in proxy response?	Reference
Schleinsee	Germany	Varve/radiocarbon	~250-300 yrs	Correlated to GRIP/GISP	Temperature	Within sampling error (0-20 yrs)	Tinner and Lotter (2001)
Soppensee	Switzerland	Varve/radiocarbon	~250-300 yrs	Correlated to GRIP/GISP	Temperature	Up to 40 yrs	Tinner and Lotter (2001)
Cooney Lough	Ireland	Radiocarbon	250 yrs	Compared to GRIP/NGRIP	Temperture	N/A	Ghilardi and O'Connell (2013)
Lake Rouge	Estonia	Varve/ palaeomagnetic/ radiocarbon	320 yrs	δ^{18}O Calcite	δ^{18}O Lakewater	Not determined	Veski et al. (2004)
Haweswater	England	U-series	No pollen response	δ^{18}O Calcite	δ^{18}O Lakewater	N/A	Marshall et al. (2007)
				Chironomid-inferred temperature	July temperature	N/A	Lang et al. (2010)
Ammersee	Germany	Varve	N/A	δ^{18}O Ostracod	Annual temperature	N/A	von Grafenstein et al. (1998)
Holzmaar	Germany	Varve	Not determined	Micro-facies: Calcite	Summer temperature	N/A	Litt et al. (2009)
				Micro-facies: Aluminuim	Winter dryness		Prasad et al. (2009)
Hojby So	Denmark	Radiocarbon	250 yrs	Magnetic Susceptibility	All a proxy for precipitation/inwash	200-250 yrs	Hede et al. (2010)
				Chlorophyll A			
				Diatom AR			
Igelsjon	Sweden	Radiocarbon	N/A	δ^{18}O/ δ^{13}C Calcite	Precipitation/ evaporation	N/A	Hammarlund et al. (2005)
				% Total organic carbon and minerogenic	Summer precipitation		
Motterudsjarnet	Sweden	Varve/radiocarbon/tephra/ palaeomagnetic	N/A	Magnetic Susceptibility	Winter precipitation	N/A	Zillen and Snowball (2009)
Kalksjon	Sweden	Varve/radiocarbon	N/A	% Total organic carbon	Both proxy for winter precipitation	-50 years	Snowball et al. (2010)
				Titanium			

Figure 2.11 shows good agreement between the location of the OHO/NAP phase at Marks Tey and the location of the 8.2 ka event at Hockham Mere, which both occur during the early temperate phase of both diagrams (Turner and West, 1968). Furthermore, there is also general agreement between the timing of both events relative to the establishment of temperate forests. The 8.2 ka event occurs approximately 2,800 years after the establishment of temperate forest at Hockham Mere (Fig. 2.11). In comparison the onset of the OHO/NAP based on average sedimentation rates from the proposed chronology for Marks Tey (Shackleton and Turner 1967; Turner, 1970, 1975), occurred ca. 3,000-4,150 years after the establishment of temperate forest at Marks Tey (in agreement with the observation of Koutsodendris et al., 2012).

The absolute age of the OHO/NAP phase is more difficult to determine, due to the issues that arise when dating sediments from this time period (Rowe et al., 1999; Kamer and Marra, 2003; Geyh and Muller, 2005, 2006; Scourse, 2006). Ashton et al. (2008) have attempted to circumvent this problem by aligning the Marks Tey record (amongst others) to those of Velay (Reille and de Beaulieu, 1995; Reille et al., 2000) and MD01-2447 (Desprat et al., 2005), by assuming that 1) the development of temperate forest coincides with the onset of MIS 11c (~424 ka BP), 2) the onset of this development is synchronous between the Mediterranean and the British Isles, and 3) the suggested 30,000 year duration of the Hoxnian (Shackleton and Turner, 1967; Turner, 1970, 1975) is accurate. This tuning process gives an approximate age for the OHO/NAP phase of around 416ka BP, 8ka after the onset of the interglacial (Fig. 2.12). Instead of tuning the records, another method is to use the suggested lamination counts by Turner (1970) for the Marks Tey sequence record. Using the same assumption as Ashton et al. (2008) about the onset of the interglacial, the OHO/NAP phase occurs somewhere between ~6,900 to 11,900 years after the onset of the interglacial woodland expansion, giving a chronological position somewhere between ~417-412ka BP.

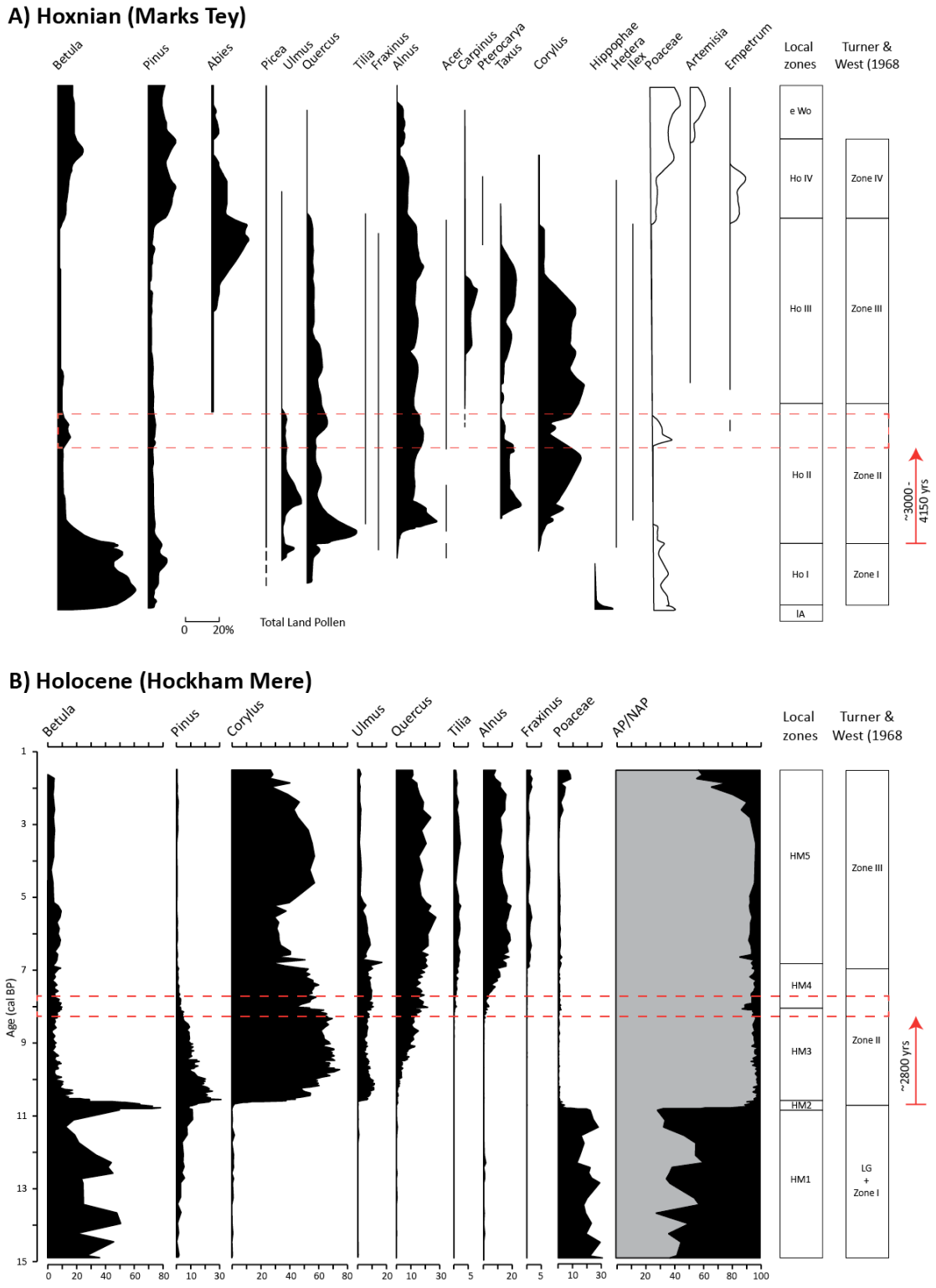

Figure 2.11. *Comparing the location of the NAP phase in the Hoxnian pollen sequence from Marks Tey (data from Turner, 1970) with the location of the 8.2 ka event in a Holocene pollen record from the same region, Hockham Mere (data from Bennett, 1983), which appears to show a response to the event (Giesecke et al., 2011). Calibration of radiocarbon dates from Hockham Mere was undertaken by Ian Matthews (RHUL). Local pollen zones are also accompanied by the general scheme of zoning interglacial pollen diagrams of Turner and West (1968), and applied by West (1970) to Holocene sequences. The boundary between Zone II and III in Hockham Mere marks the onset of the elm decline. Red arrows indicate timing of both events relative to the development of temperate forest (zone II).*

This method of alignment seems to work well for Marks Tey, because the 30,000 year duration of MIS 11c suggested by estimating sedimentation rates conforms to the duration suggested by orbitally tuned records (e.g. Imbrie et al., 1984; EPICA, 2004; Lisiecki and Raymo, 2005). The method also appears to work for Ossowka, Poland, where varve counts suggest the Holsteinian/MIS 11 lasted for between 35-39,000 years (Nitychoruk et al., 2005). In their investigation, Nitychoruk et al. (2005) suggest the OHO/NAP phase occurs at ~406-410ka BP (Fig. 2.12). Like Marks Tey, the chronology at Ossowka should be considered with caution, as detailed micro-facies analysis of the laminated sediments have not yet been published.

The method of Ashton et al. (2008) does not appear to work so well for the Holsteinian sequences in Germany, however, where the duration of interglacial conditions are thought to only last for 15,000 ± 1500 years, and the OHO/NAP phase occurs ~7,000 years after the onset of interglacial conditions (Koutsodendris et al., 2012). Koutsodendris et al. (2012) explore the possibility of two alignment scenarios for the vegetation record at Dethlingen. Using the rationale of Ashton et al. (2008), where the development of temperate forest coincides with the onset of MIS 11c (~424 ka BP), the OHO/NAP phase occurs at ~418ka BP, towards the end of the first insolation peak of MIS 11c, in agreement with the lower estimates based on the lamination counts of Turner (1970) (Fig. 2.11a). However, Koutsodendris et al. (2012) argue against this positioning because the shorter duration of temperate woodland would mean that interglacial conditions in the Luneburger Heide region would end before the second insolation peak of MIS 11c, when ice core, relative sea level, sea-surface temperature and regional pollen records indicate the warmest conditions occur (Fig 2.12 a, b, c and f). Koutsodendris et al. (2012) therefore advocate the alignment of the central European MIS 11c vegetation records to the second insolation peak (~415ka to 397ka BP), citing that there is a lag between the onset of marine and terrestrial interglacials (Tzedakis et al., 2004; Skinner and Shackleton, 2006).

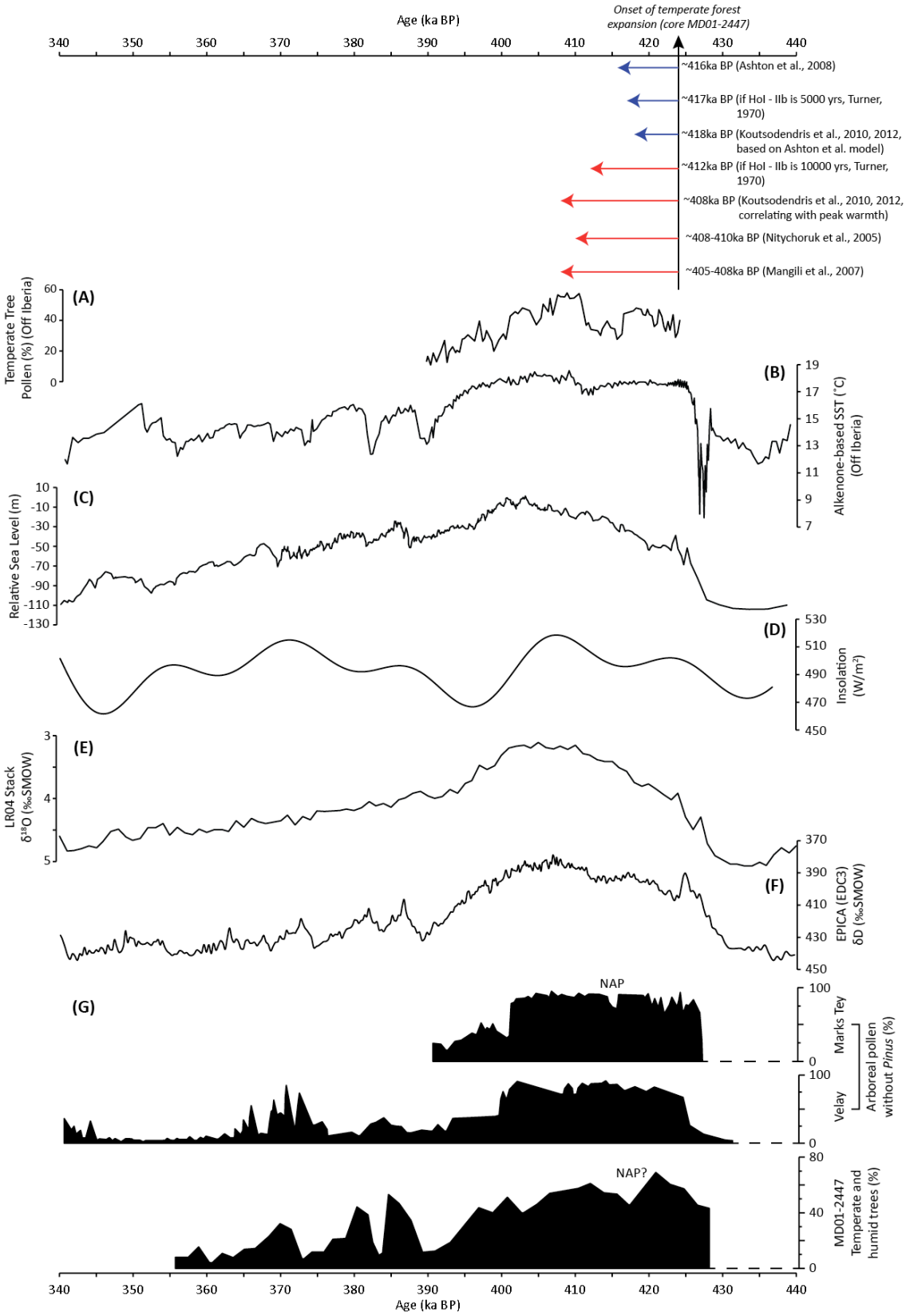

Figure 2.12. *Diagram showing different possibilities regarding the timing of the OHO/NAP phase during MIS 11c. Blue arrows relate to suggestions that place the event in the first half of the interglacial, whereas the red arrows relate to the second half (see text for discussion). A) Temperate tree pollen abundance at site MD01-2443, off Iberia (Tzedakis, 2010), B) alkenone-based sea surface temperature record from MD03-2699, off Iberia (Rodrigues et al., 2011, C) Red Sea relative sea level reconstruction (Rohling et al., 2010), D) Insolation curve June 21, 65N (Laskar et al., 2004), E) LR04 stacked benthic marine records (Lisiecki and Raymo, 2005), F) EPICA EDC3 timescale (Jouzel et al., 2007), G) selected records from the tuning undertaken by Ashton et al. (2008).*

Koutsodendris et al. (2011; 2012) also highlight that temperate forest was not well-established in Southern Europe during the first part of MIS 11c (Tzedakis, 2010) and the mid-MIS 11c decline in temperate forest pollen, which coincides with the temperature drop seen in North Atlantic SST records, is not observed within the pollen records from Germany or the British Isles, therefore arguing against alignment with the first part of MIS 11 (Fig. 2.12a). Although not discussed by Mangili et al. (2007), the positioning of Pianico Isotopic Oscillation (PIO) III agrees with the model advocated by Koutsodendris et al. (2012).

This method of alignment by Koutsodendris et al. (2010, 2012) gives a revised age of ~408ka for the OHO/NAP phase. Assuming this scenario is correct, it raises questions as to the existence of the sedimentary record of the first part of MIS 11c in the Luneburger Heide region. Assuming also that the OHO and NAP phase are synonymous, it has major implications for British pollen records during the first part of MIS 11. If the assumption is made that the lower end of Turner's (1970) duration estimates for Ho I – Ho IIb are more likely, there must either be a hiatus in the sedimentary record at Marks Tey, or there was a significant gap between the onset of MIS 11c and the initiation of sedimentation in the basin. At the other end of the scale, the upper estimate of the duration of the early part of MIS 11c by Turner (1970) would be an underestimate of ~4,000 years. Given that this would require boreal forest to persist for ~13,000 years during the first part of MIS 11, it raises important questions as to the suitability of the first part of the interglacial as an analogue for the Holocene.

2.4.2.5. Potential forcing mechanisms for the OHO/NAP phase

Since the discovery of the OHO/NAP phase, a number of different forcing mechanisms have been proposed to explain its occurrence. Kelly (1964), working on the lacustrine sequence at Nechelles, Birmingham, suggested that the event could be the result of a fall in lake level, exposing and reworking earlier cold climate lake sediments and associated pollen, or a climatically driven event. A climatic origin was also advocated by Muller (1974), based on pollen work at Munster Breloh, Germany. More recently, a review by Kukla (2003) favoured a climatic origin for the event, in which he postulated

the potential for Heinrich-like events as a forcing mechanism. Detailed work at Marks Tey by Turner (1970) suggested that, based on the vegetation response and the presence of charcoal fragments around the onset of the event, the OHO/NAP phase was more likely to be the result of a wildfire event, but this suggestion is tempered by the acknowledgement of the spatial extent of the event, making it difficult to envisage fire on such a large scale. If the OHO/NAP phase is the result of a large-scale wildfire then extreme events such as bolide impacts may need to be considered, which have been suggested as the forcing mechanism for the Younger Dryas (GS-1) (e.g. Firestone et al., 2007). It should be noted that currently, however, charcoal remains have only been found in association with the OHO/NAP at British Hoxnian sites.

A further suggestion is that the OHO/NAP phase may relate to volcanic activity, with the discovery of a large tephra deposit below the vegetation event at Dottingen, in the Eiffel region of Germany (Diehl and Sirocko, 2007). Such a suggestion would therefore imply large-scale volcanism in Europe during this time. Much like the wildfire hypothesis, the appearance of thick tephra deposits is restricted and only seems to occur at this single site.

One of the key issues surrounding these suggestions about the forcing mechanism for the OHO/NAP phase is that, until recently, no evidence was available from independent proxies to aid interpretations. In their study at Dethlingen, Germany, Koutsodendris et al. (2012) determined stratigraphical variations in $\delta^{18}O_{silica}$ from diatoms, which have been demonstrated to provide records of temperature and precipitation (e.g. Leng and Barker, 2006; Bailey et al., 2014), to further investigate the forcing mechanism. What is evident from the $\delta^{18}O_{silica}$ record is that there is a period of 90 years where the isotope values fall consistently below the long-term mean of the dataset, which Koutsodendris et al. (2012) interpret as a temperature driven reduction in the $\delta^{18}O$ value of lake water (see Fig 2.13 and chapter 3).

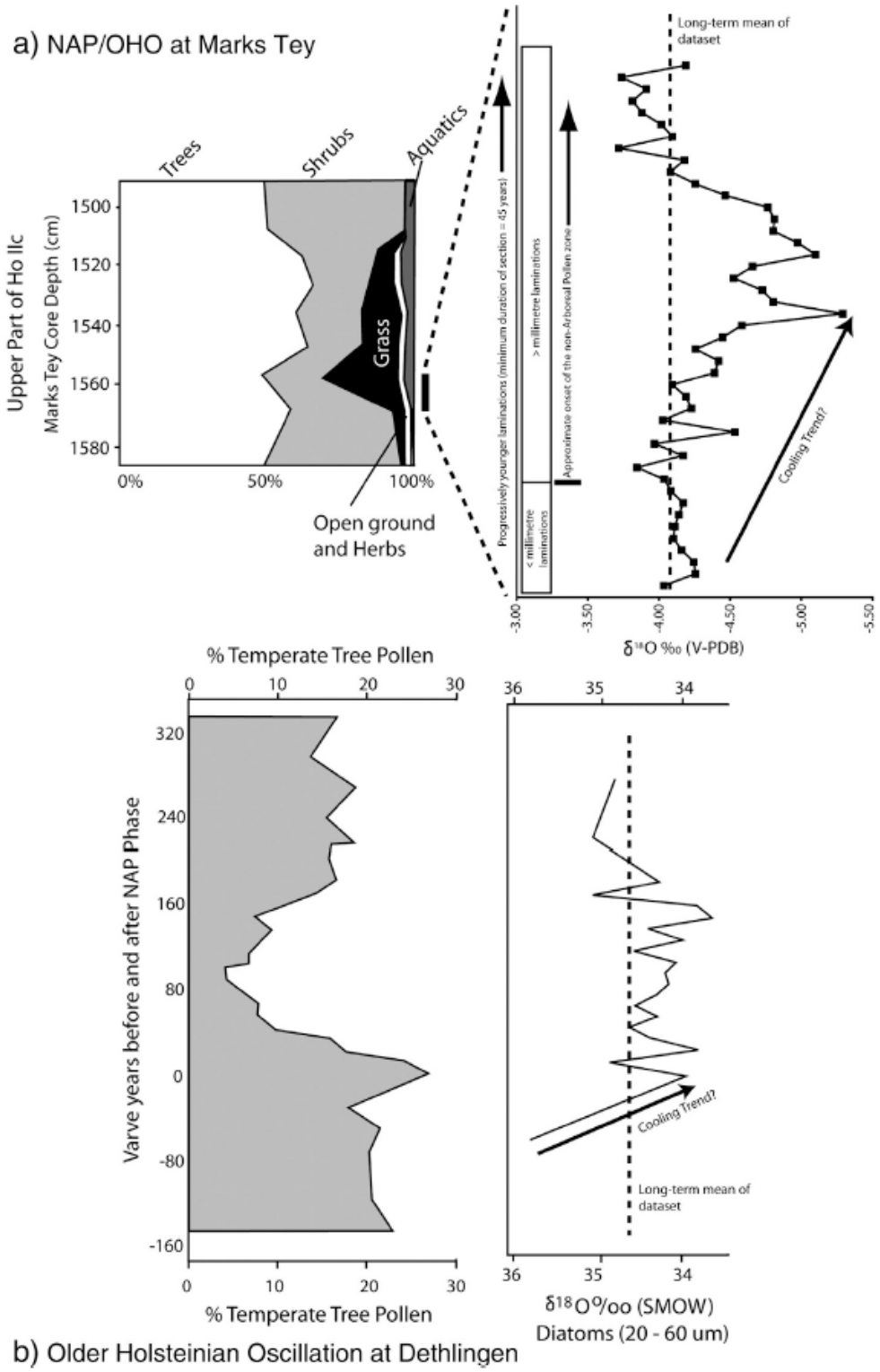

Figure 2.13. *Expression of a) the NAP phase at Marks Tey (Turner, 1970; Candy, 2009) and b) the OHO at Dethlingen (Koutsodendris et al., 2010; 2012). Plotting the stable oxygen isotope data from Candy (2009) against depth reveals a decreasing trend in the* $\delta^{10}O$ *of carbonate around the onset of the NAP phase at Marks Tey, which may indicate a cooling trend. The* $\delta^{10}O_{diatom\ silica}$ *record from Dethlingen also exhibits values consistently below the long-term mean of the dataset during the OHO phase. See text of a discussion of these records.*

Candy (2009) also undertook stable isotope work on a short section of Marks Tey sediments borehole GG of Turner (1970). This data was re-plotted as stratigraphical variations in $\delta^{18}O$ around the OHO/NAP phase by Candy et al. (2014), although the duration of the event could not be quantified and no direct comparison with the pollen event could be made. Like the results from Dethlingen, there appears to be an isotopic depletion away from average dataset values, which may be indicative of a climatic event (see Leng and Marshall, 2004; Marshall et al., 2007 and chapter 3). The issue with the dataset of Candy (2009) is that the $\delta^{18}O$ and $\delta^{13}C$ values show a high degree of co-variance (r^2=0.77), which could suggest that evaporation is the dominant control on the stable isotopic values of the authigenic carbonates, or that there is contamination of the signal by detrital carbonate from the catchment (see chapter 3).

2.4.2.6. Duration of the isotopic event

The potential forcing mechanism for the OHO/NAP phase also needs to be considered. The isotopic data presented by Koutsodendris et al. (2012) provides strong evidence in favour of a climatic origin for the OHO/NAP phase. The issue that needs to be discussed here is if the OHO/NAP is climatic in origin, what drives it if it is comparable to that at the 8.2 ka event? While the comparison by Koutsodendris et al. (2012) of the OHO/NAP phase with the central cooling phase of the 8.2 ka event in Greenland may seem reasonable (Table 2.2, Fig 2.10 and 2.13), it does assume that the climatic event and pollen event occurred contemporaneously. That is to say that isotopic analysis was only carried out on a short section of the core, the OHO/NAP zone itself, so the variations in isotopes before and after this are unknown. Nothing is known about the longer-term trends in both isotope data sets and whether or not these events are significant in relation to longer-term trends. While the duration of the stable isotope event is unknown in the Ossowka sequence (Nitychoruk et al., 2005), Mangili et al. (2007) found a period of low oxygen isotope values that lasted for 780 years in the Piánico-Sèllere sequence, which based on their correlation with MIS 11, shows good agreement with the preferred timing of Koutsodendris et al. (2012) for the OHO/NAP phase (Fig. 2.12). However, there is currently an issue with the Piánico-Sèllere sequence in terms of its age. Based on the dating of tephra layers found in the sequence, Brauer et al. (2007a, b) assigned it to MIS 11, whereas previous dates place the sequence in MIS 19 (Pinti et al., 2001, 2003, 2007), a suggestion more recently

corroborated by palaeomagnetic work at the site (Scardia and Muttoni, 2009). Irrespective of whether or not the Piánico-Sèllere record is assigned to MIS 11 or MIS 19, it highlights the need to extend the isotope records from Dethlingen and Marks Tey to determine the long-term climatic trend either side of the NAP/OHO phase.

With reference to the 8.2 ka event, Koutsodendris et al. (2012) note some key similarities with the OHO/NAP phase in terms of the impact of the cooling event on the terrestrial and aquatic ecosystems. While the magnitude of the impact of the 8.2 ka event on vegetation varies regionally, a general trend, and duration similar to that of the OHO, an increase in boreal trees at the expense of temperate taxa is seen at sites from Scandinavia through to the Mediterranean (Table 2.2, 2.3) (Koutsodendris et al., 2012 and references therein). While the climatic event, reconstructed using $\delta^{18}O_{silica}$, appears to occur contemporaneously with the pollen event at some sites (e.g. Tinner and Lotter, 2001; Veski et al., 2004), as do proxies for changes in lake catchment processes (e.g. Prasad et al., 2009), this is not always the case. For example, at Højby Sø, Denmark, proxies of detrital in-washing, which may be linked to climatic deterioration (e.g. Hammarlund et al., 2005), indicate a marked increase up to 250 years before the pollen event occurred (Hede et al., 2010). Furthermore, complexities with the terrestrial response to the 8.2 ka event in some Scandinavian sequences indicate lake catchment instability commenced after the onset of the climatic event (e.g. Snowball et al., 2010), while proxy evidence in other records appear to show the presence of two or three cooling episodes around 8,000 cal. yr BP (e.g. Ojala et al., 2008; Zillen and Snowball, 2009).

While regional variations in terrestrial response to the 8.2 ka event are to be expected, they further highlight the need to increase the temporal resolution of proxy records for the OHO/NAP phase. This is certainly the case for both the $\delta^{18}O_{silica}$ record at Dethlingen and the $\delta^{18}O_{calcite}$ record at Marks Tey. While the evidence from Dethlingen suggests that the lake catchment was relatively stable during the OHO/NAP phase, apart from the noted increase in lamination set thickness associated with the OHO/NAP phase at Marks Tey (Turner, 1970), the stability of the lake catchment is not currently known.

2.4.2.7. Alternative forcing mechanisms

The evidence presented so far would indicate that a climatic deterioration is the most likely forcing mechanism for the OHO/NAP phase. However, this suggestion would need to consider the following; 1) the occurrence of charcoal fragments at the start of the OHO/NAP which indicates wild fires as a major cause, 2) the absence of lag time proxy records from sites that would corroborate a climatic origin, 3) the fact that it if, as proposed by Koutsodendris et al. (2012), the event occurred 17,000 years after the termination of MIS 12 the key driving mechanism, the input of freshwater from melting glaciers may not be present.

While it is unlikely that a pan-European wildfire was responsible for the OHO/NAP phase, the fact remains that charcoal fragments occur in many Hoxnian sequences around the onset of the OHO/NAP phase (e.g. Turner, 1970). The exact location of these charcoal fragments and their relationship to the vegetation event therefore needs to be determined. Furthermore, given the proposed timing of the OHO/NAP phase at ~408,000 yrs BP and the suggestion that it was forced by meltwater input into the North Atlantic (Koutsodendris et al., 2012), a source for this meltwater would be required during the second part of MIS 11c. Given that the sea level record indicates continued sea level rise across MIS 11c (Fig. 2.12c) (Rohling et al., 2010; Koutsodendris et al., 2011; 2012), it is conceivable that the input of meltwater could trigger an event at this time. Evidence for a prolonged sea level rise during MIS 11 comes from species turnover rates in the British Isles, which indicate the existence of a land bridge with the continent during this interglacial (e.g. White and Schreve, 2000; Schreve, 2001a,b). Evidence from the sea level record is further supported by pollen and sedimentological evidence from marine records close to Greenland, which indicate that the Greenland ice sheet retreated during the second part of MIS 11c (de Vernal and Hillaire-Marcel, 2008; Reyes et al., 2014) Furthermore, shoreline evidence from Bermuda and the Bahamas suggests that the Greenland ice sheet may have completely collapsed during MIS 11c (Raymo and Mitrovica, 2012). While the precise mechanism for this is uncertain, prolonged sea ice coverage in the Nordic Seas during the first part of MIS 11c (e.g. Kandiano et al., 2012) and an increase in heat transport to the high northern latitudes during the second part of the interglacial (Dickson et al., 2009) could provide mechanisms. Considering that melting of the Greenland ice sheet may have also

contributed meltwater to the North Atlantic during the 8.2 ka event (Ebbeson et al., 2008), it is therefore conceivable that such a situation could also occur during MIS 11c, although suggesting any link between the two is currently speculative.

2.5. Summary

- Based on the similarity of orbital parameters between the two interglacials, MIS 11 is considered to be one of the most suitable analogues for natural climate variability during the Holocene.
- Despite the high correlation between orbital parameters, some regions (e.g. the Nordic Sea) show very different climatic records for MIS 11 when compared to the Holocene. An investigation of the merits and limitations of MIS 11, as well other interglacials, as analogues for the Holocene is, however, beyond the scope of this thesis.
- If MIS 11 is a good analogue, high-resolution terrestrial archives deposited during the interglacial offer ideal sites to investigate natural climate variability during a Holocene-like interglacial.
- A number of terrestrial records from western and central Europe contain evidence for and abrupt event (OHO/NAP Phase) during full interglacial conditions of MIS 11c, which may be analogues to the 8.2 ka event. Such events may provide important insights into climate variability during previous interglacial periods, as well as future climate variability of the Holocene.
- Questions remain, however, as to the timing, duration and forcing mechanism of this event. While the event has long been recognised in many British MIS 11 sequences, it remains understudied. There is, therefore, a need to re-investigate these sequences to provide more data about the structure and impact of this event.

Chapter 3. Environmental reconstruction using stable isotopes of lacustrine carbonates

Chapter overview

The use of stable isotopic analysis as a tool for environmental reconstruction from marine carbonates has revolutionised our understanding of climatic variability during the Quaternary Period (e.g. Hays et al., 1976; Shackleton, 1987; Jouzel et al., 2007; Rasmussen et al., 2008). Until relatively recently, oxygen and carbon isotopic analysis of lacustrine carbonates has been an under-utilised technique. Such studies can, however, investigate the impact that abrupt climate events identified in the ice core records have on the terrestrial environment (e.g. Marshall et al., 2002, 2007; Veski et al., 2004; Diefendorf et al., 2006; Candy et al., in press). The ability of lacustrine carbonates in the temperate mid-latitudes to record abrupt climatic events is primarily due to: 1) the linear relationship that exists between air temperature and the isotopic composition of precipitation, 2) the minimal lag time involved for the temperature change to register in the $\delta^{18}O$ value of rainfall, and 3) temperature control on $\delta^{18}O$ fractionation that occurs during calcite precipitation.

Although intensive pollen work has been carried out at Marks Tey and this work has revealed possible evidence for climatic instability during MIS 11 (Turner, 1970, 1975), the palaeoenvironmental proxy that has the greatest potential to inform us about rapid climate change during this interglacial is the $\delta^{18}O$ of the carbonate laminations that occur through this lacustrine sequence. The work of Turner (1970) provided important information about the paleoecology and stratigraphy of the site. The work was, however, carried out before stable isotopic analysis of lacustrine carbonates was widely applied to such deposits.

This chapter is divided into the following sections: Firstly, basic principles about stable isotopes are discussed. Secondly, because carbonate is the key mineral used in this study for isotopic analysis, the basic process of carbonate formation and the factors that control the $\delta^{18}O$ and $\delta^{13}C$ of carbonates are highlighted. In lacustrine systems of temperate regions, such as the British Isles, it is primarily the $\delta^{18}O$ of the carbonate

that gives the more detailed palaeoclimatic information (e.g. Leng and Marshall et al., 2004; Candy et al., 2011). In freshwater systems, the $\delta^{18}O$ of carbonate is primarily driven by the $\delta^{18}O$ of the water it precipitates from and, consequently, the factors that control the $\delta^{18}O$ of freshwaters are discussed. Because the $\delta^{13}C$ value of lacustrine carbonates is relatively insensitive to temperature changes (e.g. Romanek et al., 1992), it is not widely discussed in many palaeoclimate studies. While this chapter will briefly refer to some of the key processes that can control the $\delta^{13}C$ of lacustrine carbonate, the most applicable aspect of the $\delta^{13}C$ value of lacustrine carbonates to this thesis is its usefulness in detecting issues that can limit stable isotopic analysis as a palaeoenvironmental proxy; namely detrital contamination and lake basin hydrology. Some practical issues that need to be considered when interpreting the stable isotopic signal from lacustrine carbonates are then discussed, before the potential for using the $\delta^{18}O$ of lacustrine carbonate as a palaeoenvironmental proxy at Marks Tey is illustrated by reviewing published examples from the British Isles (late glacial/ early Holocene) and Europe (MIS 11).

3.1. Introduction

Stable isotopic analysis of minerals, gasses and other substances that accumulate in a range of depositional environments constitute a very important area of research in palaeoclimatology (e.g. Swart et al., 1993; Clark and Fritz, 1997; Leng, et al., 2006). This is primarily because stable isotope studies of marine and ice cores have revealed evidence for the nature of Quaternary climate variability (e.g. Bond et al., 1993; EPICA, 2004; Lisiecki and Raymo, 2005). Building on early ideas about the existence of isotopes (e.g. Soddy, 1913; Thompson, 1913), to the first precise measurements of stable isotope ratios (Nier, 1936), the potential that oxygen isotopes could be used in palaeoclimatic reconstruction was first realised, through the discovery of the temperature dependence of oxygen isotope fractionation during calcium carbonate formation (Urey, 1947, McCrea, 1950). By applying oxygen isotope analysis to foraminifera remains in marine sediment cores, researchers were able to validate the theory that orbital forcing was the main driving force behind glacial/interglacial cycles (Emillani, 1955; Shackleton and Opdyke, 1973; Hayes et al., 1976; Imbrie et al., 1984; Imbrie, 1985). As a palaeoclimatic tool, it has therefore been responsible for a

paradigm shift in our knowledge of how long-term climate has evolved throughout the Quaternary period.

Although the oxygen isotopic composition of marine microfossils has provided the most extensive palaeoclimate datasets, stable isotopes can also be applied to a range of continental sediment sequences, including freshwater carbonates (Leng and Marshall, 2004; Leng et al., 2006). This is due to the isotopic fractionation that occurs during evaporation of the source water (ultimately sea water) and the control that temperature has on the $\delta^{18}O$ of rainfall (Dansgaard, 1964). In the temperate mid-latitudes, and without significant modification of the $\delta^{18}O$ signal of meteoric waters, terrestrial freshwater carbonates can provide a proxy for temperature, a relationship that has been demonstrated by a number of studies (e.g. Marshall et al., 2002, 2007; Candy et al., 2011). While temperature can be considered the primary control, there are factors that alter this relationship, which must be taken into consideration (Leng and Marshall, 2004). Despite the potential for the oxygen isotopic value of freshwater carbonates to provide terrestrial equivalents to the marine/ice core records, they have remained underexploited until relatively recently. Apart from the complexity of the isotopic system, one of the biggest issues surrounding the use of terrestrial sequences is their often-fragmented nature, which can often lead to disagreements over the age of the records, particularly when they are at, or beyond, the limits of dating techniques (Geyh and Muller, 2005; Scourse, 2006; Preece et al., 2007; Candy et al., 2014). If this issue can be overcome, then the oxygen isotopic signal of terrestrial archives has the potential to generate high-resolution palaeoclimate records.

This is particularly relevant for abrupt climatic events. One theme that runs through recent scientific literature is the detection of abrupt climatic events that punctuate the early Holocene (e.g. 9.3 and 8.2 ka events). Such events are observed in the ice/marine records and a number of terrestrial archives (e.g. speleothems and lakes). The issues surrounding the study of these events in the Holocene and the need to find analogous events in previous interglacials have already been discussed in chapter 2. The discussion here will focus on why isotopes are important in the study of abrupt events and why Marks Tey represents a unique opportunity to study these events in a pre-Holocene interglacial. The oxygen isotopic composition of freshwater carbonates have

the ability to record abrupt climatic events due to absence of an effective lag time between a climatic shift and corresponding shift in the isotopic composition of precipitation. For example, the ~160 year isotopic shift associated with the 8.2 ka event (Thomas et al., 2007) is not recorded by the pollen assemblage at Hawes Water, northern England (Jones et al., 2011). In contrast, $\delta^{18}O$ values of authigenic carbonates from the same site reveal a ~150 year period of significantly low $\delta^{18}O$ values around 8,200 cal. yr BP, interpreted as an abrupt climatic deterioration (Marshall et al., 2007). The study of abrupt events during the early Holocene is made easier due to the potential for reliable chronology construction.

Studying such events in previous interglacials, like MIS 11, is complicated by chronological issues, as well as the fact that ice core records are of a comparatively low resolution (e.g. Pol et al., 2011). In the case of MIS 11, the varved record at Dethlingen has shown that the OHO has a similar duration to the 8.2 ka event, and may therefore provide an analogue for it (Koutsodendris, et al., 2012). The issue with using pollen records as a proxy for climate change is that, particularly when considering centennial scale events, the magnitude and duration of the climatic shift may not be sufficient to produce a clear expression in the pollen record. This is why researchers studying abrupt events have begun to look at $\delta^{18}O$ values. Koutsodendris et al. (2012) do present $\delta^{18}O_{silica}$ data, but only for the OHO itself and core depths immediately adjacent to it. Consequently it is difficult to determine the nature of the climatic pattern for before and after the pollen event, and whether or not the isotopic shifts and pollen response are related. Marks Tey provides a unique opportunity to study this event (the NAP Phase in Hoxnian sequences); like Dethlingen (Koutsodendris et al., 2012), the event is expressed in the pollen record and the sequence is considered to be varved. In contrast to Dethlingen, however, Marks Tey contains authigenic carbonate laminations as part of the varve structure. These carbonate laminations can be easily sampled for isotopic analysis and are relatively quick to analyse, enabling the construction of a long-term environmental record for early MIS 11 in the British Isles. Due to the rate at which the oxygen isotopic composition of lacustrine carbonates can record climatic shifts, such records have the potential to provide more detailed records of climatic variability, as well as the timing of abrupt climatic events.

There is therefore a strong scientific basis for studying abrupt climatic events using oxygen and carbon isotopes from freshwater terrestrial carbonates, but first it is important to understand how they form, and what controls their stable isotopic signature. This review will focus on the formation of authigenic calcite in lakes, but it should be noted that a number of other processes produce calcitic features/remains in the freshwater environment (tufa, travertine, molluscs).

3.2. Stable isotopes and the formation of carbonate in lacustrine environments

3.2.1. Basic chemical principles

The application of stable isotope analysis to palaeoclimatic reconstruction is based on the principle that the same element can exist in two or more different forms (isotopes), where the element has the same number of protons and electrons, but a different number of neutrons, resulting in different weights (mass numbers) (Fig. 3.1). The most commonly used stable isotopes in Quaternary studies are oxygen and carbon isotopes (Fig. 3.1). The two main species of oxygen isotope are ^{16}O and ^{18}O, which both have eight protons, but ^{18}O has two more neutrons than ^{16}O, and is less abundant (Fig. 3.1) (Mook, 2000). Because the isotopes are of the same element, they are chemically identical, but the differences in mass are large enough for a number of physical and biological processes or reactions to alter (fractionate) the relative proportions of isotopes (Kendall and Caldwell, 1998).

Fractionation of stable isotopes can occur when compounds undergo phase changes. For example, the stable oxygen isotopic value of water will change as H_2O moves from the liquid to gas phase (evaporation), and the stable isotopic composition of carbon will change when it changes from one compound to another (gas to organic molecules during photosynthesis) (e.g. Mook, 2006). The reason that isotopes fractionate during phase changes is due to mass differences in the nucleus between the lighter (e.g. ^{16}O) and heavier (e.g. ^{18}O) isotopes. This difference in mass means that ^{18}O has a greater binding energy than ^{16}O, so is less mobile and requires more energy to undergo phase changes, a characteristic known as mass dependent fractionation (Fig. 3.2a, Craig, 1953).

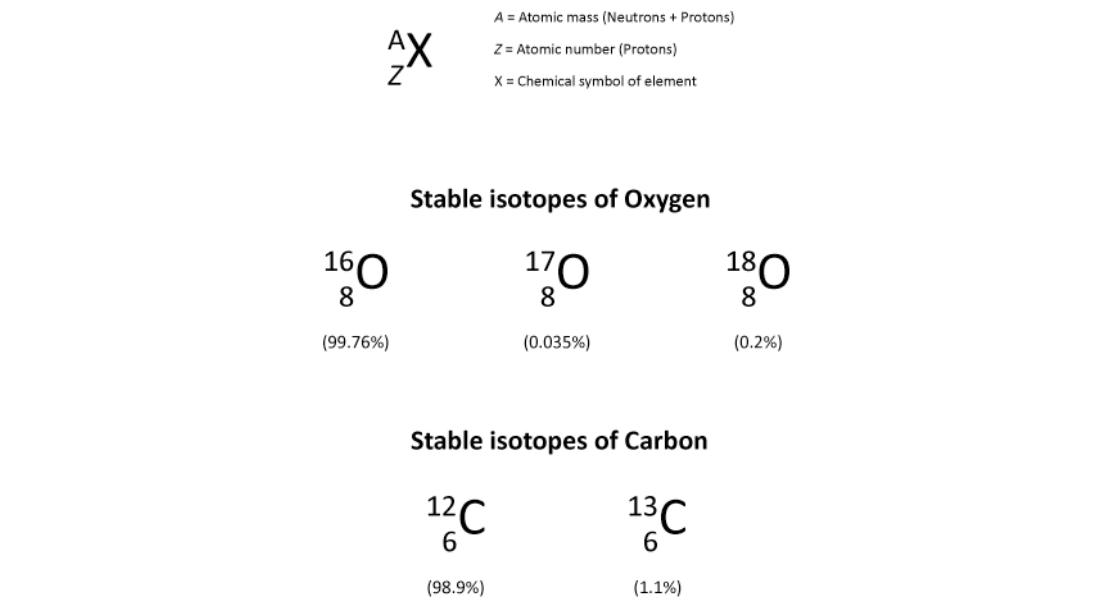

Figure 3.1. *The standard nuclear notation of an element, along with the stable isotopes of oxygen and carbon. The numbers in brackets represent the approximate natural abundance of each stable isotope (data from Mook, 2006).*

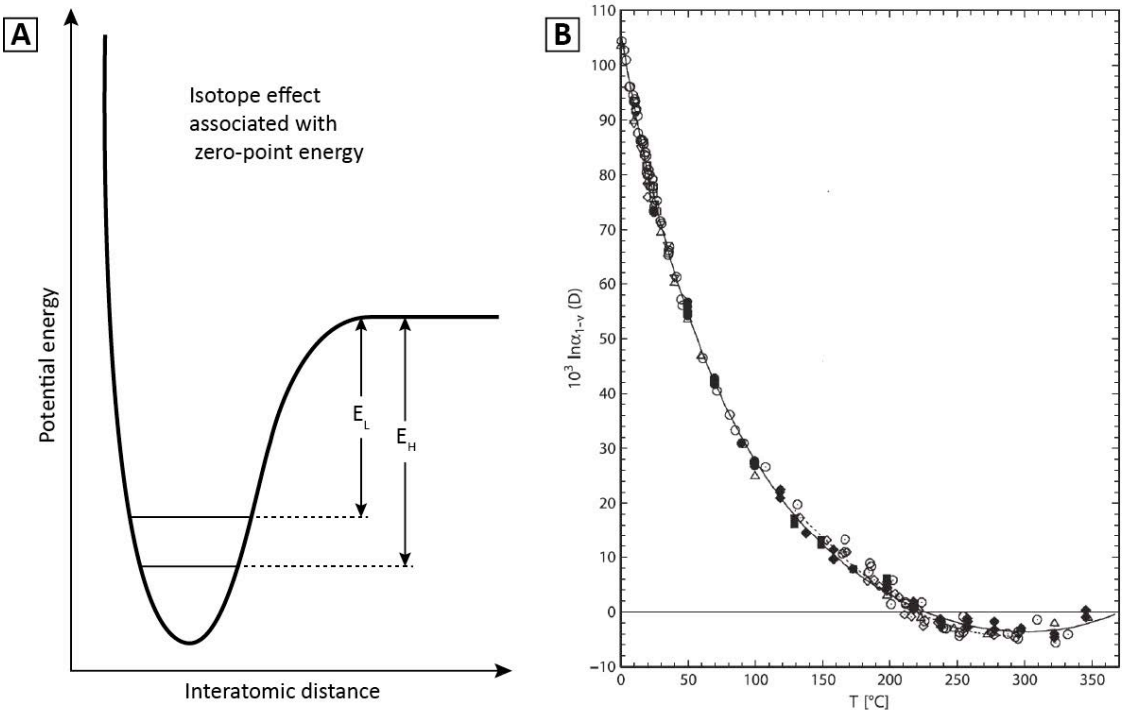

Figure 3.2. *A) Schematic representation of isotope binding energy of a light (E_L) and heavy (E_H) isotope of the same element. The heavier isotope has a lower zero-point energy than the lighter isotope (horizontal lines). This difference in potential energy means that bonds formed by the lighter isotope are weaker. During a chemical reaction, the lighter isotope will, therefore, react more readily than the heavy isotope. Re-drawn from Hoefs (2009). B) Graph showing fractionation factors for $^{18}O/^{16}O$ between liquid and vapour water phases, determined by a number of laboratory experiments. Fractionation ($10^3 ln\alpha_{l\text{-}v}$(D)) is greater at lower temperatures, resulting in an evaporate with a relatively depleted $\delta^{18}O$ value, whereas the degree of fractionation reduces with increasing temperature, resulting in an evaporate with relatively enriched $\delta^{18}O$ value. Modified from Horita and Wesolowski (1994).*

The resulting effect of this is that the lighter isotope will react faster than the heavier isotope, and in the case of a phase change from liquid water to gas, will therefore fractionate (evaporate) more easily (O'Neil, 1986). Importantly, at higher temperatures the differences between binding energies of isotope molecules becomes smaller (Fig. 3.2b) (e.g. Horita and Wesolowski, 1994). This is why, at higher temperatures, water evaporating from a source will have a relatively enriched $\delta^{18}O$ compared to water evaporating at lower temperatures.

3.2.2. Equilibrium, kinetic and non-equilibrium fractionation

There are three processes that can cause isotopic fractionation: equilibrium fractionation, kinetic fractionation and non-equilibrium fractionation (Fig. 3.3, Mook, 2006).

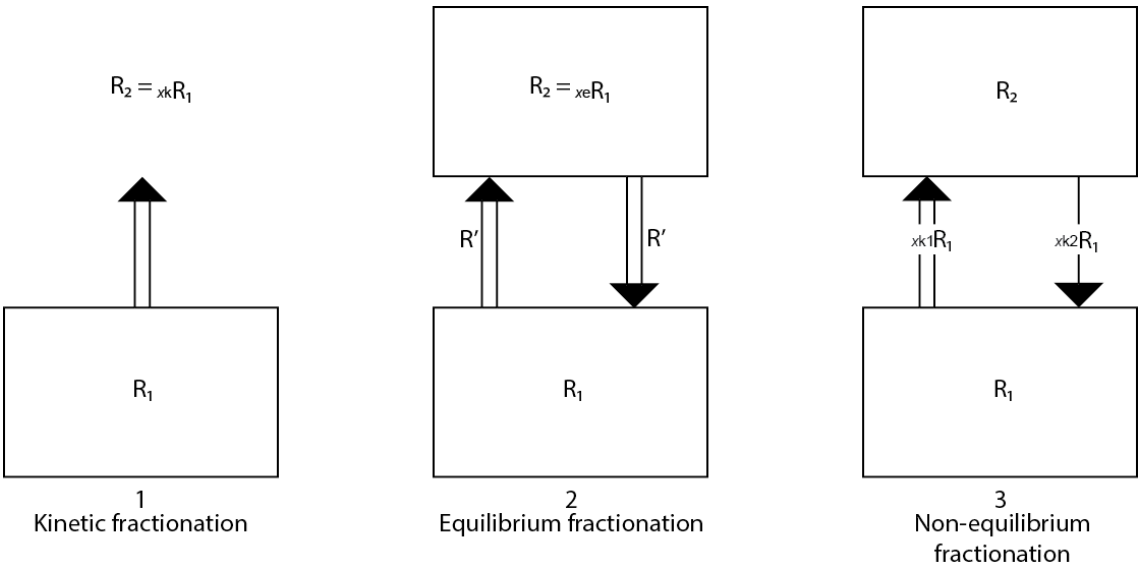

Figure 3.3. *Schematic diagram illustrating the three processes that can cause isotopic fractionation. 1) Kinetic fractionation (χ_k), which involves one-way mass transport (irreversible), 2) Equilibrium fractionation (χ_e), involving equal transfer of isotopes in forward and backward reaction, and 3) Non-equilibrium fractionation (χ_{k1} and χ_{k2}), which involves net transport, but the product is not isolated from the source. Redrawn from Mook (2006).*

Equilibrium fractionation of stable isotopes between a reactant (e.g. water) and product (e.g. calcite) is reached when the ratio of light to heavy isotopes in both end-members is equal. For equilibrium conditions to be attained, three preconditions must be met:

1) There must be both a forward and backward reaction between a reactant and product, where the forward and backward flux of isotopes must be equal (chemical equilibrium);
2) These reactions must have occurred enough times to ensure the isotopes are well mixed between each reservoir (ratios are equal); and
3) Each reservoir must itself be well mixed, to ensure temporal equilibrium conditions (Clark and Fritz, 1997).

While the forward and backward reactions must be equal, the absolute number (isotopic compositions) of molecules in the two groups may not be, as long as the ratio between the light and heavy isotopes is constant (Kendall and Caldwell, 1998). Calcite precipitation under equilibrium conditions is a fundamental condition for using its isotopic composition as a proxy for temperature.

Kinetic fractionation of stable isotopes is a one-way (irreversible) process where, due to lower zero-point energies, the reaction product (assuming it is isolated from the reactant) becomes enriched in the lighter isotope compared to the reactant (e.g. Kendall and Caldwell, 1998; Mook, 2006). In the context of lacustrine carbonates, biological processes are predominantly unidirectional and kinetic isotope effects can occur during the fixation of CO_2 during photosynthesis (Clark and Fritz, 1997). As will be discussed later, it is also possible that kinetic fractionation occurs during the precipitation of calcite, which may inhibit palaeoclimatic interpretations (e.g. Dietzel et al., 2009; Watkins et al., 2013).

A third type, non-equilibrium fractionation, lies somewhere between equilibrium and kinetic fractionation. An example of non-equilibrium fractionation is the evaporation of a lake surface, where the evaporate (product) is not isolated from the lake water (reactant) due to condensation (not kinetic), and there is no identical reverse reaction due to net evaporation (not in equilibrium) (Mook, 2006).

3.2.3. Isotope measurement and reporting

Oxygen and carbon isotope ratios are measured and reported against carbonate standards, to ensure comparison of results between different laboratories. The current

international carbonate standard is Vienna Pee Dee Belemnite (VPDB) (Friedman et al., 1982). The ratio of $^{18}O/^{16}O$ or $^{13}C/^{12}C$ in the sample is determined in a mass spectrometer by dissolving the sample with phosphoric acid, converting it to CO_2 (e.g. Clark and Fritz, 1997). These ratios are then compared to ratios found in standards that are run in the same batch and are expressed as a δ values. When a sample is depleted in the heavier isotope (e.g. ^{18}O, ^{13}C) relative to the standard, the δ value will be negative, whereas a positive δ value indicates that the sample is enriched in the heavier isotope relative to the standard. The δ value is calculated using the following equation (e.g. Urey, 1948; McKinney et al., 1950):

$$\delta^{18}O = 1000 \times \left(\frac{\left(\frac{^{18}O}{^{16}O}\right)_{sample} - \left(\frac{^{18}O}{^{16}O}\right)_{standard}}{\left(\frac{^{18}O}{^{16}O}\right)_{standard}} \right)$$

Because the fractionation of isotopes is so small, δ values are quoted in parts per thousand (per mil, ‰), so a sample with a $\delta^{18}O$ value of +1‰ is 0.1% enriched in ^{18}O relative to the standard.

3.2.4. Calcium carbonate formation

Calcium carbonate will routinely precipitate within freshwater environments where the underlying bedrock is dominated by limestone (i.e. limestone bedrock, or carbonate rich till/loess) (e.g. Smith et al., 1976; Dean and Fouch, 1983). Groundwaters in such regions become enriched in Ca^{2+} during recharge, resulting in spring, river or lake waters that are also Ca^{2+} rich. The precipitation of solid calcium carbonate from this water body occurs when physical and/or biological factors cause the surface waters to become supersaturated with respect to Ca^{2+} ions (e.g. Deocampo, 2010). The reactions that lead to this situation are summarised below. The process leading to calcite formation starts with reactions that occur in the atmosphere. Carbon dioxide combines with water to form a weak carbonic acid (Equation 3). Chemical weathering of the carbonate parent material in the catchment by the carbonic acid enriches the surface runoff, and therefore the lake water, in calcium (Ca^{2+}) and bicarbonate

($2HCO_3^-$) (e.g. Hakanson and Jansson, 1983) (Equation 1, e.g. Wetzel, 1975; Horne and Goldman, 1983).

$$CaCO_3 + CO_2 + H_2O \Leftrightarrow Ca^{2+} + 2HCO_3^- \quad (1)$$

This chemical reaction can be divided into the following equations:

$$CO_2\,(g) \Leftrightarrow CO_2\,(l)$$ • Dissolved CO_2 equilibrates with atmospheric CO_2 (2)

$$CO_2 + H_2O \Leftrightarrow H_2CO_3$$ • Formation of weak carbonic acid (3)

$$H_2CO_3 \Leftrightarrow H^+ + HCO_3^-$$ • 1st dissociation stage creating bicarbonate (↑ pH) (4)

$$HCO_3^- \Leftrightarrow H^+ + CO_3^{2-}$$ • 2nd dissociation stage forming carbonate (↑ pH) (5)

$$Ca^{2+} + CO_3^{2-} \Leftrightarrow CaCO_3$$ • Precipitation of calcium carbonate (6)

A number of physical (CO_2 degassing, evaporation) and/or biologically mediated (photosynthesis) processes may cause the supersaturation and precipitation of calcium carbonate ($CaCO_3$) out of solution. The effects of temperature and/or photosynthesis on the concentration of dissolved CO_2 are important factors (e.g. Brunskill, 1969; Kelts and Hsu, 1978; Dean and Fouch, 1983; Hakanson and Jansson, 1983; Hsu, 1989). Firstly, the concentration of dissolved CO_2 is temperature dependent. Increasing the temperature of the lake water will lead to a loss of CO_2, as its solubility is reduced. Secondly, photosynthetic plants and organisms will remove CO_2 from the water column. However, these two processes are likely to occur together, as biological productivity is at its maximum during the warmest months of the year. CO_2 removal lowers the concentration of carbonic acid in the lake water, which also lowers the concentration of the hydrogen ions, thus pH increases. Carbonic acid will dissociate its first hydrogen ion between pH 6-8, and second hydrogen ion above pH 8 (Fig. 3.4, equations 4 and 5) (e.g. Wetzel, 1975; O'Sullivan, 1983, Horne and Goldman, 1994). This process concentrates the calcium and carbonate ions until they become supersaturated, combine with the calcium ions, and precipitate out of solution (Equation 6).

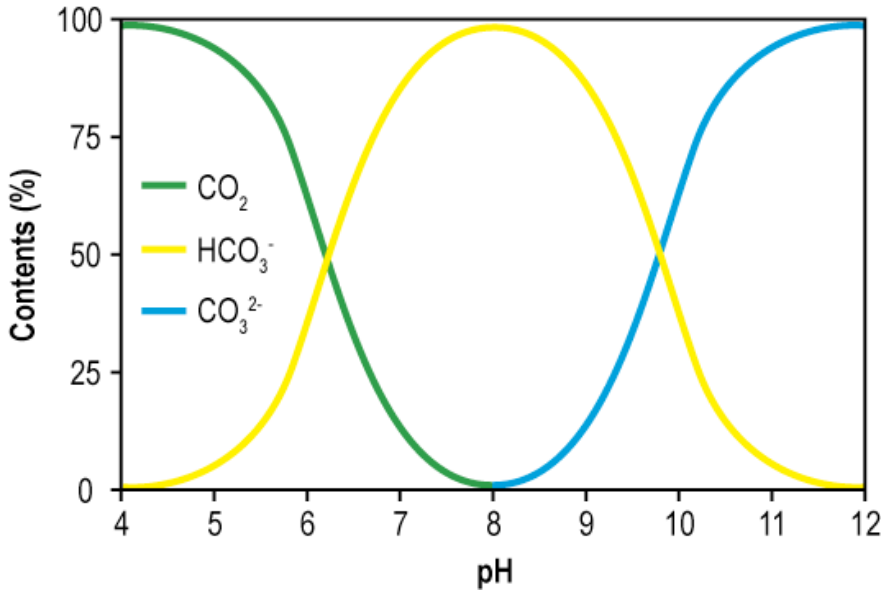

Figure 3.4. *Relationship between pH and the relative proportions of inorganic carbon species of CO_2 in solution in hard water lakes (from Wetzel, 1975). Two stages of dissociation of H^+ ions occur between pH 6-8 and above pH 8. If the lake water becomes supersaturated in CO_3^{2-} then $CaCO_3$ will precipitate.*

It is important to consider the source of the oxygen and carbon that makes up the bicarbonate when interpreting the isotopic composition of a freshwater carbonate. As the bicarbonate is derived from dissolution of CO_2 in water, the carbon isotopic composition is generally considered to record a signal of the $\delta^{13}C$ of the dissolved inorganic carbon, whereas the oxygen isotopic composition records the $\delta^{18}O$ of the source water (Candy et al., 2011.). It should be noted that it is also possible for oxygen to come from CO_2. There is, however, far more natural variability in the $\delta^{18}O$ of water compared to the $\delta^{18}O$ of carbon dioxide, so any variation in the $\delta^{18}O$ of carbonates is likely to reflect the $\delta^{18}O$ of the lake water.

3.3. Factors that control the $\delta^{18}O$ of freshwater carbonates

As the $\delta^{18}O$ value of lacustrine carbonates record the $\delta^{18}O$ of lake waters, the potential for interpreting the palaeoclimatic signature of the $\delta^{18}O$ value of these carbonates is linked to our understanding of the environmental controls over the $\delta^{18}O$ value of that lake water. Broadly speaking, use of the $\delta^{18}O$ value of lacustrine carbonate to reconstruct past environments is based on the following principles:

1) The $\delta^{18}O$ of mineral calcite precipitated in equilibrium from solution is related to the $\delta^{18}O$ of the lake water, where the process of precipitation includes a

fractionation effect controlled by the water temperature (e.g. Urey, 1947; Bigeleisen and Mayer, 1947; McCrea, 1950; Urey et al., 1951; Epstein et al., 1953; Kim and O'Neil, 1997; Leng and Marshall 2004);

2) The $\delta^{18}O$ of lake water is, in turn, controlled by the $\delta^{18}O$ of water that recharges the lake (direct recharge, surface/sub-surface runoff, rivers and groundwater), which is primarily controlled by the $\delta^{18}O$ of precipitation (Rozanski et al., 1997; Darling et al., 2003; Darling, 2004; Froehlich et al., 2005); and
3) In temperate regions like Northwest Europe, a positive linear relationship exists between $\delta^{18}O$ of precipitation and local air temperature (Craig, 1961; Dansgaard, 1964; Rozanski et al., 1992, 1993; Fricke and O'Neil, 1999; Darling and Talbot, 2003; Darling, 2004).

The result of these relationships is that, in temperate mid-latitude regions like the British Isles, there should be a link between temperature and the $\delta^{18}O$ of the carbonate precipitated in lacustrine environments. While temperature in such regions can by considered the primary control over the $\delta^{18}O$ of lake waters, and therefore the $\delta^{18}O$ of carbonates, the relationship is not always straightforward, as a number of variables can alter the $\delta^{18}O$ signal as water moves through the system (e.g. Leng, 2003; Leng and Marshall, 2004; Leng et al., 2006). These will be covered in this chapter. It is important to note here that the $\delta^{18}O$ value of lacustrine carbonates can only be used as a qualitative proxy for temperature because of the range of factors that may control $\delta^{18}O$. In regions where evaporation is an important process (Jones et al., 2005), or where the amount effect occurs (Higgins and MacFadden, 2004), the $\delta^{18}O$ of freshwater carbonates does not reflect temperature.

3.3.1. $\delta^{18}O$ of rainfall

The $\delta^{18}O$ of meteoric waters can be influenced by a number of factors, including changes in ocean water $\delta^{18}O$ and evaporation, air mass trajectory and atmospheric circulation, continentality and the 'amount effect' (Ito, 2001; Higgins and MacFadden, 2004; Leng and Marshall, 2004, Leng et al., 2006). The effects that these factors have on the $\delta^{18}O$ of rainfall are summarised below.

3.3.1.1. Evaporation of source water

Using the basic principle of mass dependent isotope fractionation covered in section 3.2.1, changes in temperature can alter the isotopic composition of water being evaporated from the surface of the ocean. Because ^{16}O is lighter than ^{18}O and has a higher zero-point energy (Fig. 3.2a), it will evaporate more readily, resulting in the water vapour becoming enriched in ^{16}O, while the ocean is left depleted in ^{16}O (and enriched in ^{18}O) (Craig and Gordon, 1965; Merlivat and Jouzel, 1979). Over longer timescales, the $\delta^{18}O$ of the ocean evolves over glacial/interglacial cycles due to the 'ice-volume' effect, where ^{16}O gets stored in glaciers and ice-caps, leaving the ocean enriched in ^{18}O (Shackleton and Opdyke, 1973; Shackleton, 1975, 1987; Rozanski, 1985; Stuiver et al., 1995; Darling et al., 1997; Rozanski et al., 1997).

3.3.1.2. Temperature and latitude

The ability to use variations in $\delta^{18}O$ of lake carbonate as a proxy for temperature is based on the principle that the $\delta^{18}O$ of precipitation is strongly correlated with local air temperature. This relationship was first proposed in the 1960s (Craig, 1961; Dansgaard, 1964), where latitudinal variations in the $\delta^{18}O$ and $\delta^{2}H$ (deuterium) of precipitation co-vary along a global meteoric water line (GMWL), with this relationship being defined by the following equation (Fig. 3.5):

$$\delta^{2}H = 8.13\ \delta^{18}O + 10.8$$

This relationship has subsequently been refined Rozanski et al. (1992, 1993), but the fundamental principles remain the same. The relationship holds true for the temperate mid-latitudes, but not the tropics, where the amount of rainfall becomes more significant (Dansgaard, 1964; Rozanski et al., 1992, 1993; Bowen and Wilkinson, 2002). Based on long-term observational data from the IAEA/WMO network of stations, Rozanski et al. (1992, 1993) (building on the previous work of Dansgaard, 1964) calculated that, for temperate mid-latitudes such as Northwest Europe, this relationship equates to an approximately +0.58‰ increase in $\delta^{18}O$ per °C (Fig. 3.5).

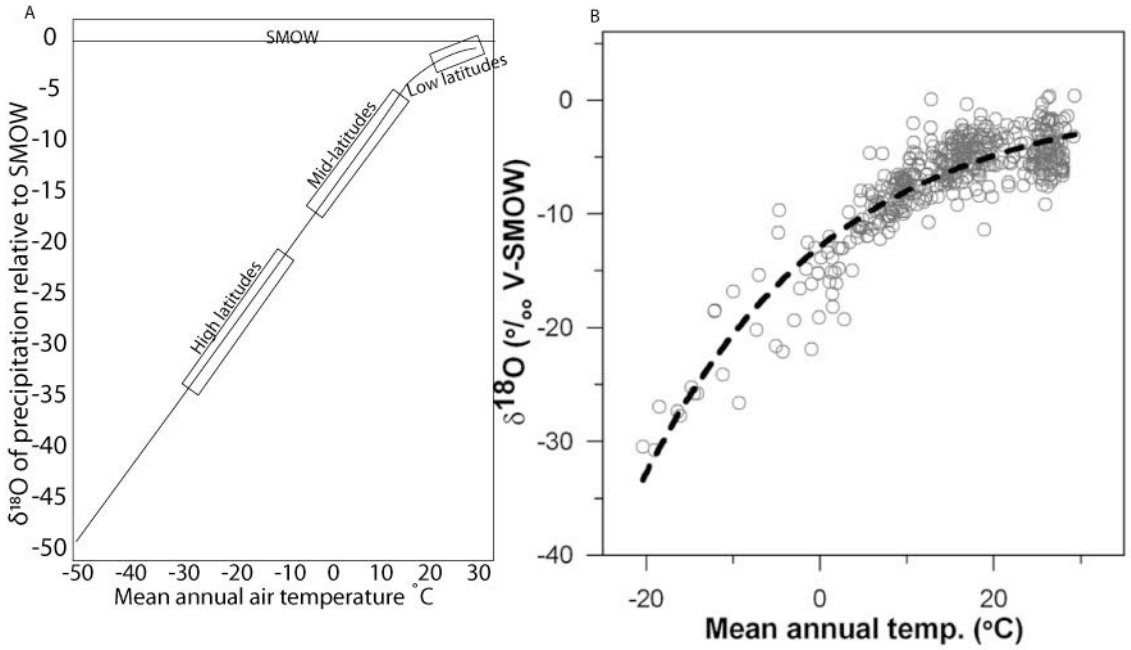

Figure 3.5. *The relationship between mean annual air temperature and $\delta^{18}O$ of precipitation (SMOW). A) Schematic of the relationship (Dansgaard, 1964), and B) Relationship obtained from worldwide data (van der Veer et al., 2009).*

This gradual partitioning of ^{18}O and ^{2}H as air masses cool and form precipitation between the low and high latitudes is known as "rainout" (Clark and Fritz, 1997) and can account for global variations in $\delta^{18}O$ of precipitation of up to 50‰ (Fig. 3.5) (Bowen and Wilkinson, 2002). As water molecules containing heavier isotopes will condense more readily, the heavier ^{18}O (and ^{2}H) will be preferentially removed from the air mass according to Rayleigh-type distillation, leading to enriched rain falling from a progressively depleting air mass (Rozanski et al., 2003). This continual depletion of the air mass will still lead to enriched rain relative to the vapour, but the rain will be depleted in respect to previous rain from the same air mass (Clark and Fritz, 1997).

3.3.1.3. Continentality and altitude

There are also physical factors that can influence the $\delta^{18}O$ of precipitation. Eustatic changes and sea-level rise/fall can alter the distance of a site in relation to the ocean. Increasing the distance of the precipitation source to the site will result in greater rain out of heavier isotopes, resulting in isotopically lighter rainfall at the site (Fig. 3.6) (e.g. Talbot, 1990; Gat, 1996; Hoefs, 1997). In Europe, for example, increasing continentality has the effect of decreasing the $\delta^{18}O$ of precipitation by around 0.002‰ per km,

whereas sampling stations located in oceans and coastal areas vary only slightly from the isotopic composition of the first precipitation event (Rozanski et al., 1993).

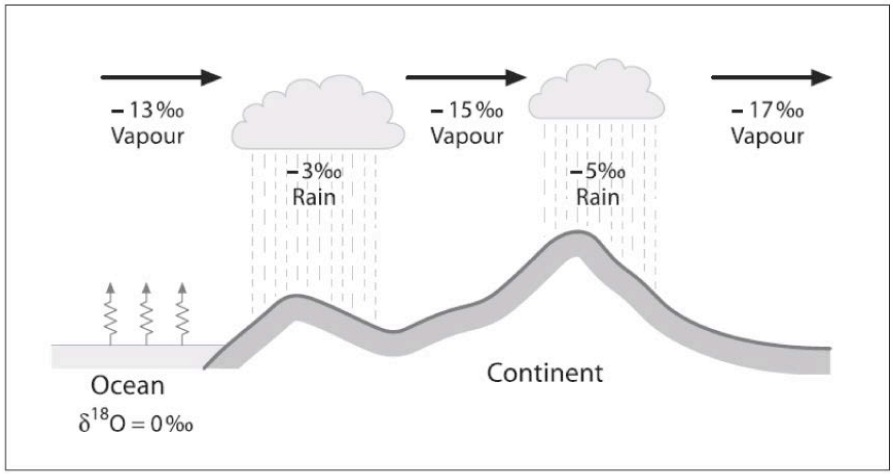

Figure 3.6. *Schematic representation of the continental effect, demonstrating the increasingly negative $\delta^{18}O$ values of precipitation with distance from the source (ocean). Taken from Hoefs (1997).*

The effect that altitude has on the $\delta^{18}O$ of precipitation is the same process that is responsible for rain out and continentality, but an air mass is increasingly depleted with respect to ^{18}O due to the added effect of adiabatic cooling resulting from increasing altitude (Clark and Fritz, 1997). The global relationship between the $\delta^{18}O$ of precipitation and altitude is -2.8‰ per 100m (Fig. 3.7) (Poage and Chamberlain, 2001), but regional and local relationships may vary significantly from this (e.g. Darling and Talbot, 2003; Darling et al., 2003).

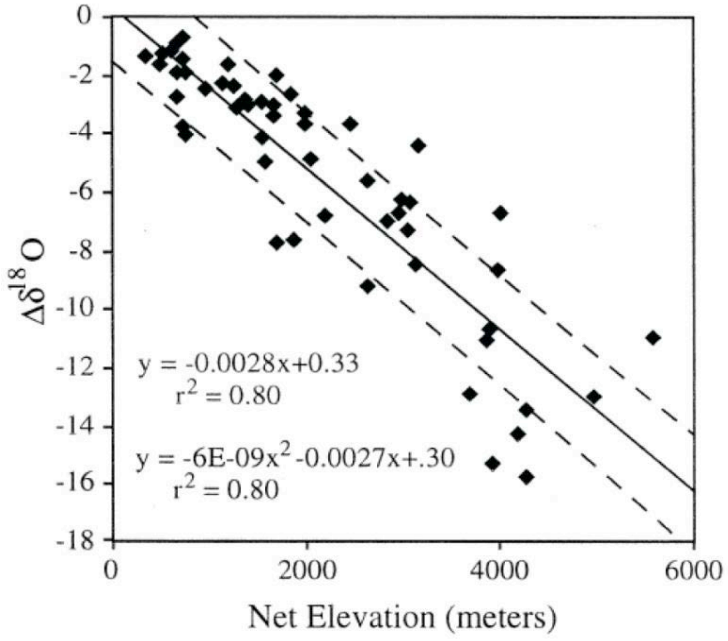

Figure 3.7. *Relationship between the $\delta^{18}O$ values of precipitation with increasing altitude, compiled from a number of sites in Europe and America. Taken from Poage and Chamberlain (2001).*

3.3.1.4. Amount effect, seasonality and atmospheric circulation

The amount effect was first noted by Dansgaard (1964) and describes the relationship between the amount of rainfall and its isotopic composition. The idea is that the relationship between the amount of precipitation and its isotopic composition is primarily controlled by evaporation from the cloud base, and from falling precipitation (e.g. Rozanski et al., 1993; Hoefs, 1997). During periods of low amounts of rainfall, evaporative enrichment of precipitation is more effective through the preferential removal of ^{16}O, whereas during periods of high rainfall, this evaporative enrichment is less effective, leading to lower $\delta^{18}O$ values (Fig. 3.8, Rozanski et al., 1993). This effect is the dominant control over the $\delta^{18}O$ of precipitation in tropical regions, where the amount of precipitation can be the dominant control in its isotopic composition (Rozanski et al., 1993).

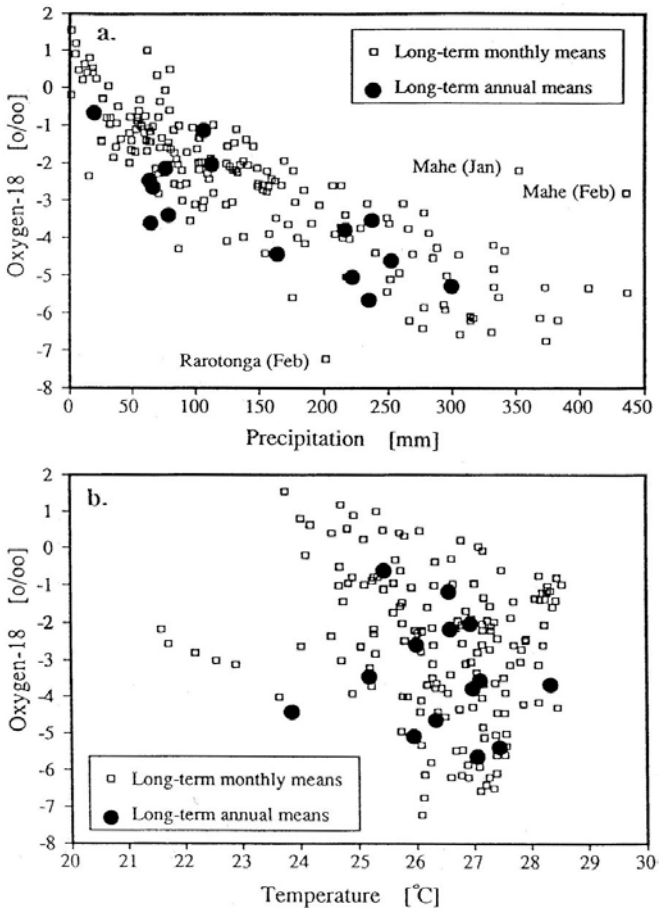

Figure 3.8. *Graphical representation of the amount effect as the dominant control over the $\delta^{18}O$ of precipitation (Rozanski et al., 1993). Long term monthly and mean annual $\delta^{18}O$ values from tropical island stations plotted as a function of A) Average monthly amount of precipitation (mm), and B) Average monthly temperature. A) Low amounts of precipitation have high $\delta^{18}O$ values and visa versa. B) There is no correlation between the $\delta^{18}O$ of precipitation and temperature.*

As section 3.3.1.2 demonstrates, the dominant control over the $\delta^{18}O$ of precipitation in the temperate mid-latitudes is temperature. This temperature effect over the $\delta^{18}O$ of precipitation also displays a seasonal variation, where warmer temperatures during summer months lead to relatively enriched $\delta^{18}O$ values in precipitation compared to winter precipitation (lower diagram in Fig 3.9) (Rozanski et al., 1993). This relationship can be modified, however, by a seasonal amount effect (upper diagram in Fig. 3.9, Higgins and MacFadden, 2001). In this situation, where temperatures pass a threshold of 20°C and there is significant precipitation and/or high humidity, the $\delta^{18}O$ of precipitation decreases due to lower levels of evaporative enrichment of rainfall (Rozanski et al., 2003; Higgins and MacFadden, 2001).

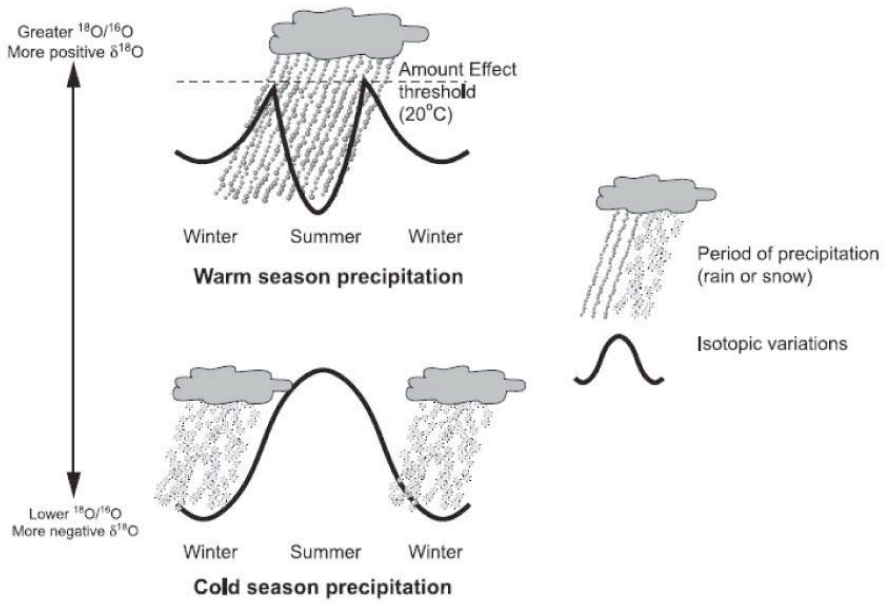

Figure 3.9. *The relationship between seasonality and the $\delta^{18}O$ of precipitation (taken from Higgins and MacFadden, 2004).*

Changes in the relative seasonal contributions of rainfall can therefore alter the isotopic composition of recharge water, lake water, and ultimately the $\delta^{18}O$ of carbonates independently of temperature (see section 4.7 below for discussion). These shifts in seasonality of rainfall can result from changing atmospheric circulation patterns, changing conditions at the water source area, vapour transport history and the mixing of air masses with distinctive $\delta^{18}O$ precipitation values (Dansgaard, 1964; Gat and Gonfiantini, 1981; Rozanski et al., 1993). For example, significant negative shifts away from expected $\delta^{18}O$ values from the mid 19th to late 20th century for two lakes in Switzerland were suggested to be the result of a shift in the North Atlantic

Oscillation (NAO) to a more positive mode (McKenzie and Hollander, 1993; Teranes and McKenzie, 2001). The resulting increased influence of westerly winds would alter the seasonality of rainfall in favour of isotopically depleted winter precipitation, which would filter through the system, leading to lower $\delta^{18}O$ values of calcite (McKenzie and Hollander, 1993; Teranes and McKenzie, 2001). It should be noted, however, that such inferences are only possible due to the chronological control in these sequences, as well as the availability of independent datasets for comparison.

3.3.2. $\delta^{18}O$ of recharge waters

As the discussion in section 3.3.1 demonstrates, the $\delta^{18}O$ of precipitation at a given location is primarily controlled by: 1) the isotopic composition of the source water, 2) the temperature of condensation during precipitation formation, and 3) the rainout history of the air mass. The way that this precipitation recharges lake basins will also lead to distinctive $\delta^{18}O$ values, as lakes are recharged by freshwater in a number of different ways, and by varying amounts; directly from precipitation, by surface run-off and from groundwater (Darling et al., 2003). However, very few lake systems in western Europe are primarily fed by direct recharge. Most of these systems derive their water from groundwater, either by direct recharge into the basin by phreatic water, or inflow by rivers/streams that are also derived from groundwater (Bernasconi and McKenzie, 2011). Consequently, in order to understand the factors that control the $\delta^{18}O$ of lake water, an understanding of the way in which the $\delta^{18}O$ of rainfall is transferred and modified during groundwater recharge is essential.

Once rain has fallen, it will percolate through soils and recharge aquifers and ground waters (Andrews, 2006). During this process, seasonal variations that occur in the $\delta^{18}O$ of rainfall (Clark and Fritz, 1997; Darling and Talbot, 2003) will become averaged out, resulting in groundwater containing a $\delta^{18}O$ value that is characterised by the average $\delta^{18}O$ value of annual rainfall. It has been demonstrated in the UK that there is a strong relationship between the $\delta^{18}O$ value of groundwater and the average annual $\delta^{18}O$ value of rainfall (Darling et al., 2003; Darling, 2004; Candy et al., 2011; Waghorne et al., 2012). This relationship suggests that the $\delta^{18}O$ of recharge waters that enter rivers and lakes is, generally speaking, a reflection of the mean isotopic composition of rainfall, the $\delta^{18}O$ value of which is controlled by temperature. One possible complicating factor

for this relationship is evaporative modification of the $\delta^{18}O$ value when it reaches the surface, either before and/or after it has passed through the aquifer. Although evaporation will undoubtedly alter the isotopic composition of recharge water to some degree, the climate of the UK (and indeed western Europe) is rarely sufficiently warm or dry enough to cause large evaporative isotope effects on surface waters (Darling and Talbot, 2003).

3.3.3. $\delta^{18}O$ of lacustrine waters

When considering the $\delta^{18}O$ value of surface waters, lacustrine systems are more complicated than rivers and steams. Fluvial systems are moving bodies of water that are constantly being recharged from groundwater, so reflect the $\delta^{18}O$ value of that groundwater, which in perennial systems like western Europe, have a relatively constant $\delta^{18}O$ value (see section 3.3.3) (White et al., 1999; Darling et al., 2003; Waghorne et al., 2012). On the other hand, lakes are relatively still bodies of water, so the regularity with which the water is recharged by groundwater and other sources can determine its susceptibility to isotopic modification (Darling et al., 2003).

The biggest influence on the $\delta^{18}O$ of lake water relates to its hydrological regime. Two basin types are recognised: endorheic (closed) and exorheic (open) basins, although they represent end-members of a continuum (Table 3.1, Leng and Marshall, 2004). Closed basins have low water turnover rates (long residence times) because they have no outflow; the only way water exits the basin is by seepage and evaporation. Closed lakes are characterised by a negative water balance and are a common feature in arid environments. A high precipitation:evaporation ratio will lead to isotopic fractionation in favour of ^{16}O, therefore increasing lake water $\delta^{18}O$. At the same time, evaporation reduces the volume of lake water, having the knock-on effect of reducing the solubility of CO_2, resulting in degassing, which also increases the $\delta^{13}C_{DIC}$ (Talbot, 1990; Leng and Marshall, 2004). The increase in both the $\delta^{18}O$ value of water and the $\delta^{13}C$ of DIC can lead to isotopic covariance, a common indicator of hydrological closure (e.g. Talbot, 1990; Li and Ku, 1997).

Table 3.1. *Summary of lake features and the environmental records that authigenic calcites precipitated within them are likely to produce (Leng and Marshall, 2004 and references therein).*

Lake-water volume	Very small	Small-medium open lakes	Small-medium closed lakes	Large
Residence time	<1 year ('open' lake)	≥1 year	10's years	100's years ('closed' lake)
Predominant forcing	*S, T, δp*	*T, δp*	*P/E*	*P/E*
$\delta^{18}O$ ranges through the Holocene	Often –ve values, small range of 1-2‰, possibly large range in ‰ for materials precipitated in different seasons	Often –ve values, small range of 1-2‰	-ve to +ve values, large swings (5 to > 10‰)	+ve values, subdued signal homogenised by buffering of large lake volume
	e.g., Lake Chuma (Kola Peninsula)[a], lake Abisko (Sweden)[b]	e.g., Hawes Water (UK)[c], Lake Ammersee (Germany)[d]	e.g., Greenland lakes[e], Lake Tilo (Ethiopia)[f], Lake Golhisar (Turkey)[g]	e.g., Lake Malawi[h], Lake Turkana (Kenya)[i]

S = seasonality, *T* = temperature, *δp* = isotope composition of precipitation, *P/E* = amount of precipitation relative to evaporation.

At the other end of the continuum, open lakes have both an inflow and an outflow, as well as much shorter water residence times (Table 3.1). Consequently, in such systems, there is less opportunity for isotopic modification by evaporation, so the $\delta^{18}O$ of lake water in open systems is more likely to retain the $\delta^{18}O$ of precipitation, which is primarily controlled by air temperature (Craig, 1961; Dansgaard, 1964; Rozanski et al., 1993; Darling and Talbot, 2003; Darling, 2004). Consequently, the $\delta^{18}O$ of carbonates precipitated in open lake systems is likely to reflect large-scale temperature changes. This may be further complicated by the relative size of the lake water body in relation to the annual water flow through it (Stuiver, 1968; Pearson and Coplen, 1978). If the volume of a basin is large in comparison to the annual water flow through it, any seasonal variation in recharge water $\delta^{18}O$ will be averaged out, whereas smaller lakes are likely to display greater seasonality (Pearson and Coplen, 1978). In terms of inter-annual variability, this is not considered to be a factor that significantly affects the British Isles, for the reasons detailed in the previous section.

Another important factor that can influence the $\delta^{18}O$ of lake water is the stratification of the water column and the degree to which vertical mixing of lake water occurs. Seasonal water column dynamics can have the effect of amplifying any modifications made to the $\delta^{18}O$ of lake water by other processes. If a lake is deep enough, increasing temperatures and productivity during the summer months can lead to stratification of the water column (Lindell, 1980, Hakanson and Jansson, 1983, Anderson et al., 1985).

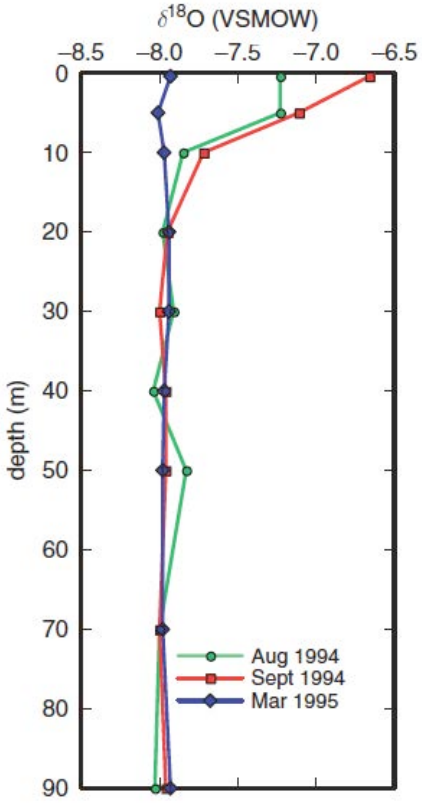

Figure 3.10. *Vertical profile of seasonal variations in water column $\delta^{18}O$ values from Lake Lugano, Switzerland. The development of water column stratification during the summer results in the increase of $\delta^{18}O$ values buy up to 1.5‰. Taken from Bernasconi and McKenzie (2007).*

Because the lake water is not being mixed, the epilimnion becomes cut off from the rest of the lake, which can lead to distinctive seasonal vertical profiles of $\delta^{18}O$ in the water column (Fig. 3.10) (McKenzie, 1982; Teranes et al., 1999; Teranes and McKenzie, 2001; Leng and Marshall, 2004; Bernasconi and McKenzie, 2007; Bluszcz et al., 2009).

3.3.4. Controls over the $\delta^{18}O$ of calcite during mineral precipitation

As highlighted in section 3.3, the $\delta^{18}O$ of water entering a lake basin is primarily a function of the $\delta^{18}O$ of precipitation, which is temperature controlled. The fractionation of carbon during calcite precipitation is insensitive to temperature and almost negligible (Emrich et al., 1970; Romanek et al., 1992), so is not considered here. The process of calcite precipitation from solution does, however, impart a fractionation effect of $\delta^{18}O$, which is temperature dependent (Urey, 1947; Bigeleisen and Mayer, 1947; McCrea, 1950; Urey et al., 1951; Epstein et al., 1953; Craig, 1965; Hays and Grossman, 1991; Kim and O'Neil, 1997; Leng and Marshall, 2004). This is due to the thermodynamic behaviour of isotopes, where lower water temperatures produce a greater fractionation effect between ^{16}O and ^{18}O, producing carbonates

with higher $\delta^{18}O$ values than those precipitated in warmer water (Fig. 3.2b, Clark and Fritz, 1997; Leng and Marshall, 2004). Numerous studies have revealed that there is a depletion of between 0.24-0.28‰ in $\delta^{18}O$ of calcite per +1°C, assuming fractionation under equilibrium conditions.

Temperature is therefore responsible for the isotopic composition of meteoric water (which becomes lake recharge water) and the isotopic composition of authigenic calcite, but the two processes work in opposing directions. However, as the air temperature control (+0.58‰ per +1°C) is greater than the influence of fractionation during calcite precipitation (-0.24-0.28‰ per +1°C) (Andrews, 2006), increasing air temperatures in the temperate mid-latitudes should result in increasing $\delta^{18}O$ values of calcite, albeit slightly muted by the fractionation effects (Andrews, 2006; Marshall et al., 2002, 2007; Leng and Marshall, 2004; Candy et al., 2011).

3.3.5. Summary: temperature and the $\delta^{18}O$ of lake water in temperate regions

Section 3.3 represents a significant portion of this chapter and has been dedicated to the processes by which water is transported from the ocean to lacustrine systems, the factors that influence the $\delta^{18}O$ value of water during this transport history, and the fractionation of oxygen that occurs during carbonate precipitation from solution. As the review highlights, oxygen isotopes in freshwater carbonates appear to be strongly controlled by prevailing temperature, albeit with the potential to be modified by non-temperature related factors. It is this relationship, which holds true for western Europe, between local air temperature and the $\delta^{18}O$ of meteoric waters that offers the potential to use $\delta^{18}O$ values of freshwater carbonates as a proxy for changes in the prevailing temperature regime.

3.4. Factors that control the $\delta^{13}C$ of freshwater carbonates

Interpreting the $\delta^{13}C$ of authigenic lacustrine carbonates is complicated by the fact that their $\delta^{13}C$ values are predominantly controlled by the $\delta^{13}C$ of the dissolved inorganic carbon content ($\delta^{13}C_{DIC}$) of the lake water (Leng and Marshall, 2004), which can be influenced by a variety of lake catchment and within-lake processes that modify

the isotopic composition of recharge waters (e.g. Teranes et al., 1999; Bade et al., 2004; Leng and Marshall, 2004).

3.4.1. Lake catchment processes

The $\delta^{13}C$ value of recharge water that enters a lake will be determined by the relative contributions of carbon from geological sources (Hammarlund, 1994; Hammarlund et al., 1997) and from soils and vegetation (Cerling et al., 1989; Cerling and Quade, 1993). As already mentioned at the start of this chapter, lakes that precipitate authigenic calcite are often located in catchments that contain limestone bedrock (Smith et al., 1976). During periods where productivity on the landscape is relatively low (e.g. glacial/stadial climates), the main source of carbon will be from these geological carbonates. Geological (marine) carbonates typically have $\delta^{13}C$ values within the range of -3 to +3‰ (Andrews et al., 1997, Leng et al., 1999b, Clark and Fritz, 1997; Leng and Marshall, 2004); therefore regions, where the $\delta^{13}C_{DIC}$ of groundwater is predominantly derived from geological sources, will have relatively high values (Hammarlund, 1994; Hammarlund et al., 1997). In such a setting, with little vegetation cover, there is also the increased possibility allogenic material being washed into the lake, contaminating the isotopic signal (Mangili et al., 2010a; Leng et al., 2005). Landscape stabilisation and soil development during interglacial conditions in temperate environments such as Britain will result in groundwater with lower $\delta^{13}C$ values, due to the reduced contribution of geologically derived carbon, and an increase in the contribution of isotopically light CO_2 from the soil zone (Cerling et al., 1989; Cerling and Quade, 1993; Andrews, 2006). The reason that recharge water in stable, vegetated landscapes tends to have lower $\delta^{13}C$ values is because CO_2 in the soil zone is derived from plant respired CO_2, which is depleted with respect to $\delta^{13}C$, due to fractionation caused by the preferential uptake of ^{12}C during photosynthesis (Cerling and Quade, 1993; Andrews, 2006). In climatic settings such as Britain, C3 plants dominate the landscape, which have typical $\delta^{13}C$ values of between -24 to -30‰, with an average of -27‰ (Cerling and Quade, 1993; Vogel, 1993). CO_2 in the soil zone will be characterised by these "low" $\delta^{13}C$ values due to soil respiration and the decay of organic matter. The high partial pressure of CO_2 in the soil zone will cause this isotopically depleted CO_2 to be taken up by soil water as it percolates through the soil zone during groundwater recharge (Clark and Fritz, 1997; Andrews, 2006). This phase change (from gas to liquid)

imparts a further diffusion, dissolution and temperature controlled fractionation effect of between +10‰ (Romanek et al., 1992) and +14‰ (Cerling et al., 1989; Cerling and Quade, 1993). As a result, groundwater $\delta^{13}C$ values in climatic settings such as Britain will typically have values in the range of -12 to -10‰ (Candy et al., 2011).

3.4.2. Within-lake processes

Once water enters a lake basin from its catchment, it will start to equilibrate with atmospheric CO_2 (e.g. Leng and Marshall 2004). The extent to which atmospheric CO_2 is equilibrated with lake water DIC is dependent on the residence time of the lake water and can be an indication of whether the lake is a hydrologically open or closed system (see discussion above, Talbot, 1990, Li and Ku, 1997). If the residence time is sufficient to enable equilibration of lake water DIC with atmospheric CO_2, which had a pre-industrial value of approximately -6.5‰ (Friedli et al., 1986) (modern day values are around -8.3‰, NOAA website), lake water DIC would have a value between approximately -0.2 and +2‰, similar to values of marine carbonates.

There are a number of other processes that occur within a lake that can alter the $\delta^{13}C_{DIC}$ value of lake water, including:

1) The preferential removal of ^{12}C from the water column during photosynthesis (McKenzie, 1982, 1985; Hollander and McKenzie, 1991; Teranes et al., 1999; Colleta et al., 2001; Myrdo and Shapley, 2006).
2) The removal of CO_2 from the water column also increases the alkalinity of the solution, changing the ratio of inorganic carbon species present ($CO_{2(aq)}$: HCO_3^-: CO_3^{2-}, Fig. 3.4,) and, therefore, the $\delta^{13}C_{DIC}$ of lake water (Zhang et al., 1995; Teranes et al., 1999; Bade et al., 2004).
3) Much like $\delta^{18}O$, the $\delta^{13}C$ of lacustrine carbonates can also be altered by water column stratification, producing very similar vertical profiles (McKenzie, 1982, Teranes and McKenzie, 2001). Stratification also influences processes like the oxidation/reduction of organic matter (Hollander and McKenzie, 1991; Meyers and Ishiwatari, 1993; Anderson and Leng, 2004) and methanogenesis (e.g. Whiticar et al., 1986; Herczeg, 1988), which alter water column $\delta^{13}C_{DIC}$.

While the $\delta^{13}C$ of lacustrine carbonates can provide important information about the lacustrine carbon cycle, it doesn't provide a direct link to climate, because the fractionation that occurs between DIC and mineral calcite is only very weakly temperature dependent (Romanek et al., 1992; Wachniew and Rozanski, 1997; Bernasconi and McKenzie, 2007). As a result, it is very rarely discussed in any great detail in palaeoclimatic studies. Carbon should not be disregarded completely, however, as when combined with the corresponding $\delta^{18}O$ values of the carbonate sample, they can provide important information about lake hydrology (section 3.3.3) and possible detrital contamination of the authigenic isotopic signal (section 3.5.3).

3.5. Practical issues to consider when interpreting lacustrine stable isotope records

A number of factors need to be taken into consideration when interpreting stratigraphical variations in $\delta^{18}O$ and $\delta^{13}C$ from lacustrine archives. While $\delta^{13}C$ values of authigenic carbonates have the potential to provide useful information about the carbon cycle in freshwater lacustrine systems, the fact that the $\delta^{13}C$ of authigenic calcite represents the balance between a variety of interrelated processes that can influence $\delta^{13}C_{DIC}$, it becomes difficult to interpret such records in a quantitative manner (Wachniew and Rozanski, 1997). Although both carbon and oxygen isotopes can contain important environmental information, it is oxygen isotopes that are most closely linked to temperature changes and climate.

3.5.1. Timing and depth of calcite precipitation

As has already been discussed, the processes that alter the $\delta^{18}O$ and $\delta^{13}C_{DIC}$ of lake water will vary seasonally, to a greater or lesser degree. Lake monitoring studies have revealed large seasonal variations in the $\delta^{18}O$ and $\delta^{13}C$ of calcite (Teranes et al., 1999; Bluszuz et al., 2009), as well as vertical changes with water column depth (e.g. McKenzie, 1982; Lehmann et al., 2004). Therefore changes in the timing and depth of peak calcite precipitation can influence the isotopic signal preserved in the sedimentary record. When studying fossil lacustrine sequences, assumptions have to be made about the timing and depth of calcite precipitation, as well as the equilibrium conditions under which the mineral precipitated.

3.5.2. (Dis)Equilibrium conditions

For authigenic lacustrine carbonates to be considered a reliable proxy for the $\delta^{18}O$ of lake water (and therefore temperature), it must be assumed that the $\delta^{18}O$ values of authigenic calcite were in equilibrium with lake water $\delta^{18}O$, a situation only possible by direct measurements of water temperature and $\delta^{18}O$, and calcite $\delta^{18}O$ during lake monitoring studies (Hodell et al., 1998; Teranes et al., 1999a and b; Marshall et al., 2002, 2007). The rate at which calcite crystals precipitate from solution can influence its $\delta^{18}O$ value. Laboratory experiments have produced contradictory results, concluding that higher rates of precipitation can either enrich the mineral phase in ^{16}O (McCrea, 1950), or have little effect on its isotopic composition (Tarutani et al., 1969). While some studies find that, within errors, calcite precipitation occurs in isotopic equilibrium with lake water (Hodell et al., 1998; Marshall et al., 2002, 2007), this is not always the case. Other studies have noted that kinetic effects are linked increasing productivity (Fronval et al., 1995; Teranes et al., 1999b).

3.5.3. Composition of lacustrine carbonates in sediment cores

Authigenic carbonates that form as a result of the supersaturation of $CaCO_3$ in surface waters will typically be fine-grained and will fall from suspension to form thick sediment sequences. Because in most cases carbonates are mixed in with other materials such as organic matter and siliciclastic grains, the deposits are referred to as marls (e.g. Verrecchia, 2007). In many lacustrine environments, however, authigenic calcite is not the only form of carbonate present. While not discussed in this review, other forms such as algal carbonates (e.g. Coletta et al., 2001; Andrews et al., 2004), ostracod shells (e.g. Holmes, 2001) and mollusc shells (e.g. Leng et al., 2010) can also get incorporated into the sediments, as well as detrital carbonates washed in from the catchment (section 3.4.1.). The problem this poses for stable isotope studies is that different forms of carbonate will record different $\delta^{18}O$ values under the same environmental conditions (vital offsets), or precipitate during different seasons, therefore contributing different isotopic signals to the sediments. Sampling and preparation methods to isolate the carbonate form of interest for isotopic analysis will therefore be dictated by the sedimentology of the sequence to be sampled, as well as the carbonate forms present (e.g. Candy, 2009; Mangili et al., 2010a; Candy et al., in press).

Techniques that aim to remove detrital carbonates before analysis have been summarised by Mangili et al. (2010a) and include separation of carbonate fractions by sieving, thin section analysis, XRF measurements and using phosphoric acid to remove detrital dolomite, although this technique is only significant in areas of dolomite bedrock. Thin section analysis is an effective way of characterising the microfacies of both laminated carbonates and marls, aiding sampling strategies (e.g. Mangili et al., 2010a; Candy et al., in press). Sieving is also effective in removing larger fractions of biogenic and detrital carbonates, as is XRF or XRD in determining detrital material with a distinctive mineralogy (Mangili et al., 2010a). While these pre-analysis methods will provide effective results in some cases, none of them will be able to identify and remove fine-grained detrital carbonates that are of similar particle size and chemical composition to the authigenic carbonates.

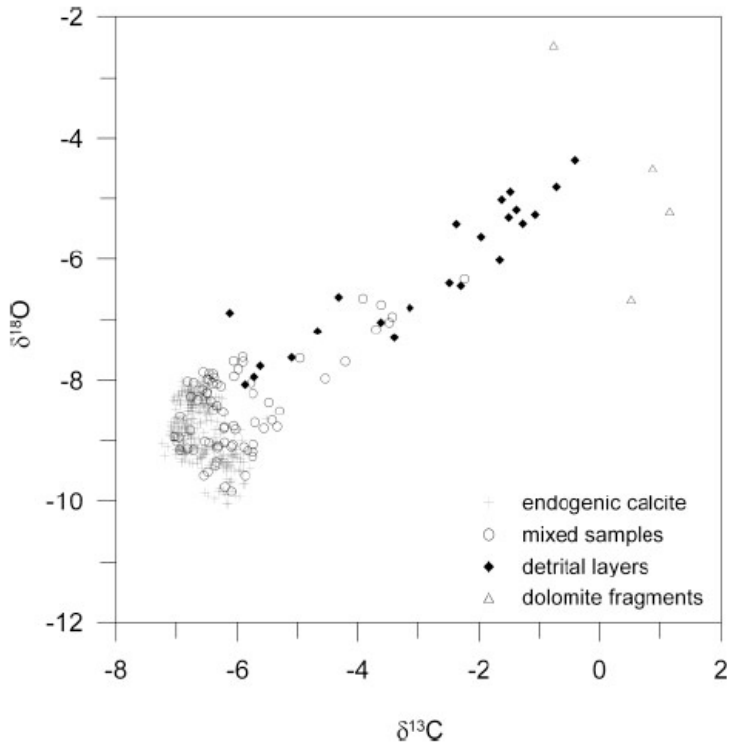

Figure 3.11. *Example of bi-plot showing distinctive isotopic signatures for authigenic and detrital calcite. The $\delta^{18}O$ and $\delta^{13}C$ will covary along a mixing line between the two populations, depending on the degree of detrital contamination (from Mangili et al., 2010a).*

Limestone bedrock is primarily of marine origin and typically has much higher $\delta^{13}C$ values than freshwater carbonates (e.g. Clark and Fritz, 1997). Because of the distinctive values, a lake carbonate record that has been contaminated by detrital

material will consist of two end-member populations (authigenic and detrital). Depending on the degree to which samples have been contaminated, they plot along a 'mixing line' between the two end-members in which the $\delta^{18}O$ and $\delta^{13}C$ values co-vary (Fig. 3.11).

In temperate regions, where isotopic covariance is unlikely to occur, this can be considered an effective way to test for, and remove contaminated samples (Mangili et al., 2010a). This is not always the case though, for two reasons. The first is that it has been suggested that climatically driven changes in seasonality can be responsible for isotopic covariance in temperate, open lake systems (Drummond et al., 1995). In this model, Drummond et al. (1995) suggest that a shift to the dominance of enriched summer rainfall, coupled with increased carbon values due to increased lake productivity in a Holocene record from a lake in Michigan, USA, caused the co-variance. The second is that while typical $\delta^{13}C$ values for marine carbonates are distinctive from $\delta^{13}C$ values for freshwater carbonates, there is a degree of overlap at higher values (Clark and Fritz, 1997). The $\delta^{13}C$ value of lake carbonates, because of the equilibration of DIC with atmospheric CO_2, can therefore exhibit similar $\delta^{13}C$ values to the marine limestone, which is the main source of contamination. Consequently, using covariance as a test for detrital contamination can be complicated by authigenic carbonates with high $\delta^{13}C$ values.

As isotopic covariance by itself is not necessarily indicative of detrital contamination, other studies have compared the isotopic composition of bulk samples to biogenic carbonates, as these are not subjected to detrital contamination from catchment bedrock (Hammarlund and Lemdahl, 1994; Hammarlund et al., 2002; Leng et al., 2010). Further to this, periods of high magnetic susceptibility can correlate with shifts in the isotopic signal, indicating that in-wash of siliciclastic material from the catchment affect the isotope signal (Eastmond et al., 2007; Leng et al., 2010).

3.5.4. Core sedimentology and its influence on the isotopic signal

One further possibility to consider when interpreting oxygen isotope records from sediment archives is the control that changes in sedimentology can have over the isotopic signal. Sequences with distinct changes in sedimentology can also be

accompanied by distinct changes in the isotopic signal, without the need to invoke climate as a forcing mechanism (e.g. Anderson and Leng, 2004; Mangili et al., 2010b). In the case of Anderson and Leng (2004), who present a stable isotope record from a lake in Greenland, a shift in core sedimentology to the preservation of distinctly laminated sediments also coincides with increased $\delta^{13}C$ values, which they suggest relates to the development of water column stratification and bottom water anoxia, leading to a decrease in the oxidation of organic matter. Another consideration related to core sedimentology is the issue of sample resolution. Mangili et al. (2010b) sampled a varved sequence at varying temporal resolutions (annual to decadal), which resulted in a $\delta^{18}O$ signal that became increasingly smoothed (less scatter) as the samples covered a greater period of time. By extension, if an isotopic record is generated from a core that contains both varved and non-varved (marl) sediments, care needs to be taken when interpreting isotopic shifts, as an increase in the scatter of $\delta^{18}O$ values may not reflect climatic instability, but rather changes in the style of sedimentation and, therefore, the resolution of sampling. In a varved sequence the clear seasonal structure of the sediments mean that each lamination, and its consequent $\delta^{18}O$ value, represents a single summer, whilst in a structureless marl a single sample, and its $\delta^{18}O$ value, may represent an average of years or decades. This is because inter-annual shifts in the $\delta^{18}O$ value of authigenically precipitated calcite will be averaged out if deposited as marl, which may represent a number of years worth of calcite precipitation and deposition.

3.6. Key lacustrine sequences in the British Isles and Europe

The application of stable isotopic analysis to authigenic lacustrine carbonates from pre-Holocene interglacials in the British Isles is not commonly undertaken (although see Candy, 2009; Candy et al., 2011). The first part of this section will focus on what environmental information can be gained from stable isotope studies of freshwater carbonates in the British Isles. As has already been discussed, the Hoxnian Interglacial as defined for the British Quaternary record is routinely correlated with MIS 11. While no terrestrial stable isotope stratigraphies currently exist for MIS 11 in the British record, there are some available from Southern (Mangili et al., 2007, 2010b) and Central Europe (Nitychoruk et al., 2005).

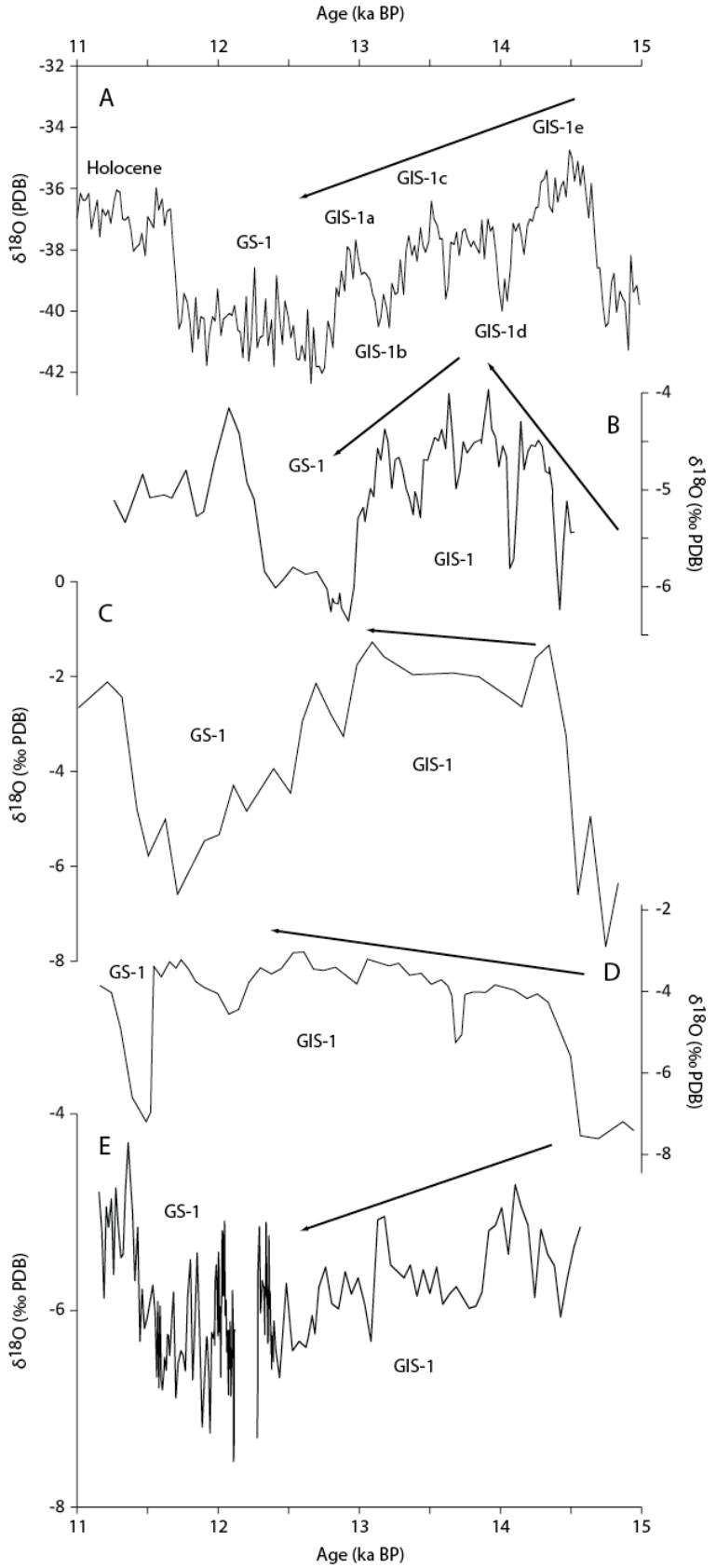

Figure 3.12. *Structure of the Lateglacial Interstadial (GIS-1) in lacustrine $\delta^{18}O_{calcite}$ records from the British Isles compared to the Greenland ice core record. A) Greenland (GICC05) (Rasmussen et al., 2006), B) Hawes Water, England (Marshall et al., 2002), C) Loch Gur, Ireland (Ahlberg et al., 2001), D) Fiddaun, Ireland (van Asch et al., 2012), and E) Loch Inchiquin, Ireland (Diefendorf et al., 2006). Modified from Darvil et al., in prep. For ease of communication Greenland nomenclature is used to define periods in he different records.*

3.6.1. Key sequences from the British Isles

While the published literature on high-resolution stable isotope records from lacustrine carbonates in the British Isles is confined to the Last Glacial-Interglacial transition (LGIT) and Holocene, it is nevertheless important to determine what environmental signal the oxygen isotopes from these sequences record, and how these reflect climatic variability. Figure 3.12 and 3.13 show the $\delta^{18}O$ signal of British LGIT/early Holocene marl records against GRIP. These include sites from the west coast of Ireland (Diefendorf et al., 2006; 2008), west coast of England (Lake District, Marshall et al., 2002; 2007), east coast of England (North Yorkshire, Candy et al., in press) and southeast Scotland (Whittington et al., 1996).

While the records are of varying resolution and completeness, they have, when compared to the Greenland ice core record for the same time period, the same general trend. This general trend consists of the following features:

1) An increase in $\delta^{18}O$ associated with the transition from Greenland Stadial 2 (GS-2) to Greenland Interstadial 1 (GI-1);
2) Generally high $\delta^{18}O$ values during GI-1, with varying amounts of sub-stage variability;
3) A drop in $\delta^{18}O$ values associated with GS-1, displaying values similar values to those that occurred during GS-2; and
4) The subsequent recovery of $\delta^{18}O$ values associated with the onset of the Holocene (Fig. 3.12).

As the general trend in isotopic changes in Greenland is also mirrored in the lacustrine sequences in figure 3.12, it can be inferred that authigenic calcites precipitated in lacustrine systems in western Europe provide a qualitative proxy for temperature shifts. While the general trend described above holds true, recent work comparing a new stable isotope record from lacustrine marls at Star Carr to these sequences found some key differences between the lacustrine marl records themselves, as well as the independent temperature record of Greenland (Fig. 3.13) (Candy et al., in press). The major differences are:

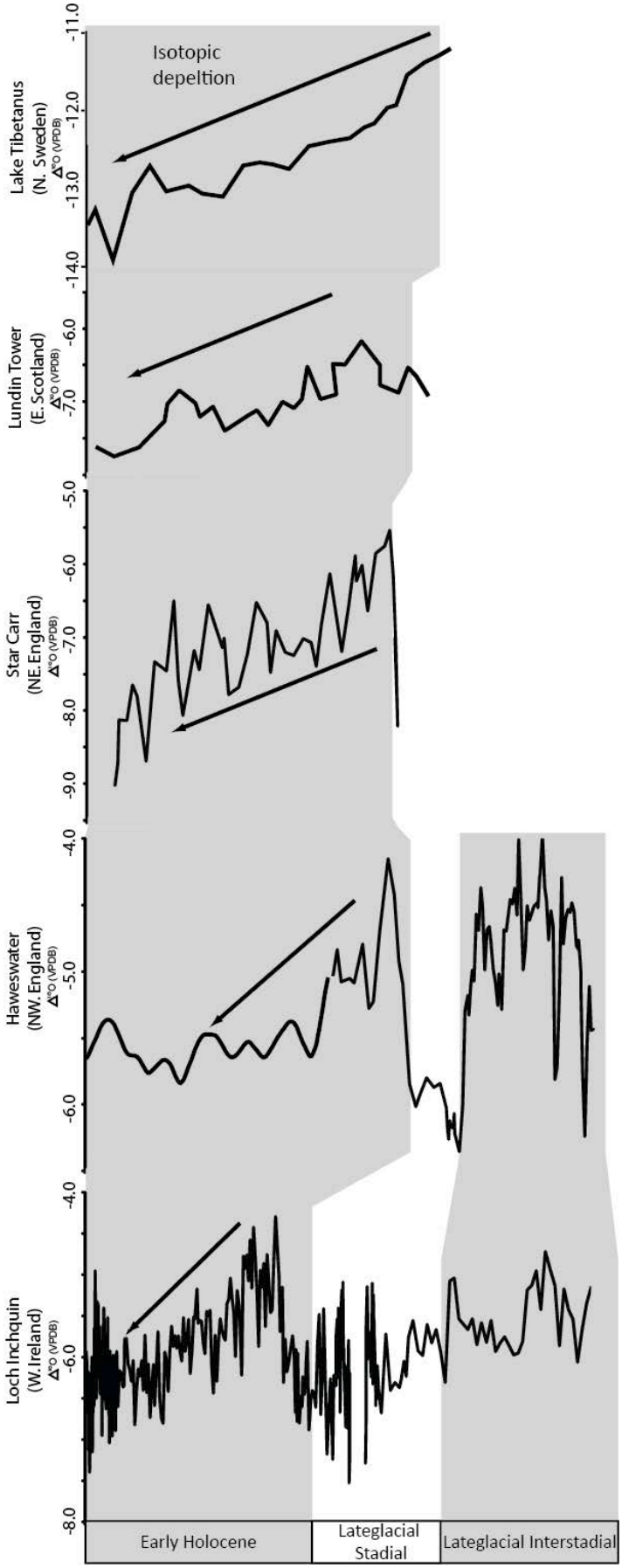

Figure 3.13. *Lacustrine $\delta^{18}O_{calcite}$ records highlighting an early Holocene isotopic depletion trend (shown by the arrows). Modified from Candy et al., in press.*

1) The climatic structure of GIS-1 varies, with Greenland and Star Carr showing a cooling trend as the interstadial progresses, whereas Fiddaun and Loch Gur show a warming trend. The signal from Hawes Water is complicated, with the calcite $\delta^{18}O$ showing peak warmth in the middle of GIS-1, while the chironomid temperature reconstruction follows the pattern seen in Greenland and Star Carr.
2) While the increase in temperature associated with the onset of the Holocene peaks and stabilises in the Greenland $\delta^{18}O$ record, all of the marl isotope records diverge from this trend, showing an early Holocene isotopic depletion to levels similar to GS-1.

The inter-site differences seen in the isotopic pattern seen during GIS-1 appear to be related to their location. Darvill et al (in prep) suggest that the distinctive warming trend seen in Fiddun and Loch Gur are due to their close proximity to northward flowing Atlantic water, the temperature of which could be influenced by increasing insolation patterns across the interstadial (a trend also seen in marine records during this period, e.g. Halfidason et al., 1995). Like Greenland, Star Carr (also Lundin Tower) would have been located in a more continental setting during this period, so would be less effected by the influence of these north Atlantic currents, which may explain the similarity in the isotopic patterns seen (Darvill et al., in prep).

Focusing on the distinctive isotopic trend during the Holocene, Candy et al. (in prep.) suggest that, because this depletion trend occurs in basins of different sizes (as well as from extant and palaeo-basins), it is probably unlikely to result from changes in lake basin hydrology. Further to this, the deviation of the marl isotope records (fig. 3.13) away from the independent temperature records (fig. 3.12a) indicate 'non-Dansgaard' effects (Hammarlund et al., 2002), suggesting that this section of the records does not represent temperature variations. Instead, it is likely that changes in the precipitation regime are more likely to explain this trend (Hammarlund et al., 2002; Diefendorf et al., 2006; Candy et al., in prep.). As summarised by Candy et al. (in press), reducing the amount of summer rainfall (which has lower $\delta^{18}O$ values), or increasing the amount of winter rainfall (higher $\delta^{18}O$ values), can shift the $\delta^{18}O$ of groundwater to lower values. To explain the isotopic pattern seen in this section of the marl sequences, the early

Holocene precipitation regime would be more seasonal (high summer, low winter rainfall) in a continental style climate, whereas a reduction in seasonality resulting from one of the two situations described previously; increasing winter precipitation and/or decreasing summer precipitation, would lead to a more maritime precipitation regime (lower $\delta^{18}O$ values) (Candy et al., in press).

Although large reorganisations in the climate system during the early part of the Holocene appear to be recorded in British lacustrine carbonates as non-Dansgaard effects, sequences do record temperature shifts as well. For example, after the early Holocene isotopic depletion event observed in the Hawes Water sequence (Fig. 3.14), the 9.3 ka and 8.2 ka events are clearly expressed periods of ~50 and ~150 years, respectively, where $\delta^{18}O_{calcite}$ reaches values up to 1.1‰ lower than the background signal (Fig. 3.14a) (Marshall et al., 2007).

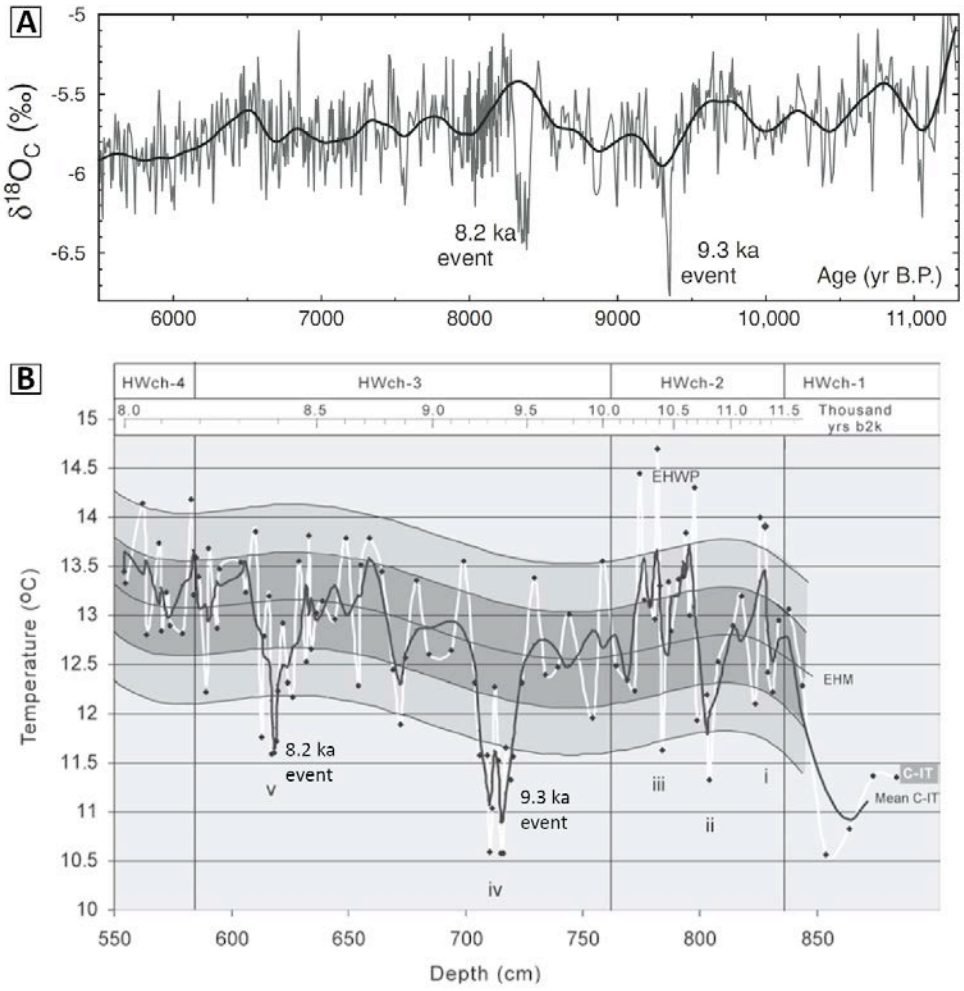

Figure 3.14. *The 9.3 and 8.2 ka events recorded in Hawes Water, England. A) The $\delta^{18}O_{calcite}$ record of Marshall et al. (2007), and B) chironomid-inferred summer temperature record for the same sequence.*

It has been demonstrated that the $\delta^{18}O$ value of modern lake water is a reflection of average monthly rainwater $\delta^{18}O$ and that contemporary calcite precipitates in isotopic equilibrium with the water and summer temperature (Marshall et al., 2007). Assuming, therefore, that this relationship holds true for the fossil record, as does the relationship between temperature and the isotopic composition of rainfall, the $\delta^{18}O$ of carbonates precipitated after the early Holocene depletion should record prevailing temperatures. This suggested temperature relationship has further been corroborated by chironomid inferred summer temperature reconstructions from the sequence, which also presents shifts in species assemblages associated with both events (3.14b) (Lang et al., 2010).

While the available isotopic records from lacustrine marl sequences in Western Europe appear to record temperature throughout most of their sequences, it is important to note that these records cannot always be considered as purely a temperature driven proxy, as temperature cannot always explain trends or shifts in the isotopic signatures. What is clear is that to identify these possible forcing mechanisms, it is desirable to have some form of independent proxy evidence to compare the isotope records to (e.g. Hammarlund et al., 2002, Candy et al., in press).

3.6.2. Key lacustrine sequences from MIS 11

As the previous section highlights, there are now a number of stable isotope records from lacustrine archives in the British Isles that record late Quaternary environmental change, but that the signal does not always reflect temperature changes. Isotope stratigraphies of inorganic freshwater carbonates from MIS 11 are still very rare, with only three studies knowingly published; Candy (2009) presented initial stable isotopic work undertaken on a small section of borehole GG of Turner (1970), while longer records have been published from Ossowka in eastern Poland (Nitychoruk et al., 2005) and Piánico-Sèllere from the southern Alps in northern Italy (Mangili et al., 2007).

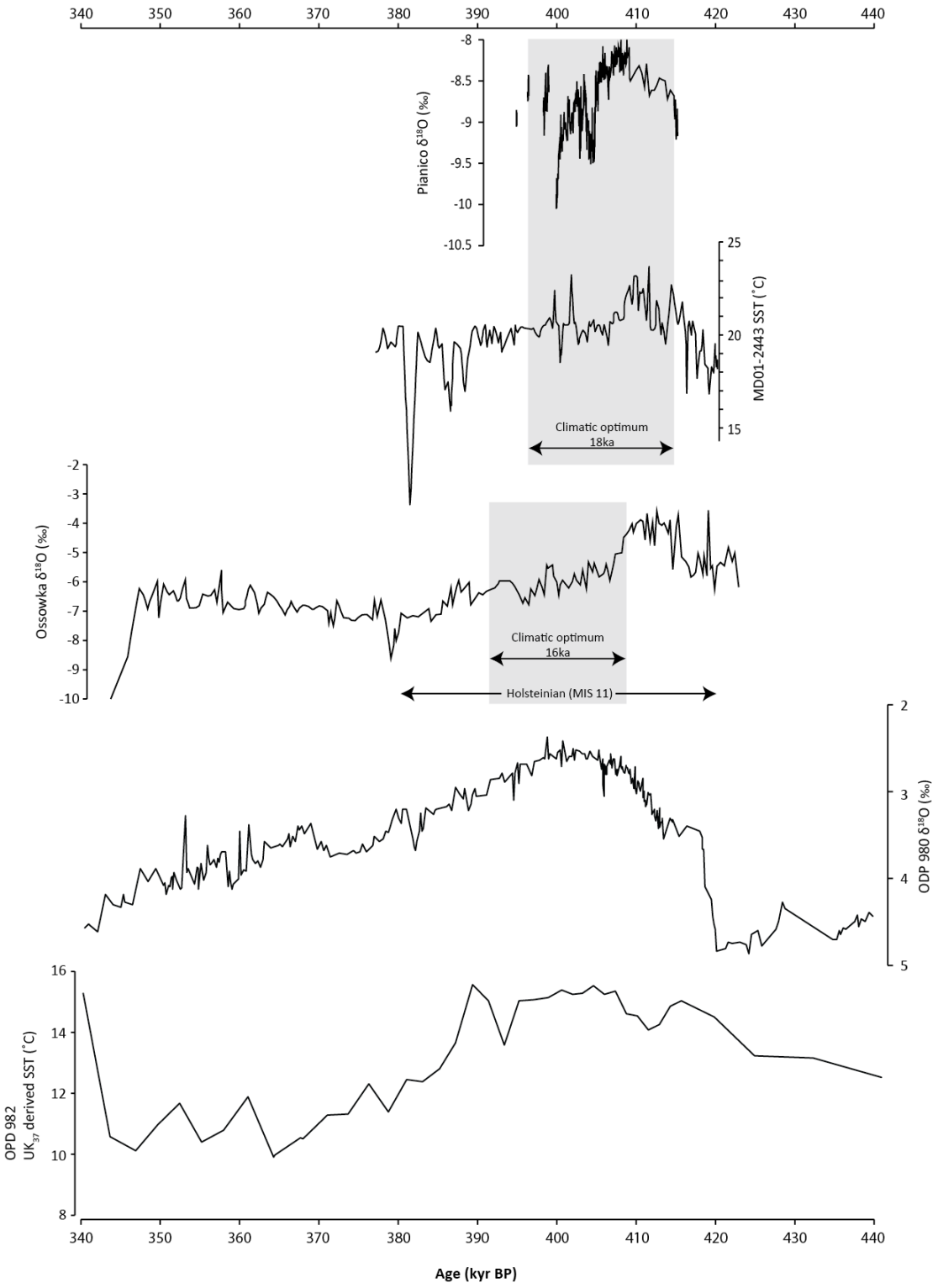

Figure 3.15. *Comparison between the two available $\delta^{18}O$ lacustrine carbonate records from MIS 11. The record from Piánico-Sèllere (Mangili et al., 2007) is plotted alongside the SST record of MD01-2443 from the Iberian Margin (de Abreu et al., 2005), as it was in the paper. The record from Ossowka (Nitychoruk et al., 2005) is plotted alongside the $\delta^{18}O$ record from ODP 980 (Oppo et al., 1998), as in the paper. The SST record from ODP 982 (Lawrence et al., 2009) has also been included in this graph. The grey shaded bars indicate the relative position and duration of the climatic optimum inferred for both sites. All records are plotted against their own inferred age models.*

While these records come from very different geographic and climatic settings, they both appear to record abrupt isotopic events that may be climatically driven. The isotopic record from Piánico-Sèllere is plotted alongside the closest sea-surface temperature record from the Iberian margin in figure 3.15 (as it was in Mangili et al., 2007). Based on the stable isotope data, Mangili et al. (2007) suggest that temperature is likely to be the dominant control over the $\delta^{18}O$ values of the authigenic carbonate, but also discuss other possible controls. The general trend in the Piánico record also appears similar to the sea-surface temperature record from core MD01-2443 (de Abreu et al., 2005). Mangili et al (2007) found evidence for 4 isotopic oscillations in the sequence, three short (125-195 varve years) and one much longer oscillation (780 varve years), which also corresponds to a shift in the pollen assemblage. The issue with this record, however, is that there is uncertainty about its age; with support for both an MIS 11 age (Brauer et al., 2007a, b), or a correlation with MIS 19 (Pinti et al., 2003; 2007, Scardia and Muttoni, 2009).

Figure 3.15 also presents the stable isotope record from Ossowka plotted with the ODP $\delta^{18}O$ record of Oppo et al. (1998) (as it was in Nitychoruk et al., 2005), and the sea-surface temperature record from ODP 982 (Lawrence et al., 2009). Interestingly, the trend in the isotopic record appears similar to the early Holocene records from the British Isles with an early peak, then gradual depletion away from independent temperature records (Fig. 3.15). Nitychoruk et al. (2005) suggest this trend is indicative of a switch in climatic regime from a more continental climate to a more maritime climate. If this is the case, other processes, in conjunction with temperature, affect the record at Ossowka. The only abrupt event described in the paper occurs at the onset of the climatic optimum (Fig. 3.15). Nitychoruk et al. (2005) also highlight a shift in the pollen assemblage at this stage, and hint that it is analogous to other events in European pollen records that have been correlated with the NAP phase at Marks Tey (Koutsodendris et al., 2012). This may well be the case, but no detailed reconstruction of the timing or duration of this event are given, which would enable a comparison to be made.

While it is difficult to compare lacustrine carbonate isotopic records from different geographical locations, some general points can be made about the environmental

information they record: 1) Isotopic records from MIS 11 lacustrine carbonate sequences have the ability to record the environmental structure of the interglacial, 2) these isotopic trends may be driven by temperature, but other factors such as continentality and seasonal distribution of rainfall should be considered, and 3) these sequences have the ability to record abrupt climatic events.

3.7. Summary

The above review highlights a number of points that are important when using the δ18O and δ13C of lacustrine carbonate to reconstruct past climate variability.

- The $\delta^{18}O$ of freshwater lacustrine carbonates in temperate mid-latitudes like British Isles reflects the $\delta^{18}O$ of lake water, which in turn reflects the $\delta^{18}O$ of precipitation, which is primarily controlled by temperature. Although other environmental controls are also important and may vary with time.
- $\delta^{13}C$ is more complicated and reflects productivity in the lake, as well as the lake catchment, giving an indication of lake hydrology and how water enters the lake.
- There are a number of possible sources of contamination to the isotopic signal, but if it can be demonstrated that they have no effect, then $\delta^{18}O$ and $\delta^{13}C$ values of calcite represent hydrological conditions within a lake system.
- Assuming the same hydrological conditions prevailed in the British Isles during geological record, stable oxygen isotopes can be used as a qualitative proxy for temperature, but caution should be taken, because other environmental factors may complicate the signal.
- Although from different geographical and climatic settings, published examples demonstrate the potential of using stable isotope records of lacustrine carbonate in the study of climatic variability during MIS 11.

Chapter 4. Varved sediments

Chapter overview

As well as the significance that Marks Tey has in the British Quaternary record in terms of its palaeobotanical evidence and possible temporal coverage of the Hoxnian Interglacial, sections of the sequence are also reported to contain annually laminated (varved) sediments (Shackleton and Turner, 1968; Turner, 1970; 1975). This view is based on thin section descriptions and preliminary unpublished pollen analysis from short sections of the core (Turner, 1970). Turner (1970) noted, however, some of the lamination structures were vague, which raises questions about the processes that generated them. Despite this uncertainty, estimates of the number of varves in the sequence have been used to determine the duration of MIS 11 in the British Isles (Shackleton and Turner, 1967; Turner, 1970; Turner, 1975). It is therefore necessary to determine whether or not the model for varve formation suggested by Turner (1970) is applicable to the sections of the sequence suggested to be annually resolved, and how many varves are preserved. Furthermore, the varve chronology can then be applied to investigate the duration and rates of landscape response during the NAP Phase, located in the pre-temperate phase of the pollen record.

This chapter is, therefore, divided into the following sections. The first section will discuss how and why varves are preserved in lacustrine settings. This will include typical varve types that are encountered, with the main focus being on biochemical varves, in line with the descriptions of Turner (1970). Due to the uncertainty over some of the sedimentary structures in the sequence, methods for demonstrating seasonal processes in laminated sediments are then discussed. The process by which varve chronologies are constructed will then be covered, before showing examples of how varve chronologies have been used to investigate the duration of abrupt climatic events, and how varve micro-facies can be used as a climatic proxy in its own right.

4.1. Introduction

Varved sediments are deposited and preserved under specific environmental conditions in a number of sedimentary settings: marine, estuarine and lacustrine environments (O'Sullivan, 1983). Varved sediments were first discovered and described in Sweden during the 19th century, but were not related to annual climate change until the work of Gerard De Geer (1912). De Geer noted the vertical repetitiveness and lateral continuity of the couplets composed of silt and clay (clastic, glaciolacustrine varves), similar to tree rings, which convinced him their formation was controlled by annual variations in climate, which controlled meltwater discharge and therefore varve thickness (De Geer, 1912). The term 'varve' can now be applied to annually laminated sediments that form from a number of different processes, under varying climatic regimes (e.g. O'Sullivan, 1983; Saarnisto, 1986; Zolitschka, 2003, 2007; Brauer, 2004). While varved sediments have also been reported from marine (e.g. Hughen et al., 1996; Dean et al., 2001, 2004) and estuarine (e.g. Sander et al., 2002) environments, this review will focus on lacustrine environments, as Marks Tey, the focus of this thesis, is a palaeolake basin.

Because of the resolution attainable, varved sediments have the potential to provide high-precision records of environmental change. They therefore have a number of important applications within climate science. The determination of the number of varves preserved within a sequence can provide fixed or floating chronologies for sedimentary archives (Zolitschka, 1991; Lotter et al., 1997; Brauer et al., 1999a; Lamoureux, 2001). Once varve chronologies are constructed, they can be used to determine the structure and duration of climatic events at a number of different scales (Lotter, 1991; Brauer et al., 1999b, 2007; Prasad et al., 2009; Palmer et al., 2010; Koutsodendris et al., 2012), act as a calibration tool for other dating techniques, such as the radiocarbon timescale (Goslar et al., 2000; Bronk Ramsey et al., 2012; Staff et al., 2013), palaeomagnetic variations (Saarinen, 1998; Snowball et al., 2007), and constrain the age of tephra layers (Zillen et al., 2002; Dorfler et al., 2012). Furthermore, it has been demonstrated that variations in varve microfacies can record climatic information at a range of different frequencies (Brauer et al., 2008b; Palmer et al., 2012; Koutsodendris et al., 2011; Neugebauer et al., 2012), therefore providing a climatic proxy in their own right.

Varved sedimentary sequences are, therefore, ideally suited to the study of abrupt climatic events, particularly in pre-Holocene interglacials where the ability to produce high-resolution chronologies is greatly reduced. In the case of MIS 11, varves have proved critical in the ability of researchers to determine the duration of abrupt isotopic events (Mangili et al., 2007). They have also enabled the duration of abrupt events in pollen records to be determined, which may provide analogues for the type of climatic events that punctuate the early Holocene (Koutsodendris et al., 2012). As has already been discussed, the NAP phase is thought to be the British equivalent to the OHO event investigated by Koutsodendris et al. (2012). The fact that this event is recorded in the sequence at Marks Tey, and the sequence is thought to be varved, will enable reconstruction at the same resolution. The intriguing situation with the NAP phase is that, based on estimated sedimentation rates, it lasts for approximately 300-350 years (Turner, 1970), which is significantly longer than the OHO (220 years, Koutsodendris et al., 2012). This seemingly different duration raises a number of questions, such as: 1) the suitability of linking the events, 2) whether local factors can explain the differences; and 3) whether pollen is a suitable proxy for recording such abrupt events. Before any discussion on the significance of this event can commence, it is vital that its duration is determined by micro-facies analysis and varve counts.

4.2. Preconditions for varve formation

The formation and preservation of varved sediments is the result of seasonal changes in regional climate, which influence the style of sediment input, formation and deposition within a lacustrine environment (Hakanson and Jansson, 1983). The resulting varve is made up of individual laminations that characterise these seasonal changes in climate throughout the year, where the laminations are arranged as couplets, triplets, or a larger number of laminations depending on the scale and frequency of climatic events (Zolitschka, 2003). The nomenclature used in this thesis to describe varve structure is as follows; a single varve is composed of a set of laminations, with each sub-lamination within this lamination set referred to as a lamination type (Palmer et al., 2012) (Fig. 4.1).

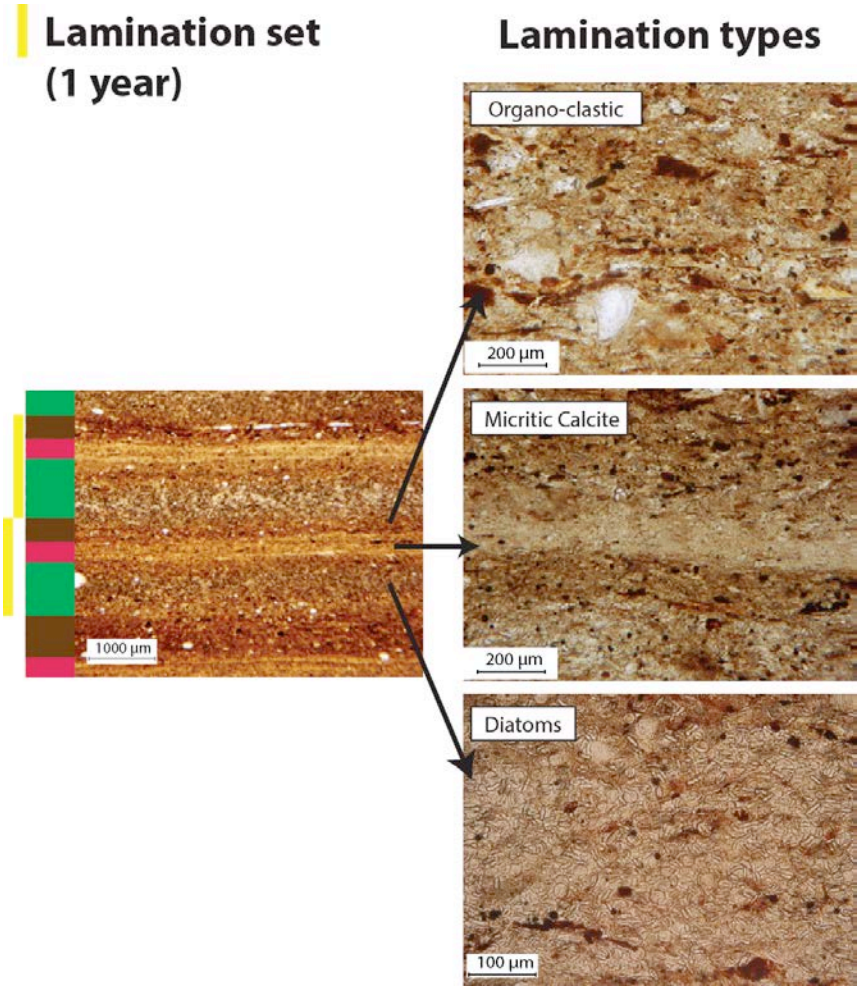

Figure 4.1. *Nomenclature used in this thesis as part of the micro-facies analysis of varved sediments based on Palmer et al., (2012). Each year is composed of sub-laminations that represent the season they were deposited during. These are referred to as lamination types. These lamination types are combined to produce a lamination set, which represents a single years worth of sedimentation.*

In principle, sedimentation is rhythmical in all lakes where climate influences production within the lake and/or the input of allocthonous material from the catchment (Saarnisto, 1986; Simola, 1992). However, while the seasonal climatic variability is a prerequisite for the formation of varved sediments, they do not occur in all lakes. This is because sediment can be disturbed by mixing from benthic organisms (*in situ* vertical mixing), re-suspension and transport of material by gravity, waves and currents (vertical and horizontal mixing) and by gas formation (e.g. CO_2 and CH_4) in the sediment resulting from the decomposition of organic material (or of volcanic origin) (O'Sullivan, 1983; Larsen and MacDonald, 1993; Brauer, 2004).

4.2.1. Sediment supply and distribution

The most basic prerequisite for varve formation is the availability of suspended matter in the water column of a lake, the source of which and how it is distributed in the water column is summarised in figure 4.2 (Kuenen, 1951; Sturm, 1979). The source and character of this sediment is controlled by the prevailing climate conditions within the lake catchment, as well as seasonal variations in climate during the year and limnological conditions within the lake itself (e.g. O'Sullivan, 1983; Saarnisto, 1986). It is the variation in the character of sediments deposited at different times during the year that create the varved structure (Petterson et al., 1993; Anderson, 1996; Ojala and Saarnisto, 1999).

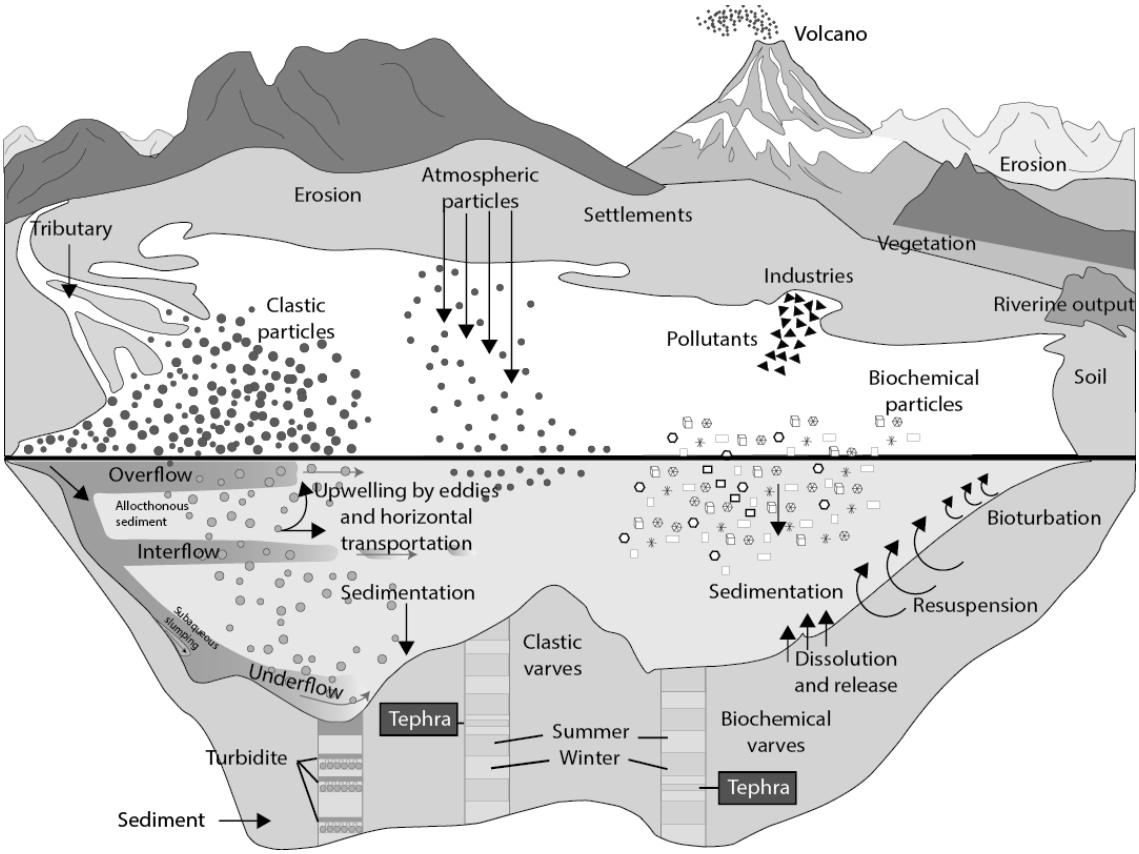

Figure 4.2. Internal and external sources and the influence of environmental factors on suspended sediments, sediment formation and deposition in a lake basin. Redrawn and modified from Bloesch (2004), originally published in Sturm and Lotter (1995).

The processes that produce material, which then forms sediment sequences, can be split into three domains; mechanical, bio/chemical and a mixture of the two (Fig. 4.3) (Anderson, 1996). The mechanical domain dominates under cold climate conditions

that prevail in proglacial and periglacial areas (e.g. Arctic or high Alpine regions), where material deposited in the lake basin, and preserved in the varve structure, is likely to be clastic sediment from allocthonous sources (Zolitschka, 2007). This is because under such conditions, physical weathering and a lack of vegetation are likely to characterise the catchment, providing large amounts of minerogenic material that can be washed into the lake in suspension and traction bed in streams (Sturm, 1979; Sturm and Lotter, 1995). As the climate is cold, lakes in which clastic sediments dominate are likely to be nutrient poor, with little or no organic productivity (Boygle, 1993). The methods by which sediments distribute across the lake basin after entry are dependent on the relationship between the density of the inflowing 'plume' (water and sediment mix) and the stratification characteristics of the water column. The larger the difference in density is between the two sources, the greater the energy that is required to mix them, and thus the plume can travel great distances into the lake as a distinct density current (Ashley et al., 1985; Best et al., 2008). The inflowing plume may disperse by three different methods; hypopycnal flows (overflows), hyperpycnal flows (underflows), mesopycnal flows (interflows) (Fig. 4.2) (Bates, 1953, Ashley et al., 1985; Mulder and Alexander, 2001).

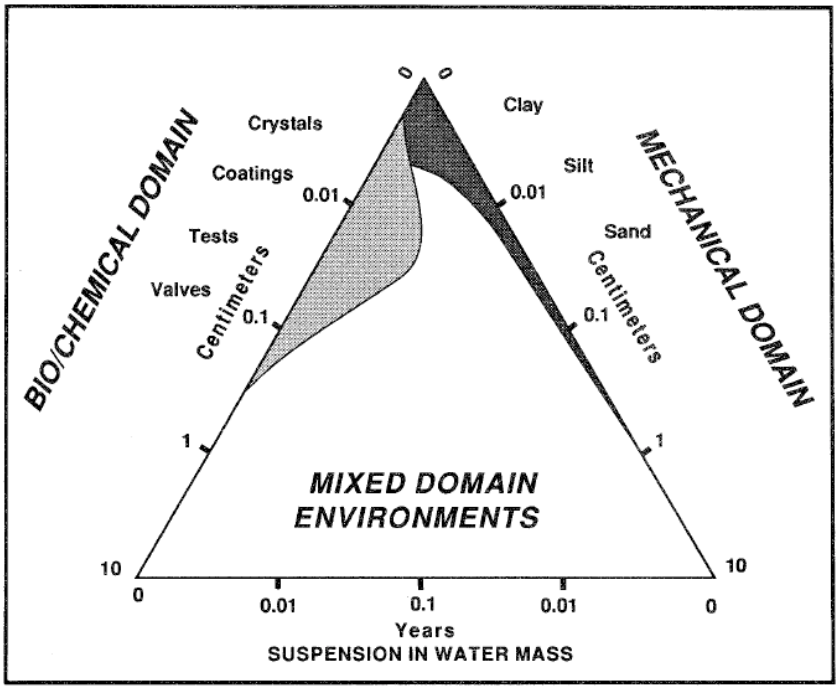

Figure 4.3. *Ternary plot highlighting the two main sources (domains) of sediments deposited in a lake basin. The mechanical domain corresponds to clastic material (mineral, soil, organic), which moves as a result of a forcing mechanism like slumping and air/water currents. The bio/chemical domain relates to particle production within the lake by biological fixation or chemical precipitation. The mixed*

domain represents a continuum between the two end members and is the domain that reflects most depositional environments (Anderson, 1996).

As climate ameliorates, physical weathering ceases and so, therefore, does the production of minerogenic material. The lake catchment will also become vegetated, reducing the amount of minerogenic material transported into the lake basin (Anderson and Dean, 1988). The source of material for the formation of clastic laminations is therefore cut off and organic sediments start to dominate the record. The trophic status of lakes is also likely to change with climate. It is generally agreed that the two most important elements involved in changing the trophic status of a lake (eutrophication) are nitrogen and phosphorus (e.g. O'Sullivan, 1995). Vegetation will introduce nitrogen to the lake catchment by biological fixation from the atmosphere, while phosphorus is released from bedrock in the catchment by chemical weathering, which becomes more effective in temperate climates (O'Sullivan, 1995, Zolitschka, 2003). This increase in nutrients entering lake waters will lead to increased primary productivity, changing its trophic status from oligotrophic to mesotrophic/eutrophic/hypertrophic, depending on nutrient levels (Padisak, 2004). The lake sediments will therefore start to incorporate material of an autochthonous origin, like diatoms, green and blue-green algae, and chemical precipitates (Sturm, 1979, Zolitschka, 2003; Brauer, 2004), indicative of the bio/chemical domain (Fig.4.3) (Anderson, 1996). While these two domains provide a way of categorising seasonal laminations, they are end-members of a continuum where varves are likely to be composed of a mixture of material from both sources (Anderson, 1996).

4.2.2. Basin morphometry

One of the most important requirements for the preservation of varves is the shape of the lake basin. An ideal basin should have a flat bottom to prevent post depositional slumping of sediment, and should be deep enough in relation to its surface area so that circulation in the water column due to storms or seasonal mixing are not sufficient enough to disturb the accumulating sediments (O'Sullivan, 1983, Saarnisto, 1986, Ojala *et al*., 2000). Other factors that may aid preservation include a bedrock basin, small lake catchment and no significant inflow (Saarnisto, 1986). Changes in basin morphometry over time can have an impact on the thickness of varves, as well as their composition (Nuhfer et al., 1993). In a study at Elk Lake, Minnesota, Nuhfer et al.

(1993) noted that as basin morphometry changes through time thicker varves tend to get deposited, which may suggest that sediment re-suspension becomes an important factor in varve formation.

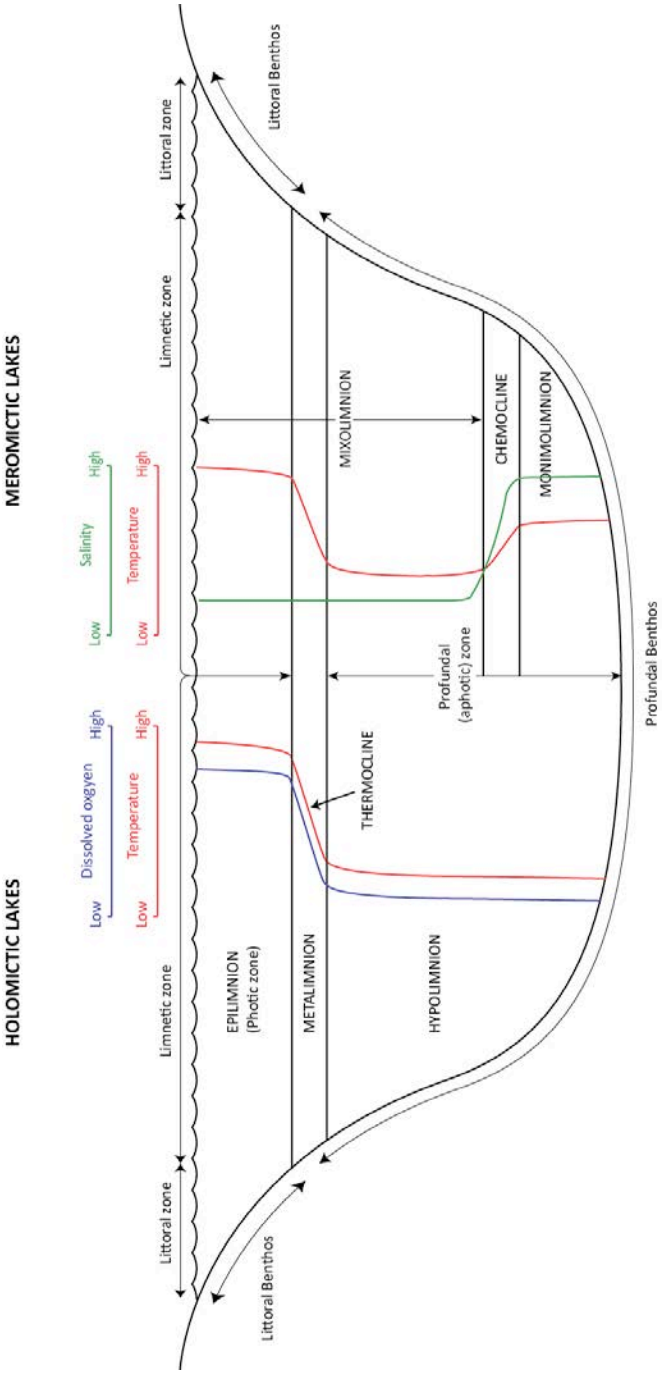

Figure 4.4. Schematic diagram depicting the types of thermal stratification patterns in holomictic and meromictic lakes. When holomictic lakes (mix at least once per year) stratify, they are characterised by three layers of water; the warmer (less dense) epilimnion, colder (more dense) hypolimnion and an intermediate layer (thermocline) called the metalimnion. Meromictic lakes are characterised by a layer of bottom water that hasn't mixed for at least one annual cycle. This is due to the build-up of dissolved substances in the bottom waters, held there by hydrostatic pressure, known as a chemocline/halocline/pycnocline, depending on whether a salinity/chemical/density gradient is the cause. Drawn using information from Boygle (1993) and Boehrer and Schultze (2008).

4.2.3. Thermal stratification of the water column

For varved sediments to preserve in the sedimentary record the lake water column should ideally be seasonally or permanently stratified, which reduces the effect of turbulence in the profundal zone, therefore limiting sediment disturbance (Boygle, 1993). Whether or not a lake will stratify is dependent on the temperature and density of the water column, which has a maximum at +4°C (Lindell, 1980), as well as the morphometry of the lake basin.

The thermal layering of a lake is made up of three components; 1) the epilimnion, which represents the lighter surface waters that are heated by the sun, 2) the metalimnion, where the warming from the sun decreases with depth (producing a temperature gradient called the thermocline), and 3) the hypolimnion, which is not heated by the sun and is therefore comparatively cold to the upper layers (Fig. 3). Lakes are classified in terms of mixing (mixis) properties and can be classified as holomictic (mix at least once a year) or meromictic (never fully mix). The different lake types are summarised in table 1. For example, the most common lake type observed in the UK is a dimictic lake.

Table 4.1. Lake mixing types (Information from Hakanson and Jansson, 1983, Anderson *et al*., 1985).

Lake Type	Lake Circulation	Thermal characteristics	Geographical Location
Amictic	Never circulate, always frozen	Inversely stratified	Antarctica, Arctic
Cold monomictic	Only during summer	Water temperature never exceeds +4°C	Cold areas and/or high altitudes. Often connected with glaciers and permafrost
Dimictic	Twice a year, generally during spring autumn	Directly stratified in summer and inversely stratified in winter	Most common type of stratification in cool temperate regions
Warm monomictic	Once a year	Water temperature never drops below +4°C	Temperate zones, mountains in subtropical latitudes, areas influenced by oceanic climates.
Polymictic	Frequent circulation	Cold polymictic: temperatures close to +4°C Warm polymictic: > +4°C	Regions with rapidly alternating winds, large daily temperature variations and small seasonal variations
Oligomictic	Irregular and/or rare circulation	Temperatures well above +4°C	Tropical regions
Meromictic	Do not undergo complete mixing. Only the Mixolimnion circulates.	Lake stratified due to chemical gradient: Chemocline	No specific geographical location, lake morphometry appears to be most important factor.

The level of oxygen present in the lake water is related to its thermal stratification and can also be an important factor for varve preservation. Circulation of the epilimnion by wave action oxygenates the water, whereas oxygen in the hypolimnion is removed by aerobic activity and is not replaced due to the lack of circulation, causing anoxic conditions (Nichols, 2009). Anoxic conditions prevent varve structure from being disturbed by benthic organisms (bioturbation) (Lamoureux and Bradley, 1996, Zolitschka, 2003). While anoxic conditions are seen as an important factor for the preservation of varves, it is not essential, as varved sediments have been observed in lakes that do not contain permanently anoxic conditions. For example, dimictic lakes can contain varved sediments. Productive lakes may also contain varved sediments if the sedimentation rate is higher than the rate of bioturbation. As well as varve preservation, the seasonal pattern of water column stratification and mixing will control the cycling of nutrients and duration of productivity within the lake, which are important factors in influencing seasonal sedimentation (Nuhfer et al., 1993).

4.3. Varve types

The balance between the dominant sediment sources discussed above will determine the varve types that are deposited (Fig. 4.3). A number of different varve types have been reported in the literature (Fig. 4.5) (O'Sullivan, 1983, Saarnisto, 1986, Anderson and Dean, 1988, Boygle, 1993) and can be grouped into three main varve types: clastic, biogenic (diatomaceaous, calcitic or iron-rich) and evaporitic varves (O'Sullivan, 1983; Zolitschka, 2003, 2007; Brauer, 2004). Clastic varves are characterised by regular alternations in coarse and fine clastic particles, where the coarse lamination represents in-wash from the catchment during the spring/summer, and the fine lamination represents the settling of clay out of suspension during winter, when the lake is ice covered (Smith, 1978; Sturm, 1979; Smith and Ashley, 1985; Hsu, 1989; Ringberg and Erlstrom, 1999; Palmer et al., 2008; 2010; Macleod et al., 2010). Evaporitic varves are a characteristic of arid climates where mineral precipitation during the summer months is driven by high evaporation rates (Anderson and Dean, 1988; Brauer, 2004). This section on varve types will focus on biogenic (biochemical) varves, however, as it is this varve type that has been described at Marks Tey (Turner, 1970).

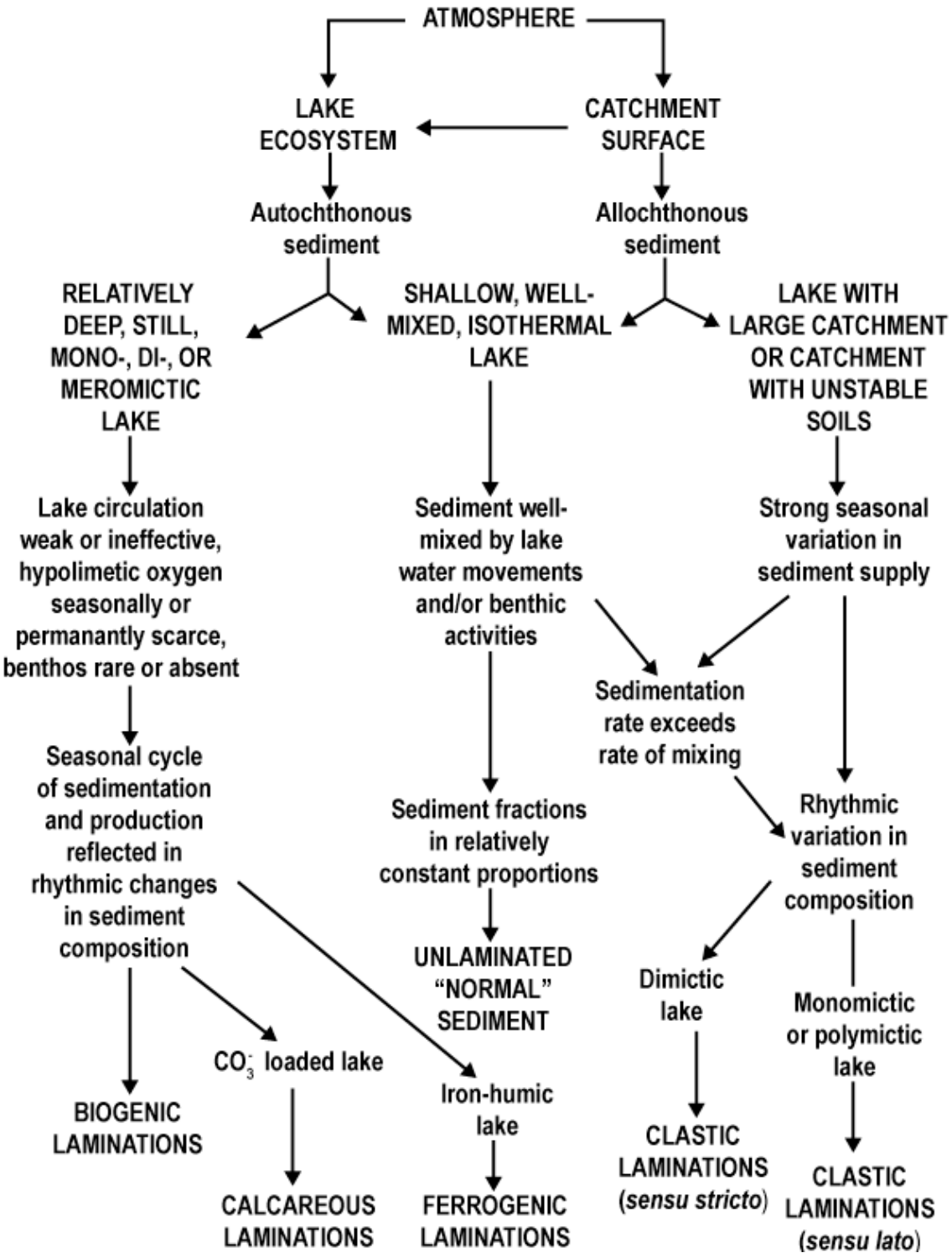

Figure 4.5. Schematic diagram showing the process of how annually laminated sediments are deposited in lakes. Re-drawn from O'Sullivan (1983).

4.3.1. Model for varve formation at Marks Tey: biochemical varves

The model proposed by Turner for varve formation at Marks Tey is shown in figure 4.1. The lamination set (varve) is composed of three lamination types (seasonal sub-laminations); 1) a diatom-rich lamination composed predominantly of *Stephanodiscus* spp. in a calcite matrix, 2) a layer composed almost entirely of fine grained calcite crystals, and 3) a lamination composed of a mixture of organic debris, diatoms and calcite crystals.

The sequence described by Turner (1970) is analogous to that found in biochemical varves, which have been described from a number of sites located in temperate regions (Ludlam, 1969; Kelts and Hsu, 1978; O'Sulivan, 1983; Peglar et al., 1984; Lotter, 1989; Nuhfer et al., 1993; Lotter et al., 1997; Zolitschka, 2003; Brauer and Cassanova, 2001; Brauer, 2004; Teranes et al., 1999; Giguet-Covex et al., 2010; Neugebauer et al., 2012) and are common in lakes where there is a local source of carbonate (i.e. limestone bedrock or carbonate-rich till/loess) (Smith et al., 1976; Dean and Fouch, 1983). The geographical distribution of sites where biochemical varves have been found will obviously lead to varve structures and species compositions that are site-specific (Table 4.2). The sub-annual arrangement of lamination types can also vary through time within a sequence (see Neugebauer et al., 2012). At the most basic level, however, the timing of seasonal diatom blooms and chemistry of the water column control the basic structure of a biochemical varve.

4.3.1.1. Diatom blooms

Diatoms form one component of the phytoplankton community whose growth periods are controlled by a number of physical (light, temperature, water column mixing), chemical (nutrient availability) and biological processes (competition and grazing) (Sommer et al., 1986; Lampert et al., 1986; Marshall and Peters, 1989; Vanni and Temte, 1990; Arhonditsis et al., 2003) The timing and nature of these processes tend to follow predictable patterns in lakes of a similar morphology and trophic level, that occur under similar climatic conditions (Reynolds, 1984).

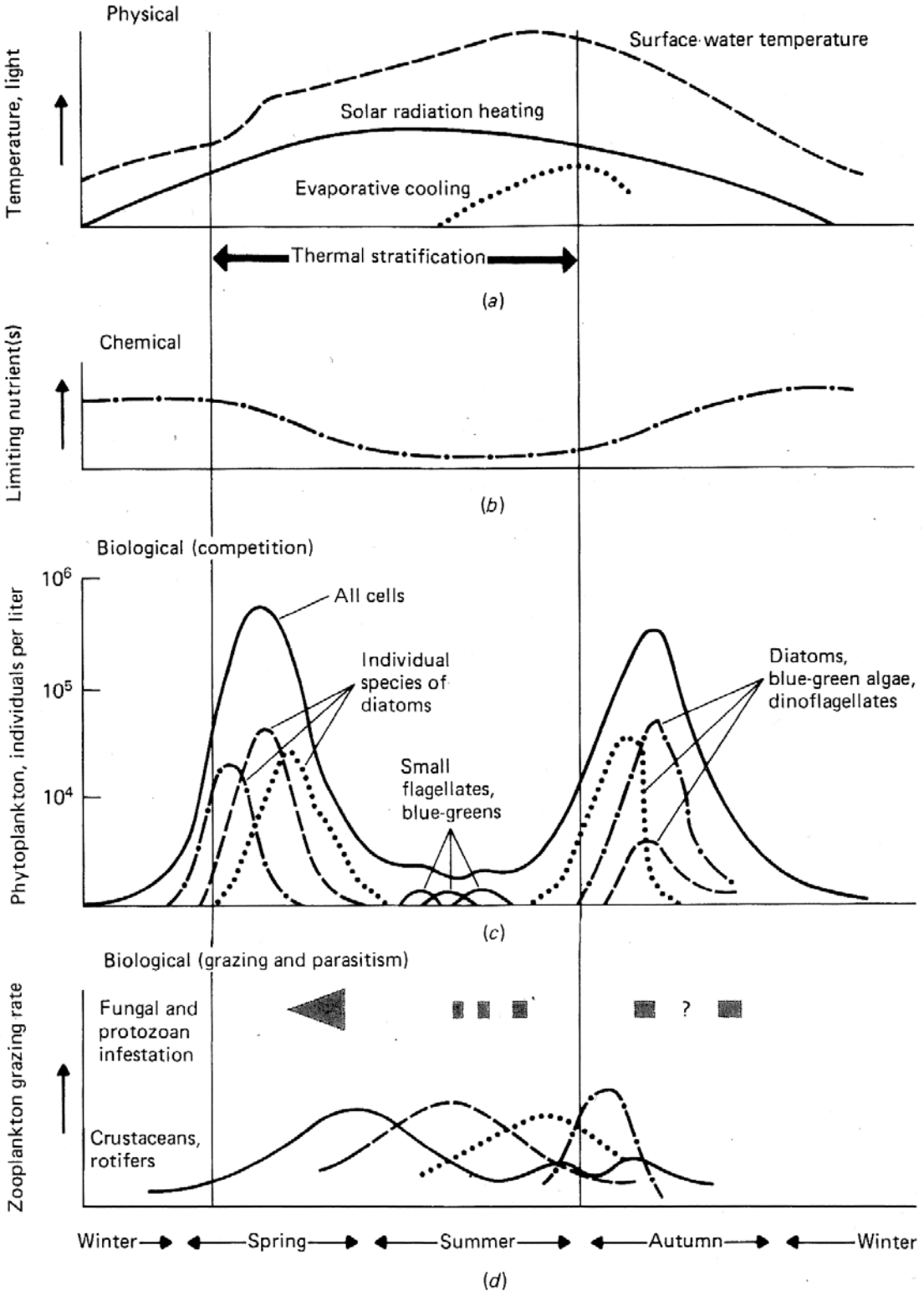

Figure 4.6. *Schematic diagram representing the annual cycle of (a) physical, (b) chemical and (c,d) biological factors that regulate the seasonal cycle of phytoplankton in a temperate lacustrine system. Diatoms show two distinct bloom periods (c), during the spring and autumn. Figure taken from Horne and Goldman, 1994.*

Lakes in temperate (and polar) regions are characterised by distinctive seasonal patterns of diatom blooms, which occur during spring and autumn water column mixing periods, while water column stratification during the summer months results in a shift of dominance to other algal communities (Fig. 4.6) (Hitchinson, 1967; Reynolds, 1984; Sommer et al., 1986; Marshall and Peters, 1989; Willen, 1991; Maberly et al., 1994). As section 4.2.3 demonstrates, the most common lakes in temperate regions are dimictic lakes, which undergo periods of mixing during the spring and autumn (Lewis, 1983). It could therefore be expected that varves deposited in dimictic lakes will contain evidence for diatom blooms in both the spring and autumn. Although diatom laminations are a common feature of the spring layer in biochemical varves (e.g. Kelts and Hsu, 1978; Lotter et al., 1997; Neugebauer et al., 2012), they do not, however, always produce another lamination relating to a second bloom during the autumn period (c.f. Giguet-Covex et al., 2010). One possibility to account for this is that diatom blooms during the autumn lake mixing period tend to be weaker than during spring overturn (Fig. 4.6) (Horne and Goldman, 1994; Kirilova et al., 2009) and may get obscured by other materials that compose the autumn/winter layer (section 4.3.1.3).

4.3.1.2. Calcite precipitation

The chemistry of non-clastic calcium carbonate precipitation was covered in chapter 3. With its relevance to varve structure, calcite precipitation occurs in lakes during the warmest months of the year, between late spring and early autumn. This has been demonstrated in extant lakes by analysing sediment traps, where calcite crystals are collected as they precipitate (Brunskill, 1969, Kelts and Hsu, 1978, Anderson and Dean, 1988, Teranes et al., 1999), and by relating sediment trap results to the sediments deposited on the lake floor (Ludlam, 1969). The sedimentology of calcite laminations varies, as calcite can either form a single lamination, or multiple sub-laminations over a single season (Teranes et al., 1999a, b; Brauer et al., 2008b).

Furthermore, it appears that the size of the calcite crystals may be used to infer timing of precipitation, as some researchers have noted an upward-fining pattern in crystal size within the calcite layer (Peglar et al., 1984, Lotter, 1989, Lotter et al., 1997, Teranes et al., 1999b; Giguet-Covex et al., 2010). Coarse crystals tend to be associated

with late spring and are often found in the spring diatom layer (Kelts and Hsu, 1978; Lotter et al., 1997). The precise mechanism for the upward-fining secession is unclear. It may relate to low levels of supersaturation in the late spring, where lower temperatures/less biological productivity enable slow crystal growth, whereas during the summer, increasing temperature/biological activity increase the degree of supersaturation, favouring rapid growth of smaller crystals (Folk, 1974, Kelts and Hsu, 1978; Peglar et al., 1984). Another possibility is that increased phosphorous concentrations during spring inhibit calcite precipitation, and the subsequent precipitation due to reducing concentrations leads to high rates of crystal growth (McConnaughhey and Whelan, 1997; Teranes et al., 1999b). While both of these mechanisms account for a simple normally graded calcite lamination, the situation is further complicated by the micro-facies descriptions of Brauer et al., (2008b), who describe repeating cycles of calcite crystal size patterns.

The mechanism for the production of multiple calcite laminations over a single season is unclear, but any explanation would need to consider the influences over calcite supersaturation states, such as nutrient levels, algal productivity, temperature and pH. The best way to study this would of course be to monitor extant lakes that undergo multiple whiting events. Multiple whiting (authigenic calcite precipitation) events have been noted in some lakes (Romero et al., 2006) and multiple calcite sub-laminations have been noted in others (Teranes et al., 1999a, b), but no study has yet linked lake monitoring to the sedimentary record in this respect.

4.3.1.3. Organic/detrital material

After the spring diatom bloom and subsequent period of peak calcite precipitation during the summer months, the autumn/winter layers in calcitic biogenic varves are typically composed of a mixture of particles from both autochthonous and allocthonous sources. Autochthonous sources include organic material that settles out of the water column after peak periods of biological production, as well as debris of reworked littoral material, including calcite and diatom frustules (Kelts and Hsu, 1979; Renberg, 1981, 1982; Petterson et al., 1993; Zolitschka and Negendank, 1996; Lotter et al., 1997; Merkt and Muller, 1999; Bloesch, 2004; Luder et al., 2006; Brauer et al., 2008a). As noted earlier, if the autumn diatom bloom is strong enough, it will also

form a discrete layer within this mixture (e.g. Giguet-Covex et al., 2010). Laminations formed during the autumn/winter months also often contain material in-washed from allocthonous sources, which can include plants remains (e.g. leaves, stems and twigs), humic particles eroded from catchment soils and minerogenic/detrital carbonate particles (Zolitschka and Negendank, 1996; Brauer et al., 1999b; Lücke and Brauer, 2004; O'Sullivan, 2004; Brauer et al., 2008a).

4.3.1.4. Examples of other structural components in calcitic biogenic varves

The succession of structural components described above, while providing a possible explanation of the mechanism of sediment deposition at Marks Tey, should only be regarded as one example of how biochemical varves can form, as other seasonally specific components have been noted. Table 2 shows examples of some of the other structural components that have been noted in biochemical varves.

Table 4.2. *Examples of other structural components found in calcitic biogenic varves. See text for references.*

Season	**Basic succession**	Extra calcite layer	Second diatom bloom	Chrysophytes	Blue-green algae	Detrital layers
Spring	**Diatom bloom**	X		X		X
Summer	**Calcite**			X	X	X
Autumn	**Organic/**		X	X	X	X
Winter	**detrital**					X

As well as the occurrence of a secondary discrete diatom bloom during autumn lake circulation, calcite crystals of a larger size have also been found to form a spring layer that is separated from the summer layer (Neugebauer et al., 2012). Chrysophyte cysts (golden brown algae) have also been noted as structural components of biochemical varves (Tippett, 1964; Batarbee, 1981; Peglar et al., 1984; Lotter, 1989). While their preservation in distinctive layers of laminated sediments has been used as a line of evidence to demonstrate a varved nature, it is questionable whether they should be used solely as an indicator of seasonal processes (Pitkanen and Huttunen, 1999), as in many of the studies referred to above, no genetic identification of the cysts was

carried out. This is because, unlike diatoms for example, chrysophyte cysts have been relatively understudied, and knowledge of taxonomy, provenance and identification is still being developed (Adam and Mahood, 1981, Smol, 1988, O'Sullivan, 2004).

Like diatoms, green and blue-green algae also form an important part of lacustrine phytoplankton, in which they tend to dominate during the summer-autumn period of the seasonal cycle (Fig. 4.6). This algae is easily decomposed and, as a result, not often preserved (Zolitschka, 2003, 2007), but has been found in varved sediments under high magnifications, where it is restricted to the layers corresponding to the summer/autumn months (Kelts and Hsu, 1978; Simola, 1979; Merkt and Muller, 1999).

4.4. Determination of the seasonal signal in laminated sediments

A number of different methods have been used to demonstrate the annual character of laminated sediments, including direct observations of water column particle fluxes, radiometric dating of contemporary sequences and counting back from the present day, process-based models, and identifying seasonal successions of microfossils (e.g. pollen and diatoms) within the laminations. Based on the discussion in the previous section, it may seem reasonable to accept the assertion of Turner (1970) about the varved nature of the lamination sets at Marks Tey. While the model of Turner (1970) is analogous to the processes that produce calcitic biogenic varves, it is based on thin sections from short sections of the sequence, as well as preliminary unpublished high-resolution pollen analysis. As yet, no quantitative evidence has yet been published to validate the proposed model of varve formation.

The development of a depositional model for varve formation is a fundamental step in the goal of constructing a varve chronology, as it ensures that the repetitive sequence of structures preserved in sediments can be assigned to seasonal processes (Lotter and Lemcke, 1999; Lamoureux, 2001; Brauer et al., 2009), and are not a function of other processes that can produce non-annual laminations in sediment sequences (Lambert and Hsu, 1979; Mulder and Alexander, 2001). This process is particularly important for fossil lake archives, such as Marks Tey, where the varved nature cannot be anchored by counting back to annually controlled marker horizons like ^{137}Cs peaks

and/or ^{210}Pb activity (Erten et al., 1985, Lotter, 1997; Tylmann et al., 2013), or by lake monitoring studies (Ludlam, 1969; Kelts and Hsu, 1978; Nuhfer et al., 1993; Stockhecke et al., 2012). Both of these techniques are limited in their scope to extant lakes where varves are currently forming.

4.4.1. Micro-facies descriptions

An important step in the process of developing a robust model for seasonal depositional processes is the characterisation of micro-scale changes in the structural components of the lamination sets, a process known as micro-facies analysis (Brauer, 2004). As Brauer (2004) indicates, variations in sub-lamination composition or structure can result from climatic induced change in the lacustrine depositional environment, therefore providing a proxy for climate, which has been demonstrated by a number of studies (Lucke and Brauer, 2004; Brauer et al., 2008a; Martin-Puertas et al., 2012; Neugebauer et al., 2012; Rach et al., 2014). As highlighted by Brauer et al. (2009), the main limitation of micro-facies analysis is that it only produces semi-quantitative data. This limitation can be overcome by combining microscope descriptions with micro X-Ray fluorescence (μ-XRF) data, however, as stratigraphical changes in elemental composition can aid interpretations (Brauer et al., 2009).

The introduction of continuous core scanning techniques for the generation of μ-XRF data has been a significant development in the study of lacustrine sequences, providing a sub-millimetre, non-destructive method for the relatively fast generation of variations in sediment elemental composition (Croudace et al., 2006; Croudace and Rothwell, 2010). The resulting data can provide high-resolution records of catchment stability, as well as within-lake processes such as primary productivity and palaeo-redox conditions (Brauer et al., 2009; Francus et al., 2009). The particular benefit of applying this technique to varved sediments is that: 1) it supports micro-scale sediment descriptions by characterising seasonal layer composition (e.g. Brauer et al., 2009; Neugbauer et al., 2012); 2) the varve chronology can be used to quantify the rate and duration of changes in elemental composition, which may have a climatic significance (e.g. Brauer et al., 2008a; Martin-Puertas et al., 2012); and 3) it can provide a novel approach to aid varve chronology construction (Guyard et al., 2007; Marshall et al., 2012).

4.4.2. Other methods for developing a depositional model

A number of methods have been used to demonstrate the annual signal in laminated lake sediments that occur in fossil basins. A common technique is to compare the micro-facies descriptions of stratigraphical variations in microfossils and minerals from sediment thin sections (also SEM images) and relate them to their seasonal characteristics in modern environments (Tippett, 1964; Card, 1997; Brauer et al., 1999b; Koutsodendris et al., 2011; Neugbauer et al., 2012; Flower et al., 2012). A quicker alternative to producing thin sections involves the use of sediment tape-peels, where the stratigraphic succession of microfossils adhered to the tape can be determined using a microscope (Simola, 1979, 1992). A further method involves sub-sampling core material and splitting laminations into horizontal sub-samples to produce microscope slides for microfossil identification (Nipkow, 1927, Tippett, 1964, Peglar et al., 1984, Lotter, 1989, Gauthier and Munoz, 2009). This method may be preferred in a situation where the sedimentology of a sequence (e.g. the abundance of calcite) makes it difficult to identify microfossils by *in situ* observations alone.

4.5. Construction of varve chronologies

If it can be demonstrated that the lamination sets in a sediment sequence are varves, a chronology can then be constructed. Methods commonly used for chronology construction are summarised by Lamoureux and Bradley (1996) and Lamoureux (2001). Despite the importance of this process, the methodologies by which varve chronologies are constructed are not always reported in sufficient detail in the published literature, and errors associated with the chronologies are sometimes omitted (e.g. Leemann and Niessen, 1994). The accuracy of a varve chronology is dependent on assessing counting error introduced as a result of sedimentation processes that operate within the lake, technical problems during core recovery and correlation, and errors introduced during the counting process (Sprowl, 1993; Lamoureux and Bradley, 1996; Lamoureux, 2001; Zolitschka, 2003):

1) **Errors introduced by style of sedimentary processes:** Very high sedimentation rates can produce varves with multiple sub-annual laminations that may be

interpreted as more than a single varve during the counting process (**Type A error**). Very low sedimentation rates can produce varves that are thin, increasing the likelihood that varves will be missed during counting (**Type B error**). Spatial variations in sedimentation patterns can also affect the varve counts, resulting in extra or fewer varves being preserved. Similarly, areas of the core where varve quality is low and the structure is difficult to identify will also introduce uncertainties, as these areas may require interpolation;

2) **Errors introduced by depositional events:** Erosion from turbidity currents, tephra deposition or movement within the sediment stack itself can result in the removal of varves from the whole sequence (**Type C error**). This can only be truly assessed by extracting multiple cores from the lake basin and the error quantified by using independent dating techniques to validate the chronology through establishing hiatuses in the sediment sequence. If restricted to localised areas, taking multiple cores can circumvent these errors;
3) **Errors introduced by technical issues:** Which are introduced due to incomplete recovery of a sequence (gaps between coring runs and coring artefacts) or by incorrect core correlation, which can be overcome if appropriate coring techniques are used, or multiple overlapping cores are studied.

Constructing a robust varve chronology to minimise the associated errors requires selection of the most appropriate techniques throughout the whole process, from obtaining the sediment cores, to sub-sampling, varve counting, and verifying the resulting chronology.

4.5.1. Core collection

The first step of any investigation is the collection of sediment cores. Cores are usually taken from the deepest part of the lake basin, below the thermocline (or chemocline), where sediment disturbance is minimal and there is the greatest potential for varve preservation (O'Sullivan, 1983, Saarnisto, 1986, Petterson et al., 1993, Lamoureux and Bradley, 1996, Ojala *et al*., 2000, Tian et al., 2005). The key objective is to obtain a continuous sediment record. When drilling long sequences with a number of core segments, overlapping cores should be extruded to ensure that breaks between coring runs are covered (Merkt and Muller, 1999, Zolitschka, 2003). Another important

consideration is the number of cores to be taken. Using a single core requires the assumption that it will be an accurate representation of sedimentation in the basin as a whole. As sedimentation patterns in lakes are dependent on a number of factors, results from such variability studies differ, with some suggesting that a single core can be representative of a basin (Petterson et al., 1993), with others demonstrating significant lateral variability, therefore advocating the multiple core approach (Lamoureux, 1999; Neugbauer et al., 2012). The advantage of using multiple cores is that it reduces to likelihood of Type C counting errors (Leonard, 1997, Lamoureux and Bradley, 1996). The collection of multiple cores can, however, be expensive.

4.5.2. Counting methods

A number of different analytical methods have been applied to varved sediments to enable varve counts to be made. The method(s) selected will depend on the preference of the user, but will also be driven by the level of structural detail required, as well as the quality and thickness of the varves preserved. Whichever methods are selected, there are some important tasks that should be carried out prior to, and during counting:

1) Preliminary sedimentological observations of the core should be undertaken to construct a model for varve formation that all counters can work from. By assembling the structural components described in section 3, the result is a set of sedimentological criteria that will make the counting process more objective, as the recognition of what actually constitutes an individual varve can be subjective (Lotter and Lemcke, 1999, Cockburn and Lamoureux, 2007, Lamoureux, 2001).
2) Prominent laminations within the sequence should be marked on the core (or thin sections if made). These act as boundaries, in between which the counts can be carried out and compared over short sections (Lamoureux and Bradley, 1996; Brauer et al., 1999a; Ojala and Saarnisto, 1999). The distance between the marker beds/layers obviously depends on where they occur in the core, but they should ideally cover regular intervals (Lamoureux and Bradley, 1996, Lamoureux, 2001).
3) The number of counts made along the sequence, and by how many workers, needs to be agreed upon. Published methodologies can vary, with some providing only vague methods for the number of counts made (Ojala and Saarnisto, 1999, Tian et

al., 2005). The most common practice seems to be multiple counts along one or more transects by multiple workers (Lamoureux and Bradley, 1996, Zolitschka, 1996, Lamoureux and Cockburn, 2007).

4) While the counting is taking place, a note should be made of varve quality, as well as unusual or vague structures and sediment colour (Lotter and Lamoureux, 2001). The scale used for varve quality estimation varies, and will depend on operator preference (Lotter and Lemke, 1999; Brauer and Cassanova, 2001; Nakagawa et al., 2011). Depending on the counting method employed, varve thickness measurements should also be undertaken, as they can provide another important line of evidence (e.g. Brauer et al., 1999b; Hu et al., 1999).

These processes are important, as it can highlight sections of the core that contain the potential for chronological error (Lamoureux, 2001). In terms of undertaking the varve counts, a number of methods have been employed.

Two of the simplest methods used are counting directly from the core surface and from enlarged photographs, but this should only be applied where varves are relatively thick (>1mm) and the structure easy to distinguish (Pike and Kemp, 1996, Ojala and Saarnisto, 1999; Zolitschka, 2003). More time-consuming methods include counting from images produced by scanning sediment thin sections (Cockburn and Lamoureux, 2007) and semi-automated techniques, such as ITRAX core scanning (Guyard et al., 2007; Marshall et al., 2012). One of the limitations of these methods is that fine-scale detail, such as the composition of sub-annual laminations, may be missed (Lotter and Lemcke, 1999). It has become an increasingly standard technique to undertake varve counts on overlapping sediment thin sections under high magnifications (Brauer et al., 1999a; Brauer and Cassanova, 2001; Mangili et al., 2005; Martin-Puertas et al., 2008; Palmer et al., 2008, 2010; Koutsodendris et al., 2011; Neugebauer et al., 2012; Czymzik et al., 2013). This method not only enables counting to be completed, but micro-facies descriptions to be undertaken at the same time (Brauer, 2004).

4.5.3. Estimating counting error and chronology validation

Much like the counting methods employed, there is no standard method for reporting errors associated with varve counts. Reviews by Lotter and Lemcke (1999), Lamoureux (2001) and Ojala et al. (2012) cover some of the methods that have been employed. Whatever the preferred method is, it requires multiple counts using a single core (e.g. Cockburn and Lamoureux, 2007), or multiple cores (e.g. Neugbauer et al., 2012) from the same site. If independent chronological proxies are available, these can be compared to the varve counts as an independent form of calibration (e.g. Brauer et al., 2000a; Stanton et al., 2010).

While some studies provide only qualitative estimates of counting error (Huttunen, 1980; Leonard, 1997), the majority provide quantitative estimates of uncertainties. Quantitative methods include presenting the error by displaying counting deviations in terms of ±number of varves by counting segment (Brauer et al., 1999a; Mangili et al., 2005) or percentage deviations (Ojala and Saarnisto, 1999). This data can be presented in terms of count differences over these specified depth intervals (e.g. Brauer et al., 1999a), or over a specified time interval, e.g. 100 years (Palmer et al. 2010) or 200 years (Fig. 4.7) (Ojala and Tiljander, 2003). The counting errors associated with each counting segment can also be presented as cumulative error with varve age (e.g. Sprowl, 1993; Ojala and Saarnisto, 1999), or as a percentage error for the sequence (e.g. Brauer et al., 1999a). The advantage of splitting cores into these smaller counting intervals is that it highlights sections of the core that may contain greater chronological uncertainties (Lamoureux, 2001).

One of the biggest challenges with varve chronologies, even if compiled using multiple cores from the same site, is the possibility that Type C errors (varves missed in all cores studied) could still affect the sequence (Lamoureux, 2001). One way to address this, if possible, is to validate the chronology with independent dating techniques. Stanton et al. (2010) used Lead (Pb) dating to anchor the varve chronology from Kälksjön, Sweden, and palaeomagnetic secular variations (PSV). As a result of the Pb dating, 250 years were added to the very top of the sequence (thought to be a hiatus due to human activity and indistinct varves) and PSV results lead to the removal of 230 years from the early Holocene (multiple sub-laminations interpreted as varves) (Stanton et

al., 2010). Radiocarbon calibration has also been used at Holzmaar, for example (Hajdas et al., 1995). Disagreement between the two chronologies resulted from low sedimentation rates and indistinctive lamination structures, with 878 years added to the varve chronology (Hajdas et al., 1995). Furthermore, Brauer et al. (2000a) validated the varve chronology from Meerfelder Maar with radiocarbon dating, which indicated a possible loss of 240 varves due to a micro-disturbance and low varve quality, while Brauer et al. (1999b) correlated the varve chronology with the Greenland ice core by using the Laacher See Tephra, demonstrating good agreement between the two chronologies. It should be noted, however, that the methods and records used for calibration also have errors associated with them. A more relevant point for this study though is that the sequence at Marks Tey is at or beyond the limits of most dating techniques. Furthermore, age uncertainties associated with techniques that do extend to this time period (ca 410,000 years BP), preclude validation of the record with independent techniques.

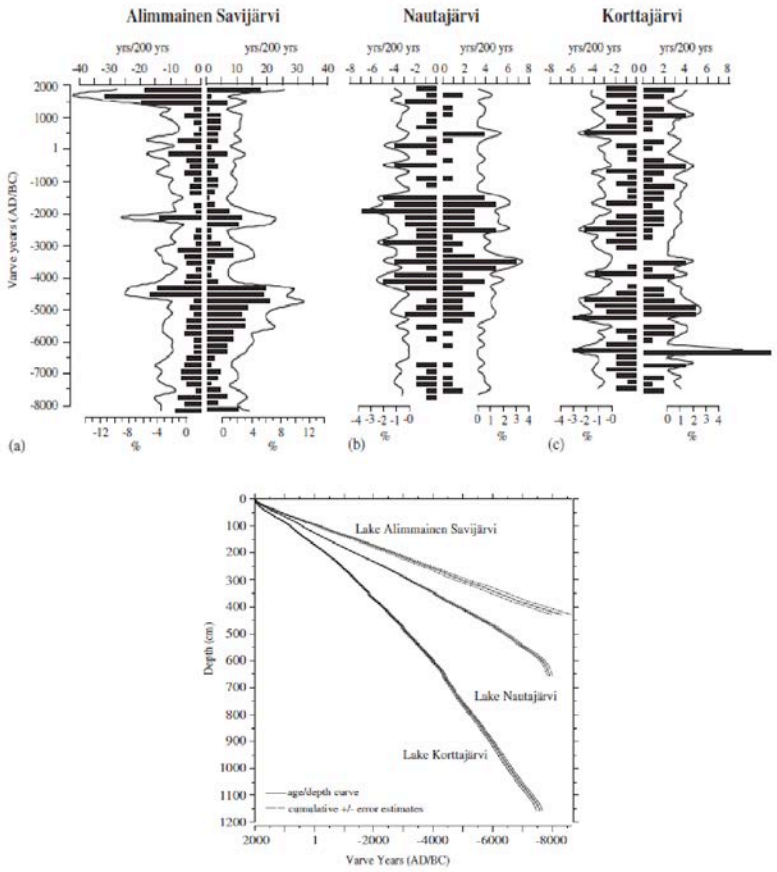

Figure 4.7. *Examples of how error estimates from multiple varve counts can be presented, from three Finnish lakes. Error estimates are presented as possible extra or missing varves per 200 years (percentage deviations are also shown by the lines) (top). This data can also be presented as an age/depth function (bottom). From Ojala and Tiljander, 2003.*

4.6. The application of varved sediments to the study of abrupt events

Once a varve chronology has been constructed, it can be used to investigate a number of different questions, as highlighted in the introduction. Varved lacustrine sediment records have proved particularly useful when investigating the structure, duration and proxy response to abrupt climatic events, such as the 8.2 ka event, abrupt events in previous interglacial periods, as well as the last-glacial-interglacial transition (LGIT).

4.6.1. The 8.2 ka event

Due to the potential precision attainable from varve chronologies, they provide the ideal tool to reconstruct abrupt climatic events (i.e. the 8.2 ka event). Varves should, where possible, be combined with other techniques to demonstrate their reliability as a chronological tool. A good example of such an approach is the studies of the 8.2 ka event in Holzmaar, Germany (Prasad et al., 2006, 2009). Based on micro-facies analysis alone, Prasad et al. (2006) suggested that the sedimentological response to the 8.2 ka event; cooler summers (cessation of calcite formation) and drier winters (reduced in-washing of clay) occurred simultaneously.

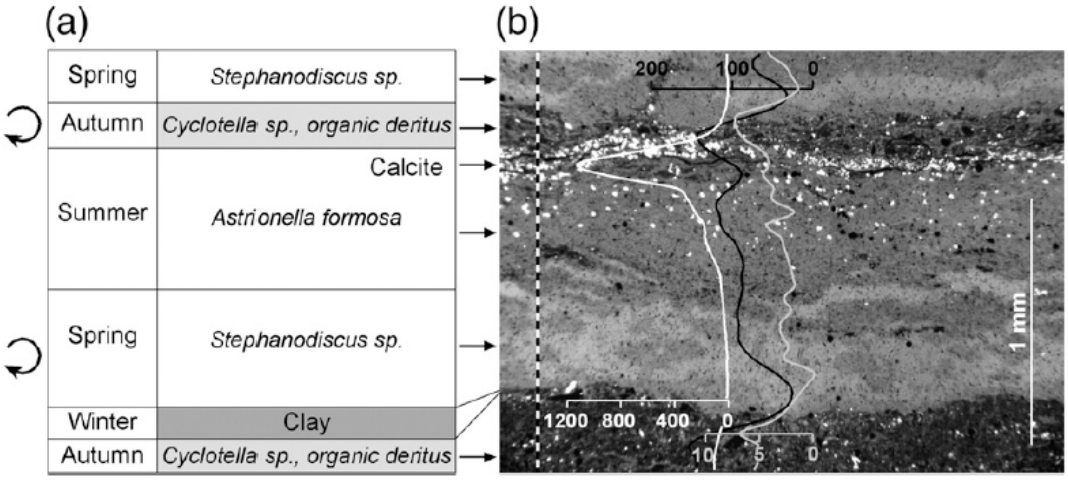

Figure 4.8. *a) Schematic showing the composition of seasonal laminations in the Holzmaar sequence. (b) Thin section photograph showing the sediments that correspond to the descriptions in (a), with µ-XRF data superimposed ontop (Ca: white, Si: black, Al: grey). From Prasad et al., 2009.*

By combining µ-XRF with the microfacies analysis, however, Prasad et al. (2009) were able to interpret previously unidentified clastic fragments in some of the late summer/early autumn layers as calcite crystals (Fig. 4.8). These new results indicated that summer cooling (and by extension, the onset of response to the 8.2 ka event)

began ca. 28 years before the onset of drier winters (Prasad et al., 2009). These studies therefore provide an example of how useful μ-XRF data can be when combined with micro-facies analysis (Brauer et al., 2009).

4.6.2. The Last Glacial to Interglacial Transition

Due to the amount of work undertaken, as well as the range of proxies used, the Maar lakes located in the Eifel region of Germany provide excellent examples of how varved sediment sequences can be used to document the impact of climate change on the terrestrial and aquatic environment during the Last Glacial to Interglacial Transition (LGIT). For this review, studies at Meerfelder Maar (MFM) (e.g. Brauer et al., 1999a; Brauer et al., 2008a; Rach et al., 2014) are chosen. Based on micro-facies analysis of the varved sequence at MFM, Brauer et al. (1999b) report distinctive changes in the seasonal structure of varves (Fig. 4.9a), supported by a number of other proxies (Fig. 4.9b), from the late Allerød interstadial through to the early Holocene (Preboreal), which can be summarised as follows:

1. **Late Allerød**: This time period is characterised by thin, organic varves with summer layers composed of organic matter, chrysophyte cysts and occasional planktonic diatoms, while winter layers are composed of authigenic minerals (siderite and vivianite) (Fig. 4.9a);
2. **Early Younger Dryas**: is characterised by a marked increase in varve thickness (Fig. 4.9a), driven by stronger diatom blooms (biogenic opal in Fig. 4.9b) and an increase in allocthonous material and epiphytic diatoms (Sediment accumulation rate (SAR) and Total Organic Carbon (TOC) in Fig. 4.9b), indicative of eutrophication during climatic cooling in response to increased erosion of the catchment/littoral zone, supplying nutrients to the lake. Lake catchment instability is inferred from increasing Non-Arboreal Pollen (NAP) values at this time, while the gradual decreasing trend in varve thickness is attributed to reducing nutrient supply due to a reduction in the availability of erodible soil (Fig. 4.9b);
3. **Late Younger Dryas**: The depositional system changed with thinner varves being deposited (Fig. 4.9a) and a significant reduction in the diatom component and increase in clastic material (Fig. 4.9b). This shift in varve type to clastic/organic varves, is thought to have possibly been the result of the Meerbach stream starting

to drain into the lake, as well as a higher potential for erosion due to increased precipitation;

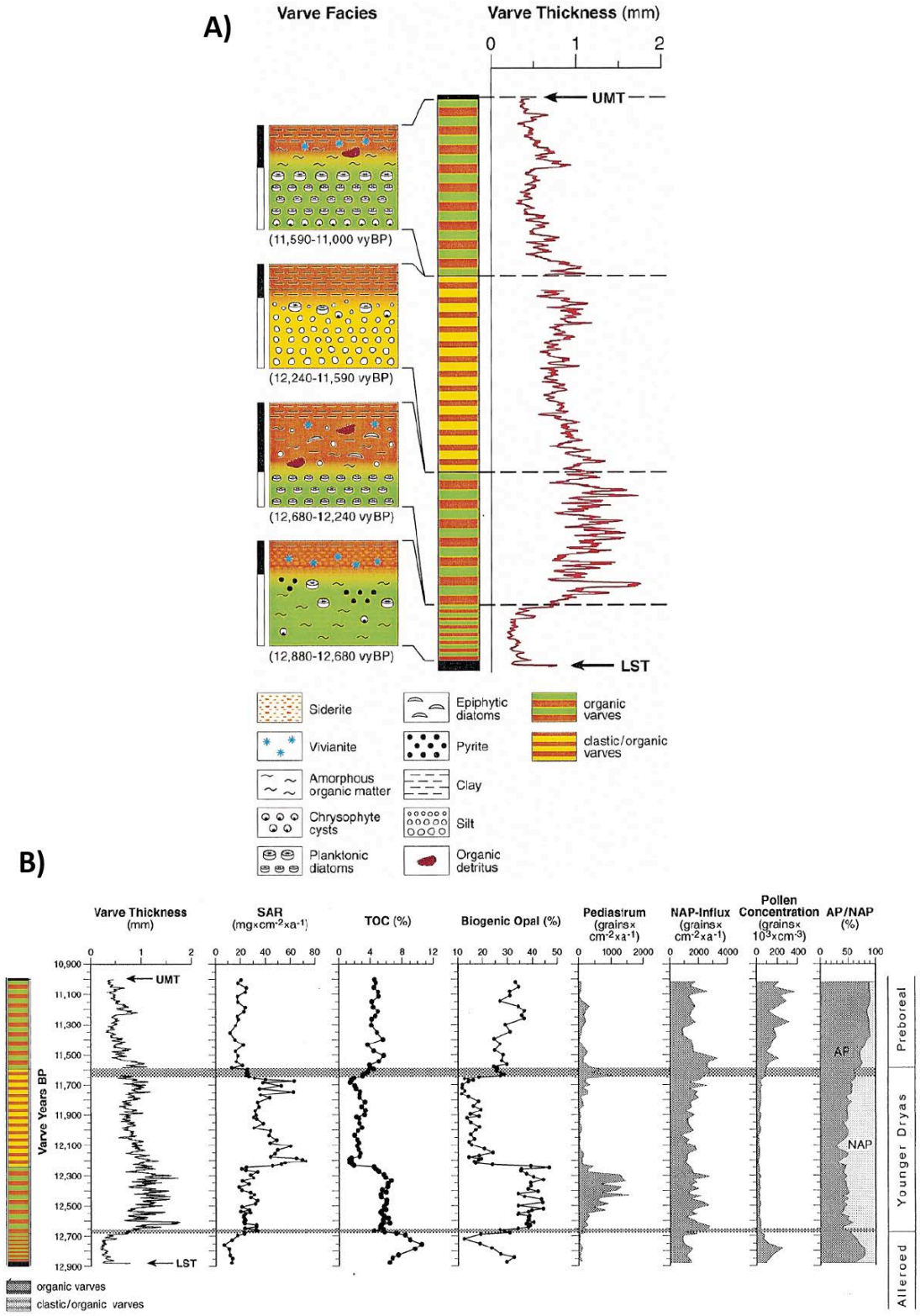

Figure 4.9. *A) Varve micro-facies variations in the Meerfelder Maar sequence from the Late Allerød through to the Preboreal, alongside varve the varve thickness record, and B) Sedimentological and palynological data for the same section. From Brauer et al., (1999b).*

4. **Preboreal**: The depositional system reverts back organic varves with spring/summer layers composed of planktonic diatoms and chrysophyte cysts, autumn layers composed amorphous organic matter (also siderite and vivianite), and winter clay layers (Fig. 4.9a and b). This shift in varve type is explained by eutrophication caused by climatic amelioration.

By combining the micro-facies descriptions with µ-XRF data, Brauer et al. (2008a) suggest the micro-facies shift that occurs at the onset of the Younger Dryas is caused by increased wind shear disrupting water column stability, preventing the formation of siderite (indicative of anoxic bottom water) and also re-suspending nutrients causing the large diatom blooms (Fig. 49a). This increased storminess is linked to a shift in westerly winds in the North Atlantic to a stronger, zonal jet during the Younger Dryas (Brauer et al., 2008a). Furthermore, the varve chronology at MFM has enabled lags in proxy response to the climatic cooling in Greenland to be quantified (Rach et al., 2014). Such changes occur on time scales within the error limits of many dating techniques; therefore highlighting how important varve chronologies can be in environmental reconstruction. What the studies at MFM demonstrate is how sensitive some varved records are to climatic events and how, by combining varve micro-facies descriptions with other proxies, very detailed records of terrestrial response to abrupt climatic events can be reconstructed.

4.7. Summary

An extensive literature exists on varve formation and analysis. This review has focussed on biochemical varves as these are the most relevant to Marks Tey. The following points are highlighted:

- Varved sediment sequences form in a variety of depositional and geographical settings and have the potential to provide exceptionally detailed records of environmental change at a variety of scales.
- They are particularly suited to the investigation of abrupt events in previous interglacials, where the temporal resolution of long climate records from ice and ocean cores is reduced.

- Varved records offer the potential to reconstruct terrestrial response to abrupt events in great detail, due to the range of climatic/environmental proxies they can contain.
- Before varve chronologies can be constructed, however, the first step is to produce a robust depositional model for varve formation.

Chapter 5. Methodology

5.1. Introduction

This chapter will outline the methods used to obtain the results presented in this thesis. There are five main objectives to this research project at Marks Tey:

1) To retrieve a core and characterise the macro-sedimentology and bulk sedimentology of the lacustrine sequence at Marks Tey.
2) To determine whether the sequence contains varved sediments by testing the model for seasonal sedimentation suggested by Turner (1970).
3) Characterisation of the micro-scale sedimentology and the production of a varve chronology.
4) Stable oxygen and carbon isotope analysis of the carbonate laminations of the *in situ* early/mid Hoxnian sediments.
5) Combining the varve chronology and stable isotope results with proxy evidence produced by other contributors to investigate the timing and forcing mechanism for, as well as the rates of proxy response during the NAP Phase as defined by Turner (1970).

This chapter will therefore be split into four sections, covering the techniques used to meet the first four objectives. The fifth objective requires data generated by other researchers (pollen, diatoms and charcoal). The palynological work was carried out by Professor Pete Coxon (University College Dublin), with the aim of investigating landscape evolution during the early part of the Hoxnian. This also served the purpose of correlating the new sequence with the original palynological investigation of Turner (1970). Samples for charcoal and diatom analyses were then taken from the section of the core where the NAP Phase was located. Charcoal samples were taken to investigate possible forcing mechanisms of the NAP Phase. These samples were processed and analysed by Dr Mark Hardiman (RHUL, Portsmouth University). To assess the limnological response of the lake to this event, Dr Dave Ryves and Katie Loakes (Loughborough University) sampled the core for diatom analysis.

5.2. Coring, correlation and macro-sedimentology

5.2.1. Coring

The aim of the fieldwork at Marks Tey was to retrieve a sediment sequence comparable to that recovered in borehole GG of Turner (1970). This is the deepest known part of the basin and the only location within the brick pit where sediments older than pollen zone Ho III are currently known to exist. Coring from the deepest part of the basin is also considered advantageous for varve chronological work, as this position will naturally be located below the thermocline (or chemocline), where sediment disturbance is minimal and there is the greatest potential for varve preservation (O'Sullivan, 1983; Saarnisto, 1986; Petterson et al., 1993; Lamoureux and Bradley, 1996; Ojala et al., 2000; Tian et al., 2005).

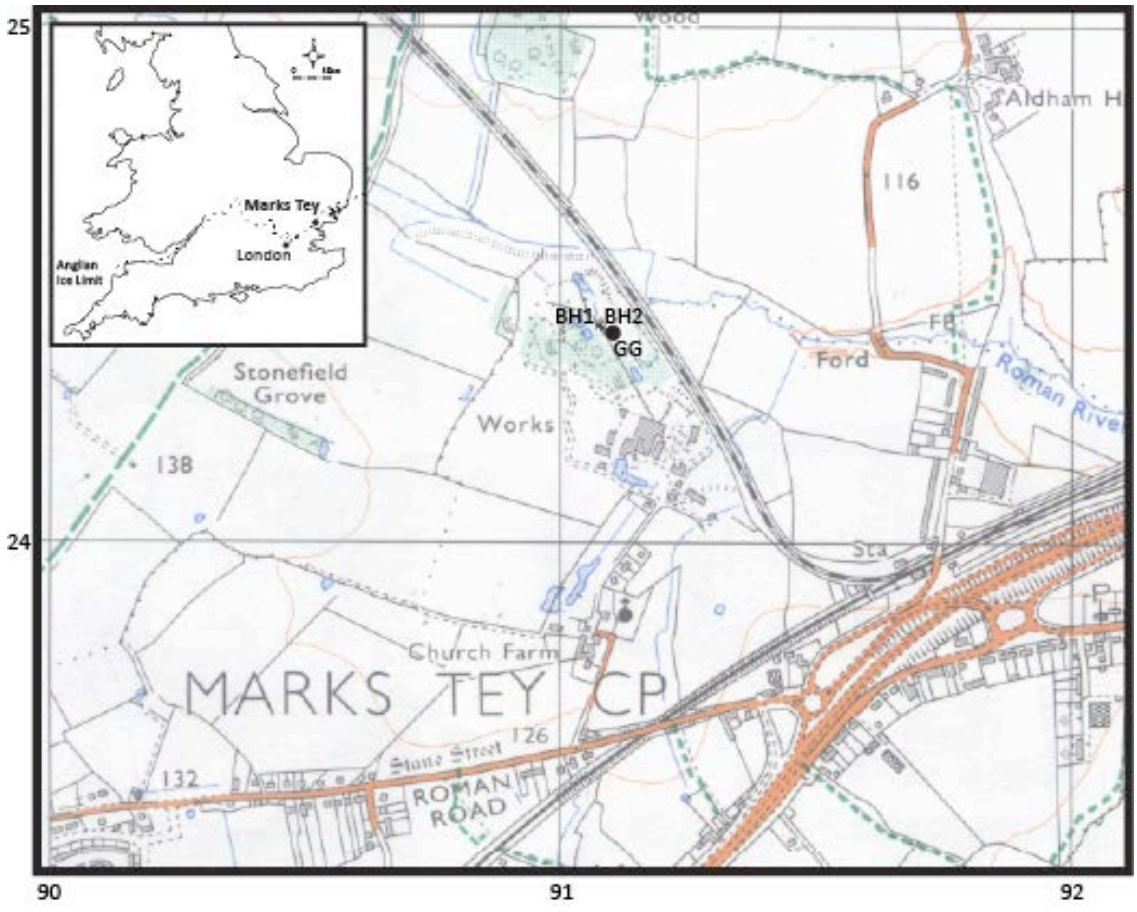

Figure 5.1. *Map showing the location of the coring sites for BH1 and BH2 (core MT-2010). The location of borehole GG (Turner, 1970) is also shown. BH1 (TL 91081, 24431) and BH2 (TL91082, 24432).*

A sediment sequence composed of two overlapping boreholes drilled 5m apart was obtained in 2010, approximately 15m from the location of borehole GG of Turner (1970) (Fig. 5.1). The cores were drilled by Ecologia Environmental Solutions Ltd. using a wet rotary drilling rig (Fig. 5.2), recovering sections in three-meter lengths, which

were then sawn in half for transport. The boreholes were levelled to determine the altitudinal range of the sequence in relation to an Ordnance datum using a Topcon total station.

Figure 5.2. *Photograph of the drilling rig used to recover the sediment sequence at Marks Tey.*

A hand auguring survey was also carried out using a spiral auger in the immediate lake catchment to collect samples of Anglian Till, from which chalk intra-clasts and chalk-rich matrix were sampled. This work was carried out to determine the stable isotopic composition of clastic carbonate from the lake catchment. If material from these sources enters the lake in clastic form, it retains the stable isotopic signature of the

parent material, and may contaminate the authigenic signal. This can have a significant effect on the ability to use stable isotope data from lacustrine sequences as a proxy for environmental/climatic changes (e.g. Candy, 2009; Mangili et al., 2010a).

5.2.2. Correlation and macro-sedimentology

The sediment cores from the two overlapping boreholes were correlated by the identification of key marker beds present in both sequences, which when combined produced a profile 18.5m in length. The sequence was then logged and described to determine the visible lithofacies architecture by describing the structural (e.g. bedding, unit contacts) and textural (e.g. colour, sorting, grain size) properties using standard methods (Jones et al., 1999; Evans and Benn, 2004).

5.2.3. Calcium carbonate and organic carbon

1cm^3 samples for calcium carbonate and organic carbon content were taken to characterise the bulk sedimentology of the sequence. Calcium carbonate content measurements were measured using a Bascomb Calcimiter (Gale and Hoare, 1991) and the total organic carbon content was determined by titration (Walkley and Black, 1934).

5.2.4. µ-XRF core scanning

While the whole sequence was characterised in terms of macro-scale sedimentological variations, only the lowest 6.5m will be investigated in detail as it is this section that contains *in situ* laminated sediments and the location of the OHO/NAP phase. As well as the other methods of core characterisation, micro X-ray fluorescence (µ-XRF) core scanning analysis was used on the lowest 6.5m of the core.

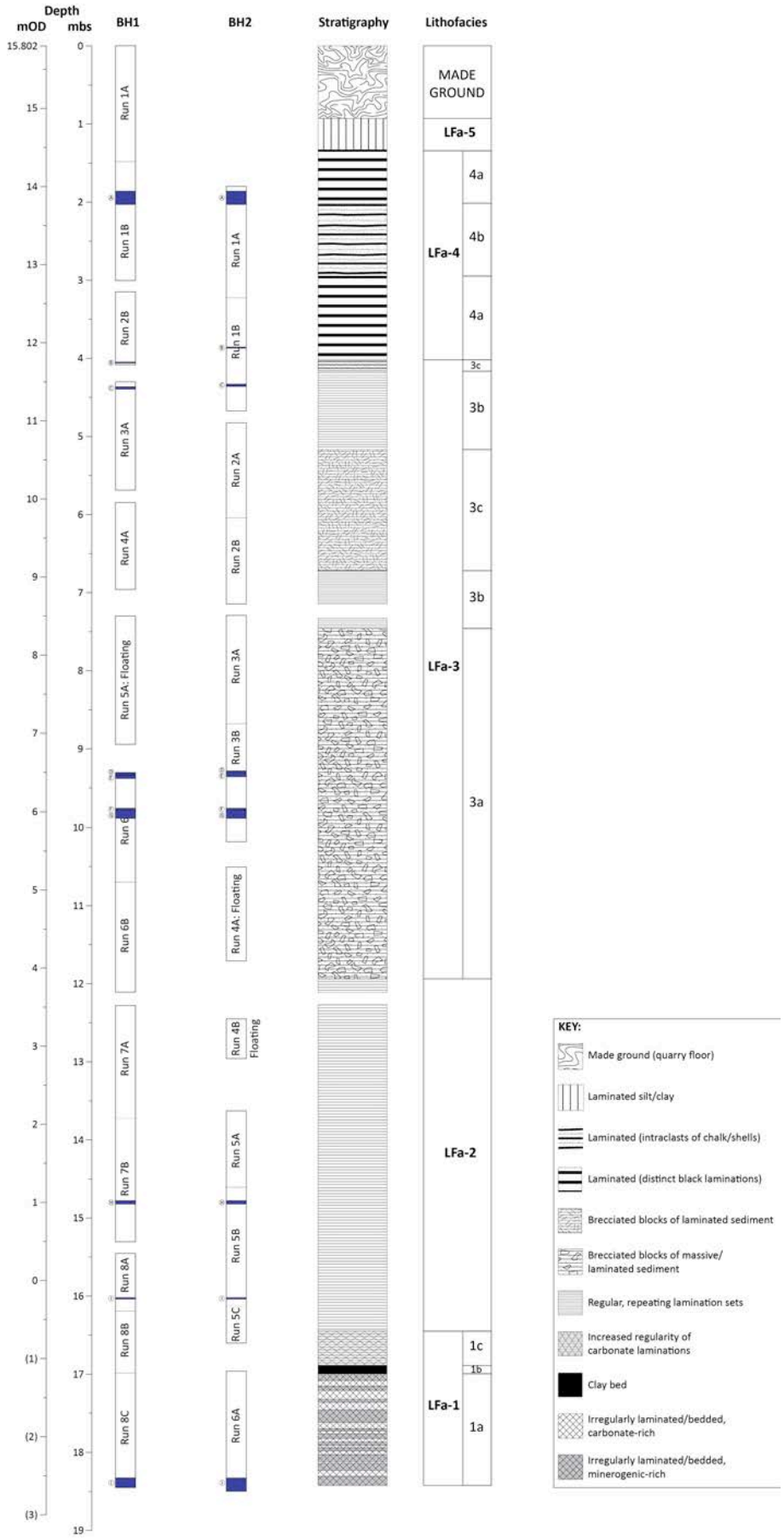

Figure 5.3. *Diagram showing the composite sediment stratigraphy (MT-2010) described from borehole (BH) 1 and 2. BH1 and BH2 were correlated using key marker horizons (blue shading).*

The technique works by irradiating the sediment with a focused X-ray beam; the resulting energy of the fluorescent radiation spectrum detected then provides a measure of the relative proportions of elements within the sample (Croudace et al., 2006; Rothwell et al., 2006). In this study, analysis was undertaken with a 3 kV molybdenum (Mo) target tube, 45 kV X-ray voltage and 30 mA X-ray current and 30-second count time using a flat X-ray beam focused to a 20 x 0.2mm rectangle. The combination of a Mo-tube and 30-second count time provides suitable conditions to detect both light and heavy elements from Aluminium (Al) through to Lead (Pb) (Rothwell et al., 2006). Incremental step-size of the X-ray beam varied from 1mm for the lowest 1.5m of the sequence, with the remaining 5m scanned at 200µm resolution. The larger step-size was chosen for the lowest 1.5m of the sequence because the micro-scale sedimentology of this section of the core indicated that varved sediments are not present (see chapter 5). The analysis was undertaken using the ITRAX™ Core Scanner at the British Ocean Sediment Core Research Facility, National Oceanography Centre, under the supervision of Dr Suzanne MacLachlan and Dr Guy Rothwell. Post-scanning filtering and reduction of data were carried out using ItraX-PLOT data visualisation software, to remove data from gaps and cracks in the samples, as well as data for elements with count rates below 200 kcps and/or a validity value of 0 (S. MacLachlan, pers. comm.).

Although the technique has the ability to generate high-resolution records of element variations within a sedimentary sequence, there are some important steps to take when processing the raw data output, as well as considerations to bear in mind when assessing what the signal generated actually represents. Changes in core surface topography, surface sediment mineral heterogeneity, grain-size changes and variations in water content can all influence the resulting signal (Croudace et al., 2006; Weltje and Tjallingii, 2008; Hennekam and Lange, 2012). Furthermore, ageing of the X-ray tube also influences the counts measured, which can make comparisons between sections of the same core difficult unless processed at similar times (Lowemark et al., 2010). These issues, combined with the fact that elemental variations are measured as elemental intensity (counts per second), not concentrations, means that µ-XRF provides only semi-quantitative data (Croudace et al., 2006; Lowemark et al., 2010).

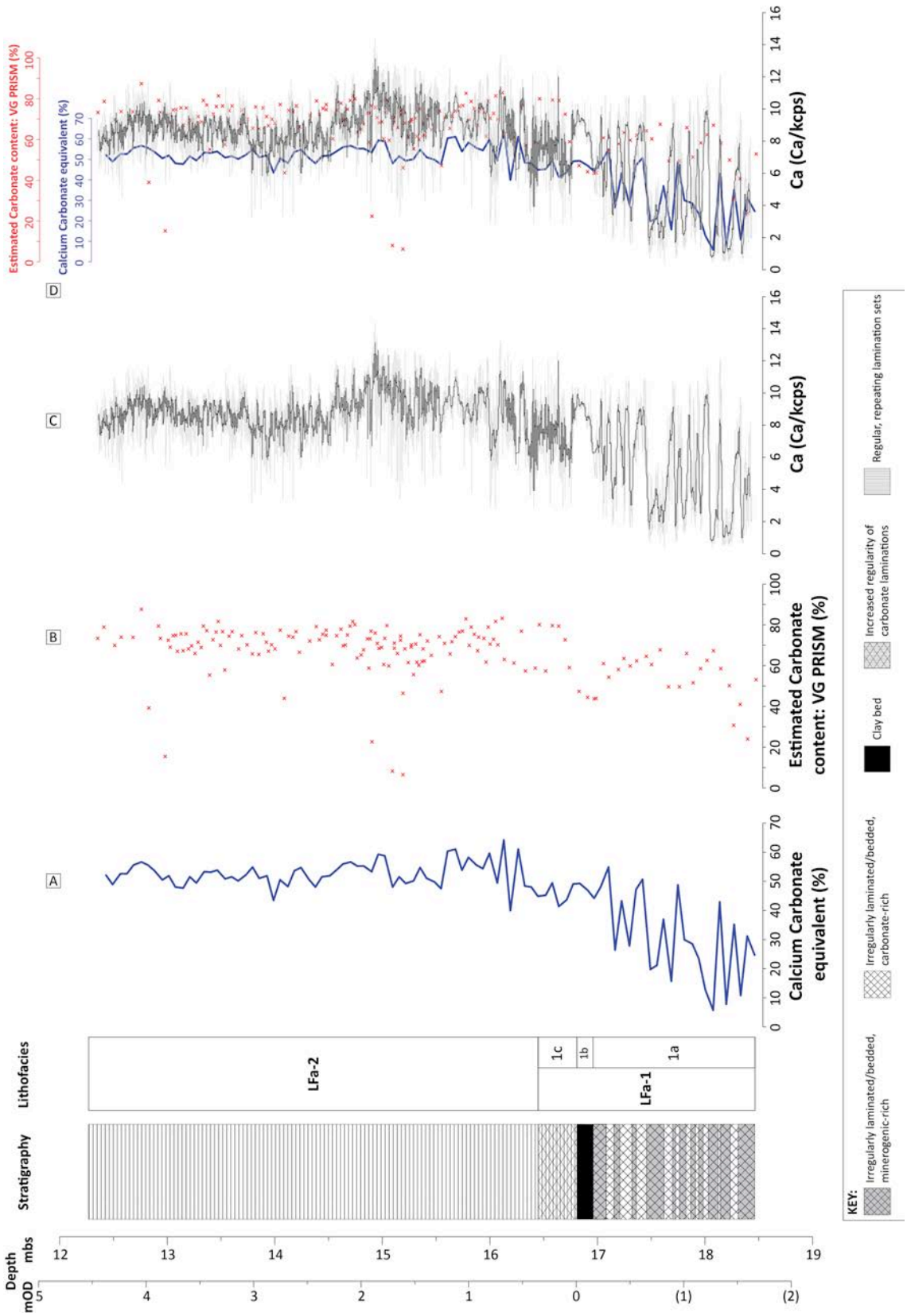

Figure 5.4. *Comparison of A) calcium carbonate equivalent data (Bascomb Calcimiter), B) estimated carbonate content during isotopic measurements (VG PRISM), C) Ca element intensity (μ-XRF core scanning), and D) All three datasets overlaid.*

Some of these factors, however, are not considered to be an issue. Firstly, grain-size variations are unlikely to effect the results, because 1) the consistently silty/clayey nature of the sediments at Marks Tey make them suitable for such analysis, and 2) the spot size of the incident X-ray beam is far greater that the largest grains within the sequence (Weltje and Tjallingii, 2008). Heterogeneity in lateral sediment composition is also not an issue as the majority of sediment is finely and horizontally laminated (although see below for vertical inhomogeneity) (Haug et al., 2001; 2003). Issues that arise from variable core surface roughness and water content are circumvented in this instance by using polished resin-impregnated blocks from the production of thin sections (Brauer et al., 2009). Not only does this enable direct comparisons to be made between the µ-XRF data and micro-facies descriptions, the resin-impregnation of the sediment prevents geochemical alteration that can occur during sediment storage (Brauer et al., 2009).

5.2.4.1. Calibration of µ-XRF data

To adjust for the sedimentological characteristics and methodological limitations, the raw data sets can be compared to element concentration data generated from the core (e.g. ICP-MS measurements; Weltje and Tjallingii, 2008), or standardised to another element or parameter. This is particularly relevant where significant changes in the content of organic material occur (Lowemark et al., 2011). As discussed by Lowemark et al. (2011), carbon is beyond the detection limit of the technique, so can dilute the signal from other elements. Lowemark et al. (2011) therefore suggest normalising counts to a stable element, such as aluminium (Al). If Al is not present in sufficient quantities, other studies have used rubidium (Rb) (Rothwell et al., 2006; Guyard et al., 2007), while parameters including the measures of incoherent and coherent scattering (inc/coh) (Melles et al., 2012), as well as thousands of counts per second (kcps) (Bouchard et al., 2011), which gives a single unit to which all the elements are compared. In this study, organic material only makes up a minor sedimentary component, so kcps is used as the normalising parameter. It was not possible to determine element concentrations by Inductively Coupled Plasma Mass Spectrometry (ICP-MS) in this study, but the calcium carbonate content measured from bulk samples, as well as carbonate content estimates generated from carbonate samples taken for isotopic analysis, provide a means of comparison for the µ-XRF Ca

counts (Fig. 5.4). Although some variability is evident due to the different methods used, all three datasets follow the same general trends (Fig. 5.4).

5.3. Investigating the annual nature of the laminated sediments in the sequence

The laminated sediments in the sequence at Marks Tey are generally considered to be varves (Turner, 1970, 1975), however, no quantitative evidence has yet been published to demonstrate this. This work therefore forms an important part of this thesis, as a fundamental step in the process of constructing a varve chronology is the development of a depositional model demonstrating that the repetitive sequence of structures preserved in sediments are annual in nature (Lamoureux, 2001), and not a function of other processes that can produce laminations in sediments (Lambert and Hsu, 1979; Mulder and Alexander, 2001).

This process is complicated in fossil basins, where the varved nature cannot be confirmed by counting back to known annually controlled marker horizons (Erten et al., 1985; Lotter, 1997; Tylmann et al., 2013), or by lake monitoring studies (e.g. Stockheke et al., 2012). Both of these techniques are limited in their scope to extant lakes where varves are currently forming. In the case of varved records where such methods are not applicable, other methods have been employed to relate the structural components of laminated sediments to their seasonal characteristics in modern environments. These methods are covered in more detail in the literature review on annually laminated sediments in chapter 4.

SEM analysis of split sediment blocks covering multiple lamination sets (to produce a fresh surface) provided insufficient detail to characterise the structural components within the lamination types and identify microfossils (pollen and diatoms) to species level. Furthermore, the high calcite content of the sediment also obscured these microfossils in thin section. Thus, due to the nature of the sediments at Marks Tey, it was decided the best method to use would be to sample individual lamination types for stable isotope analysis, as well as the preparation of slides for diatom and pollen analysis.

5.3.1. Core sampling

A single block of sediment (50 x 30 x 20mm) spanning five lamination sets was removed from the core at 14.75 metres below surface (mbs). This section of the core was chosen for sampling due to the quality of lamination structure preserved and because this section of the core contained the thickest lamination sets. This made the identification of boundaries between lamination types easier and sub-sampling more straightforward (Fig. 5.5).

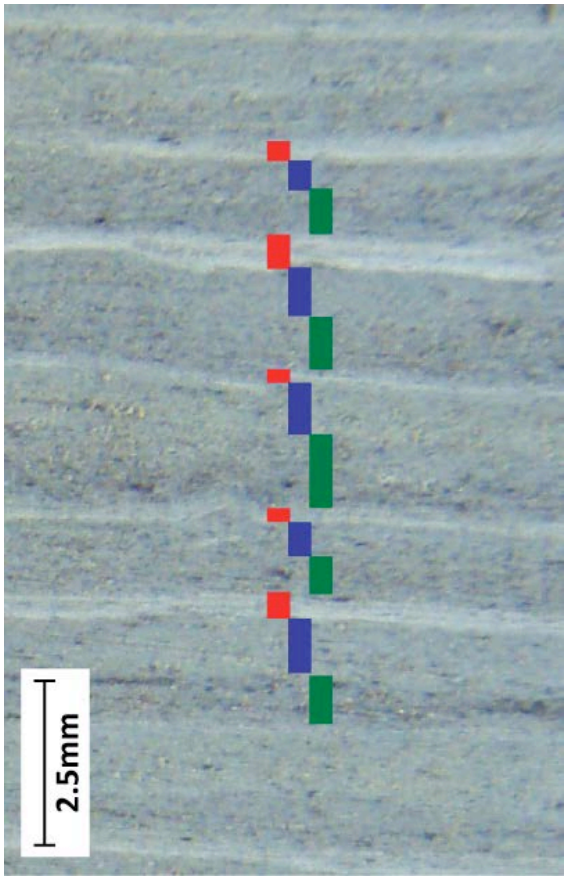

Figure 5.5. *Photograph of the sediment block containing the five lamination sets that were sampled. The green line represents the organic detrital lamination type, the blue line represents the diatom lamination type and the red line represents the calcite lamination type.*

The block was allowed to air dry and the lamination sets split into individual lamination types using a scalpel and dissection needle under a low magnification microscope (Tippett, 1964; Peglar et al., 1984; Lotter, 1989), and providing a total of 15 samples.

5.3.2. Diatom preparation

Diatom samples were prepared using the waterbath method (Renberg, 1990) and slides were mounted in Naphrax®. Determination of diatom concentration (valves/g)

was made possible by the addition of divinylbenzene microspheres (Battarbee and Kneen, 1982). Slides were analysed using oil-immersion, phase contrast optics at 1000x magnification at the Department of Geography, University College London. Diatoms were identified following the standard guidelines set out in Krammer and Lange-Bertalot (1988, 1991a,b, 1999).

5.3.3. Pollen preparation

Pollen samples were prepared following standard techniques, including sample weighing, treatment with sodium pyrophosphate ($Na_4P_2O_7$), hydrochloric acid (HCL, 10%), hydrofluoric acid (HF, 40%), heavy-liquid separation with sodium polytungstate ($Na_6[H_2W_{12}O_{40}]$, acetolysis ($C_2H_4O_2$), and slide preparation using glycerine jelly. The samples were spiked with *Lycopodium* spores to enable concentrations (grains/g) to be calculated. These slides were analysed by Professor Pete Coxon (TCD).

5.3.4. Stable isotope analysis

As well as producing a stable oxygen and carbon isotope stratigraphy for the lower 6.5m of the sequence (see section 5.5 for details on preparation and analysis procedures), samples were also taken from the lowest three lamination sets shown in figure 5.5 for stable oxygen and carbon isotope analysis. Three samples were taken from each lamination type, to access the reproducibility of the data. These samples were taken for two reasons: 1) to investigate whether any seasonal signal is preserved in the lamination types, and 2) whether detrital contamination may be an issue.

5.3.4. Statistical analysis

Statistical techniques were applied to investigate whether any relationships existed within the diatom and pollen data and the lamination sets they were sampled from. Species were removed if they made up less than 1% of sample counts, or were present on no more than one slide. Multivariate techniques were used as the diatom and pollen samples could be analysed without making any assumptions about relationships prior to analysis (Birks, 2003). This was achieved using ordination, which arranges sites/samples along axes on the basis of species or environmental composition data (Kent and Coker, 1994). As only species data was available, indirect ordination methods were used. Firstly, detrended correspondence analysis (DCA) (Hill and Gauch,

1980) was performed to establish the gradient length of the first axis (a measure of beta diversity/species turnover) (ter Braak and Smilauer, 2002). If the gradient length is greater than 2 standard deviation (SD) units, species are deemed to exhibit a non-linear response, and unimodal methods were used (e.g. Correspondence Analysis (CA), DCA) (Birks, 1998). If gradient lengths were less than 2 SD, species are deemed to exhibit a linear response, therefore Principle Component Analysis (PCA) was performed (Birks, 1998). Ordinations were performed using CANOCO 4.5 (ter Braak and Smilauer, 2002) on concentration data that had been square-root transformed. All ordinations were performed using concentration data, as percentage data co-varies (the constant sum problem) (e.g. Aitchison, 1986), while square-root transformation restricted the influence of species with large variances (Korhola et al., 2000).

5.4. Varve micro-facies analysis and chronology construction

Thin section micromorphology has increasingly become a standard technique in the study of varved sediments, because of the unparalleled levels of sedimentary detail it offers (e.g. Brauer et al., 2008a,b; Palmer et al., 2010, 2012; Martin-Puertas et al., 2012; Neugebauer et al., 2012). In some instances, due to varve thicknesses being too great for example, it is combined with other methods (e.g. MacLeod et al., 2010). The rationale for using the technique extensively in this thesis is because of the variability of sedimentology noted at the macro-scale, as well as the varves being too thin/indistinct to count by eye. The production of thin sections also allows accurate thickness measurements to be made.

5.4.1. Thin section micromorphology

The micromorphology of sediments in the sequence was determined by microscopic analysis of thin sections. 119 thin sections were prepared from fresh sediment blocks (100 x 30 x 20mm) cut out from the core using metal tins specifically made for this purpose. It was ensured that each sample had at least a 2cm overlap with the preceding one, in which distinctive marker laminations were visible for correlation purposes (Fig. 5.6c). Processing techniques involved air drying and acetone replacement where necessary, following standard methods developed in the Centre for Micromorphology at Royal Holloway, University of London (Palmer et al., 2008).

The compact nature and low water content of the sediments prevented core splitting, so a flat surface was made along the outside edge of the cores, from which the metal tins were carved into (Fig. 5.6a-d). These sediment characteristics ensured minimal shrinkage during processing, but did result in the incomplete impregnation of some samples, which were then subject to the surface impregnation method described by Carr and Lee (1998).

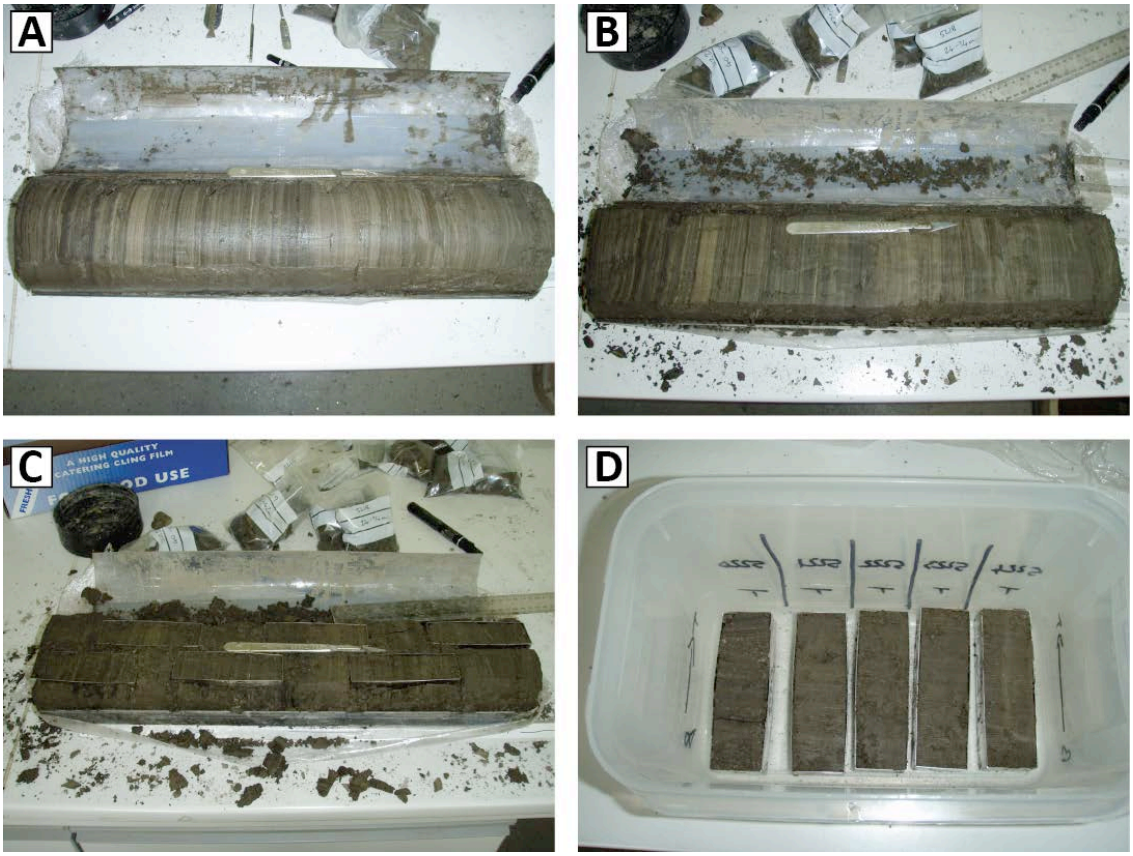

Figure 5.6. *Photograph showing the sampling method for thin sections: a) fresh core surface, b) flattened surface ready to carve blocks from, c) metal tins carved into the core (note 2cm overlaps), and d) fresh sediment blocks removed from the core and ready for thin section production.*

Thin sections were analysed using an Olympus BX-50 microscope with magnifications from 20x to 200x and described using the micro-facies approach (e.g. Brauer, 2004; Palmer et al., 2012). This approach adopts the same descriptive method to that detailed in section 5.2.2, but applies it at the micro-scale. Essentially each varve is made up of a number of different lamination types which when combined, produce a lamination set (Fig. 5.7) (Palmer et al., 2012). The aim of the micro-facies descriptions was to characterise the range of lamination types that exist in the sequence at Marks Tey.

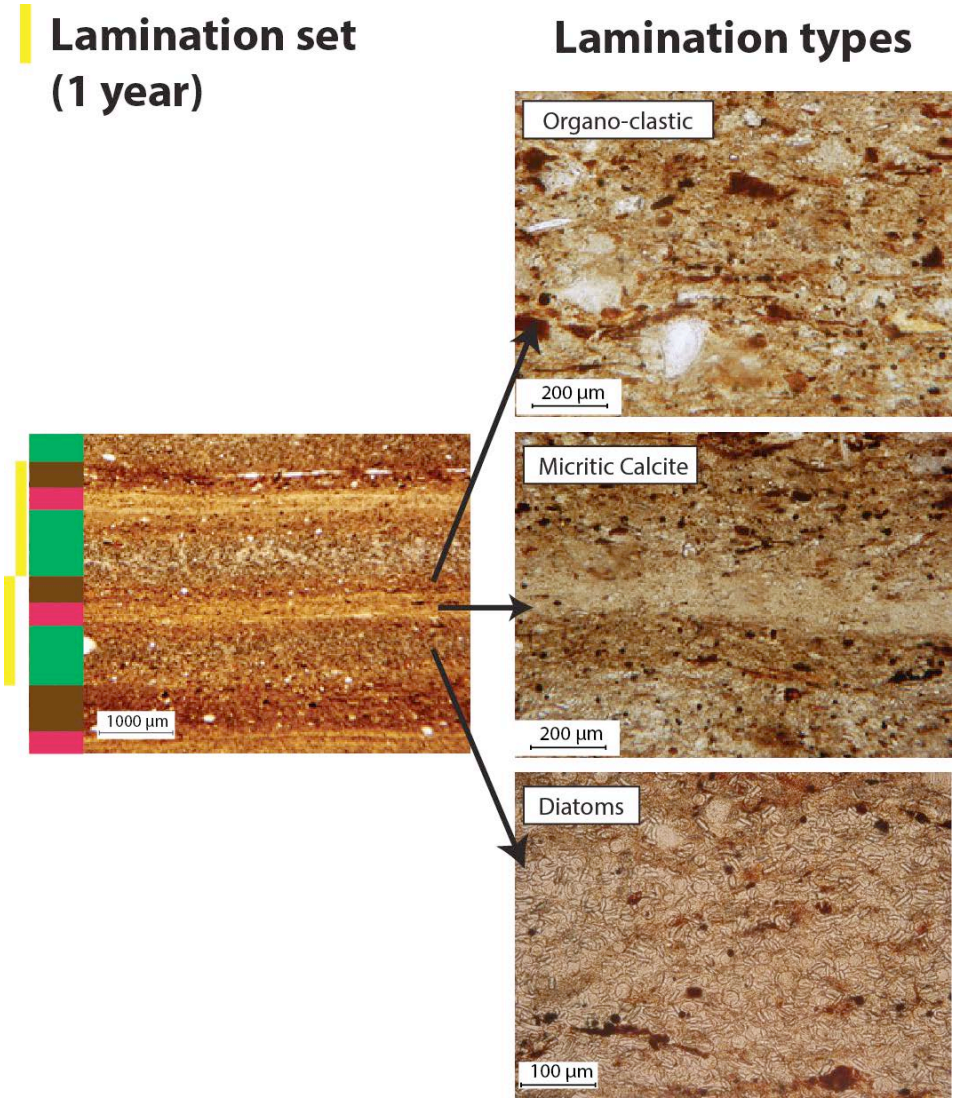

Figure 5.7. *Photomicrographs showing the descriptive terminology used for the micro-facies analysis in this thesis. A single varve year (lamination set) is composed of a number of sub-laminations representative of changes in seasonal sedimentation patterns (lamination types). This model is based on the descriptions of Turner (1970), who suggests that the primary structure of the varves at Marks Tey is composed of three lamination types; diatoms, micritic calcite and organic detritus.*

The possible combinations of these lamination types (to produce lamination sets) then produced specific varve groups (Palmer et al., 2012), which were plotted as a function of depth to investigate changes in micro-scale varve sedimentology through time.

5.4.2. Chronology construction

As detailed in chapter 4, there is no standard method for constructing a varve chronology, as it will depend on the techniques considered most appropriate to the individual sediment sequence (Lotter and Lemke, 1999; Lamoureux, 2001). The aim should be to construct a robust chronology by limiting potential errors during the

counting process (Lamoureux and Bradley, 1996; Lamoureux, 2001). The process of constructing the varve chronology at Marks Tey followed the procedure outlined below:

5.4.2.1. Core collection

Two overlapping boreholes were drilled in close proximity to each other to ensure a continuous sediment sequence was recovered (Merkt and Muller, 1999; Zolitschka, 2003). While some researchers advocate a multiple core approach to account for possible spatial variability in sedimentation patterns within a lacustrine system (Lamoureux and Bradley, 1996; Leonard, 1997; Lamoureux, 1999), it was only possible to recover one complete profile from the basin for this project. However, both boreholes were sampled for thin sections, to cover overlaps between drilling runs, as well as providing some replicated sections for varve counting, enabling partial fulfilment of the multi-core approach.

5.4.2.2. Pre-counting procedure

Thin sections were examined using a light box, where the overlaps (approximately 2 cm) between each sample were verified by marking prominent laminations visible on both slides (the carbonate lamination type was the most distinctive, so was routinely used). The correlated slides were traced onto to a roll of paper to replicate the borehole correlation. This enabled any changes in the correlation (due to faulting, slumping, or compression) to be easily determined. Once the correlation was complete, each thin section was split into a series of regularly spaced smaller, counting sections and numbered. These smaller sections enabled counts to be easily compared, and any counting errors easily identified and constrained (Lamoureux and Bradley, 1996; Brauer et al., 1999; Ojala and Saarnisto, 1999).

5.4.2.3. Counting procedure

As chapter 4 highlights, published methodologies for counting techniques vary, although the most common practice seems to be multiple counts along one or more slide transects by multiple workers (Lamoureux and Bradley, 1996, Zolitschka, 1996, Lamoureux and Cockburn, 2007). In this study, a total of four counts were made, using the following process:

1) Two counts were made of the whole sequence, one month apart (borehole 1 and overlaps from borehole 2), with the second count carried out along a transect parallel to the first.
2) The third count came exclusively from borehole 2, as an exercise to determine between core variability (although this borehole is not as extensive due to core recovery issues).
3) An independent count (in progress at submission date) was undertaken by Dr Adrian Palmer (RHUL) as a comparative count to the method outlined in bullet point 1.

While varve counting was being carried out, a note was made of varve quality and any unusual or vague structures (e.g. Lotter and Lamoureux, 1999). Photomicrographs were taken during counting with a Pixera Penguin 600es camera. Varve lamination type thickness measurements were made from these photos using Image-Pro® Express image analysis software.

5.4.2.4. Error estimation and varve interpolation

Because variable levels of varve quality and subjective interpretations complicate the process of varve counting, it can be difficult to quantify counting errors for a varved sediment record (Brauer et al., 1999a). The counting method used in this study, where the sequence is split up into smaller counting sections, enables the direct comparison of repeated counts over short intervals, therefore isolating sections of the core where counts vary most (Brauer et al., 1999a; Ojala and Tiljander, 2003; Palmer et al., 2010). The difference between the counts then gave a counting error as a percentage of the whole sequence.

For sections of the varved interval of the core where varve preservation was too poor to determine the seasonal structure, or where the sediments had been deformed during thin section processing or as an artefact of coring, interpolations were made. These interpolations were based on the average varve thickness of 10 varves above and below the disturbed section.

5.5. Production of a stable isotope stratigraphy for the sequence

The stable isotopic composition of lacustrine carbonates can provide important environmental information and, in some circumstances, can be used to infer qualitative temperature variations (chapter 3). The possibility of obtaining a palaeoclimate record for MIS 11 in Britain is very important because, not only would it represent the first terrestrial record of high-resolution climatic variability of MIS 11 in the British Isles, it would also offer the opportunity to investigate the forcing mechanism behind the period of landscape instability expressed in Hoxnian (and other) pollen records known as the NAP Phase (see chapter 2).

5.5.1. Core sampling

When taking bulk samples for stable isotope analysis, samples are routinely sieved to remove coarser fractions from detrital sources (e.g. detrital carbonate, shells, chara) (e.g. Leng et al., 2011). Sieving is not considered suitable for the sediments at Marks Tey for the following reasons; 1) the consistently fine particle size of all sediments within the carbonate laminations precludes sieving, as any detrital carbonate present would be of the same particle size as the authigenic fraction; 2) thin-section analysis was undertaken to avoid sampling any carbonate laminations that contained obvious evidence for in-washed layers or shell fragments; and 3) sampling was restricted to the carbonate lamination, thus avoiding any detrital material that occurred in the other lamination types.

Samples for stable isotope analysis in this project were therefore taken from individual carbonate laminations using a magnifier stand, fine-bladed scalpel and needle. Furthermore, to test for contamination from fine detrital carbonate, the stable isotopic composition of carbonate from the catchment was characterised by sampling chalk intra-clasts and till matrix from the Anglian Till that underlies the immediate catchment (Fig. 5.8).

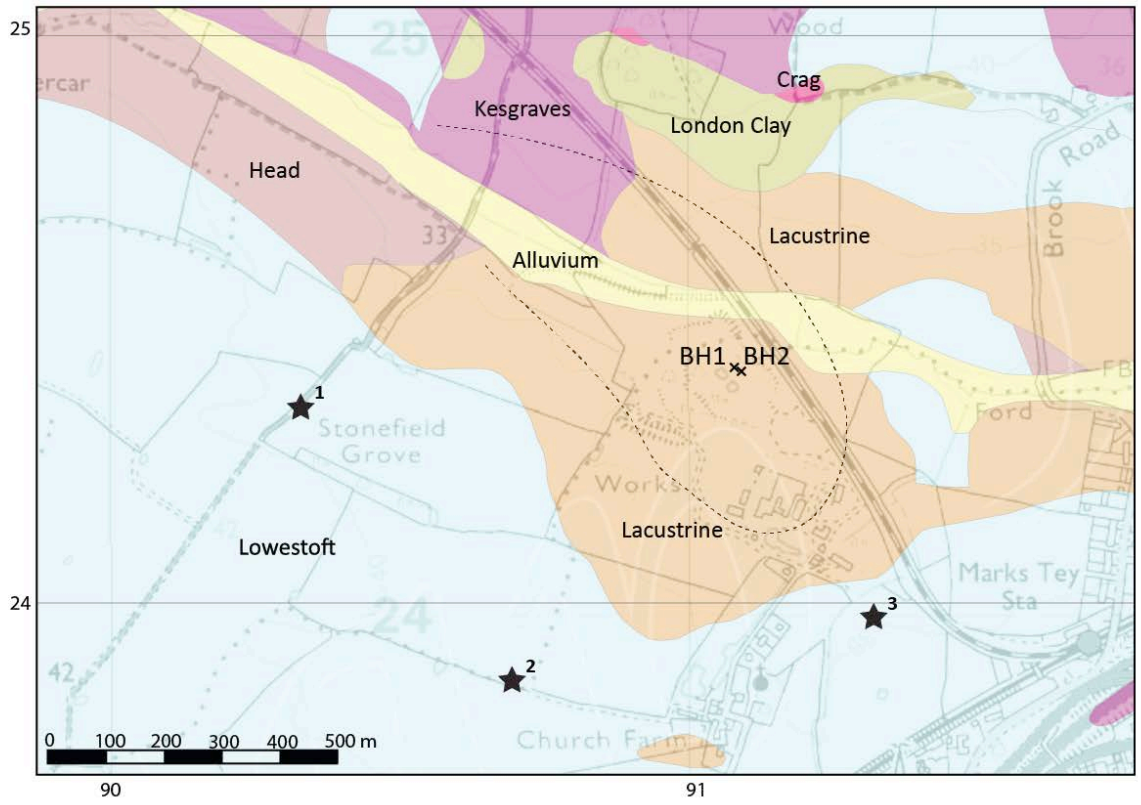

Figure 5.8. *Location of isotope samples taken of detrital carbonates from Lowestoft Till matrix and chalk intra-clasts within the till (shown by numbered stars). The surficial sedimentary deposits are overlaid on top of the map. The location of BH1 and BH2 are also shown, along with the suggested basin limit (Ellison and Lake, 1986).*

5.5.2. Sample preparation and analysis

Samples were left to dry, powdered, and then weighed using a Mettler Toledo XP6 microbalance. The $\delta^{18}O$ and $\delta^{13}C$ composition was determined by analysing CO_2 generated from the reaction of the sample with phosphoric acid at 90°C using a VG PRISM series 2 mass spectrometer in the Earth Sciences Department at Royal Holloway. Internal (RHBNC) and external (NBS-19, LSVEC) standards were analysed every 18 samples, and the isotope data presented in this study are quoted against VPDB (Vienna PDB). The instrumental error associated with this analysis is ±0.07‰ for $\delta^{18}O$ and ±0.04‰ for $\delta^{13}C$.

5.6. Calibrating other proxies using the varve chronology

As well as providing an indication of how many varves are preserved in the sequence at Marks Tey, the value of a varved record is that it can provide a chronology for other proxy data generated from the sequence; therefore enabling the development of the first annually-resolved environmental record of the early part of MIS 11 in the British

Isles. The varve chronology developed for Marks Tey will be utilised in the following ways for this thesis:

1) When combined with the pollen record, it will enable the quantification of the duration of the NAP Phase, which has been estimated to last for approximately 350 years (Turner, 1970).
2) As the isotope samples in the varved section of the core are taken from individual carbonate laminations, an annually-resolved environmental record can also be constructed. The timing and duration of climatic events can therefore be constrained.
3) When the datasets are combined, it will be possible to develop a model of the timing, duration and leads and lags in proxy response to abrupt events in MIS 11 in the British Isles.

Chapter 6. Stratigraphy, bulk sedimentology and pollen results

Chapter overview

This chapter will present the lithostratigraphy and biostratigraphy of the MT-2010 sequence. The correlation of the two overlapping boreholes is proposed and a macro-scale description (supported by % $CaCO_3$ and TOC content) of the whole sequence is presented. The main focus of this study is the section of the Marks Tey sequence that are: 1) *In situ* and undisturbed; and 2) purported to be varved (Turner, 1970). Consequently, more detailed analysis is restricted to the lowermost 6.25m of the MT-2010 sequence, where intact and finely laminated sediments occur. The micro-scale sedimentology, i.e. the thin section analysis, of these sediments is presented along with µ-XRF core scanning data of elemental composition. A pollen diagram of the lowermost 6.25m (produced by Prof. P. Coxon, TCD) is also presented. This diagram is used to: 1) provide a palaeoenvironmental context to the MT-2010 sequence, and 2) allow correlations to be made with the GG borehole of Turner (1970).

This chapter is, therefore, divided into the following sections. Firstly, the location of the two overlapping boreholes is presented within the context of the palaeo-lake basin and the rationale for borehole correlation is discussed. Secondly, the lithostratigraphy/macro-scale sedimentology of the MT-2010 record is presented. Thirdly, the micro-scale sediment descriptions and µ-XRF elemental variations of the lowermost 6.25m of MT-2010 are compared to the biostratigraphy of the sequence as derived from the new pollen diagram. The chapter then discusses the data presented in terms of variations in depositional process and lake development during the early part of MIS 11.

6.1. Introduction

Marks Tey is located in eastern England, approximately 60 miles (96.5km) to the northeast of London and 6 miles (9.6km) east of Colchester (Fig. 6.1). The coring site is located in a palaeo-lake basin that is actively quarried for brickmaking by W.H. Collier Ltd.

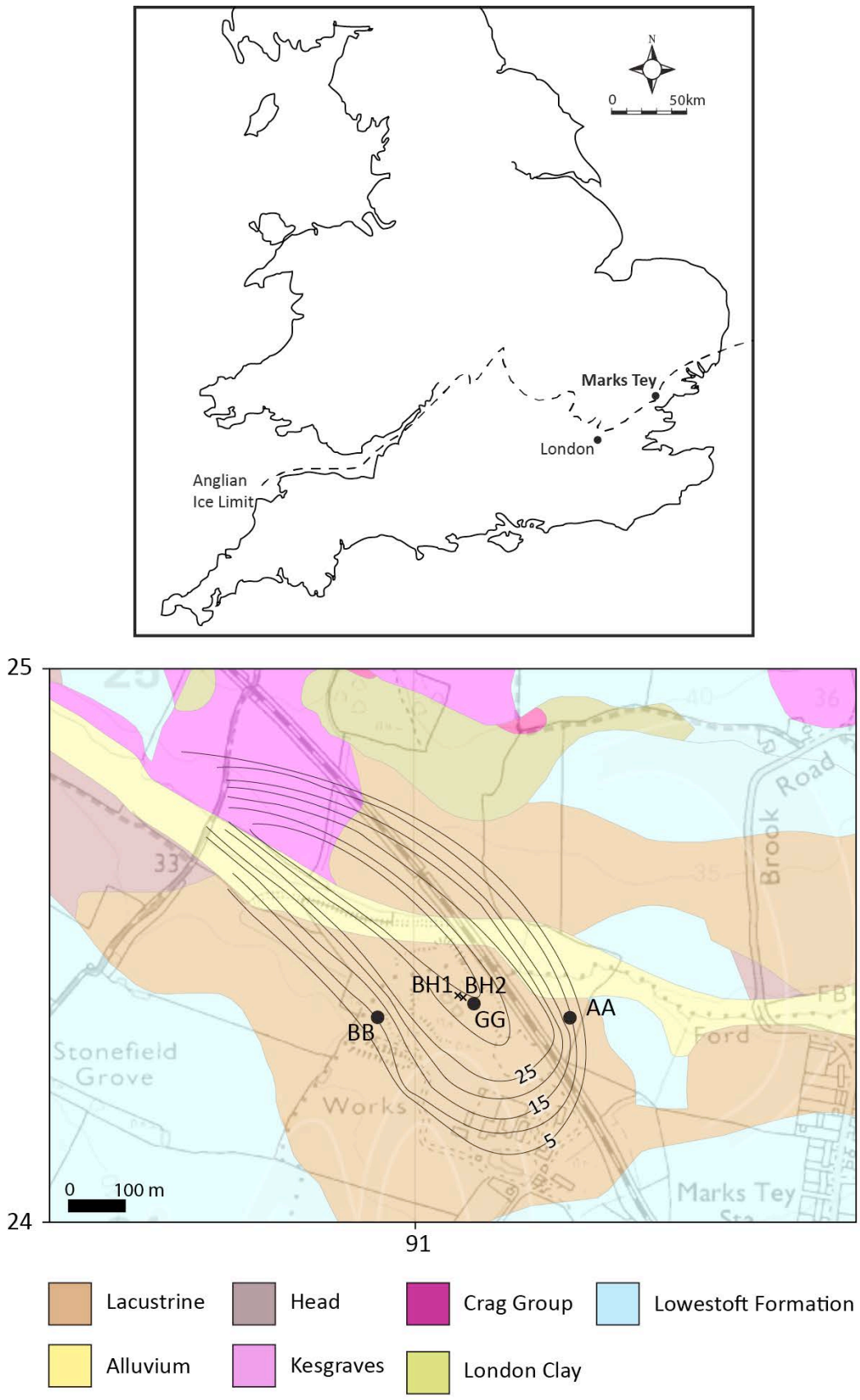

Figure 6.1. *Maps showing the location of Marks Tey within the British Isles and location of the Anglian (MIS 12) ice limit (Ehlers and Gibbard, 2001). The geometry of the basin is also shown (Ellison and Lake, 1986), along with the location of boreholes GG, AA, BB (Turner, 1970) and the boreholes drilled as part of this study (BH1 and BH2). This data is superimposed on top of a geological map of the immediate area surrounding the basin.*

Figure 6.1 shows the location of the two boreholes drilled for this study, along with the location of boreholes GG, AA and BB (Turner, 1970). The Quaternary geology of the site comprises lacustrine sediments situated in depressions formed in the Anglian till (Fig. 6.1). The Marks Tey basin itself is approximately 1km long, 0.4km wide, 35m at its deepest point, with a long axis that trends northwest to southeast (Turner, 1970; Ellison and Lake, 1986). Other geological units surrounding the site include recent alluvium associated with the Roman River (a tributary for the Colne), Kesgrave sand and gravel deposits from the proto-Thames (e.g. Rose et al., 1999), small outcrops of un-differentiated Crag deposits (Early-Middle Pleistocene), as well as outcrops of London Clay (Eocene), the unit that forms the bedrock geology of the area (Fig. 6.1).

The basin is one of a number of depressions that formed during the preceding glaciation, MIS 12 (the Anglian glaciation) (Pawley et al., 2008), when ice extended across East Anglia (Fig. 6.1) (Perrin et al., 1979; Rose, 1987, 2001; Ehlers and Gibbard, 2001; Clark et al., 2004; Gibbard and Clark, 2011). A number of topographic depressions formed in the till (Lowestoft Formation in figure 6.1) around the margin of this ice mass by sub-glacial scouring, dead-ice features and glaciofluvial processes, which subsequently in-filled with sediment during MIS 11 (the Hoxnian interglacial) (e.g. West, 1956; Turner, 1970).

6.2. Core correlation and macro-scale sediment description

The sequence recovered from Marks Tey for this study is composed of two overlapping boreholes obtained in 2010 (Fig. 6.1). Each drilling run recovered a core three meters in length, which was then cut in half for transport. The cores were correlated by the identification of key marker beds present in both sequences, which when combined, produced a profile from the quarry floor to 18.47 metres below surface (mbs) (15.802 to -2.668m O.D.) (Fig. 6.2). Two gaps in the stratigraphy occur between 714.5-729.5mbs and 12.13-12.28mbs, the depths of which were determined by measuring the amount of core loss between each drilling run using an electronic plumb bob. Based on changes in macro-sedimentology through the sequence, the core can be sub-divided into five lithofacies units (Fig. 6.2), which form the basis for the summary descriptions in table 6.1.

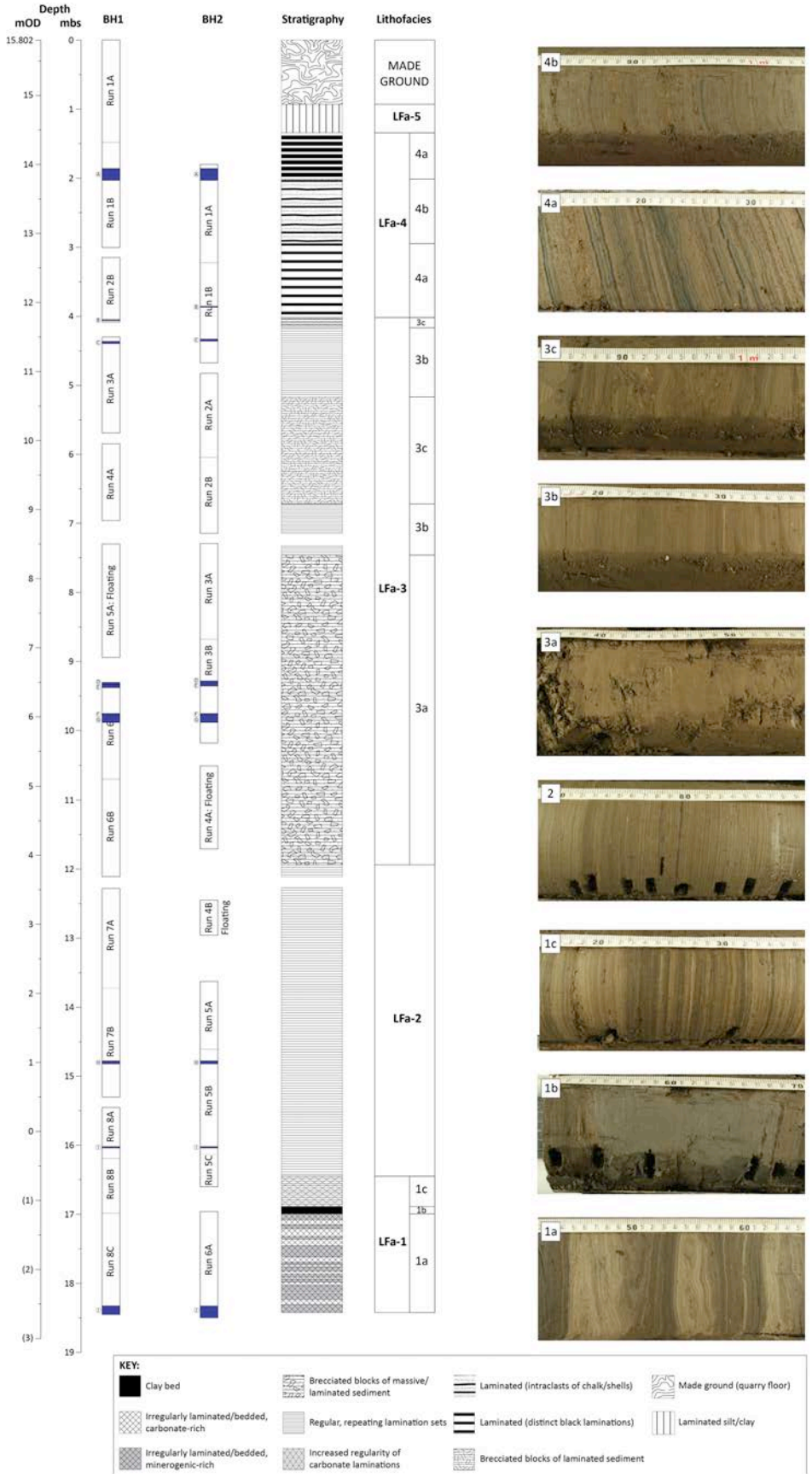

Figure 6.2. *The stratigraphy of core MT-2010 with lithofacies zones and core photographs. The stratigraphy is compiled from two overlapping boreholes that have been correlated based on the identification of key marker beds visible in both boreholes (blue bands). Due to incomplete core recovery, two gaps in the stratigraphy occur between 714.5-729.5mbs and 12.13-12.28mbs. Depths for the stratigraphy are in meters below coring surface (mbs) and meters Ordnance Datum (mOD).*

Table 6.1. *Summary of the lithological characteristics for core MT-2010, compared to the lithological characteristics of borehole GG (Turner, 1970)*

LF		Sediment characteristics core MT-2010 (this study)		Sediment characteristics of borehole GG (Turner, 1970)	
		Depth (mbs)		**Depth (mbs)**	
				21.44-21.41	• Finely bedded, silty, grey clay.
				21.41-21.20	• Medium-coarse grey sand with fine chalk gravel (Cretaceaous forams and sponge spicules.
				21.20-20.87	• Sandy to silty grey clay with thin seams of sand and fine chalk.
				20.87-20-10	• Firm grey clay, faintly laminated. Occasional shell fragments, thin re-deposited carbonate laminae and fine inorganic black specking.
1	a	18.47-16.99	• Beds ranging from 3-18cm thick that display distinct alternations in colour; alternate between very dark grey (10YR 3/1) and grey (10YR 6/1), within which laminations occur. • Very dark grey beds: Texture from fine sand to clay, dominated by clastic and organic material. Structure varies between weakly and well-defined laminations (<mm to mm-scale) and beds (cm-scale) with massive structure. • Grey beds: Silty-clay texture, dominated by carbonate-rich beds (cm-scale) and lamiantions (<cm-scale). Laminated structure defined by thin laminations (mm-scale) of organic material.	20.10-18.92	• Banded and laminated silty clay, becoming a moreeven coloured brownish grey laminated clay below 19.81 m.
	b	16.99-16.91	• Bed with a massive structure and clayey texture that has a 2.5Y 4/1 dark grey colour. Carbonate-rich (reacts with HCL) with sharp upper and lower contacts.	18.92-18.80	• Silty grey clay with seam of dark grey sand and angular flint.
	c	16.91-16.45	• Transitional unit between LFa-1a and LFa-2. Carbonate laminations occur with increasing frequency through the section and consistently display more regular (<mm-mm-scale) thicknesses	18.80-18.45	• Laminated dark to khaki-brown and grey clay mud showing irregular alternating grey and brown bands. Lamination often poorly developed.
2		16.45-12.00	• Distinctive, repeating laminations that display regular thicknesses. The structure is defined by thin (<mm-scale) carbonate laminations (2.5Y 7/2 light grey) that have a sharp lower contact and more diffuse upper contact, and thicker (>mm-scale), 2.5Y 4/2 dark greyish brown laminations.	18.45-12.54	• Finely laminated (rather fissile) dark, khaki or grey-brown clay mud. Fine, silty, organic, brown laminae alternate with grey, buff-yellow or while laminae; each pair generally <1mm thick. • Below 17.07 m the lamination becomes finer and sometimes indistinct.

Table 6.1. *Continued*

3	a	12.00-7.50	• Characterised by rotated soft sediment intraclasts/blocks of massive clayey silt (cm-scale) within a massive silty matrix. Intraclasts also occasional contain structures analogues to LFa-2.	12.54-8.42	• 12.54-12.51: Contoured seam of grey clay containing brecciated fragments of brown clay mud. • 12.51-8.42: Faintly laminated, brecciated khaki-brown clay mud blocks with lenses of dark grey silt between them.
	b	7.50-6.67	• Return to laterally continuous, horizontally laminated sediments analogous to LFa-2	8.42-7.71	• Faintly laminated khaki-brown clay mud. Dip of the laminations about 50°; probably a single large inclined block of clay mud with the breccia.
	c	6.67-5.20	• Unit is similar to LFa-3a below, but with increased frequency of soft sediment intra-clasts that have laminated structure analogous to LFa-2.	7.71-7.17	• Khaki-brown clay mud, brecciated into angular fragments (1-10cm across), in a matrix of finer fragments of the same material. Most fragment show well defined lamination.
	b	4.20-4.10	• Same as 7.50-6.67 above.		• N/A
4	a	4-10-3.00	• Laminated structure characterised by (>mm-scale) olive grey (2.5Y 4/3) and black (7.5YR 2.5/1) laminations, with both sharp and diffuse upper and lower contacts. Black laminations occur more frequently towards the base of the unit. Carbonate laminations occur occasionally.	7.17-4.04	• Distinctly and finely laminated grey clay and grey-brown clay mub. Lighter coloured layers of grey silty clay (0.3-2cm), alternate with grey-brown, brown or blackish layers of silt (0.3-1cm). • Towards the base of the bed the darker bands become more pronounced and the lighter ones thinner. • Darker layers contain platy reworked fragments of brown, silty (sometimes shelly) clay mud and grey clay. Lighter layers also conatin re-worked material.
	b	3.00-2.11	• Similar to LFa-4a, but also contains discrete beds (10-50mm) of olive brown (2.5Y 4/3) clay intraclasts/aggregates and organic fragments. Small chalk intraclasts also present.		
	a	2.11-1.35	• Return to 4.10-3.00 above.		
5		1.35-0.98	• Alternating low angle silty clay beds (2.5Y 4/2 dark greyish brown, 2-10mm thick) with sharp lower and sharp/diffuse upper contacts. Clayey beds contain multiple sub-layers (mm-scale) of 5Y 5/2 olive grey, greenish grey (gley/1/4/1) colour sediment with diffuse/graded lower and sharp upper contacts.	4.04-3.14 3.14-1.77	• Unevenly banded grey, orange-grey and grey-brown clay (5-10cm thick) in irregular order, which merge indistinctly into one another. • Sometimes contains fine brecciated flakes and nodules of orange-grey clay and clay mud. • Laminated medium dark grey clay, with distinct light grey clay layers (2.54 and 1.94-1.86cm). • Mottled orange-grey clay.
		MADE GROUND	• The final unit of the sequence is composed of heavily deformed beds of dark greyish brown (2.5Y 4/2) and dark greenish grey (gley/1/4/1) silty clay that have a moderate to high angle of repose. Iron staining evident.	1.77-0	• Mottled orange-grey clay

The summary descriptions in table 6.1 for core MT-2010 are also compared to those of Turner (1970) for borehole GG. Despite subtle differences in the sediment descriptions from both sequences, core MT-2010 displays the same lithological units as those present in borehole GG. The difference between the two records is that borehole GG is deeper than core MT-2010, with an extra 1.34m of sediment recovered by Turner (1970). When borehole GG was recovered, the coring rig struck artesian water between 21.41-21.44 mbs (Turner, 1970). It was decided that during the recovery of MT-2010, therefore, to cease drilling before this depth, to avoid the possibility of drilling into the aquifer.

6.3. Sedimentology of LFa-1 and LFa-2

The sediment descriptions of the lowermost 6.25m of the Marks Tey sequence, which covers LFa-1 and LFa-2, are based on the bulk sediment results from calcium carbonate (CC) and total organic carbon (TOC) analyses, selected element data from μ-XRF analysis (Fig. 6.5), as well as thin section descriptions. Microphotographs of sediments representative of each lithofacies zone are shown in figure 6.3, 6.4, 6.6.

6.3.1. Lithofacies 1 (18.47 – 16.45mbs)

Lithofacies (LFa) 1 comprises the basal section of the core and is subdivided into two main sub-facies (LFa-1a and 1c), based on subtle variations in sedimentology, that occur either side of a distinctive bed of massive clayey silt (LFa-1b).

6.3.1.1. LFa-1a (18.47 – 16.99mbs)

The sediments contained within LFa-1a are characterised by an irregular bedded and laminated structure and alternations in colour. The sequence is composed of beds that alternate in colour between very dark grey (10YR 3/1) and grey (10YR 6/1) (Fig. 6.2), within which laminated structures occur. The very dark grey beds range from 3 to 18cm in thickness, displaying variable thicknesses through LFa-1a (Fig. 6.2). The beds are predominantly composed of massive to weakly laminated organic and clastic (fine sand-clay) material, with carbonate making up a minor component (Fig. 6.3a). These sections of the sequence are also commonly associated with bioturbation structures

(Fig 6.3b). Where carbonate laminations occur in these beds, they have variable structures and are composed of calcite crystals that range in size from micrite to spar (<4μm - >50μm), mixed with siliciclastic grains and organic fragments (Fig. 6.3c-e). Carbonate either occurs as 1) intra-clasts within a massive matrix of organic and minerogenic material (lower part of photo, Fig. 6.3c); 2) laterally continuous laminations of the same material (upper part of photo, Fig. 6.3c); 3) normally graded laminations that exhibit decreasing quartz grain-sizes from fine sand to slit/clay (Fig. 6.3d), or 4) laterally discontinuous laminations (Fig. 6.3e), between which laminations of amorphous organic matter, quartz grains and a heterogeneous mix of benthic (e.g. *Epithemia* and *Rhopalodia* sp.) and planktonic (*Cyclotella* sp.) diatoms occur (Fig. 6.3f).

The calcium carbonate content is variable in LFa-1a (mean = 30.8%, SD = 14.5) and displays an increasing trend from values of ~10% at the base, to ~50% at the top of the unit, while organic carbon, although variable, displays no broad trend (mean = 7%) (Fig. 6.5a,b). The datasets do, however, vary with changes in bed composition. The calcium carbonate and organic carbon contents display a negative relationship in the very dark grey beds, with low values of calcium carbonate content (e.g. 5.76% at 18.07mbs and 19.79% at 17.48mbs) corresponding to high values of organic carbon content (e.g. 9.16% at 18.07mbs and 11.63% at 17.48mbs) (Fig. 6.5a,b).

The μ-XRF data also shows a clear trend in LFa-1a, with Si, Ti and K all displaying decreasing trends, while the Ca and Mn/Fe data exhibit regular variations (Fig. 6.5). Ca values are low within the dark grey beds (Fig. 6.5c), which correspond with peaks in Si, Ti, K and the Mn/Fe ratio (Fig. 6.5d,e,f,g).

The grey beds that interdigitate with the very dark grey beds range in thickness from 3 to 10cm and display a general increase in thickness through LFa-1a (Fig. 6.2). These beds are characterised by an increase in the frequency of carbonate, which has variable lamination structures. The most common facies in these beds are carbonate laminations with a massive structure (organic, clastic, diatom and shell material is rare) and a range of calcite crystal sizes (micrite to spar) (Fig. 6.4a), in between which are fine (<mm-scale) laminations where the frequency of diatom frustules increases (Fig. 6.4b). The composition of these diatom layers is similar to figure 6.3f (Fig. 6.4b). Where

there is more structure within the grey bed, multiple carbonate laminations (micrite-spar crystals) are interrupted by distinctive laminations of amorphous organic material (Fig. 6.4c). The laminated structure of the carbonate is defined by multiple sub-laminations of *Cyclotella* sp. (Fig. 6.4b).

The calcium carbonate and organic carbon content display a similar relationship to the one seen in the very dark grey beds, although the opposite trend is apparent in the grey beds. The grey beds are associated with peaks in calcium carbonate content and relatively low values of organic carbon content (Fig. 6.5a,b). The calcium carbonate content results are also mirrored by high values of Ca in the µ-XRF data (Fig6.5c). These high values of calcium carbonate and Ca correspond to relatively low values of Si, Ti, K and a low Mn/Fe ratio (Fig. 6.5d,e,f,g).

6.3.1.2. LFa-1b (16.99 – 16.91mbs)

LFa-1b is a distinctive bed of dark grey (2.5Y 4/1) silty-clay that has sharp contacts with LFa-1a and LFa-1c. The unit is poorly sorted, with the matrix composed of calcite in the size range of micrite to micro-spar, and mineral grains with a particle size range from clay to very fine sand (Fig. 6.6a). Occasional lenses composed predominantly of re-worked spar crystals also occur (Fig. 6.6b), along with calcified plant stems (Fig. 6.6c). This unit is unique within the sediment sequence as it contains very low percentages of pollen grains, while pre-Quaternary microfossils (PQM) account for almost 80% of countable material on the pollen slides (P. Coxon, pers. comm.).

Calcium carbonate content rises slightly from 44% to 49% through the unit (Fig.6.5a) (2 data points), while organic carbon content shows a marked drop to values of 0.97% and 1.58% (Fig. 6.5b). The trend in calcium carbonate content is mirrored by the Ca values, which display an increasing trend through the unit (Fig. 6.5c). Si, Ti and K values also have high values in this unit, with K displaying a particularly prominent peak (Fig. 6.5,e,f), while the Mn/Fe ratio exhibits the lowest values seen in the sequence (Fig. 6.5g).

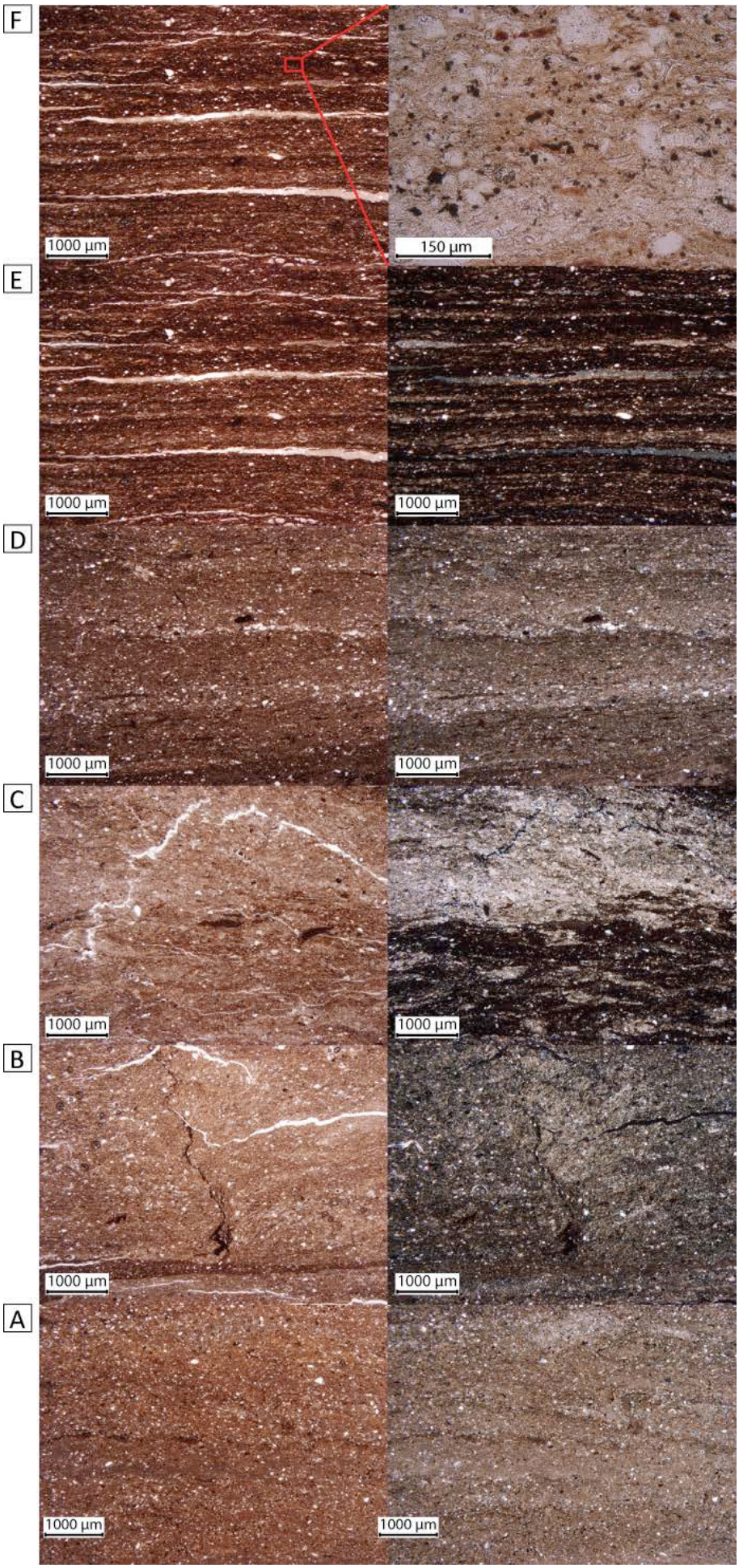
F
1000 µm
150 µm
E
1000 µm
1000 µm
D
1000 µm
1000 µm
C
1000 µm
1000 µm
B
1000 µm
1000 µm
A
1000 µm
1000 µm

Figure 6.3. *Photomicrographs of the sediment structures that characterise the very dark grey beds in LFa-1. The figure contains paired images (a-e) taken in plain polarised light (left) and cross polarised light (right). Image f is a copy of image e (plain polarised light), alongside which is a high magnificent image of the organic matter, quartz grains and diatoms found between carbonate laminations. (a) weakly laminated organic and clastic dominated sediment, which is associated with bioturbation structures (b). Lower part of (c): carbonate intra-clasts in a matrix of organic and minerogenic material, upper part of (c): laterally continuous laminations of same material, (d): normally graded laminations, (e): laterally discontinuous laminations of calcite, in between which organic matter, minerogenic material and diatoms occur (f).*

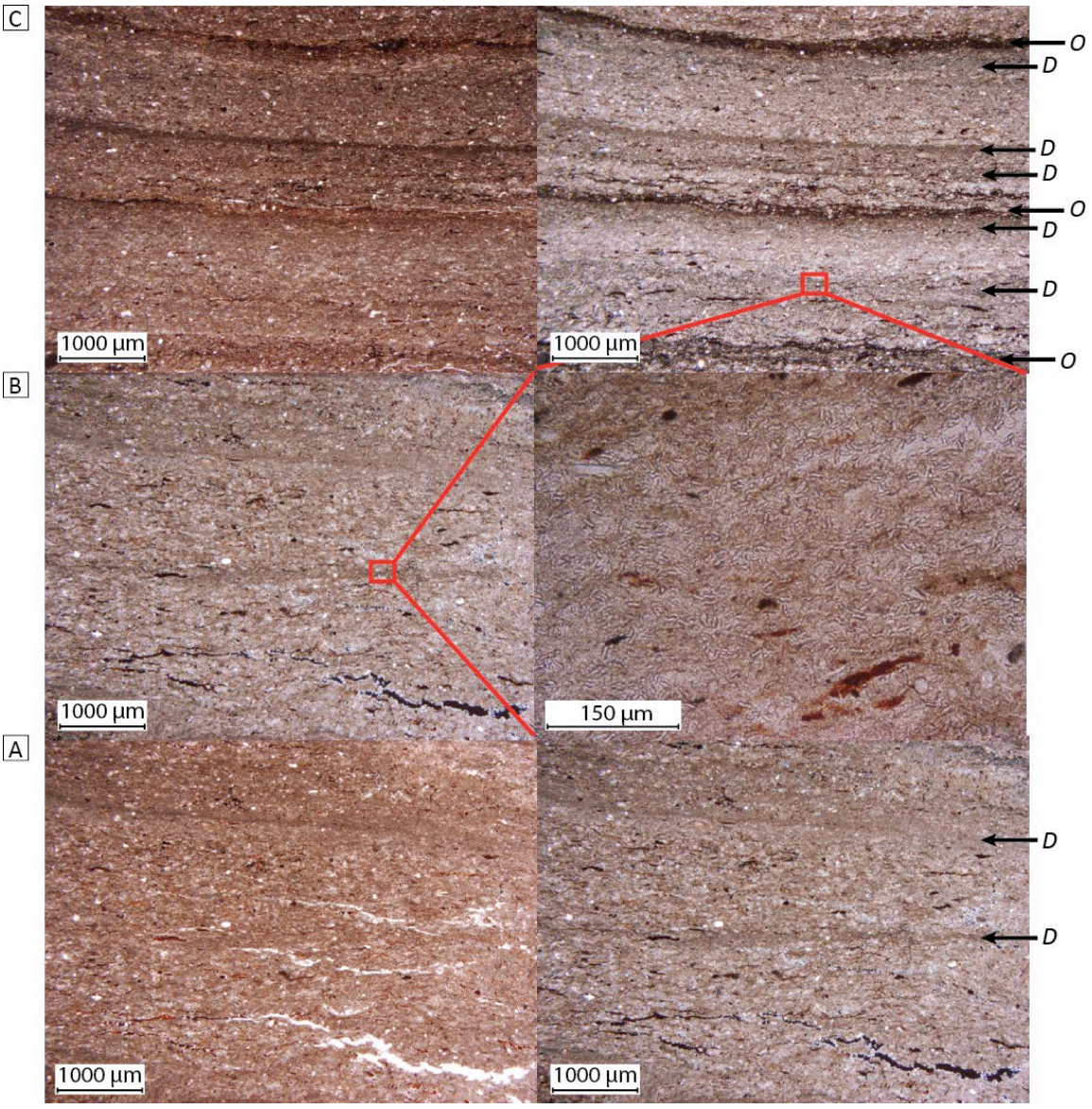

Figure 6.4. *Photomicrographs of the lamination structures that characterise the grey beds contained within LFa-1a. (a) carbonate laminations with a massive structure, which alternate with diatom rich (Cyclotella* sp.*) laminations. These diatom rich laminations are highlighted by arrows (D) in image (a),with a high magnification image in (b). (c) carbonate laminations separated by laminations of amorphous organic material, highlighted by arrows (O). The carbonate laminations contain multiple sub-laminations of diatoms, also highlighted by arrows (D), with a similar composition to those in image (b).*

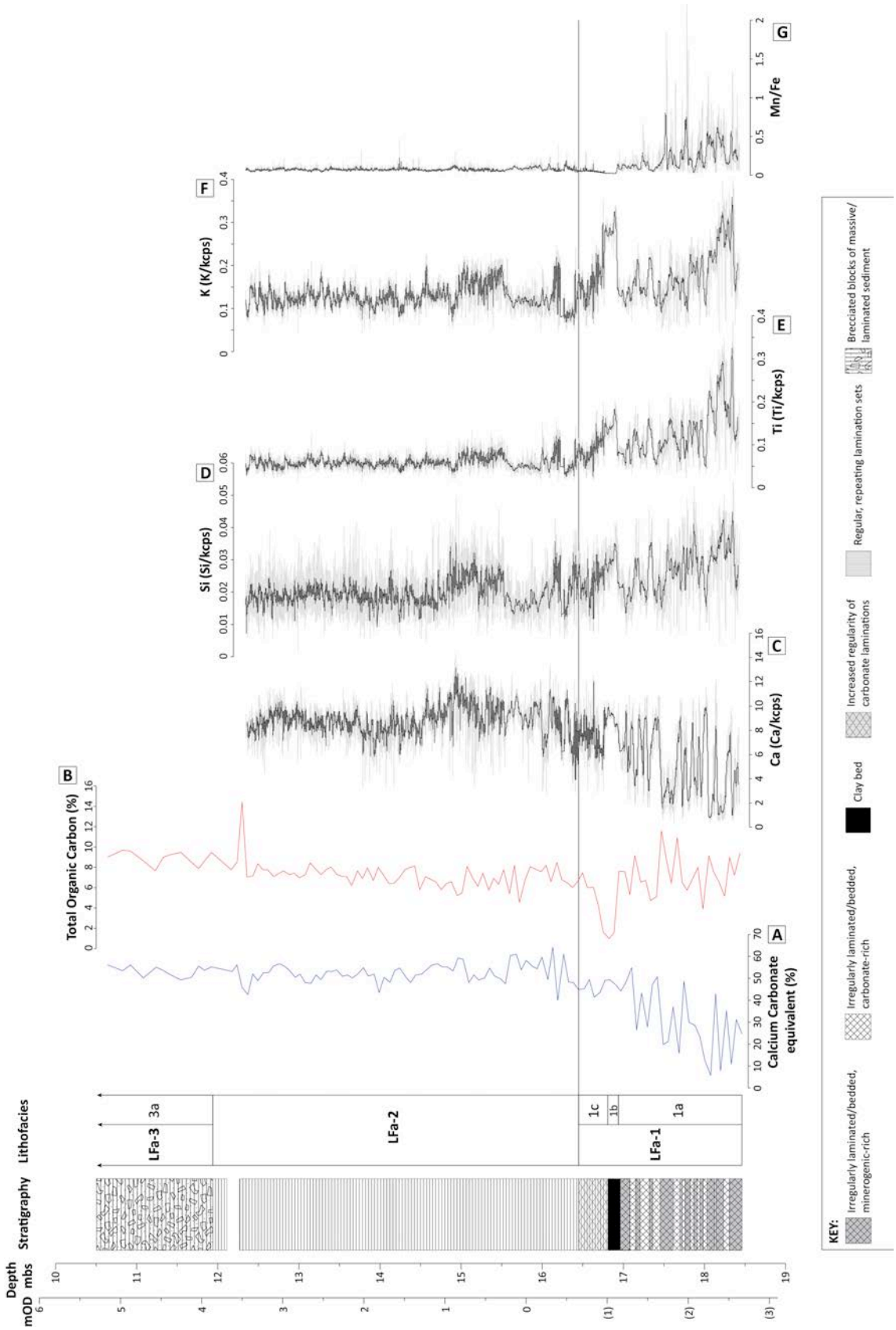

Figure 6.5. *Figure showing results of bulk sedimentological characteristics and µ-XRF element intensity data for the lowermost 6.25m of core MT-2010. A) calcium carbonate content, B) total organic carbon content. C, D, E and F show elemental intensity data (standardised to kcps) for Ca, Si, Ti and K. G) Mn/Fe ratio.*

6.3.1.3. LFa-1c (16.91 – 16.45mbs)

LFa-1c is characterised by an increase in the regularity of the sediments, indicating a transition between the irregular nature of LF 1a and the ordered nature of laminations in LFa-2. The sedimentology of LFa-1c does bear some similarities to that of the weakly laminated sediments of LFa-1a (see Fig. 6.3e), however, carbonate laminations (<mm to mm-scale) occur at more regular intervals in LFa-1c (Fig. 6.d,e). Furthermore, this lithofacies zone is characterised by the appearance of carbonate laminations that are composed almost entirely of micritic calcite (Fig. 6.6d,e).

Carbonate content continues to show stable values (mean = 46%) (Fig. 6.5a), while organic carbon content increases from 1.61% to 7.49% through the unit (Fig. 6.5b). The µ-XRF results show a slight increasing trend in Ca values (Fig.6.5c), while Si, K and Ti all exhibit decreasing trends, and the Mn/Fe ratio remains low (Fig. 6.5d,e,f,g).

6.3.2. Lithofacies 2 (16.45 – 12.00mbs)

Micromorphological descriptions of the laminations in LFa-2 show that they occur as part of repeating lamination sets, composed of three broad lamination types: LT1, LT2 and LT3. Micro-facies descriptions of vertical variations in the structure of these lamination types are presented in chapter 7, but in brief; LT1 is predominantly characterised by high abundances of centric diatom frustules, LT2 is composed of fine-grained micritic (<4µm) calcite, and LT3 is characterised by material from a number of sources (e.g. amorphous and particulate organic material, mineral grains, centric and pennate diatom frustules) (Fig. 6.6f).

Both carbonate content and organic carbon content is stable in this part of the sequence, with average carbonate values of 52% and average organic carbon values of 7%; the one exception to this trend is an anomalous value of 14.44% for organic carbon content at 12.28mbs (Fig. 6.5a,b). The trend in carbonate content and the organic carbon content are also exhibited by the µ-XRF data, which shows a fairly consistent trend within LFa-2, with less variability than LFa-1. Ca continues the increasing trend seen in LFa-1, with peak values reached at 14.95 mbs. Ca counts then show a decreasing trend until 13.90 mbs, before increasing again to another peak at 12.80 mbs, with a subsequent decrease through to the end of LFa-2 (Fig. 6.5c).

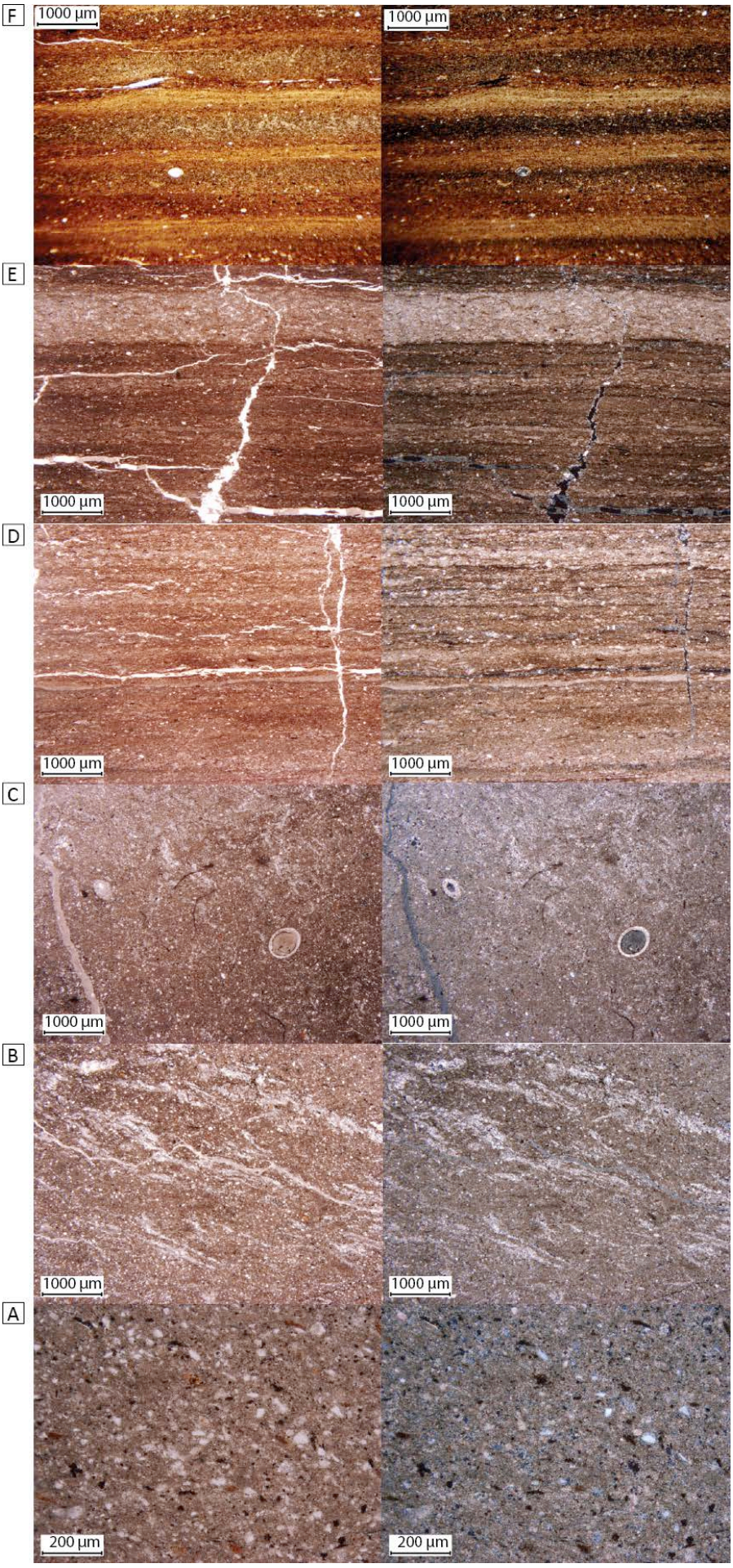
F
1000 µm
1000 µm
E
1000 µm
1000 µm
D
1000 µm
1000 µm
C
1000 µm
1000 µm
B
1000 µm
1000 µm
A
200 µm
200 µm

Figure 6.6. *Photomicrographs of the sediment structures that characterise LFa-1b (a-c) and LFa-1c (d and e). (a) photo of the matrix from LFa-1b, which is poorly sorted, carbonate rich and contains minerogenic material in the range clay – very fine sand. (b) lenses composed of re-worked spar crystals, and (c) calcified plant stem. (d and e) photos showing the increase in regularity of core sedimentology. This section of the core marks the first appearance of carbonate laminations composed almost entirely of micritic calcite (d). (f) Regular and repeating lamination sets from LFa-2.*

After initial peaks centred on 16.20 mbs, Si, Ti and K show consistent values throughout LFa-2, apart from a zone between 15.55-14.90mbs where, although subtle, all three elements display values consistently elevated from the long-term trend (6.5d,e,f). The Mn/Fe ratio continues to stay low throughout this lithofacies zone (Fig. 6.5g).

6.4. Pollen results

Results of pollen analysis for the base of the sequence from 18.45 – 10.88mbs are presented in figure 6.7, with the summary diagram produced by Turner (1970). The section of core MT-2010 relevant to this thesis contains sediments from Ho I (18.46 – 16.74 mbs), Ho II (16.74 – 13.50 mbs) and the first part of Ho III (13.50 – 10.88 mbs) (Fig. 6.7).

6.4.1. Description of the vegetation succession in core MT-2010

1) **Ho I (18.46 – 16.74mbs, Pre-temperate zone):** Although core MT-2010 contains sediment from Ho I, the boundary with the preceding Late Glacial zone (Fig. 6.7b) is not present in the core, with the basal sample (18.45mbs) containing a pollen assemblage where AP exceeds NAP (Fig. 6.7a). The zone is characterised by high percentages of *Betula*, which reaches 65% at 17.47mbs, before decreasing to 42% at the end of the zone. *Pinus* also shows an increasing trend from 10% to 30% between 18.45 – 17.07mbs, before reducing to 7% at 16.74mbs. *Poaceae* is also present throughout this zone, reaching 20% at 18.45mbs, before declining to 8% at the transition to Ho II. *Quercus*, which only exhibits values <5% for most of the zone, shows a marked increase to 16% between 17.07 – 16.74mbs (Fig. 6.7a).

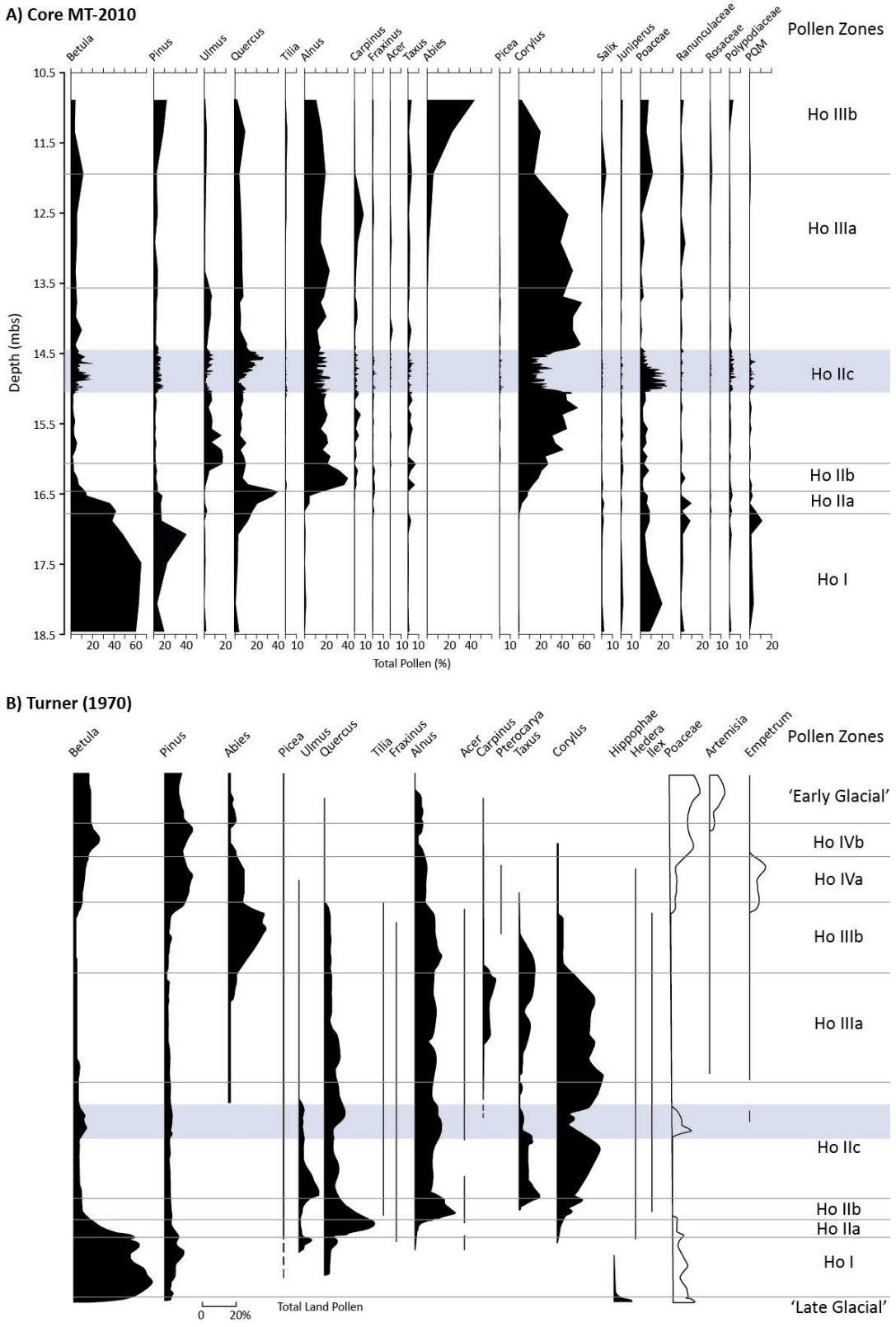

Figure 6.7. *A) Pollen diagram for core MT-2010 from 10.88-18.45mbs (this study), which contains sediments from pollen zones from Ho I – early Ho IIIa. B) The summary diagram of Turner (1970), representing a composite record of a number of boreholes from the basin. Although core MT-2010 represents a higher-resolution record for Ho IIc, it is directly comparable to the pollen diagram of Turner (1970) for the early part of the Hoxnian, but does not contain pollen from the 'Late Glacial' zone.*

2) **Ho II (16.74 – 13.50mbs, Early-temperate zone)**: This zone is characterised by mixed oak forest. Based on variations in vegetation composition, the zone is divided into three sub-zones;
    a. ***Ho IIa (16.74 – 16.47mbs)*** is characterised by a drop in *Betula* (42-13%), which is mirrored by a rapid rise of *Quercus* pollen (16-39%). *Pinus also stays low* (~6%), while *Alnus* and *Corylus* start to expand (Fig. 6.7a);
    b. ***Ho IIb (16.47 – 16.07mbs)*** is characterised by an increase in *Alnus*, which peaks mid-zone (16.27mbs) at 40% and a gradual increase in *Corylus* through the zone from 9-27%, which corresponds to a marked decrease in *Quercus* from 39-9% (Fig. 6.7a);
    c. ***Ho IIc (16.07 – 13.50mbs)*** is characterised by an early peak in *Ulmus* (17% at 15.97mbs) and the presence of Quercus and Alnus. These three species show a general decline through this zone due to the continued increase in *Corylus*, which becomes the most dominant taxa, reaching values of up to 58%. The vegetation succession during Ho IIc is interrupted between 15.05 – 14.50mbs, where *Birch, Pinus* and particularly *Poaceae* values increase at the expense of *Corylus*, which shows the most striking response from AP to the event (Fig. 6.7);
3) **Ho III (13.50 – onwards, Late-temperate zone)**: This zone can also be divided into sub-zones, although the transition between Ho IIIb and Ho IV does not occur in this part of the sequence.
    a. ***Ho IIIa (13.50 – 11.93mbs)*** is characterised by the expansion of *Carpinus* as well as low values of *Abies*. Values of *Alnus* remain stable throughout this zone, while *Ulmus, Quercus* and *Corylus* show gradual declining trends (Fig. 6.7a);
    b. **Ho IIIb (11.93 onwards)** is not present in its entirety in figure 6.7a, but the section of the zone that is, is characterised by the marked increase in *Abies* pollen, while *Ulmus, Quercus, Alnus* and *Corylus* continue their declining trends. *Pinus* and *Poaceae* also start to become present on the diagram again (Fig. 7.a).

6.5. Synthesis

The results presented in this chapter enable a discussion of the sedimentology from the new core drilled at Marks Tey in terms of: 1) the location in the sequence of laminated sediments for further micro-facies analysis, to test the model for varve formation proposed by Turner (1970); 2) the location of the NAP phase in core MT-2010, as defined by Turner (1970) in borehole GG; and 3) preliminary interpretations about lake development during the early part of MIS 11.

6.5.1. Correlation of core MT-2010 with borehole GG

Comparing the sediment descriptions in table 6.1 and the pollen results in figure 6.7 for core MT-2010 with those for borehole GG (Turner, 1970) reveals excellent agreement between both sequences, and thus establishing that the material in the two boreholes are comparable. The only significant difference between the two records, as stated earlier, is that borehole GG contains an extra 1.34m of sediment at the base of the sequence (Table 6.1). The result of this is that the transition between the Late Glacial pollen zone (MIS 12) and pollen zone Ho I is not recorded in core MT-2010, a situation that was unavoidable given the groundwater conditions discussed in section 6.2. Key to this study is the fact that the NAP phase that Turner (1970) recognised in the sequence is replicated in core MT-2010, between 15.10 – 14.50 mbs in LFa-2 (blue shading, Fig. 6.7a,b).

6.5.2. Location and extent of varve-like sediments and the NAP phase

The focus of this chapter has been to characterise the whole MT-2010 sequence at the macro-scale, before presenting more detailed descriptions of the lowermost 6.25m. The analysis of the sequence from 18.47 to 12.28mbs has revealed a section of the sequence between 16.45 – 12.27mbs (LFa-2) that contains laminated sediments with regular and repeating structures, which will be the focus of the next two chapters (chapters 7 and 8). Although the sediments of LFa-1 are laminated, the structure of these laminations is irregular and not varved, so will not be considered for further micro-facies analysis, as section 6.5.2 will demonstrate.

6.5.3. Lake development at Marks Tey during early MIS 11

By combining thin section micromorphological analysis with the bulk sedimentological data (calcium carbonate, organic carbon and μ-XRF data) and the pollen data, it is possible to make some preliminary interpretations about lake development during the early part of MIS 11. These interpretations are preliminary as a detailed diatom record, which will add additional proxy information, is not yet available. Preliminary descriptions about the changes in diatom flora have been made from thin section descriptions, however, which, when combined with previously published data allow some initial observations to be made, and to provide some context for subsequent sediment descriptions and interpretations.

The sedimentology of the sequence indicates at least three phases of lake development during the early part of MIS 11. Phase 1 relates to LFa-1a and 1b, which occurred during the pre-temperate pollen zone Ho I (Fig. 6.8). Phase 2 corresponds to the sediments associated with LFa-1c, which were deposited during Ho IIa of the early-temperate phase, while the third phase is typified by LFa-2, which was deposited during Ho IIb and c of the early-temperate phase and the first part of the late-temperate phase (Ho IIIa) (Fig. 6.8).

6.5.3.1. Phase 1 (18.47 – 16.91mbs, LFa-1a, Ho I)

Phase 1 represents the initial period of sedimentation in the lake basin at Marks Tey following the Anglian glaciation, during pollen zone Ho I (Fig. 6.8). The sedimentology of this part of the sequence indicates a system that alternates between periods of relatively stable and unstable conditions.

The very dark grey beds that dominate the sediments in LFa-1 (particularly at the base of the sequence) indicate periods of unstable conditions within both the lake catchment and the basin itself. Peaks in Ti and K counts indicate input of detrital clastic material from the catchment (Fig. 6.8) (Arnaud et al., 2012; Neugebauer et al., 2012; Czymzik et al., 2013; Schlolaut et al., 2014). High Si counts in these beds may indicate detrital input, however, using Si as a proxy for detrital input at Marks Tey is complicated by the fact that diatom silica will also contribute to these Si counts (Peinerud, 2000; Kylander et al., 2011; Wennrich et al., 2014).

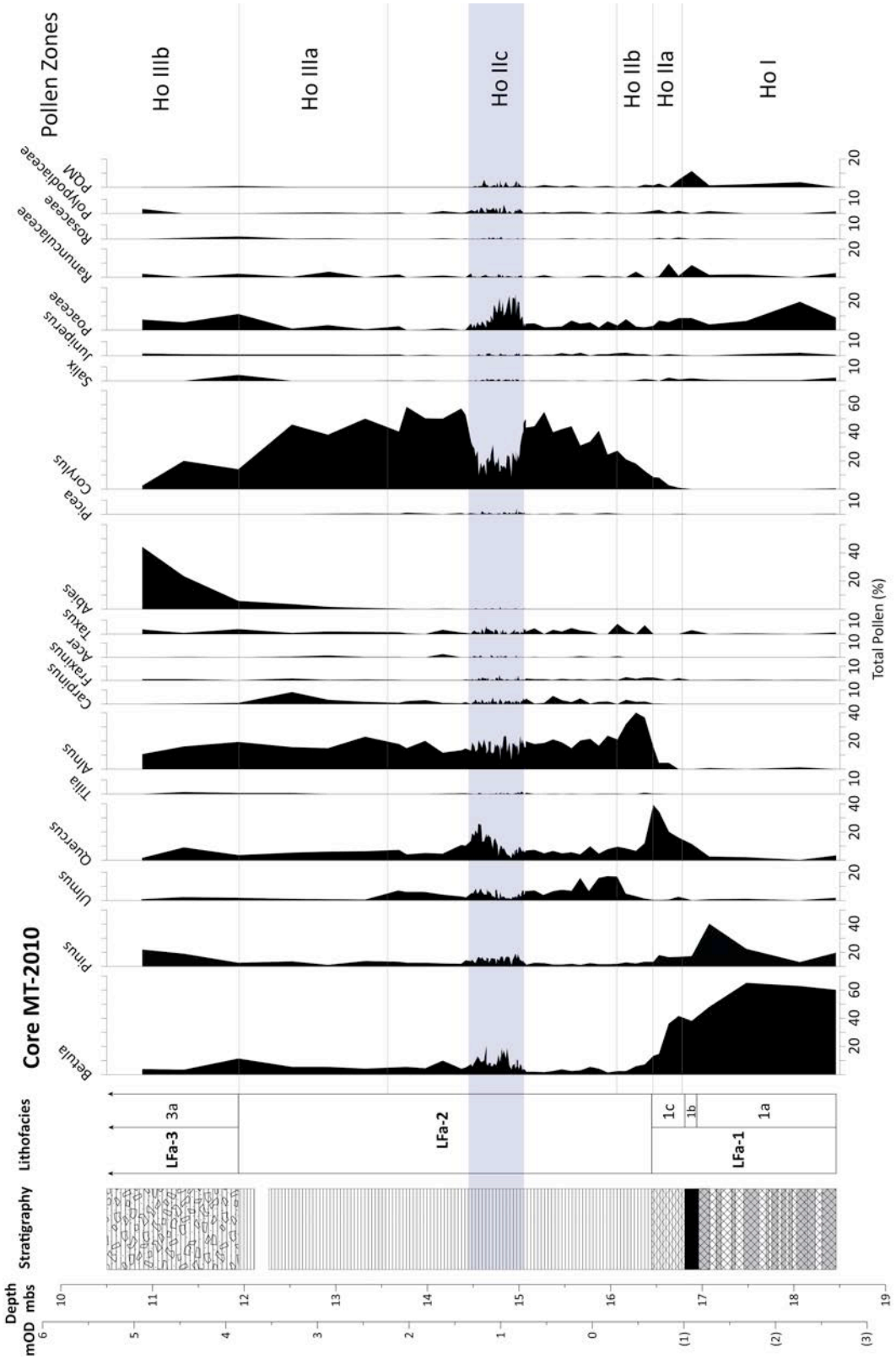

Figure 6.8. *Percentage pollen diagram for the MT-2010 sequence, sub-divided into the pollen zones contained within the lowermost 6.25m of the record. The pollen diagram is plotted alongside core lithostratigraphy, which also has also been sub-divided into lithofacies zones (see figure 6.5 for key to lithostratigraphic log).*

There is, however, a strong positive relationship between Si and the detrital indicators K and Ti throughout this section of the sequence (R^2=0.65 and R^2=0.59, respectively), indicating that it can also be used as a proxy for detrital input. Lake catchment instability during Ho I is also shown by a dominance of birch forest, a pioneer community on unstable, newly deglaciated terrain (Pennington, 1969; West, 1980; Bennett, 1983; Atkinson, 1992), as well as persistent traces of pre-Quaternary microfossils (Fig. 6.8). Furthermore, the normally graded laminations in these beds suggest the likely operation of underflows as an important method of sediment delivery during these periods (Sturm, 1979) (Fig. 6.3d).

Low peaks in carbonate content and Ca counts also suggest low levels of productivity in the lake during these periods (Hodell et al., 1998; Prasad et al., 2009; Neugebauer et al., 2012) (Fig. 6.8). Peaks in the Mn/Fe ratio associated with these beds may also indicate an unstable water column, as both elements are sensitive to changes in redox conditions (Davison, 1993; Olsen et al., 2012; Naeher et al., 2013). Using the Mn/Fe ratio alone is problematic as Fe can also represent detrital input (e.g. Jouve et al., 2013). The sedimentology of these beds does support the trend seen in the Mn/Fe ratio, however, as poorly preserved laminations and the presence of bioturbation structures also indicate oxic conditions at the sediment/water interface (Fig. 6.3a, b).

The grey, carbonate-rich beds that represent a larger proportion of sedimentation from 17.45 – 16.99 mbs, indicate the development of more stable conditions in the lake and its catchment during the later stages of Ho I (Fig. 6.8). These beds show low K, Ti and Si counts, indicative of lower levels of detrital input, while peaks in both calcium carbonate concentration and Ca counts suggest increased levels of productivity (Fig 6.9). It should be noted, however, that large changes in calcium carbonate content will have a dilution effect on these elements, as the µ-XRF data only records relative proportions of the elemental composition of the sediment (e.g. Croudace et al., 2006; Lowemark et al., 2010). While the dilution effect will influence the dataset, the appearance of oak and elm trees in the catchment during the later part of Ho I suggests increased catchment stability (Fig. 6.8) (e.g. West, 1980).

Low Mn/Fe ratios also indicate water column stability with anoxic bottom waters, as Mn is preferentially reduced under anoxic conditions (Davison, 1993; Olsen et al., 2012; Naeher et al., 2013). This is also reflected in the sedimentology of these beds, with the preservation of lamination structures and absence of bioturbation structures (Fig. 6.4). Despite the preservation of laminations within these beds, the structure is irregular, and they do not represent the deposition of annually-laminated sediments. This is suggested because *Cyclotella comensis* represents the dominant planktonic diatom species during Ho I (D. Ryves, pers. comm.) and occurs as multiple sub-laminations within the carbonate (Fig. 6.4b). *Cyclotella comensis* also dominates planktonic assemblages of some UK lakes during early stages of lake development following the Last Glacial Maximum (LGM) (e.g. Sabater and Haworth, 1995; Galloway et al., 2011) and has been found in high abundances in shallow, polymictic lakes (Werner and Smol, 2006). Evans (1972) also noted a dominance of *Cyclotella* spp. at Marks Tey during the early-temperate phase, indicative of a lower lake level at this time. The presence of a relatively shallow, polymictic lake during Ho I therefore preclude the ability to demonstrate a depositional model with clear seasonality. This supports the suggestion that these laminations are not varved.

The dark grey clay bed that separates LFa-1a and LFa-1c is the most distinctive unit in the lower part of the Marks Tey sequence (Fig. 6.2, 6.6a-c). The poorly sorted nature of the unit, combined with its very low organic carbon content, suggest the unit was deposited rapidly. The pollen evidence also suggests this, with little (P. Coxon pers. comm.) or no (Turner, 1970) pollen present. The unit does, however, contain high percentages of PQMs (P. Coxon, pers. comm), as well as a distinctive peak in K counts (and smaller peaks in Ti and Si), which suggests an allocthonous origin for the sediment. The unit also contains an autochthonous component, with lenses of re-worked spar crystals and calcified plant stems, suggesting the re-working of deposits from sediments from the littoral zone. It is difficult to provide a precise explanation of its origin, because the unit is not diamictic, so does not, therefore, relate directly to the Anglian Till. The sedimentology also indicates that the sediments are not purely derived from autocthonous lake deposits. Based on the sedimentology, this unit probably represents an event deposit that originated in the catchment and entrained littoral lake sediments.

6.5.3.2. Phase 2 (16.91 – 16.45mbs, LFa-1c, Ho IIa)

This phase of lake development indicates a transition between the irregular sediments of LFa-1a and b and the regularly laminated sediments of LFa-2. The detrital elements (K, Ti and Si) all show a decreasing trend throughout this phase, after the peaks seen in LFa-1b (Fig. 6.8), suggesting further stabilisation of the lake catchment. The pollen data corroborates this, with a rapid decrease in birch (and pine to a lesser extent) coinciding with the expansion of oak trees at the beginning of the phase, while alder and hazel begin to expand towards the end of this period (Fig. 6.8).

The calcium carbonate concentration and Ca counts continue the increasing trend seen during the later stages of phase 1 and the Mn/Fe ratio is persistently low during this phase, indicative of increasing productivity and a stable water column. The increased carbonate content of the sediments meant that diatom frustules were not readily visible in thin section, but Evans (1972) noted a progressive shift in the assemblage during Ho IIa from *Cyclotella* sp. to *Stephanodiscus* sp. Future work needs to be undertaken to corroborate these findings, but they are in keeping with the sedimentology of this section of the core. A shift in dominance from *Cyclotella* to *Stephanodiscus* species indicates increasing nutrient supply to the lake and, therefore, increasing levels of productivity (e.g. Anderson, 1990; Scheffler et al., 2005). Evans (1972) also suggested that this shift in assemblage coincided with an increase in lake level at the site. This may in part also explain the sedimentology. An increase in lake productivity and deepening water column will lead to increasing potential of the preservation of seasonal lake stratification, as indicated by the Mn/Fe ratios.

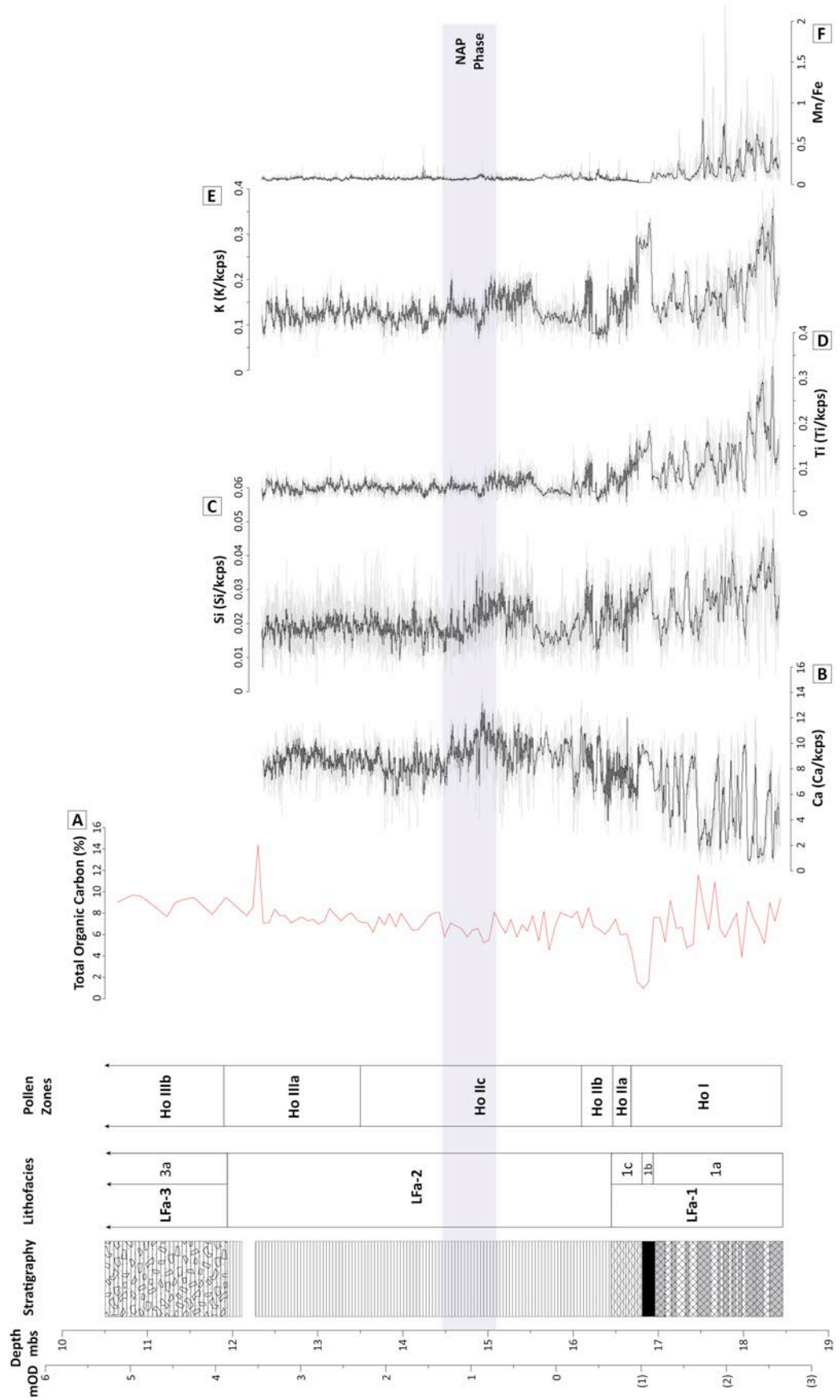

Figure 6.9. *Figure showing how litholofacies zones in core MT-2010 relate to changing vegetation composition. The figure is same as figure 6.4, apart from the removal of the calcium carbonate data (as Ca counts can also be used) and the addition of the pollen zones and the location of the NAP phase (blue shaded area). See figure 6.5 for key to lithostratigraphy.*

6.5.3.3. Phase 3 (16.045 – 12.28mbs, LFa-2, Ho IIb, c and IIIa)

The final phase of lake development in this section of the core coincides with the persistent preservation of the regular and repeating lamination sets in LFa-2 (Fig. 6.8). Si is unlikely to provide a good indicator of detrital input during this phase of lake development, due to the regular occurrence of diatom-rich laminations (Fig.6.6f). This is reflected in the biplots for this section of the core, where the relationship between K and Si (R^2=0.31) and Ti and Si (R^2=0.32). K and Ti show a fairly stable trend through this part of the sequence. Lake catchment stability is further indicated by the further expansion of hazel to become the dominant taxa, while yew, alder oak and elm also make up forest composition.

Calcium carbonate concentrations and Ca counts also remain high throughout this phase, while the Mn/Fe ratio remains consistently low. This is indicative of a productive lake, with a stable water column and anoxic bottom waters. The sedimentological data is further supported by the diatom data of Evans (1970) and the micro-facies analysis in this thesis, where the dominance of *Stephanodiscus* sp. suggests a nutrient-rich, eutrophic lake.

As noted in the results, there is a period between 15.55 – 14.90mbs where the K and Ti counts show persistently elevated values compared to the long-term trend, suggesting a period of increased detrital input into the lake. This trend in the detrital elements overlaps with the first 20 cm of the NAP phase (15.10-14.50mbs) (Fig. 6.8) and will be discussed in detail in chapter 10).

6.6. Chapter Summary

The key characteristics of the MT-2010 core can be used to correlate this sequence to that of Turner (1970) and suggest some key observations about the evolution of the lake basin and its catchment.

- This chapter has presented lithostratigraphical and biostratigraphic results from MT-2010, a new core extracted from the palaeo-lake basin at Marks Tey.
- Data from a number of different techniques has allowed the sedimentology of the sequence to be determined at both the macro- and micro-scale, indicating variations in depositional process.

- These descriptions have identified sedimentary structures in LFa-2 (16.45 to 12.00 mbs) that are analogues to annually-laminated sediments (Turner, 1970). These sediments will be the focus of chapters 7 and 8.
- The sedimentology of LFa-1, however, is too irregular for these sediments to be considered varved.
- The palynological data has allowed the correlation of the MT-2010 sequence with borehole GG (Turner, 1970) and provides the environmental context for further the subsequent chapters in this thesis.
- Initial observations about the lake development at Marks Tey during the early part of MIS 11 indicate the transition from a relatively unstable, oligotrophic water body during the initial stages after deglaciation to a eutrophic system as a result of increased catchment stability and an input of nutrients related to the development of temperate forest during MIS 11.

Chapter 7. Developing a depositional model for varve formation

Chapter overview

Chapter 6 has shown that LFa-2 in the MT-2010 sequence is characterised by regular, repeating lamination sets. It is these laminations that are proposed to be varves, the sediments at LFa-1 are too irregular in structure to be varved. This chapter aims, through micro-facies analyses, coupled with high precision pollen, diatom and O/C isotopic analysis, to examine whether these regular lamination sets do, in fact, contain a seasonal signal. The author, under the supervision of Prof. Anson Mackay (UCL), carried out the diatom analysis in this chapter.

This chapter is, therefore, divided into the following sections. Firstly, the lamination sets are characterised (thin section descriptions and μ-XRF data) in terms of their composition (lamination types) and how it varies throughout LFa-2. It is the variability in lamination set structure that is used to determine the sampling strategy for the diatom, pollen and O/C isotopic analyses. Secondly, the results of these analyses are described in terms of variations in microfossil and isotopic composition of the individual lamination types. Finally, the chapter concludes by discussing the data presented to produce a model for sediment deposition within LFa-2.

7.1. Introduction

As the literature review on varve formation in chapter 4 demonstrates, the development of a robust model for varve formation is a key step in the process of producing a varve chronology. This is particularly important for the Marks Tey sequence (which is purportedly varved), where estimations about the number of laminations preserved have been used to determine the length of MIS 11c (Shackleton and Turner, 1967; Turner, 1970; 1975). The depositional model of Turner (1970) is based on thin section descriptions for selected core depths and unpublished high-resolution pollen analysis (Fig. 7.1). While the sediment structures described by Turner (1970) are analogous to processes that produce biochemical varves in modern environments (Kelts and Hsu, 1978; Lotter et al., 1997; Brauer, 2004; Giguet-Covex et al., 2010), no quantitative evidence has been published to validate this model.

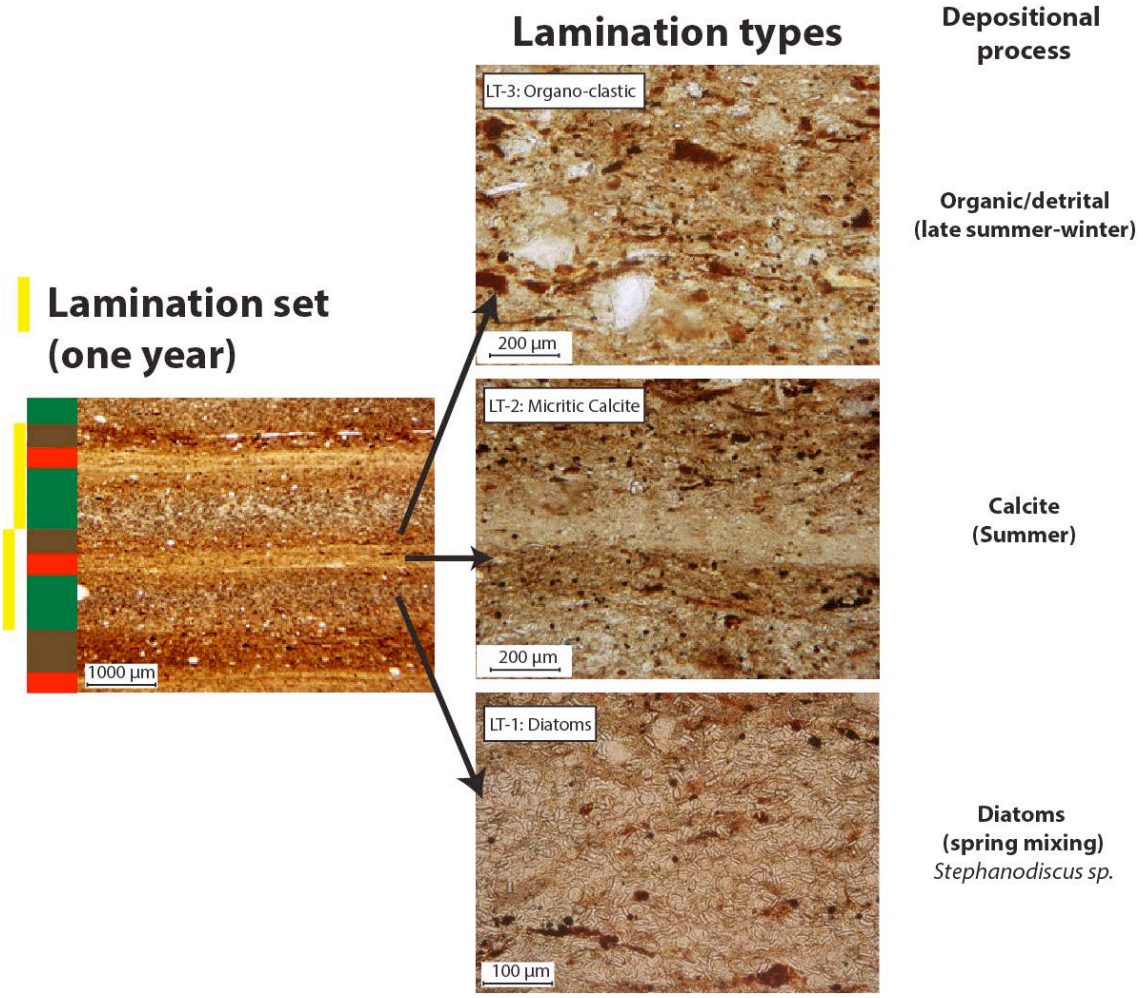

Figure 7.1. *Thin-section images highlighting the model for varve formation proposed by Turner (1970). Each varve is composed of three lamination types: LT-1) a diatom-rich lamination composed of Stephanodiscus spp., formed during the late winter/spring, LT-2) a calcite lamination formed during the summer, and LT-3) a lamination of organic and detrital (organo-clastic) material formed during later summer/winter.*

Furthermore, the sedimentary structures in parts of the sequence are ambiguous; the irregularly bedded and laminated sediments contained within LFa-1, for example (see figure 6.3 in chapter 6). It has already been demonstrated in chapter 6 that the sediments in LFa-1 are not varved, but a detailed micro-facies investigation of LFa-2 is also required to provide quantitative evidence for the repetition of seasonal depositional processes.

7.2. Micro-facies descriptions of LFa-2

This section presents more detailed micro-facies descriptions of the lamination sets preserved in LFa-2, than the basic structure (three lamination types) that was outlined in chapter 6. In this study, the sediments are divided into lamination sets (combinations of lamination types that make up a repeating set). The basic lamination types comprise the same sediment components (diatoms, calcite, organic debris, mineral grains), however, it is the arrangement of these different types in varying patterns/thicknesses that generate different lamination sets (Fig. 7.2). This data is presented in table 7.1 and figure 7.2; the prominent characteristics of each lamination type are described below.

7.2.1. Lamination Type 1 (characterised by diatoms)

LT-1 is characterised by the dominance of centric diatoms (predominantly *Stephanodiscus* sp.), which compose between 10 - >50% of the lamination (Table. 7.1, Fig. 7.1), with variable amounts of calcite and organic debris. Variation in the structure of LT-1 is the result of changes in the relative abundance of diatom frustules compared to the calcite and organic material. LT-1 can be split into two sub-lamination types: LT-1.1 and LT-1.2. In LT 1.1, the lower unit contact is sharp (occasionally diffuse) while the upper contact is diffuse (Table 7.1). These contacts are the result of diatom abundances that compose <50% of the lamination, with rest of the lamination composed of amorphous organic detritus (30-50%), with occasional calcite crystals (up to 30%) (Table 7.1, Fig 7.2). LT-1.2 is characterised by sharp lower contacts (occasionally diffuse), sharp upper contacts and high abundances of centric diatom frustules (>50%), while amorphous organic debris and calcite crystals account for the minor component of the lamination (<10 – 50%) (Table 7.1, Fig. 7.2).

The µ-XRF data in figure 7.3 provides an example of how the major elements that comprise the sediments in the core vary over six lamination sets. The only component to show a distinctive peak associated with LT-1 is the Mn/Fe ratio, while Si, Ti and K all show decreasing trends (Fig. 7.3). The trend in Si is particularly interesting, given the presence of diatom silica. This trend is likely due to the increase in Ca counts that are observed through LT-1, which may have a dilution effect on the Si (Fig. 7.3).

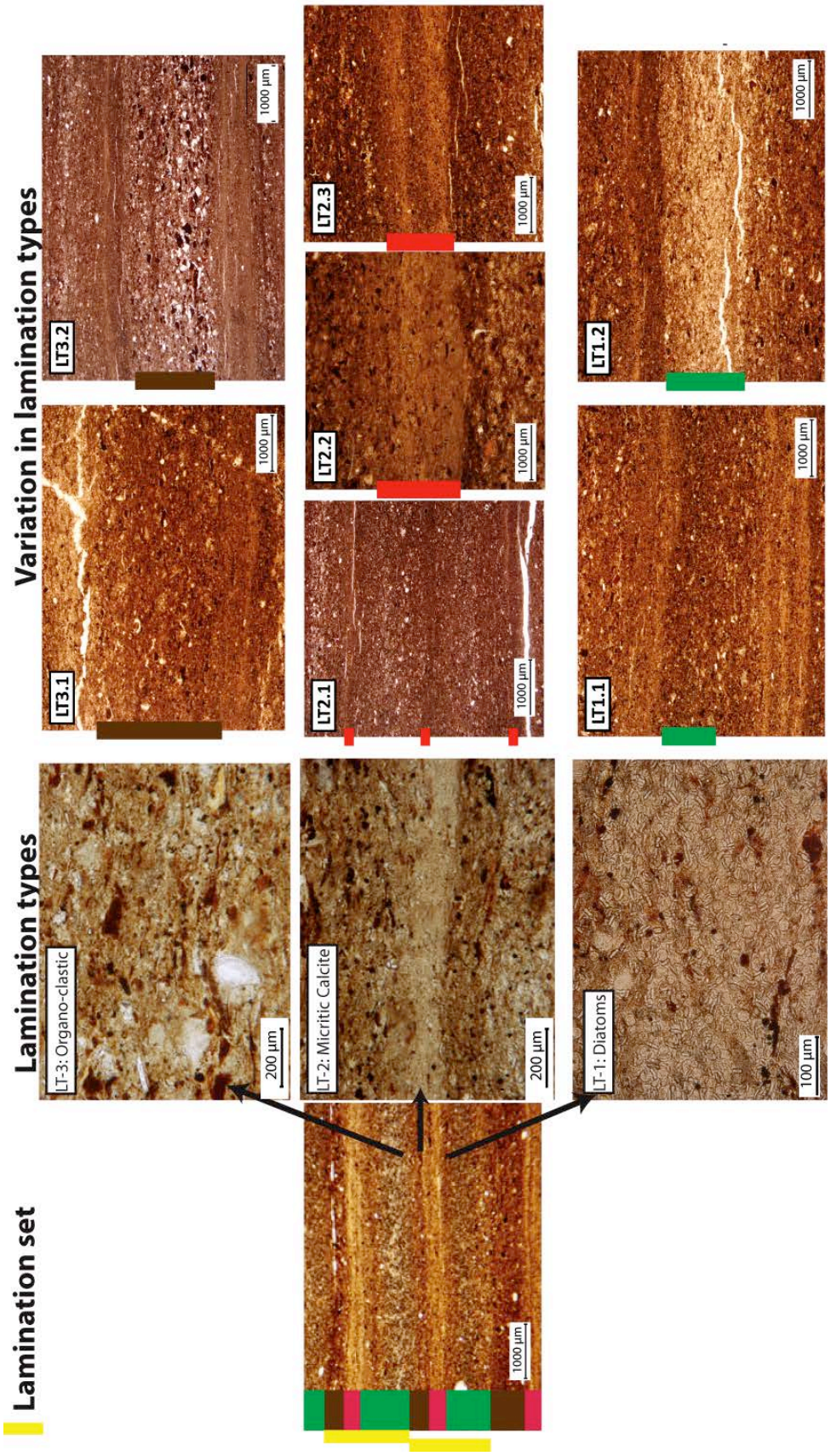

Figure 7.2. *Thin section images showing variations in structure of the lamination types in LFa-2. LT-1 is characterised by the abundance of diatoms (LT-1.1: <50%, LT-1.2: >50%), LT-2 is sub-divided on the basis of calcite abundance (LT-2.1: ≤30%, LT2.2 and 2.3: >50%) and the presence of multiple calcite sub-laminations (LT-2.3). LT 3 is sub-divided on the basis of the abundance of minerogenic material (LT-3.1: ≤10% and LT3.2: 10-30%).*

Table 7.1. *Summary of the criteria used to describe and divide the lamination types (LT-1, LT-2, LT-3) into sub-lamination types (e.g. LT-1.1, LT-1.2). The symbols used are explained in the key below.*

Lamination Type (LT)	Unit contacts		Diatoms			Calcite			Organic			Mineral grains					Notes
	Lower	*Upper*	*Abundance*	*Type*	*Sorting/ Grading*	*Abundance*	*Type*	*Sorting/ Grading*	*Abundance*	*Type*	*Sorting/ Grading*	*Abundance*	*Type*	*Size*	*Sorting/ Grading*	*Roundedness*	
LT-1																	
1.1	Shp/Diff in places	Diff	C-F	Ct	Ps	Ra-C	M/MS (occasional Sp).	M	Ab	AM, Fg, Pt	S	Ra	Qtz	Mz	M	SR	Diatom layer, but heavily masked by organic matter and calcite crystals. Diatoms don't form distinct layer, making up less than 50% abundance.
1.2	Shp/Diff in places	Shp/Diff	Ab	Ct	Ws	C-F	M/MS (occasional Sp)	M	R-C	AM, Fg, some Pt	S	Ra	Qtz	Mz-Cz	M	SA-R	Matrix consists of diatoms and calcite crystals with small amounts of organic material. Diatoms are the most abundant component, consistently composing >50% of the lamination.
LT-2																	
2.1	Diff	Diff	Ra	Pn	-	C	M	S	F-Ab	AM, Fg, Pt	S	Ra	Qtz	Mz	M	SR	Lamination contains a mixture of calcite crystals and organic material. Calcite does not form a pure layer, but rather is scattered throughout a matrix of mainly amorphous organic material. The material in the lamination is sorted, which makes it distinctive.
2.2	Shp/Diff	Diff	Ra	Pn	-	A	M	WS/N	Ra	AM, Fg, Pt	-	Ra	Qtz	Fz	M	SR	Lamination of almost pure micritic calcite, characterised by generally sharp basal contact. Upper contact is gradational due to increase in abundance of organic material.
2.3	Shp/Diff	Diff	Ra	Pn	-	A	M	WS/Lam	Ra	AM, Fg	S/Lam	Ra	Qtz	Fz-Mz	M	SA-SR	Pure micritic calcite. Appears laminated due to sub-laminations (diffuse contacts) of more organic rich material. Contains 2-3 sub-laminations of calcite.
LT-3																	
3.1	Diff	Shp/Diff	Ra	Pn/Ct	-	C-F	M,MS, Sp, Sh	M	Ab	AM,Fg, Pt	PS	C	Qtz	Fz-Mz	M	SR-SA	Organo-clastic lamination composed of a mixture of organic material, calcite (including shell fragments) and mineral grains. Diatoms are not readily observed. Massive structure, occasional fine lenses of mineral material.
3.2	Diff	Shp/Diff	Ra	Pn/Ct	-	F-Ab	M, MS, Sp, Sh	PS	F-Ab	AM, Pt, Fg	PS	F	Qtz	Fz-VFSa	M	A-SR	Characterised by the increase in size of mineral,organic and calcite grains. Also contains more frequent shell material (still rare on scale used). Frequently displays a massive structure
Detrital layers																	
1	Shp	Shp	Ra-C	Pn/Ct	Ps	F-Ab	M, MS, Sp, Sh	PS	F	Pt, Fg	PS	F-Ab	Qtz	Mz - MSa	M	A-SR	Lamination characterized by sharp upper and lower contacts. Mixture of calcite grains of all sizes (including shell fragments) and mineral grains that can reach MSa particle size.

KEY:

Abundance:
Ab = Abundant (>50%)
F = Frequent (30-50%)
C = Common (10-30%)
Ra = Rare (<10%)

Sorting/Grading/Contacts:
Ws = Well sorted
S = Sorted
Mso = Moderately sorted
Ps = Poorly sorted
N = Normal grading
Lam = Laminated
M = Massive
Diff = Diffuse
Shp = Sharp

Diatoms:
Ct = Centirc
Pn = Pennate

Calcite crystals:
M = Micrite (<4um)
MS = Microspar (4-50um)
S = Spar (>50um)
Sh = Shell

Organic material:
AM = Amorphous
Fg = Fine grained
Pt = Particulate

Mineral grains/Size/Roundedness:
Qtz = Quartz
VFz = Very fine silt
Fz = Fine silt
Mz = Medium silt
Cz = Coarse silt
VFSa = Very fine sand
MSa = Medium sand
A = Angular
SA = Subangular
SR = Subrounded
R = Rounded

7.2.2. Lamination Type 2 (calcite dominated)

LT-2 is characterised by an increase in the concentration of micritic calcite (Fig. 7.2). Variation in the structure of LT-2 is due to the relative abundance of these calcite crystals, as well as the number of calcite sub-laminations that occur (fig. 7.2), resulting in the identification of three sub-lamination types. LT-2.1 is characterised by diffuse upper and lower contacts, the result of low concentrations of calcite crystals (up to 30%), with the rest of the lamination dominated by amorphous organic material (30 - >50%) (diatom frustules are rarely observed in thin section) (Table 7.1, Fig. 7.2). LT-2.2 represents a single lamination composed almost entirely of fine-grained micritic calcite crystals (>50%) that displays sharp/diffuse lower contacts and diffuse upper contacts (Table 7.1, Fig. 7.2). This lamination type occurs most frequently throughout the sequence, its form and structure analogous to the calcite lamination described by Turner (1970); a sharp basal contact and diffuse upper contact with LT-3. The calcite found in the third sub-lamination, LT-2.3, is very similar in terms of its abundance (>50%) to LT 2.2, also has sharp/diffuse lower and diffuse upper unit contacts, but occurs as multiple sub-laminations (two or three have been observed), between which fine layers of amorphous organic detritus occur. Contacts between the sub-laminations in LT 2.3 are diffuse (Fig. 7.2). Peaks in Ca counts highlight the increase in abundance of calcite within this lamination type, while the Mn/Fe ratio is low and Si, Ti, K and display generally low counts (Fig. 7.3).

7.2.3. Lamination Type 3 (organo-clastic dominated)

LT-3 is an organo-clastic lamination characterised by an abundance of amorphous and particulate organic matter (30 - >50%), as well as minerogenic material (10 - >50%) (Table 7.1, Fig 7.2). Diatoms (both centric and pennate) are present in the matrix, but do not occur in high enough concentrations to form a discrete sub-layer (<10%). LT-3 has diffuse lower and sharp/diffuse upper contacts and can be divided into two sub-lamination types, based on variations in the concentration of mineral grains, which range in size from medium silt to fine sand (Table 7.1, Fig 7.1). LT-3.1 contains mineral grains that compose up to 10% of the lamination with particle sizes from fine to medium silt, whereas LT-3.2 contains mineral grains in concentrations between 10-30%, with particle sizes that range from fine silt to coarse sand (Table 7.1).

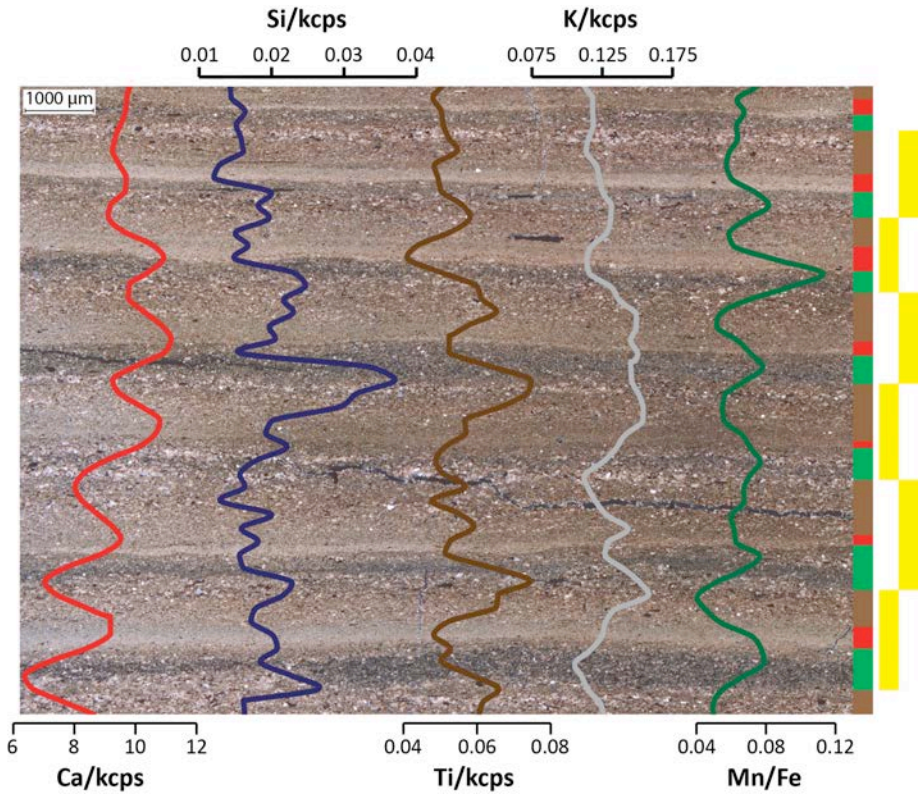

Figure 7.3. *µ-XRF element count data plotted on top of a thin section image (cross-polarised light) of six lamination sets (highlighted by yellow bars to the right of the image). Individual lamination types are also highlighted on the right hand side of the image: LT-1 (green bars), LT-2 (red bars) and LT-3 (brown bars). Count data for Ca (red), Si (blue), Ti (brown) and K (grey) are normalised to kilo counts per second (kcps). The Mn/Fe ratio (green) is also shown.*

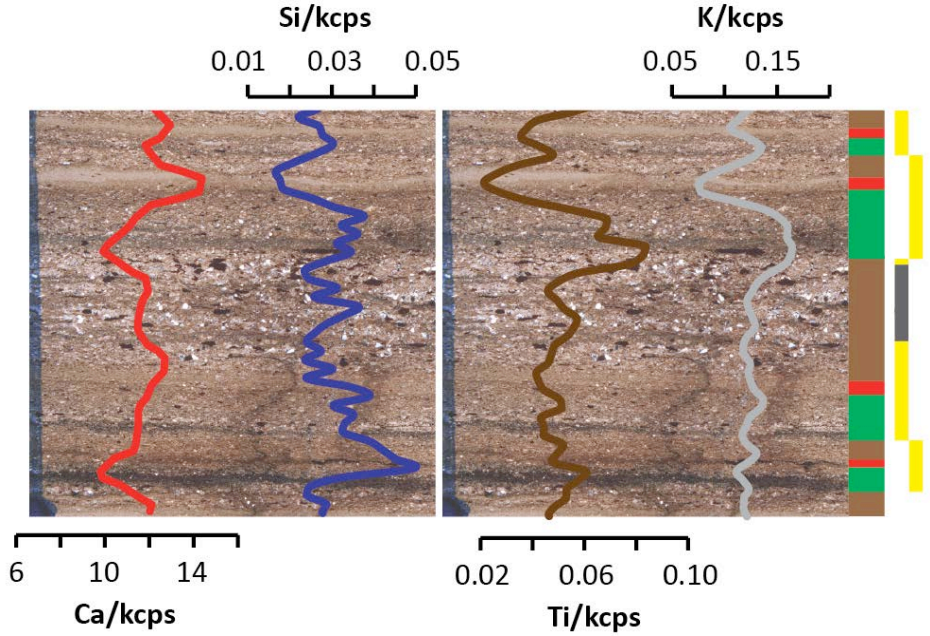

Figure 7.4. *µ-XRF element count data characterising the elemental composition of detrital layers that can occur within the lamination types. Element counts for Ca (red), Si (blue), Ti (brown) and K (grey) are plotted on top of a thin section image (cross-polarised light) of four lamination sets (highlighted by yellow bars to the right of the image). Individual lamination types are also highlighted on the right hand side of the image: LT-1 (green bars), LT-2 (red bars) and LT-3 (brown bars). The grey bars on top of the yellow bars indicate the location of detrital layers that can occur within the lamination types. The figure shows one detrital layer in LT-3 of the second lamination set of the sequence.*

There is a distinct overlap in particle roundness between the two sub-lamination types, with LT-3.2 containing more angular grains (Table 7.1). The μ-XRF data for this LT shows a decrease in the count rate of Ca, while the Mn/Fe ratio also low (Fig. 7.3). The Si, Ti and K graphs indicate elevated counts in LT-3, with Si and Ti often displaying multiple peaks (Fig. 7.3).

7.2.4. Detrital layers

The basic sequences of lamination types that compose the lamination sets described above represent the dominant, repeating pattern of sedimentation that occurs throughout LFa-2. This depositional succession can be interrupted, however, by the occurrence of detrital layers, which form discrete sub-laminations within the three lamination types (Fig. 7.4). These detrital layers are distinct from the lamination types in terms of their structure and composition. These layers are characterised by sharp lower and upper contacts and have a massive structure. They contain carbonate (30 to >50%) with a range of crystal sizes (micrite to spar), as well as particulate organic fragments, shell fragments, pennate/centric diatoms and mineral grains (Table 7.1 and Fig 7.4). The structure is also shown by the μ-XRF data in figure 7.4. The detrital layers are characterised by peaks in SK, Ti and Si, and to a lesser extent Ca (Fig.7.4).

7.2.5. Use of micro-facies descriptions to direct sampling strategy for microfossil analysis

The micro-facies descriptions show that the lamination sets present within LFa-2 are composed of three main lamination types; LT-1: which is characterised by the dominance of centric diatom frustules, LT-2: which is dominated by micritic calcite, and LT-3: which is characterised by organic matter and minerogenic material. As it was not possible to document the variation in diatom and pollen species with lamination type by analysing the thin sections alone, it was decided that a block of sediment would be cut from the core and the lamination sets split into lamination types, to prepare microscope slides for diatom and pollen analyses. Due to the consistency in lamination set structure throughout LFa-2, a single block of sediment was cut from the core where the thickest lamination sets occurred (14.75 – 14.80mbs) and the contacts between the lamination types were readily visible (Fig. 7.2).

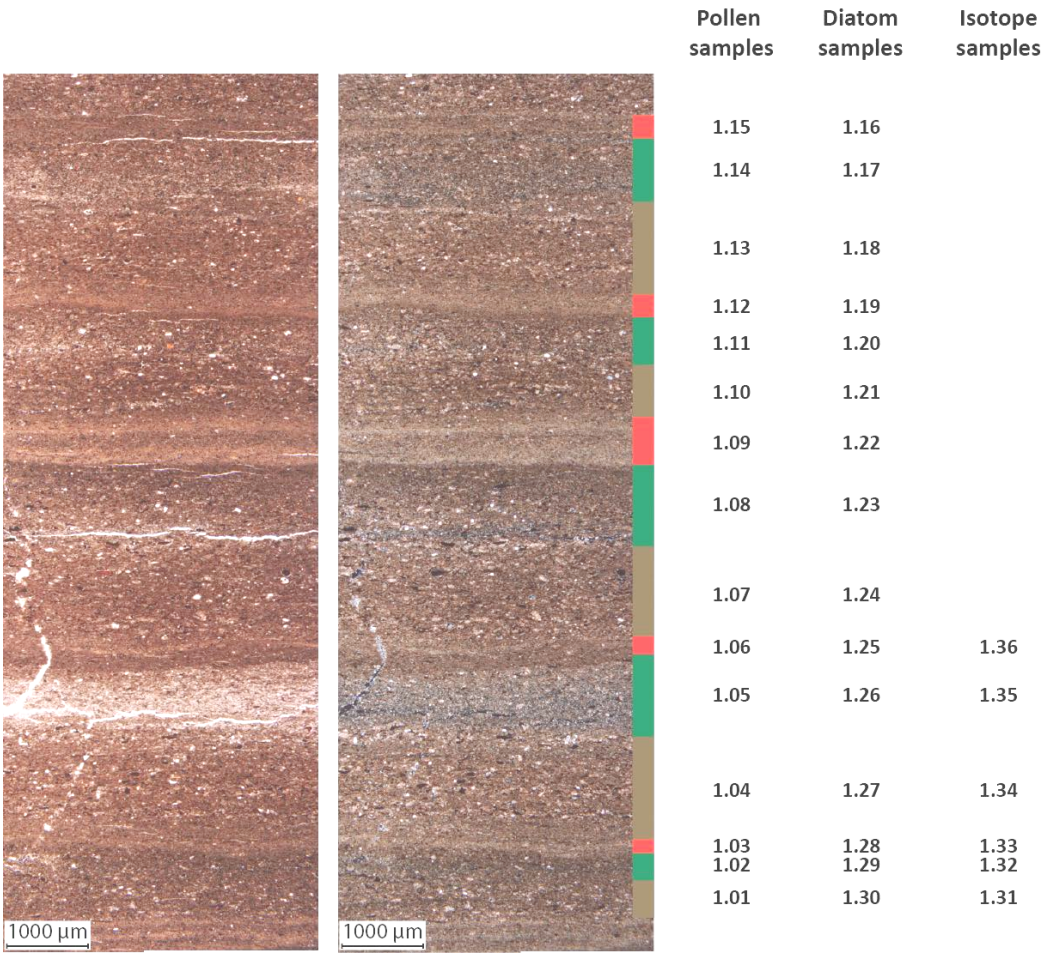

Figure 7.5. *Paired microphotographs showing the lamination types sampled for pollen, diatom and O/C isotopic analysis. The image on the left is taken under plain-polarised light and the image on the right under cross-polarised light. Lamination types are highlighted by the coloured bars to the right of the cross polarised image (LT-1 = green, LT-2 = red and LT-3 = brown). The corresponding sample numbers are shown to the right hand side of the figure.*

7.3. Diatom and Pollen analysis of the lamination types

Results of the diatom and pollen counts from individual lamination types are presented as stratigraphical variations in percentage composition and concentrations in figures 7.6 and 7.8. The results of principal component analysis (PCA) on the concentration data for both is also presented in figure 7.7 and 7.9.

7.3.1. Diatoms

Apart from some centric species that occur in low percentages and concentrations (e.g. *Cyclotella radiosa*, *C. comensis*, *Aulacoseira subarctica*), there are no distinctive changes in the composition of dominant species between the lamination types, as all contain a similar diatom flora (Fig. 7.3). There are, however, obvious species trends in both the relative abundance and valve concentration data with lamination type.

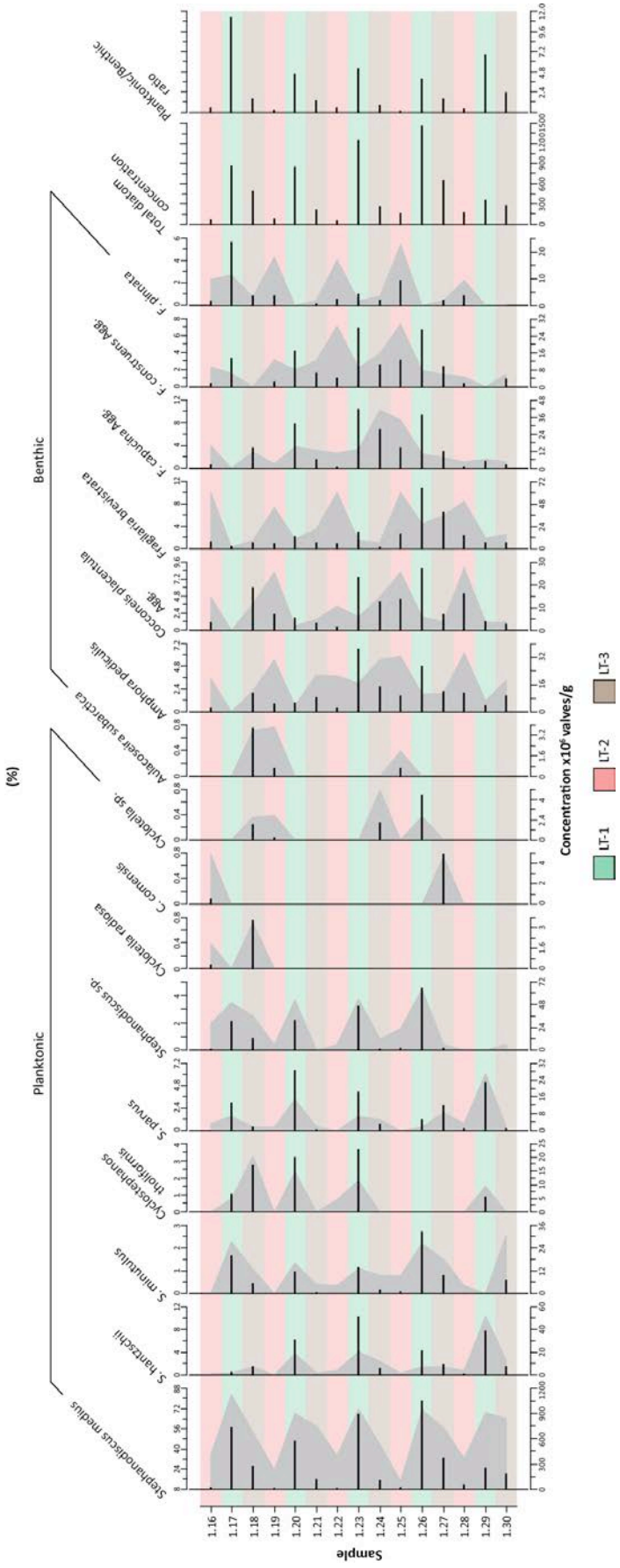

Figure 7.6. *Results of diatom counts from the lamination types of selected taxa, presented as percentage (grey silhouette) and concentration (black lines) data. Each sample is shaded to represent the lamination type it came from.*

7.3.1.1. Lamination Type 1

Apart from sample 1.29, taken from the thinnest LT-1 sampled (Fig. 7.5), LT-1 contains the highest concentrations of diatoms in the dataset (Fig. 7.6). This LT is dominated by *Stephanodiscus medius*, a planktonic diatom that accounts for between 68 – 83% of species composition and concentrations of at least twice that of LT-2 and LT-3 (504 – 1057 x 10^6 valves/g) (Fig. 7.6). *S. hantzschii* and *S. parvus* also occur in all of the samples counted, but do not always occur in higher percentages or concentrations relative to the LT's adjacent to them. Peaks are also observed in *S.minutulus* and *Cyclostephanous tholiformis*, although these species do not occur in every sample (Fig. 7.6). LT-1 is also characterised by generally low peaks in the percentage composition of benthic species when compared to LT-2 and LT-3, such as *Cocconeis placentula, Fragilaria brevistrata, F. construens* and *F. pinnata* (Fig. 7.6).

Concentrations are variable for these species; *C. placentula, F. brevistrata* and *F. construens,* for example, show the opposite trend to the percentage data, with relatively low percentage composition corresponding to peaks in the concentration data (Fig. 7.3). It should be noted, however, that benthic species occur in concentrations one to two orders of magnitude lower than the planktonic species in LT-1.

7.3.1.2. Lamination Type 2

In contrast to LT-1, LT-2 contains the lowest diatom concentrations of the dataset (~62-182 x 10^6 valves/g). This large drop is caused by very low concentrations of the planktonic species in this LT, in particular *S. medius*, which occurs in concentrations of 22-60 x 10^6 valves/g (Fig. 7.6). The trend in the planktonic species concentration data is also shown by the percentage data, where planktonic species account for 18-40% of species composition (Fig. 7.6). LT-2 is therefore characterised by benthic species; with *C. placentula, F. brevistrata* and *F. pinnata* all showing peaks in percentage composition (Fig. 7.6). The benthic community is composed of a diverse flora, with 96 species identified. As a result, most of these species occur in very low numbers and concentrations but, when combined, dominate the assemblage.

7.3.1.3. Lamination Type 3

In terms of total concentration, LT-3 consistently contains higher diatom concentrations than LT-2, but lower concentrations than LT-1 (Fig. 7.6). This intermediate position is characterised by an increase in the percentage composition (50-79%) and concentration of planktonic species (135-417 x 10^6 valves/g), in particular *S. medius* (Fig. 7.6). *S. minutulus*, *C. tholiformis* and *S. parvus* all show isolated peaks in both percentage composition and concentration, but these are anomalous in terms of the dominant trend in these species (Fig. 7.6). The *Cyclotella* species and *Aulacoseira subarctica* also show a preference for this LT, but these species only occur sporadically throughout the dataset (Fig. 7.6).

7.3.1.4. Statistical analysis of the diatom data

The diatom data presented in figure 7.6 shows clear trends in both species composition and abundance with lamination type. These relationships were also explored statistically to determine the main gradients within the dataset using multivariate statistical analyses. Performing DCA on the concentration data indicated that axis 1 had a short gradient (1.48 SD), so PCA was used to explore patterns in the diatom species data (Birks, 1998). The scatter-plot of the first two principal component axes in figure 7.7 shows the PCA of the diatom concentration data. PCA axis 2 accounts for only 7.4% of the variance, with no clear pattern observed (Fig. 7.7). Axis 1, however, accounts for 66.3% of variance within the dataset, with a clear trend observed in the location of lamination types along the axis. LT-1 (positive scores) and LT-2 (negative scores) exhibit the greatest difference in species composition, while LT-3 (and sample 1.29 from LT-1) occurs as an intermediate group between them (Fig. 7.7). *S. medius (StepMedi)* is the most important species for axis 1, while other planktonic species such as *S. minutulus (StepMinu)* and *S. hantzschii (StepHant)* are also important, and *S. parvus (StepParv)* and *C. tholiformis (CyclThol)* are important for both axis 1 and 2 (Fig. 7.7). Samples from LT-1 are all characterised by the presence of these centric species (1.17, 1.20, 1.23 and 1.26), with samples 1.17 and 1.20 characterised by greater concentrations of *S. hantschii* and *S. parvus*, while sample 1.26 shows a greater correlation with *S. minutulus* (Fig. 7.7).

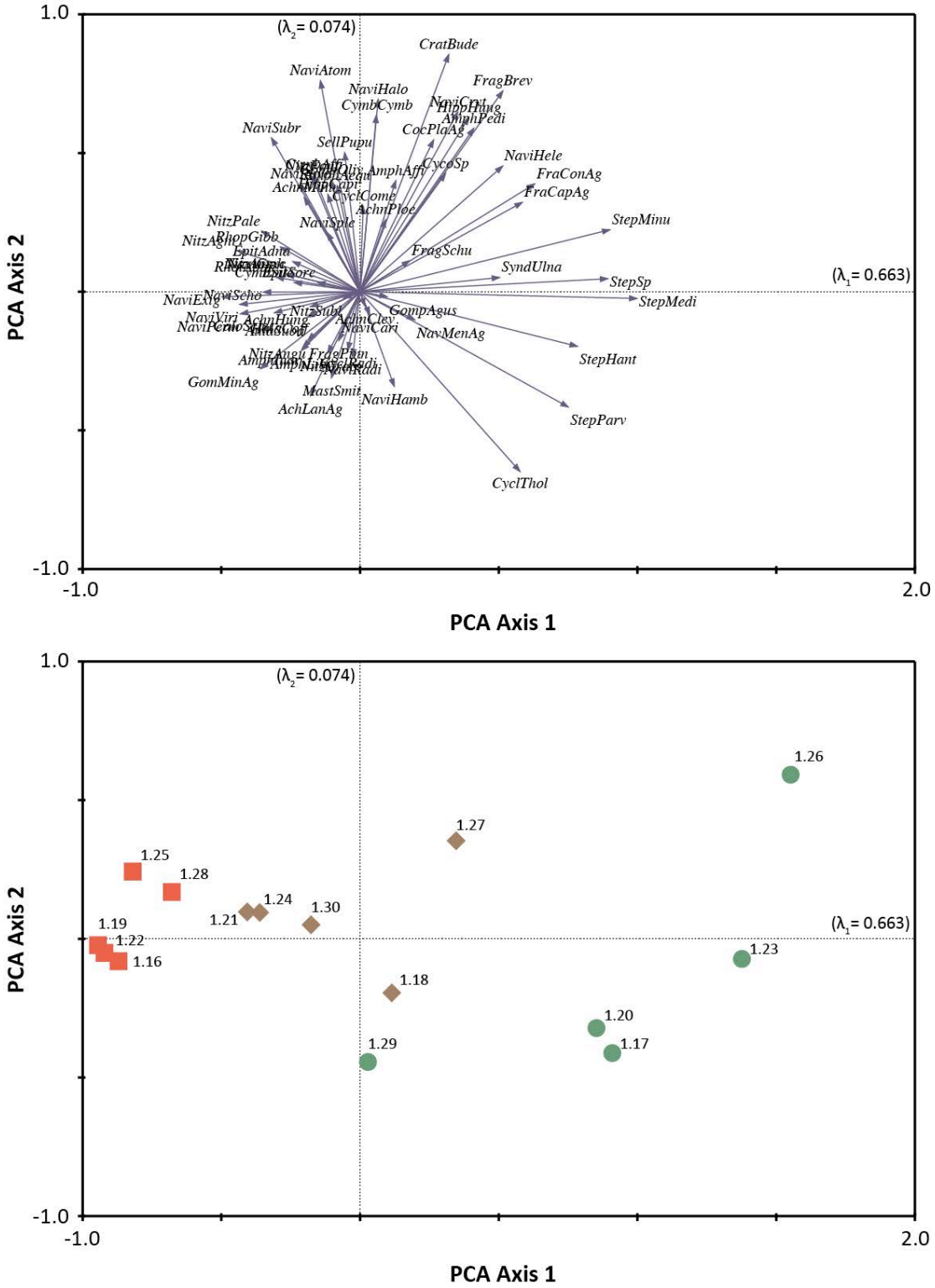

Figure 7.7. *Plot of PCA axis 1 and 2 of the diatom concentration data from individual lamination types, plotted as A) species and B) lamination type. The colour code for lamination types is consistent with figure 7.3, with LT-1 indicated by green dots, LT-2 by red squares and LT-3 by brown diamonds. Axis 1 accounts for 66.3% of total variance experienced by the dataset, while axis 2 accounts for 7.4%.*

Diatoms with the strongest negative correlations on axis 1 are the Naviculiod species *N. perminuta*, *N. exigua, N. viridula var. lineata* and *N. schoenfeldi* (Fig. 7.7). These benthic species occur in association with the samples from LT-2, which are all closely grouped with one another (Fig. 7.7). Along with sample 1.29, the samples from LT-3 form an intermediate group between LT-1 and LT-2 (Fig. 7.7). Samples 1.21, 1.24 and 1.30 have negative scores on axis 1 and show a greater affinity for benthic species, while 1.18, 1.27 from LT-3 and 1.29 from LT-1 have positive axis 1 scores and are characterised by higher concentrations of planktonic species. Sample 1.29 from LT-1 is the only sample that overlaps with another lamination type (LT-3). Sample 1.29 has a high planktonic/benthic ratio (6.88), but total valve concentrations are relatively low when compared with other samples from LT-1, so is therefore more comparable to those from LT-3 (Fig. 7.6, 7.7). Sample 1.29 also appears to be unique in terms of its sedimentology, with the thin section image in figure 7.5 indicating that the lamination has low diatom concentrations, as well as being the thinnest LT-1 sampled.

7.3.2. Pollen

Results from pollen analysis of the lamination types are presented as stratigraphical changes in percentage composition and concentration in figure 7.8. *Betula, Quercus, Alnus, Corylus and Poaceae* dominate the assemblage.

7.3.2.1. Lamination Type 1

LT-1 is characterised by peaks in concentrations of *Betula, Ulmus, Alnus, Quercus* and *Corylus*, with percentage composition variable. *Ulnus and Alnus* display a clear trend in LT-1, with peaks in concentration (up to 26 x 10^3 and 154 x 10^3 grains/g, respectively) and percentage composition occurring in four of the five laminations sampled (sample 1.02, 1.05, 1.11 and 1.14), when compared to the lamination types adjacent to them (Fig. 7.8). The highest concentrations of *Quercus* also occur in LT-1 (up to 94 x 10^3 grains/g), with peaks in four laminations (1.05, 1.09, 1.11 and 1.14) (Fig. 7.9). The same relationship is observed for *Betula, Corylus* and Poaceae, with peaks occurring in three of the five laminations sampled (1.05, 1.11 and 1.14) (Fig. 7.8).

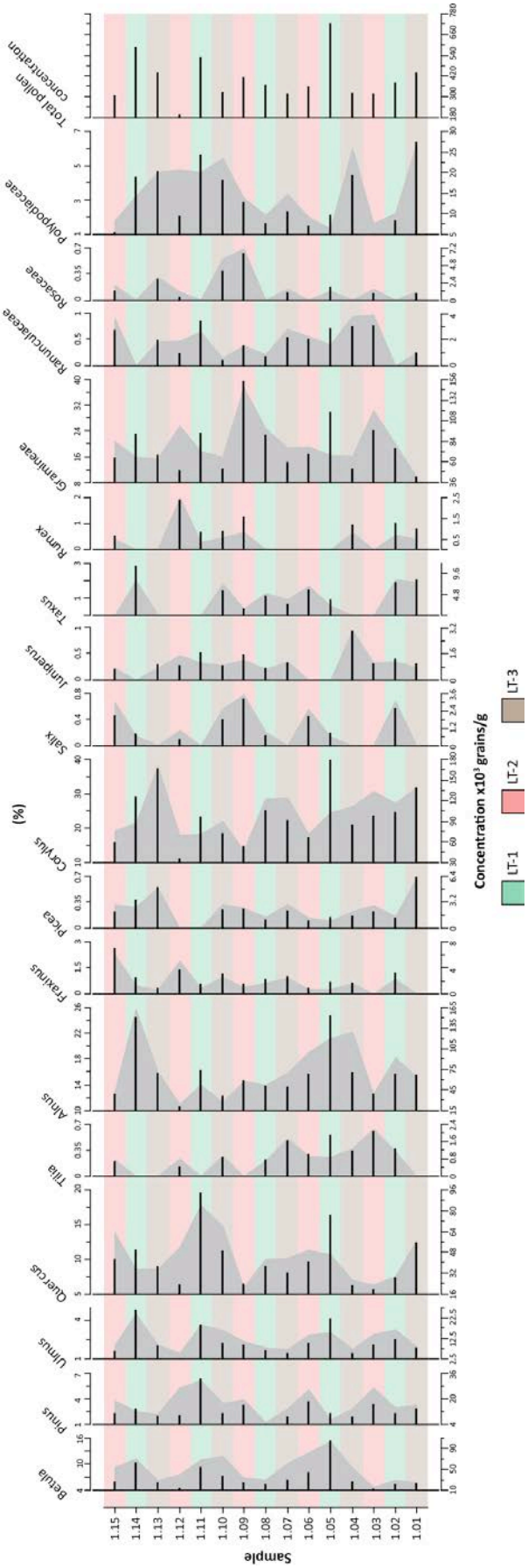

Figure 7.8. *Results of pollen counts from the lamination types of selected taxa, presented as percentage (grey silhouette) and concentration (black lines) data. Each sample is shaded to represent the lamination type it came from.*

The peaks in concentration of *Betula* (samples 1.05, 1.11 and 1.14) represent the highest concentrations for the species in the dataset (up to 107 x 10^3 grains/g) (Fig. 7.8). While the peaks seen in *Corylus* (samples 1.05, 1.08 and 1.11) and *Poaceae* (samples 1.05, 1.11 and 1.14) are distinctive in terms of the laminations adjacent to them, the concentrations are not consistently higher than the dataset as a whole (Fig. 7.8).

7.3.2.2. Lamination Type 2

LT-2 is characterised by the presence of *Rumex, Pinus, Tilia, Ranunculaceae, Fraxinus, Rosaceae and Poaceae*. Total pollen concentrations are generally lower than LT-1 and LT-2 also contains the lowest concentrations of the dataset (sample 1.12; 200 x 10^3 grains/g) (Fig. 7.8). The exception to this trend is sample 1.09, the thickest calcite lamination sampled (Fig. 7.5), which contains higher pollen concentrations than both the laminations adjacent to it (Fig. 7.9). The most distinctive species in LT-2 is *Rumex* which, although occurring in low concentrations (up to 2.3 x 10^3 grains/g), peaks in three of the five laminations (1.09, 1.12, 1.15). It is not present, however, in samples 1.03 and 1.06 (Fig. 7.9). Both *Tilia* (samples 1.03, 1.12 and 1.15) and *Ranunculaceae* (samples 1.03, 1.09 and 1.15) reach their highest concentrations (2.1 and 3.2 x 10^3 grains/g) in this LT, although *Tilia* occurs in lower concentrations and is not present in sample 1.09 (Fig. 7.8). *Pinus* is present in every sample, with concentrations between 10 and 18 x 10^3 grains/g, although the highest concentrations for this taxa are observed in LT-1 (sample 1.11), with peaks evident in samples 1.03, 1.06 and 1.09 (Fig. 7.8). *Fraxinus* (samples 1.12 and 1.15), *Rosaceae* (samples 1.03 and 1.09) and *Poaceae* (samples 1.03 and 1.09) also reach their greatest concentrations in LT-2, but only display distinctive peaks in two of the five laminations (Fig. 7.8).

7.3.2.3. Lamination Type 3

LT-3 contains variable total pollen concentrations and is characterised by peaks in *Umbelliferae, Picea, Corylus* and *Polypodiaceae,* with minor contributions from *Quercus, Tilia* and *Juniperus*. *Picea* represents a low proportion of the dataset in terms of both percentage contribution and concentration, but is present in all of the samples taken from LT-3, where it is present in the highest percentages (1.15%) and

concentrations (6.3 x10^3 grains/g), displaying peak values in samples 1.01, 1.07 and 1.13 (Fig. 7.8).

Polypodiaceae and *Umbelliferae* also have peaks in concentration (up to 27 and 3.1 x10^3 grains/g, respectively) and percentage composition (up to 6.2 and 1%, respectively) in four of the five laminations sampled (samples 1.01, 1.04, 1.07 and 1.13), although *Umbelliferae* is not present in sample 1.10 (Fig. 7.8). *Corylus* occurs in higher concentrations than *Picea* and *Umbelliferae* (up to 168 x10^3 grains/g), but only displays peak values in two of the laminations sampled (1.01 and 1.13). *Tilia* is not present in samples 1.01 and 1.13, but does occur as peaks in concentration and percentage in samples 1.07 and 1.10 (Fig. 7.9). *Quercus*, although occurring in relatively high percentages and concentrations in this LT (12.7% and 56 x10^3 grains/g, respectively), only displays a peak that is distinctive from the laminations adjacent to it in sample 1.01 (Fig. 7.9).

7.3.2.4. Statistical analysis of the pollen data

The pollen concentration data was also explored statistically to determine the main relationships between the taxa and lamination type. As with the results obtained from statistical analysis of the diatoms, a DCA on the pollen concentration data indicated that axis 1 had a short gradient (0.61 SD), so PCA was used to explore patterns in the pollen data (Birks, 1998). The first two principal component axes for the pollen taxa and sample data are presented in figure 7.9. The first principal component axis explains 44.4% of variation in the dataset, while axis 2 represents 14.5% of the variation. Positive axis scores dominate axis 1 for *Alnus, Betula, Ulmus, Quercus* and to a lesser extent *Taxus*, which correspond to samples 1.05, 1.11 and 1.14 from LT-1 (Fig. 7.9). Corylus, *Carpinus, Poaceae, Pinus* and *Sparganium* are important for both axis 1 and 2. *Rumex, Juniperus* and to a lesser extent *Tilia*, *Rosaceae* and *Ranunculaceae* are also important for axis 1, displaying negative axis scores, which correspond to samples 1.03, 1.12 and 1.15 from LT-2 (Fig. 7.9). The dispersion of these samples along axis 1, along with those from LT-1 described above (1.05, 1.11, 1.14), indicate that they contain different species compositions, while samples 1.02 and 1.08 (LT-1) and 1.06 (LT-2) hold intermediate positions and plot close together, therefore indicating floristic compositions that are also intermediate between the two groups (Fig. 7.9).

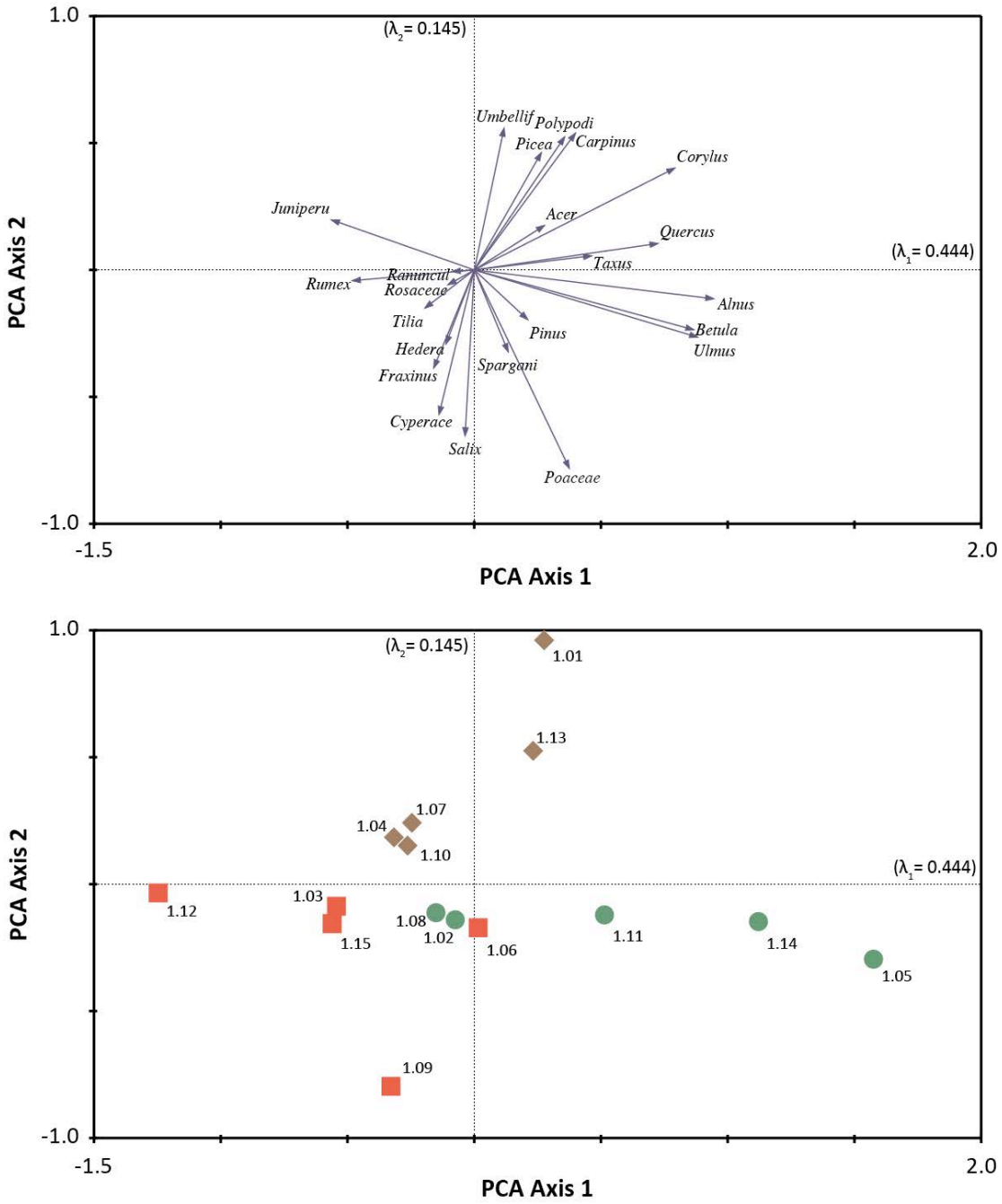

Figure 7.9. *Plot of PCA axis 1 and 2 of the pollen concentration data from individual lamination types, plotted as A) species and B) lamination type. The colour code for lamination types is consistent with figure 7.5, with LT-1 indicated by green dots, LT-2 by red squares and LT-3 by brown diamonds. Axis 1 accounts for 44.4% of total variance experienced by the dataset, while axis 2 accounts for 11%.*

Samples from LT-3 are the most dispersed along axis 2 in comparison with LT1 and LT2, which all have positive axis scores, while the samples from LT-1 and LT-2 all have negative scores (Fig. 7.9). *Umbelliferae* and, to a lesser extent, *Picea, Polypodiaceae* and *Carpinus*, are important for axis 2, displaying positive axis scores which correspond to samples 1.01 and 1.13 from LT-3, while the other samples from this LT (1.04, 1.07 and 1.10) have a slightly different species composition, characterised by *Juniperus* (Fig.

7.9). *Salix* and *Cyperaceae* are also important for axis 2, allied to *Poaceae, Sparganium, Fraxinus* and *Hedera*, which all have negative axis scores (Fig. 7.9). These species are characteristic of sample 1.09 from LT-2 (Fig. 7.9).

7.3.3. Stable isotopes

Figure 7.10 presents the oxygen and carbon stable isotope results, which are plotted as a biplot, as well as stratigraphically by lamination type. Figure 7.8a also shows the results of samples taken from calcareous rich Anglian till that forms the major exposed sediment body in the immediate catchment. Although based on a small dataset, $\delta^{18}O$ does not co-vary with $\delta^{13}C$ (R^2 = 0.064, n = 18) for the dataset from the lamination types (Fig. 7.10a). There is also an interesting relationship between this dataset and the results from samples of the Anglian till. $\delta^{18}O$ values of the LT samples have a range -4.03 to -3.43‰, whereas the samples from the catchment have a greater range, from -4.39 to -2.69‰. The same is true for $\delta^{13}C$, where the LT samples range from 0.01 to 0.83‰, whereas the catchment samples range from 0.09 to 1.35‰. The dataset from the lamination types therefore plot within the range of values from the catchment samples.

When plotted by lamination type, it is clear that there is variation in both the $\delta^{18}O$ and $\delta^{13}C$ values within each lamination type, a trend more apparent in the $\delta^{18}O$ data (Figure 7.10b). The average $\delta^{18}O$ values (black data points) in figure 7.10b indicate that LT2 exhibits lower $\delta^{18}O$ values (-3.85 to -3.91‰) than LT1 and LT3 (-3.43 to -3.64‰) and apart from sample 1.35 (LT1), LT1 and LT3 exhibit values that cannot be separated when analytical errors are taken into consideration. There is far greater variability, however, when the individual samples within lamination types are considered (grey data points). Including analytical errors, all but one of the lamination types sampled overlap to varying degrees, making them indistinguishable from one another. The only exception to this is sample 1.33 (LT-2), which overlaps with sample 1.36 (also from LT-3), but displays consistently lower $\delta^{18}O$ values (-3.85 to -4.03‰) than samples from LT-1 and LT-3 (Figure 7.10b).

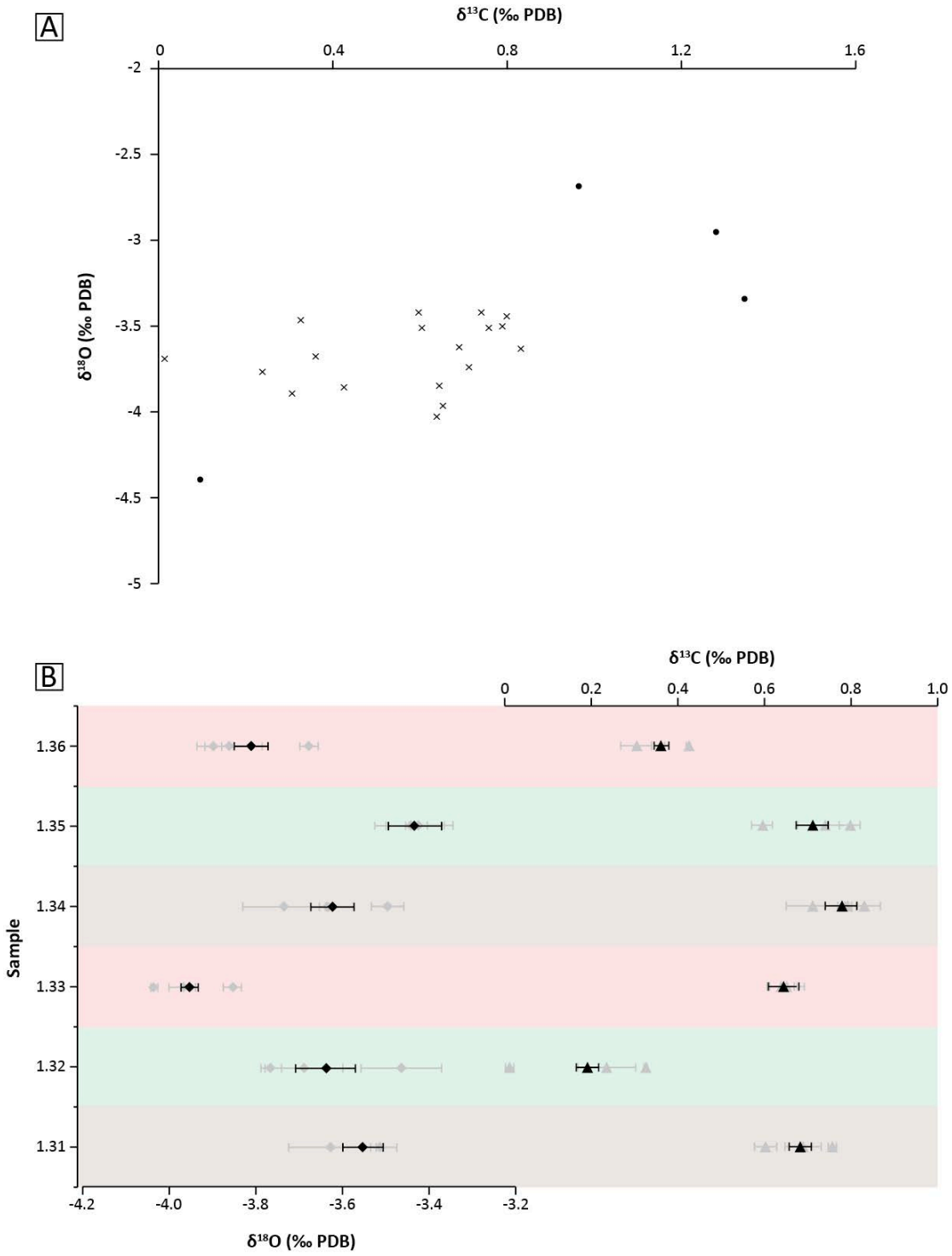

Figure 7.10. *Oxygen and carbon isotope results from six contiguous lamination types, the location of which are shown in figure 7.2. Three samples were taken from each lamination type, giving 18 samples in total. This data (crosses) is plotted as an oxygen vs. carbon biplot (R^2 = 0.064) (A), along with four samples of detrital carbonate taken from Anglian till in the immediate catchment (circles). The data is also plotted by lamination type (B). Each lamination type contains three individual samples (grey data points), with the average of these three data points also shown (black data points). Samples shaded in green are from LT-1, red from LT-2 and brown are from LT-3.*

The $\delta^{13}C$ values from individual samples within the lamination types (grey data points) in Figure 7.10b are less variable than the $\delta^{18}O$ values. The average $\delta^{13}C$ values for each lamination type indicate that sample 1.32 (LT-1) has the lowest $\delta^{13}C$ value (0.19±0.03‰) while sample 1.36 (LT-2) is also distinctive, with an average value of 0.36±0.02‰ (Figure 7.10b). Within the rest of the dataset, sample 1.34 (0.78±0.04‰) displays higher values than sample 1.33 (0.64±0.04‰), but both overlap with samples 1.31 (LT-3) and 1.35 (LT-1) (Figure 7.10b). When the variation in the individual samples is taken into consideration, sample 1.32 (LT-1) and 1.36 (LT-2) still exhibit distinguishably lower $\delta^{13}C$ values than the rest of the dataset, but show some degree of overlap with each other (Figure 7.10b). For the rest of the dataset, the distinction between samples 1.33 (LT-2) and 1.34 (LT-3) disappears and, along with samples 1.31 (LT-3) and 1.35 (LT-1), cannot be distinguished from each other (Figure 7.10b).

7.3.4. Synthesis

The results from diatom and pollen counts, in addition to the oxygen and carbon isotope data, allow the development of a depositional model for the laminated sediments in LFa-2. The diatoms give information about the thermal regime of the water column (periods of mixing and stratification) and when these changes occur. Data from the pollen analysis provides information on the timing of pollen dispersal, which can be seasonally specific, and the oxygen and carbon isotope data can highlight seasonal changes in the $\delta^{18}O$ of lake water, while $\delta^{13}C$ values should reflect seasonal variations in dissolved organic carbon (DIC) in the lake.

7.3.4.1. Diatoms and pollen

The diatom results presented in figure 7.6 and 7.7 indicate a clear relationship between diatom species composition and lamination type. This relationship is summarised by the first principal component axis in figure 7.7; samples that have positive axis 1 scores are characterised by planktonic diatoms, which indicate periods of lake mixing, whereas samples that have negative axis 1 scores are characterised by benthic species and lake stratification. The pollen results also provide some important evidence for seasonality within the lamination types, although the signal is more complicated than for the diatoms.

7.3.4.1.1. Lamination Type 1

LT-1 is characterised by high concentrations of *Stephanodiscus* sp., with *S. medius* dominating the assemblage, while *S. hantzschii*, *S. parvus* and *S. minutulus* constitute a minor component (Fig. 7.6). *Stephanodiscus medius* prefers high phosphorous (P) and low silica (Si) concentrations (low Si:P ratios), indicating that the Marks Tey lake was eutrophic during the deposition of LFa-2 (Anderson, 1990; Bennion, 1994). These planktonic diatoms are non-motile and require turbulent water to maintain buoyancy, therefore providing the clearest indication of lake water mixing. Peaks in the Mn/Fe ratio during LT-1 also indicate lake water mixing, as Fe is preferentially oxidised compared to Mn during oxic lake water conditions (Davison, 1993; Olsen et al., 2012; Naeher et al., 2013). The *Stephanodiscus* sp. that occur in LT-1 also commonly dominate the phytoplankton during water circulation in the spring, although the exact timing can vary from late winter to early summer (Sommer, 1985, 1986; Bradbury, 1988; Stoermer, 1993; Stoemer et al., 1996; Rioual et al., 2007; Kirilova et al., 2008; St Jacques et al., 2009; Lenard and Wojciechowska, 2013). Furthermore, the high concentrations of diatom frustules that characterise LT1 are also a feature of the spring mixing period, often associated with the highest annual diatom accumulation rates (Kirilova et al., 2008).

The pollen results for the lamination types reveal a mixed signal. Three of the samples (1.05, 1.11 and 1.14) are characterised by the occurrence of *Alnus, Betula*, *Ulmus, Quercus* and to a lesser extent *Taxus*, which all flower from early to late spring (Hyde and Williams, 1944; Emberlin et al., 1990). These samples are also characterised by taxa that occur in other lamination types. *Corylus*, *Carpinus* and to a lesser extent *Acer* are also important for samples 1.01 and 1.13 from LT-3 (Fig. 7.9). *Corylus* is spring pollinated, but can produce pollen as early as Februry (Hyde and Williams, 1944; Hyde, 1952). In contrast, *Carpinus* (late spring) and *Acer* (late spring-summer) typically pollinate later in the year (Emberlin et al., 1990). Samples 1.05, 1.11 and 1.14 from LT-1 also contain *Poaceae*, which is also found in sample 1.09 of LT-2 (Fig, 7.8, 7.9). *Poaceae* has a long pollination period, peaking during the summer months (Hyde and Williamson, 1944; Stace, 1991). The results of the pollen analysis from samples 1.05,

1.11 and 1.14 from LT-1 therefore indicate that these laminations are likely to have been deposited during the spring, as does the diatom data.

In contrast, samples 1.02 and 1.08 from LT-1 have negative axis 1 scores and overlap with sample 1.06 from LT-2 and have a similar taxa composition to sample 1.09 (LT-2). These samples are characterised by the occurrence *Cyperaceae, Tilia, Salix* and *Fraxinus* (Fig. 7.9). With the exception of *Fraxinus*, which pollinates during the spring, samples 1.02 and 1.08 are characterised by the late spring/early summer pollinating taxa *Cyperaceae* and *Salix* (Bonny, 1980), as well as *Tilia*, which pollinates during the summer months (Emberlin et al.,1990). The presence of these taxa in samples from LT-1 suggests that these lamination types were deposited later in the year. This contrasting signal from the pollen taxa could be related to the variable times of the year that water circulation occurs. As noted above, although the *Stephanodiscus* sp. noted above typically bloom in the spring, blooms can occur from late winter to early summer.

7.3.4.1.2. Lamination Type 2

LT-2 exhibits a distinct change in diatom species composition, as highlighted by the PCA in figure 7.5. LT-2 is characterised by benthic diatom species (e.g. *Navicula* sp*., Nitzschia* sp*., Achnanthes* sp.), therefore lowering the planktonic/benthic ratio, as well as a significant reduction in total diatom concentrations, between one to two orders of magnitude (Fig. 7.6). This distinct change in diatom abundance and decline in planktonic species indicates a shift in the hydrological conditions of the lake. Significant reductions of planktonic diatoms in the epilimnion can result from processes such as nutrient limitation and overgrazing, resulting in a shift in dominance to other algal communities (Hutchinson, 1967; Reynolds, 1984; Sommer et al., 1986; Marshall and Peters, 1989). Increasing temperatures will also lead to the development of water column stratification, which is also likely to play a major role as the heavy, non-motile diatoms will fall from suspension (Hutchinson, 1967; Padisak et al., 1998). The development of water column stratification is a characteristic feature of temperate lakes during the summer months, which is supported by the sedimentology of LT-2 and the μ-XRF data, which is characterised by the deposition of fine-grained micritic calcite (Fig. 7.2), high Ca counts and a low Mn/Fe ratio (Fig. 7.3). Increasing

temperatures and biological activity result in the supersaturation and precipitation of calcite, with peak precipitation rates occuring during the summer months, as noted in a number of studies (Brunskill, 1969; Kelts and Hsu, 1978; Teranes et al., 1999a). Lake water stratification also leads to oxygen depletion and anoxia in the bottom waters, an important condition for varve preservation (Boygle, 1993; Nuhfer et al., 1993; Lamoureux and Bradley, 1996).

Apart from sample 1.06 and 1.09, samples 1.03, 1.12 and 1.15 are characterised by taxa that pollinate later in the year. These samples are characterised by *Juniperus* and *Rumex*, which both flower during the early summer (Fig. 7.9) (Bonny, 1980; Goldberg et al., 1988). These samples are also characterised, to a lesser extent, by *Rosaceae*, which pollinates during late spring/early summer (Kurohura et al., 2013) and *Tilia*, which is characteristic of the summer season (Emberlin et al., 1990). The taxa associated with LT-2 therefore suggest that this lamination type was deposited during the summer months of the year.

7.3.4.1.3. Lamination Type 3

Interpreting the diatom species composition of LT-3 is more complicated, as samples from this LT occupy an intermediate position on principal component axis 1, indicating that the diatom assemblage of LT-3 falls somewhere between LT-1 and LT-2 (Fig. 7.5). The slight increase in total concentration and plantonic/benthic ratio indicates the re-appearance of planktonic diatoms, suggesting the lake water has undergone a second period of mixing. The lower concentrations in LT-3 suggest that this bloom was less pronounced or shorter than the spring bloom in LT-1. Following stratification of the water column during the summer months (LT-2), secondary diatom blooms often occur during late summer/autumn mixing periods, when an excess of nutrients is available during the erosion of water column stratification (Sommer et al., 1986). A weaker/shorter bloom may also result from reduced temperature and light conditions during this time (Kirilova et al., 2008). In contrast to LT-1, the Mn/Fe ratio does not peak again in LT-3 (Fig. 7.1). If the lake underwent another period of mixing, it might be expected that the Mn/Fe ratio would respond. If the mixing period is shorter/weaker, however, it may not have significantly altered redox conditions in the bottom water to produce a clear chemical response. No distinctive shift in the

composition of planktonic species occurs in LT-3, which like LT-1, is also characterised by *Stephanodiscus* sp. Although the *Stephanodiscus* sp. present in LT-3 are commonly found in the phytoplankton during spring mixing periods, they have also been observed in low concentrations during lake mixing in the autumn (Kirilova et al., 2008).

Samples from LT-3 are characterised by two distinctive assemblages. Samples 1.04, 10.7 and 1.10 are characterised by *Juniperus*, which pollinates during the early summer (Fig. 7.9) (Bonny, 1980; Goldberg et al., 1988). Samples 1.01 and 1.13 are characterised by *Umbelliferae* and *Picea*, which pollinate during the mid/late summer (Bonny, 1980), and *Carpinus*, which pollinates during the spring (Emberlin et al., 1990). *Corylus* (also important for LT-1) also occurs in these lamination types and starts to pollinate early in the year (February) (Hyde and Williams, 1944; Hyde, 1952). LT-3 therefore contains pollen from taxa that pollinate during the early spring to the late summer.

7.3.4.1.4. Oxygen and carbon isotopes

Before discussing whether a seasonal signal is preserved in the stable isotopic values, it is necessary to consider what environmental factors are likely to be controlling the $\delta^{18}O$ and $\delta^{13}C$ values from the lamination types. Detrital contamination from biological and allocthonous carbonate is a concern for lacustrine isotopic records, as it can have a large impact on the isotopic signal (Leng et al., 2010; Mangili et al., 2010a). This is particularly true for this study, as samples were taken from all three lamination types. It is difficult to rule out the possibility of detrital contamination from allogenic carbonates because the $\delta^{13}C$ values of the LT samples, although different from the $\delta^{13}C$ values of samples from the Anglian Till samples, fall within the range of $\delta^{13}C$ values for the detrital source (Fig. 7.10). Detrital contamination is considered unlikely, however, because the $\delta^{13}C$ values from the LT samples are typical of lacustrine carbonates where the lake water has undergone equilibration with atmospheric CO_2 (Leng and Marshall, 2004) and will, therefore, have similar values to carbonates of marine origin (Clark and Fritz, 1997). Further to this, the micro-sedimentology of these lamination sets shows no evidence of in-washed event layers (Fig. 7.2). The overlap of the LT dataset with that from catchment carbonates is therefore considered coincidental.

In the absence of detrital contamination, the $\delta^{18}O$ composition of the carbonates at Marks Tey will reflect the isotopic composition of water recharging the lake water, and the temperature at which carbonate precipitation occurs. The high $\delta^{13}C$ values imply that the lake water underwent equilibration with atmospheric CO_2 and a lack of co-variance in the dataset suggests that lake water $\delta^{18}O$ and $\delta^{13}C$ was not sensitive to the balance between precipitation and evaporation and underwent regular recharge from ground/ surface water flow (Fig. 7.10) (Talbot, 1990: Talbot and Kelts, 1990; Li and Ku, 1997, Anderson and Leng, 2004), so should therefore be considered a hydrologically open system (Marshall et al., 2002, 2007; Leng and Marshall, 2004; Diefendorf et al., 2006). Although water in modern British lakes does undergo minor modification by evaporation (Marshall et al., 2002, 2007), these changes are not enough to significantly alter the $\delta^{18}O$ and $\delta^{13}C$ of lake water, so the $\delta^{18}O$ value of carbonates at Marks Tey should reflect the $\delta^{18}O$ value of recharge water that enters the basin, fractionated at a value related to the temperature of mineralisation.

The effect that temperature has over the $\delta^{18}O$ value of precipitation in the temperate mid-latitudes is well known (Craig, 1961; Dansgaard, 1964; Rozanski et al., 1992, 1993; Bowen and Wilkinson, 2002). This temperature control over the $\delta^{18}O$ of precipitation also has a seasonal component, whereby rain falling during colder months will have lower $\delta^{18}O$ values compared to higher $\delta^{18}O$ values expected of rain falling in warmer months (Rozanski et al., 1993), a relationship that has also been observed in the British Isles (Darling and Talbot, 2003; Darling, 2004). If the $\delta^{18}O$ value of lake water at Marks Tey represented seasonal changes in the $\delta^{18}O$ composition of precipitation, the data in figure 7.8 indicates calcite found in LT-1 and LT-3 formed during the warmer months of the year, whereas the calcite in LT-2 formed during colder months. This data contradicts the evidence from the diatoms and pollen, however, which suggest LT-2 was deposited during the summer months.

Such a scenario is unlikely to occur, however, as modern analogue studies have demonstrated seasonal variations that occur in the $\delta^{18}O$ value of rainfall will be averaged out as water percolates through soils to recharge aquifers and groundwater (Darling et al., 2003). The $\delta^{18}O$ value of resulting surface waters that recharge rivers and lakes will, therefore, represent the average annual $\delta^{18}O$ value of rainfall (White et

al., 1999; Darling et al., 2003; Darling, 2004; Candy et al., 2011; Waghorne et al., 2012). Although some modification due to seasonality or evaporation may occur, this relationship therefore suggests that the $\delta^{18}O$ value of water recharging modern lake basins is fairly consistent throughout the year. Assuming this relationship can be applied at Marks Tey, the isotopic composition of calcite should relate to temperature dependent isotopic fractionation during mineral precipitation (Urey, 1947; McCrea, 1950; Urey et al., 1951; Epstein et al., 1953; Kim and O'Neil, 1997; Leng and Marshall, 2004). Due to the temperature controlled isotopic fractionation that occurs during calcite precipitation, the warmest months would therefore produce calcite with more negative values than colder months.

While this interpretation is consistent with the $\delta^{18}O$ values for sample 1.33 from LT-2, the $\delta^{18}O$ values obtained from sample 1.36 overlap with sample 1.32 from LT-1 and both samples from LT-3 (Fig. 7.8). Although it is not possible to provide a definitive answer to the trend observed in these lamination types, the overlap is not the result of sample contamination, as they were taken from individual lamination types. It is possible, however, that lake water temperatures were relatively mild during the formation of LT-1 and LT-3 over these two lamination sets. It is also possible that calcite precipitated during the summer months is re-suspended and deposited during periods of lake mixing during the autumn and spring (Teranes et al., 1999), therefore 'contaminating' the signal of any authigenic calcite precipitated in the lake water during these months.

7.3.4.1.5. Model Summary

The results from diatom, pollen, sedimentology and isotope analysis confirm that the laminated sediments in LFa-2 are varved. A comparison of the model suggested by Turner (1970) with the results of this study shows a consistency between the two (Fig. 7.9). Sampling the lamination types for microfossil analysis has revealed a detailed seasonal signal for deposition of the lamination sets at Marks Tey. The diatoms give the clearest indication of seasonality between the lamination types. The evidence from Marks Tey is also consistent with the concept that lakes of the same morphology and trophic level, which occur in similar climatic regimes, will follow a predictable pattern (Reynolds, 1984; Harris, 1988).

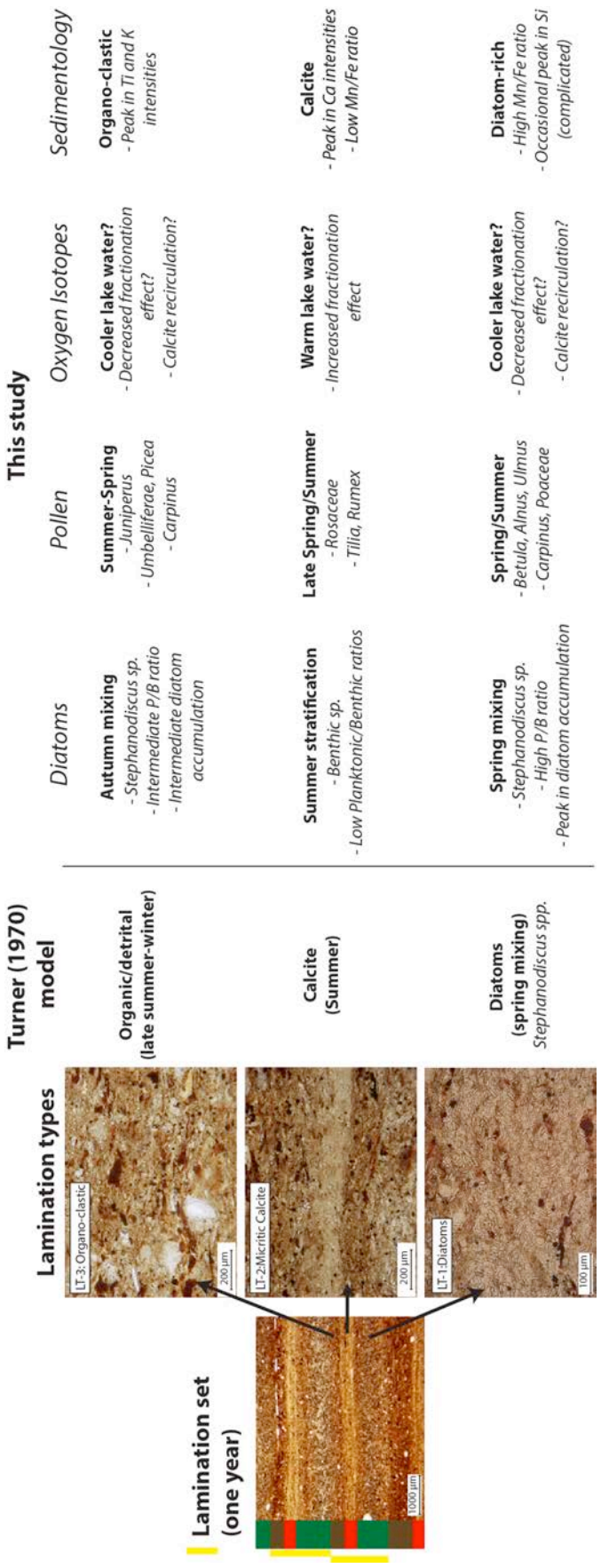

Figure 7.11. *Comparison between the model for varve formation suggested by Turner (1970) and the model developed in this study. The current work has confirmed the basic succession described by Turner (1970) and demonstrated a seasonal signal for sediment deposition. Although the pollen and isotopic results reveal a mixed signal, they do generally support the diatom results.*

The British Isles is located in the temperate mid-latitudes and the diatom flora present in the lamination types sampled, which are dominated by *Stepanodiscus* sp., indicate that the lake was eutrophic (e.g. Anderson, 1990; Bennion, 1994) and dimictic (Lewis, 1983). Productive lakes in temperate regions are characterised by this distinctive seasonal pattern, which results from annual solar, hydrological and temperature cycles that dictate the thermal structure of lake water (Boehrer and Schultze, 2008). Under such conditions, diatoms bloom during spring and autumn water column mixing periods, while water column stratification characterises the summer and winter periods, when planktonic communities are replaced by other algae (Fig. 7.11) (Hitchinson, 1967; Reynolds, 1984; Sommer et al., 1986; Bradbury, 1988; Marshall and Peters, 1989; Willen, 1991; Maberly et al., 1994; Boehrer and Schultze, 2008).

The sedimentological results should not be used in isolation to invoke seasonal processes, but the microfacies descriptions do suggest, as Turner (1970) did, that the lamination sets are analogous to biochemical varves (Kelts and Hsu, 1978; Lotter et al., 1997; Brauer, 2004; Giguet-Covex et al., 2010). Although the pollen results are not as clear, the results do suggest a similar seasonal signal. The pollen data does, however, indicate a summer component in all three lamination types. For LT-1, the spring diatom lamination type, this may be due to the timing of the diatom bloom. Although the *Stephanodiscus* sp. that dominate the assemblage commonly bloom during the spring, the timing of this bloom can vary from late winter to early summer (e.g. Sommer, 1985, 1986; Kirilova et al., 2008). The assumption with this type of analysis is also that the pollen present within the lamination types is representative of taxa that are flowering during the time that the lamination type is being formed, that there is no significant lag between pollen release and transport to the lake (Tauber, 1967), and that pollen is deposited at the sediment surface soon after entering the lake (Tippett, 1964). Such lags in pollen recruitment and deposition may, therefore, cause the mixed signal. Furthermore, the isotopic signal may be contaminated by the recirculation of calcite precipitated in the summer months during the two periods of lake mixing in the spring and autumn (Teranes et al., 1999).

7.4. Summary

- Multi-proxy analysis of the regular and repeating lamination sets that characterise LFa-2 confirm the suggestion of Turner (1970) that the Marks Tey sequence contains varved sediments. This study has, however, demonstrated the seasonal nature of the lamination types, based on a combination of lithological and biological proxies.
- The biochemical varves at Marks Tey are composed of a spring diatom bloom (LT-1), calcite deposition during the summer months (LT-2) and the late summer/autumn deposition of organo-clastic material, with evidence for a second, smaller diatom bloom in the autumn.
- Counting of the varves in LFa-2 can, therefore, produce an annually-resolved chronology for the early-temperate phase of the Hoxnian, as well as the first part of the late-temperate phase (Ho IIIa).

Chapter 8. Chronology construction and varve micro-facies stratigraphy

Chapter overview

The results presented in chapter 7 have demonstrated that the repeating lamination sets contained within LFa-2 in the MT-2010 sequence are varved. This chapter will present results from the counting of the varved sediments with the aim of producing a chronology for the sequence. Furthermore, stratigraphical variations in sub-annual structure from the micro-facies data will be presented. The first section of this chapter focuses on the process of chronology construction: from varve counts, to the assessment of counting error and the interpolation of sections that display poor varve preservation. The second section of this chapter will present temporal stratigraphical changes in the varve micro-facies structure and thickness, allied to the varve quality and the presence of event layers, with the aim of determining how these properties vary through time. These data will then be discussed in terms of their palaeoenvironmental significance to the dynamics and processes in the lake catchment.

8.1. Introduction

The sediments preserved within the palaeo-lake basin at Marks Tey represent an important MIS 11 sequence in the British Isles, as the laminated sediments it contains have been used to estimate the duration of interglacial conditions (Shackleton and Turner, 1967; Turner, 1970, 1975). It has been estimated that the early part of the sequence at Marks Tey (Ho I to Ho IIIa), where varved sediments are purportedly preserved, contains between 9,500 and 14,500 varves (Fig. 8.1) (Shackleton and Turner, 1967; Turner, 1970). Extrapolating these estimated sedimentation rates through the whole sequence gives an estimated duration of between 30,000-50,000 years for MIS 11 (Shackleton and Turner, 1967; Turner, 1970), although this figure was subsequently reduced to 25,000 years (Turner, 1975).

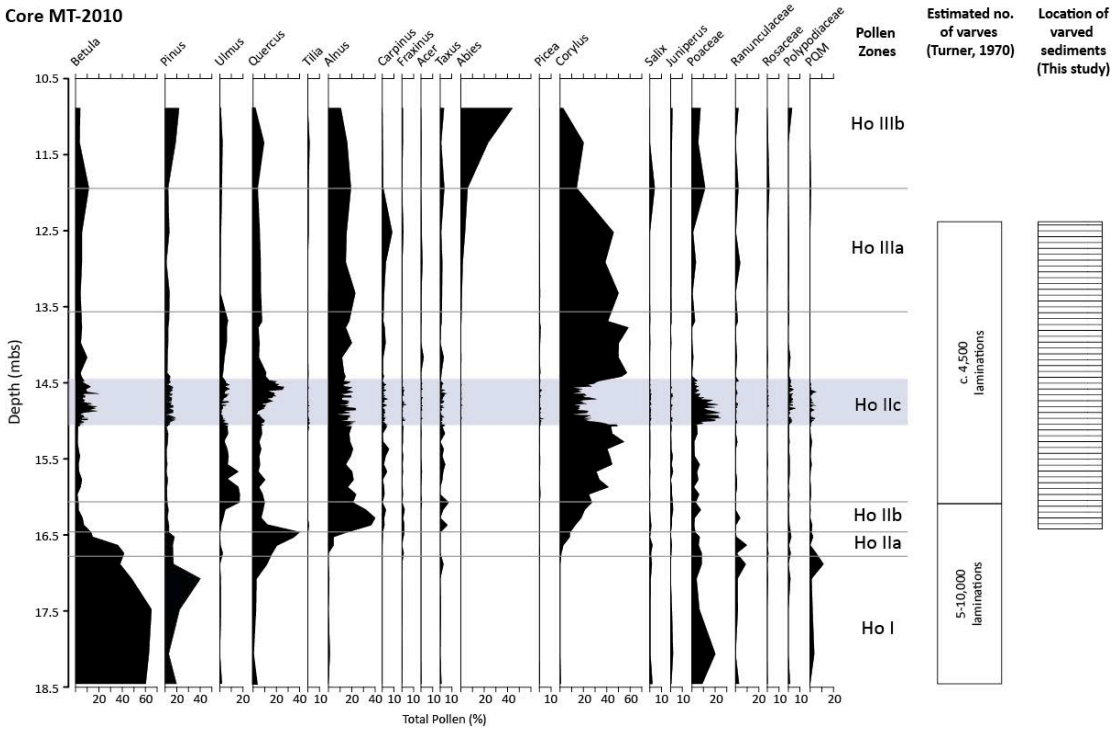

Figure 8.1. *Summary pollen diagram from the lowest 6.25m of core MT-2010, which has been subdivided into the local Hoxnian pollen zones present. The location and number of laminations preserved, as estimated by Turner (1970), are also shown. Based on these estimates, Turner (1970) suggested that pollen zones Ho I to Ho IIb contained 5-10,000 varves, while Ho IIc and a large part of Ho IIIa contained c. 4,500 varves. The shaded box beside these estimates represents the location of varved sediments as determined from the results in chapters 6 and 7. In contrast to the observations of Turner (1970), varves are only preserved in the Marks Tey sequence from Ho IIb to Ho IIIa.*

Despite the subsequent reduction of estimated duration, it is still significant, given that interglacial conditions during MIS 11 are often reported to have lasted for longer than any other interglacial that occurred during the Middle and Late Pleistocene, and is often regarded as one of the best climatic analogues for the Holocene (e.g. Droxler and Farrell, 2000; Berger and Loutre, 2002, 2003; EPICA, 2004).

The issue with estimating the duration of MIS 11 in this manner is that it assumes that 1) all of the laminated sediments contained within Ho I to Ho IIIa are varved; and 2) these sedimentation rates provide accurate estimates of those in the upper part of the sequence. The second point is difficult to address, given that the sediments are not *in situ* from 12.00 to 4.10mbs (LFa-3 in table 6.1 figure 6.2 of chapter 6). Chapters 6 and 7, have however, been able to demonstrate that varved sediments only occur between 16.45 – 12.28 mbs (LFa-2), during pollen zones Ho IIb to Ho IIIa (chapters 6 and 7, Fig. 8.1). This chapter will not, therefore, be able to test estimates for the duration of the

interglacial. It will however, be able to determine how many varves are present in the sequence and determine the duration of pollen zone Ho IIc.

8.2. Varve chronology construction

The varve chronology for Marks Tey presented in this thesis is a floating chronology determined from a composite profile of BH1 and BH2 (Fig. 8.2). Varve counts were based on varve micro-facies descriptions and thickness measurements of 85 sediment thin sections for each lamination type at magnifications between x20 to x200. Two counts were undertaken on thin sections prepared from BH1 (Run 8B, A and 7B, A), which represents the most complete record of the varved interval, while thin sections from BH2 were used to cover gaps in BH1 that resulted from core breaks between drilling runs (red shading on varve thickness data, Fig. 8.2) and coring artefacts identified while micro-facies descriptions were being undertaken (black shading on varve thickness data, Fig. 8.2 A and B). Thin sections were also prepared for parts of BH2 that were not used for the first two counts (un-shaded area, Run 5C, B and A) (Fig. 8.2). These thin sections were counted and compared to the varve counts for BH1 as a method of varve count verification (Fig. 8.2c). To aid varve counting, each sediment thin section was split up into a series of short (1-2cm) intervals by identifying prominent calcite laminations and marking them with a pen. This procedure was carried out for BH1 and BH2, so that the counting sections from both boreholes are directly comparable to each other.

8.2.1. Counts 1 and 2

The first two counts of the Marks Tey sequence were undertaken on the whole varved sequence (359 counting sections) (Fig. 8.2a and b). The first varve count resulted in the identification and measurement of 3432 varves (Fig. 8.2a). One month after the first count, a second count was undertaken along a different transect on the same thin sections. This count resulted in the identification of 3483 varves, 51 more varves than count 1 (Fig. 8.2b), with a maximum counting error of 131 varves (when both positive and negative deviations are considered). The deviation in the number of varves counted when count 2 is compared to count 1 is shown in figure 8.3, where the deviations are delimited by the counting section. Figure 8.3 also contains the varve

quality index (0-3) for varves counted within each counting section, which has been averaged and plotted above the deviation data for comparison.

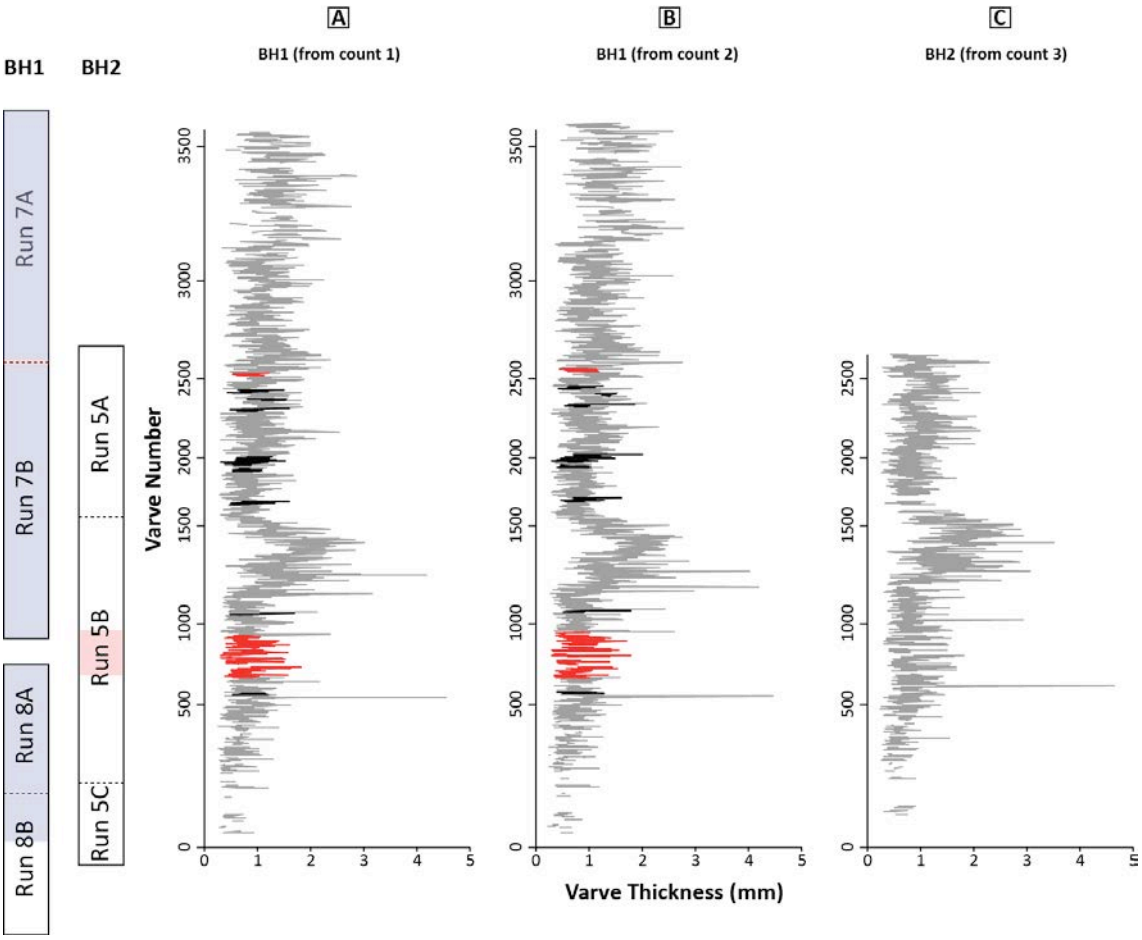

Figure 8.2. *Results of the varve counts made on the Marks Tey sequence. The first two counts (A and B) represent the composite stratigraphy, which is composed of BH1 (blue shading on borehole correlation), while BH2 was used to cover gaps introduced during core recovery (red shading, on borehole correlation). Other sections of the sequence where BH2 was used to fill gaps resulting from coring artefacts in BH1 are shown as black shading in A and B. The varve thickness record in C was taken exclusively from BH2 and used for a comparison with BH1.*

The deviation data indicates that during count 2, 34 of the 359 counting sections contained fewer varves, whereas the identification of extra varves occurred in 55 counting sections. When extra varves were identified, there was a tendency for counting deviations to be greater than for fewer varves, with the largest deviation being 6 varves (counting section 309, Fig. 8.3). Counting deviations are also unequally distributed throughout the sequence, with the greatest difference between count 2 and 1 occurring from counting sections 359-290, located in the basal section of the sequence, and sections 45-1, located at the top of the sequence (Fig. 8.3). Both of these areas of the core contain varves that are generally of a lower quality, when compared with the counting sections between 289-46 (Fig. 8.3).

8.2.1.1. Sources of error in count 1 and 2

Analysis of varve counts using varve thickness data is considered to be a precise method of analysis, enabling counts to be compared on a varve-to-varve basis (Brauer et al., 2000a; Martin-Puertas et al., 2012) and was undertaken on count 1 and 2.

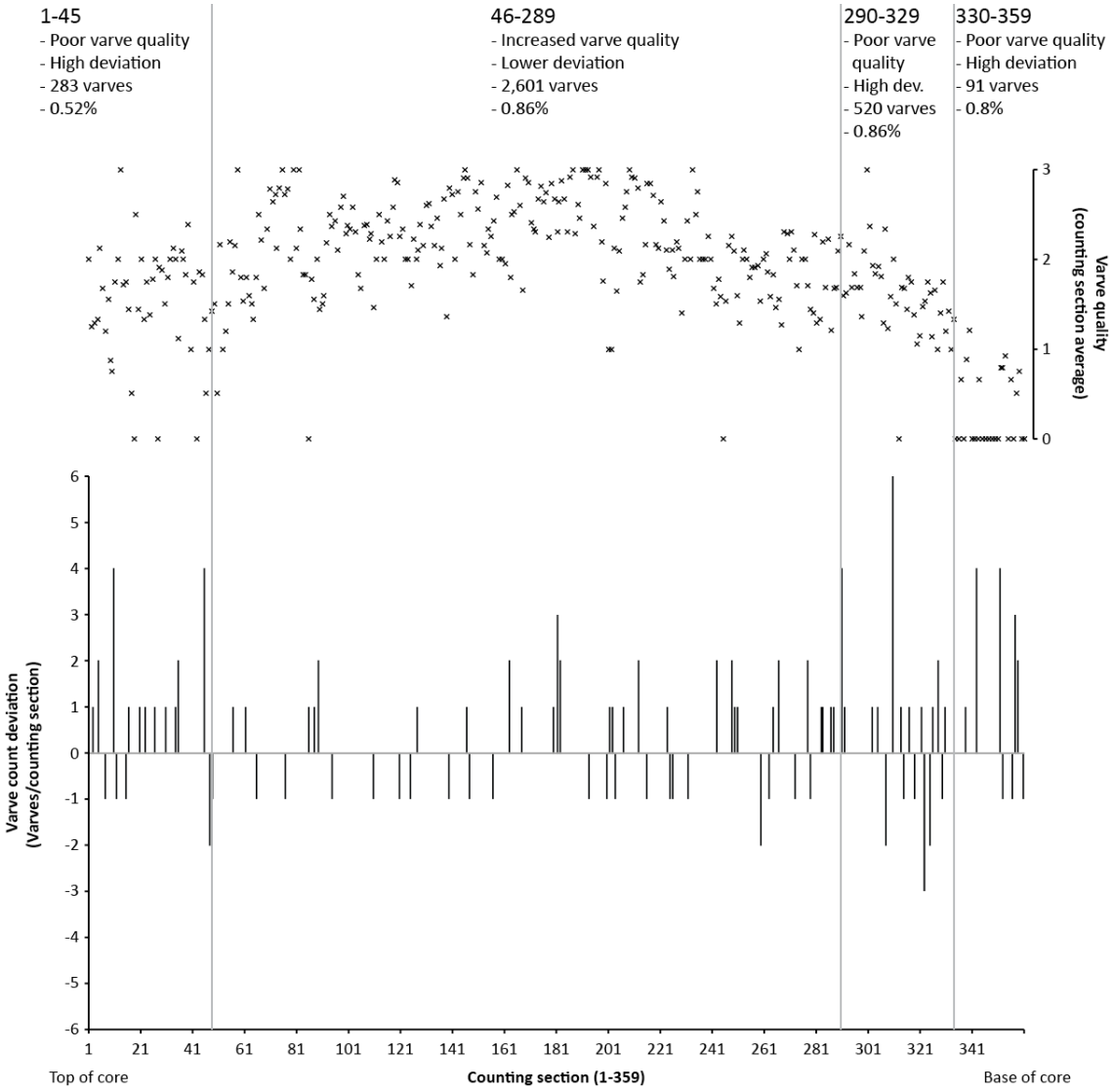

Figure 8.3. *Deviation in number of varves through the sequence when count 2 is compared to count 1. Each back bar represents a difference in number of varves counted within individual counting sections marked out on the thin sections, the boundaries of which are delimited by prominent calcite laminations. Increasing counting section numbers relate to increasing depth through the sequence. Average varve quality for varves within each counting section has also been determined for comparison to the counting deviation data. The sub-division of the data (grey lines) highlights the main source of counting deviation, which occur in areas of poor varve quality. 283 varves occur in counting sections 1-45 and represent 0.52% deviation. Despite only containing 611 varves, counting sections 290-359 have the greatest deviation between count 1 and 2 and has represents 1.66% error. In contrast, counting sections 46-289 cover areas of higher varve quality. The counting deviations in this section are lower and the 2,601 varves represent 0.86% error. Total error for the counts is the sum of these figures (3.75%).*

By comparing the thickness datasets for both counts, in conjunction with the corresponding counting sections on the thin sections, the sources of counting error could be determined. The main sources of counting error were a result of misidentification of varve boundaries in either of the BH1 counts, predominantly in counting sections of poor varve quality; counting sections 1-45 and 290-359. Varve boundaries were particularly difficult to identify in counting sections 330-359, where varve structures form a minor component of the sediment sequence.

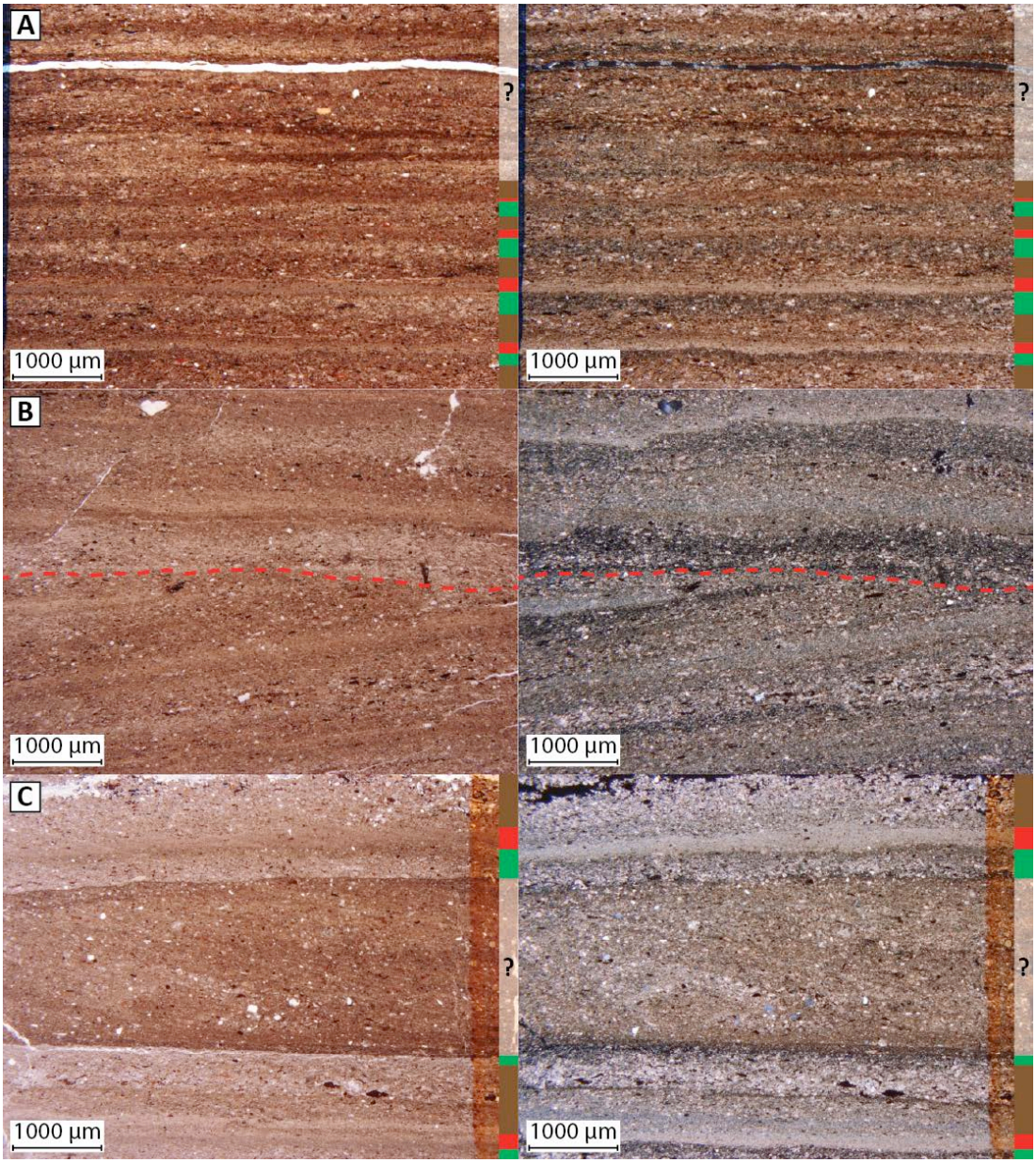

Figure 8.4. *Paired photomicrographs (plain (left) and cross polarised light) of the varved sediments, showing examples of where chronological errors may occur. A) The transition between areas of high and low varve quality, which can result in extra/missed varves; B) Small-scale disturbances in the core, which result in the 'pinching out' of varves between counting transects; and C) Coring artefacts introduced to the sequence due to the drilling method. The rotary action of the drill occasionally sheered the sediment core during extrusion.*

In counts 1 and 2, a chronology of 3,495 varve years was constructed, with a total counting error of 131 years; a 3.75% error for this sequence. Of this percentage error, 2.18% can be explained by the poor varve quality in the counting sections 1-45 and 290-359, whilst the remaining 0.86% is the result of missing or additional varves in counting sections 46-289 (Fig. 8.3).

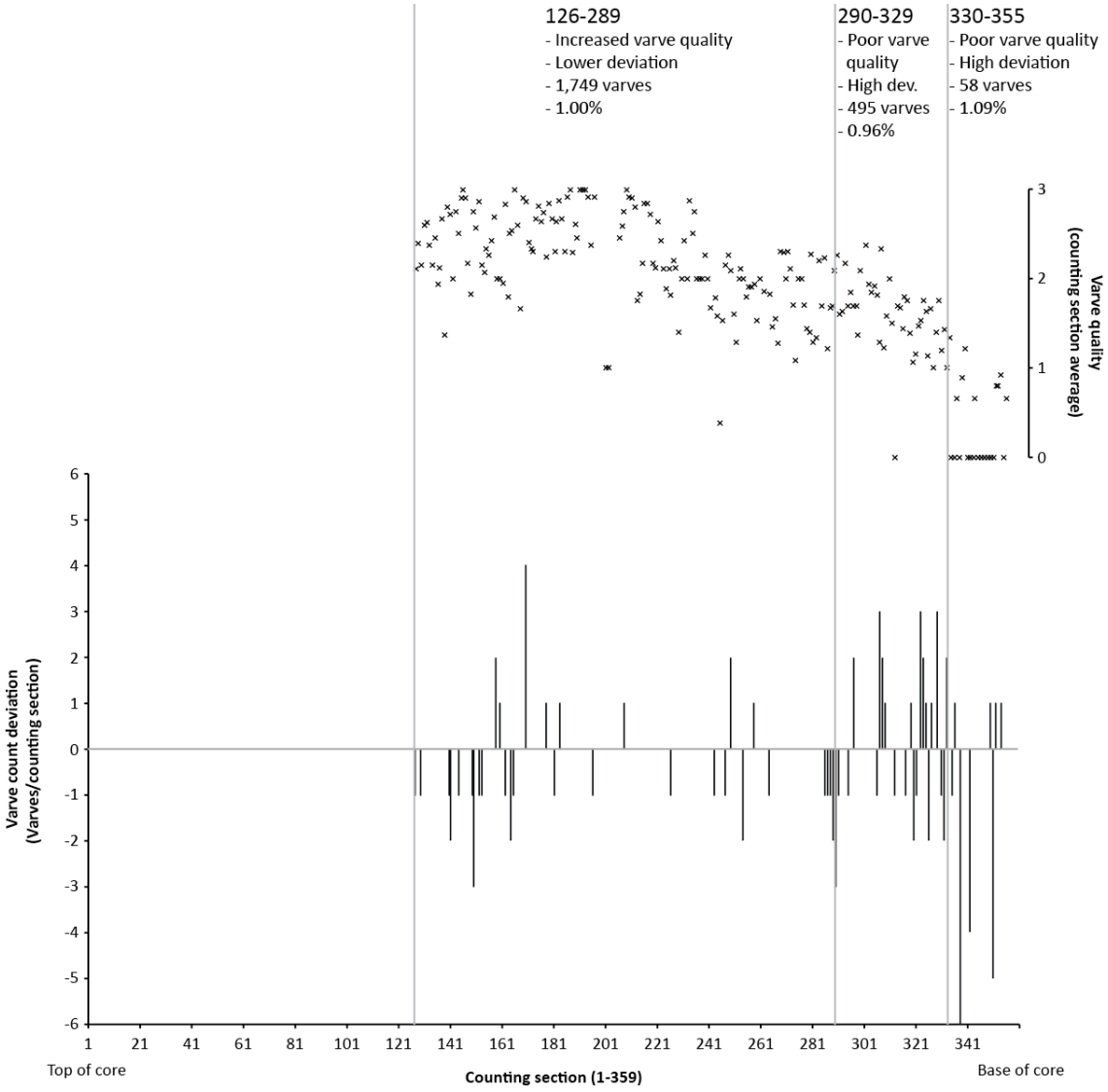

Figure 8.5. *Deviation in number of varves through the sequence when count 3 is compared to the combined counts from counts 1 and 2. Due to incomplete core recovery and coring artefacts in BH2, replicate counting sections for varve verification were only available for counting sections 126 to 355. Increasing counting section numbers relate to increasing depth through the sequence. Average varve quality for varves within each counting section has also been determined for comparison to the counting deviation data. The sub-division of the data (grey lines) highlights the main source of counting deviation, which occur in areas of poor varve quality. Counting sections 290-355 have the greatest deviation between count 3 and the combined counts from BH1; containing 553 varves, but accounting for 2.05% error. In contrast, counting sections 126-289 cover areas of higher varve quality. The counting deviations in this section are lower and the 1,749 varves represent 1% error. Total error for the counts is the sum of these figures (3.05%).*

8.2.2. Count 3

Count 3 was undertaken exclusively on BH2. Due to incomplete core recovery, the first 125 counting sections are missing from this count. The last four counting sections (355-359) were also omitted due to artefacts introduced by the coring process. The third count was therefore undertaken on counting sections 126 to 355 (Fig. 8.2). The total number of varves counted in count 3 was 2,302, which is comparable to the counts for the same counting sections in count 1 (2,290±12) and count 2 (2,323 ±21). The results from count 3 were then compared to the combined chronology for counts 1 and 2, with the deviation shown in figure 8.5. The data shows that 27 of the 229 counting sections contained more varves, while 42 of the counting sections contained fewer varves, with a maximum counting deviation of 101 varves when both positive and negative deviations are considered (Fig. 8.5). In comparison to the first two counts, the greatest frequency of count deviations in count 3 also occurs at the base of the sequence, from counting sections 290 to 355, which like BH 1, coincides with the interval of the sequence where varve quality is comparably low (Fig. 8.5).

8.2.2.1. Sources of counting error in count 3

As with BH1, the key sources of error within the sequences was predominantly misidentification of varves due to poor varve quality at the base of the sequence, which accounts for 2.05% of the total error, whilst the remaining 1% is in counting sections 126-289. Count 3 in BH2 highlights the value of using a multiple core approach to varve chronology construction. By comparing the varve thickness data and thin sections from this count with the chronology generated from the first two counts, 38 extra varves were identified. Of these 38 varves, 27 were located in the counting sections 290-355, where varve quality and preservation is generally low. Between counting sections 126-289, 11 extra varves were identified; with seven varves missed during both counts on BH1 (a possible Type C error), and a further four varves probably the result of coring artefacts. Since the cores were extracted in close proximity to one another, allied to the lack of independent dating of the core, it is difficult to quantify the nature of Type C error in this sequence. As such, the errors quoted are most likely to be the product of either Type A or Type B.

8.3. Synthesis: Master varve chronology for the Marks Tey sequence

Results of the three varve counts allow for the construction of a master varve chronology for the Marks Tey sequence (referred to as MTSC-2014). Analysis of the varve thickness data for each count, in conjunction with the counting sections marked on the thin sections, generates a count of 3533 varve years (vyr). A total counting error, by combining counts from BH 1 and BH2, of 201 vyr gives a counting error of 5.7% for this master chronology.

While the error for the sequence is large compared to other varved records, which often have counting precisions of ~1% (e.g. Brauer et al., 1999a; Ojala and Tiljander, 2003; Martin-Puertas et al., 2012), the counting error for the Marks Tey varve chronology is not equally spaced throughout the sequence. Varve thickness data for the master chronology is plotted by both depth and varve number in figure 8.6. The depth data is compared to varve quality data generated as part of the micro-facies analyses, which reveals a number of intervals between 16.45 – 15.06 mbs and 13.46 – 12.39 mbs where varve quality is 0 (Fig. 8.6a). This is particularly prevalent between 16.45 – 15.06 mbs, where the largest gaps in varve counts occur, due to the poor preservation of varve structure. The chronological uncertainty for this part of the sequence can be illustrated by splitting the total counting errors for the sequence into 100-year intervals (Fig. 8.6b). Figure 8.5b shows that for the majority of the sequence (3,133 varve years), counting error remains below 5yrs/100years. The first 400 years of the chronology (16.45 – 15.72 mbs) contains the largest counting errors, which when combined, account for 39.8% of the total counting error for the sequence (Fig. 8.6b).

8.2.3.1. Interpolation through non-varved sections of the core

The varved interval of the Marks Tey sequence, between 16.45 – 12.39 mbs, contains sections where varve structures are interrupted and varve quality is too low to provide continuous counts. Within these sections of the sequence it is therefore valid to estimate the number of years between the varved sections by interpolation. A common method to estimate the number of missing varves is to use average sedimentation rates determined from well-defined varves adjacent to these sections (e.g. Hughen et al., 2004; Koutsodendris et al., 2011).

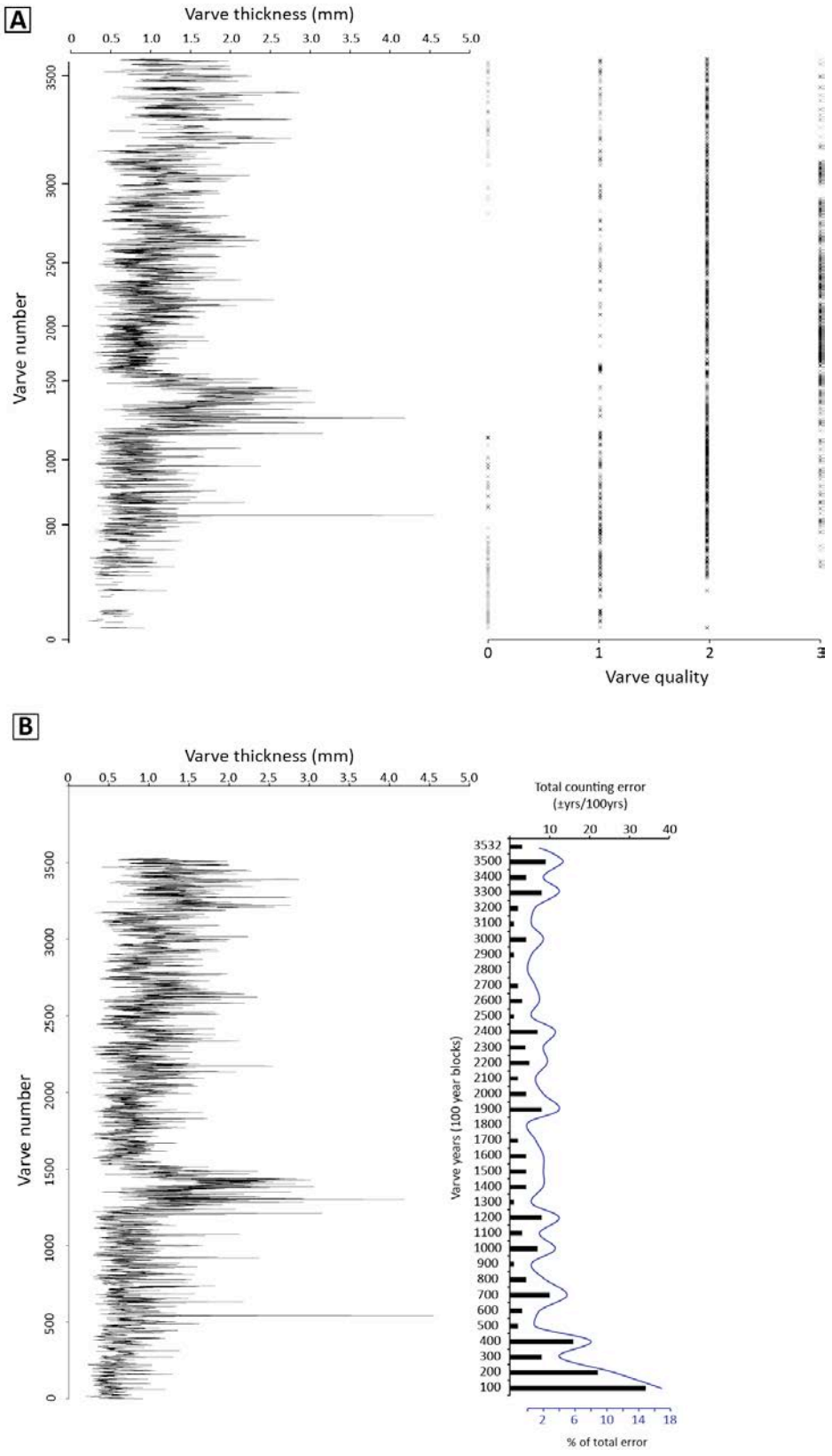

Figure 8.6. *Master varve chronology for Marks Tey, plotted as varve thickness against depth (A) and varve thickness against varve number (B). A) Plotting the varve thickness data against depth highlights sections of the sequence where gaps in varve sedimentation occur (particularly 16.45 – 16.00 mbs). Varve quality determinations have also been presented for comparison. B) Plotting the varve thickness data by varve number and comparing this to total counting error per 100 year intervals allows for the determination of where in the sequence greatest counting errors occur. For the majority of the sequence, counting error remains below 5yrs/100years. The first 400 varve years contain the greatest counting errors, which account for 39.8% of counting deviations for the whole sequence.*

Between 16.00 – 15.06 mbs and 13.47 – 12.36 mbs, varves represent the dominant mode of sedimentation in the sequence, so interpolation was undertaken based on the average thickness of 10 varves that occur immediately above and below these sections. This method resulted in the estimation of 267 varves between 16.00 – 15.06 mbs and 197 varves between 13.47 – 12.36 mbs (464 varves in total), giving a total of 3,850 years between 16.00 – 12.36 mbs (Fig. 8.7.). The interval between 16.45 – 16.00 mbs complicates the interpolation process, because varves identified only represent 20.5% sediments deposited.

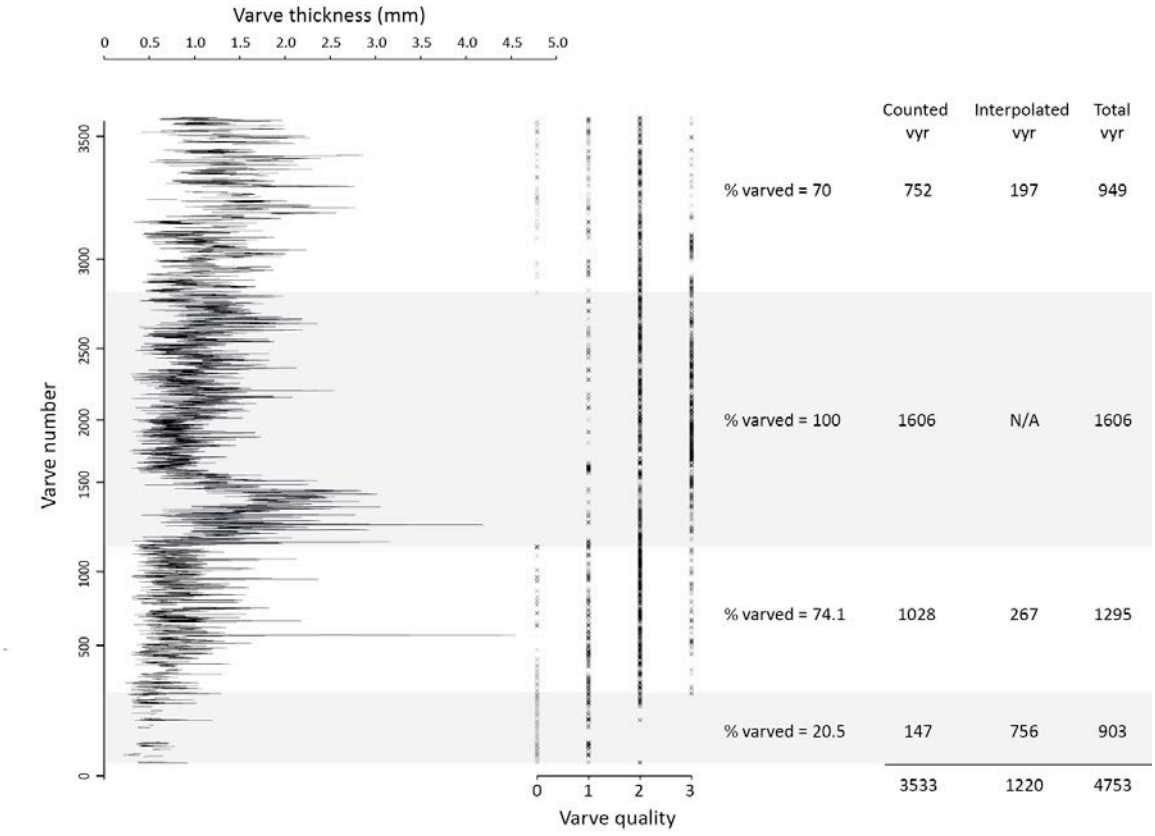

Figure 8.7. *Summary of results from interpolation through sections of the sequence where low varve quality prevented identification and counting. Between 16.00 – 15.06 mbs and 13.47 – 12.36 mbs, where varves dominate sediment deposition (at least 70%), 464 extra varves were calculated based on average sedimentation rates of 10 varves immediately above and below the gap. Interpolation from 16.45 – 16.00 mbs is more uncertain, as varves only compose 20.5% of the sequence. Averaging varve thickness throughout this section of the core results in the calculation of 756 extra varves to fill the gaps in the sequence.*

Based on average sedimentation rates determined from all of the varves identified in this interval (147), an extra 756 years are assumed to be missing (Fig. 8.7), which gives a total of 4,753 vyrs for the entire record (16.45 – 12.36 mbs). When compared to the number of counted varves (3,533 vyrs), this increases the chronology by 35%. Given

the large gaps that occur in this section of the sequence, these estimates should be considered tentative. The development of an annually-resolved model for the NAP Phase in chapter 10 will be based on the interpolated chronology. The model will be constructed from the onset of Ho IIc, which occurs at 16.07 mbs. Ho IIc begins in varved sediments of low varve quality and therefore interpolation is required to develop a chronology for this section (MTSC-2014^{INT}). The discussion in chapter 10 will use this interpolated model because, despite using later parts of the varved sequence (above 16.07 mbs), there is a 7cm section of the chronology (between 16.07 to 16.00 mbs) that requires interpolation. The interpolation is, however, only for 50% of the varves for this zone, in comparison to the lower part of the zone, where varves account for 20.5% of the chronology.

8.4. Stratigraphical changes in varve micro-facies

Descriptions of the sub-annual laminations (lamination types) that compose the varves (lamination sets) in the Marks Tey sequence reveal the occurrence of seven lamination types: two for the diatom-rich lamination type (LT-1), three for the calcite-rich lamination type (LT-2); and two for the organo-clastic lamination type (LT-3). These were described in chapter 7, but are summarised here in figure 8.8. These individual lamination types can be combined to produce 12 observed lamination sets that occur within the sequence (Table 8.1; Fig. 8.9). This section will describe the variation in these lamination sets through the sequence and summarise the environmental signal that they contain. In contrast to the MTSC-2014^{INT} chronology that will be used in chapter 10, this section is based on the number of counted varves in the sequence (MTSC-2014). This is because stratigraphic variations in varve structure can only be assessed from descriptions on counted varves. Furthermore, although it has been demonstrated that the lamination sets within LFa-2 are varves, for consistency in descriptive terms, lamination set will continue to be used. Variation in the lamination sets present through the sequence is plotted according to the MTSC-2014 chronology in figure 8.9. Figure 8.9 has been sub-divided into four main lamination set zones, based on the frequency at which the individual lamination sets occur within them (Table 8.1).

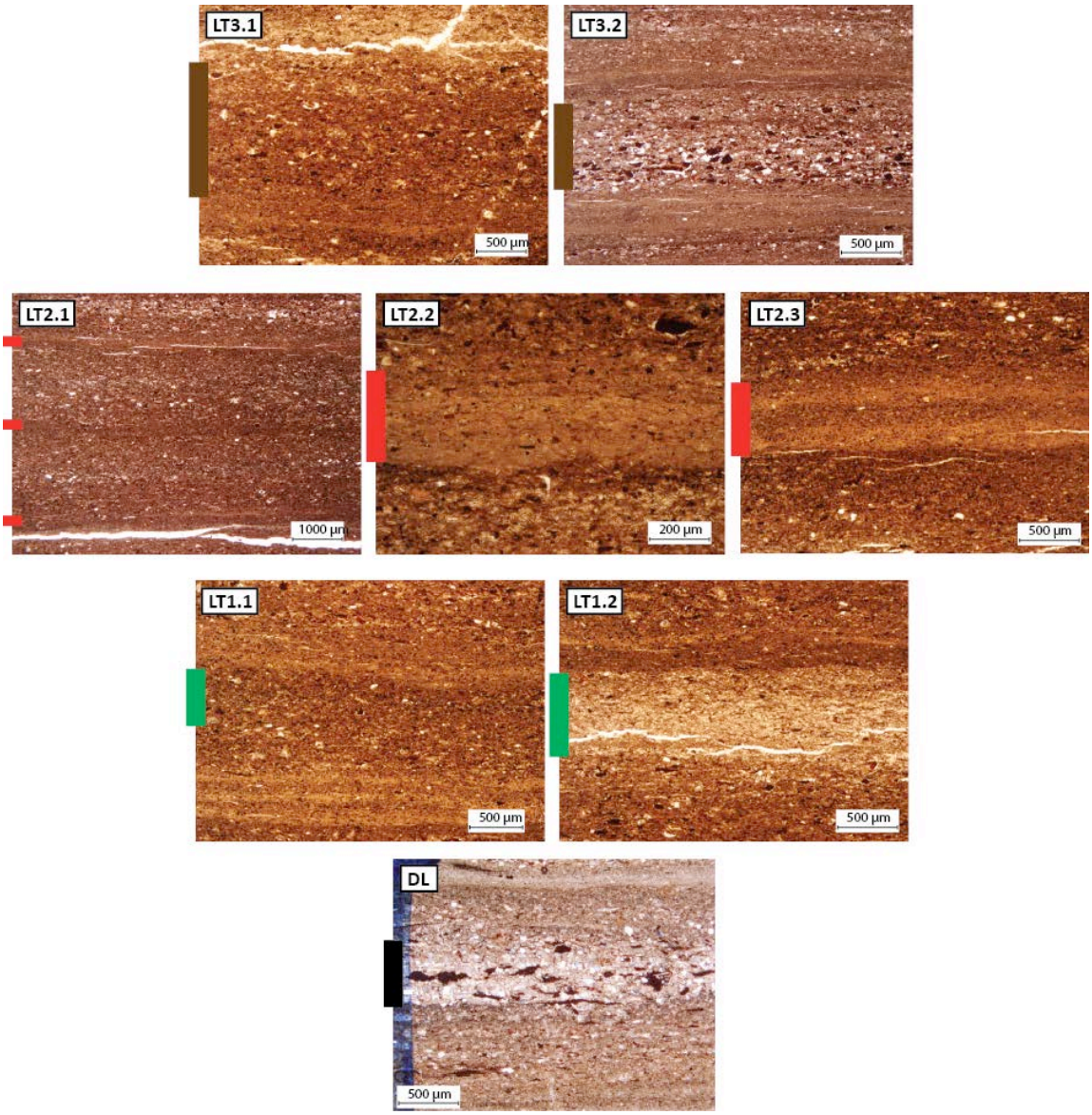

Figure 8.8. *Thin section images showing the variations in structure and composition of the lamination types that compose the varves in the Marks Tey sequence. LT-1 can be sub-divided based on the abundance of diatoms present (LT-1.1: <50%, LT-1.2: >50%), LT-2 is sub-divided on the basis of calcite abundance (LT-2.1: ≤30%, LT2.2 and 2.3: >50%) and the presence of multiple calcite sub-laminations (LT-2.3). LT 3 is sub-divided on the basis of the abundance of minerogenic material (LT-3.1: ≤10% and LT3.2: 10-30%). There are 12 possible lamination sets that can be produced by combining these lamination types. Detrital layers (DL) also occur within the lamination types (see section 7.2.4 in chapter 7). The image here is of a detrital layer present between LT-3.3 and the proceeding LT-1.1.*

8.4.1. Lamination set zone 1 (1,214 vyrs)

Zone 1 corresponds to the lowermost section of the varved sequence, covering the first 1,214 vyrs of MTSC-2014 (Fig. 8.9) and occurring from the later part of pollen zone Ho IIb to the first part of Ho IIc (early-temperate phase) (Fig.8.10). The zone is characterised by thin varves (average thickness ~700µm; Fig. 8.10b) that contain LT-1.1 (<50% diatom abundance) (Table 8.1; Fig. 8.10d), LT-2.1 (≤30% calcite abundance)

(Table 8.1; Fig. 8.11d) and LT-3.1 (organo-clastic laminations with ≤10% mineral grain abundance) (Table 8.1; Fig. 8.12d). As well as these lamination sets, zone 1 is also characterised, to a lesser extent, by varves that contain LT-2.2 (>50% calcite abundance) (Table 8.1; Fig. 8.10d) and LT-3.2 (organo-clastic laminations with 10-30% mineral grain abundance) (Table 8.1; Fig. 8.12d). The zone also contains a number of detrital layers, which occur in 13% of the varves present (Fig. 8.12f).

Table 8.1. *Relative percentages of each lamination set that comprise the lamination set zones identified in the varved interval of the Marks Tey sequence (MTSC-2014), as defined in figure 8.7. The cells shaded in green represent lamination sets that comprise more than 10% of those zones, while those shaded in red indicate the most commonly occurring lamination set. The graph can be viewed in two halves: from lamination sets 1-6 and 7-12. Lamination sets 1-6 are characterised by LT-1.1 (<50% diatom abundance) and the possible combinations of LT-2 and LT-3, whereas lamination sets 7-12 are characterised by LT-1.2 (>50% diatom abundance) and possible combinations of LT-2 and LT-3.*

	Lamination Sets (%)											
	1	2	3	4	5	6	7	8	9	10	11	12
MF Zones	1.1/2.1/3.1	1.1/2.1/3.2	1.1/2.2/3.1	1.1/2.2/3.2	1.1/2.3/3.1	1.1/2.3/3.2	1.2/2.1/3.1	1.2/2.1/3.2	1.2/2.2/3.1	1.2/2.2/3.2	1.2/2.3/3.1	1.2/2.3/3.2
Zone 1	36.7	21.1	17.7	5.2	3.7	1.1	4.0	1.9	5.0	1.5	1.7	0.6
Zone 2	14.8	4.0	22.8	14.0	7.6	2.1	3.2	2.3	12.9	8.0	5.3	3.0
Zone 3	9.0	1.7	11.6	2.2	4.1	0.6	11.5	2.3	32.1	7.2	15.1	2.6
Zone 4	22.0	2.2	20.7	3.2	4.1	0.0	11.0	1.2	22.0	3.9	8.8	1.0

8.4.2. Lamination set zone 2 (478 vyrs)

Lamination set zone 2 occurs from varve number 1,210 – 1,687, during the middle of the early-temperate phase (Ho IIc), as identified by the pollen assemblage (Fig.8.10a). Based on lamination type characteristics and varve thickness changes, the zone can be sub-divided into three sections (Table 8.2; Fig. 8.13).

8.4.2.1. Zone 2a (1,210 – 1,350 vyrs)

The transition between zone 1 and 2a is marked by an increase in varve thickness (~1.22mm) (Fig. 8.14a), which also coincides with the onset of the NAP phase (blue shading in Fig. 8.9a). The most frequently occurring lamination set in this zone is composed of lamination types LT-1.1, LT-2.2 and LT-3.2 (Table 8.2; Fig. 8.14d, g, j). The zone is also characterised by varves that contain LT-3.1 and, to a lesser extent, LT-1.2 (Table 8.2; Fig. 8.14e, i). Detrital layers form a significant proportion of sedimentation during this zone, occurring in 54% (73) of the varves (Fig. 8.14k), and provide a large contribution (20.6%) of overall varve thickness in this zone (Fig. 8.14b).

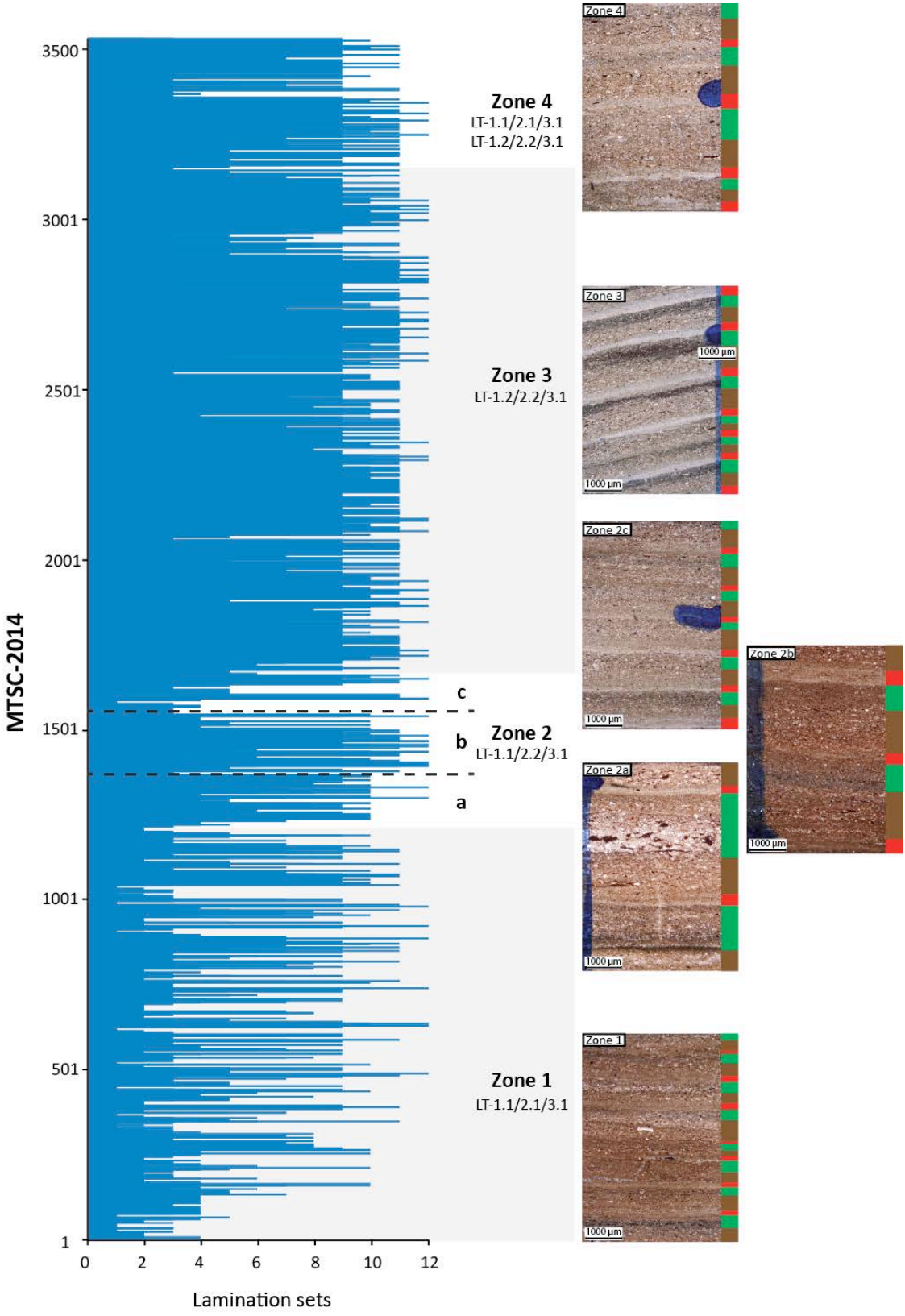

Figure 8.9. *Graphical representation of how the varve micro-facies vary throughout the sequence. There is a general trend for increasing lamination set numbers from zone 1 to zone 3, which then changes to a trend towards lower lamination set values in zone 4. Zone 2 has been divided into three sub-zones and represents a distinctive phase of increased lamination set numbers that is superimposed on the long-term trend, which is discussed in section 8.4.2. The lamination sets that characterise each zone are shown, along with photomicrographs illustrating the variation in varve-microfacies structure that occurs through the sequence.*

8.4.2.2. Zone 2b (varve 1,351 – 1,532)

Zone 2b is characterised by a second, larger peak in varve thickness, with average thickness values of ~1.47mm (Fig. 8.14a). The lamination set composition of this zone differs from 2a in terms of the organo-clastic lamination (LT-3). Whereas zone 2a is characterised by LT-3.2, zone 2b is characterised by organo-clastic laminations with lower abundances of mineral grains (LT3.1) (Fig. 8.14i). The zone is also characterised by a trend towards higher lamination type values, with varves composed of diatom-rich laminations (LT-1.2) and calcite-rich laminations; both with single (LT-1.2) and multiple laminations (Table 8.2). Detrital layers occur less frequently in this zone, occurring in 24% (43) of the varves (Fig. 8.14k). Despite the generally thicker varves that occur during this zone, detrital layer sedimentation accounts for only 5.6% of total varve thickness (Fig. 8.14b).

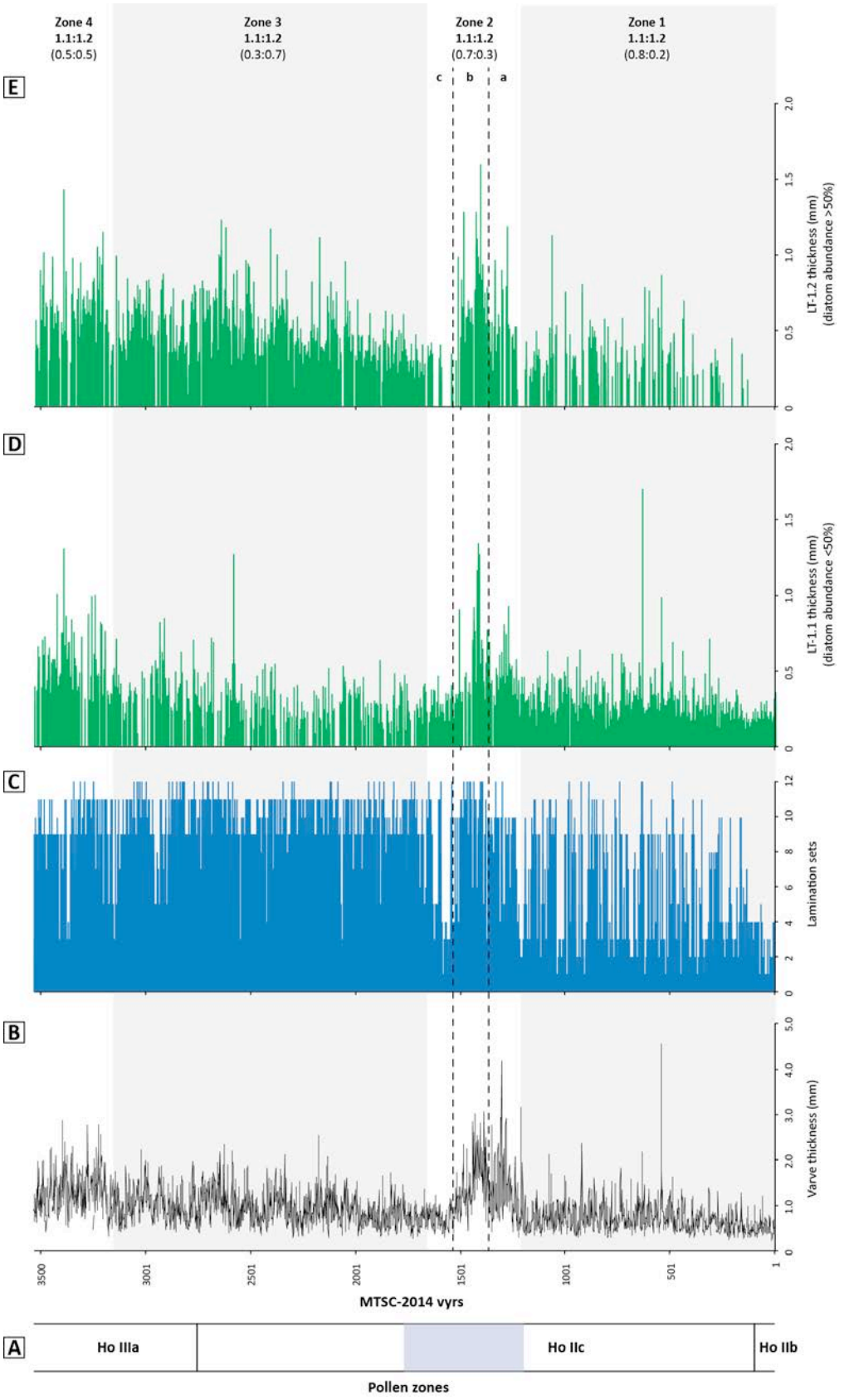

Figure 8.10. *Micro-facies analysis of LT-1, which can be sub-divided based on the abundance of diatoms present. A) pollen zones covered by the varved interval; B) total varve thickness; C) variation in lamination sets present (black line is a 50-point moving average); D) variation in LT-1.1 (<50% diatom abundance) through the sequence; E) variation in LT-1.2 (>50% diatom abundance) through the sequence. The sequence can be sub-divided into four lamination set zones, based on the lamination set data presented in C. The sub-zones of zone 2 are also highlighted (dashed lines).*

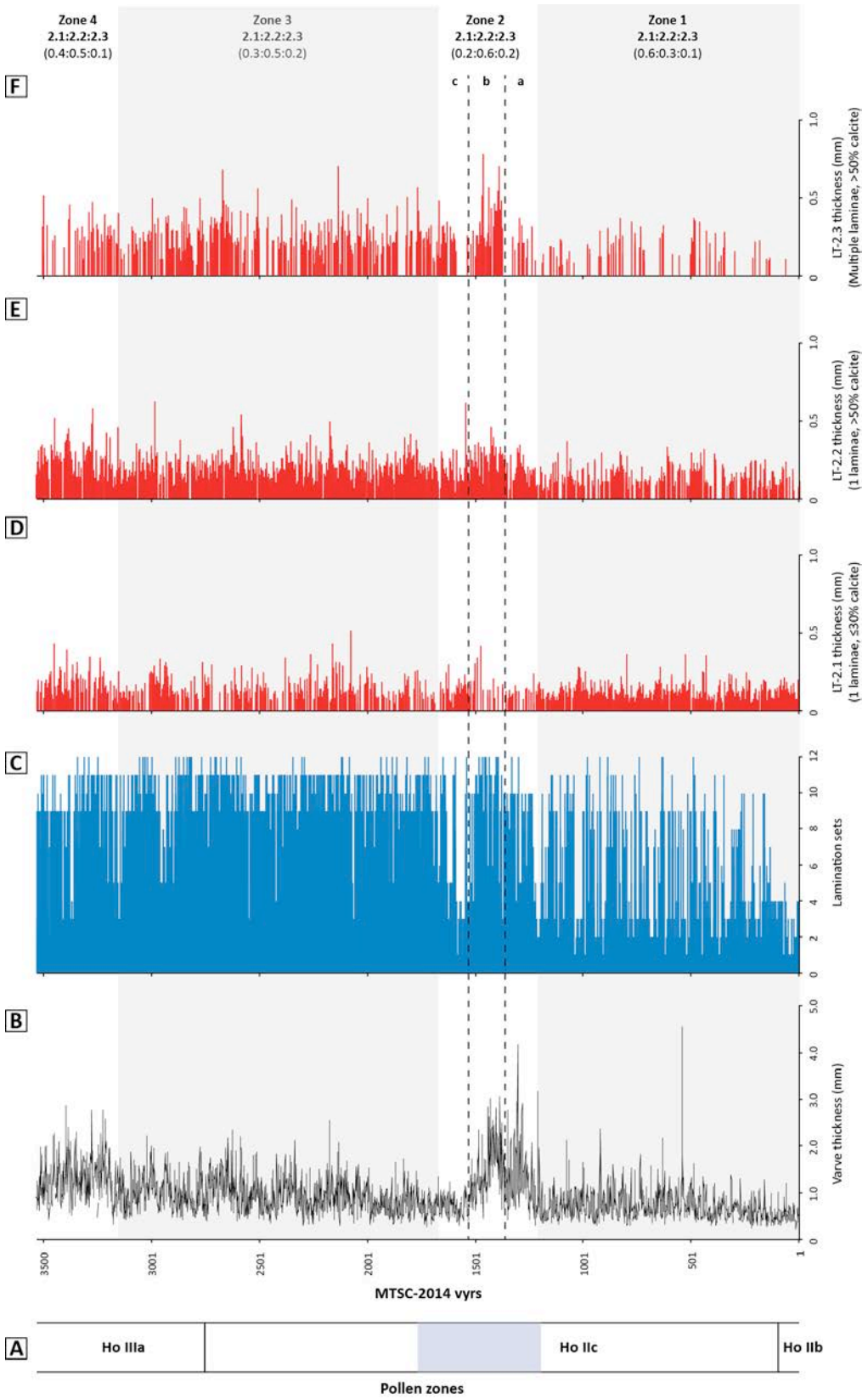

Figure 8.11. *Micro-facies analysis of LT-2, which can be sub-divided based on the abundance and number of calcite lamination present. A) pollen zones covered by the varved interval; B) total varve thickness; C) variation in lamination sets present; D) variation in LT-2.1 (≤30% calcite, 1 lamination) through the sequence; E) variation in LT-2.2 (>50% calcite, 1 lamination) through the sequence; F) variation in LT-2.3 (>50% calcite, multiple laminations) through the sequence. The sequence is sub-divided into four lamination set zones, based on the lamination set data presented in C.*

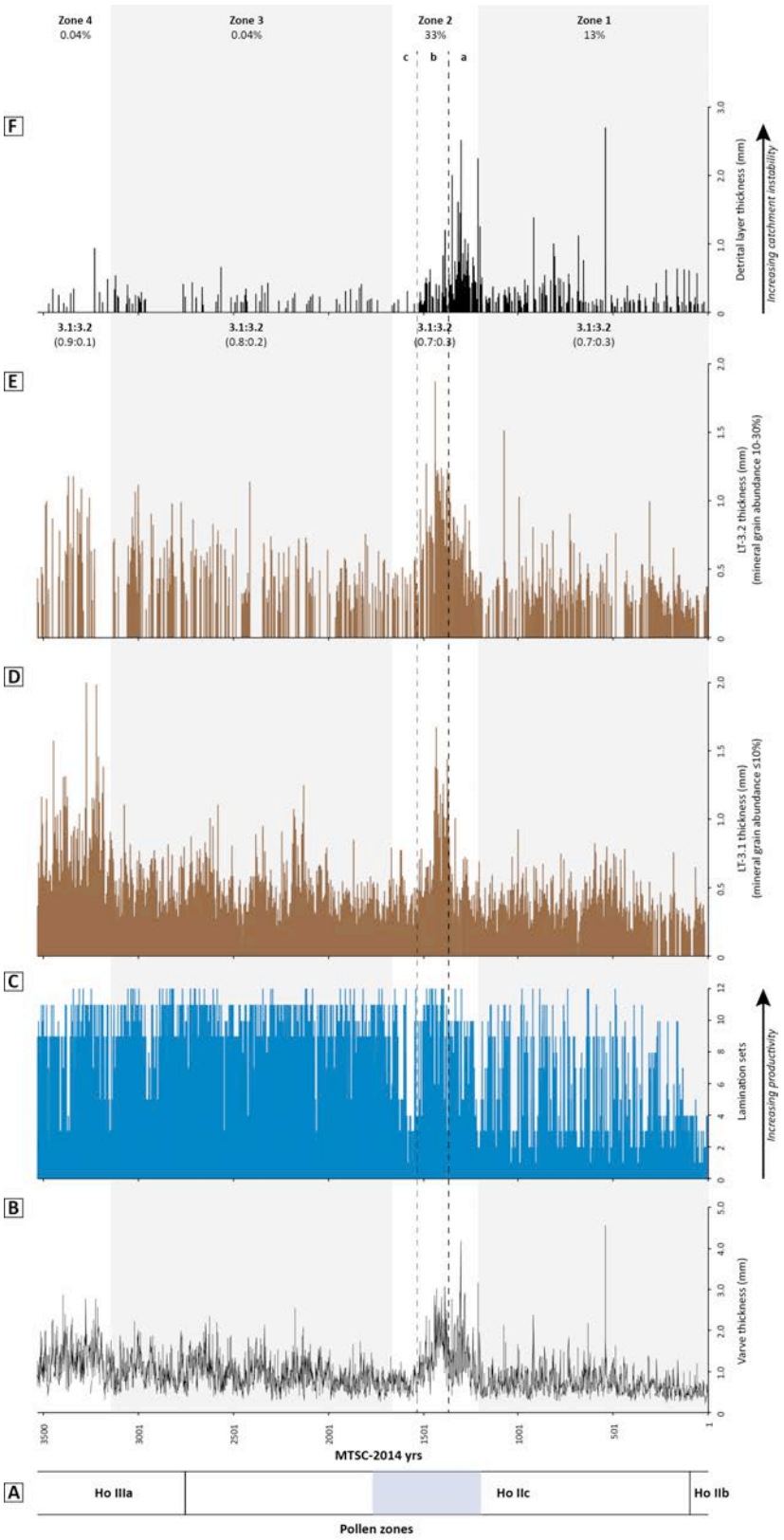

Figure 8.12. *Micro-facies analysis of LT-3, which can be sub-divided based on the abundance of minerogenic material present in the organo-clastic laminae. A) pollen zones covered by the varved interval; B) total varve thickness; C) variation in lamination sets present; D) variation in LT-3.1 (<10% mineral grain abundance) through the sequence; E) variation in LT-3.2 (10-30% mineral grain abundance) through the sequence; F) variation in location of detrital layers through the sequence. The sequence can be sub-divided into four lamination set zones, based on the lamination set data presented in C.*

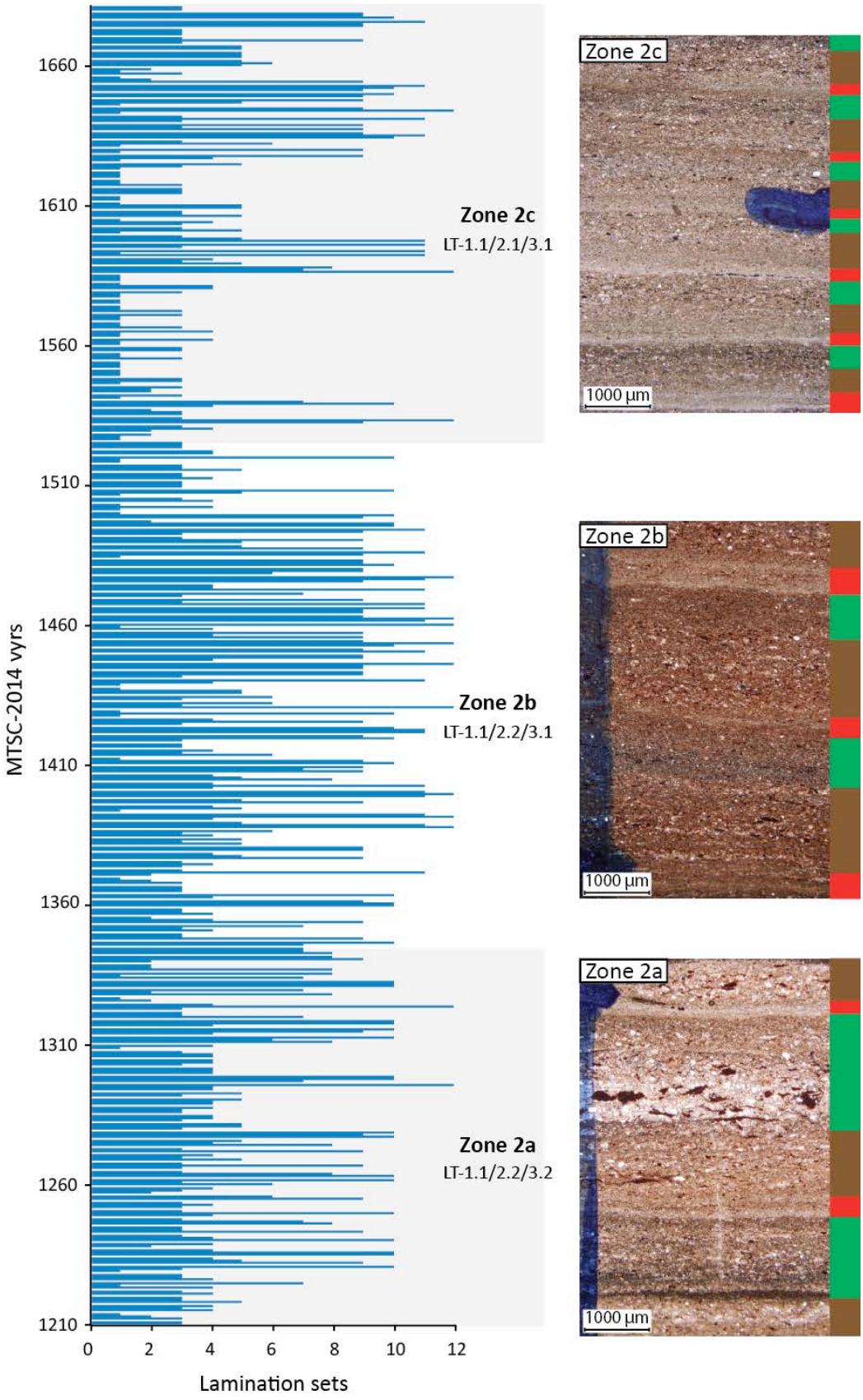

Figure 8.13. *Graphical representation of how varve micro-facies vary through zone 2. There is a trend for increasing lamination set numbers from zone 2a to 2b. Zone 2c is characterised by lamination sets with generally lower values when compared to zone 2a and 2b.*

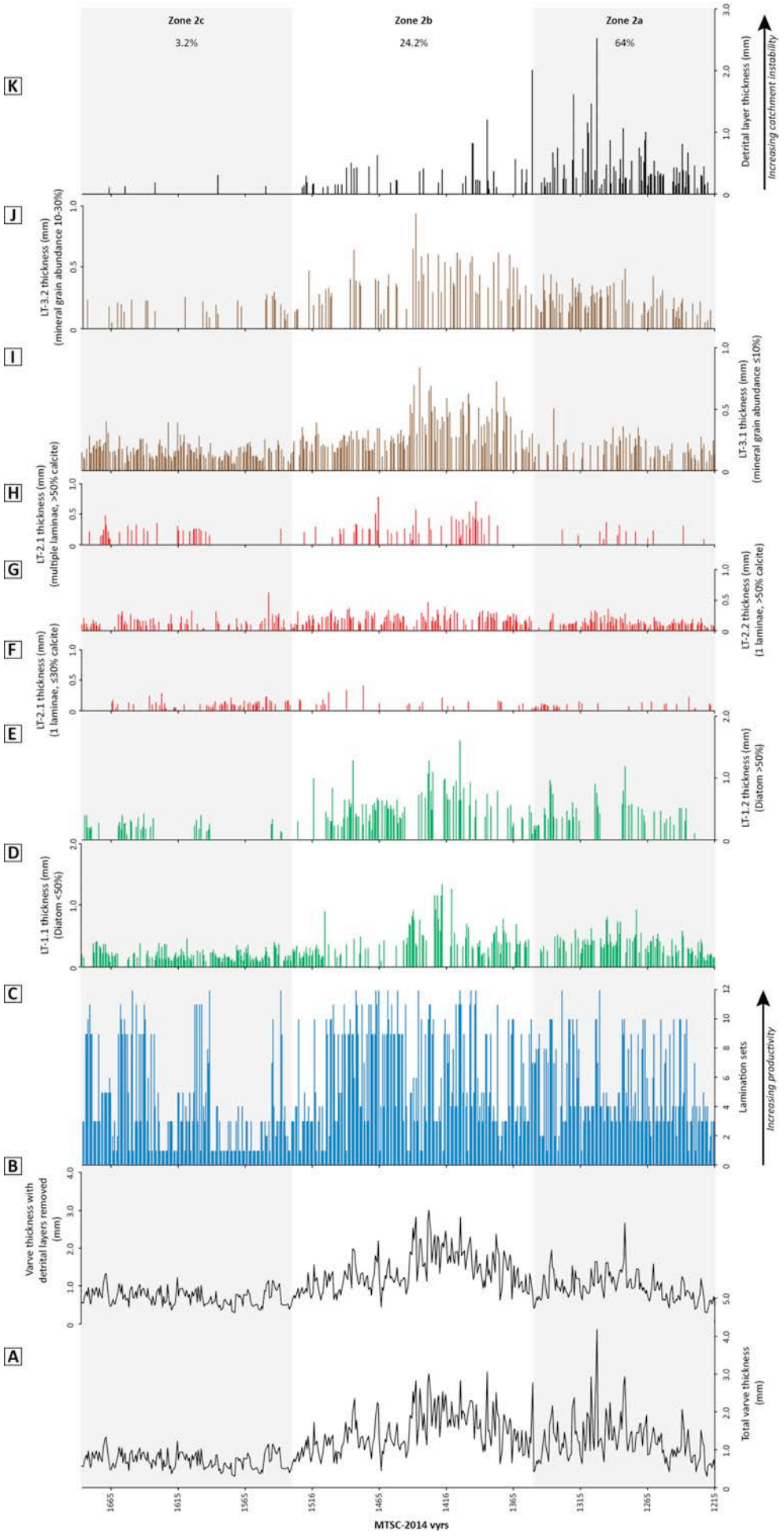
Zone 2c
3.2%
Zone 2b
24.2%
Zone 2a
64%
K
Detrital layer thickness (mm)
Increasing catchment instability
J
LT-3.2 thickness (mm)
(mineral grain abundance 10-30%)
I
LT-3.1 thickness (mm)
(mineral grain abundance ≤10%)
H
LT-2.1 thickness (mm)
(multiple laminae, >50% calcite)
G
LT-2.2 thickness (mm)
(1 laminae, >50% calcite)
F
LT-2.1 thickness (mm)
(1 laminae, ≤30% calcite)
E
LT-1.2 thickness (mm)
(Diatom >50%)
D
LT-1.1 thickness (mm)
(Diatom <50%)
C
Lamination sets
Increasing productivity
B
Varve thickness with
detrital layers removed
(mm)
A
Total varve thickness
(mm)
1665
1615
1565
1516
1465
1416
1365
1315
1265
1215
MTSC-2014 vyrs

↑ ***Figure 8.14.*** *Micro-facies analysis of zone 2, which shows the variation in varve micro-facies during the NAP phase. A) Total varve thickness; B) total varve thickness with detrital layers removed; C) variation in lamination sets present; D) variation in LT-1.1 (<50% diatom abundance); E) variation in LT-1.2 (>50% diatom abundance; F) variation in LT-2.1 (≤30% calcite, 1 lamination); G) variation in LT-2.2 (>50% calcite, 1 lamination); H) variation in LT-2.3 (>50% calcite, multiple laminations); I) variation in LT-3.1 (<10% mineral grain abundance); J) variation in LT-3.2 (10-30% mineral grain abundance); K) variation in location of detrital layers through the zone. The zone has been sub-divided into three lamination set zones, based on the lamination set data presented in C and the varve thickness data in A.*

Table 8.2. *Relative percentages of each lamination set that comprise the lamination set sub-zones identified in zone 2, based on the data in figure 8.12. The cells shaded in green represent lamination sets that comprise more than 10% of those zones, while those shaded in red indicate the most commonly occurring lamination set. The graph can be viewed in two halves, from lamination sets 1-6 and 7-12. Lamination sets 1-6 are characterised by LT-1.1 (<50% diatom abundance) and the possible combinations of LT-2 and LT-3, whereas lamination sets 7-12 are characterised by LT-1.2 (>50% diatom abundance) and possible combinations of LT-2 and LT-3.*

	Lamination Sets (%)											
	1	2	3	4	5	6	7	8	9	10	11	12
MF Zones	1.1/2.1/3.1	1.1/2.1/3.2	1.1/2.2/3.1	1.1/2.2/3.2	1.1/2.3/3.1	1.1/2.3/3.2	1.2/2.1/3.1	1.2/2.1/3.2	1.2/2.2/3.1	1.2/2.2/3.2	1.2/2.3/3.1	1.2/2.3/3.2
Zone 2a	4.5	6.1	23.5	24.2	6.1	2.3	5.3	6.8	6.1	13.6	0.0	1.5
Zone 2b	8.2	2.2	20.3	13.7	7.1	2.7	2.7	0.5	19.8	7.5	10.0	4.9
Zone 2c	30.8	4.4	25.2	5.7	9.4	1.3	1.9	0.6	10.7	3.1	5.0	1.9

8.4.2.3. Zone 2c (varve 1,533 – 1,687)

Zone 2c has similar lamination set characteristics to zone 1, with lamination set 1 (LT-1.1, LT-2.1, LT-3.1) the most frequently occurring varve type (Table. 8.2). Varves in this zone also commonly contain LT-2.2 (25.2%), and occasionally LT 1.2 (10.7%) (Table 8.2). This zone is also characterised by reduced varve thicknesses (~730µm) and the occurrence of detrital layers in only 3.4% (5) of the varves (Fig. 8.14k).

8.4.3. Lamination set zone 3 (1,433 vyrs)

Lamination set zone 3 covers varve number 1,688 – 3,121 and occurs during the latter part of Ho IIc and the early part of the late-temperate phase (Ho IIIa) in the sequence (Fig. 8.12a). Lamination set zone 3 is characterised by the dominance of lamination sets 6-12, which are all driven by laminations that contain >50% diatom abundance (Fig. 8.9). Varve thickness also displays a general increasing trend through this zone, with average thickness values of ~0.94mm (Fig. 8.10). The dominant varve architecture in this zone is composed of LT-1.2 (Fig. 8.10e), LT-2.2 (Fig. 8.11e) and LT-3.1 (Fig. 8.12d), which accounts for 32.1% of the varved sediment (Table 8.1). Varves in this zone are also characterised by the presence of multiple calcite sub-laminations (LT-2.3, Fig. 8.11e), which occur in frequencies above 10% in lamination set 11 (15.1%) (Table

8.1), with varves containing LT-2.1 (Fig. 8.11d) composing 11.5% of varves in the interval (Table 8.3). Although this zone is dominated by varves containing LT-1.2, LT-1.1 is also present (Table 8.1). Zone 3 is also characterised by the infrequent occurrence of detrital layers, which occur in 0.04% of varves in the zone (Fig. 8.12f).

8.4.4. Lamination set zone 4

The final lamination set zone in the sequence covers varve number 3,122 – 3,533, occurs during Ho IIIa and is characterised by intermediate lamination set values between zone 1 and 3, containing both LT-1.1 and LT-1.2. The increasing varve thickness trend observed in zone 3 continues, with an average thickness of ~1.27mm (Fig. 8.10b). Varves in this zone are characterised by lamination sets that dominate both zone 1 (lamination set 1) and zone 3 (lamination set 9) (Table. 8.1). Much like zone 3, detrital layers also occur infrequently (0.04%) (Fig. 8.12f).

8.5. Synthesis of lamination set variations

Stratigraphical changes in the sub-annual structure of varved sediments can be used as a proxy for temporal changes in environmental conditions within lakes and their catchments (e.g. Brauer et al., 1999b; Lucke and Brauer, 2004; Palmer et al., 2010). This is also possible at Marks Tey, where variations in the dominant lamination sets that compose the varved sediments indicate changing environmental conditions during the early-temperate (Ho IIc) and early part of the late-temperate (Ho IIIc) pollen phases. The lamination set data reveals two major changes in environmental conditions; the first is a long-term trend that occurs throughout the sequence, which is punctuated by a second, short-term trend associated with lamination set zone 2, which forms part the NAP Phase.

8.5.1. Long-term environmental signal

The long-term environmental signal contained within the varved sediments is one of increasing lake catchment stability and within-lake productivity during Ho IIc and the early part of Ho IIIa (zones 1-3), with possible changes in lake level occurring during Ho IIIa (zone 4). Lake development has already been discussed in chapter 6, in which changes in macro-scale sedimentology from LFa-1 (non-varved sediments) to LFa-2

(varved sediments) indicate the gradual stabilisation of the lake catchment and increasing productivity within the lake (chapter 6, section 6.5.3). While more obvious changes occur in the sequence from LFa-1 to LFa-2 that are identifiable at the macro-scale, micro-scale observations of the lamination sets described in this chapter also reveal changes in landscape stability and lake productivity during LFa-2.

Although the presence of repeating lamination sets was suggested to indicate the development of stable catchment conditions and a productive lake, the lamination set data suggests that during varve deposition in the first part of Ho IIc (zone 1), the lake catchment remained relatively unstable (Fig. 8.12c), as indicated by the presence of detrital layers within the varves (Fig. 8.12f), as well as the presence of organo-clastic laminations with higher abundances of minerogenic material (LT-3.2, lamination set 2) (Fig. 8.12e). During this period, lake productivity also remained relatively low, as suggested by the dominance of varves that contain lamination types LT-1.1 (<50% diatom abundance) and LT-2.1 (≤30% calcite abundance).

The less frequent occurrence of detrital layers during zone 3 indicates the development of stable catchment conditions, and is supported by a trend towards higher lamination set numbers in zone 3, which indicates that the lake became more productive during the second part of Ho IIc, following the NAP phase (Fig. 8.12c). This is because lamination sets 6-12 are characterised by LT-1.2 (>50% diatom abundance). Further evidence for a more productive system come from the tendency for varves to contain calcite laminations LT-2.2 (single lamination, >50% calcite) and LT2.3 (multiple laminations, >50% calcite). The presence of multiple calcite sub-laminations during a single summer is intriguing, as a mechanism must exist to promote multiple pulses of calcite precipitation in the water column. Multiple whiting events have been observed in some lakes (Romero et al., 2006) and multiple calcite sub-laminations have been noted in varved sequences (Brauer et al., 2008b; Teranes et al., 1999a, b), but the mechanism for these observations is uncertain. In a productive lake with long growing seasons, a number of changes within lake waters can alter $CaCO_3$ saturation levels, including changing nutrient levels, algal productivity, temperature and pH. One possibility is the influence that changing meteorological conditions can have on $CaCO_3$ saturation levels (Gruenert and Raeder, 2014). In this study, observations at three

hardwater lakes in Germany found that periods of increased wind activity during water column stratification reduced epilimnetic pH and, therefore, the level of $CaCO_3$ saturation in the water column.

The trend towards lower lamination set values that occured during zone 4 (pollen zone Ho IIIa) is also interesting, as it may suggest that levels of productivity within the lake were decreasing during the early part of the late-temperate pollen phase of the Hoxnian. The shift is driven by a change from lamination types that are characterised by LT-1.2 (>50% diatom abundance) to those that contain (<50% diatom abundance) (Fig. 8.10d). The varve thickness record also appears contradictory, as zone 4 contains varves that are almost as thick as those during zone 2 (the NAP phase) (Fig. 8.12b). In contrast to zone 2, varve thickness is not driven by the deposition of detrital layers (which occur in only 0.04% of varves in the interval). Changes in varve thickness during this zone are, therefore, caused by an abundance of organic material in LT-1 (Fig. 8.10d) and the deposition of thick organo-clastic laminae in LT-3 (8.12d). Furthermore, the late-temperate phase (Ho IIIa) is characterised at a number of Hoxnian sites by the occurrence of thermophilous plant taxa (e.g. *Trapa natans*) that suggest peak interglacial conditions occurred during this time period (Coxon, 1985). In the absence of significant input of detrital material during this zone, another mechanism is required to explain the changes in varve thickness observed.

Temporal changes in basin morphometry, caused by basin infilling and changing water depths, can lead to changes in varve thickness and composition (Nuhfer et al., 1993). Given that the maximum water depth at Marks Tey would have been ~35m, it is considered unlikely, over the 4m depth interval of continuous varve preservation, that basin infilling could account for such changes. A change in the proximity of sediment input due to changing lake level is considered more likely, as a number of Hoxnian sites (including Marks Tey) display evidence for water level changes during MIS 11 (West, 1956; Turner, 1970; Gibbard and Aalto, 1977; Gibbard et al., 1986; Boreham and Gibbard, 1995). At Marks Tey, water level changes are indicated by sediment slumping and lake bed brecciation (Turner, 1970), as well as a decrease in planktonic/benthic diatom ratios (Evans, 1972), during pollen sub-zone Ho IIIb. Although the varves in zone 4 occur during the preceding pollen sub-zone (Ho IIIa), the microfacies may

indicate that water levels were lowering at this time. As well as the changes in varve thickness, varve quality also reduces during zone 4 (Fig. 8.7). The reduction in varve quality and the cessation of continuous varve preservation during this zone suggests that anoxic bottom water conditions were not maintained, possibly a result of lowering lake levels.

8.5.2. Short-term environmental signal: the NAP phase

Changes in lake productivity indicated by the varve micro-facies are punctuated in Ho IIc by a section of the core that does not follow this long-term trend. This section of the core relates to the NAP phase, the structure of which will be described in chapter 10. To summarise the varve micro-facies changes, the event is characterised by short-term variations in lake catchment stability and lake productivity. Varve thickness demonstrates two distinct peaks in thickness during this interval, with average thicknesses of ~1.22µm (zone 2a) and ~1.47µm (zone 2b). The first peak in varve thickness is associated with low lamination set numbers, driven by diatom abundances in LT-1 of <50%, suggesting low levels of productivity. This zone is also characterised by the presence of detrital layers, which contribute a significant proportion to overall varve thickness, suggesting an unstable lake catchment. The second peak (zone 2b) is characterised by fewer detrital layers and an increase in the frequency of varve structures indicative of greater lake productivity, with diatom abundances >50% in LT-1 and calcite laminations containing calcite concentrations >50%. The final stage of this interval (zone 2c) is characterised by decreasing varve thicknesses, infrequent detrital layer deposition and low lamination set values. The lack of detrital layers and varves characterised by organo-clastic laminations (LT-3.1) indicates increased catchment stability, while lower levels of productivity within the lake are indicated by varves characterised by diatom abundances of <50% in LT-1.

8.6. Summary

- Varve counting undertaken on the Marks Tey sequence identified 3533 varves. A total counting error of 201 varves over the three counts gives a counting error for the chronology of 5.7%.

- Between 15.99 – 12.36 mbs, varves represent the dominant sedimentary structures preserved (at least 70%), and interpolation based on average sedimentation rates gives an estimated 467 missing varves.
- Between 16.45 – 15.99 mbs, varves only represent only 20.5% of the sediment sequence. Based on estimated sedimentation rates for the whole of this section of the core, and using interpolation, 903 varves are missing from the sequence.
- Two varve chronologies have been developed for the MT-2010 sequence. The first is based only on counted varves (MTSC-2014), while the second includes an estimate of the numbers of varves missing from micro-hiatuses in varve sedimentation (MTSC-2014^{INT}).
- Changes in varve micro-facies show the long-term development of landscape stability and increasing lake productivity during the latter stage of pollen zones Ho IIb through Ho IIc (early-temperate phase) and the first part of Ho IIIa (late-temperate phase).
- This long-term lake and catchment development is punctuated during Ho IIc by the NAP phase, with varve micro-facies showing distinctive short-term variations during the event. The first part of the NAP phase is characterised by landscape instability low lake productivity, the second zone by increasing landscape stability and increased lake productivity, and the final stage with a stable catchment and low levels of lake productivity.

Chapter 9. Stable isotope stratigraphy

Chapter overview

Marks Tey is one of the few Hoxnian lacustrine sites in Britain where the sediments contain a significant component of authigenic carbonate. Consequently, it is one of the few sites of this age that can be analysed at high precision for oxygen and carbon isotopes to: 1) produce a record of environmental change for the early part of MIS 11; and 2) investigate potential forcing mechanisms for the NAP phase.

This chapter therefore presents results from oxygen and carbon isotopic analysis of *in situ* carbonate laminations that characterise the lowermost 6.5m of the Marks Tey sequence. The aim of this analysis is to develop a stable isotope stratigraphy for the first part of MIS 11 in the British Isles, from the pre-temperate (pollen zone Ho I) to early late-temperate phase (Ho IIIa). The first section of this chapter will present and describe the main patterns in the $\delta^{18}O$ and $\delta^{13}C$ data and to compare this to changes in the lithostratigraphy. The patterns that occur within the isotope data are used to sub-divide the sequence into two main isotope zones. The chapter then discusses the factors that may drive both the $\delta^{18}O$ and $\delta^{13}C$ signal, with respect to lake basin hydrology, detrital contamination and climate. The chapter then concludes by discussing the climatic significance of this record in the context of other MIS 11 records in Britain and Europe.

9.1. Introduction

Chapter 3 reviewed the application of oxygen and carbon isotopic analysis to lacustrine carbonates and highlighted the potential of these archives to generate detailed palaeoenvironmental records, as well as their potential to record abrupt climatic events. The construction of a $\delta^{18}O/\delta^{13}C$ stratigraphy for the lowermost 6.25m of the MT-2010 sequence is crucial to this thesis for two reasons: 1) it has the potential to determine the underlying forcing mechanism for the NAP Phase, and 2) to determine the environmental structure of the first part of the Hoxnian interglacial (Ho I to Ho IIIa) at a resolution that has been hitherto unattainable (see Candy et al., 2010; 2014).

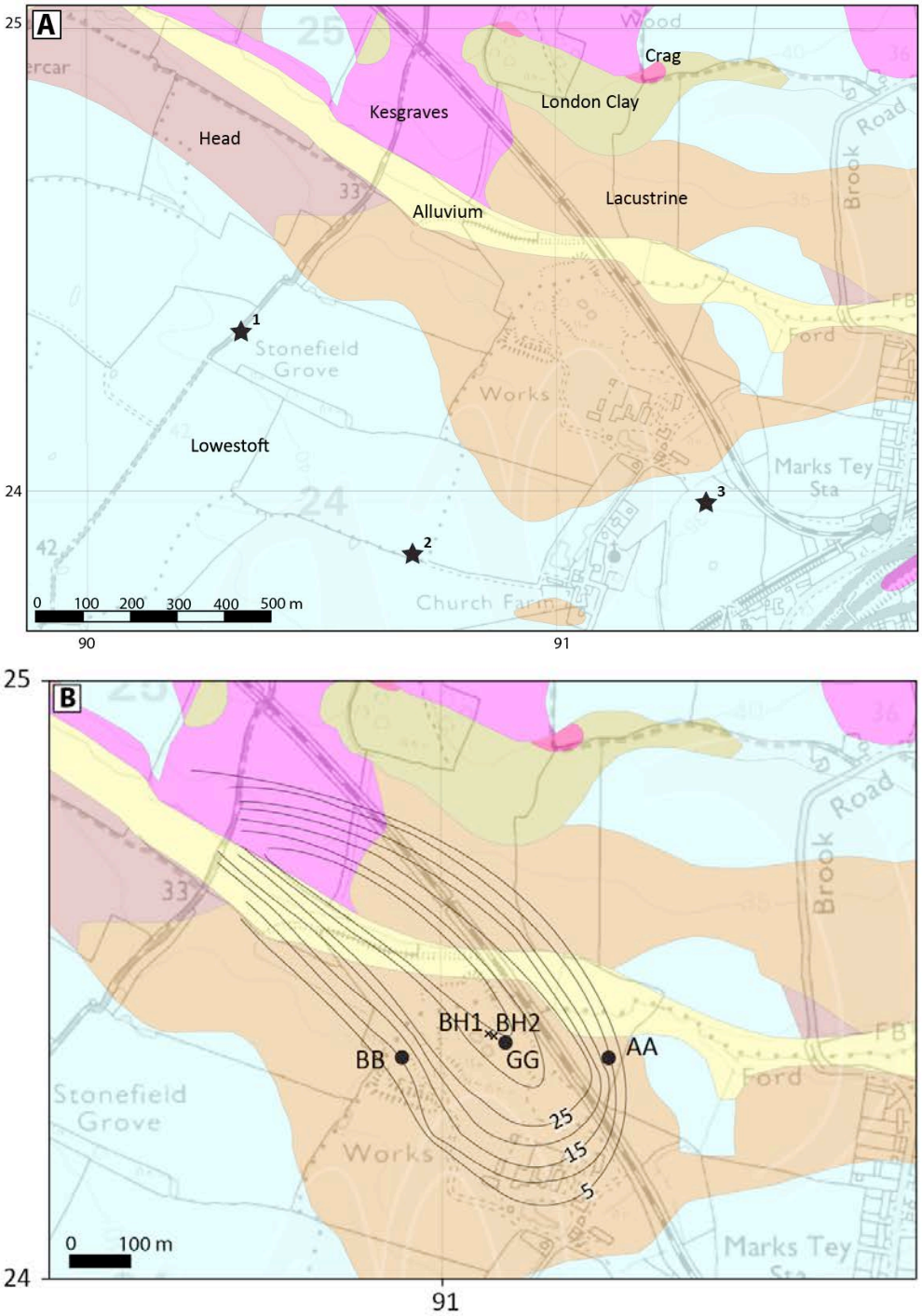

Figure 9.1. *Location maps with surface sediment geology overlays showing A) The locations in the immediate basin catchment (numbered stars) where samples were taken of Lowestoft Till (till matrix and chalk intra-clasts), the likely source of allogenic carbonate that could contaminate the authigenic signal, and B) The location of BH1 and BH2 (MT-2010), along with borehole GG, AA and BB of Turner (1970), within the context of the suggested geometry of the basin (Ellison and Lake, 1986).*

Figure 9.1 shows two location maps for the site. Figure 9.1a shows the location in the immediate basin catchment where samples of chalk-rich Lowestoft Till (MIS 12) were augured to provide samples for the determination of oxygen and carbon isotopic

values of detrital carbonates analogues to those that may have been washed into the basin and contaminated the authigenic signal (Fig. 9.1a). The suggested geometry of the basin is also shown (Ellison and Lake, 1986), along with the location of BH1 and BH2 (sequence MT-2010) and boreholes GG, AA and BB of Turner (1970).

9.2. $\delta^{18}O$ and $\delta^{13}C$ values of the lacustrine carbonates

The oxygen and carbon isotope results from the lowest 6.5m of the Marks Tey sequence are presented in figure 9.2, alongside the composite core stratigraphy, lithofacies zones and pollen zones. The isotope record has been sub-divided into two isotopic zones (MTIZ's), based on a visual inspection of the patterns present in the descriptive statistics of the $\delta^{18}O$ data. Essentially, at a depth of 15.90 mbs there is a shift in both; 1) the scatter present in the dataset (as represented by the standard deviation), and 2) the five point running average within the dataset. MTIZ 1 (18.47 to 15.90 mbs) is characterised by a higher mean $\delta^{18}O$ value and a lower 1σ standard deviation than MTIZ 2 (15.90 to 12.34 mbs). The $\delta^{18}O$ data, rather than the $\delta^{13}C$ data, was used to sub-divide the isotopic record because, in Western Europe, it is the shift in $\delta^{18}O$ values within lacustrine carbonates that gives the clearest palaeoenvironmental signal. Consequently, zoning the oxygen isotopic data should allow key environmental transitions to be identified.

9.2.1. MT isotopic zone 1 (18.47 – 15.90 mbs, LFa-1 – LFa-2, pollen zone Ho I – early Ho IIc)

The $\delta^{18}O$ (mean = -3.13‰) and $\delta^{13}C$ (mean = 2.32‰) values in MTIZ 1 are relatively high, with $\delta^{13}C$ having a higher standard deviation than $\delta^{18}O$ ($\delta^{13}C$ 1σ = 1.31; $\delta^{18}O$ 1σ = 0.37) (Fig. 9.2, Table 9.1). The higher standard deviation in $\delta^{13}C$ is the result of a pronounced decreasing trend through the zone, from 3.62‰ at 18.47 mbs to a value of 1.68‰ at 15.90 mbs. Although the $\delta^{18}O$ standard deviation is lower, it also exhibits a decreasing trend through the zone, from 18.40 mbs (-2.65‰) to 15.90 mbs (-3.41‰) (Fig. 9.2). The relationship between $\delta^{18}O$ and $\delta^{13}C$ is shown in figure 9.3 and summary statistics in Table 9.1. There is no significant co-variance between $\delta^{18}O$ and $\delta^{13}C$ in MTIZ-1 (r^2 = 0.14) (Table 9.1).

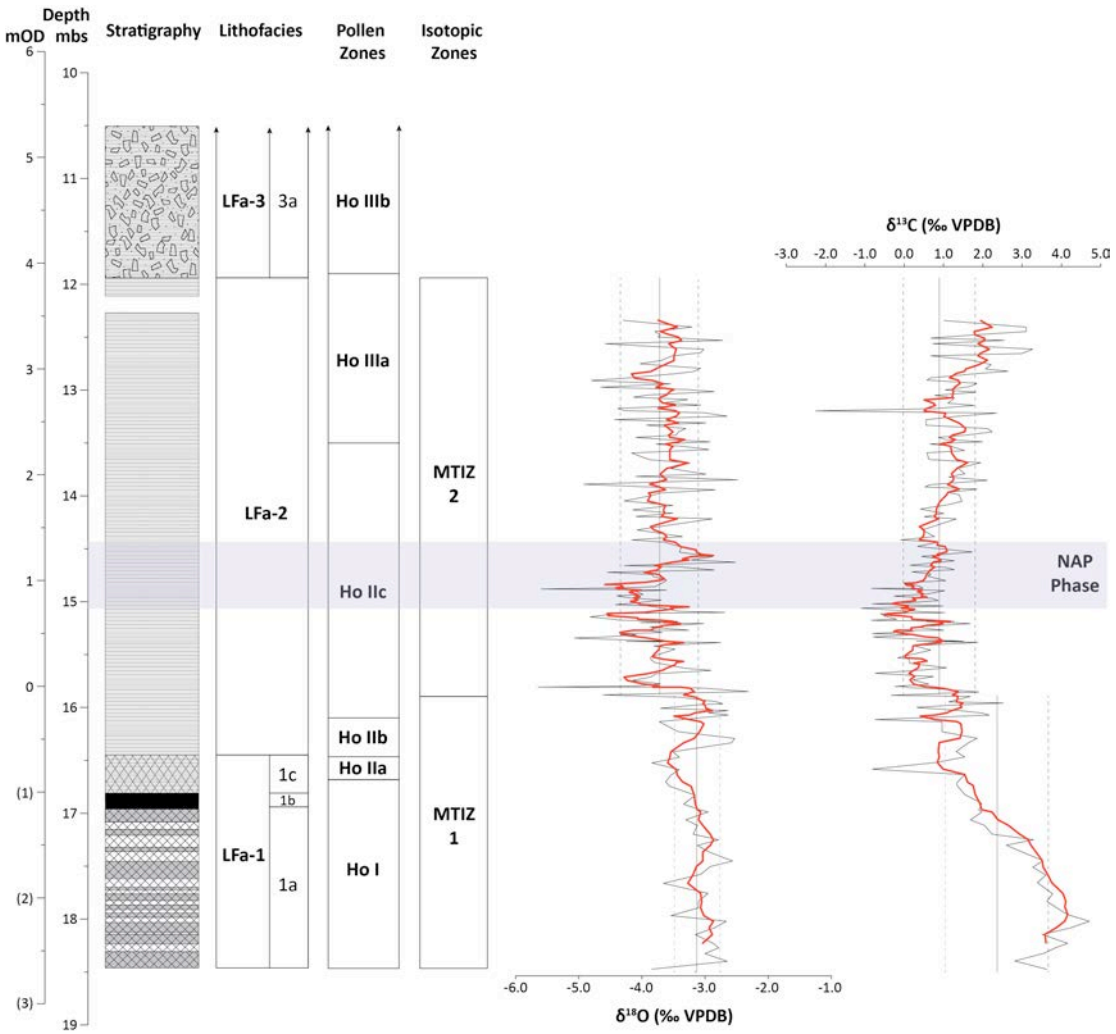

Figure 9.2. *$\delta^{18}O$ and $\delta^{13}C$ datasets plotted against core stratigraphy, alongside the lithofacies, pollen and isotopic zones. The mean (solid grey line), standard deviation (dashed grey line, 1σ) and 5-point moving average (red line) of the $\delta^{18}O$ and $\delta^{13}C$ datasets from both isotopic zones are also plotted. The location of the NAP Phase is indicated by blue shading.*

9.2.2. MT isotopic zone 2 (15.90 – 12.34 mbs, LFa-2, pollen zones Ho IIc – IIIa)

MTIZ 2 is characterised by average $\delta^{18}O$ and $\delta^{13}C$ values that are lower than MTIZ 1 ($\delta^{18}O$ mean = -3.73‰ and $\delta^{13}C$ mean = 0.86‰). The standard deviation in $\delta^{18}O$ increases from that of MTIZ 1 ($\delta^{18}O$ 1σ = 0.62), whilst the standard deviation of $\delta^{13}C$ decreases, but is still high ($\delta^{13}C$ 1 σ = 0.92). $\delta^{13}C$ values continue to decrease across the boundary between MTIZ 1 and 2, reaching a low of -1.10‰ at 15.06 mbs, after which they increase across the rest of this zone. There is no clear trend in the $\delta^{18}O$ signal within MTIZ 2; however, the 5-point moving average highlights an interval between 15.80 to 14.80 mbs where $\delta^{18}O$ values regularly plot below the average $\delta^{18}O$ value for the zone, after which they recover and follow the dataset average between 14.80 to 12.34 mbs (Fig. 9.2).

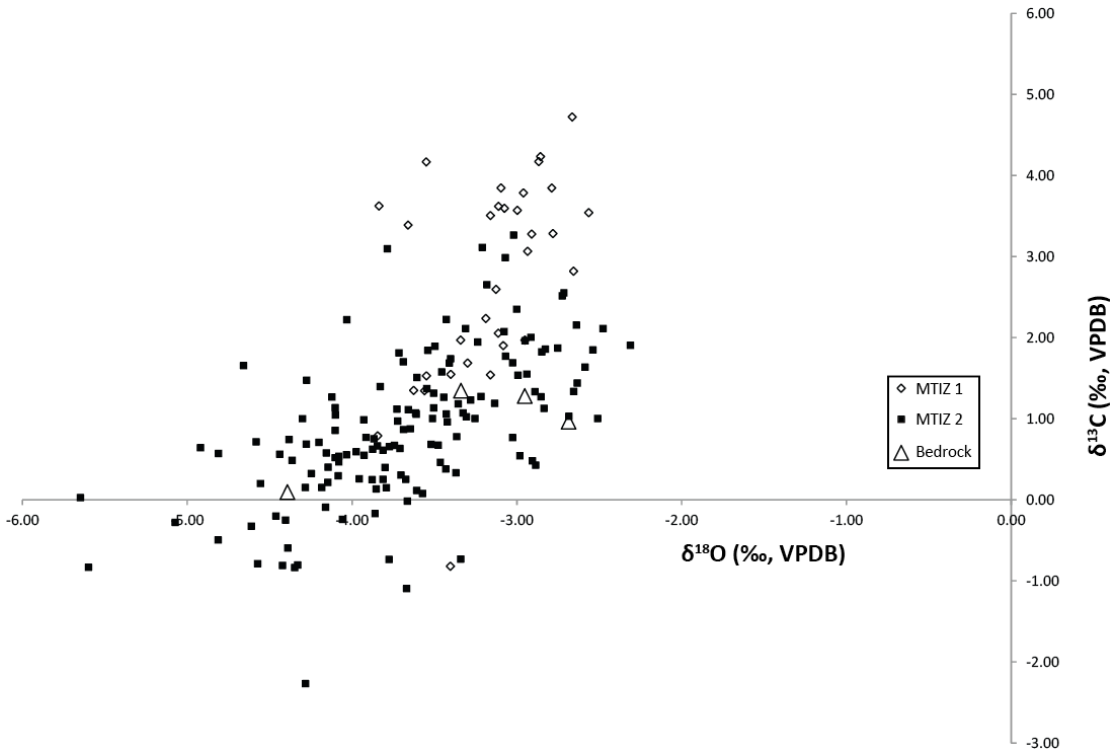

Figure 9.3. *Bi-plot showing the $\delta^{18}O$ and $\delta^{13}C$ composition of carbonate samples from Marks Tey. Samples are plotted according to isotopic zone. Samples taken from the Lowestoft Till are also plotted.*

The lower part of this zone (15.80 to 14.80 mbs) has a lower mean $\delta^{18}O$ value (-3.95‰) than the uppermost part (14.80 to 12.34 mbs), which has mean $\delta^{18}O$ values of -3.61‰ (0.34‰ higher). The lower mean $\delta^{18}O$ value of 15.80 to 14.80 mbs is a function of two factors; 1) the fact that the lowest individual $\delta^{18}O$ values within MTIZ 2 occur between these depths, and 2) the occurrence of a 24 cm section of the core, from 15.04 to 14.80 mbs, where $\delta^{18}O$ values are persistently low (mean $\delta^{18}O$ value = -4.12‰). These low values occur in association with the NAP phase (blue shaded area in Fig. 9.2). No significant co-variance occurs between $\delta^{18}O$ and $\delta^{13}C$ values (r^2 = 0.35) in this zone (Fig. 9.3, Table 9.1).

Table 9.1. *Summary statistics for the $\delta^{18}O$ and $\delta^{13}C$ datasets by isotope zone and for the whole dataset.*

Isotope Zone	N	$\delta^{18}O$	SD (1σ)	$\delta^{13}C$	SD (1σ)	R^2
1	45	-3.13	0.37	2.32	1.31	0.14
2	129	-3.73	0.62	0.86	0.92	0.35
Dataset	174	-3.57	1.23	0.62	1.22	0.38

9.2.3. Isotopic composition of bedrock samples

The $\delta^{18}O$ and $\delta^{13}C$ values of bulk and chalk clast samples taken from carbonate-rich Anglian Till that forms the underlying geology of the area are shown along with the results from MTIZ 1 and 2 in figure 7.2. The $\delta^{18}O$ values of these samples range between -4.39 and -2.69‰, while $\delta^{13}C$ values range between 0.09 and 1.35‰. These values place the bedrock samples within the range of $\delta^{18}O$ and $\delta^{13}C$ values from MTIZ 2 (Fig. 9.3).

9.3. Environmental signal from the $\delta^{18}O$ and $\delta^{13}C$ record

As discussed in chapter 3, the $\delta^{18}O$ and $\delta^{13}C$ value of authigenic lacustrine carbonates can be influenced by a number of factors. These included seasonality of rainfall, evaporation, vegetation development in the lake catchment, within lake productivity, changing sedimentology and detrital contamination. Before the isotopic record from Marks Tey can be discussed in terms of palaeoenvironmental conditions, the key factors influencing $\delta^{18}O$ and $\delta^{13}C$ values of the carbonate need to be determined.

9.3.1. Basin hydrology

When considering the hydrological regime of a lacustrine system, the degree of covariance between $\delta^{18}O$ and $\delta^{13}C$ can be used as a measure of whether a lake basin is hydrologically open or closed. The palaeoclimatic significance of this is that the isotopic composition of carbonates precipitated in hydrologically closed lakes may be strongly influenced by the balance between precipitation and evaporation. As these processes will affect both the $\delta^{18}O$ and $\delta^{13}C$ values of the carbonates precipitated in such a setting, the isotopic values of these carbonates typically show a strong degree of co-variance (Talbot, 1990; Talbot and Kelts, 1990; Li and Ku, 1997; Anderson and Leng, 2004). Conversely, the $\delta^{18}O$ and $\delta^{13}C$ values of authigenic carbonates precipitated in hydrologically open basins will not co-vary. In these settings, the $\delta^{18}O$ of the carbonate should be a record of the $\delta^{18}O$ of the lake water, which should closely relate to the $\delta^{18}O$ of rainfall, whereas in a closed lake system, evaporation will strongly modify the $\delta^{18}O$ signal. In open system lakes the $\delta^{13}C$ of the carbonate provides a record of the $\delta^{13}C$ of the DIC pool (Marshall et al., 2002, 2007; Leng and Marshall, 2004; Diefendorf et al., 2006). The isotopic properties of the Marks Tey sequence are

typical of an open lake basin, with no relationship between $\delta^{18}O$ and $\delta^{13}C$ values (R^2 value for the whole dataset is 0.38; MTIZ 1 = 0.14; MTIZ = 0.35) (Fig. 9.3; Table 9.1). While it is important to note that modern British surface waters do undergo minor modification by evaporation (Marshall et al., 2002, 2007; Darling et al., 2003), significant temperature shifts (and the role these shifts play in the $\delta^{18}O$ of rainfall and meteoric water) should still be the main expression of climate change within these systems. Furthermore, the lack of co-variance implies that the lake water is regularly recharged by ground/surface water, with a form of outflow (Talbot, 1990; Leng and Marshall, 2004).

9.3.2. Detrital contamination

Detrital contamination from biological and allocthonous carbonate is a concern for any lacustrine isotopic records, as it can have a large impact on the isotopic signal (Leng et al., 2010; Mangili et al., 2010a) Detailed micro-facies analysis of the carbonate laminations indicates a general absence of biological carbonates, particularly the varved sediments in LFa-2 (see figure 7.2 and 7.3 in chapter 7). Sections of the core where biological carbonate was noted were avoided when sampling. The results from Marks Tey make it difficult to rule out detrital contamination of the isotopic signal from allocthonous sources, as equilibration of lake water with atmospheric CO_2 results in authigenic carbonates with $\delta^{13}C$ values similar to those typical of marine limestones, one of the main sources of detrital carbonate (Candy et al., in press). As a result, the $\delta^{18}O$ and $\delta^{13}C$ values of bulk samples and chalk clasts from the Lowestoft Till matrix overlap with the values from the sediment sequence (Fig. 9.3). Despite this overlap, it is considered unlikely that detrital contamination is an issue in the Marks Tey sequence. The overlap occurs in association with samples from MTIZ 2 (Fig. 9.3), which are taken from clearly defined, individual carbonate laminations in the varved section of the sequence (LFa-2). The lithofacies zone that contains the greatest potential for sediment in-washing, due to its variable carbonate and organic content, as well as high µ-XRF intensities for detrital elements (see chapter 6), is LFa-1. The $\delta^{18}O$ and $\delta^{13}C$ values of samples taken from this unit, however, have very different values to those of the Lowestoft Till samples (Fig. 9.3). The varved sediments of LFa-2, on the other hand, contain pure authigenic carbonate laminations; enabling sampling with relative confidence that contamination is negligible. It is suggested, therefore, that the overlap

of the $\delta^{18}O$ and $\delta^{13}C$ values from LFa-2 with samples from the Lowestoft Till is the result of natural environmental processes and therefore coincidental. Consequently, it is argued that detrital contamination is not an issue in the Marks Tey isotopic record.

9.3.3. Core sedimentology and its influence on the isotopic signal

Changes in the pattern of sedimentation within a lake basin may also have an influence on the isotopic signal. In the case of the section of the Marks Tey sequence analysed here, the major sedimentological shift is from the non-varved to varved sediments, which occurs at ca 16.45 mbs. This shift in sedimentation style does not, however, coincide with the transition from MTIZ 1 to MTIZ 2, which takes place at 15.90 mbs (Fig. 9.2). The change in the pattern observed in the $\delta^{18}O$ values (from relatively high $\delta^{18}O$ values/low 1σ to relatively low $\delta^{18}O$ values/high 1σ) appears, therefore, to be unrelated to changes in core sedimentology. It is, however, worth noting that 1σ is typically higher in the varved section than the non-varved section (Table 9.1.). This is not unsurprising as each sample in the varved section represents $\delta^{18}O$/ $\delta^{13}C$ of a single summer, whereas in the non-varved section, a sample may reflect an average of multiple, may be decades worth of summers. The fact that the increase in 1σ does not occur at the boundary between the varved and non-varved sediments can be explained by the fact that, in the first 55cm of LFa-2, sampling resolution is low. It has been shown by Mangili et al. (2010a) that in carbonate varves, 1σ will typically increase with increased sampling resolution (Fig. 9.4). Although the change from non-varved to varved sediments can explain the shift in 1σ values, it cannot explain the shift in average $\delta^{18}O$ values, as the effect of averaging removes the imprint of changing sample resolution. Consequently, the pattern showed by the 5/10 point moving average is real and the shift in $\delta^{18}O$ values at 15.90 mbs is a true environmental shift (Fig. 9.5).

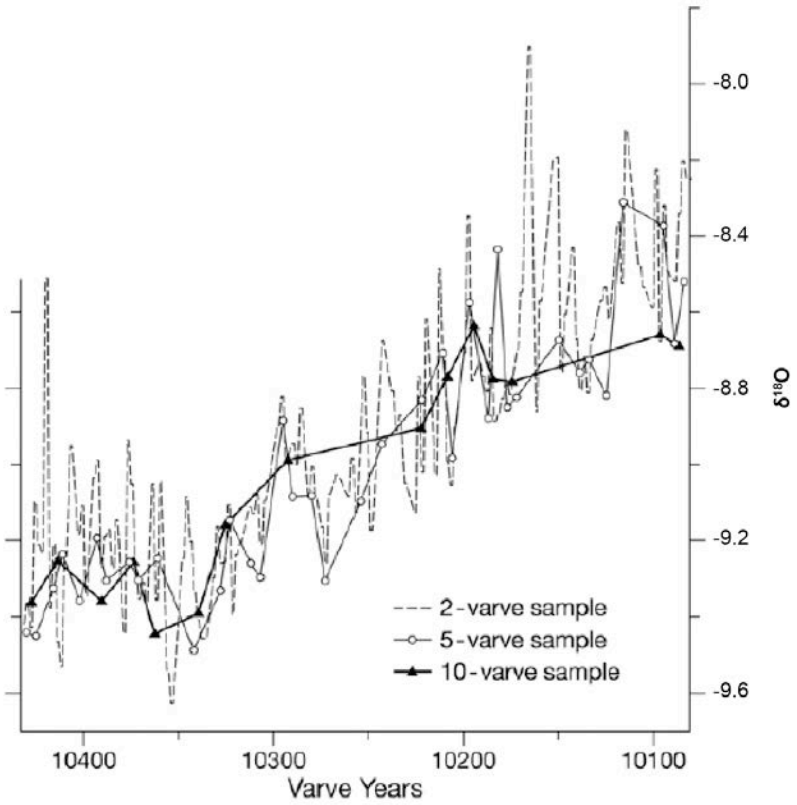

Figure 9.4. *Stratigraphical variations in the $\delta^{18}O$ value from samples of varying temporal resolution in the varved sequence at Pianico-Sellere, Italy. The data shows that samples taken across 2 varves (dashed line) have a high degree of variability, whereas samples that average 10 years worth of carbonate sedimentation (solid black line) pick out the main trend in the dataset, but with far less variability. Modified from Mangili et al. (2010a).*

Another issue to consider for the Marks Tey record is the effect that changing water column dynamics may have on the isotopic signal. The switch from non-varved to varved sediments is likely to result from the development of seasonal or permanent water column stratification (Boygle, 1993; Nuhfer et al., 1993; Lamoureux and Bradley, 1996), which can significantly alter the isotopic composition of carbonates (McKenzie, 1982; Teranes et al., 2001; Anderson and Leng, 2004; Bluszcz et al., 2009), without the need to invoke climate as a forcing mechanism. This is not considered to be an issue at Marks Tey because the decreasing trend observed in both $\delta^{18}O$ and $\delta^{13}C$ starts during LFa-1 and continues across the boundary with LFa-2 (Fig. 9.2). If the change in isotopic record were a function of water column stratification then an abrupt shift in both $\delta^{18}O$ and $\delta^{13}C$ at the boundary between LFa-1 and LFa-2 would be expected to occur. Furthermore, if stratification of the water column had a significant effect on $\delta^{18}O$ and $\delta^{13}C$ values, they would be expected to increase, due to the isolation of the epilimnion and preferential removal of ^{12}C during photosynthesis and evaporation of ^{16}O

(McKenzie, 1982; Teranes et al., 2001). The opposite trend, however, is apparent at Marks Tey (Fig. 9.2).

9.3.4. Summary

The isotopic data from LFa-1 and LFa-2 suggest that the authigenic carbonate found within the lacustrine sediments at Marks Tey were precipitated in a hydrologically open lake basin. There is negligible evidence for detrital contamination from biogenic and allogenic carbonates, so the isotopic record can be interpreted as a purely authigenic signal. Carbonate $\delta^{18}O$ values should, therefore, record the $\delta^{18}O$ of lake water, fractionated in association with water temperature, which will be strongly controlled by the $\delta^{18}O$ of rainfall, while $\delta^{13}C$ values should act as a proxy for lake water DIC ($\delta^{13}C_{DIC}$). Finally, although the switch from non-varved (LFa-1) to varved (LFa-2) sedimentation influences, to some degree, the variability within the $\delta^{18}O$ and $\delta^{13}C$ signal, this should not affect the environmental significance of the mean isotopic values. This can be highlighted by the nature of the isotopic trend across the boundary from LFa-1 to LFa-2, as well as the 5-point averages of both datasets, which show that although the standard deviation of isotopic data changes across these two lithofacies the pattern of the isotopic trend does not. Averaging of the isotopic signal, therefore, removes the potential impact of changing lamination resolution on the interpretation of the environmental/climatic trend.

9.4. $\delta^{13}C$ stratigraphy of the Marks Tey sequence

The range of $\delta^{13}C$ values from the authigenic carbonate laminations at Marks Tey plot within expected ranges of lacustrine carbonates (Stuiver, 1970; Talbot, 1990, Clark and Fritz, 1997; Leng and Marshall, 2004; Candy et al., 2011). One of the most striking aspects of the $\delta^{13}C$ stratigraphy is the pronounced decreasing trend that occurs throughout LFa-1, during the pre-temperate phase (HoI) of MIS 11 (Fig. 9.2). Such a trend has also been noted in $\delta^{13}C$ records from the early Holocene, where increasing landscape stabilisation and soil development result in the progressive lowering of recharge water $\delta^{13}C$ values, due to the reduced contribution of geologically derived carbon (Hammarlund, 1993; Hammarlund et al., 1997), and an increase in the

contribution of isotopically light CO_2 from the soil zone (Cerling et al., 1989; Cerling and Quade, 1993; Andrews, 2006).

While stratigraphical variations in the $\delta^{13}C$ values of lacustrine carbonates can provide information about the lacustrine carbon cycle, they are often not considered in any level of detail in palaeoclimatic studies in Western Europe. This is because the fractionation that occurs between DIC and mineral calcite is only very weakly temperature dependent, and doesn't provide a direct link to climate (e.g. Romanek et al., 1992; Wachniew and Rozanski, 1997; Bernasconi and McKenzie, 2007). In this study, $\delta^{13}C$ has been used as a tool to give information about lake hydrology and detrital contamination, as discussed in section 9.3 above.

9.5. $\delta^{18}O$ stratigraphy of the Marks Tey sequence

Discussion about the environmental significance of the isotopic data in section 9.3 suggests that the Marks Tey lake basin was a hydrologically open system, unlikely to have been subject to detrital contamination and modification by evaporation, with carbonate $\delta^{18}O$ values therefore a proxy for the $\delta^{18}O$ of water recharging the lake. The key to being able to use such isotopic records as palaeoclimatic proxies is, therefore, dependent on identifying the main controls over the $\delta^{18}O$ value of lake recharge water.

9.5.1. Factors controlling the $\delta^{18}O$ of lake recharge water

Isotopic shifts that occur in $\delta^{18}O$ records from authigenic lacustrine carbonates from late Quaternary archives in Western Europe are regularly interpreted in terms of temperature changes (Marshall et al., 2002, 2007; Leng and Marshall, 2004; Leng et al., 2005; Candy, 2009; Candy et al., 2011; van Asch et al., 2012). This is because the $\delta^{18}O$ value of authigenic carbonate will reflect the $\delta^{18}O$ value of the lake water it precipitated from (Kim and O'Neil, 1997), the value of which is primarily controlled by the $\delta^{18}O$ of precipitation (Darling and Talbot, 2003; Darling et al., 2003; Darling 2004), which ultimately recharges the lake through surface/ground waters. In temperate, mid-latitude regions like Western Europe, the $\delta^{18}O$ value of precipitation is strongly correlated with air temperature, such that an increase in 1°C will result in an enrichment of rainwater by approximately 0.58‰ (Dansgaard, 1964; Rozanski et al.,

1992, 1993; Darling 2004), an effect which is slightly dampened by the depletion of $\delta^{18}O$ (approx. -0.24‰/°C) during carbonate formation in the water column (Craig, 1965, Hays and Grossman, 1991, Kim and O'Neil, 1997). This relationship between prevailing air temperature and the $\delta^{18}O$ of authigenic lacustrine carbonates has been demonstrated from a number of sites across the British Isles, where the timing and magnitude of $\delta^{18}O$ shifts during the last glacial-interglacial transition are comparable to those found in the Greenland ice core records (e.g. Marshall et al., 2002).

Assuming this modern (and late Quaternary) relationship can be applied to lacustrine carbonates of MIS 11 age, an increase in prevailing air temperature will result in higher $\delta^{18}O$ values in carbonates formed in the Marks Tey palaeolake basin, with the opposite effect apparent for lower temperatures. If these assumptions are accepted and the $\delta^{18}O$ record from Marks Tey is interpreted purely in terms of temperature shifts, then: 1) the relatively high $\delta^{18}O$ values observed in MTIZ 1 indicate a temperature peak early in MIS 11 (Ho I, pre-temperate zone), 2) the subsequent decline through MTIZ 1 indicates a general climatic cooling, 3) the consistent, but lower, $\delta^{18}O$ values during MTIZ 2 indicate relatively stable temperatures during the early-temperate (Ho II) and early late-temperate (Ho IIIa) phases, and 4) the persistent low $\delta^{18}O$ values between 15.80 and 14.80 mbs imply a particularly cool interval punctuated by short-lived cold events. While these trends are apparent, it should be noted that the isotopic shifts which occur between these two zones are relatively small (0.50‰) (MTIZ 1 average = -3.13‰; MTIZ 2 = -3.73‰). This equates to an approximate temperature shift of potentially <2°C, the result of a net increase in $\delta^{18}O$ of carbonates of ~0.30 – 0.34‰, based on the temperature dependence on the oxygen isotopic composition of precipitation (+0.58‰/°C) and the temperature dependent fraction that occurs during the precipitation of mineral calcite (-0.24 – 0.28‰/°C).

Although temperature is likely to play a major role in the $\delta^{18}O$ record from Marks Tey, it is important to consider other factors that may influence the $\delta^{18}O$ of water recharging the basin, such as the seasonal distribution of precipitation throughout the year, as well as changes in the $\delta^{18}O$ of source water. Changes in sea level and the re-arrangement of atmospheric systems that occur during glacial-interglacial transitions can both alter the $\delta^{18}O$ value of water in the hydrological system (Dansgaard, 1964;

Gat and Gonfiantini, 1981; McKenzie and Hollander, 1993; Rozanski et al., 1993; Teranes and McKenzie, 2001). This may provide an alternative explanation to the decreasing trend observed through MTIZ-1. Such changes may have influenced $\delta^{18}O$ values of meteoric water in the British Isles during the last glacial-interglacial transition, a suggestion recently made by Candy et al. (in review). The lacustrine carbonate sequences from this region display an early Holocene peak in $\delta^{18}O$ values, followed by a decreasing trend until approximately 8,000 yrs BP, after which the isotopic signal stabilises (Fig. 3.12 in chapter 3) (Candy et al., in review). This decreasing trend contradicts the Greenland ice core records for the same time period, which show a temperature increase during the glacial-interglacial transition, followed by relatively stable temperatures.

Candy et al. (in review) have suggested that the divergence of the lacustrine $\delta^{18}O$ records from the Greenland ice core record reflects a shift in the seasonality in rainfall across the early Holocene. In this model, more "continental" rainfall patterns (low levels of rainfall in winter but high levels in summer) existed during the onset of the Holocene and more "maritime" rainfall patterns (relatively consistent levels of rainfall across the year) occurred during the later part of the early Holocene. Such a shift in seasonality would generate a major decrease in the $\delta^{18}O$ value of surface waters. This is because the $\delta^{18}O$ value of rainfall in mid-latitude regions varies across the year with air temperature, with higher $\delta^{18}O$ values in the summer and lower $\delta^{18}O$ values in the winter (Rozanski et al., 1992,1993; Darling, 2004). Consequently, lake waters that are recharged under a "continental" rainfall regime will have relatively high $\delta^{18}O$ values, because the lake systems are receiving a greater proportion of water from summer rainfall (which is enriched in $\delta^{18}O$), than from winter rainfall (which is depleted with respect to $\delta^{18}O$). Conversely, lake waters recharged under a "maritime" rainfall regime; receiving relatively similar proportions of water from both enriched summer and depleted winter rainfall, will have relatively low $\delta^{18}O$ values (see Higgins and MacFadden, 2004).

It is likely that the shift from "continental" to "maritime" rainfall patterns which occurred across the early Holocene is a function of both changing insolation patterns, which operate to reduce seasonality across this interval, and rising sea levels that

make the British Isles progressively less continental. It is, therefore, possible that the early peak in $\delta^{18}O$ values that occurs during Ho I (LFa-1) and subsequent decline that occurs between 17.34 – 16.42 mbs, does not represent an early temperature peak and subsequent cooling, but rather a shift in the seasonality of precipitation early on in the interglacial that is comparable to that seen in early Holocene lake records in Britain (Candy et al., in review).

In all probability, the factors that are responsible for the seasonality shift during the early Holocene are likely to have been amplified during the early part of MIS 11. Low sea levels, and, therefore, enhanced continentaility in Britain, are likely to persist for longer during the Hoxnian interglacial, given that the transition between MIS 12 and 11 (Termination V) is characterised by a uniquely long deglaciation and consequently a protracted rise in sea level (Imbrie et al., 1984; Lisiecki and Raymo, 2005; Rohling et al., 2010; Raymo and Mitrovica, 2012). Evidence for a protracted sea level rise during MIS 11 also comes from the high species turnover that occurred in the British Isles during the Hoxnian, which indicates that a land bridge with the continent existed for a large part of this interglacial. (e.g. White and Schreve, 2000; Schreve, 2001a,b). As highlighted by Candy et al. (2014), the unique pattern of deglaciation that characterised MIS 11, which lasted ca 30,000 years, is put into context when, during all other late Middle and Late Pleistocene interglacials, only ca 12,000 years elapses between the last major stadial of the preceding glacial and the sea level peak of the subsequent interglacial. The result is that lower sea levels persisted for longer in MIS 11 than during any other interglacial (Rohling et al., 2010).

This unique characteristic of MIS 11 has two important consequences for the early part of the Marks Tey isotopic record. Firstly, it will potentially enhance and extend the occurrence of continental climates during the early Hoxnian resulting in the enrichment of the $\delta^{18}O$ value of freshwater carbonate as outlined above. Changes in the seasonality of rainfall have also been suggested to explain the $\delta^{18}O$ trend observed during the early stages of MIS 11 in the lacustrine record from Ossowka, Poland (Nitychoruk et al., 2005). Like Marks Tey, the $\delta^{18}O$ values at Ossowka are high during the early the early part of MIS 11, followed by a decline. Nitychoruk et al. (2005) interpret this pattern as a result of an increase in the influence of oceanic climate,

resulting in the increase of lake inflow from river/ground water and/or a decrease in the influence of evaporative processes. The shift in $\delta^{18}O$ values at Ossowka occurs over a much greater range than Marks Tey (~2‰), however, this might be due to the more continental location of the site.

Secondly, the persistence of relatively high ice volume into the early part of MIS 11 will mean that Atlantic waters, the source of British precipitation, will remain relatively enriched with respect to $\delta^{18}O$. This is because a significant proportion of $H_2{}^{16}O$ is still held within the residual ice masses. This may mean that, during the early Hoxnian the $\delta^{18}O$ value of rainfall is enriched, not necessarily because of high temperatures, but because the $\delta^{18}O$ value of the source water still "inherits" a glacial stage signature. This would result in the persistence of rainfall with high $\delta^{18}O$ values during the early part of the Hoxnian until significant ice melt has occurred.

In summary, the most basic interpretation of the high $\delta^{18}O$ values that occur in MTIZ 1 is through the occurrence of an early temperature peak. However, given our understanding of the isotopic shifts that occur within lacustrine carbonate records of the early Holocene and the protracted deglaciation that occurs during MIS 11 this early peak could also be explained by; 1) a shift from a "continental" to a "maritime" rainfall regime; 2) persistence of enriched source waters in the North Atlantic; and 3) a combination of both of these factors. Interpretation of the Marks Tey $\delta^{18}O$ record during MTIZ-1 is therefore speculative, because 1) the isotopic shift that occurs between MTIZ-1 and MTIZ-2 is relatively small, indicating fairly stable climatic conditions that can be explained by both temperature and seasonality changes, and 2) core MT-2010 does not extend to the base of pollen zone Ho I or beyond, so no data is available for the isotopic trend that occurred during the MIS 12-11 transition.

9.5.2. Evidence for abrupt climatic events during MIS 11c

As discussed in chapter 2, the OHO/NAP phase represents the clearest evidence for the occurrence of an abrupt event in European (and possibly Mediterranean) pollen records from pre-Holocene interglacials. The existence of the event has long been known, yet its forcing mechanism has been the subject of much debate; i.e. climate or non-climate. In this context, the $\delta^{18}O$ record of MTIZ-1 and 2 is crucial, as it may

provide the palaeoclimatic context to this event. As highlighted in section 9.5.1, the $\delta^{18}O$ signal within the varved section (LFa-2) of core MT-2010 contains a high degree of scatter, which reflects the inherent variability that seasonal samples will produce, a characteristic of other varved isotopic records of MIS 11 (Mangili et al., 2010b). Thus, when identifying climatic events or trends, the occurrence of a single sample with a significantly high or low $\delta^{18}O$ value is not significant. It is, instead, the occurrence of a number of low/high $\delta^{18}O$ values in a varved record that allow climatic shifts to be identified (see Marshall et al., 2007; Mangili et al., 2009 for examples).

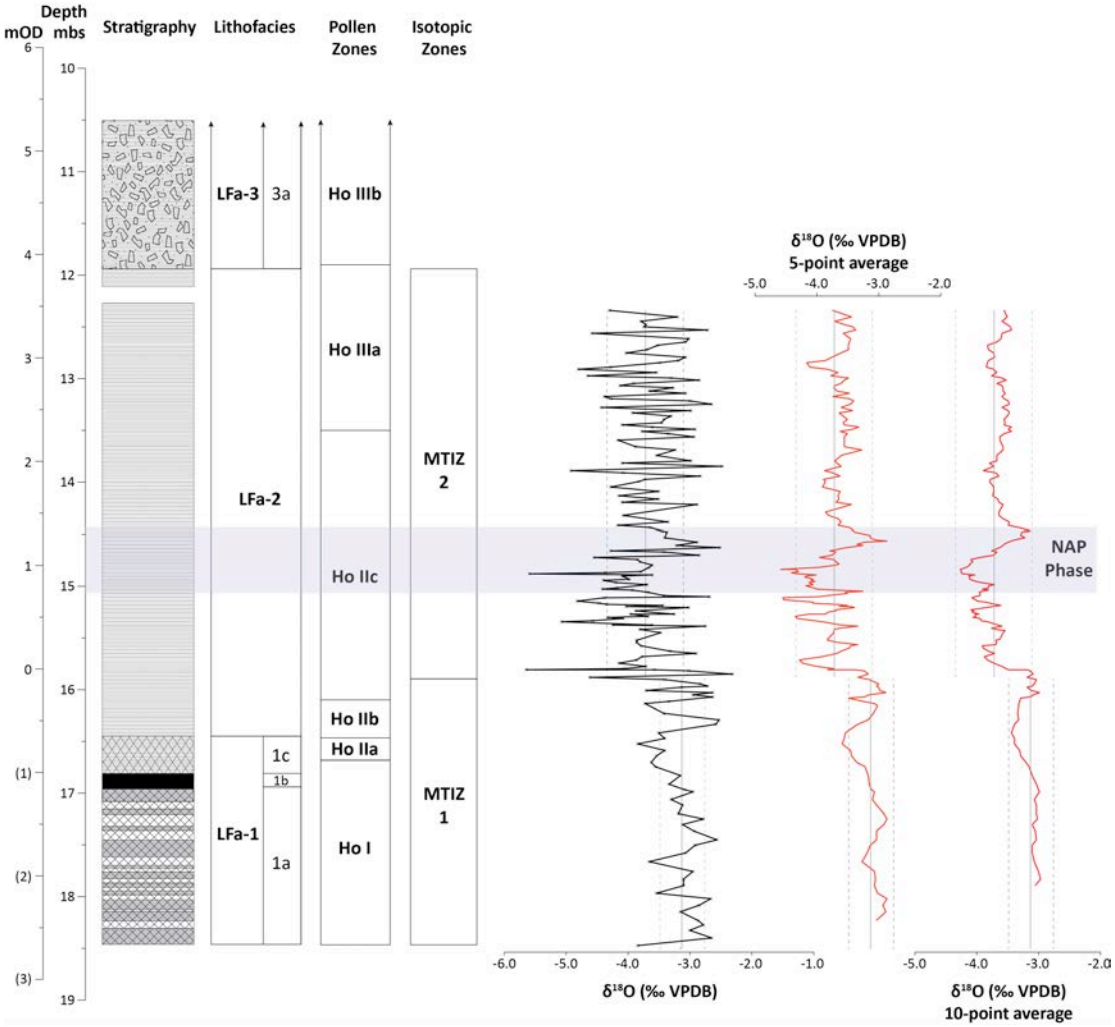

Figure 9.5. *$\delta^{18}O$ dataset plotted against core stratigraphy, along with the lithofacies, pollen and isotopic zones. The 5-point and 10-point moving averages are plotted separately to highlight the main trends in the dataset. The mean (solid grey line) and standard deviation (dashed grey line, 1σ) for MTIZ 1 and MTIZ 2 are also plotted. The location of the NAP Phase is indicated by blue shading.*

The NAP phase (15.05 – 14.42 mbs) occurs during MTIZ 2, which has an average $\delta^{18}O$ value of -3.73‰ (Fig. 9.5). The NAP section of the core, from 15.05 – 14.80 mbs,

coincides with a period of $\delta^{18}O$ values that plot consistently below this average. The NAP section represents a relatively unique trend within the context of MTIZ 2, as low $\delta^{18}O$ values occur throughout this zone, but these rarely form part of a consistent pattern of low values (Fig. 9.5). This is demonstrated by the difference between the mean $\delta^{18}O$ value of the section of core relating to the NAP phase and the mean value of MTIZ 2 as a whole (-4.04‰ and -3.73‰, respectively), a difference of 0.31‰. Furthermore, the occurrence of a $\delta^{18}O$ excursion, or event, in association with the NAP phase can be clearly seen if a 5 or 10 point running average is plotted through the dataset (Fig. 9.5). Plotting these running averages removes the "noise" from the dataset and identifies areas or persistently low or high values. The NAP phase is characterised by a pronounced low in $\delta^{18}O$ values and is followed by a return to higher mean $\delta^{18}O$ values, however, the pattern of $\delta^{18}O$ variations prior to the NAP phase is relatively complicated. This section of the sequence is characterised by three zones of low $\delta^{18}O$ values, all below the mean value of MTIZ-2, separated by short-lived increases (Fig. 9.5). If it is assumed that these decreases in $\delta^{18}O$ values reflect cold events, then the NAP phase does not occur in association with a single cold event, but is part of a more complex series of cold/warm oscillations that occur during the early part (early-Temperate phase) of this interglacial.

Part of the problem associated with resolving the forcing mechanism for the OHO/NAP phase has been the absence of a palaeoclimatic proxy that is independent of vegetation. The $\delta^{18}O$ signal of the lake sequences that the OHO/NAP phase occurs within would address this issue, but carbonate precipitates are absent in many of these sequences. Koutsodendris et al. (2012) attempted to address this by analysing the $\delta^{18}O$ value of diatom silica across the OHO interval at Dethlingen. Although a reduction in $\delta^{18}O$ values was evident during the pollen event, the section of the sequence analysed was short, making it difficult to establish whether this shift was significant in the context of long-term trends within the $\delta^{18}O$ signal. The Marks Tey data presented in this thesis allows; 1) the NAP phase to be directly compared to the $\delta^{18}O$ value of lacustrine carbonate, and 2) the $\delta^{18}O$ values associated with the NAP phase to be placed into the context of the $\delta^{18}O$ signal from the early-Temperate phase (Ho I) through to the early part of the late-Temperate phase (Ho IIIa). As outlined above, the NAP phase is associated with an interval of persistently low $\delta^{18}O$ values

and, therefore, occurs during a period of climatic cooling. The 10 and 5 point running average indicates that rather than a single interval during Ho IIc where $\delta^{18}O$ values are low, there is a period where three episodes of persistently low $\delta^{18}O$ values occur, each separated by a short lived increase in $\delta^{18}O$ values (Fig. 9.5). It is therefore suggested that a number of abrupt cooling events occur during Ho IIc, and the NAP phase occurs in association with the last of these.

9.6. Summary

A high-resolution $\delta^{18}O$ and $\delta^{13}C$ carbonate stratigraphy has been produced fro Ho I to early Ho IIIa in the Marks Tey sequence. The main findings of this study are:

- $\delta^{18}O$ and $\delta^{13}C$ data for the lowermost section of sequence MT-2010, between 18.47 to 12.34 mbs indicates that authigenic calcite precipitation at Marks Tey occured in a hydrologically open lacustrine system that is unlikely to have been affected by detrital contamination.
- Carbonate $\delta^{18}O$ values should therefore record the $\delta^{18}O$ of lake water, which will act as a proxy for the $\delta^{18}O$ of rainfall.
- If the $\delta^{18}O$ record is purely driven by temperature changes, then early MIS 11 is characterised by a peak in temperature, followed by a gradual cooling and stabilisation of temperature, which is punctuated by a number of short-lived cold events.
- This interpretation, however, is complicated by other possible influences, such as changes in the seasonal distribution of precipitation throughout the year, as well as changes in the $\delta^{18}O$ of source water that can occur during the early stages of an interglacial.
- The running averages elucidate trends in dataset, indicating that the NAP Phase occurred in association with the last of a number of abrupt cooling events that punctuated the Hoxnian pre-temperate phase; the relationship between these events and the pollen record will be investigated further in the next chapter.

Chapter 10. The Non-Arboreal Pollen Phase

Chapter overview

This chapter will focus on the Non-Arboreal Pollen (NAP) phase at Marks Tey. This thesis is based on the construction of a varve chronology and the development of an isotope stratigraphy for the early part of the Hoxnian at Marks Tey, but secondary data from other contributing researchers allows for a detailed reconstruction of the NAP phase. Pollen data (P. Coxon, Trinity College Dublin) provides the framework for understanding the event, while diatom analysis (K. Loakes and D. Ryves, Loughborough) provides evidence for the limnological response to the event. By combining the MTSC-2014^{INT} varve chronology with this secondary data, it is possible to investigate the timing and rates of palaeoecological response across the NAP phase. The varve thickness and μ-XRF data provide information about landscape stability, while the stable isotope stratigraphy for the sequence is combined with the charcoal data (M. Hardiman, Portsmouth) to investigate the forcing mechanism for the NAP phase.

10.1. Introduction

In this chapter, the reconstruction of the NAP phase in the MT-2010 sequence will be based on descriptions of changes that occur in environmental and sedimentological proxies over a 1.9m section of the record, between 16.07 and 14.17 mbs. This depth interval was chosen as 16.07 mbs represents the onset of pollen zone Ho IIc and 14.17 mbs enables descriptions to be made about changes that occur in the proxy data during the first 25cm after the NAP Phase has finished (Fig. 10.1). In this study, the NAP Phase in the MT-2010 sequence is defined in terms of percentage changes that occur in *Corylus* during pollen zone Ho IIc. The rationale for this was discussed in chapter 2 (section 2.4.2.3).

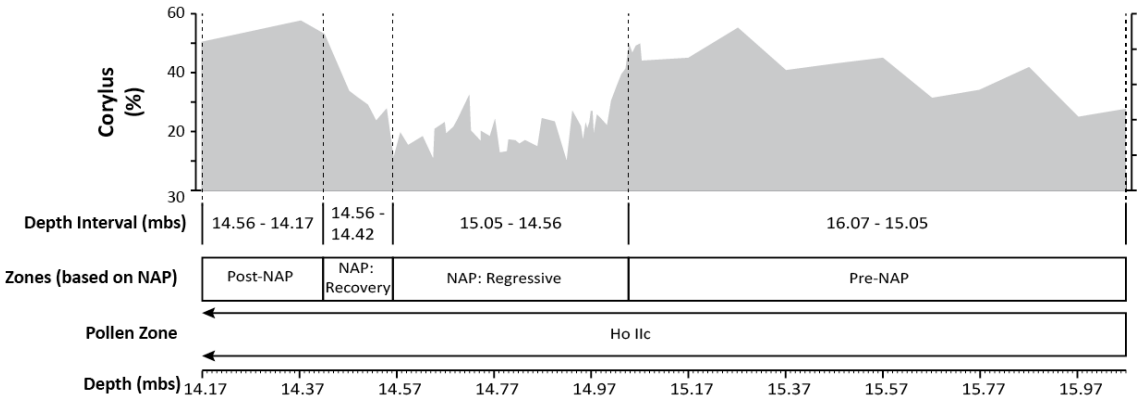

Figure 10.1. *Sub-division of the MT-2010 sequence from 16.07 to 14.17 mbs, which provides the framework for descriptions of environmental and sedimentological proxy data in this chapter. This section of the sequence covers the first 1.9m of pollen zone Ho IIc and has been sub-divided based on changes that occur in the Corylus percentage data.*

Figure 10.1 shows the changes that occur in *Corylus* percentage data over the first 1.9m of pollen zone Ho IIc (16.07 to 14.17 mbs). The pre-NAP Phase (16.07 to 15.05 mbs) zone is characterised by an increase in *Corylus*, from 21.2 to 48.5% (peak values of 54.8% occur at 15.27 mbs). The NAP Phase occurs between 15.05 and 14.42 mbs and is sub-divided into regressive and recovery zones (Fig. 10.1). The regressive zone is characterised by a decline in *Corylus* from 48.5 to 8.5% over the first 0.13m (15.05 to 14.92 mbs). Although percentages fluctuate (between 8.5 and 31.4%), *Corlyus* remains low until 14.56 mbs (the end of the regressive zone) (Fig. 10.1). The recovery zone (14.56 to 14.42 mbs) is defined by increasing *Corylus* percentages from 9.6% to pre-NAP values (52.8 %). The first 0.2m of the post-NAP zone of the core is also included in the description of proxy evidence, where *Corylus* percentages are ca 50% (Fig. 10.1).

10.2. Palaeoenvironmental evidence

This section will build a model of the NAP phase based on its palaeoenvironmental characteristics. The pollen data provides the framework for the event, within which the charcoal, diatom and isotope data can be placed. It should be noted that because samples for individual proxies were taken at different resolutions, the depths (in mbs) quoted in this section are reported to two, three and four decimal places.

10.2.1. Pollen

Results from selected taxa are plotted as both relative pollen composition and concentrations in figure 10.2, with both datasets displaying trends over the depth interval considered in this chapter.

10.2.1.1. Pre-NAP Phase Zone (16.07 – 15.05 mbs)

The pre-NAP zone of the sequence is dominated by *Corylus*, which rises from 27.3% at 16.07 mbs to 54.8% at 15.27 mbs, before falling slightly to 48.5% at 15.05 mbs (Fig. 10.2). This zone is also characterised by *Ulmus* and *Quercus*. *Ulmus* reaches peak values of 17.2% occurring at 14.97 mbs, before gradually declining to 3.2% at 15.05 mbs, while *Quercus* remains relatively stable, with values between 4 and 9.7% (Fig. 10.2). *Taxus* is also present, displaying peak values of 7.3% 16.07 mbs, but remains below 4.5% for the rest of the zone (Fig. 10.2). *Betula* (max. 6.6%), *Pinus* (max. 3.8%) and *Poaceae* (max. 7.8%) are present in this section of the core, but represent minor contributions to the assemblage.

Total pollen concentrations display fluctuations by orders of magnitude in this zone, between 1413 x 10^3 grains/g (15.57 mbs) and 346 x 10^3 grains/g (15.17 mbs) (Fig. 10.2). With the exception of 15.07 mbs, where total concentrations reach 1,253 x 10^3 grains/g, there is a general trend of decreasing pollen concentrations between 15.57 mbs (1,413 x 10^3 grains/g) and 15.05 mbs (719 x 10^3 grains/g). This trend is exemplified by *Corylus*, which increases in terms of relative composition, but decreases in terms of its concentration in the core (Fig. 10.2).

10.2.1.2. NAP Phase (15.05 – 14.42 mbs)

This zone contains the NAP phase, which is expressed in temperate tree taxa by a reduction of *Corylus* and to a lesser extent *Quercus* and *Ulmus*, while there is an increase in the % contribution of *Poaceae* and disturbed ground indicators (*Betula* and *Pinus*) (Fig. 10.2). The pollen response during the NAP phase can be split into two phases: a regressive zone and a recovery zone.

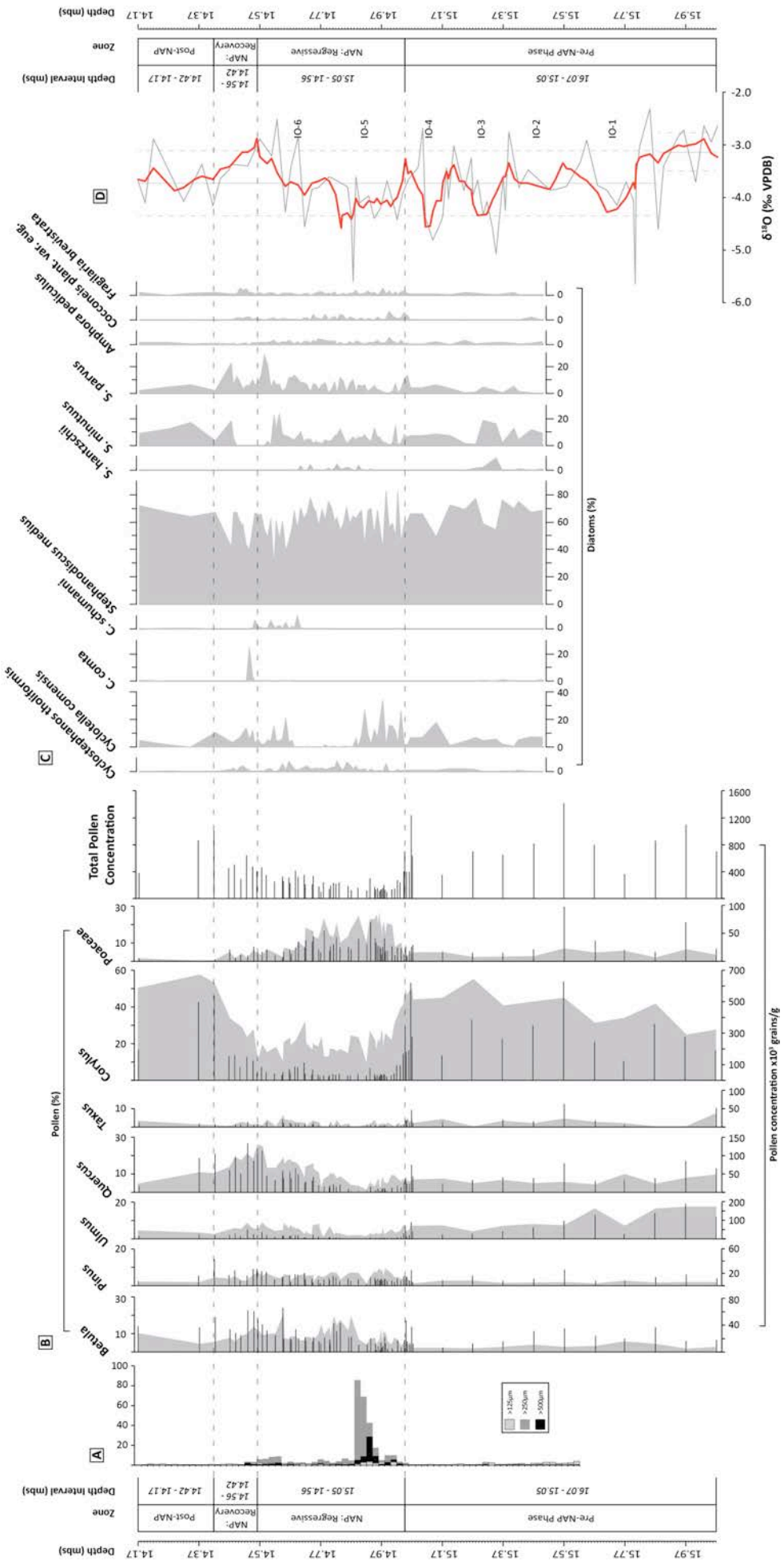
Depth (mbs)
Zone
Depth Interval (mbs)
Pre-NAP Phase
NAP: Regressive
NAP: Recovery
Post-NAP
16.07 - 15.05
15.05 - 14.56
14.56 - 14.42
14.42 - 14.17
δ18O (‰ VPDB)
IO-1
IO-2
IO-3
IO-4
IO-5
IO-6
Diatoms (%)
Cyclostephanos tholiformis
Cyclotella comensis
C. comta
C. schumanni
Stephanodiscus medius
S. hantzschii
S. minutulus
S. parvus
Amphora pediculus
Cocconeis plant. var. eug.
Fragilaria bevistrata
Pollen (%)
Betula
Pinus
Ulmus
Quercus
Taxus
Corylus
Poaceae
Total Pollen Concentration
Pollen concentration x10³ grains/g
>125µm
>250µm
>500µm
A
B
C
D

↑ ***Figure 10.2.*** *Palaeoenvironmental proxy results for the Marks Tey sequence between 16.07 – 14.17 mbs. The sequence has been sub-divided based on the information in Fig. 10.1. A) Macro-charcoal counts undertaken between 15.62 – 14.18mbs have been plotted by particle size fraction (>125µm, >250µm, >500µm); B) Selected pollen taxa for the whole interval, plotted as percentage contribution (silhouette) and concentration (lines, x10^3 grains/g); C) Selected diatom species from counts undertaken between 15.50 – 14.18 mbs, plotted as percentage contribution; and D) Oxygen isotope values for the whole interval, plotted as raw data (grey line) with the main trend in the data highlighted by a 5-point moving average (red line). The location of the isotopic oscillations (IO) presented in Table 10.1 has also been noted.*

10.2.1.2.1. NAP Phase: Regressive Zone (15.05 – 14.56 mbs)

The regressive zone of NAP phase is most clearly expressed by *Corylus*, which declines from 48.5% to 8.5% from 15.05 to 14.92 mbs (Fig. 10.2). Apart from a peak of 31.4% at 14.72 mbs, *Corylus* values remain low (average of 9.6%) until 14.56 mbs. Other temperate tee taxa that decrease during the regressive phase are *Quercus* and *Ulmus*, while *Taxus* remains low throughout the zone (Fig. 10.2). *Quercus* declines from 6% at 15.05 mbs to reach its lowest value of 1.1% at 14.92 mbs, while *Ulmus* decreases from 3.2% to 0.92% over the same depth interval. In contrast to *Corylus*, *Quercus* and *Ulmus* percentages gradually increase between 14.92 – 14.56 mbs. *Quercus* increases from 1.1% to 25.8% during this interval, and *Ulmus* increases from 0.92% to a peak of 8.4% before Quercus, at 14.57 mbs (Fig. 10.2).

The decline in *Corylus*, *Quercus* and *Ulmus* from 15.05 – 14.92 mbs coincides with a large increase in % contribution of *Poaceae*, rising from 2.2% to 24.8%. The response of *Betula* and *Pinus* is more complicated, with both taxa increasing to values of 10.7% and 8.9% at 14.9775 mbs, before declining to 3.7% and 0.7% at 14.92 mbs, respectively (Fig. 10.2). From 14.92 – 14.56 mbs, *Poaceae* values gradually decline from 24.8% to 3.9%, while *Pinus* values remain stable. In contrast, *Betula* increases to 18.6% at 14.47 mbs, before declining and remaining relatively stable until 14.56 mbs (11.9%) (Fig. 10.2).

The pollen concentration data for individual taxa during the regressive zone follows the same general pattern as the % data (Fig. 10.2). Total pollen concentrations also reveal an interesting trend. The regressive zone is characterised by decreasing pollen concentrations. With the exception of one sample (14.93 mbs; 306 x 10^3 grains/g) the interval from 15.05 – 14.92 mbs is characterised by pollen concentrations less than

250 x 10^3 grains/g (lowest values approx. 100 x 10^3 grains/g) (Fig. 10.2). From 14.92 – 14.56 mbs, concentrations gradually rise to 407 x 10^3 grains/g.

10.2.1.2.2. NAP Phase: Recovery Zone (14.56 – 14.42 mbs)

The recovery zone of the NAP Phase is characterised by increasing *Corylus* values, from 9.6% (14.56 mbs), to pre-NAP phase values at 14.42 mbs (52.8%) (Fig. 10.2). In contrast to *Corylus*, both *Quercus* and *Ulmus* values decrease, falling from 25.8% and 8.4% (14.56 mbs), to 10.3% and 2.1% (14.42 mbs), respectively. The recovery zone is also characterised by decreasing values for *Poaceae* (3.9-0.3%), *Betula* (11.9-5.2%) and *Pinus* (6.7-4.3%) between 14.56 – 14.42 mbs (Fig. 10.2). Pollen concentrations remain stable during the recovery zone, between 14.56 – 14.47 mbs, before increasing by an order of magnitude at the end of the zone (1,019 x 10^3 grains/g) (Fig. 10.2).

10.2.1.3. Post-NAP Phase Zone (14.42 – 14.17 mbs)

The first 25cm of the sequence after the NAP phase is dominated by the occurrence of *Corylus*, which accounts for over 50% of the pollen assemblage (Fig. 10.2). *Quercus*, *Ulmus* and *Taxus, Poaceae, Betula* and *Pinus* also return to pre-NAP percentage and concentration values (Fig. 10.2).

10.2.2. Macro-charcoal

Macro-charcoal counts were undertaken on contiguous samples of 2cm^3 from 15.62 – 14.18 mbs and have been presented by size fractions >125µm, >250µm and >500µm (Fig. 10.2).

10.2.2.1. Pre-NAP Phase Zone (15.62 – 15.05 mbs)

The pre-NAP Phase zone is characterised by very low counts in all three size fractions. Average charcoal particle counts for this section of the sequence are 2.5 particles/cm^3, which are dominated by the >125µm size fraction (1.3) and >250µm size fraction (1), while the >500µm size fraction contains an average of 0.2 particles/cm^3. The sample from 15.32 – 15.30 mbs contains the greatest number of charcoal fragments (6 particles/cm^3), 3 of which are >125µm, 2 are >250µm and 1 >500µm (Fig. 10.2).

10.2.2.2. NAP Phase: Regressive and Recovery Zones (15.05 – 14.42 mbs)

The interval of the sequence covering the NAP phase contains the greatest number of charcoal particles, with average counts of 15.1 particles/cm^3 (>125µm = 1.8; >250µm = 10.6; >500µm = 2.7 particles/cm^3). There is a distinctive period of elevated charcoal particle counts between 15.04 – 14.88 mbs, which can be sub-divided into two peaks based on the particle size data; the first peak occurs between 15.04 to 14.96 mbs and the second, larger peak occurs between 14.96 to 14.88 mbs (Fig. 10.2).

The first charcoal peak is characterised by peak particle counts for the >500µm fraction (5.6 particles/cm^3) that occur between 15.02 – 15.00 mbs, with particle counts then gradually declining to 1.4 particles/cm^3 in the sample from 14.98 – 14.96 mbs (Fig. 10.2). The >250µm fraction displays a wider peak of 10 particles/cm^3 between 15.02 – 14.98 mbs, which then fall to 5.3 particles/cm^3 between 14.98 – 14.96 mbs (Fig. 10.2). The >125µm fraction reaches its highest values for this peak between 15.00 – 14.98 mbs (4.4 particles/cm^3).

The second, larger charcoal peak follows the same pattern as the first, with an early peak in particles >500µm, followed by a later peak in the >250µm fraction (Fig. 10.2). The peak in the >500µm fraction occurs between 14.94 – 14.92 mbs and contains 29 particles/cm^3, before declining to counts of 5.4 particles/cm^3 between 14.90 – 14.88 mbs (Fig. 10.2). Peak values in particles >250µm progressively increase from 17.5 particles/cm^3 at 14.96 – 14.94 mbs to reach peak values of 86 particles/cm^3 from 14.90 – 14.88 mbs (Fig. 10.2).

The remainder of this interval (14.88 – 14.42 mbs) is characterised by the presence of charcoal, but counts are lower compared to those between 15.04 – 14.88 mbs, particularly for the >500µm fraction (Fig. 10.2). Despite these low values, there is a section of the sequence between 14.64 – 14.52 mbs where charcoal particles increase in frequency. This section of the sequence is characterised by the persistent presence of particles >500µm (0.3 – 1.1 particles/cm^3). There is also an increase frequency of the >250µm and >125µm fractions, which display peak of 8.9 and 2.4 particles/cm^3 at 14.62 – 14.52 mbs, before declining gradually to values of 0.9 and 0.55 particles/cm^3 at 14.54 – 14.52 mbs, respectively (Fig. 10.2).

10.2.2.3. Post-NAP Phase Zone (14.42 -14.17 mbs)

Much like the section of the sequence before the NAP phase, the post-NAP zone is characterised by very low counts in all three size fractions. Average counts for this section of the sequence are 1.7 particles/cm^3 (>125µm = 0.6; >250µm = 0.7; >500µm = 0.3). The sample from this zone that contains the largest number of charcoal particle was taken from 14.26 – 14.24 mbs and contains 2.3 particles/cm^3 (>125µm = 1.1; >250µm = 0.9; >500µm = 0.3) (Fig. 10.2).

10.2.3. Diatoms

Diatom counts were undertaken from 15.50 – 14.18 mbs and 268 species/sub-species were identified, with selected species plotted as percentage composition in figure 10.2. In general, the diatom assemblage from this section of the sequence is dominated by planktonic diatoms, which account for 64.9 – 94.3% of the assemblage.

10.2.3.1. Pre-NAP Phase Zone (15.50 – 15.05 mbs)

This zone is dominated by *Stephanodiscus medius*, which exhibits a slight decreasing trend in abundance, from 69% at 15.50 mbs, to 61% at 15.055 mbs (Fig.10.2). Other important taxa that reach abundances greater than 10% are *S. minutulus* and *Cyclotella comensis*. There are two sections of this zone where *S. medius* declines, between 15.345 – 15.302 mbs, where values fall to 54.7% and 58.8% respectively, and 15.15 mbs, where values drop to 49.3% (Fig.10.2). The first of these declines in *S. medius* is associated with the increases in abundance of *S. hantzschii* and *S. parvus*, while the second decline is associated with an increase in *C. comensis* (Fig. 10.2).

10.2.3.2. NAP Phase: Regressive and Recovery Zones (15.05 – 14.42 mbs)

The interval associated with the NAP phase is characterised by complex changes in the diatom flora within the lake, which exhibit a number of short-term fluctuations in species composition. There are, however, some general trends that will be highlighted in this section, with the sequence subdivided into three sections.

10.2.3.2.1. 15.05 – 14.915 mbs

Although displaying variable percentage compositions, *S. medius* represents the dominant species during this section of the core (up to 82.7%). There are depths in this

section of the sequence, however, where percentage contributions for *S. medius* fall below 50% (e.g. 15.035 mbs: 45%; 14.975 mbs: 41.3%; 14.915 mbs: 42.7%) (Fig. 10.2). These sections of the sequence are characterised by increases in percentage contribution from *C. comensis*, which is present throughout the interval, reaching peak values of 34.3% at 14.975 mbs (Fig. 10.2). *Stephanodiscus minutulus* (15% at 15.015 mbs) and *Stephanodiscus parvus* (10.5% at 15.045 mbs) also occur infrequently through the interval, as does *Cyclostephanos tholiformis* (5.7% at 14.985 mbs) (Fig. 10.2). Benthic diatoms compose only a minor proportion of the diatom flora in the sequence, with *Amphora pediculus*, *Cocconeis placentula var. eugulpta* and *Fragilaria brevistrata* found in greatest abundances (up to 6.1%) (Fig. 10.2).

10.2.3.2.2. 14.915 – 14.665 mbs

This interval of the NAP phase is characterised by the continued dominance of *S. medius*, which displays more stable percentages (54 – 78.1%) when compared to the previous zone (Fig. 10.2). *S. minutulus,* which reaches 12.3% at 14.835 mbs, remains present, as does *S. parvus*, which displays maximum abundances of 13.5% at 14.685 mbs. *C. tholiformis* occurs more regularly in this interval, reaching a maximum abundance of 7.8% at 14.825 mbs (Fig. 10.2). The characteristic feature of this interval is the decline and disappearance of *C. comensis* from the record. Coeval with the decline in *C. comensis* is the reappearance of *Stephanodiscus hantzschii*, which reaches maximum abundances of 4.8% at 14.824 mbs, although it is not present at every depth sampled (Fig. 10.2). In a trend continued from the previous interval, the periphyton remains low.

10.2.3.2.3. 14.665 – 14.42 mbs

The final interval of the NAP phase is characterised by a similar species composition to *15.05 – 14.915 mbs*. Variable and lower percentage contributions from *S. medius* (28.8 – 67.2%) coincide with the reappearance of *C. comensis*, which varies between 3.67 – 21% abundance (Fig. 10.2). A distinctive feature of this interval is the persistent presence of small percentages (0.3 – 5%) of *Cyclotella schmanni* from 14.655 – 14.535 mbs (Fig. 10.2). Although variable, *S. parvus* exhibits its highest percentage contributions in this interval (28.2% at 14.585 mbs and 22.3% at 14.475 mbs), as does *S minutulus* (23.8% at 14.635 mbs), which disappears from the record between 14.585

– 14.495 mbs (Fig. 10.2). After reaching a peak value of 7.3% at 14.665 mbs, *C. tholiformis* displays a decreasing trend, and is not present at 14.42 mbs (Fig. 10.2). The benthic species in figure 10.2 continue their presence in the assemblage, but only in small percentages (up to 5.05%).

10.2.3.3. Post-NAP Phase (14.42 – 14.18 mbs)

The post-NAP section of the sequence is again dominated by *S. medius*, which comprises between 64.1-72.1% of the assemblage. *S. munutulus* and *S.* parvus continue to occur, with both peaking in abundance at 14.345 mbs; *S. munutulus* (17%) and *S. parvus* (6.5%). This section of the sequence is characterised by the decline of *C. comensis*, which decreases at the start of the interval and remains low (0 – 4.7%) (Fig. 10.2c).

10.2.4. Oxygen isotopes

The environmental signal contained within the oxygen isotopic composition of the carbonates at Marks Tey has been discussed in chapter 9. Based on this discussion, it is considered that the $\delta^{18}O$ record for the depth interval presented in figure 10.2 can be used as a qualitative indicator for temperature shifts. Due to the degree of scatter in the dataset, a 5-point moving average has been used to highlight the main trends in the raw data.

10.2.4.1. Pre-NAP Phase Zone (16.07 – 15.05 mbs)

The first section of this interval, between 16.07 – 15.898 mbs, covers the last ca 20cm of MTIZ 1 (see Fig. 9.2 in chapter 9), which is characterised by $\delta^{18}O$ values that have an average value of -3.13‰, 0.44‰ higher than the dataset average (-3.57‰) (Fig. 10.2d). The remainder of this section of the core is located in MTIZ 2, which is characterised by an average $\delta^{18}O$ value of -3.73‰, 0.16‰ below the dataset average (Fig. 10.2d). Due to the degree of scatter in the $\delta^{18}O$ values in MTIZ 2 ($1\sigma = 0.62$), a 5-point moving average is plotted to highlight trends in the dataset (Fig. 10.2d). This average reveals the presence of four negative isotopic oscillations from 15.803 – 15.089 mbs, where $\delta^{18}O$ values are lower than the average value for MTIZ 2, separated by periods of $\delta^{18}O$ values higher than the MTIZ 2 average (Fig. 10.2d). Fig. 10.3 shows the $\delta^{18}O$ record from Fig. 10.2d, highlighting the locations and depth intervals of the

individual isotopic oscillations. The depth intervals and summary statistics associated with these oscillations are presented in Table 10.1.

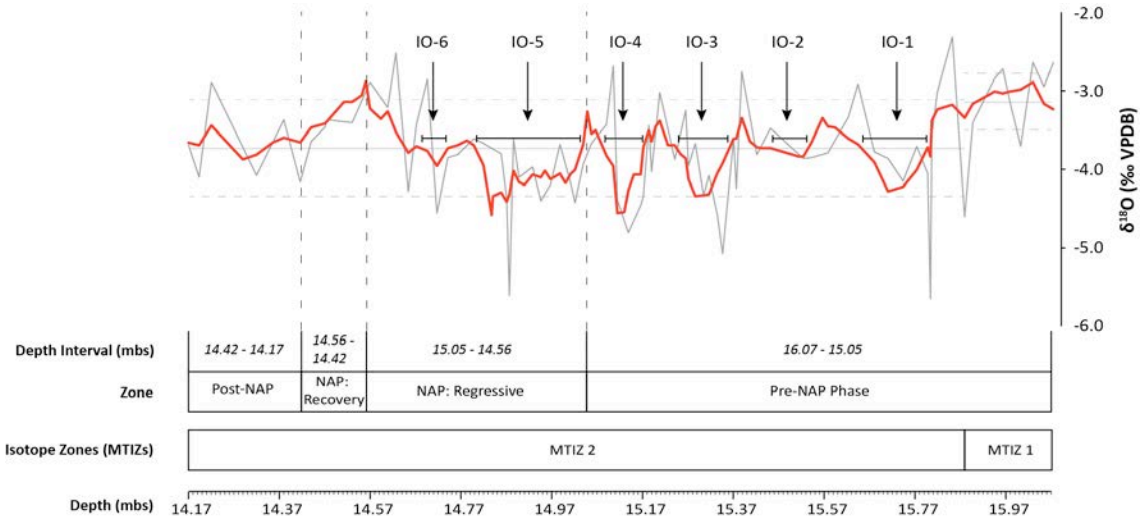

Figure 10.3. *The $\delta^{18}O$ record from Fig. 10.2, highlighting the location of isotopic oscillations (IO) that occur between 16.07 – 15.898 mbs and corresponding depth intervals (marked by the black lines). The oscillations begin when the 5-point moving average (red line) crosses below the dataset average for MTIZ 2 (-3.73‰) and end when the 5-point average crosses back above the average. IO-1 to IO-4 occur during the pre-NAP zone and IO-5 and IO-6 occur during the NAP Regressive zone.*

The first two oscillations (OI-1 and OI-2), while displaying values lower than the long-term mean, do not exceed the standard deviation for the dataset (1σ = 4.34‰) (Fig. 10.3 and Table 10.1). The next two oscillations (OI-3 and OI-4 in Fig. 10.3), which occur from 15.346 – 15.089 mbs, do exceed the standard deviation; with oscillation 4 reaching more depleted average $\delta^{18}O$ values (-4.55‰) than oscillation 3 (-4.35‰) (Table 10.1).

Table 10.1. *Characteristics of the oscillations that occur in the 5-point moving average of the $\delta^{18}O$ record between 16.07 – 14.17 mbs in the Marks Tey sequence.*

Isotopic Oscillation (IO)	Depth starts (mbs)	Depth most depleted values occur (mbs)	Depth finishes (mbs)	Duration of event (cm)	Duration of event (years)	Significant at 1σ?
1	15.803	15.711 (-4.28‰)	15.644	15.9	219	N
2	15.543	15.525 (-3.83‰)	15.453	9.0	117	N
3	15.346	15.285 (-4.35‰)	15.241	10.5	128	Y
4	15.172	15.113 (-4.55‰)	15.089	8.3	109	Y
5	15.038	14.836 (-4.59‰)	14.798	24	183	Y
6	14.740	14.717 (-3.96‰)	14.653	8.7	62	N

10.2.4.2. NAP Phase: Regressive Zone (15.05 – 14.56 mbs)

The $\delta^{18}O$ values in this zone reveal the presence of two further oscillations in the Marks Tey sequence. With the exception of two data points (-3.61‰ at 14.886 and -3.69‰ at 14.988 mbs), $\delta^{18}O$ values during the interval from 15.05 – 14.798 mbs plot consistently below the long-term average, which results in an oscillation picked out by the 5-point moving average that is unique when compared to those preceding it (Fig. 10.2, 10.3 and Table 10.1). This oscillation (IO-5 in Fig 10.3) lasts for 24cm, a greater depth interval than the four that precede it (Table 10.1), as well as having a different structure (Fig. 10.2, 10.3). While the first four oscillations are relatively symmetrical, the oscillation that occurs at the onset of the NAP phase displays a more complicated structure, with a sharp depletion in average $\delta^{18}O$ values occurs from -3.68 to -4.18‰ (15.038 – 14.999 mbs), with these low values maintained until 14.929 mbs, when they lower again to attain values lower than the 1σ error (-4.59‰ at 14.836 mbs). Values then also recover rapidly, returning to average dataset values at 14.798 mbs (Table 10.1 and Fig. 10.2, 10.3).

The recovery of $\delta^{18}O$ values after oscillation 5 is then followed by a more subdued oscillation, between 14.740 – 14.653 mbs, with the lowest average $\delta^{18}O$ values reaching -3.96‰ at 14.717 mbs (IO-6 in Fig, 10.2, 10.3 and Table 10.1). Following this oscillation, the average $\delta^{18}O$ values continue to rise until the end of the regressive zone (14.56 mbs) (-2.87‰).

10.2.4.3. NAP Phase: Recovery Zone (14.56 – 14.42 mbs)

The recovery zone is characterised by a decreasing trend, following the peak reached at the boundary between the regressive and recovery zones (-2.87‰). After this peak values gradually fall to values comparable with the MTIZ 2 average at the end of the zone (Fig. 10.2, Fig 10.3).

10.2.4.4. Post-NAP Phase Zone (14.42 – 14.17 mbs)

This zone is characterised by relatively stable $\delta^{18}O$ values. Apart from one value (-2.89‰ at 14.22 mbs), the data points for this interval of the sequence plot within uncertainties (±1σ) and average $\delta^{18}O$ values hover around the dataset average (Fig. 10.2, 10.3).

10.3. Sedimentological evidence

This section will focus on the sedimentological variations that occur in the Marks Tey sequence between 16.07 – 14.17 mbs. Varve micro-facies analysis (thickness measurements and lamination set characteristics) and μ-XRF data provide evidence for changes in lake catchment stability and lake productivity. The descriptions will follow the same basic sub-division employed in section 10.2 (pre-NAP Zone: 16.07 – 15.05 mbs; NAP Phase Zone: 15.05 – 14.42 mbs, and post-NAP Phase Zone: 14.42 – 14.17 mbs) (Fig. 10.3). Further sub-division will be made based on distinctive changes in the proxy data.

10.3.1. Pre-NAP Phase Zone (16.07 – 15.05 mbs)

The pre-NAP Phase zone of the sequence presented in Fig. 10.4 is characterised by varves with an average thickness of 0.705mm (Fig. 10.4b), lamination sets that are dominated by LT-1.1 (<50% diatom abundance), LT-2.1 (≤30% calcite abundance) and LT-3.1 (organo-clastic laminations with ≤10% mineral grain abundance) (see section 8.4.1 in chapter 8) (Fig. 10.4c), as well as detrital layers with an average thickness of 0.275mm, which occur in 14.1% of varves in the interval (Fig. 10.4d). The μ-XRF data for Ca, Ti and K show distinctive patterns throughout this zone. Although fluctuations occur, Ca intensities are relatively consistent (9.44 Ca/kcps) (Fig. 10.4e). In contrast, Ti and K exhibit low values between 16.07 – 15.53 mbs (averages of 0.06 Ti/kcps and 0.13 K/kcps), after which they exhibit small increases to average values of 0.07 Ti/kcps and 0.16 K/kcps between 15.53 – 15.05 mbs (Fig. 10.4e). The increase in Ti and K intensities between 15.53 – 15.05 mbs is also associated with a small increase in the frequency of detrital layer deposition (87 layers in 562 varves, 15.5%) compared to 16.07 – 15.53 mbs (60 layers in 570 varves, 10.5%). It should be noted, however, that the occurrence of fewer detrital layers within the lamination sets between 16.07 – 15.53 mbs may be due to poor varve quality between 16.07 – 16.00 mbs (Fig. 10.4d).

10.3.2. NAP-Phase: Regression and Recovery Zones (15.05 – 14.42 mbs)

This zone can be split into three sub-sections, based on changes observed in total varve thickness and the lamination set data described in chapter 8.

10.3.2.1. 15.05 – 14.86 mbs

This interval is associated with the first peak that occurs in the varve thickness record, which has an average varve thicknesses of ~1.22mm (Fig. 10.4b). The varves in this interval are characterised by lamination sets containing lamination types LT-1.1 (<50% diatom abundance) and to a lesser extent, LT1.2 (>50% diatom abundance), LT-2.2 (>50% calcite abundance, single lamination) and LT-3.2 (organo-clastic, 10-30% mineral abundance) (Fig. 10.4c). Detrital layers, which have an average thickness of 0.415mm, occur in 54% varves in this zone and contribute to 20.6% of the total varve thickness.

From 15.05 – 14.96 mbs, the μ-XRF data for K, Ti and Ca continue the trend of elevated intensities observed between 15.53 – 15.05 mbs (Fig. 10.4e). From 14.96 – 14.89 mbs, however, K and Ti intensities decrease (from 0.11 to 0.07 K/kcps and 0.04 to 0.03 Ti/kcps), while Ca intensities increase from 10.75 to 12.25 Ca/kcps, which coincides with the period of maximum varve thicknesses (Fig. 10.4b) and the deposition of the thickest (up to 4.19mm) detrital layers (Fig. 10.4e). The final section of this interval, between 14.89 – 14.86, is characterised by decreasing Ca counts (to 11.10 Ca/kcps) and increasing K and Ti counts (to 0.13 K/kcps and 0.05 Ti/kcps) (Fig. 10.4e).

10.3.2.2. 14.86 – 14.60 mbs

This interval is defined by the second peak that occurs in varve thickness, with average thicknesses of ~1.47mm (Fig. 10.4b). This interval is also characterised by different lamination sets, with a switch from organo-clastic laminations (LT-3) with 10 – 30% mineral grain abundance to those with ≤10% (Fig. 10.4c).

↓ ***Figure 10.4.*** *Sedimentological data for the Marks Tey sequence between 16.07 – 14.17 mbs. The sequence has been sub-divided based on the information in Fig. 10.1. A) Selected pollen taxa, plotted as percentage contribution (silhouette) and concentration (lines, x10^3 grains/g); B) Total varve thickness (the two distinctive peaks during the NAP Regressive phase have been highlighted); C) Summary of the main lamination sets identified in the sequence, plotted as a 50-point moving average; D) The location and thickness of detrital layers contained within the varves; E) μ-XRF count data for Ca, Ti and K, which have been standardised to kilo counts per second (kcps), plotted as raw data (grey line) with a 20-point moving average (black line); F) Oxygen isotope values for the whole interval, plotted as raw data (grey line) with the main trend in the data highlighted by a 5-point moving average (red line).*

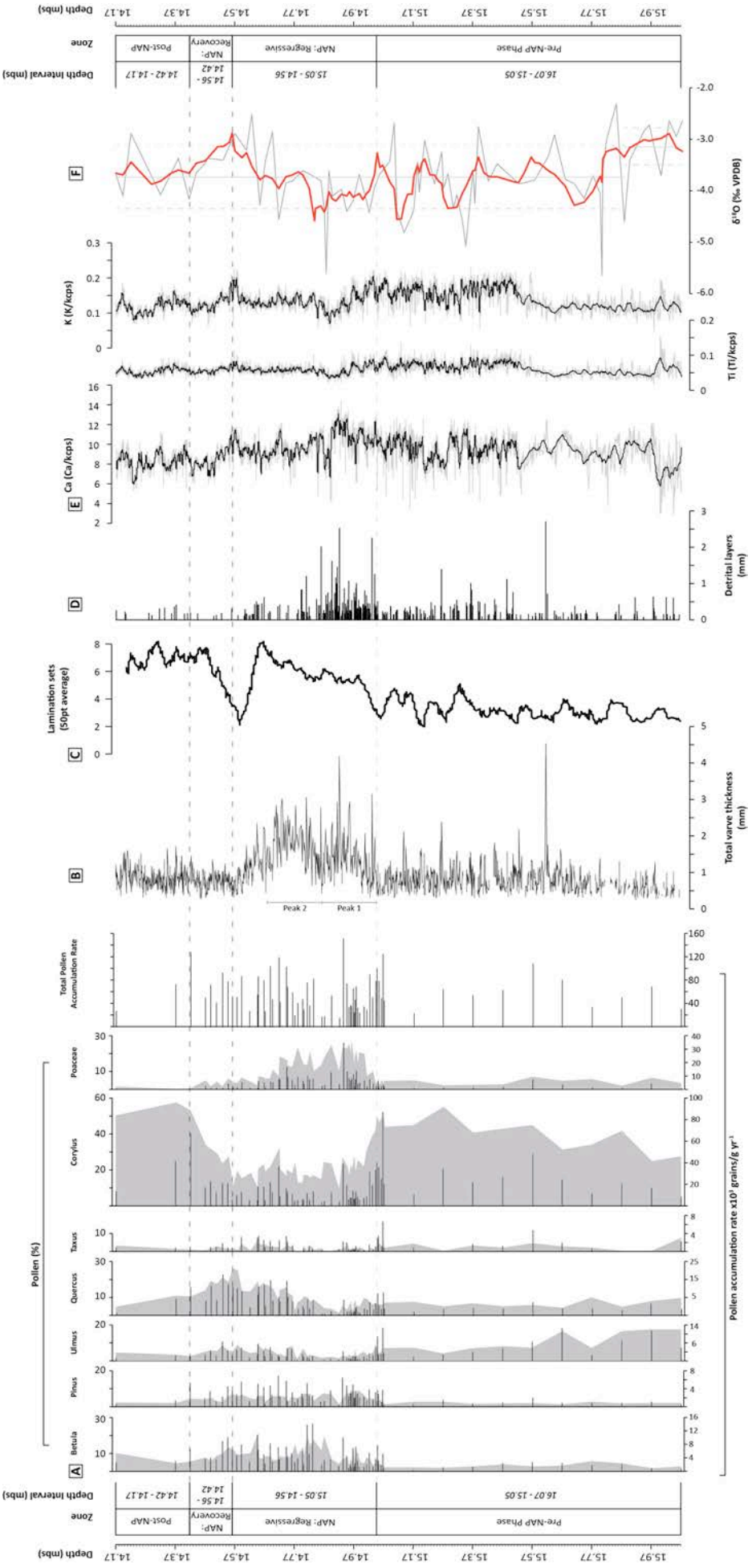
Depth (mbs)
14.17
14.37
14.57
14.77
14.97
15.17
15.37
15.57
15.77
15.97
Zone
Post-NAP
NAP: Recovery
NAP: Regressive
Pre-NAP Phase
Depth interval (mbs)
14.42 - 14.17
14.56 - 14.42
15.05 - 14.56
16.07 - 15.05
F
δ18O (‰ VPDB)
-2.0
-3.0
-4.0
-5.0
-6.0
K (K/kcps)
0.3
0.2
0.1
0
Ti (Ti/kcps)
0.2
0.1
0
E
Ca (Ca/kcps)
16
14
12
10
8
6
4
2
D
Detrital layers (mm)
3
2
1
0
C
Lamination sets (50pt average)
8
6
4
2
0
B
Total varve thickness (mm)
5
4
3
2
1
0
Peak 2
Peak 1
Total Pollen Accumulation Rate
160
120
80
40
Poaceae
30
10
40
30
20
10
Corylus
60
40
20
100
80
60
40
20
Taxus
10
8
4
Quercus
30
10
25
15
5
Ulmus
20
14
6
Pinus
20
8
4
Betula
30
10
16
12
8
4
A
Pollen (%)
Pollen accumulation rate x10³ grains/g yr⁻¹

The trend towards higher lamination set numbers in this interval is the result of diatom-rich laminations (>50% abundance, LT-1.2) and calcite rich lamination types (both LT-2.2 and 2.3) (Fig. 10.4c). Detrital layers are thinner (average of 0.341mm) and occur less frequently in this interval (23% of the varves) (Fig. 10.4d). The µ-XRF data for K and Ti show consistent elemental intensities across the interval, with average values of 0.13 K/kcps and 0.06 Ti/kcps, returning the same average values as those for the interval between 16.07 – 15.53 mbs. The Ca series is more variable, displaying a decreasing trend from 11.10 to 9.9, with average values of 9.48 Ca/kcps, comparable to those for the interval from 16.07 – 15.53 mbs (Fig. 10.4e).

10.3.2.3. 14.60 – 14.42 mbs

This interval is characterised by thin varves (~0.73mm) and the infrequent occurrence of detrital layers, which occur in 3.4% of varves that cover the interval and have an average thickness of 0.175mm (Fig. 10.4d). The start of this zone is characterised by lamination set compositions similar to those between 16.17 – 15.05 mbs, with LT-1.1 (<50% diatom abundance), LT-2.1 (≤30% calcite abundance) and LT-3.1 (organo-clastic laminations with ≤10% mineral grain abundance) (Fig. 10.4c). There is then a trend towards varves with higher lamination set values, which are composed of LT-1.2 (>50% diatom abundance), LT-2.2 (>50% calcite abundance) and LT-3.1 (organo-clastic laminations with ≤10% mineral grain abundance) (Fig. 10.4c). After peaks in the intensity of both K and Ca (0.18 K/kcps and 11.06 Ca/kcps) at 14.56 mbs, both elements decrease throughout the zone to values of 0.12 K/kcps and 8.16 Ca/kcps (Fig. 10.4e). This trend is also observed in the Ti data, although the scale of the shift is lower (from 0.07 to 0.05 Ti/kcps) (Fig. 10.4e).

10.3.3. Post-NAP Phase Zone (14.42 – 14.17 mbs)

The post-NAP interval of the sequence is characterised by a continuation of the average varve thicknesses and lamination sets observed towards the end of the previous interval, with average varve thicknesses of ~0.79µm and varves characterised by diatom-rich laminations (LT-1.2, >50% diatom abundance) and calcite-rich laminations (>50% calcite abundance) that occur as single (LT-2.2) or multiple sub-laminations (LT-2.3) (Fig. 10.4e). Furthermore, detrital layers only occur in 3.7% of the

varves located in this zone. The µ-XRF data also reveals a consistent trend through this interval, with all three elements displaying relatively consistent trends throughout (8.32 Ca/kcps, 0.12 K/kcps and 0.06 Ti/kcps) (Fig. 10.4e).

10.4. Annually-resolved model for the NAP phase at Marks Tey

The first part of this chapter has described results from the analysis of Palaeoenvironmental and sedimentological proxies from 16.07 -14.17 mbs in core MT-2010. This section will bring this data together and place it in a temporal framework, based on the MTSC-2014^{INT} varve chronology developed in chapter 8. The palaeoenvironmental and sedimentological changes that occur during the NAP phase (15.05 – 14.42 mbs) will be summarised in relation to the regressive and recovery phases of the pollen assemblage. Variations in these proxies will also be placed into a temporal framework for the pre-NAP Phase section of the sequence (16.07 to 15.05 mbs), as this provides important information about possible forcing mechanisms for the NAP phase.

As the MTSC-2014^{INT} varve chronology is floating, it will be anchored to the onset of the NAP Phase, as defined by the onset of decreasing *Corylus* percentages at 15.05 mbs (Fig. 10.1). This depth will therefore be 0±6 vyrs. All events that occur prior to this point (the pre-NAP Phase) will, therefore, be reported as negative varve years and all events that occur after this point will be reported as positive varve years. Furthermore, figures in brackets indicate timing of events after the commencement of varve formation in the sequence (Fig. 10.5). Figure 10.5 is a summary diagram of selected palaeoenvironmental and sedimentological proxies that highlight the main changes that occur from the pre-NAP Phase zone through to the post-NAP Phase zone of the sequence.

⬇***Figure 10.5.*** *Summary figure showing selected palaeoenvironmental and sedimentological proxies that highlight the main trends that occur during the pre-NAP, NAP and post-NAP Phase zones of the MT-2010 sequence. The sequence has been sub-divided based on the information in Fig. 10.1. A) Macro-charcoal counts undertaken from -766±5 vyrs have been plotted by particle size fraction (>125µm, >250µm, >500µm), B) Selected pollen taxa, plotted as percentage contribution (silhouette) and PAR (lines, x10^3 grains/g y^{-1}); C) Selected diatom species of counts from -616±5 vyrs, plotted as percentage contribution, D) Total varve thickness; E) The location and thickness of detrital layers contained within the varves; and F) Oxygen isotope values for the whole interval, plotted as raw data (grey line) with the main trend in the data highlighted by a 5-point moving average (red line). Locations of the isotopic oscillations (IO) are also annotated.*

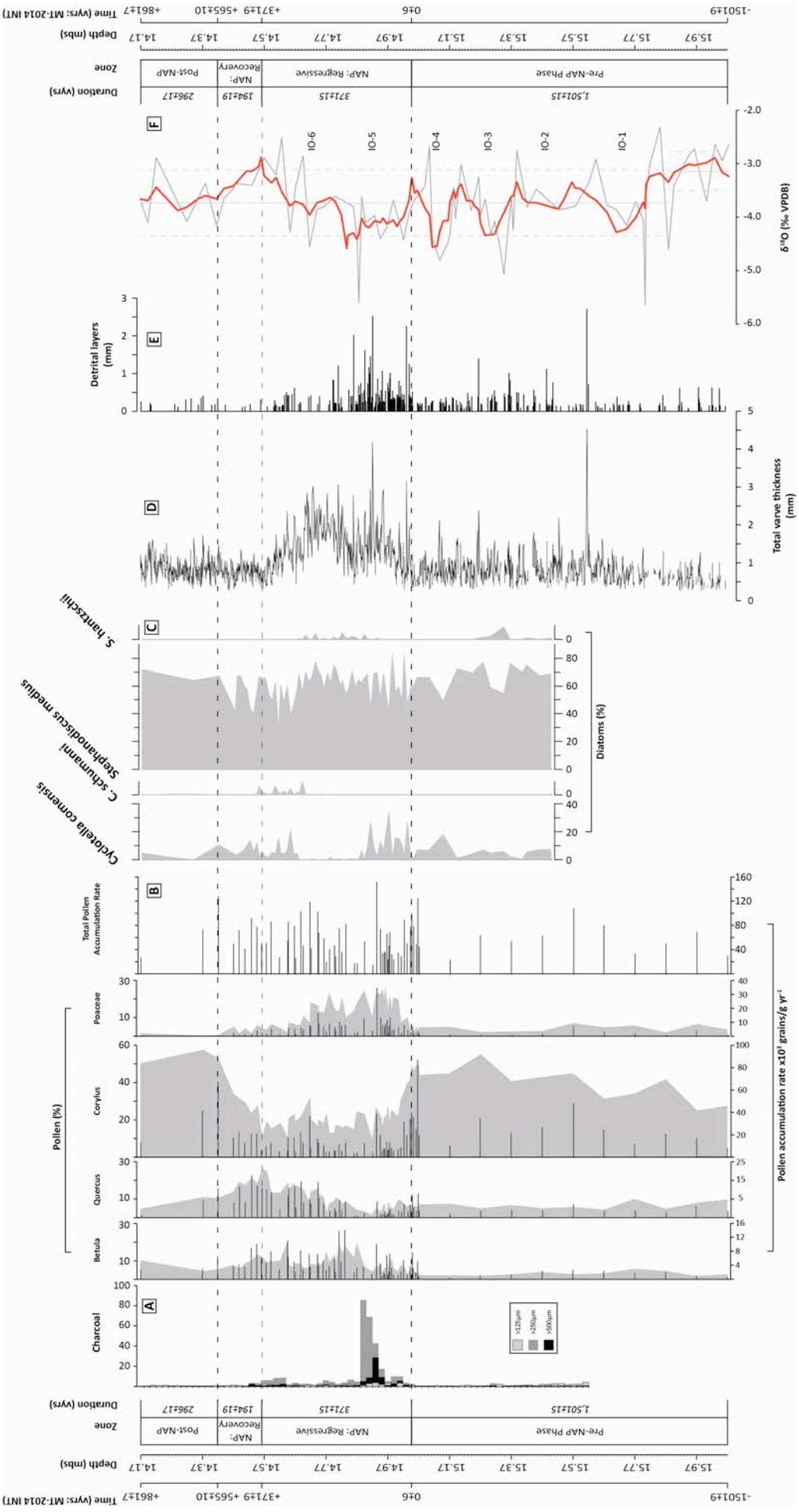
Time (yrs: MT-2014 INT)
Depth (mbs)
Zone
Duration (yrs)
Pre-NAP Phase
NAP: Regressive
NAP: Recovery
Post-NAP
1,501±15
371±15
194±19
296±17
IO-1
IO-2
IO-3
IO-4
IO-5
IO-6
δ18O (‰ VPDB)
Detrital layers (mm)
Total varve thickness (mm)
Diatoms (%)
S. hantzschii
C. schumanni
Stephanodiscus medius
Cyclotella comensis
Total Pollen Accumulation Rate
Poaceae
Corylus
Quercus
Betula
Pollen (%)
Pollen accumulation rate x10³ grains/g yr⁻¹
Charcoal
>125µm
>250µm
>500µm

The ± error associated with the duration and timing of events stated in this section relates to the number of varves contained within samples taken from the core. To aid the descriptions in this section, two further figures have been produced. Figure 10.6 is a copy of figure 10.5, with the addition of annotations to highlight the timing of key events and, in some cases, the duration. Figure 10.7 also provides this information in a tabular format. As these are only summary diagrams they only contain the key pollen, diatom and varve micro-facies data. Where data that is not contained in these figures is referred to in the text, reference will be made to figures 10.2 and 10.4.

10.4.1. Pre-NAP phase (16.07 – 15.05 mbs, -1,501±15 vyrs)

This zone of the MT-2010 sequence from 16.07 – 15.05 mbs represents the period from the onset of pollen zone Ho IIc to the onset of the NAP phase and contains 1,501±15 years. The chronology for the first 174 vyrs (59 counted, 115 interpolated) is based on average sedimentation rates from the first point that varve structures were identified in the core (16.45 mbs) to 16.00 mbs, due to varves making up only a minor component of the sequence (see chapter 8). The next section (16.00 – 15.05 mbs) composes 1,327 vyrs (1,062 counted, 265 interpolated varves).

10.4.1.1. Pollen

As described in section 10.2.1.1, the pre-NAP phase of the sequence is characterised by vegetational development during the early part of Ho IIc, with an early peak in *Ulmus* at the onset of the pollen zone, the presence of *Quercus* and *Ulmus* and increasing percentages of *Corylus*, which reaches a peak percentage contribution of 54.8% at -325±12 vyrs (1,798 vyrs after varve formation commences). The zone is also characterised by low percentages of *Betula* (max. 6.6%), *Pinus* (max. 3.8%) and *Poaceae* (max. 7.8%).

🡻***Figure 10.6.*** *Summary diagram (from Fig. 10.5) of selected proxies highlighting main trends that occur during the pre-NAP, NAP and post-NAP Phase zones of the MT-2010 sequence. This figure contains the location of key events that occur through the sequence, which have been annotated with the timing in vyrs before (-) and after (+) the onset of the NAP Phase (figures in brackets indicate timing of events after the commencement of varve formation in the sequence). A) Macro-charcoal counts undertaken from -766±5 vyrs have been plotted by particle size fraction (>125µm, >250µm, >500µm), B) Selected pollen taxa, plotted as percentage contribution (silhouette) and PAR (lines, x10^{3} grains/g y^{-1}); C) Selected diatom species of counts from -616±5 vyrs, plotted as percentage contribution, D) Total varve thickness; E) The location and thickness of detrital layers contained within the varves; and F) Oxygen isotope values for the whole interval, plotted as raw data (grey line) with the main trend in the data highlighted by a 5-point moving average (red line). Locations of the isotopic oscillations (IO) are also annotated.*

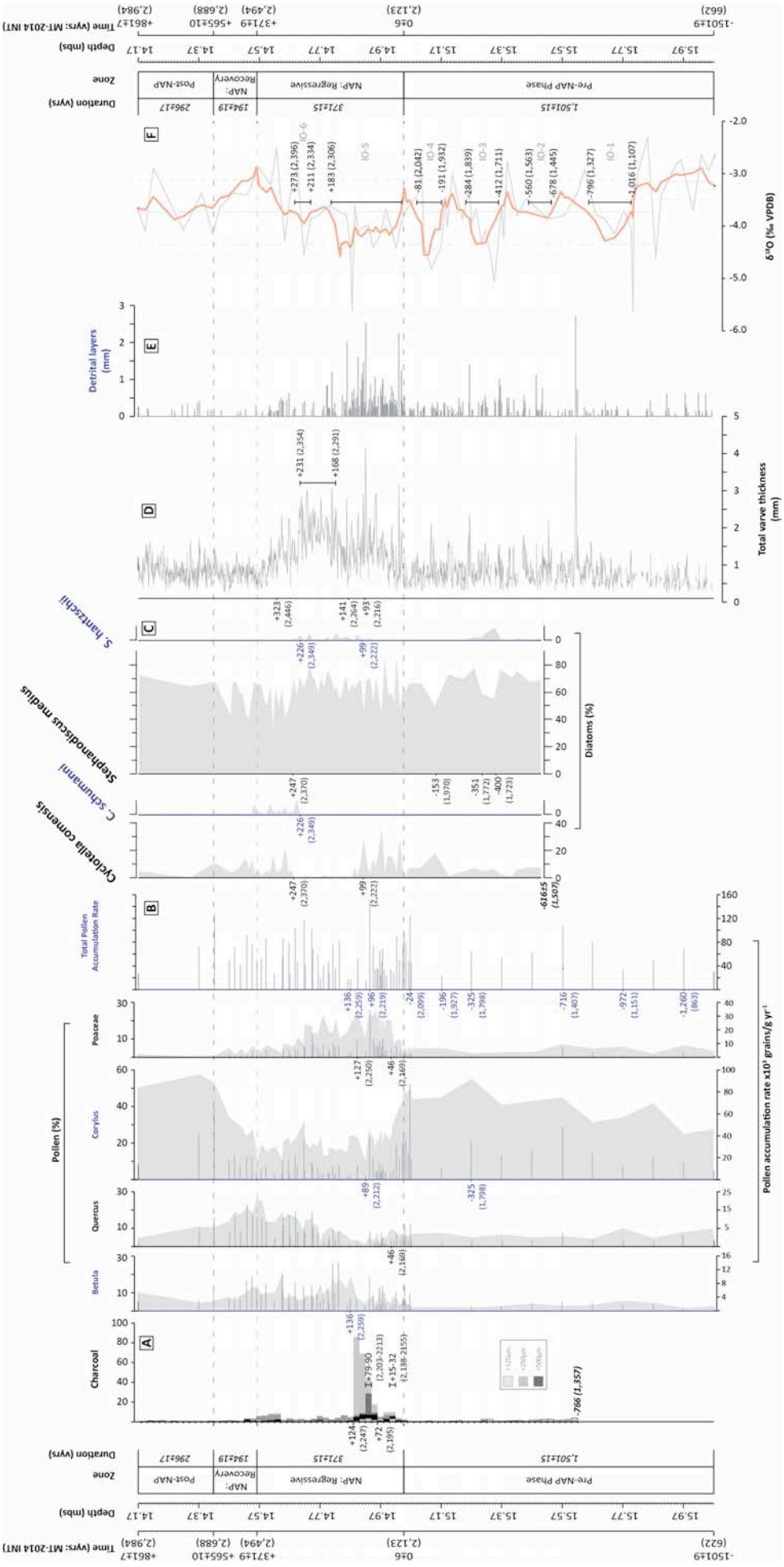
Time (yrs: MT-2014 INT)
Depth (mbs)
Zone
Duration (yrs)
Pre-NAP Phase
NAP: Regressive
NAP: Recovery
Post-NAP
δ18O (‰ VPDB)
Detrital layers (mm)
Total varve thickness (mm)
Diatoms (%)
S. hantzschii
Stephanodiscus medius
C. schumannii
Cyclotella comensis
Total Pollen Accumulation Rate
Poaceae
Corylus
Quercus
Betula
Pollen (%)
Pollen accumulation rate x10³ grains/g yr⁻¹
Charcoal

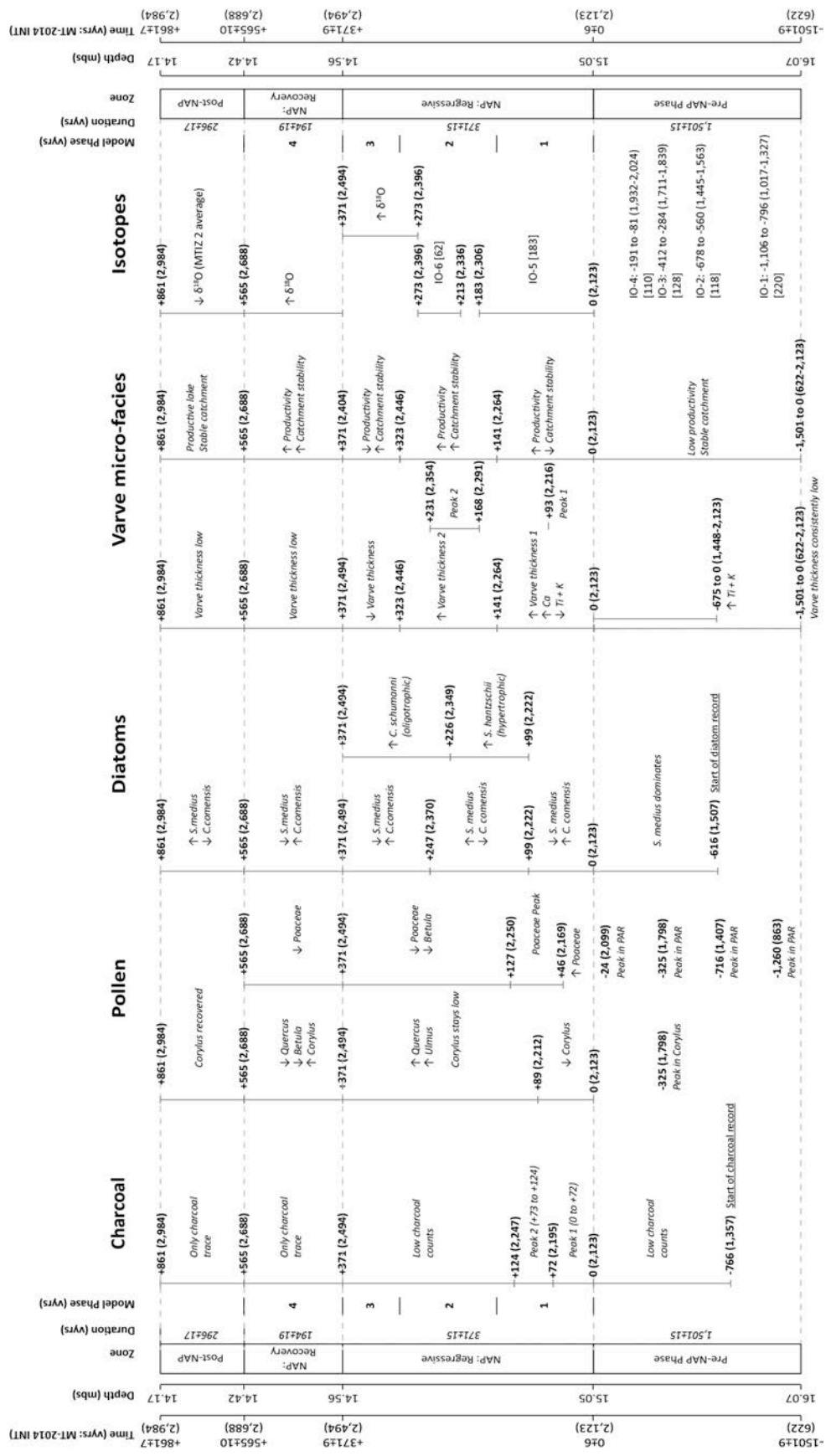

Figure 10.7. *Summary of the relationship between the timing and phasing of proxy response during the Pre-NAP, NAP and post-NAP Phase zones of the MT-2010 sequence shown in figure 10.7 (figures in brackets indicate timing of events after the commencement of varve formation in the sequence). The arrows represent either an increase of decrease in the associated proxy. All shifts in the pollen data relate to percentage changes, except for where PAR is stated.*

Although the percentage data reveals the expansion of temperate tree taxa during Ho IIc, total pollen accumulation rates (PAR) vary. After reaching a peak of 69 x 10^3 grains/g y^{-1} at -1,260±21 vyrs (863 vyrs after varves begin to form), PAR then decreases to 33 x 10^3 grains/g y^{-1} at -972±14 vyrs. This is then followed by another increase to 109 x 10^3 grains/g y^{-1} at -716±11 vyrs, before then declining to 23 x 10^3 grains/g y^{-1} at -196±12 vyrs. This decreasing trend is interrupted -325±12 vyrs, where PAR increases to 64 x 10^3 grains/g y^{-1}. PAR then increases to a final peak of 125 x 10^3 grains/g y^{-1} at -24±9 vyrs, before declining to 90 x 10^3 grains/g y^{-1} at the onset of the NAP phase (0±6 vyrs).

10.4.1.2. Macro-charcoal

Macro-charcoal counts for the sequence started -766±5 vyrs. This interval contains very low charcoal counts (average of 2.5 particles/cm^3).

10.4.1.3. Diatoms

Diatom analysis was undertaken from -616±5 vyrs. During this interval, the assemblage is dominated by *S. medius*. The first interval where *S. medius* percentages decline occurs from -400±9 to -351±9 vyrs, where *S. hantzschii* and *S. minutulus* increase to 9.1-2.3% and 16.2-18.6%, respectively. The second interval occurs at -153±8 vyrs, where *C. comensis* increases to 17.7%.

10.4.1.4. Oxygen isotopes

The oxygen isotope record is characterised by four negative oscillations during Ho IIc, before the onset of the NAP phase, which occur during the 1,016 years that precede it (Fig. 10.8).

- Oscillation 1 begins at -1,016±6 vyrs and ends at -796±6 vyrs (220 year duration);
- Oscillation 2 starts at -678±6 vyrs and ends at -560±6 vyrs (118 year duration);
- Oscillation 3 starts at -412±6 vyrs and ends at -284±6 vyrs (128 year duration); and
- Oscillation 4 begins at -191±6 vyrs and ends at -81±6 vyrs (110 year duration) (Table. 10.1).

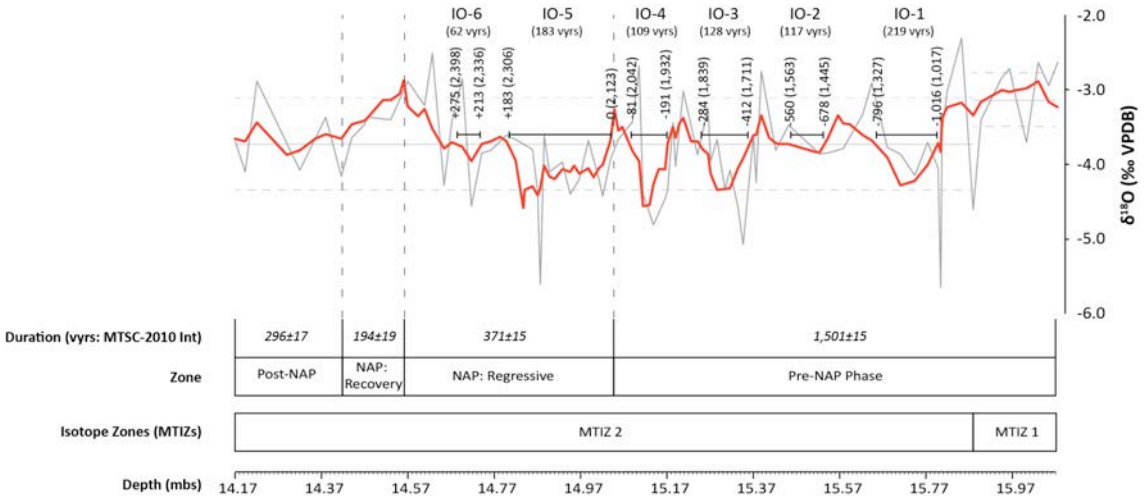

Figure 10.8. *The $\delta^{18}O$ record from Fig. 10.3, with the MTSC-2014^{INT} varve chronology applied to it. The figure highlights the timing and duration of the isotopic oscillations during the pre-NAP Phase and NAP Phase: Regressive Zone.*

The oxygen isotope record therefore contains evidence for four centennial-scale oscillations from -1,016±6 vyrs to the onset of the NAP phase. The first two are not significant at 1σ, while oscillations 3 and 4 are (Table 10.1).

10.4.1.5. Sedimentology

The pre-NAP Phase zone is characterised by average varve thicknesses of ~0.7mm and the varve structure is characterised by lamination types indicative of relatively low levels of lake productivity (LT-1.1, LT-2.1). While the µ-XRF element intensities for Ca fluctuate, it maintains a consistent trend (average of 9.44 Ca/kcps) throughout. The shift that occurs in the Ti and K series at -675±5 vyrs, with average intensities changing from 0.06 to 0.07 Ti/kcps and 0.13 to 0.16 K/kcps (Fig. 10.4e).

10.4.2. The NAP phase (15.05 – 14.42 mbs, +565±12 vyrs)

As identified in the introduction to this chapter, the NAP phase in the Marks Tey sequence can be delimited by changes that occur in *Corylus* percentages (Fig. 10.1). Based on the MTSC-2010^{INT} varve chronology, the duration of the NAP is 565±12 vyrs. To allow comparisons to be made with the OHO, the NAP phase has been sub-divided into a regression and recovery zone (Koutsodendris et al., 2012).

10.4.2.1. NAP: Regressive Zone (15.05 – 14.56 mbs, 371±15 vyrs)

10.4.2.1.1. Pollen

The regressive zone of the NAP phase lasts for 371±15 years. It is represented by an initial decrease in *Corylus* percentages from 48.5 to 8.5% after +89±12 vyrs. Over the same time period, *Ulmus* also declines from 6 to 1.1%, while *Quercus* exhibits a delayed response (from 9.15 to 0.92%), at +46±9 vyrs after the onset of the regressive zone. From +89±12 to +371±15 vyrs, although variable, *Corylus* percentages remain consistently below 25%. In contrast, *Quercus* and *Ulmus* percentages gradually increase during this time interval from 1.1 to 25.8% and 0.92 to 8.4%, respectively (Fig. 10.2).

In contrast to *Corylus, Quercus* and *Ulmus*, *Poaceae* percentages increase rapidly during the first part of the regression zone, from 2.2 to 19.6%, between the onset and +46±9 vyrs. *Poaceae* percentages remain high until +127±8 vyrs, before gradually declining from 24.1 to 3.9% over the next 244±14 vyrs until the end of the regressive zone (at +371±15 vyrs) (Fig. 10.5b). The decline in *Poaceae* percentages is marked by an increase in *Betula*, which remains low (ca 10%) for the first +127±7 vyrs of the regressive zone, before increasing rapidly to 18.6% over the next 9±7 vyrs (+136±7 vyrs). During the next 235±15 vyrs, *Betula* percentages gradually fall and reach 11.9% at the end of the zone. In contrast to *Poaceae* and *Betula*, no obvious trend is apparent in *Pinus* percentages throughout the regressive phase, which remain below 10% (see Fig. 10.3).

The PAR data for individual taxa follow the same general trend seen in the percentage data, but the PAR data does reveal some interesting trends during the regressive zone. Apart from a peak in PAR of 153 x 10^3 grains/g y^{-1}, which occurs at +80±6 vyrs, the regressive zone of the NAP phase is characterised by decreasing PARs, which decrease to 17 x 10^3 grains/g y^{-1} after +136±11 vyrs. PAR then returns to pre-NAP levels for the next 234±17 years until the end of the regressive phase.

10.4.2.1.2. Macro-charcoal

The two charcoal peaks present in the NAP phase occur in the regressive zone. The first (and smaller) of these two peaks occurs, within error, at 0±6 vyrs and lasts for +72 vyrs, with peak counts reached between +15 to +32 vyrs. The second, larger charcoal peak follows immediately afterwards (due to sampling resolution) and lasts from +73 to +124 vyrs (51 vyrs), with peak counts occurring between +79 and +90 vyrs. The two peaks in charcoal accumulation therefore occur during the first +124 vyrs of the regressive zone, which also coincides with the period of peak *Poaceae* percentages described above.

10.4.2.1.3. Diatoms

Between 0±6 and +99±7 vyrs of the regressive zone (coeval with the decrease in *Corylus*), the characteristic feature of the assemblage is the increase in percentage contribution of *C. comensis* (up to 34.3%) at the expense of *S. medius* (down to values of 41.3%). From +99±7 to +247±7 vyrs, *S. medius* percentages recover and remain stable (54 to 78.1%). This time interval is characterised by the decline and disappearance of *C. comensis* from the record, and the appearance of *S. hantzschii* (up to 4.8%) between +99±7 to +226±6 vyrs, which is then replaced by *C. schumanni* (up to 10%) from +226±6 vyrs until the end on the regressive zone (371±15 vyrs), during which time *S. medius* percentages again become lower and more variable (28.8 to 67.2%). During this time period, where *C. schumanni* is present, *C. comensis* also reappears, from +247±7 vyrs until the end of the regressive phase. There are also peaks in *S. minutulus* at +279±6 (23.8%) and +297±7 (22.4%) vyrs, which then disappears from the assemblage, and a distinctive peak in *S. parvus* (28.2%) at +330±8 vyrs.

10.4.2.4. Oxygen isotopes

The regressive zone is associated with isotope oscillations 5 and 6 (Fig. 10.6), identified in the oxygen isotope stratigraphy between 15.038 to 14.798 mbs and 14.740 to 14.653 mbs, respectively. Oscillation 5 lasts for approximately 183 vyrs (Table 10.1, Fig. 10.8), with the 5-point average moving below the average $\delta^{18}O$ value for MTIZ-2 (-3.73‰) in conjunction with the onset of the regressive phase (0±6 vyrs), reaching a $\delta^{18}O$ value of -4.18‰ at +41±6 vyrs. The $\delta^{18}O$ values then remain low and decrease to

a value of -4.59‰ at +161±6 vyrs ($\delta^{18}O$ remains low for 120 years), before recovering to average values for MTIZ-2 at +183±6 vyrs (recovery takes 22 vyrs) (Table 10.1, Fig. 10.8). The 5-point average then fluctuates, again moving below the dataset average from +213 to +275 vyrs (62 years), reaching $\delta^{18}O$ values of -3.96% after which it increases to -2.85‰ at the end of the regressive phase.

10.4.2.1.5. Sedimentology

The regressive zone is characterised by the two distinct peaks that occur in varve thickness. The first peak in varve thickness occurs at 0±6 vyrs (within pollen sampling errors) and lasts until +141±5 vyrs. Peak varve thicknesses attained at +93±5 vyrs, which also coincides with peak values in the µ-XRF Ca intensities and corresponding low values in K and Ti (Fig. 10.4e). The first peak in varve thickness is characterised by lamination sets indicative of relatively low levels of productivity (Fig. 10.4c) and the frequent deposition of detrital layers.

The second peak in varve thickness occurs between +142±5 and +323±5 vyrs. Peak varve thicknesses occur at +175±5 vyrs, however, a broad interval of elevated varve thickness (ca 2,000µm) occurs from +168 to +231±5 vyrs. As discussed earlier, the varves in this second peak are characterised by lamination sets indicative of increasing lake productivity and a relatively stable lake catchment (Fig. 10.4c). The K and Ti µ-XRF data is stable throughout this section of the regressive phase (average intensities 0.13 K/kcps and 0.06 Ti/kcps), returning to the same average values for the interval from -1,501±15 to -675±5 vyrs (16.07 to 15.53 mbs in Fig. 10. 4e). In contrast, Ca is more variable during this interval, displaying a decreasing trend from 11.10 to 9.9, with average values of 9.48 Ca/kcps, comparable to those for the interval from 1,501±15 to 675±5 vyrs (Fig. 10.4e). As varve thickness decreases during the latter part of the regressive phase, from +231 to +371±5 vyrs, the lamination sets also shift towards varve structures indicative of lowering levels of productivity (Fig. 10.4c).

10.4.2.2. NAP: Recovery Zone (14.56 – 14.42 mbs, 194±19 vyrs)

10.4.2.2.1. Pollen

The recovery zone lasts for 194±19 vyrs (+371±9 to +565±10 vyrs) and is characterised by a recovery in *Corylus* from 9.6 to 52.8%, and decreasing percentages of both

Quercus and *Ulmus*, from 25.8 10.3% and 8.4 to 2.1%, respectively (Fig. 10.5b, see Fig. 10.4a for *Ulmus* response). The 194±19 vyr duration of the recovery zone is also characterised by decreasing percentages for *Poaceae* (3.9 to 0.3%), *Betula* (11.9 to 5.2%) and *Pinus* (6.7 to 4.3%) (see Fig. 10.4a for *Pinus* response).

10.4.2.2.2 Macro-charcoal

The recovery zone is characterised by very low charcoal counts.

10.4.2.2.3. Diatoms

The recovery zone is characterised by the continuation of variable and generally lower percentages of *S. medius* and the presence of *C. comensis* that occurred during the last 145±19 vyrs of the regressive zone (+226±6 to +371±15 vyrs) (Fig. 10.5c). This zone is also characterised by the disappearance of *C. schumanni* at +371±15 vyrs. *S. minutulus* reappears in this zone at +460±14 vyrs (18.3%), which also coincides with a peak in *S. parvus* (22.3%) (Fig. 10.3c). Furthermore, *C. comta* appears for the first time, reaching 24.8%, at +323±19 vyrs (Fig. 10.3c).

10.4.2.2.4. Oxygen isotopes

The recovery zone of the NAP phase is characterised by a decrease in average $\delta^{18}O$ values from -2.85‰ at the end of the regressive zone (+371±9 vyrs), to values of -3.66‰ at +194±19 vyrs.

10.4.2.2.5. Sedimentology

The sedimentology of the recovery zone of the NAP phase is characterised by a return to varve thicknesses similar to those of the pre-NAP zone (0.736mm). From +371±9 to +527±11 vyrs (156±11 vyr duration), varve structure changes from varves characterised by lamination types indicative of low productivity (LT-1.1 and LT-2.1) to those indicative of higher levels of productivity (LT-1.2 and LT-2.2) (Fig. 10.4c). The recovery zone is also characterised by the infrequent deposition of detrital layers (6 occur), as well as the decrease of all three element intensities, from 0.18 K/kcps, 0.07 Ti/kcps and 11.06 Ca/kcps at the start of the zone, to values of 0.12 K/kcps, 0.05 Ti/kcps and 8.16 Ca/kcps at the end of the recovery zone (Fig. 10.4e).

10.4.2.3. Post-NAP Phase Zone (14.42 – 14.07 mbs, 296±17 vyrs)

The first 296±17 vyrs after the NAP phase is dominated by the occurrence of *Corylus*, which accounts for over 50% of the pollen assemblage. *Quercus*, *Ulmus* and *Taxus, Poaceae, Betula* and *Pinus* also return to pre-NAP percentage and concentration values. Charcoal counts are low throughout this zone (~1.7 particles/cm^3) and *S. medius* again dominated the phytoplankton assemblage, while *C. comensis* declines. This zone is further characterised by relatively stable $\delta^{18}O$ values, which plot within uncertainties (±1σ) and average $\delta^{18}O$ values hover around the dataset average (Fig. 10.6).

The sedimentology of the post-NAP phase zone is characterised by a continuation of the average varve thicknesses and lamination sets observed towards the end of the previous interval, with average varve thicknesses of ~0.79mm and varves characterised by diatom-rich and calcite-rich laminations, while detrital layers do not occur frequently (Fig 10.4). The μ-XRF data for all three elements (8.32 Ca/kcps, 0.12 K/kcps and 0.06 Ti/kcps) display a fairly consistent trend throughout the zone (Fig. 10.4e).

10.5. Model summary

This chapter has brought together the sedimentological and isotopic data generated in this thesis and other environmental data generated by other researchers (pollen, diatoms and macro-charcoal) and developed an annually resolved model for the 1.9m section of core MT-2010 from 16.07 to 14.17 mbs, which is summarised below.

10.5.1. Environmental and sedimentological characteristics during the pre-NAP phase zone (16.07 – 15.05 mbs, 1,501±15 vyrs)

- The pre-NAP phase zone of core MT-2010 covers the depth interval 16.07 to 15.05 mbs and is characterised by the occurrence of four isotopic events during the 1,016 years preceding the NAP Phase:
- Isotopic oscillation 1 (not significant at 1σ) occurs from -1,016 to -796±6 vyrs (220 vyr duration) and coincides with a period of low PAR (33 x 10^3 grains/g y^{-1}) at -972±14 vyrs;

- Isotopic oscillation 2 (not significant at 1σ) occurs from -678 to -560±6 vyrs (118 vyr duration) and coincides with the onset of decreasing PARs after a peak of 109 x 10^3 grains/g y^{-1} at -716±11 vyrs. This oscillation also coincides with the onset of increasing K and Ti intensities at -675±5 vyrs (from 0.06 to 0.07 Ti/kcps and 0.13 to 0.16 K/kcps) (see Fig. 10.4);
- Isotopic oscillation 3 (significant at 1σ) occurs from -412 to -284±6 vyrs (128 vyr duration) and broadly coincides with PARs of 54 x 10^3 grains/g y^{-1} at -445±9 vyrs. The diatom assemblage changes during this event, with *S. minutulus* and *S. hantzschii* increasing (16.2-18.6% and 9.1-2.3%, respectively) at the expense of *S. medius* from -400 to -351±9 vyrs;
- Isotopic event 4 (significant at 1σ) occurs from -191 to -81±6 vyrs (191 vyr duration) and coincides with a further decrease in PARs to 23 x 10^3 grains/g y^{-1} at -196±12 vyrs. This event also coincides with an increase in percentages of *C. comensis* to 17.7%, which occurs at -153±8 vyrs.

10.5.2. Environmental and sedimentological characteristics during the NAP phase zone (15.05 – 14.42 mbs, 565±12 vyrs)

The NAP phase zone covers the depth interval from 15.05 to 14.42 mbs and lasts for 565±12 vyrs. The NAP Phase has been sub-divided into regressive and recovery zones.

10.5.2.1. Regressive zone (0±6 – +371±9 vyrs)

- The regressive zone lasts for 371±15 vyrs and is characterised by the following changes:
- A decrease in *Corylus* (48.5 to 8.5%), *Ulmus* (6 to 1.1%) and *Quercus* (9.15 to 0.92%) over the first +89±12 vyrs, while *Poaceae* increases from 2.2 to 19.6% over the first +46±9 vyrs (and remains high until +127±8 vyrs), with *Betula* showing a delayed response, increasing to 18.6% from 10% over 9±7 vyrs after +127±7 vyrs. PARs start to decrease after a peak of 125 x 10^3 grains/g y^{-1} at -24±9 vyrs, falling to 15 x 10^3 grains/g y^{-1} after +80±12 vyrs. During the first +99±7 vyrs of the regressive zone, the percentage contribution of *C. comensis* increases (up to 34.3%) at the expense of *S. medius* (down to values of 41.3%). The two charcoal peaks occur during the first +124±5 vyrs; the first (smaller peak) occurring during the initial +72 vyrs (peak from +15 to 32±5 vyrs) and the second from +73 to 124±5 vyrs (peak

from +79 to 90±5 vyrs). *C. comensis* disappears from the record after this second charcoal peak. These charcoal peaks also coincide with the first peak in varve thickness, which occurs during the first +141±5 vyrs. Peak varve thicknesses occur after +93±5 years, which further coincide with peak values in the µ-XRF Ca intensities and corresponding low values in K and Ti (see Fig. 10.4e). The first peak in varve thickness is characterised by lamination sets indicative of relatively low levels of productivity and the frequent deposition of detrital layers. These events occur during isotopic oscillation 5, the onset of which coincides with 0±6 vyrs, with $\delta^{18}O$ values falling to -4.18‰ after +41±6 vyrs. The $\delta^{18}O$ values then remain low and decrease to a value of -4.59‰ after +161±6 vyrs ($\delta^{18}O$ remains low for 120 vyrs).

- The recovery of $\delta^{18}O$ values after isotopic event 5 happens in two stages. During the first stage, $\delta^{18}O$ values return to average dataset values for MTIZ 2 at +183±6 vyrs (recovery takes 22 vyrs), which then remain stable until +275±6 vyrs. During this period *Corylus* percentages remain low (below 25%, except for a peak of 31.4% at 224±8 years), *Quercus* and *Ulmus* increase (from 8.6 to 17.9% and 2.9 to 5.1%), *Poaceae* and *Betula* decrease (9.8 to 6.4% and 17.2 to 8.3%), while PARs return to pre-NAP levels (80-120 $x10^3$ grains/g y^{-1}). This interval is characterised by stable percentages of *S. medius* (54-78.1%), the continued absence of *C. comensis* and the re-appearance of *S. hantzschii* (up to 4.8%). This interval also coincides with the second increase in varve thickness (+141 to 323±6 years), which has a period of elevated varve thickness (~2mm) that occurs from +168 to 231±6 years (60 vyrs), as well as varve structures indicative of increased levels of productivity (LT-1.2 and LT-2.2/3) and a reduction in the thickness and frequency of detrital layers (average thickness of 0.341mm, occur in 23% of the varves).
- The second stage of isotopic increase after event 5 occurs between +275 and 371±15 vyrs (the end of the regressive zone), where average $\delta^{18}O$ values increase further, to -2.85‰. During this final interval of the regressive zone, *Corylus* percentages continue to stay low (below 25%), *Quercus* and *Ulmus* continue to increase (17.9 to 25.8% and 5.1 to 8.4%) and *Poaceae* percentages fall (6.4 to 3.9%). This interval of increasing isotope values coincides with the appearance of *C. schumanni*, the reappearance of *C. comensis* and the disappearance of *S. hantzschii* (from +247±7 vyrs). During this 96±15 vyr interval, varve thickness decreases from

~1mm to ~0.5mm, varve structure also changes to lamination types indicative of lower levels of productivity (LT-1.1 and LT-2.1), while the elemental intensity data for Ca, K and Ti remain stable.

10.5.2.2. Recovery zone (+371±15 – +565±10 vyrs)

- The recovery zone lasts for 194±19 vyrs and is characterised by the following changes:
- The recovery zone is characterised by decreasing isotope values, from peak values of -2.85‰ at the onset, to -3.66‰ by the end of the zone. *Corylus* recovers from 9.6 to 52.8%, *Quercus* and *Ulmus* decrease (25.8 10.3% and 8.4 to 2.1%, respectively), as does *Poaceae* (3.9 to 0.3%), *Betula* (11.9 to 5.2%) and *Pinus* (6.7 to 4.3%). The variable percentages of *S. medius* and presence of *C. comensis* that characterised the last 145±19 years of the regressive phase (+226±6 to +371±15 vyrs) continue. *C. schumanni* disappears at the onset of this zone, replaced by the reappearance of *S. minutulus* and peaks in *S. parvus* (22.3%). *C. comta* appears for the first time, reaching 24.8% at +23±19 vyrs.
- The sedimentology of the recovery zone indicates a return to varve thicknesses similar to those of the pre-NAP Phase zone (0.736mm). During the first +156±11 vyrs of the recovery phase, varve structure changes from varves characterised by lamination types indicative of low productivity (LT-1.1 and LT-2.1) to those indicative of higher levels of productivity (LT-1.2 and LT-2.2). The recovery zone is also characterised by the infrequent deposition of detrital layers (6 occur), as well as the decrease of all three element intensities, from 0.18 K/kcps, 0.07 Ti/kcps and 11.06 Ca/kcps at the start of the zone, to values of 0.12 K/kcps, 0.05 Ti/kcps and 8.16 Ca/kcps at the end of the recovery zone.

10.5.2.3. Post-NAP Phase Zone (+565±10 – +867±7 vyrs)

- The first 296±17 vyrs of the post-NAP Phase zone of the sequence is characterised by the following changes:
- The zone is characterised by relatively stable $\delta^{18}O$ values, which plot within uncertainties (±1σ) and average $\delta^{18}O$ values hover around the dataset average. *Corylus* maintains its pre-NAP percentage (over 50% of the pollen assemblage), as does *Quercus*, *Ulmus* and *Taxus. Poaceae, Betula* and *Pinus* also return to pre-NAP

percentage and concentration values. Charcoal counts are low throughout this zone (~1.7 particles/cm^3) and *S. medius* dominates the phytoplankton assemblage, while *C. comensis* declines.

- Average varve thicknesses increases slightly (~0.79µm) and are characterised by diatom-rich and calcite-rich laminations, while detrital layers do not occur frequently. The µ-XRF data for all three elements (8.32 Ca/kcps, 0.12 K/kcps and 0.06 Ti/kcps) display a fairly consistent trend throughout the zone.

10.6. Summary

- This chapter has described changes in environmental and sedimentological proxies that occur from 16.07 –to14.17 mbs of the MT-2010 sequence.
- Applying the MTSC-2014^{INT} chronology to the proxy descriptions has allowed for the development of an annually-resolved palaeoenvironmental record for the first 2,363±16 vyrs (-1,501±9 to +861±7 vyrs) of pollen zone Ho IIc.
- The sequence records proxy changes that occur during the pre-NAP Phase zone (-1,501 to 0±6 vyrs), the NAP Phase Regressive zone (0±6 to +371±15 vyrs), the NAP Phase Recovery zone (+371±15 to +565±10 vyrs) and the post-NAP Phase zone (+565±10 to +861±7 vyrs).
- This model forms the basis of the next chapter, which will focus on the palaeoenvironmental significance of the NAP Phase.

Chapter 11. Palaeoenvironmental significance of The Non-Arboreal Pollen Phase

Chapter overview

This discussion chapter will focus on the palaeoenvironmental significance of the NAP Phase at Marks Tey in terms of its forcing mechanism, the nature of landscape and limnological response, the duration of the event, and its chronological position in the Hoxnian (MIS 11). This discussion will then allow for comparisons to be made with the Older Holsteinian Oscillation (OHO) and the 8.2ka event. The OHO is considered to be the equivalent event to the NAP Phase in continental European, as well as providing an analogue for abrupt climatic events that punctuate the early Holocene (Koutsodendris et al., 2012). The suggestion of the occurrence of 8.2 ka-type events in pre-Holocene interglacials is currently, however, limited to the annually-resolved multi-proxy reconstruction of the OHO at Dethlingen, Germany (Koutsodendris et al., 2012), as well as a preliminary stable isotopic study from the annually-laminated carbonates at Marks Tey (Candy, 2009; Candy et al., 2014). The multi-proxy reconstruction of the NAP Phase developed in this thesis expands the current discussion about abrupt events in pre-Holocene interglacials, by: 1) extending the temporal coverage of current isotopic records beyond the immediate vicinity of the pollen regression event to investigate environmental (possibly climatic) variability during early MIS 11, and 2) investigating the role that wildfire may play during abrupt events, and the impact it has on the landscape and aquatic environment.

11.1. Introduction

The NAP phase represents an important event in many British (and European) pollen diagrams from MIS 11, as it interrupts the natural vegetational succession during fully interglacial conditions (Duigan, 1956; West, 1956, 1961; Kelly, 1964; Turner, 1970; Horton, 1974, 1989; Phillips, 1976; Coxon, 1979, 1985, 1993; Thomas, 2001). In the British terrestrial record of MIS 11, the NAP phase occurs in pollen zone Ho IIc (early temperate pollen phase), where NAP briefly expands at the expense of AP (Fig. 11.1).

As discussed in chapter 2, different forcing mechanisms have been suggested to explain this pollen response, including; 1) climatic deterioration (Kelly, 1964; Muller, 1974; Kukla, 2003; Koutsodendris et al., 2012), 2) volcanic activity (Diehl and Sirocko, 2007), and 3) wildfire (Turner, 1970). Until recently, one of the key issues surrounding the debate about the forcing mechanism was that no evidence was available from independent temperature indicators to test the climatic hypothesis.

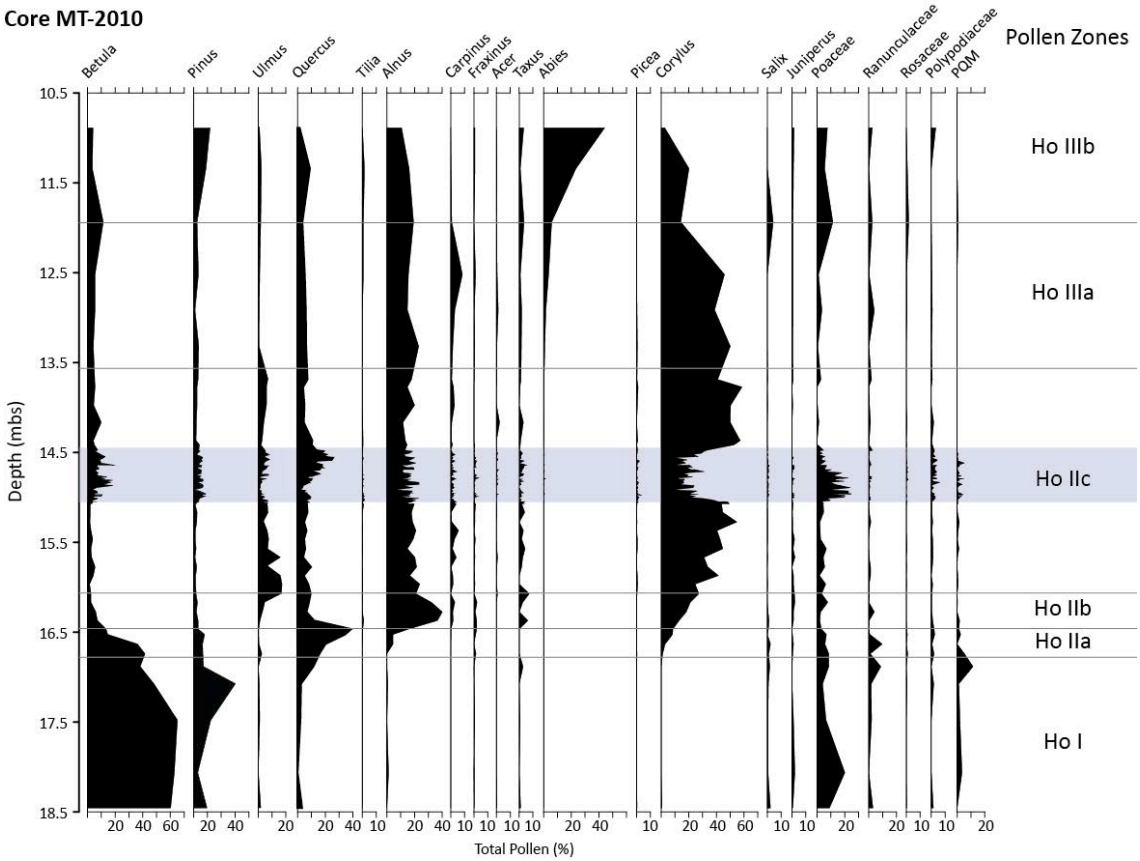

Figure 11.1. *Summary pollen diagram from the lowest 7.5m of core MT-2010, which covers pollen zones Ho I to Ho IIIb. The NAP phase is located in Ho IIc, indicated by the blue shaded area.*

Evidence from $\delta^{18}O_{silica}$ at Dethlingen, Germany (Koutsodendris et al., 2012) and $\delta^{18}O_{calcite}$ from Marks Tey (Candy, 2009; Candy et al., 2011, 2014) suggests that the OHO/NAP phase occurs in association with depleted isotopic values. The data therefore suggests that the event is likely to be climatically forced, possibly analogous to the 8.2 ka event (Koutsodendris et al., 2012). Before a climatic origin can be accepted for this event, a number of issues need to be addressed. These are; 1) the short temporal resolution of both isotopic datasets, which limit our understanding of the long term climatic trends, 2) the fact that the isotope record of Candy (2009)

displays a high degree of co-variance between $\delta^{18}O$ and $\delta^{13}C$ values (r^2=0.77), 3) the relationship between the occurrence of charcoal and the onset of the NAP phase, and 4) the absence of robust quantifications of the duration of this event in Britain.

A reinvestigation of the Marks Tey sequence can address these issues and contribute to our understanding of the NAP phase in four ways: 1) by reconstructing the palaeoecological characteristics of the event and the pattern of proxy response in more detail, including diatom response to the event and the location of the charcoal fragments; 2) investigating the sedimentological response during the event using the varve micro-facies data to identify the timing of periods of landscape instability identified by Turner (1970); 3) investigate long-term variations in the $\delta^{18}O$ record to test the climatic hypothesis as a forcing mechanism; and 4) apply the varve chronology to quantify the pattern of response and identify any leads/lags in proxy response during the event.

11.2. The NAP Phase at Marks Tey

The first section of this chapter will consider the interval of core MT-2010 from 15.05 to 14.42 mbs, the location of the NAP Phase, the onset of which occurs 1,501±15 vyrs after the onset of zone Ho IIc of the pre-temperate Hoxnian pollen phase (Turner and West, 1968) and 2,123 yrs after the onset of varve formation. The environmental and sedimentological proxy data used to reconstruct the NAP Phase at Marks Tey in chapter 10 will be interpreted in this section in terms of landscape and limnological changes that occur during the pollen event. A discussion will then follow concerning the forcing mechanism for the NAP phase. The discussion in this section of the chapter will be based on figure 11.2 and 11.3. These figures contain the same information as figure 10.6 and 10.7 from the previous chapter, but have sub-divided the NAP Phase into four separate phases of lake evolution, which will be discussed below. The first three phases relate to the regressive zone, and phase four represents the recovery zone (Fig. 10.2 and 10.3). Figure 11.1 is a summary of all the palaeoenvironmental and sedimentological data described in chapter 10, and has been sub-divided into the same four phases. This figure acts as a reference for data not included in figures 11.2 and 11.3.

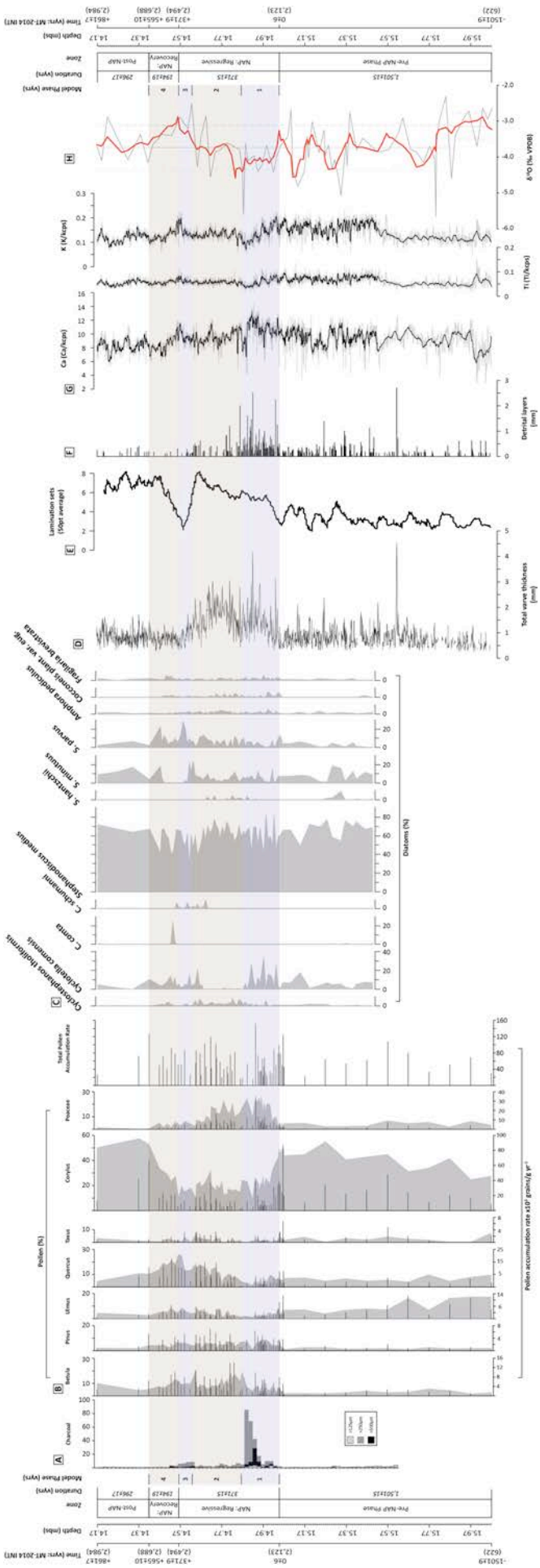

Figure 11.2. *Palaeoenvironmental and sedimentological proxy results for the Marks Tey sequence between 16.07 – 14.17 mbs (2,362 vyrs). The sequence has been sub-divided based on the information in Fig. 10.1. The regressive and recovery zones of the NAP Phase have been further sub-divided into four phases of lake evolution that occur during the NAP Phase. See text for discussion. A) Macro-charcoal counts undertaken from -766 to + 861 vyrs have been plotted by particle size fraction (>125µm, >250µm, >500µm); B) Selected pollen taxa for the whole interval (2,362 vyrs), plotted as percentage contribution (silhouette) and PAR (lines, x10^3 grains/g y^{-1}); C) Selected diatom species from counts undertaken between -616 and +861 vyrs, plotted as percentage contribution; D) Total varve varve thickness; E) Summary of the main lamination sets identified in the sequence, plotted as a 50-point moving average; F) The location and thickness of detrital layers contained within the varve structure; G) µ-XRF count data for Ca, Ti and K, which have been standardised to kilo counts per second (kcps), plotted as raw data (grey line) with a 20-point moving average (black line); and H) Oxygen isotope values for the whole interval, plotted as raw data (grey line) with the main trend in the data highlighted by a 5-point moving average (red line).*

11.2.1. Phase 1: Fire, catchment instability and oligotrophic/eutrophic lake conditions (0±6 – +141±5 vyrs)

Varve year 0±6 in the MTSC-2014 INT chronology relates to the onset of the NAP Phase at Marks Tey at 15.05 mbs, as defined by *Corylus*. The decline in temperate tree pollen (*Corylus, Quercus* and *Ulmus*) that occurs within the first +141±5 vyrs of the NAP Phase coincides with the location of the two largest charcoal peaks that occur in the sequence, which suggests that the NAP Phase at Marks Tey was the result of fire, as suggested by Turner (1970). As microscopic charcoal fragments can be transported long distances, their presence in a sequence may not always be indicative of local conditions (e.g. Butler, 2008). The results presented in this thesis are from macroscopic charcoal counts (>125µm), which provide a more reliable indication of a local fire source (Whitlock and Millspaugh, 1996; Ohlson and Tryterud, 2000; Tinner et al., 2006). The fire had the effect of destabilising the lake catchment, evidenced by both the increased frequency of detrital layer deposition and the increase in varve thickness. Maximum varve thicknesses occur at +93±5 vyrs and coincide with peak charcoal abundances of the >500µm fraction (+72 to +95±5 vyrs) and the anomalously high PAR value (153 x 10^3 grains/g y^{-1}). The first (smaller) charcoal peak is associated with varve thicknesses that are not too dissimilar to those of the pre-NAP Phase zone of the core, so probably reflect the input of wind-blown primary charcoal, whereas the second, larger peak is associated with the greatest sedimentation rates, probably indicative of secondary charcoal washed in due to destabilisation of the landscape (Whitlock and Anderson, 2003). Despite the increase in sediment accumulation rates during this period, the µ-XRF data indicates that the intensities of detrital elements K and Ti are decreasing, while Ca intensities increase (Fig. 11.1g). This is because µ-XRF

data represents only the relative elemental intensity of a sample, not the concentration (e.g. Croudace et al., 2006; Lowemark et al., 2010). As the detrital layers deposited in the sequence are characterised by high Ca intensities, presumably the result of re-working of pre-existing lake sediments, the carbonate present in the detrital layers has a dilution effect on the other elements (Weltje and Tjallingii, 2008; Lowemark et al., 2011). The abundance of authigenic components in lake cores, like diatoms (Brauer et al., 1999b; Prokopenko et al., 2001, 2006; Mackay, 2007) and calcite (Hodell et al., 1998; Prasad et al., 2009; Neugebauer et al., 2012), can be used as a proxy for productivity.

Although the micro-facies description of these components is semi-quantitative, they provide important observations about palaeo-lake productivity at Marks Tey. Micro-facies analysis reveals that varves in this section of the core contain a mixed signal. The zone is dominated by varves containing LT-1.1 (<50% diatom abundance), indicative of relatively low levels of productivity, however calcite laminations are characterised by LT-2.2 (>50% calcite), suggesting higher levels of productivity. Varves containing LT-1.2 (>50% diatom abundance) are also present (Fig. 11.1e). This suggestion is further supported by changes in the diatom assemblage during the first +99±7 vyrs of the NAP phase. The NAP Phase is characterised by the presence of *Stephanodiscus medius*, a planktonic species that prefers high phosphorous (P) and low silica (Si) concentrations (low Si:P ratios), indicating that the palaeo-lake at Marks Tey was eutrophic during the NAP Phase (Anderson, 1990; Bennion, 1994; Kirilova et al., 2010). The presence of other *Stephanodiscus* species, such as *S. parvus* and *S. minutulus,* also indicate eutrophic conditions (Anderson, 1990; Lotter, 1989; Alefs and Muller, 1999; Kirilova et al., 2010).

🡻***Figure 11.3.*** *Summary diagram (from Fig. 10.5), which shows selected environmental and sedimentological proxies that highlight the main trends that occur during the pre-NAP, NAP and post-NAP Phase zones of the MT-2010 sequence. This figure contains the location of key events that occur through the sequence, which have been annotated with the timing in vyrs. A) Macro-charcoal counts undertaken from -766±5 vyrs have been plotted by particle size fraction (>125µm, >250µm, >500µm), B) Selected pollen taxa, plotted as percentage contribution (silhouette) and PAR (lines, x10^{3} grains/g y^{-1}); C) Selected diatom species of counts from -616±5 vyrs, plotted as percentage contribution, D) Total varve thickness; E) The location and thickness of detrital layers contained within the varves; and F) Oxygen isotope values for the whole interval, plotted as raw data (grey line) with the main trend in the data highlighted by a 5-point moving average (red line). Locations of the isotopic oscillations (IO) are also annotated.*

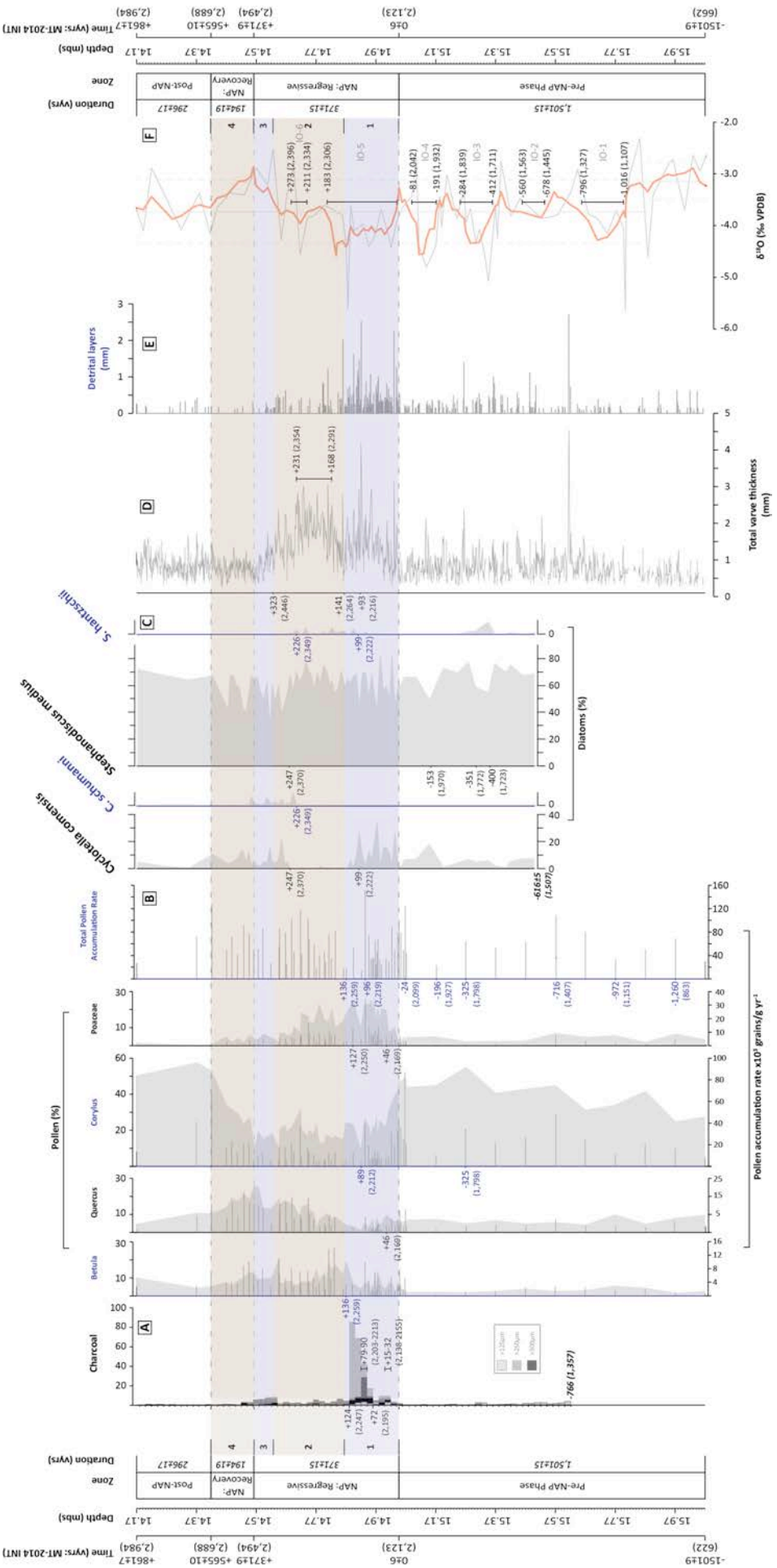
Time (yrs: MT-2014 INT)
Depth (mbs)
Zone
Duration (yrs)
Pre-NAP Phase
NAP: Regressive
NAP: Recovery
Post-NAP
δ18O (‰ VPDB)
Detrital layers (mm)
Total varve thickness (mm)
Diatoms (%)
S. hantzschii
Stephanodiscus medius
C. schumanni
Cyclotella comensis
Total Pollen Accumulation Rate
Pollen (%)
Poaceae
Corylus
Quercus
Betula
Charcoal
Pollen accumulation rate x10³ grains/g yr⁻¹

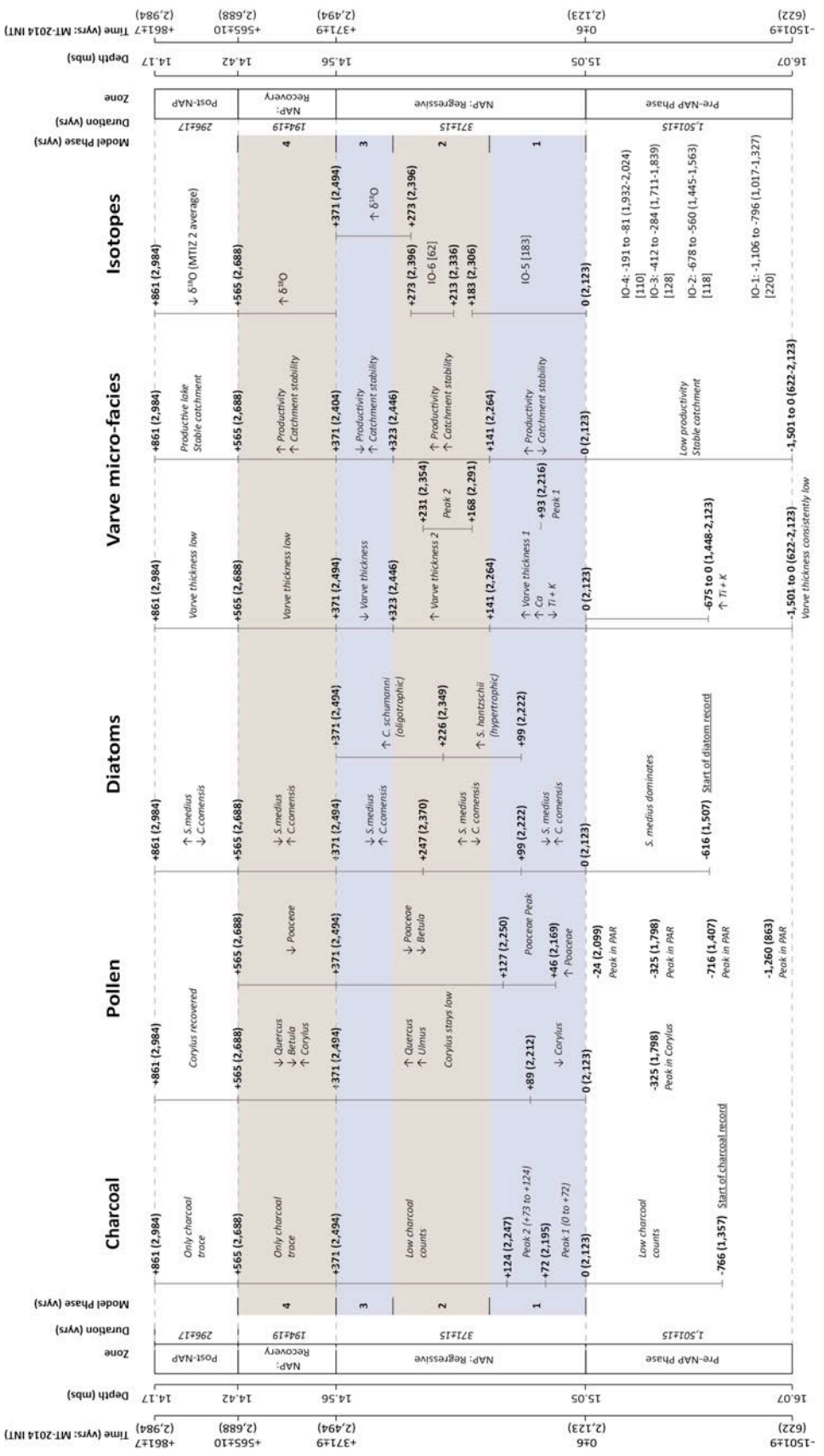

Figure 11.4. *Summary of the relationship between the timing and phasing of proxy response during the Pre-NAP, NAP and post-NAP Phase zones of the MT-2010 sequence shown in figure 11.2. The arrows represent either an increase of decrease in the associated proxy. All shifts in the pollen data relate to percentage changes, except for where PAR is stated.*

The presence of *C. comensis* for the first +99±7 vyrs, however, indicates that the first part of the regressive phase was characterised by lower lake water nutrient levels, as *C. comensis* provides an important indicator of oligotrophic lake waters (Scheffler et al., 2005; Werner and Smol, 2006).

The environmental and sedimentological evidence therefore suggests a mixed response during this phase of lake development. Although the proxies indicate relatively low levels of lake productivity, varve structures indicate a general increase in productivity when compared to the pre-NAP interval of the sequence (Fig. 11.1). The source of this increase in productivity is likely to be from the influx of nutrients from the lake catchment (as shown by the increased frequency of detrital layer deposition), as well as charcoal from the primary input event. Such a scenario has also been observed in other varved lake records, where increases in the input of material from the catchment cause nutrient conditions to increase (Brauer et al., 1999b; Lucke and Brauer, 2004).

11.2.2. Phase 2: Catchment stability and eutrophic/hypertrophic lake conditions (+142 – +323±5 vyrs)

Phase 2 of the regressive zone is characterised by increasing stability in the lake catchment, as decreases in *Poaceae* (17.1 to 7.1%) and *Betula* (18.6 to 6.4%) correspond to an expansion of *Quercus* (3.4 to 19.9%), while *Corylus* remains low but variable (between 12.6 and 31.4.%), while PARs return to values characteristic of the pre-NAP interval. Catchment stability is further indicated by low charcoal counts throughout this zone and the less frequent deposition of detrital layers (in 24% of varves in the phase), suggesting that erosion of the landscape has become a less effective method of allogenic sediment delivery.

The lake system undergoes a shift in trophic status during this phase, as the second period of increasing varve thickness is caused by thickness changes in the lamination types, rather than the input of detrital material from the catchment. The observed trend in varve micro-facies, caused by a switch to varves with lamination types abundant in biogenic silica (LT-1.2), calcite (LT-2.2 and 2.3) and organo-clastic laminations rich in organic material (LT-2.1), suggests more productive lake waters

prevailed during this zone; the source of these nutrients likely to be from the larger second charcoal peak that occurred towards the end of zone 1 (Fig. 11.1e). Shifts in the diatom assemblage also indicate nutrient loading. The disappearance of *C. comensis* from the record at the onset of the zone coincides with a slight increase (ca. 1 to 3%) in *C. tholiformis* (see Fig. 11.1c) and the appearance of *S. hantzschii* (up to 4.8%), both of which are indicator species for hypertrophic conditions (Bennion, 1994; Bennion et al., 2004; Kirilova et al., 2008). The fact that they only make up a minor component of the assemblage suggests that conditions were not fully hypertrophic, but that nutrient levels increased during this zone.

11.2.3. Phase 3: Catchment stability and oligotrophic/eutrophic lake conditions (+324 – +371±5 vyrs)

Phase 3 represents the final interval of the regressive pollen zone, from +324 to +371±5 years (48 vyr duration). The pollen, charcoal and sedimentary data indicate the continuation of landscape stability that characterised phase 3, with the continued decrease in *Poaceae* (7.1 to 3.9%) and increase in *Quercus* to a peak of 25.8%. *Corylus* remains low (between 9.5 and 20.6%), and *Betula* increases slightly 6.4 to 11.9%).

The characteristic feature of this zone is a switch from varve micro-facies indicative of increased levels of productivity to those indicative of lower levels of productivity (Fig. 11.1e). This shift is also coeval with the decline in varve thickness that occurs during the zone. The diatom assemblage is complex during this zone, with the disappearance of *S. hantzschii* and falling percentages of *C. tholiformis* (Fig. 11.1c) indicative of a drop in nutrient levels.

In a similar pattern to that seen during phase 1, *S. medius* declines and becomes more variable (fluctuating between 39 and 67%), but other taxa indicative of eutrophic conditions (*S. parvus* and *S. minutulus*) increase. Zone 3 is also characterised by the reappearance of the oligotrophic indicator *C. comensis*, as well as the appearance of *C. schumanni*. Both are present throughout the zone and *C. schumanni* provides further evidence for a switch to more nutrient poor conditions (Chen et al., 2008). Although the changes are complex, they do indicate a shift to lower nutrient levels. Given the sedimentological and palynological evidence, which both indicate continued

catchment stability during this zone, a reduction in nutrient input from the catchment may suggest that nutrient limitation might have become a factor in diatom growth.

11.2.4. Phase 4: Catchment stability and eutrophic lake conditions (+372 – +565±12 vyrs)

Phase 4 represents the final interval of the NAP Phase (+194±12 vyr duration), where *Corylus* percentages return to pre-NAP values (52.8%), *Poaceae* continues to decline (3.9 to 0.3%), as does *Quercus* (25.8 to 10.3%) and *Betula* (11.9 to 5.2%), while PARs remain consistently above 45 x 10^3 grains/g y^{-1}, suggesting the continuation of stable catchment conditions. During the first part of this interval, between +372 and +395±19 vyrs, the lake is characterised by a continuation of the relatively low nutrient levels that characterised zone 3. *C. comensis* remains present, but *C. schumanni* is replaced by *C. comta*, also commonly found in oligotrophic lakes (Brugam, 1983; Lotter, 1989), at +395±19 vyrs. The remainder of this zone (+395 to 565±10 vyrs) is characterised by a return to eutrophic conditions, with *C. schumanni* and *C. comta* replaced by *S. minutulus,* increasing percentages of *S. parvus* and a return to dominance of *S. medius* (Fig. 11.1c). The trend in nutrient conditions indicated by the shift in diatom flora is also reflected in the sedimentological data, with the varve micro-facies characteristics displaying a trend back towards varves with lamination types indicative of higher levels of lake productivity (Fig. 11.1e).

11.3. Forcing mechanism for the NAP Phase

11.3.1. Burning event or climatic event?

The discussion in section 11.2 has highlighted the landscape and limnological responses that occurred during the +565±12 vyr NAP Phase. The increase in percentage abundance of NAP at the expense of AP was caused by a burning event that triggered a series of productivity-driven changes in the aquatic environment, caused by nutrient influx from an unstable lake catchment. If the isotopic data is not considered, this interpretation is consistent with the conclusions of Turner (1970), although the spatial extent of the pollen event from the Midlands to East Anglia (Duigan, 1956; West, 1956; Kelly, 1964; Turner, 1970; Horton, 1974. 1989; Philips,

1976; Coxon, 1979, 1985) requires consideration. A climatic trigger for the event also needs to be considered (Kelly, 1964, Muller, 1974, Kukla, 2003), given the recent publication of isotopic data from borehole GG of Turner (1970) by Candy (2009) and Candy et al. (2014), as well as the multi-proxy reconstruction of the OHO at Dethlingen, Germany (Koutsodendris et al., 2012). Although both datasets provide evidence for isotopic oscillations during the pollen events, questions remain as to the significance of both oscillations in relation to long-term trends, and the fact that the $\delta^{18}O_{calcite}$ dataset from borehole GG displayed a high degree of covariance (R^2 = 0.77) with $\delta^{13}C$ (Candy, 2009; Candy et al., 2014). As highlighted in chapter 9, the $\delta^{18}O$ stratigraphy produced in this thesis therefore provides important evidence to the debate surrounding abrupt climatic events during full interglacial conditions during MIS 11.

The isotopic results presented in chapter 9 indicate that, unlike the results of Candy (2009), $\delta^{18}O$ values of carbonate samples taken from core MT-2010 do not co-vary with respect to $\delta^{13}C$ (R^2 = 0.38). The sampling strategies adopted in both studies were the same, so only calcite-rich summer lamination types should have been sampled. Although care was taken to isolate the summer calcite lamination type (LT-2) by Candy (2009), the section of borehole GG sampled was narrow and dried out, making it difficult to avoid contamination from the other two lamination types (I. Candy, pers. comm.). As a result, although the broad trend in the dataset of Candy (2009) picks out an isotopic oscillation in association with the NAP Phase, it is possible the signal may be contaminated. The need to take long-term trends in isotopic datasets into consideration, especially given the nature of high-resolution isotopic studies (Mangili et al., 2010b), has been addressed in this thesis, as the average background $\delta^{18}O$ value of -3.73‰ for MTIZ 2 (the value used to identify the isotopic events in chapters 9 and 11) is based on 129 samples taken over a ca. 3,300 year period (average sample resolution of ~25 years).

As discussed in chapter 9, variations in the oxygen isotope stratigraphy during the pre-temperate and early part of the early-temperate pollen zones (Ho I to Ho IIb) of the Hoxnian Interglacial (MIS 11) at Marks Tey could be driven by a number of factors, including temperature, seasonality of rainfall, method of lake recharge and changing

$\delta^{18}O$ of source water. The 5-point moving average plotted through the dataset reveals an interval of +183±6 vyrs, the start of which coincides with the onset of the NAP Phase, as shown by the percentage pollen diagram, where $\delta^{18}O$ values consistently plot below the background average for MTIZ 2, reaching lowest average values of -4.59‰ (0.86‰ lower than the average for MTIZ 2) for +183±6 vyrs. If it is assumed that authigenic carbonates in MTIZ 2 were precipitated under equilibrium conditions, and that the $\delta^{18}O$ value of lake water at Marks Tey was primarily a reflection of the $\delta^{18}O$ value of rainwater, which has a strong linear relationship with temperature at these latitudes, then the interval of low $\delta^{18}O$ values during the first +183±6 vyrs of the NAP Phase should represent a centennial-scale cooling event with a maximum temperature anomaly of approximately 2.5 – 2.9°C (based on the net effect of the temperature/precipitation relationship and temperature dependent fraction of mineral calcite formation, see section 9.5.1, chapter 9).

The oxygen isotope data therefore suggests that the onset of the NAP Phase occurred in association with an abrupt cooling event, as well as a burning event. The question then becomes which of these two events occurred first? It is clear from figure 11.2 and 11.3 that the start of the first peak in charcoal occurs in association with the onset of *Corylus* decline and the increase in *Poaceae,* in terms of their relative contribution to the pollen assemblage. It is, however, also evident from figure 11.2b that PARs were already declining at this point (102 x 10^3 grains/g y^{-1}), having reached a peak (125 x10^3 grains/g y^{-1}) at -24±9 vyrs, before the changes in pollen percentages occurred. The onset of declining PARs before the decline in percentage composition and, therefore, the first peak in charcoal input, indicates that climate may have had an effect on the temperate tree taxa prior to the burning event. Climatic deterioration can stress tree populations, leading to a reduction in pollen production as a consequence of unfavourable climatic conditions, although a reduction in pollen production may not necessarily lead to changes in the assemblage of species present within the landscape and, consequently, may not be seen in percentage pollen diagrams (Veski et al., 2004; Seppa et al., 2007). This stress, which can lead to the death and increased fatalities of individuals, can result in large amounts of dead wood on the landscape that would provide the necessary fuel for the ignition of wildfires (Van der Hammen, 1951, 1957; Edwards et al., 2000; Vander Hammen and Van Geel, 2008), which are usually initiated

by events such as lightning strikes (Pyne et al., 1996; Scott, 2010; Scott et al., 2014). Consequently, the following model is proposed to explain the events seen in the record of the NAP Phase at Marks Tey.

A series of cold events, as indicated by the isotopic record, occurred during Ho IIc. The last and most extreme of these, lasting for +183±6 vyrs, was not sufficient in itself to change the vegetation assemblage within the landscape, but placed stress on the ecosystem. It was this stress that lead to increased amounts of dead and dry wood lying on the landscape, which acted as fuel for one or more wildfires. It is this wildfire, the conditions for which were generated by the cold event, which caused the expression of the event in the pollen record. Based on the timing of events, it is therefore suggested that the NAP Phase at Marks Tey is the expression of a wildfire event caused by the ignition of dead wood on the landscape, which accumulated as a result of unfavourable climatic conditions caused by the climatic deterioration.

11.3.2. Multiple cooling events during early MIS 11?

The oxygen isotope, pollen, charcoal and chronological data indicate that the NAP Phase at Marks Tey is a climatically triggered wildfire event. The abrupt oscillation that occurs in association with the NAP Phase is not, however, the only isotopic oscillation that occurs during the early-temperate phase of MIS 11, but rather the fifth and final event of a more complex series of potentially cold/warm oscillations that occur during the -1,016±6 vyrs that precede the NAP Phase. Although the isotopic data in MTIZ 2 has a high degree of scatter, it is suggested that these events occurred because; 1) the 5-point moving average for these events is greater than 1σ of MTIZ 2, and 2) the 5-point moving average in MTIZ 1 and in the post-NAP Phase zone show no such excursions.

The two oscillations that immediately precede the oscillation associated with the NAP Phase (isotopic oscillation 3: -412 to -284+6 vyrs and oscillation 4: -191 to -81±6 vyrs) have durations of 128±6 vyrs and 110±6 vyrs, respectively, and are both significant at 1σ. Although the current resolution of the pollen diagram from -1,016 to 0±6 vyrs is relatively low (14 samples), drops in PAR do appear to coincide with these isotopic oscillations, in particular oscillation 4, where PAR's decrease to similar levels to those

seen during the NAP Phase (23 x 10^3 grains/g y^{-1}) at -196±12 vyrs. Furthermore, the µ-XRF element intensities for K and Ti display elevated values during this period. These elements are biologically immobile, and are often considered a proxy for in washing of detrital clastic material from the lake catchment (Arnaud et al., 2012; Neugebauer et al., 2012; Czymzik et al., 2013; Schlolaut et al., 2014), which may result from climatic cooling.

The other two oscillations that occur during Ho II c (oscillation 1: -1,016 to -796±6 vyrs and -678 to -560±6 vyrs) are more difficult to interpret, as neither is significant at 1σ. There is no diatom data for comparison in this section of the sequence, but PARs may respond to oscillation 1 (33 x 10^3 grains/g y^{-1}) at -972±14 vyrs. Interestingly, the µ-XRF element intensities for K and Ti increase in association with oscillation 2 (from 0.06 to 0.07 Ti/kcps and 0.13 to 0.16 K/kcps) at -675±5 vyrs (Fig. 11.1g). Elevated levels of in-washed detrital material have been used as a proxy for the onset of climatic deterioration (e.g. Hede et al., 2012). Despite this increase, there does not appear to be a response in the other varve micro-facies data. Although the increase observed in element intensities does not translate into visible changes in varve structure, it may relate to fine-grained detrital material distributed within the lamination types (Neugebauer et al., 2012). The shifts in these elements are relatively small, however, and further isotopic analysis in this section of the sequence to increase the sampling resolution is required before any further interpretations can be made.

11.4. Comparison of the NAP Phase with the OHO

The development of an annually-resolved model for the NAP Phase at Marks Tey allows for comparisons to be made with similar events that occurred during early MIS 11. The Older Holsteinian Oscillation (OHO) (Koutsodendris et al., 2012) provides the most suitable event to compare the NAP Phase with, given the generally accepted correlation of both the Hoxnian and Holsteinian interglacials with MIS 11 (e.g. Shackleton and Turner, 1968; Sarnthein et al., 1986; Nitychoruk et al., 2006; see Candy et al., 2014 for review). Furthermore, the OHO and NAP Phase occur at broadly similar positions in the pollen stratigraphy of their respective interglacials and, therefore, may represent responses to the same forcing mechanism (Koutsodendris et al., 2012).

Although the pattern of vegetation response during the NAP Phase, which is characterised by an increase in grassland at the expense of deciduous woodland taxa (West, 1956; Kelly, 1964; Turner, 1970), differs from that in continental Europe, where pine woodland expands at the expense of deciduous woodland (Nitychoruk et al., 2005; Koutsodendris et al., 2011; 2012; Candy et al., 2014), the two events have been correlated, with the implication being that both responses are caused by the same climatic deterioration (Koutsodendris et al., 2012).

Table 11.1. *Comparison between characteristics the OHO and NAP Phase. Table redrawn and modified from Koutsodendris et al. (2012). Sea level data derived from Rohling et al. (2010).*

Criterion	**OHO (~408 ±0.5 ka)**	**NAP Phase**
Timing after establishment of temperate forest	3100 ± 500 yrs	~2890 yrs
Sea level below present	~15-20 or ~40m	~15-20 or ~40m
Duration of climate regression	90 yrs	~183 yrs
Duration of vegetation event	220 yrs	565±12 yrs
Climate pattern in Europe	N Europe: cold and increasingly drier towards East Mountainous C. Europe: possibly wetter	?

Table 11.1 summarises the main characteristics of the OHO at Dethlingen, Germany, as presented by Koutsodendris et al. (2012), and a comparison with comparable characteristics from the NAP Phase determined in the current study. The table shows some agreement between the two events, but also some distinctive differences. Based on estimated sedimentation rates for pollen zones Ho II a,b and the first 10 cm of IIc, the NAP Phase at Marks Tey occurs approximately 2890 years after the establishment of temperate forest in MIS 11, which agrees (within error) with the onset of the OHO (Table 11.1). If it is assumed that the development of temperate forest in the British Isles and continental Europe during MIS 11 is synchronous, then the events occur in identical stratigraphic positions. The question of the absolute timing of the event during the interglacial, however, cannot currently be addressed. As discussed in chapter 2, Koutsodendris et al. (2012) align forest expansion during the Holsteinian and, therefore, the OHO (and NAP Phase) with the second insolation peak that occurs during MIS 11, giving an age of ~408±0.5 ka. This suggests the existence of a lag between the onset of marine and terrestrial interglacials (Tzedakis et al., 2004; Skinner

and Shackleton, 2006), which has major implications for landscape development in the British Isles during the first part of MIS 11. It is not possible in the current study, however, to discuss the absolute timing of this event, however, it is possible to compare the duration and the palaeoenvironmental and sedimentological characteristics of both events.

When considering the duration of both the vegetation and the climatic events at Marks Tey and Dethlingen, important discrepancies are seen. Before the varve counts undertaken in this thesis, the duration of the NAP Phase at Marks Tey was stated as lasting for no longer than ~350 years (Turner, 1970). The varve counts in the current study have demonstrated that the NAP Phase at Marks Tey lasted for +565±12 vyrs, more than 200 years longer than estimated by Turner (1970) (Table 11.1). The difference between the varve counts undertaken in this thesis and those of Turner (1970) are intriguing, given that the depth interval over which the changes in vegetation assemblage are identified are almost identical in both core MT-2010 (63cm) and borehole GG (61cm) (Turner, 1970). Furthermore, Turner (1970) refers to the ~350 year duration in terms of the length of time it took *"from the destruction of the forest to its recovery"* (Turner, 1970 p. 428), therefore suggesting it has been defined in the same way. There are, however, possible reasons for the difference: 1) pollen analysis in the current study was undertaken at a higher resolution, so despite the similar depth intervals, the precise definition of the onset/termination of the event has been defined more clearly in this study, 2) Turner (1970) notes that the duration of the NAP Phase is an approximation, based on counted varves and estimated sedimentation rates, as the coring method used tended to distort and expand the sediment extracted, which may also account for the underestimation, and 3) in this thesis, the duration of the NAP Phase has been quantified by micro-facies analysis and varve counts of sediment thin sections, rather than macro-scale counts and estimates.

This definition in structure enables the NAP Phase to be directly compared to the OHO. When the NAP Phase and OHO are compared, it is apparent that the NAP Phase lasts for more than double the length of time of the OHO (Koutsodendris et al., 2012). The apparent reason for this difference in pollen response is revealed when comparing the duration of the regression and recovery zones. The OHO is characterised by a pollen

regressive zone of 90 years, and a recovery zone lasting 130 years (Koutsodendris et al., 2012). In contrast, the NAP Phase at Marks Tey has a regressive zone lasting 371±15 vyrs, followed by a recovery zone of 194±19 yrs (see section 11.2). It would appear, therefore, that the extended duration of the regressive zone at Marks Tey accounts for the major discrepancy between the two events (~281 years). It should be noted that, in this study, *Corylus* has been used to define the NAP Phase, to allow direct correlation with the work of Turner (1970). However, Koutsodendris et al. (2012) used total % temperate tree pollen to define the OHO and not just *Corylus* variations. This is partly because pattern of vegetation response is different between the OHO and the NAP Phase, i.e. the expansion of *Pinus* in the OHO compared to *Poaceae* in the NAP Phase. If the approach of Koutsodendris et al. (2012) is applied, the relative duration of the regressive and recovery zones would change in the NAP Phase, however, the duration would be unchanged and, therefore, remain ca 300 years longer than the OHO at Dethlingen. The critical point to make here is that, despite the slight difference in methodology, both methods result in the same duration for the NAP Phase (565±12 vyrs). The extended duration of the NAP Phase is therefore likely to be a function of the burning event, which appears to be a characteristic feature at a number of sites across the UK (West, 1956; Turner, 1970), but seemingly absent from continental European archives, although charcoal analysis is not a technique that is routinely applied. Although no charcoal analysis was undertaken at Dethlingen, detailed micro-facies analysis (thickness and μ-XRF measurements) of the varved sequence suggests that the lake catchment remained stable during the OHO (Koutsodendris et al., 2011), which may indicate that fire was not a contributing factor to the changes in vegetation assemblage observed.

The other discrepancy between the two events is the duration of the climatic regression associated with the pollen events. Much like the discrepancy associated with the duration of the pollen events, the climatic oscillation as recorded by $\delta^{18}O_{calcite}$ at Marks Tey lasts for 183±6 vyrs, double that of the oscillation at Dethlingen (90 years), as recorded by $\delta^{18}O_{silica}$ (Table. 11.1). This large difference in duration raises questions as to the correlation of the two events. Another important difference is that the $\delta^{18}O_{calcite}$ record from Marks Tey covers a much longer time period than the $\delta^{18}O_{silica}$ record at Dethlingen, revealing a number of isotopic oscillations that

potentially represent multiple abrupt climatic events during early MIS 11, rather than just a single event.

An important conclusion can be drawn from comparing the NAP Phase at Marks Tey with the OHO at Dethlingen. The first relates to the use of pollen as a proxy for abrupt climatic events. Although such a practice may be suitable in some instances (e.g. Tinner and Lotter, 2001; Veski et al., 2004; Seppa et al., 2007), the assumption is made that shifts in pollen assemblages are caused by, and are synchronous with, the climatic event. This is not possible for the NAP Phase at Marks Tey because although the underlying cause is climatic, the expression and duration of the event in the sequence (and the subsequent landscape and limnoloigcal changes that occur) is the result of a burning event.

11.5. Comparison of the NAP Phase with the 8.2 ka event

There is now clear evidence for abrupt climatic events that punctuate relatively stable climatic conditions during the early part of the current interglacial (Alley and Ágústdóttir, 2005; Rohling and Palike; 2005; Fleitmann et al., 2008; Daley et al., 2011; Morrill et al., 2013). A key research question for this study is whether or not such events are common in pre-Holocene interglacials (Tzedakis et al., 2009). It has been argued that the OHO/NAP Phase provides evidence for such events, and may be analogous to the 8.2 ka event. This suggestion is based on its relative position within the pollen stratigraphy of the interglacial, the pattern of vegetation/climatic response, and the forcing mechanism (Koutsodendris et al., 2012). In light of the isotopic data generated in this thesis, which suggests the occurrence of one or more abrupt cooling events during MIS 11, this section of the discussion will focus on whether these events (the last of which is associated with the NAP Phase), like the OHO, can be considered analogous to the abrupt climatic changes that occurred during the early Holocene.

11.5.1. Relative position within the pollen stratigraphy

Due to the absence of isochronous markers linking the Marks Tey sequence to the Marine record, as well as issues that arise when dating sediments from this time period (e.g. Rowe et al., 1999; Kamer and Marra, 2003; Geyh and Muller, 2005, 2006;

Scourse, 2006), it is currently only possible to provide a discussion about the relative timing of the NAP Phase in the interglacial in terms of where it occurs within the pollen stratigraphy.

Table 11.2. *Comparison between characteristics the OHO and 8.2 ka event as presented by Koutsodendris et al. (2012), with those of the NAP Phase at Marks Tey and the expression of the 8.2 ka event in the British Isles and Ireland. Table redrawn and modified from Koutsodendris et al. (2012).*

Criterion	**8.2ka event (Continent)**	**OHO (~408 ±0.5 ka)**	**NAP Phase**	**8.2ka event (GB & I)**
Timing after establishment of temperate forest	~3500 yrs[a,b]	3100 ± 500 yrs	~2978 yrs	~2800 yrs[l]
Sea level below present	~15-20m[c]	~15-20 or ~40m[c]	~15-20 or ~40m[c,m]	~15-20m[c]
Duration of climate regression	~80 yrs[d] (160.5 yrs[i])	90 yrs	~183 yrs	~150 yrs[j]
Duration of vegetation event	~300 yrs[e,f]	220 yrs	565±12 yrs	~300 yrs[k]
Climate pattern in Europe	N. Europe: cold and dry Mountainous C. Europe: cold and wet[g,h]	N Europe: cold and increasingly drier towards East Mountainous C. Europe: possibly wetter	?	Cold and dry[h]

[a]Litt et al. (2001); [b]Lowe et al. (2008); [c]Rohling et al. (2010); [d]Kobashi et al. (2007); [e]Tinner and Lotter (2001); [f]Veski et al. (2004); [g]Magny et al. (2003); [h]Wiersma and Renssen (2006); [i]Thomas et al. (2007); [j]Marshall et al. (2007); [k]Ghilardi and O'Connell (2013); [l]I. Matthews, unpublished data; [m]Koutsodendris et al. (2012).

Table 11.2 provides information on how this was achieved for the 8.2 ka event and OHO (Koutsodendris et al., 2012), as well as for the NAP Phase at Marks Tey and the expression of the 8.2 ka event in the British Isles and Ireland (also see Fig. 11.5). It has already been noted in section 11.3 that the NAP and OHO seem to occur in similar stratigraphic conditions. Koutsodendris et al. (2012) determined the length of time that elapsed between the establishment of temperate forest and the onset of the abrupt event for both the OHO and 8.2.ka event. By their reasoning, the 8.2 ka event occurred ~3,500 years after the establishment of temperate forest in the Holocene, whereas the OHO occurred 3,100±500 years after the establishment of temperate forest during the Holsteinian (Table 11.2). If the same method is applied to the NAP Phase, it occurred ~2,890 years after the onset of Hoxnian temperate forest (Ho II), in agreement with the OHO, but approximately 500 years earlier than the 8.2 ka event (Table 11.2). However, when the timing of the NAP Phase at Marks Tey is compared to the 8.2 ka event in Hockham Mere, a Holocene record from the same region (Bennett, 1983; I. Matthews, unpublished data), the records are in relatively close agreement.

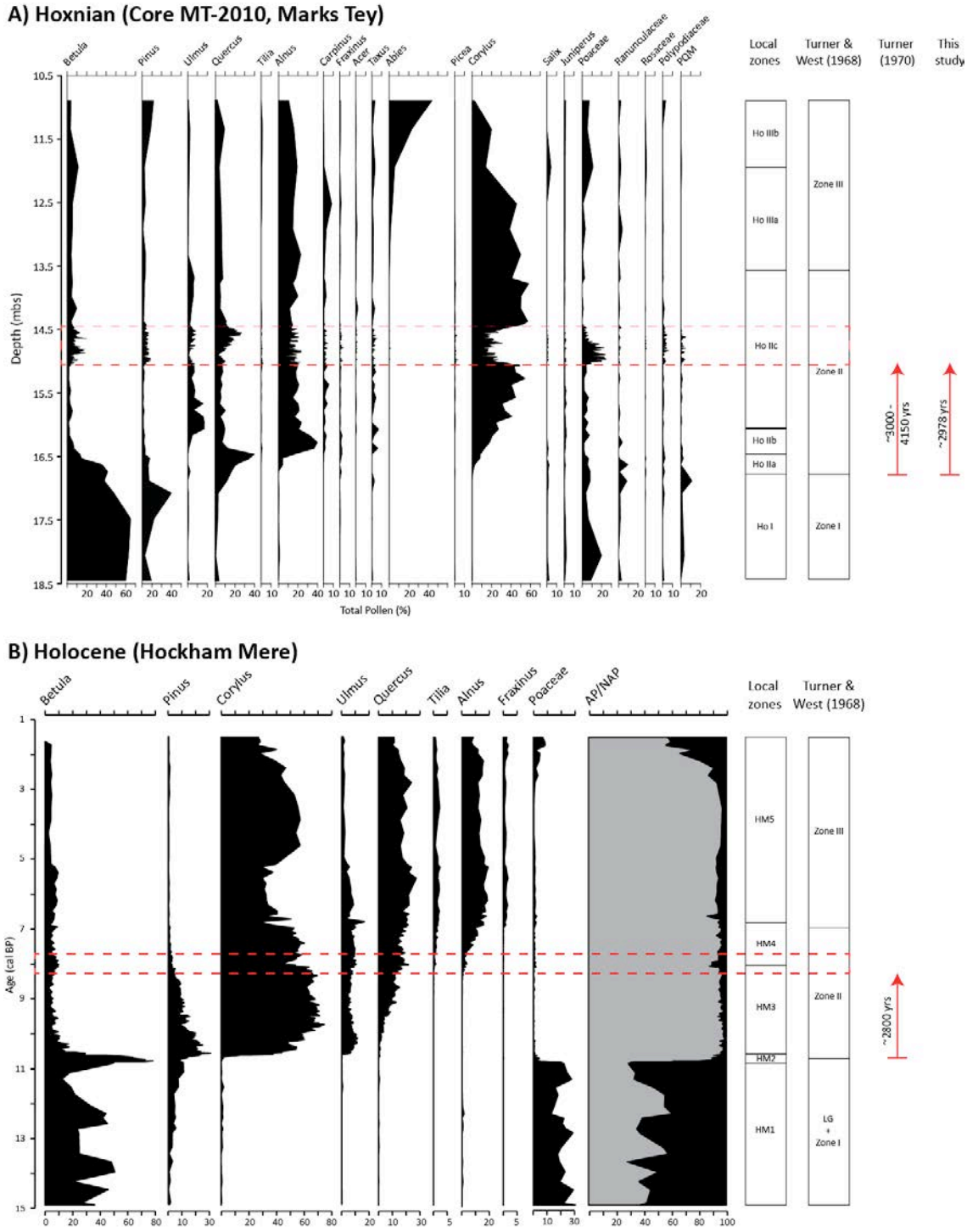

Figure 11.5. *Comparison of the Location of the NAP Phase in the Hoxnian pollen sequence from core MT-2010, with the location of the 8.2 ka event in the Holocene pollen record from Hockham Mere (data from Bennett, 1983, chronology produced by Ian Matthews). A) The timing of the NAP Phase after the onset of Ho II is based on the estimated sedimentation rates of Turner (1970), as well as the varve chronology (counted and interpolated varves) produced in this thesis. B) Timing of the 8.2 ka event in Hockham Mere.*

The re-calibrated radiocarbon dataset in figure 11.2 shows possible evidence for the 8.2 ka event at Hockham Mere, where *Corylus* percentages decline by 20% (~65 to 45%) and recover over a ~350 year period (I. Matthews, unpublished). No charcoal has been noted in the sequence (Bennett, 1983), but given the findings at Marks Tey, this clearly needs to be reinvestigated. It should be noted that the timing of the NAP Phase in relation to the onset of Ho II at Marks Tey is only an estimate, as Ho IIa and a large part of Ho IIb are not varved. The figure of 2,978 is made up of 1,150 counted varves and 1,828 interpolated years so is, therefore, tentative (Table 11.2). Despite this, there is clearly good consistency between the timing of both the NAP Phase and the 8.2 ka event relative to vegetation development in their respective interglacials.

11.5.2. Vegetation response

When comparing the vegetation responses between the OHO and 8.2 ka event, Koutsodendris et al. (2012) found reasonable agreement. Central European vegetation records indicated that the pollen regression associated with the 8.2 ka event lasted for approximately 300 years (Tinner and Lotter, 2001; Veski et al., 2004), comparable to the 220 years that the pollen regression lasted for during the OHO (Table 11.1). The difficulty in comparing the vegetation response during the NAP to that of the 8.2 ka event is the influence that the wildfire has over the structure and duration of the pollen event. It is also difficult to determine the impact, if any, that fire had on the landscape during the 8.2 ka event. Although the electrical conductivity series for the GISP2 ice core, which determines ammonia levels (a by-product of biomass burning) (Taylor et al., 1996), indicates that fire-frequency increased by 90% during the 8.2 ka event (Alley et al., 1997; Alley and Ágústdóttir, 2005), the source areas for this burning are speculative, encompassing North America, Europe and northern Asia (Taylor et al., 1996).

Few examples exist from northwest Europe of the occurrence of burning events that occur in association with the 8.2 ka event (e.g. Edwards et al., 2007; Ghilardi and O'Connell, 2013), but it is important to note that humans were also actively modifying the landscape during the early Holocene (e.g. Turney et al., 2006). One example is the radiocarbon dated lacustrine record from Cooney Lough, western Ireland, which contains evidence for a regression in the pollen assemblage during the 8.2 ka event, as

well as the presence of a peak in micro-charcoal (Ghilardi and O'Connell, 2013). Despite the similar nature of vegetation response to that of the NAP Phase (decrease in *Corylus* and increase in *Poaceae, Betula* and *Pinus*), the pollen event only lasted for ~300 years (Ghilardi and O'Connell, 2013), although the chronological uncertainty associated with the radiocarbon dates above and below this section of the sequence indicate that it could have a duration comparable to the NAP Phase. Furthermore, the charcoal was not considered to represent a local signal, as lake sedimentation processes were unaffected (Ghilardi and O'Connell, 2013). Another lacustrine sequence covering the early Holocene from the Isle of Mull, Scotland, provides evidence of a ca 560 year pollen regression associated with peaks in charcoal centred on 8,250 cal. yr BP (Fig. 11.6) (Edwards et al., 2007). There is remarkable similarity with the NAP Phase, not only between the taxa response, but also the duration of the pollen event. Independent chironomid temperature estimates suggest, however, that the burning and climatic events are not related, and that forest clearance during the Mesolithic is more likely (Edwards et al., 2007). This study potentially highlights the issue with studying such events in the Holocene, due to the impact of humans on the landscape, although it is worth noting that chironomids record summer temperatures (e.g. Brooks and Birks, 2001). If most of the temperature change during the 8.2 ka event occurred during the winter (see Denton et al., 2005; Rohling et al., 2005; Morrill et al., 2013, for example), then the signal may not be apparent in the chironomid assemblage.

A further complication associated with comparing vegetation responses to abrupt climatic events is that the vegetation does not always appear to respond. Pollen records from Holzmaar and Meerfelder Maar, for example, although both located in the Eifel region of western Germany, indicate different responses to the 8.2 ka event (Litt et al., 2009). Based on pollen-temperature reconstructions, Litt et al. (2009) found that the 8.2 ka event was not pronounced in Holzmaar. Varve micro-facies changes, however, indicated by the cessation of calcite precipitation (cooler summers) and the reduced in washing of clays from the catchment (drier winters), appear to show the event quite clearly (Prasad et al., 2006, 2009). Furthermore, the event was not detected in either the temperature reconstructions or the pollen diagram from Meerfelder Maar (Litt et al., 2009).

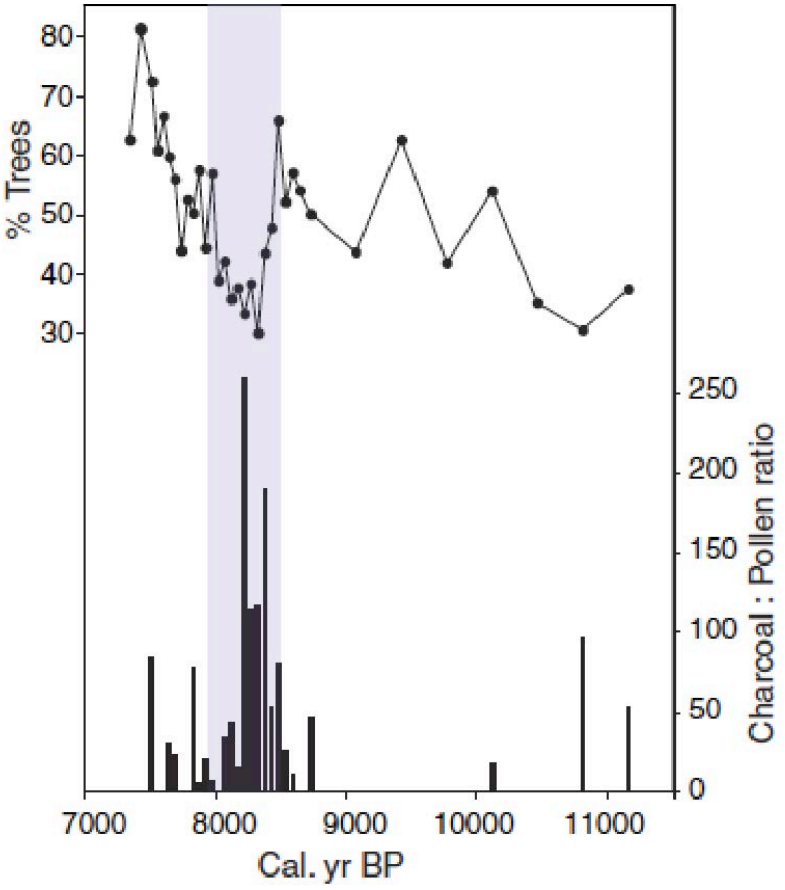

Figure 11.6. *Summary of changes in percentage tree pollen and micro-charcoal during the early Holocene at Loch an t'Suidhe, Isle of Mull, Scotland. The duration of the pollen event (ca. 560 years) is highlighted by the blue shaded area. Modified from Edwards et al. (2007).*

A similar example for the British Isles comes from Hawes Water, northern England, which provides a very detailed record of early Holocene climatic variability (Marshall et al., 2007; Lang et al., 2010; Jones et al., 2011). The $\delta^{18}O_{calcite}$ and chironomid temperature reconstructions for the sequence both show the presence of abrupt climatic events punctuating the early Holocene (Marshall et al., 2007; Lang et al., 2010), but the event does not appear to have had an impact on the forest structure (Jones et al., 2011). It should be noted, however that the pollen records for both of these studies represent changes in percentage composition and not pollen concentration/accumulation rates, which may be required to reveal possible impacts of unfavourable climates on pollen production. Due to the complications in pollen response during the NAP Phase and a lack of suitable modern analogues, comparing the two based on the isotopic response is considered more appropriate in this thesis.

11.5.3. Climatic response

If the assumption that 1) the modern relationship between local air temperature and the $\delta^{18}O$ value of precipitation in the temperate mid-latitudes can be applied to lacustrine carbonates from Marks Tey, and 2) this $\delta^{18}O$ value is not significantly modified during lake water recharge/residence or calcite precipitation, then $\delta^{18}O_{calcite}$ should provide a qualitative proxy for temperature changes. If this is the case, the magnitude of isotopic shifts that occur during the oscillations seen in the Marks Tey record can be compared to temperature anomalies for the 8.2 ka event. There are now a number of $\delta^{18}O$ stratigraphies from lacustrine sequences across Europe that record environmental conditions during the 8.2 ka event, with suggested event durations of between 150 to 200 years and maximum isotopic anomalies of between 0.4 to 1.1‰ (Table 11.3) (see Daley et al., 2011 for a review). The best example in the British Isles for comparing the isotopic events at Marks Tey to the 8.2 ka event is from Hawes Water in Lancashire (Fig. 11.6) (Marshall et al., 2002; 2007).

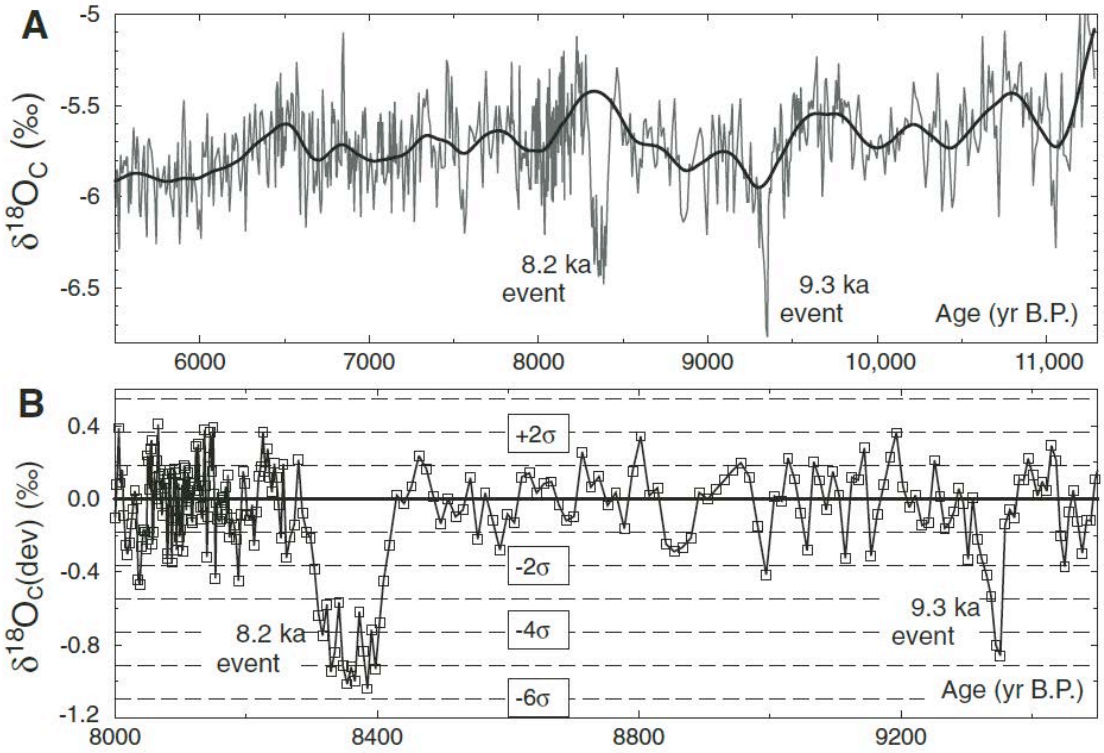

Figure 11.7. *The early Holocene $\delta^{18}O$ record from Hawes Water, Northwest England. A) Raw dataset fitted with a smoothing spline to illustrate the moving average, calculated by omitting data points from the abrupt events. B) The data plotted as deviation in $\delta^{18}O$ away from the spline. By using this method, the 8.2 and 9.3 ka events are clearly expressed, and to a lesser degree, a number of other oscillations. Taken from Marshall et al. (2007).*

Although the proximity of Hawes Water makes it a useful Holocene comparison for the isotopic oscillations at Marks Tey, it is important to note that, unlike Marks Tey, the sequence at Hawes Water is comprised of homogeneous marl and is not varved (Marshall et al., 2002; 2007). Consequently, the $\delta^{18}O$ signal derived from bulk carbonate samples, whilst containing significant noise (Fig. 11.6), does not contain the same degree of scatter that is observed in MTIZ-2 (varved section of core MT-2010) of the Marks Tey record. When the characteristics of oscillation 5 (associated with the NAP Phase) at Marks Tey are compared to those associated with the 8.2 ka event at Hawes Water, the events appear comparable in terms of duration and magnitude. The 8.2 ka event is expressed in the Hawes Water record as a ~150 year shift away from the moving average of the dataset, with a maximum isotopic anomaly of 1.1‰ (Fig. 11.6, Table 11.3), which equates to the 8.2 ka event being 33 years shorter and a maximum isotopic shift 0.24‰ greater than oscillation 5 at Marks Tey (Table 11.3). The events are therefore comparable in terms of their duration and magnitude, which may be indicative of a similar forcing mechanism (i.e. a temperature decline of similar magnitude and duration).

Table 11.3. *Summary data for isotopic characteristics from the 8.2 ka event at selected lacustrine sequences in Northern Europe, compared with data for the isotopic oscillations at Marks Tey. Modified from Daley et al. (2011).*

Site	Duration of event (years)	Maximum magnitude of isotopic anomaly (‰)	Proxy
Lake Rouge	200	0.4	$\delta^{18}O_{calcite}$
Hawes Water	150	1.1	$\delta^{18}O_{calcite}$
Lough Avolla	150	0.8	$\delta^{18}O_{calcite}$
Ammersee	160	1.0	$\delta^{18}O_{p}$ (ostracod)
Marks Tey			$\delta^{18}O_{calcite}$
Oscillation 1	219	0.55	
Oscillation 2	117	0.1	
Oscillation 3	128	0.62	
Oscillation 4	109	0.82	
Oscillation 5	183	0.86	

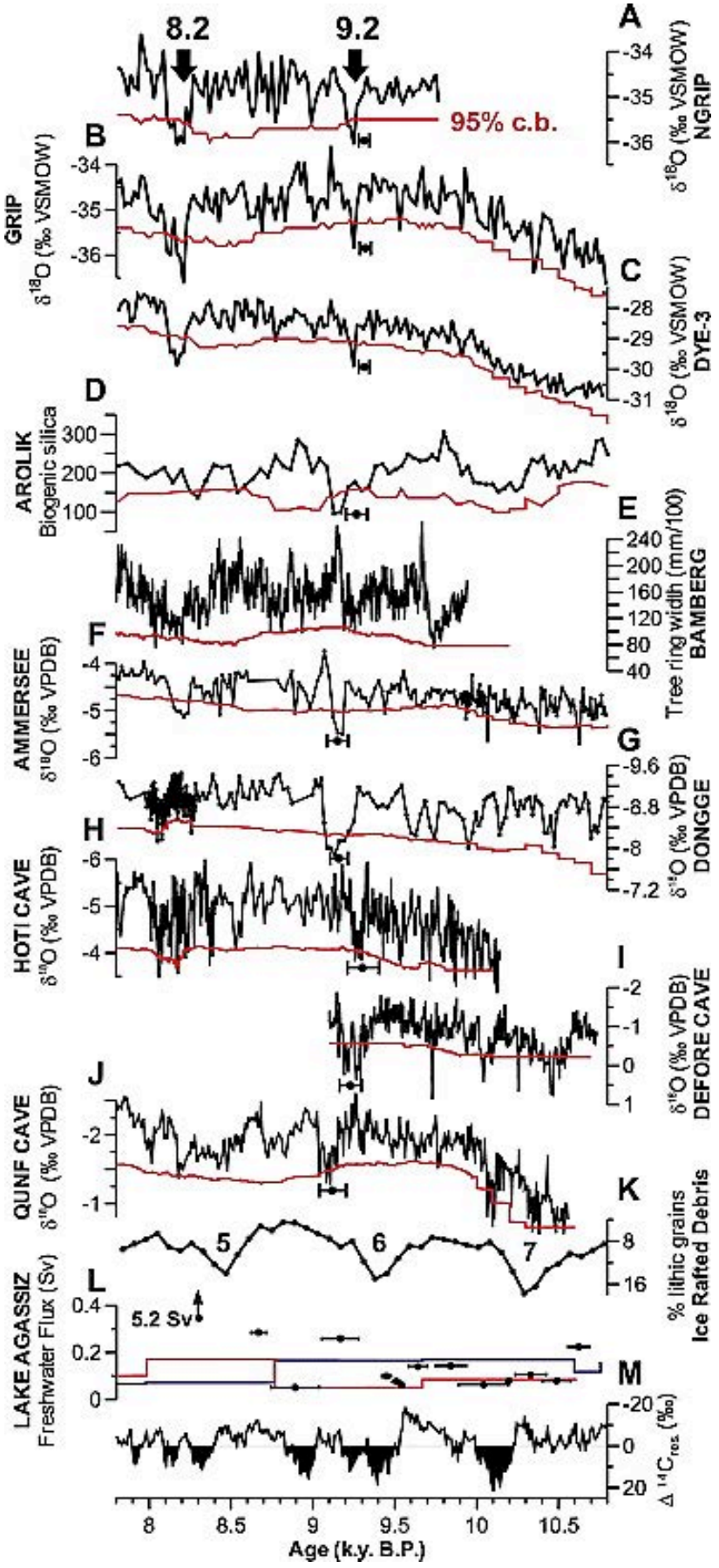

Figure 11.8. *Comparison of a number of early Holocene climate proxy records (see paper for record sources) that show evidence for the 9.2 and 8.2 ka events. The red lines mark 95% confidence bands (c.b). Figure taken from Fleitmann et al. (2008).*

The second observation that can be made about the Hawes Water $\delta^{18}O$ record is that the 8.2ka event is just one of a number of isotopic oscillations, and therefore abrupt cooling events, that occur during the early Holocene at the site (Marshall et al., 2007). As well as the 8.2 ka event, the 9.3 ka event is also expressed, as are other shorter-lived $\delta^{18}O$ oscillations that are not named. Furthermore, these events are not unique to the Hawes Water record, as the presence of multiple short-lived cooling events during this interval has also been noted in numerous other records (e.g. Rasmussen et al., 2007; Fleitmann et al., 2008), in which a number of statistically significant oscillations are apparent (Fig.11.7). The 8.2 ka event is not, therefore, an isolated cooling event, but rather one of a number of early Holocene abrupt shifts that occur during the ~1,000 year interval between the 9.3 and 8.2 ka events, a situation comparable to that seen in Ho IIc at Marks Tey.

11.5.4. Forcing mechanism

Much of the debate in the literature surrounding the NAP Phase and OHO relates to whether they represent a climatic event (Kelly, 1964; Koutsodendris et al., 2012), a regional wildfire (Turner, 1970), or are the result of volcanic activity (Diehl and Sirocko, 2007). The data presented in this thesis suggests that the underlying cause of the NAP Phase at Marks Tey, like the OHO in continental Europe (Koutsodendris et al., 2012), is climatic, but that the climatic event at Marks Tey (and other sites across eastern England and the Midlands) triggered a wildfire.

As the discussion in the previous sections highlights, there are similarities between the climatic events that occurred during the early Holocene and those that characterise Ho IIc of early MIS 11. This similarity in terms of timing, duration and magnitude of the isotopic oscillations would therefore suggest that similar forcing mechanisms might be in operation. This point was discussed by Koutsodendris et al. (2012) who suggested that, like the 8.2 ka event, the OHO/NAP Phase could be attributed to freshwater input into the North Atlantic, disrupting the AMOC and therefore reducing heat transport to the mid- to high-latitudes (Barber et al., 1999; Clark et al., 2001; Clarke et al., 2004). The similarity between the isotopic record from Marks Tey and those from early Holocene sequences therefore adds further evidence in support of such a mechanism. There is general agreement that outburst floods from ice-dammed lakes, which

formed at the margin of the decaying Laurentide ice sheet, forced the 8.2 and 9.3 ka events (e.g. Alley et al., 1997; Barber et al., 1999; Alley and Ágústdóttir, 2005, Fleitmann et al., 2008), but the possible presence of multiple climatic oscillations during the early Holocene/Ho IIc also needs to be explained. While the 8.2 and 9.3 ka events have received the greatest attention in the literature (Alley and Ágústdóttir, 2005, Rohling and Palike, 2005; Fleitmann et al., 2008; Daley et al., 2011), there is also evidence for a number of other flooding events from Lake Agassiz during the early part of the Holocene (Teller and Leverington, 2004). Based on isostatic rebound data and radiocarbon dated fossil shorelines, Teller and Leverington (2004) suggest that up to 15 flooding events from lake Agassiz occurred between the Pre-Boreal Oscillation (PBO) and 8.2 ka event, with evidence for three events occurring between the 9.3 and 8.2 ka event (Fig. 11.9).

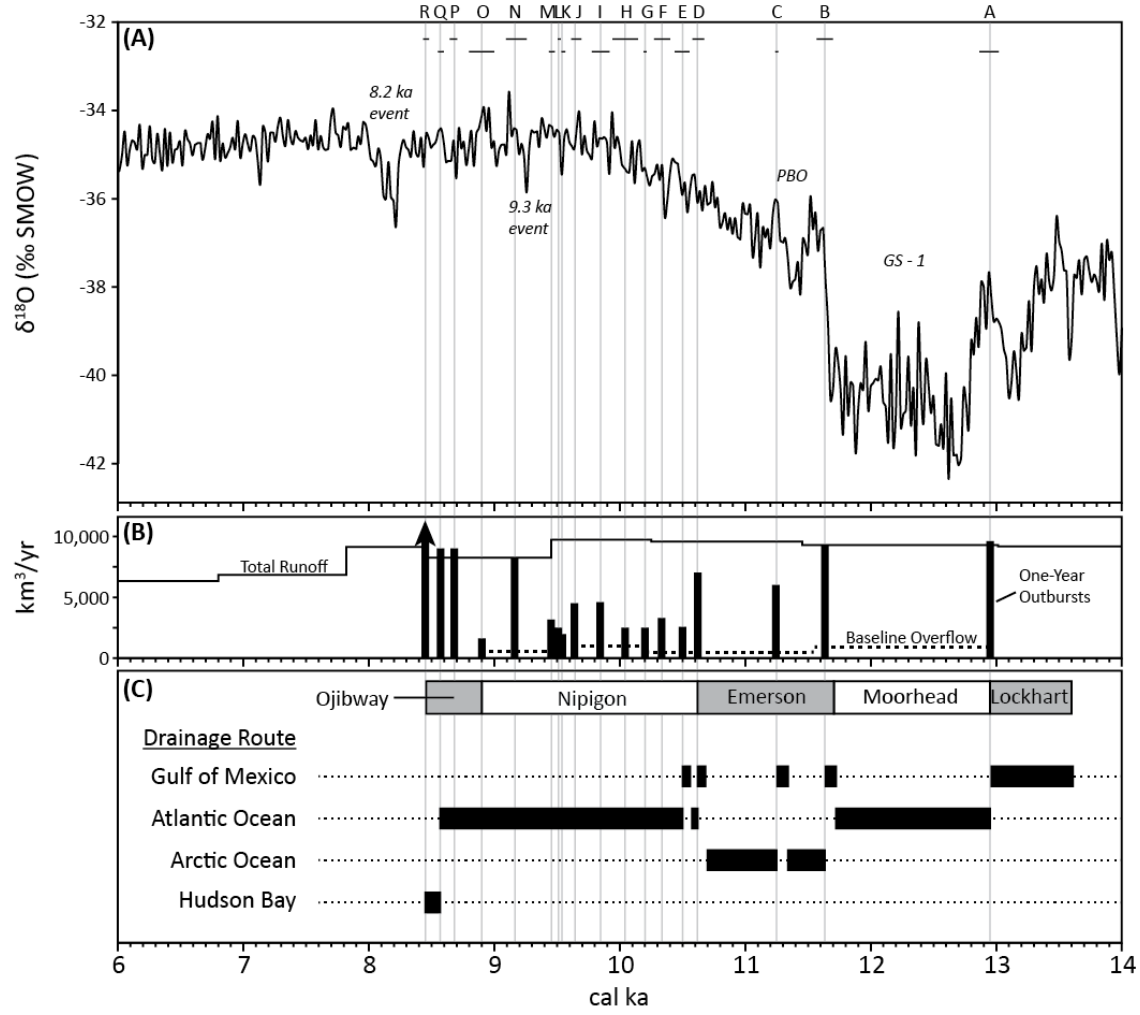

Figure 11.9. *A) The GRIP $\delta^{18}O$ record, plotted using the GIC05 age model (Rasmussen et al., 2006; Vinther et al., 2006) plotted with the outburst flood events from Lake Agassiz reconstructed by Teller and Leverington (2004) (vertical grey lines labelled A-R). B) Outburst floods from Lake Agassiz, with the height of each bar representing total volume of the outburst. C) Various lake outlets where water drained and the route it took to the ocean. Redrawn and modified from Teller and Leverington (2004).*

While the flooding associated with these events was not on the same scale as the outburst flood for the 8.2 ka event, and it is difficult to link these events to isotopic excursions in the Greenland ice cores (Teller and Leverington, 2004), the potential is there for the forcing of multiple events during the early stages of an interglacial. The 8.2 ka event occurs early in the Holocene, in association with numerous other comparable events, and that the key mechanism is suggested to be meltwater releases into the north Atlantic (e.g. Barber et al., 1999; Clarke et al., 2001; Clarke et al., 2004; Teller and Leverington, 2004; Hillaire-Marcel et al., 2007). The discussion in this chapter has highlighted similarities between the cooling associated with the NAP Phase and the 8.2 ka event in terms of: 1) their relative timing in relation to interglacial vegetation development, 2) the potentially similar impact on the landscape, 3) the duration and magnitude of isotopic response in lacustrine isotopic records, and 4) the fact that they both occur as the last event in a series of abrupt isotopic oscillations during the early part of an interglacial. Due to the number of similarities between the two events, there is good reason to believe that the cooling event associated with the NAP Phase is also driven by oceanic forcing.

This is further supported by the fact that: 1) MIS 11 is considered to be a suitable climatic analogue for the Holocene (e.g. Loutre and Berger, 2000, 2003), and 2) marine and terrestrial evidence indicates that MIS 12 was one of the most extensive glaciations of the last 1 million years (e.g. Shackleton, 1987; Perin et al., 1979; Clark et al., 2004; Lisiecki and Raymo, 2005). MIS 12 is characterised by high benthic $\delta^{18}O$ values in marine records (e.g. Shackleton, 1987; Lisiecki and Raymo, 2005) and some of the most extensive terrestrial ice limits of the last 500,000 years (e.g. Perin et al., 1979; Clark et al., 2004), which suggest a period of high global ice volume. Furthermore, the shift in benthic $\delta^{18}O$ values that occurs between the preceding glacial maximum and peak interglacial conditions represents one of the largest $\delta^{18}O$ shifts that occur during the last 800,000 years (Droxler et al., 2003). This evidence, combined with peak insolation values that occur during the second half of the interglacial, produces a glacial-interglacial transition (Termination V) that is longer and more extreme than any other of the past 450,000 years (Imbrie et al., 1984; Lisiecki and Raymo, 2005; Kandiano and Bauch, 2007). Assuming, therefore, that meltwater inputs into the north

Atlantic from glacial lake Agassiz were the primary trigger for abrupt climatic events during the early Holocene (Barber et al., 1999; Clark et al., 2001; Clarke et al., 2004; Teller and Leverington, 2004), it is possible that the extreme deglaciation that occured during Termination V may also have had the potential to produce similar events to those that occurred during the early Holocene.

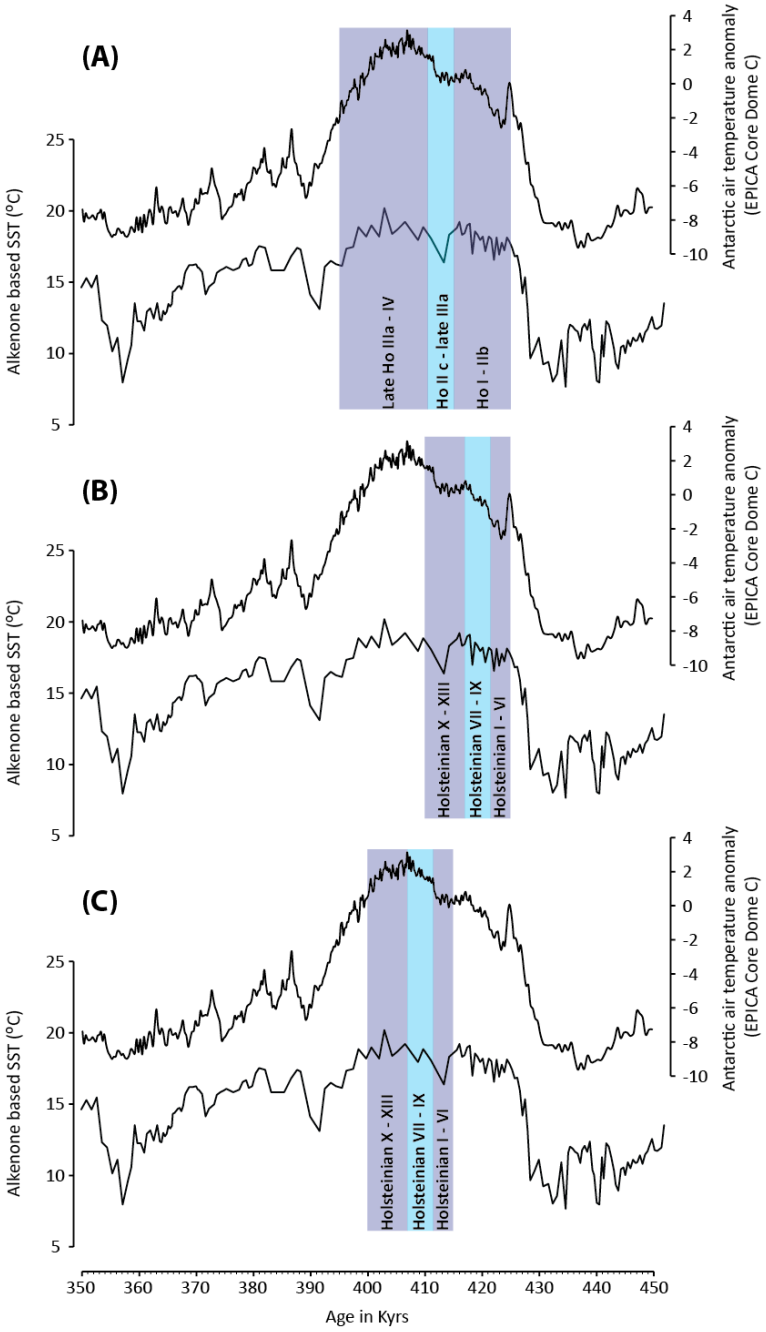

Figure 11.10. *Correlation between western and central European pollen records and EPICA Dome C (Jouzel et al., 2007) and North Atlantic SST records (U1313, Stein et al., 2009). A) Alignment of Hoxnian pollen zones with the onset of MIS IIc using the estimated duration proposed by Shackleton and Turner (1967) and Turner (1970) after Ashton et al. (2008), B) Alignment of Holsteinian pollen zones with the onset of MIS 11c (proposed but considered unlikely by Koutsodendris et al., 2012), and C) Alignment of Holsteinian pollen zones with the thermal maximum of MIS 11c (following Koutsodendris et al., 2010, 2012), and. Redrawn from Candy et al. (2014).*

What cannot currently be addressed is the absolute timing of the NAP Phase and OHO within the chronology of MIS 11. If it is accepted that both the NAP Phase and OHO are stratigraphically identical and forced by meltwater pulses, then whether they occur early or late in the interglacial is clearly important (Fig. 11.10). If they occur early then outbursts associated with the final phases of MIS 12 deglaication can be reasonably invoked as a cause. If they occur later, then such a forcing mechanism is more problematic, however, recent work on the long-term stability of Greenland may provide a potential mechanism. There is now increasing evidence that a major part of the Greenland ice sheet decayed during the climatic peak of MIS 11 (de Vernal and Hillaire-Marcel, 2008; Reyes et al., 2014; Kandiano et al., 2012; Raymo and Mitrovica, 2012). This would release freshwater into the North Atlantic and potentially cause slowing of the AMOC in a manner similar to that predicted for the future (Velligna and Wood, 2002, 2008).

Models for the timing of the NAP Phase and OHO have proposed their occurrence both early (ca 418 ka BP) (Ashton et al., 2008; Koutsodendris et al., 2012) and late (ca 408 ka BP) in MIS 11 (Koutsodendris et al., 2012) (Fig. 11.9). Although this study cannot resolve the absolute timing of this event, whether an early or late timing is involved, our current understanding of MIS 12 deglaciation and ice sheet dynamics during MIS 11 would imply the existence of a possible forcing meltwater forcing mechanism at either point.

11.5. Summary

- It has been demonstrated in this chapter that the NAP Phase, which occurs during the pre-temperate pollen zone of the Hoxnian (MIS11c) Interglacial (Ho IIc) in the British Isles, represents a wildfire driven by an abrupt cooling event.
- The abrupt cooling event that forced the wildfire lasted for 183±6 vyrs and was the last and most extreme of a series of centennial scale cooling events that occurred during the preceding -1,016±6 vyrs.
- The climatic cooling stressed tree populations, leading to reduced pollen production (observed in the PAR record) and death, providing dead wood on the landscape that was ignited by a lightning strike.

- This wildfire caused the expression of the event in the pollen record, resulting in unstable lake catchment conditions and the delivery of large amounts of allochtonous to the Marks Tey basin, resulting in a four-phase lake response, driven by changes in catchment stability and lake nutrient levels.
- The NAP Phase appears comparable to the 8.2 ka event in terms of the relative timing within the pollen stratigraphy after the onset of temperate woodland development, as well as duration and magnitude of the isotopic oscillation associated with it, but the 565±12 vyr duration of the pollen event appears to have no naturally forced analogue in the early Holocene.
- Further similarities are apparent between the isotopic oscillation that forced the NAP Phase and the 8.2 ka event, as both occur as the last in a series of abrupt isotopic oscillations during the early part of an interglacial, suggesting that both may be driven by oceanic forcing.
- It is not currently possible to determine that absolute timing of the NAP Phase and OHO within MIS 11, however, current understanding about the nature of ice sheet dynamics during Termination V and MIS 11c would suggest that a forcing mechanism existed during both the early and latter part of MIS 11c.

Chapter 12. Structure and duration of the Hoxnian and MIS 11

Chapter overview

The focus of this thesis has been to develop a varve chronology for the Hoxnian sequence at Marks Tey and then apply this chronology to investigate the structure, duration and underlying forcing mechanism for the NAP Phase. The data generated as part of this research project can also be used to provide some initial discussion about the environment and duration of the Hoxnian (MIS 11) in the British Isles. This chapter will therefore deal with the following topics: 1) the completeness of the sedimentary record contained within the palaeo-lake basin at Marks Tey, 2) how robust estimates of the duration of the Hoxnian previously derived from this sequence are, and 3) a comparison of the duration of pollen zones from Marks Tey with regional records within the Holocene.

12.1. Introduction

The duration of MIS 11c is clearly an important question, as it allows us to discuss how long the Holocene would naturally persist for. As insolation patterns will partially control the duration, climatic structure and degree of warmth/cooling that occurs within the climate system, the isotopic signals that occur in long climate records that extend beyond the limits of current dating methods are often tuned to peaks and troughs in insolation patterns, which for MIS 11c, suggests a duration of approximately 30,000 years (e.g. Hays et al., 1976; Imbrie et al., 1984; EPICA, 2004; Lisiecki and Raymo, 2005). The extended duration of MIS 11c in such records is due to the insolation patterns that occured during the interglacial. In contrast to other interglacial periods during the last 500,000 years, which are characterised by single, high amplitude early insolation peaks (MIS 5, 7 and 9), MIS 11 is characterised by lower amplitude insolation variations and two insolation peaks, with the larger second peak corresponding to peak interglacial conditions (Fig. 11.1a). As a result of tuning, climatic records from MIS 11 are therefore characterised by two temperature “plateaus” (section 2.3 in chapter 2); the first part of the interglacial indicating stable, cooler temperatures compared to the second part, which is characterised by stable, warmer

temperatures (Fig. 11.1b). Due to the relatively subdued insolation changes that occur during MIS 11, however, the "tie points" for tuning are not as clear as MIS 5 or 1, for example (e.g. Desprat et al., 2005) and the chronology for MIS 11 can, therefore, be considered less reliable than for other interglacials (Candy et al., 2014).

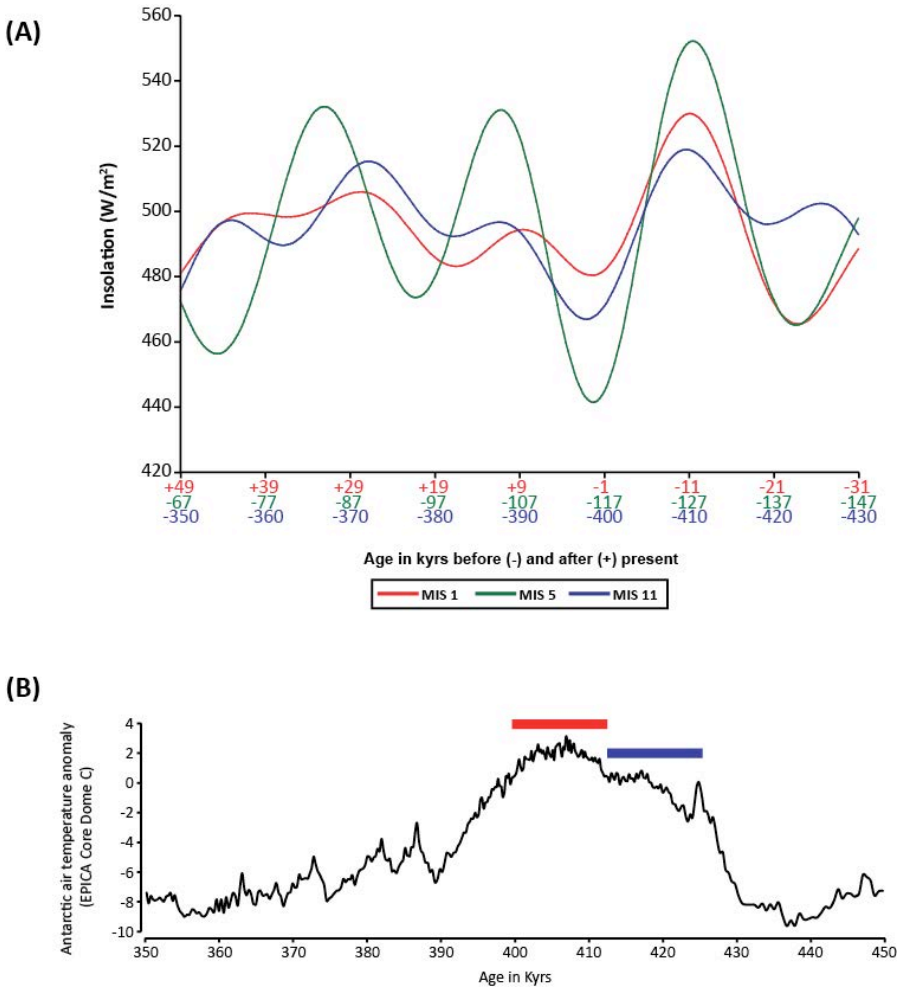

Figure 12.1. *A) June insolation values at 65°N for MIS 11, 5 and 1, aligned using the insolation maxima (approx. 410 kyrs, 127 kyrs and -11 kyrs, respectively). The data highlights differences in insolation patterns between MIS 11 and other middle-late Pleistocene interglacials. While MIS 5 and 1 are characterised by a single insolation peak, MIS 11 was characterised by two, with the second indicative of the thermal maximum. B) The climatic structure of MIS 11 in the EPICA Dome C record, plotted as temperature anomaly (Jouzel et al., 2007). The blue bar represents relatively cooler temperatures during the first half of the interglacial (first insolation peak) and the red bar indicates warmer conditions during the second half of the interglacial (second insolation peak).*

Although orbital tuning represents the predominant method for developing age models for long continuous records that extend this far back in the Quaternary, there are a number of terrestrial archives from MIS 11 that provide independent chronologies for the interglacial (Shackleton and Turner, 1967; Turner, 1970, 1975;

Nitychoruk et al., 2005; Koutsodendris et al., 2012). The partially varved record from Marks Tey has been used to estimate the duration of temperate woodland during MIS 11c, with estimates ranging from 25,000 years (Turner, 1975) to between 30,000-50,000 years (Shackleton and Tuner, 1967). Although these estimates vary significantly, they appear to confirm the long duration suggested by orbitally-tuned records. In contrast to Marks Tey, Holsteinian varved records from central and Eastern Europe suggest a much shorter duration of 15,000-16,000 years (Nitychoruk et al., 2005; Koutsodendris et al., 2012). The Ossowka sequence in Poland is purported to be continuously varved throughout MIS 11c, with peak interglacial conditions (i.e. temperate forest expansion) lasting for 16,000 years and the Holsteinian lasting for 35-39,000 years (Nitychoruk et al., 2005).

The Holsteinian varved records from central and eastern Europe therefore indicate a large discrepancy in interglacial duration (based on the duration of temperate woodland) when compared with Marks Tey and the orbitally-tuned records. There are, however, two issues with the approach to chronology at Marks Tey that need to be discussed in relation to providing estimates for the duration of MIS 11; 1) the sediment sequence at Marks Tey is not continuous and contains evidence for major hiatuses (Chapter 6; Turner, 1970), and 2) In contrast to Ossowka and the Luneburger Heide regional records, the section of the Marks Tey sequence, from Ho I to Ho IIIa, where lamination counts were undertaken (Shackleton and Turner, 1967; Tuner, 1970) has been shown in this study to be only partially varved (chapters 6 and 7).

12.2. Characteristics of the sediment record at Marks Tey: Implications for estimates of interglacial duration

The duration of the Hoxnian (MIS 11) at Marks Tey, as suggested by Shackleton and Turner (1967) and Turner (1970; 1975), is based on a estimates of: 1) counts from sections of the Marks Tey sequence where lamination sets are well developed (Ho IIc to early Ho IIIa), 2) the number of years where lamination sets are poorly developed (Ho I to Ho IIb), and 3) the number of years based on average sedimentation rates and the thickness of sedimentary units for non-laminated or brecciated beds (late Ho IIIa to IV). As stated above, these estimates, although variable (25 – 50,000 years), appear to

corroborate the orbitally tuned chronologies for an extended duration of MIS 11, but conflict with estimates based on varved records from central Europe, which suggest a duration of 15-16,000 years (Nitychoruk et al., 2005; Koutsodendris et al., 2012). There are, however, some important characteristics of the sediment sequence at Marks Tey, which combined with the new data generated as part of this the current study, raise questions about the reliability of these estimates.

The MTSC-2014 varve chronology for Marks Tey contains a total of 3,533 counted varves between 16.45 – 12.37 mbs (total counting error of 5.7%), which occur during part of pollen zone Ho IIb, through Ho IIc and the early part of Ho IIIa (Table. 12.1). The duration of pollen zone Ho IIc provides the only reliable point of comparison between the chronology generated in this thesis with the estimates of Shackleton and Turner (1967) and Turner (1970), as it is the only pollen zone in the sequence where varves compose the dominate mode of sedimentation and the sequence has not been affected by incomplete core recovery (Table 12.1). The estimate of ~2,700 years for the duration of Ho IIc by Shackleton and Turner (1967) and Turner (1970) is in close agreement with the number of varves counted by micro-facies analysis in this thesis (26 year difference), indicating that the estimates of Shackleton and Turner (1967) and Turner (1970) are reliable in this section of the sequence.

If the thickness and duration of Ho IIc is used to calculate the average sedimentation rate for Ho IIa and Ho IIb, which are not varved, then the pre-temperate phase (Ho II) lasted for approximately 4,203 years. The radiocarbon dated sequence at Hockham Mere (Bennett, 1983), located approximately 65 miles to the north of Marks Tey, which when re-calibrated (I. Matthews, unpublished data), provides a Late glacial and Holocene vegetational succession that the pre-temperate phase at Marks Tey can be compared to. The same pollen zone at Hockham Mere lasted for approximately 4,000 years, which is comparable to the same zone at Marks Tey (Table. 12.1). Although the duration of this zone at Marks Tey is partly based on average sedimentation rates, it does suggest that vegetation development during the pre-temperate zone may have occurred over similar timescales during both interglacials.

Table 12.1. *Summary of estimated durations of the pollen zones at Marks Tey, based on Shackleton and Turner (1967) and Turner (1970) and varve counts in this thesis. The Holocene equivalent of the pre-temperate phase is also stated for comparison.*

<table>
<tr><th>Pollen Zone</th><th>Shackleton and Turner (1967); Turner (1970)</th><th colspan="3">MTSC-2014 chronology</th><th>The Holocene (Hockham)</th></tr>
<tr><td></td><td>Estimated</td><td>Counted</td><td>Interpolated</td><td>Estimated</td><td>Cal. yrs</td></tr>
<tr><td>Late Ho IIIa – IV</td><td>~15,000 yrs</td><td>-</td><td>-</td><td>-</td><td>-</td></tr>
<tr><td>Early Ho IIIa</td><td>~2,000 yrs</td><td>771 yrs[b]</td><td>965 yrs[b]</td><td>-</td><td>-</td></tr>
<tr><td>Ho IIc</td><td>~2,700 yrs</td><td>2,674 yrs</td><td>3,054 yrs</td><td rowspan="3">4,203 yrs</td><td rowspan="3">~4,000 yrs</td></tr>
<tr><td>Ho IIb</td><td rowspan="3">~5,000 – 10,000 yrs</td><td>88[a]</td><td>816[a]</td></tr>
<tr><td>Ho IIa</td><td colspan="2" rowspan="2">Not varved</td></tr>
<tr><td>Ho I</td><td>-</td><td>-</td></tr>
</table>

[a]*The sediments that comprise Ho IIb are only partially varved (~20%), which is why there is a large discrepancy between the counted and interpolated figures.* [b]*The early Ho IIIa section of the MT-2014 chronology is not complete because of a section missing from the core, due to incomplete core recovery. It is therefore not possible to compare these numbers with those of Shackleton and Turner (1967).*

Although the varve counts of Shackleton and Tuner (1967) and Turner (1970) provide a reliable estimate of the duration of pollen zone Ho II, the issue with using other sections of the Marks Tey sequence to provide estimates for the duration of the Hoxnian/MIS 11 is that the sedimentology of the sequence during Ho I is very different from the early part of Ho II (Ho IIa and Ho IIb). While the sediments in Ho IIa and Ho IIb display increasing regularity in sedimentology, the sediments during Ho I are predominantly composed of beds and irregular laminations (Fig. 12.2). Using the thickness of units that contain such sedimentary structures to estimate sedimentation rates is, therefore, not possible.

The estimates of Shackleton and Turner (1967) and Turner (1970) are further complicated by the sedimentology of the sequence from late Ho IIIa to Ho IV, which consist of brecciated sediments, as well as a major hiatus in sedimentation in borehole GG. Approximately 5.4m of brecciated sediments were identified in borehole GG (as have been in core MT-2010), covering a large part of the late-temperate pollen zone (late Ho IIIa and IIIb) (Fig. 12.3b) (Turner, 1970).

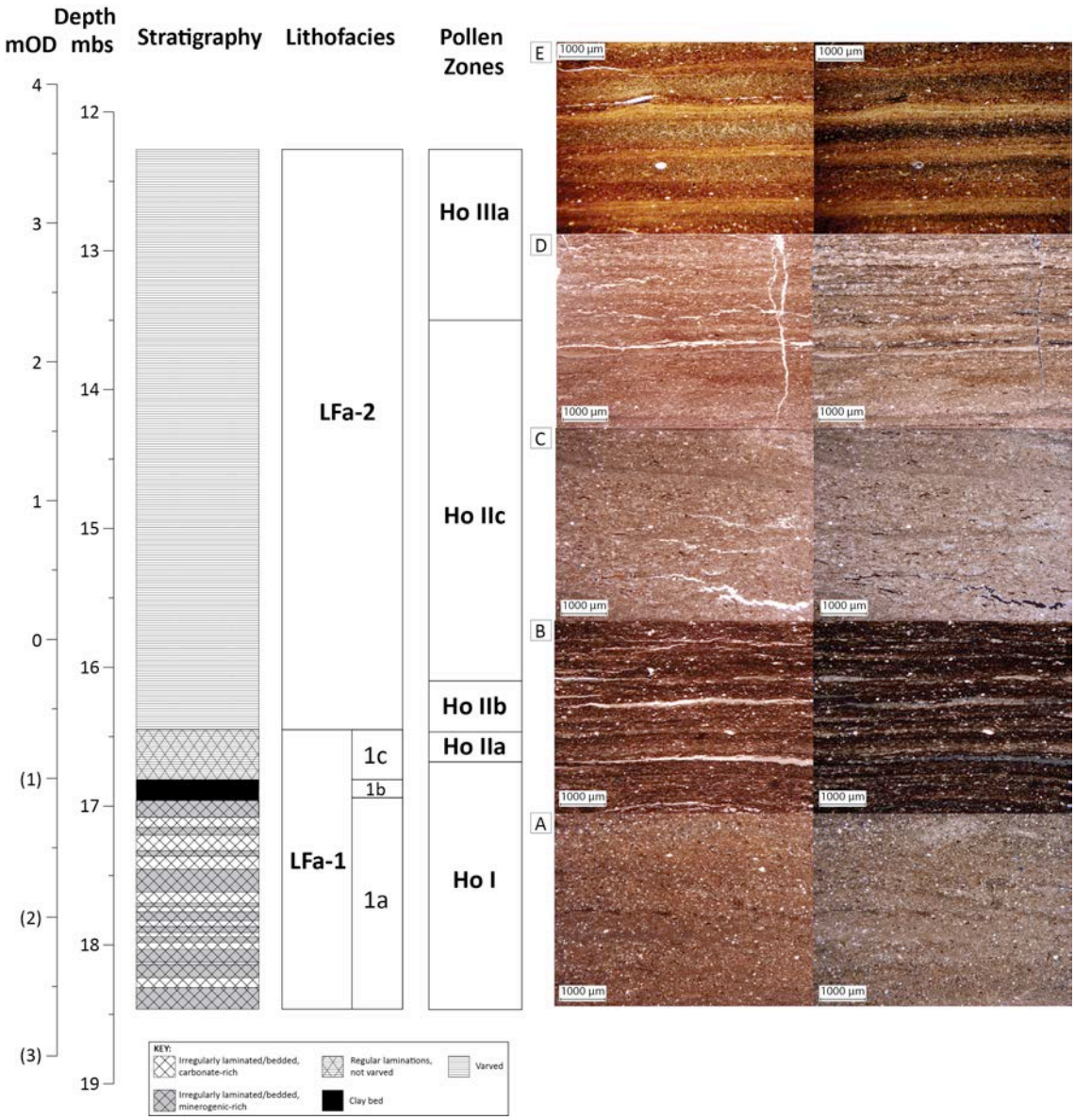

Figure 12.2. *Figure showing the MT-2010 lithostratigraphy, lithofacies zones and pollen zones with photomicrograph examples of the micro-scale sedimentology. A,B and C) Irregularly laminated sediments of LFa-1a (Ho I), D) Increasing regularity of carbonate laminations in LFa-1c (Ho II a), and E) Varved sediments that characterise LFa-2 (Ho IIc and early IIIa).*

This slumping and reworking of the lake sediments suggests the lake level fell during this period (Turner, 1970; Gibbard and Aalto, 1977; Gibbard et al., 1986), which is also indicated by a decrease in the planktonic/benthic diatom ratio during Ho IIIb (Evans, 1972). Although these brecciated sediments contain a different pollen signature to the pre-existing deposits, they are not *in situ*, so should not therefore be used to estimate the duration of these pollen zones. The final complication is that borehole GG does not contain a full sediment sequence for the Hoxnian, as there is a hiatus in sedimentation during the post-temperate phase (Ho IV) (Fig. 12.3b). Sediments containing pollen assemblages from this pollen zone were located in boreholes AA and BB, taken from

the marginal areas of the basin (Fig. 12.3a) (Turner, 1970). The Pollen record therefore represents the combined record of three sediment cores. Estimates of Ho IV duration based on the thickness of these marginal cores therefore assume that sedimentation rates are comparable across the basin, which is unlikely to be the case (e.g. Lehman, 1975; Palmer et al., 2010).

Although the varve chronology generated in this thesis cannot provide new estimates for the duration of Hoxnian (MIS 11c) in the British Isles, it has demonstrated how much of the lowest 6.25m of the sequence is annually-laminated. The sedimentological characteristics of the Marks Tey sequence described above suggest that estimates of Shackleton and Turner (1967) and Turner (1970) for the duration of temperate woodland phases during MIS 11 should be viewed with caution, as unlike the central and western European records, Marks Tey is not varved throughout the interglacial (Nitychoruk et al., 2005) and cannot be used as part of a regional varve stratigraphy (Koutsodendris et al., 2012). Assuming that the location of borehole GG and core MT-2010 represents the depocentre of the basin and, therefore, the location most suitable for the preservation of varves, then the Marks Tey sequence should not be used to provide estimates of Hoxnian duration.

There is widespread consensus that MIS 11c is an interglacial of unique duration. Marine, ice core and Mediterranean pollen records all indicate a duration of ca 25,000 – 30,000 years. All of these records are orbitally-tuned, however, with no independent ages estimates. Consequently, the fact that large numbers of records exist with evidence for extended warmth during MIS 11c does not mean that this duration has been tested by multiple independent investigations. All of these records are tuned to the same signal and will always produce similar results. The Marks Tey sequence was considered important because it was the one site where an extended duration for MIS 11c was suggested through independent chronology (i.e. varve counting). This study has shown the estimate for interglacial duration to be unsound. Consequently, all available varved lacustrine records from Europe indicate a much shorter duration for MIS 11c than the ice core records and marine sequences. This is an issue that requires further study.

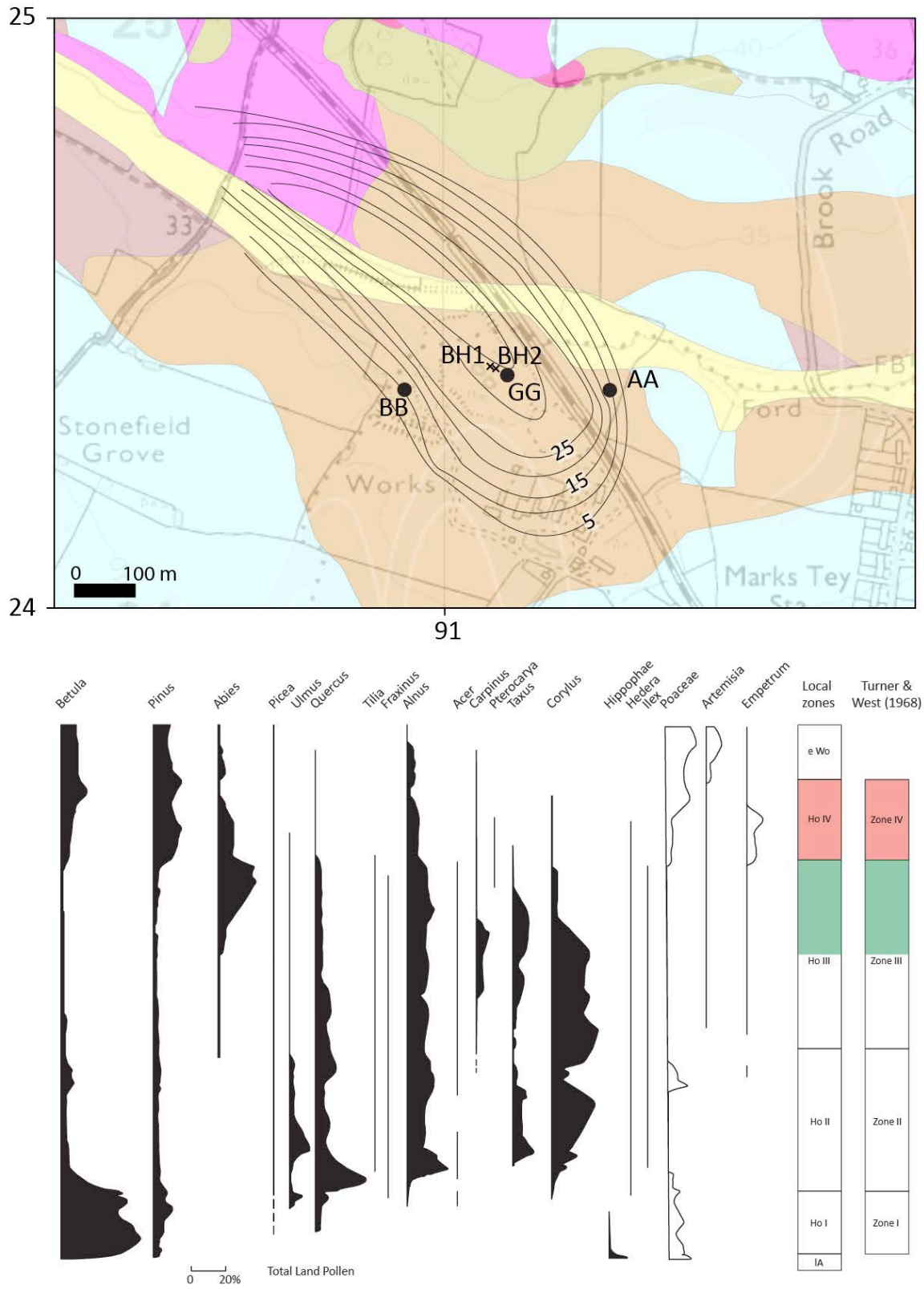

Figure 12.3. *Location map showing the location of BH1 and BH2, which produce the composite MT-2010 stratigraphy, together with the location of boreholes AA, BB and GG, which compose the composite pollen diagram of Turner (1970). Borehole GG contains Pollen zones from the Late Glacial (lA) through to the end of the late-temperate phase (Ho IIIb). There is then a hiatus, as the next pollen zone to occur is from the early part of the subsequent cold stage (eWo). The post-temperate phase (Ho IV) is missing from borehole GG, but occurs in the marginal boreholes AA and BB. The combined pollen record of Turner (1970) is shown to illustrate where the hiatus in borehole GG occurs (red shading). The location of brecciated sediments is highlighted by green shading.*

12.3. Oxygen isotope stratigraphy at Marks Tey: Environmental significance of MIS 11 in Britain, Europe and the North Atlantic

The application of oxygen isotope analysis to the authigenic lacustrine carbonates at Marks Tey has primarily focused on the environmental signal recorded by the $\delta^{18}O$ values and what the isotope stratigraphy reveals in terms of possible abrupt climatic events during the early Hoxnian/MIS 11. As well as this work, it is also possible to make some more general observations about the longer-term climatic structure and stability of the first part of MIS 11 in the British Isles, as well as compare the record from Marks Tey with other isotopic records of MIS 11 from Europe and the North Atlantic.

12.3.1. Structure of MIS 11 in the British Isles

Previous methods to investigate the climatic structure of MIS 11 in the British Isles have focused on temperature reconstructions from coleopteran (e.g. Coope and Kenward, 2007), vertebrate (e.g. Schreve, 2001a,b), floral (e.g. Candy et al., 2010) and ostracod (e.g. Horne, 2007) evidence. Such reconstructions provide important snap-shots of temperature estimates for different pollen zones, revealing that temperatures during peak interglacial (MIS 11c) conditions were not too dissimilar from the present interglacial (Fig. 12.4) (Candy et al., 2010, 2014 and references therein). The high-resolution isotope stratigraphy from Marks Tey, although not able to provide quantitative temperature estimates, can provide a more detailed record of environmental variability during early MIS 11, depending on what the primary control over $\delta^{18}O_{calcite}$ is. The oxygen isotope data presented in figure 12.4 includes seven samples taken from carbonate laminations that occur within blocks of brecciated lake sediment from Ho III (data courtesy of J. Sherriff). These samples are included as a point of comparison for the values that occur from Ho I to early Ho IIIa, but do not indicate how the environment evolved during this period. Although the pollen content indicates these sediments are younger than those below (Ho I to early Ho IIIa) and older than those above (Ho IV), the stratigraphic integrity has been lost. The $\delta^{18}O$ values of these samples, therefore, provide an indication of the isotopic characteristics of lacustrine carbonates that precipitated during Ho III.

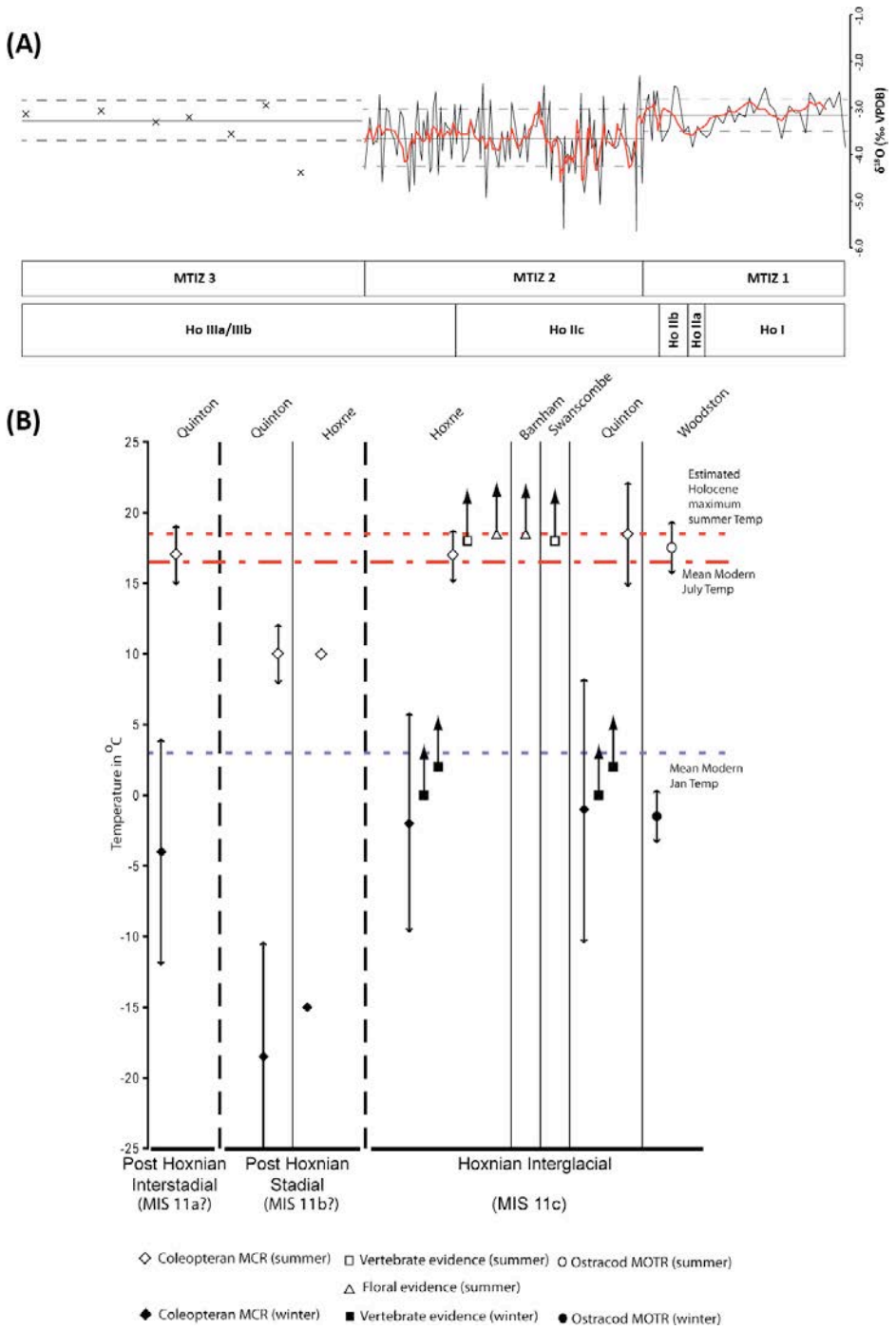

Figure 12.4. *A) The $\delta^{18}O$ from this study, combined with samples taken from blocks that contain carbonate laminations in the brecciated sediments of Ho IIIa and Ho IIIb (black crosses) (MTIZ 3). Samples from Ho IIIa/IIIb have an average $\delta^{18}O$ value of -3.37‰ (1σ = 0.49) .B) The climatic structure of MIS 11 in Britain from terrestrial proxies at a number of sites. Taken from Candy et al. (2014).*

With the addition of samples from the brecciated sediments of the late-temperate phase (Ho III), the $\delta^{18}O$ stratigraphy for the Marks Tey sequence shows two zones, MTIZ-1 Ho I to HoIIb) and MTIZ-3 (Ho III), which have high mean $\delta^{18}O$ values (-3.13‰ and -3.21‰, respectively), separated by MTIZ-2 (Ho IIc and Ho IIIa), with a lower mean $\delta^{18}O$ value of -3.73‰. The interpretation of this signal is complicated by the fact that

samples from MTIZ-3 come from brecciated fragments of lake sediments, so should therefore be considered tentative. The magnitude of isotopic decline between MTIZ-1 and MTIZ-2, through to the recovery into MTIZ-3 is relatively small (ca 0.5 – 0.7‰), suggesting that there is minimal evidence for major, long-term shifts in mean $\delta^{18}O$ values across a large part of the interglacial (Ho I to Ho III). What this means in terms of environmental signal was discussed in detail in chapter 9. Isotopic shifts in $\delta^{18}O$ records from open lacustrine systems in western Europe are frequently interpreted as temperature shifts, due to the observed control that air temperature has over the $\delta^{18}O$ of rainfall (Dansgaard, 1964; Rozanski et al., 1993; 1993; Darling and Talbot, 2003; Darling, 2004), which then becomes the groundwater that recharges lake basins (Darling et al., 2003). Assuming there is no significant modification of this $\delta^{18}O$ value by physical and biological processes as the water moves through the system (e.g. Leng and Marshall, 2004), the temperature imprint should remain.

If these assumptions are accepted, then the Hoxnian interglacial was characterised by; 1) long-term climate stability, with minimal changes in mean $\delta^{18}O$ values from Ho I through Ho III (with the exception of the centennial scale events discussed in chapter 11), and 2) the possible occurrence of two temperature peaks; one during Ho I and one during Ho III, in between which relatively cooler temperatures prevailed (Ho II). It should be noted, however, that these changes are small, so if two temperature peaks and a cooler interval occur, they must have been relatively subdued. With reference to the possible early "temperature" peak, other factors can influence the $\delta^{18}O$ values of meteoric waters (as noted in chapter 9), such as changes in seasonality of rainfall and changes in $\delta^{18}O$ of the source water. This will be particularly true during the early part of an interglacial, where large changes in ice volume, sea level and the re-arrangement of atmospheric systems may all impact on the $\delta^{18}O$ value of water passing through the hydrological system. Such changes are thought to have influenced the $\delta^{18}O$ value of lacustrine carbonates in the British Isles during the last glacial to interglacial transition (Candy et al., in press), so may well have had a similar influence over the $\delta^{18}O$ values of recharge waters during early MIS 11. Although the suggestion of a late "temperature" peak in Ho III is based on a small number of $\delta^{18}O$ analyses from brecciated sediments, this is still consistent with other proxy evidence for the temperature history of the Hoxnian. *Trapa natans* (floating water chestnut), a thermophilous plant which occurs

only in the warmest of British interglacials (i.e. Ipswichian/MIS5e and Cromerian) as it requires summer temperatures of >20°C to germinate successfully (Candy et al., 2010). It is not common in Hoxnian deposits, but where it does occur, it is found within deposits of Ho IIIb (Gibbard and Aalto, 1977; Coxon, 1985; Gibbard et al., 1986). There is, therefore, good reason to believe, based on isotope and palaeoecological data that a late temperature peak did occur in Britain during the Hoxnian.

12.3.2. Comparison with other lacustrine isotopic records from MIS 11

The lowermost 6.25m of Marks Tey shows a strong similarity, in terms of $\delta^{18}O$, to the Ossowka sequence in Poland (Fig. 12.5). That is to say an early peak followed by a decline across the interval of temperate woodland conditions (Nitychoruk et al., 2006).

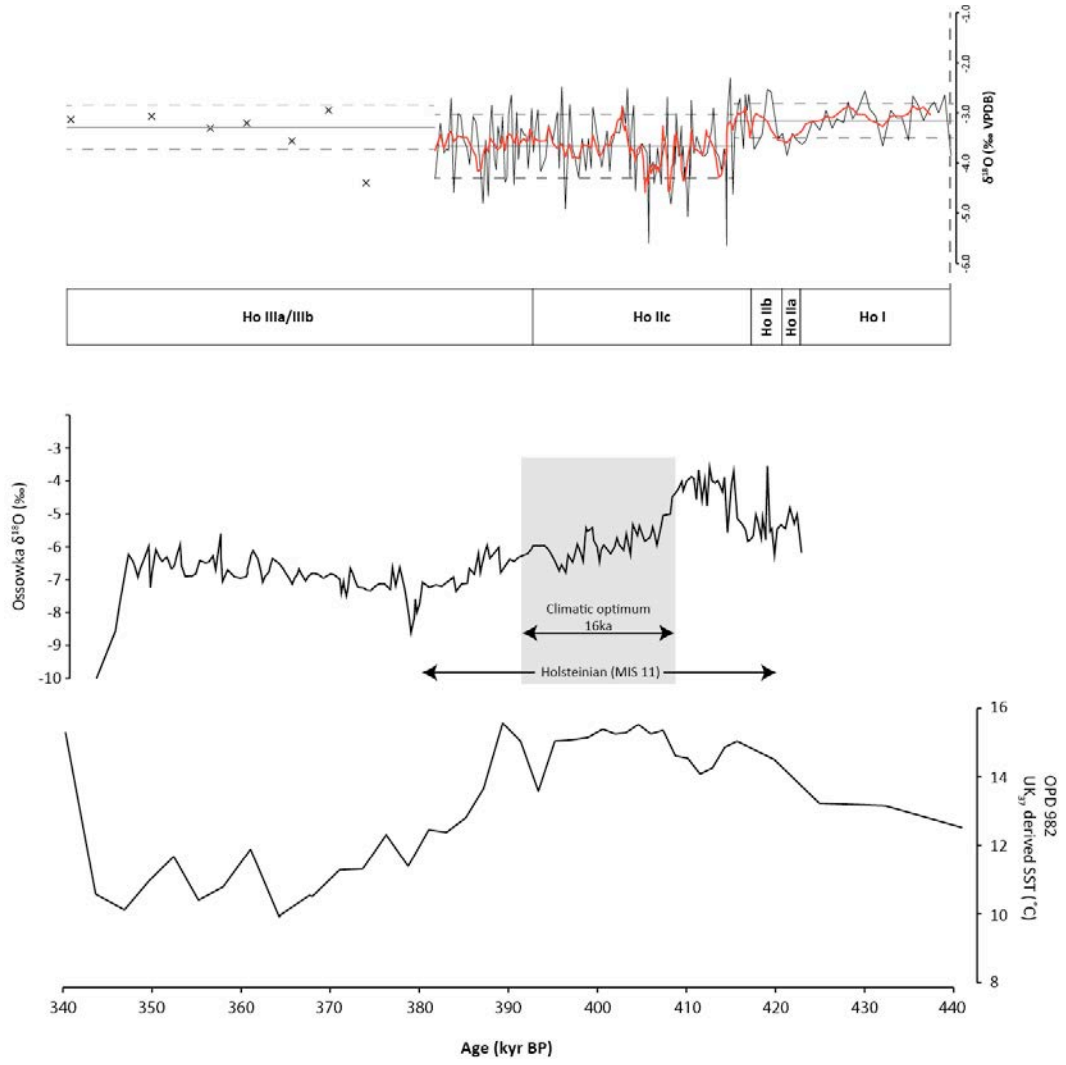

Figure 12.5. *Comparison between the $\delta^{18}O$ record from Marks Tey with Ossowka. The record from Ossowka (Nitychoruk et al., 2005) is plotted alongside the SST record from ODP 982 (Lawrence et al., 2009). The grey shaded area indicates the relative position and duration of the climatic optimum inferred from the expansion of temperate woodland.*

Nitychoruk et al. (2006) have proposed that this trend reflects a shift from continental to maritime climates during the interglacial. This has been discussed in chapter 9 and may also explain the early peak seen in the Hoxnian deposits at Marks Tey. The high $\delta^{18}O$ values seen in the brecciated beds at Marks Tey have no analogue in the Ossowka sequence (Fig. 12.5). This may suggest that the climatic structure of this interglacial varies between East and West Europe. It may, however, also indicate issues associated with isotopic analysis of the brecciated sediments.

12.3.3. The Hoxnian as an interglacial of prolonged climatic stability: comparison with N. Atlantic isotopic records

The suggestion that the Hoxnian interglacial is a time of prolonged climatic stability is consistent with a number of records from the North Atlantic (McManus et al., 1999; 2003; Martrat et al., 2007; Stein et al., 2009). The work of McManus et al. (2003) on ODP 980 has highlighted the occurrence of relatively stable sea surface temperatures at the same approximate latitude as Britain. This is consistent with the $\delta^{18}O$ signal of the Marks Tey sequence, which also shows remarkably little variation in mean $\delta^{18}O$ value across the major part of the interglacial (HoI to HoIII). The apparent occurrence of an early and late peak in $\delta^{18}O$ values at Marks Tey, if interpreted as being temperature maxima, is also consistent with many of the North Atlantic records of MIS 11c, e.g. MD01-2443 (Martrat et al., 2007), ODP 982 (Lawrence et al., 2009), U1313 (Stein et al., 2009), MD03-2699 (Voelker et al., 2010). All of these workers show that North Atlantic SSTs during MIS 11c were characterised by an early (centred on ca 425ka BP) and a late (centred on 405ka BP) temperature peak, separated by a short-lived and relatively minor cooling interval (centred on ca 413ka BP) (Fig. 12.6). It is important to note, however, that such a structure is not true for all North Atlantic SST records of this time period, particularly in the Nordic Seas (>60°N), where cold conditions and extended sea-ice cover restricted peak interglacial values to the second part of MIS 11 (i.e. Kandiano et al., 2012) (Fig 2.5 in chapter 2). Figure 12.6 shows the $\delta^{18}O$ stratigraphy from Marks Tey compared to U1313 (Stein et al., 2009) and MD992277 (Kandiano et al., 2012) (see figure 2.5 in chapter 3 for all records). These alignment methods have been discussed in section 2.4.2.4 of chapter 2.

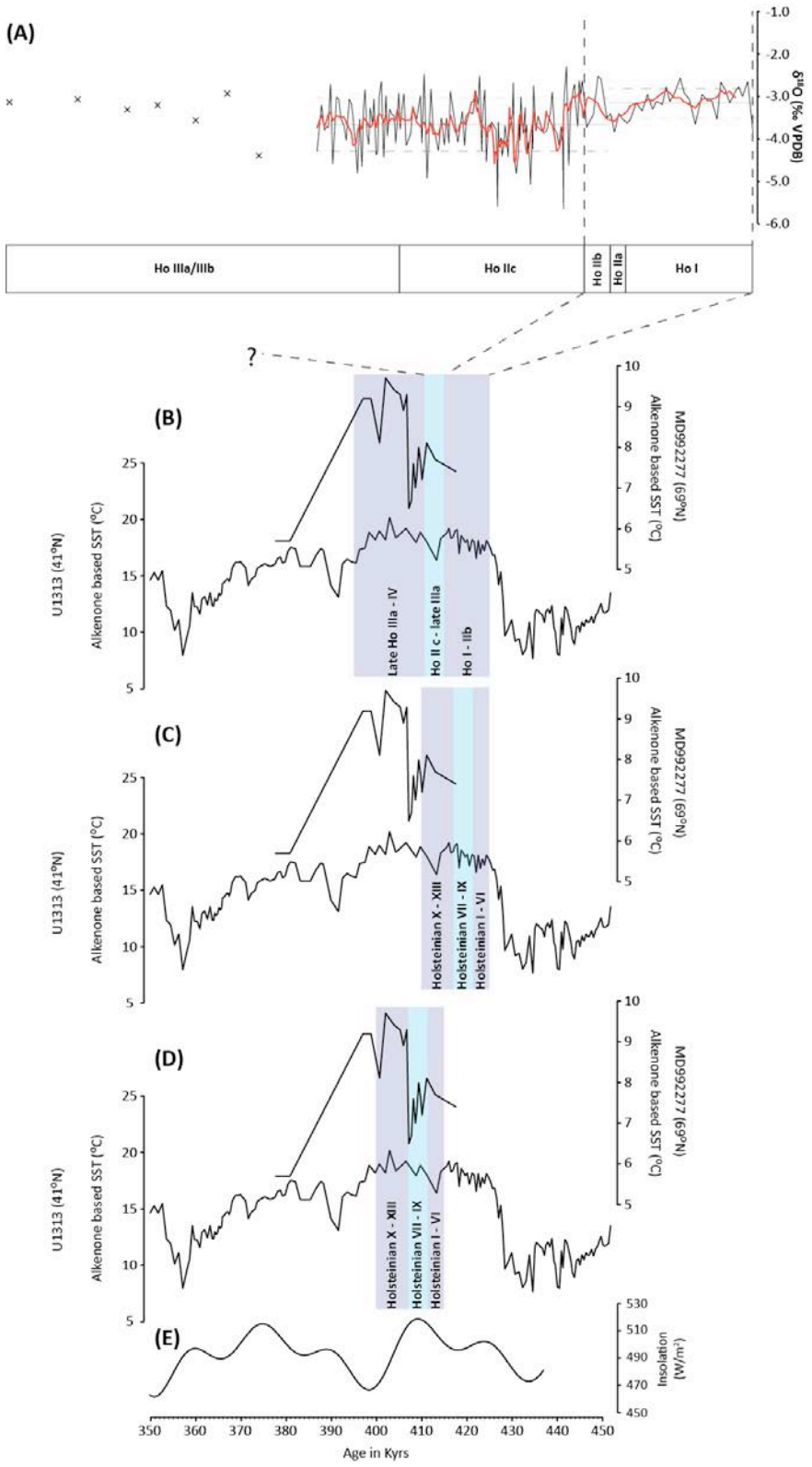

Figure 12.6. *Comparison of the $\delta^{18}O$ from Marks Tey with selected records from the N. Atlantic. Correlation between western and central European pollen records and North Atlantic SST records for U1313 (Stein et al., 2009) and MD992277 (Kandiano et al., 2012) is made using three models for alignment: A) Alignment of Hoxnian pollen zones with the onset of MIS IIc using the estimated duration proposed by Shackleton and Turner (1967) and Turner (1970), after Ashton et al. (2008), B) Alignment of Holsteinian pollen zones with the onset of MIS 11c (proposed but considered unlikely by Koutsodendris et al., 2012), and C) Alignment of Holsteinian pollen zones with the thermal maximum of MIS 11c (following Koutsodendris et al., 2010, 2012). E) Changes in insolation during MIS 11 for comparison (Laskar et al., 2004). Redrawn and modified from Candy et al. (2014).*

Discussion of the records in figure 12.6b and c is restricted by the temporal resolution of the MD992277 dataset (Kandiano et al., 2012). If it is assumed that the the Hoxnian was a prolonged Interglacial (ca 30,000 yrs), then the possible late temperature peak at Marks Tey (Ho IIIa/b, Fig. 12.6a) is consistent with North Atlantic marine records, although the high $\delta^{18}O$ values during Ho I to Ho IIb may be related to non-temperature effects. The alignment method used in figure 12.6c (Koutsodendris et al., 2012 after Ashton et al., 2008) assumes that the ca 15,000 yr duration of temperate forest during the Holsteinian occurred before peak interglacial conditions are indicated in the North Atlantic SST records (Fig. 12.6), a view considered unlikely by Koutsodendris et al. (2012). The preferred method of alignment by Koutsodendris et al. (2012) is with the second part of MIS 11, which agrees with the SST records from the North Atlantic (Fig. 12.6).

Assuming the alignment method in figure 12.6c is incorrect, the first part of MIS 11 in the North Atlantic region is characterised by lower SSTs than the latter part of the interglacial, although this discrepancy is more extreme in the Nordic Seas (core MD992277 in Fig. 12.6) (Kandiano et al., 2012). Kandiano et al. (2012) suggest that an increased SST gradient between the Nordic Seas and the Mediterranean during early MIS 11 (compared to the Holocene) was the result of a predominantly negative North Atlantic Oscillation (NAO) mode compared to the later part of MIS 11. If this is the case, then the decreasing isotopic trend that occured during Ho I through to Ho IIb (MTIZ 1) may be a result of changes in atmospheric circulation and seasonality of rainfall. A switch from predominantly negative to positive NAO conditions (an increase in pressure gradient between the Iceland low and Azores high) will result in stronger westerly winds and wetter conditions over Northern Europe, particularly during the winter (e.g. Rodwell et al., 1999; Hurell et al., 2003). An increase in the contribution of isotopically depleted winter precipitation will therefore alter the $\delta^{18}O$ value of rainwater and, therefore, the $\delta^{18}O$ value of lake water, which are likely to lead to lower $\delta^{18}O$ values of authigenic calcite. Such 'non-Dansgaard' effects have been documented in Holocene lake carbonate records (e.g. McKenzie and Hollander, 1993; Teranes and McKenzie, 2001), although such changes occurred over much shorter timescales. If this is the case, a switch from relatively dry to wet conditions that accompanies the change

in NAO mode may explain increasing water levels at Marks Tey, as suggested by sedimentological and diatom evidence from the sequence (see section 6.5.3 in chapter 6).

If, as discussed above, the high $\delta^{18}O$ values that occured early in the Hoxnian within the Marks Tey sequence are not a function of high temperatures, but a function of precipitation changes or the prolonged pattern of deglaciation, then the fact that the highest $\delta^{18}O$ values occurred in Ho III (the later part of MTIZ 2 and MTIZ 3) might imply that peak temperatures during the Hoxnian in Britain occurred relatively late in that interglacial. This would again be consistent with the SST records from the North Atlantic, which typically show that the younger temperature peak that occurs during MIS 11c contained the interglacial thermal maximum. Such a scenario is also consistent with palaeoecological evidence from some Hoxnian sites, which show tentative evidence for climates during Ho III being warmer than during HoI and Ho II (see comment in section 12.3.1). It should be noted, however, that such palaeoecological evidence is not present at Marks Tey, with evidence of warm climate conditions in Ho III heavily reliant on isotopic data from brecciated sediments. The $\delta^{18}O$ values of this data are, however, consistent with palaeoclimatic data from other Hoxnian sites.

12.4. Summary

- This study has demonstrated that the laminated sediments at Marks Tey are varved from late Ho IIb, through Ho IIc, to early Ho IIIa. This contradicts the suggestion by Shackleton and Turner (1967) and Turner (1970, 1975) that Ho I to late Ho IIb are also varved. As a result, estimates for a prolonged Hoxnian Interglacial duration based on Marks Tey are considered unsound.
- The wider implication of this is that Marks Tey was hitherto the only terrestrial sequence that contained an independent chronology for the Hoxnian/MIS 11c, which corroborated the prolonged duration suggested by orbitally-tuned marine, ice core and long pollen sequences. As a result, all available varved lacustrine records from Europe show indicate a much shorter duration for MIS 11c.
- The environmental structure of the Hoxnian, as recorded in the $\delta^{18}O$ record from Marks Tey, is consistent with the structure of a number of North Atlantic marine

records. The $\delta^{18}O$ record from Marks Tey indicates predominantly stable conditions, with two periods of high $\delta^{18}O$ values (Ho I to Ho IIa and Ho IIIa/b), in between which a period of lower $\delta^{18}O$ values occur (Ho IIc/IIa).

- If the $\delta^{18}O$ signal is interpreted purely in terms of temperature, it suggests that the Hoxnian (MIS 11c) was characterised by early and late temperature peaks, with an intervening period of cooler conditions, much like the North Atlantic SST records.
- Non-Dansgaard effects must be taken into consideration, however, due to changes that occur in the hydrological system during the early stages of an interglacial.

Chapter 13. Conclusions

13.1 Conclusions and key findings

This work has recovered a ca. 18 metre sequence of Hoxnian lake sediments from the palaeolake basin of Marks Tey, Essex, UK. This core replicates the record published by Turner (1970) in terms of both lithostratigraphy and pollen stratigraphy and indicates that this sequence records the major part of the Hoxnian interglacial, the British terrestrial correlative of MIS 11 (Candy et al., 2014). The major focus of the current study has been on the *in situ* laminated sediments that comprise the lowest 6.25 metres of this record and span pollen zones Ho I to Ho IIIa, the early temperate through to late temperate parts of this interglacial, which were originally proposed to be annually laminated, or varved (Turner, 1970). The main findings of this work are:

- Only the laminated sediments spanning Ho IIb to early Ho IIIb are varved. A varved origin has been proved through high-resolution micromorphological, stable (C and O) isotopic, pollen and diatom analysis.
- The sediments that comprise Ho I and Ho IIa are laminated but the structures are too irregular in both thickness and style of sedimentation to represent annual deposition.
- Varve counts through Ho IIb and Ho IIIb have identified 3,533 varve yrs (5.7% error), a chronological framework which has been named the Marks Tey Site Chronology (MTSC-2014). Small hiatuses occurring in the first 1.01 metres of Ho IIc mean that an interpolated chronology has been developed (MTSC-2014^{INT}).
- The Non-arboreal pollen Phase (NAP Phase) that has been reported from this site, and other Hoxnian sites in Britain, is clearly represented in the pollen stratigraphy of this sequence and the varve chronology developed for this sequence allows its duration (565 vyrs +/-12) to be accurately quantified for the first time.
- This study has shown that the NAP Phase is a highly complex event. The presence of charcoal peaks at its onset suggests that it is the vegetational response to a wildfire event and that this event produces complex landscape response (as represented by the varve thickness/type and the elemental

chemistry) and the limnology of the system (as represented by the diatom assemblages).

- Although apparently triggered by a wildfire the oxygen isotopic record produced for this sequence suggests that during Ho II a number of abrupt centennial scale climate oscillations occurred. The first four of these occurred prior to the NAP Phase whilst the 5th, and most extreme, occurs in association with the onset of this event. Isotopic values and pollen concentration values decrease prior to the expression of the NAP Phase in the percentage pollen diagram and prior to the occurrence of the charcoal peaks.
- Consequently, it is concluded that the NAP Phase is a composite response to an abrupt cooling event (ca 180 yrs in duration) that places stress on the tree population of eastern England at this time. The death of individual trees and the consequent accumulation of dead wood acts as fuel for a wildfire that is the cause of the major changes in percentage pollen that characterise the NAP Phase. Furthermore, it is the wildfire's impact on erosional processes that causes nutrient loading within the lake and, consequently, the complex patterns of sedimentation and lake productivity seen in this interval.
- The NAP Phase represents the most convincing example of an abrupt event during a pre-Holocene interglacial in the British Quaternary record and shows that climatic instability during fully interglacial conditions is not restricted to the Holocene.
- The NAP Phase has many similarities to the 8.2 ka event in the British Isles, in terms of: 1) the duration and magnitude of the isotopic event that drives it (Marshall et al., 2007); 2) its expression within pollen sequences, i.e. the possibility of associated burning events (Edwards et al., 2007) and 3) its relative position in the stratigraphy of the respective interglacial (ca 3,000 yrs after the onset of temperate woodland).
- It is, therefore, likely that, like the 8.2 ka event, the NAP Phase occurs in response to meltwater release into the North Atlantic during the final stages of deglaciation during the preceding termination. As the MIS 12 ice sheet was one of the most extensive in the Middle Pleistocene it would appear reasonable to assume that catastrophic outburst floods during Termination V would have occurred.

- The NAP Phase occurs in a similar stratigraphic setting to the older Holsteinian oscillation (OHO), seen in Holsteinian (the continental correlative of the Hoxnian (Turner, 1975)) lacustrine records from the continent. Major differences exist between the pattern and duration of these two events which are likely to reflect: 1) regional differences in the expression of the climatic event that forces these vegetational shifts; and 2) the complicating effect of wildfire that is seen at Marks Tey but not, currently, at continental sites.
- Although the absolute timing of both the NAP Phase and the OHO within MIS 11 is not currently known (Candy et al., 2014), given current views about the instability of the Greenland ice sheet during MIS 11 it is likely that meltwater pulses, that could drive such events could occur both early and late in this interglacial.

Beyond the analysis of the NAP Phase this study has shown that much of the Hoxnian sequence seen at Marks Tey is either; 1) not varved, or 2) not in situ. Consequently, there is no reason to assume that the estimates for the duration of the Hoxnian interglacial, based on earlier work by Shackleton and Turner (1967) and Turner (1970) are valid. Consequently, there is no reason to assume that the Hoxnian is an interglacial of unique extended duration, as has been proposed for MIS 11c in the North Atlantic (i.e. McManus et al., 2003).

13.2 Wider significance

MIS 11c is widely regarded as the most appropriate analogue for the current interglacial (Berger and Loutre, 2002; Candy et al., 2014). This study has shown that in a "Holocene-like" interglacial "8.2 ka like" abrupt events occur. The Marks Tey study is important as it is the first study that places an abrupt event from a pre-Holocene interglacial into the context of long-term patterns of climate change, the oxygen isotopic signal, that occur across the early and middle part of the interglacial. Furthermore, this study considers not just the climatic event itself but also the potential impact of this event on ecological, geomorphic and hydrological systems. If events such as the NAP Phase have a role to play as analogues for future abrupt climatic episodes then this second step is vital because it is the impact on the environment and landscape, not just the magnitude of cooling, that needs to be understood to allow policy makers and societies to mitigate and plan for their impacts.

This study is part of a growing body of evidence to suggest that during MIS 11c, a close Holocene analogue, abrupt events, comparable to the 8.2 ka event occurred in western and central Europe. This asks the question: are such events restricted to "Holocene-like" interglacials or are they common to all interglacials? This needs to be addressed in the future.

13.3 Further work

Marks Tey is just one of a large number of Hoxnian sites in Britain that record the NAP Phase (West, 1956; Kelly, 1964; Turner, 1970; Coxon, 1985; Candy et al., 2014). Although none of these sites are reported to be varved, they offer the potential of investigating the impact of this climatic event on a regional scale. Do all of these sites contain evidence for wildfire? Is the pattern of pollen response identical? Would sedimentary studies indicate that landscapes responded in a consistent manner? Furthermore, many of these shallower lake systems may offer other proxies that, because of the deep anoxic nature of the Marks Tey basin, could not be applied to this study. In particular is it possible to produce a chironomid or ostracod based temperature reconstruction for this interval to support the oxygen isotopic record presented here? A study that re-analysed the NAP Phase at multiple sites and introduced new proxy techniques would increase our understanding of both the regional expression of this event and its climatic structure. Finally, the work by Diehl and Sirocko (2007) has shown that, in German sites, tephra is found directly below the OHO. New advances in microtephra may now allow the same tephra to be identified in British and German sequences even though shard abundance may be low. Such an approach would allow high-precision correlation of all NAP/OHO records and allow a much greater understanding of the synchroneity of this event across Europe.

References

Adam, D.P. and Mahood, A.D., 1981, Chrysophyte cysts as potential environmental indicators, *Geological Society of America Bulletin*, Part 1, v. 92, p. 839-844

Aitchison J., 1986, *The Statistical Analysis of Compositional Data, Monographs on Statistics and Applied Probability*, Chapman & Hall Ltd, London

Alefs, J. and Müller, J., 1999, Differences in the eutrophication dynamics of Ammersee and Starnberger See (Southern Germany), reflected by the diatom succession in varve-dated sediments, *Journal of Paleolimnology*, Vol. 21, pp. 395-407

Allen, J.R.M., Brandt, U., Brauer, A., Hans-Wolfgang, H., Huntley, B., Keller, J., Krami, M., Mackensen, A., Mingram, J., Negendank, J.F.W., Nowaczyk, N.R., Oberhansli, H., Watts,W.A.,Wulg, S., Zolitschka, B.,1999. Rapid environmental changes in southern Europe during the last glacial period, *Nature,* Vol. 400, pp. 740–743

Alley, R.B. and Ágústdóttir, A.M., 2005, The 8k event: cause and consequences of a major Holocene abrupt climate change, *Quaternary Science Reviews*, Vol. 24, pp. 1123-1149

Alley, R.B., Marotske, J., Nordhaus, W.D., Overpeck, J.T., Petreet, D.M., Pielke Jr, R.A., Pierrehumbert, R.T., Rhines, P.B., Stocker, T.F., Talley, L.D. and Wallace, J.M., 2003, Abrupt climate change, *Science*, Vol. 299, pp. 2005- 2010

Alley, R.B., Mayewski, P.A., Sowers, T., Stuiver, M., Taylor, K.C. and Clark, P.U., 1997, Holocene climate instability: A prominent, widespread event 8200 yr ago, *Geology*, Vol. 25, pp. 483-486

Anderson NJ (1990) The biostratigraphy and taxonomy of small *Stephanodiscus* and *Cyclostephanos* species (Bacillariophyceae) in a European lake, and their ecological implications. *British Phycological Journal*, Vol. 25, pp. 217–235

Anderson, N.J. and Leng, M.J., 2004, Increased aridity during the early Holocene in West Greenland inferred from stable isotopes in laminated-lake sediments, *Quaternary Science Reviews*, Vol. 23, pp. 841-849

Anderson, R.J., Nuhler, E.B. and Dean, W.E., 1985, Sedimentation in a blast zone lake at Mount St. Helens, Washington – Implications for varve formation, *Geology*, Vol. 13, pp. 348-352

Anderson, R.Y. and Dean, W.E., 1988, Lacustrine varve formation through time, *Palaeogeography, Palaeoclimatology, Palaeoecology*, Vol. 62, pp. 215-235

Anderson, R.Y., 1996, *Seasonal sedimentation: a framework for reconstructing climatic and environmental change*, Kemp, A. E. S. (ed.), 1996, Palaeoclimatology and Palaeoceanography from Laminated Sediments, Geological Society Special Publication No. 116, pp. 1-15.

Andrews, J. E., Coletta, P., Pentecost, A., Riding, R., Dennis, S., Dennis, P. F., and Spiro, B., 2004, Equilibrium and disequilibrium stable isotope effects in modern charophyte calcites: implications for palaeoenvironmental studies, *Palaeogeography, Palaeoclimatology, Palaeoecology,* Vol. 204, pp. 101–114.

Andrews, J.E., 2006, Palaeoclimatic records from stable isotopes in riverine tufas: Synthesis and review, *Earth-Science Reviews*, Vol. 75, pp. 85-104

Andrews, J.E., Riding, R. and Dennis, P.F., 1997, The stable isotope record of environmental and climatic signals in modern terrestrial microbial carbonates from Europe, *Palaeogeography, Palaeoclimatology, Palaeoecology*, Vol. 129, pp. 171 - 189

Arhonditsis, G., Brett, M.T., Frodge, J., 2003, Environmental control and limnological impacts of a large recurrent spring bloom in Lake Washington, USA, *Environmental Management,* Vol. 31, pp. 603–618.

Arnaud, F., Révillon, S., Debret, M., Revel, M., Chapron, E., Jacob, J., Giguet-Covex, C., Poulenard, J. and Magney, M., 2012. Lake Bourget regional erosion patterns reconstruction reveals Holocene NW European Alps soil evolution and paleohydrology. *Quaternary Science Reviews* 51, 81-92.

Ashley, G.M., Shaw, J. and Smith, N.D., 1985. *Glacial Sedimentary Environments: Society of Economic Paleontologists and Mineralogists*. SEPM Short Course Notes No. 16, 246pp

Ashton, N., Lewis, S.G., Parfitt, S.A., Penkman, K.E.H., Coope, G.R., 2008, New evidence for complex climate change in MIS 11 from Hoxne, Suffolk, UK, *Quaternary Science Reviews*, Vol. 27, pp. 652-668.

Bade, D.L., Carpenter, S.R., Cole, J.J., Hanson, P.C. and Hesslein, R.H., 2004, Controls of $\delta^{13}C$ -DIC in lakes: Geochemistry, lake metabolism, and morphometry, *Limnol. Oceanogr.*, Vol. 49, pp. 1160–1172

Barber, D.C., Dyke, A., Hillaire-Marcel, C., Jennings, A.E., Andrews, J.T., Kerwin, M.W., Bilodeau, G., McNeely, R., Southon, J., Morehead, M.D. and Gagnon, J.M., 1999, Forcing of the cold event of 8,200 years ago by catastrophic drainage of Laurentide lakes, *Nature*, Vol. 400, pp. 344-348

Battarbee, R., 1981, Changes in the diatom microflora of a eutrophic lake since 1900 from a comparison of old algal samples and the sedimentary record, *Ecography,* Vol. 4, pp. 73-81

Bates, C.C., 1953. “Rational theory of delta formation”. *Bulletin American Association of Petroleum Geologists* 37, 2119-2162Battarbee, R.W. and Kneen, M.J., 1982, The use of electronically counted microspheres in absolute diatom analysis*, Limnol. Oceanogr*. Vol. 27, pp. 184-189

Bauch, H.A., Erlenkeuser, H., Spielhagen, R., Struck, U., Matthiessen, J., Thiede, J., Heinemeier, J., 2001, A multiproxy reconstruction of the evolution of deep and surface waters in the subarctic Nordic seas over the last 30,000 years, *Quaternary Science Reviews* Vol. 20, pp. 659–678

Bennett, K.D., 1983, Devensian Late-Glacial and Flandrian Vegetational History at Hockham Mere, Norfolk, England. I. Pollen Percentages and Concentrations, *New Phytologist*, Vol. 95, pp. 457-487

Bennion, H., 1994. A diatom-total phosphorous transfer function for shallow, eutrophic ponds in southeast England. *Hydrobiologia* 275/276, 391-410.

Bennion, H., Fluin, J. and Simpson, G.L., 2004. Assessing eutrophication and reference conditions for Scottish freshwater lochs using subfossil diatoms. *Journal of Applied Ecology* 41, 124-138.

Berger, A. and Loutre, M.F., 2002, An exceptionally long interglacial ahead? *Science*, Vol. 297, pp. 1287-1288.

Berger, A., Loutre, M.F., 2003, Climate 400,000 years ago, a key to the future? Earth's climate and orbital eccentricity: the Marine Isotope Stage 11 question, *Geophysical Monograph Series,* Vol. 137, pp. 17-26.

Berger, A., Yin, Q., 2012. Astronomical theory and orbital forcing. In: Matthews, J.A., Bartlein, P.J., Briffa, K.R., Dawson, A.G., de Vernal, A., Denham, T., Fritz, S.C., Oldfield, F. (Eds.), *The SAGE Handbook of Environmental Change*, vol. 1. SAGE, London, pp. 405–425.

Bernasconi, S.M. and McKenzie, J.A., 2007, Lake Sediments, IN: Elias, S (Ed), *Encyclopaedia of Quaternary Science*, Elsevier, Amsterdam, pp.351-359

Bigeleisen, J. and Mayer, M.G., 1947, Calculation of equilibrium constants for isotopic exchange reactions, *Journal of chemical physics,* Vol. 15, pp. 261-274

Birks, H.J.B., 1998. Numerical tools in palaeolimnology – progress, potentialities, and progress. *Journal of Palaeolimnology* 20, 307-332

Birks, H.H., 2003, The importance of plant macrofossils in the reconstruction of Lateglacial vegetation and climate: examples from Scotland, western Norway, and Minnesota, USA, *Quaternary Science Reviews*, Vol. 22, pp. 453-473

Bloesch, J., 2004. Sedimentation and lake sediment formation. In: O'Sullivan, P.E. and Reynolds, C.S. (eds.). *The Lakes Handbook volume 1: Limnology and Limentic Ecology*, Blackwell Publishing, 197-229

Bluszucz, P., Lucke, A., Ohlendorf, C. and Zolitschka, B., 2009, Seasonal dynamics of stable isotopes and element ratios in authigenic calcites during their precipitation and dissolution, Sacrower See, northeastern Germany), *Journal of Limnology*, Vol. 68, pp. 257-273

Boehrer, B. and Schultze, M., 2008, Stratification of lakes, *Reviews of Geophysics*, Vol. 46, RG2005, pp. 1-27

Bond, G., Kromer, B., Beer, J., Muscheler, R., Evans, M.N., Showers, W., Hoffman, S., Lotti-Bond, R., Hajdas, I. and Bonani, G., 2001, Persistent Solar Influence on North Atlantic Climate During the Holocene, *Science express*, p. 1-6, science.1065680

Bond, G., Showers, W., Cheseby, M., Lotti, R., Almasi, P., deMenocal, P., Priore, P., Cullen, H., Hajdas, I. and Bonani, G., 1997, A Pervasive Millennial-Scale Cycle in North Atlantic Holocene and Glacial Climates, *Science,* Vol. 278, pp. 1257-1266

Bouchard, F., Francus, P., Pienitz, R. and Laurion, I., 2011. Sedimentology and geochemistry of thermokast ponds in discontinuous permafrost, subarctic Quebec, Canada. *Journal of Geophysical Research* 116, G00M04

Bowen G. J. and Wilkinson B., 2002, Spatial distribution of $\delta^{18}O$ in meteoric precipitation, *Geology*, Vol. 30, pp. 315-318.

Bowen, D.Q (ed.) 1999. *A revised correlation of Quaternary deposits in the British Isles*. Geological Society of London Special Report No. 23.

Boygle, J., 1993, The Swedish varve chronology – a review, *Progress in Physical Geography*, Vol. 17, pp. 1-19

Bradbury, J.P., 1988. A climatic-limnological model of diatom succession for paleolimnological interpretation of varved sediments at Elk Lake, Minnesota. *Journal of Paleolimnology* 1, 115-131

Brauer, A., Endres, C. and Negendank, J.F.W., 1999a. Lateglacial calendar year chronology based on annually laminated sediments from Lake Meerfelder Maar, Germany. *Quaternary International* 61, 17-25

Brauer, A., Enders, C., Gunter, C., Litt, T., Stebich, M. and Negendank, J.F.W., 1999b. High resolution sediment and vegetation responses to Younger Dryas climate change in varved lake sediments from Meerfelder Maar, Germany. *Quaternary Science Reviews* 18, 321-329

Brauer, A., Enders, C., Zolitschka, B. and Negendank, J.F.W., 2000a. AMS Radiocarbon and varve chronology from the annually laminated sediment records of Lake Meerfelder Maar, Germany. *Radiocarbon* 42, 355-368

Brauer, A., Gunter, C., Johnsen, S.J., Negendank, J.F.W., 2000b. Land-ice teleconnections of cold climatic periods during the last Glacial/Interglacial transition. *Climate Dynamics* 16, 229-239

Brauer, A. and Cassanova, J., 2001, Chronology and depositional processes of the laminated sediment record from Lac d'Annecy, French Alps, *Journal of Paleolimnology*, Vol. 25, pp. 163–177

Brauer, A., 2004, Annually laminated lake sediments and their palaeoclimatic relevance. In: Fischer, H., Kumke, T., Lohmann, G. (eds.), *The Climate in Historical Times – Towards a Synthesis of Holocene Proxy Data and Climate Models*, Springer, Berlin, 109-128.

Brauer A, Wulf S, Mangili C, Moscariello A., 2007a, Tephrochronological dating of varved interglacial lake deposits from Piánico-Séllere (Southern Alps, Italy) to around 400 ka. *Journal of Quaternary Science,* Vol. 22, pp. 85–96.

Brauer, A., Wulf, S. and Mangili, C., 2007b, Reply: Tephrochonological dating of varved interglacial lake deposits from Piánico-Séllere (Southern Alps, Itlay) to around 400 ka, *Journal of Quaternary Science*, Vol. 22, pp. 415-418

Brauer, A., Allen, J.R.M., Mingram, J., Dulski, P., Wulf, S. and Huntley, B., 2007c, Evidence for last interglacial chronology and environmental change from Southern Europe, *Proceedings of the National Academy of Science*, Vol. 104, pp. 450-455

Brauer, A., Haug, G.H., Dulski, P., Sigman, D.M. and Negendank, J.F.W., 2008a. An abrupt wind shift in Western Europe at the onset of the Younger Dryas cold period. *Nature Geoscience* 1, 520-523

Brauer, A., Mangili, C., Moscariello, A. and Witt, A., 2008b. Palaeoclimatic implications from micro-facies data of a 5,900 varve time series from the Pianico interglacial sediment record, Southern Alps. *Palaeogeography, Palaeoclimatology, Palaeoecology* 259, 121-135

Brauer, A., Dulski, P., Mangili, C., Mingram, J. and Liu, J., 2009. The potential of varves in high-resolution paleolimnological studies, *PAGES news*, Vol. 17, pp. 96-99

Bridgland, D.R., 1994, *The Quaternary of the Thames*, Geological Conservation Review Series. Joint Nature Conservation Committee and Chapman & Hall, London.

Bridgland, D.R., 2000, River terrace systems in north-west Europe: an archive of environmental change, uplift and early human occupation, *Quaternary Science Reviews*, Vol. 19, pp. 1293–1303.

Broecker, W.S., Denton, G.H., Edwards, R.L., Cheng, H., Alley, R.B., Putnam, A.E., 2010, Putting the Younger Dryas cold event into context, *Quaternary Science Reviews*, Vol. 29, pp. 1078-1081.

Bronk Ramsey, C., Staff, R.A., Bryant, C.L., Brock, F., Kitagawa, H., van der Plicht, J., Schlolaut, G., Marshall, M.H., Brauer, A., Lamb, H.F., Payne, R.L., Tarasov, P.E., Haraguchi, T., Gotanda, K., Yonenobu, H., Yokoyama, Y., Tada, R. and Nakagawa, T., 2012, A complete terrestrial radiocarbon record for 11.2 to 52.8 kyr B.P., *Science*, Vol. 338, pp. 370-374

Brooks, S.J. and Birks, H.J.B., 2001. Chironomid-inferred air temperaturs from Lateglacial and Holocene sites in north-west Europe: progress and problems. *Quaternary Science Reviews* 20, 1723-1741.

Brugam, R.B., 1983. The relationship between fossil diatom assemblages and limnological conditions. *Hydrobiologia* 98, 223-235.

Brunskill, G.J., 1969, Fayetteville Green Lake, New York. II. Precipitation and Sedimentation of Calcite in a Meromictic Lake with Laminated Sediments, *Limnology and Oceanography*, Vol. 14, pp. 830-847

Butler, K., 2008. Interpreting charcoal in New Zealand's palaeoenvironment – What do those charcoal fragments really tell us? *Quaternary International* 184, 122-128

Candy, I., 2009, Terrestrial and freshwater carbonates in Hoxnian interglacial deposits, UK: micromorphology, stable isotopic composition and palaeoenvironmental significance, *Proceedings of the Geologists' Association*, Vol. 120, pp. 49-57

Candy, I., Coope, G.R., Lee, J.R., Preece, R.C., Rose, J. and Schreve, D.C., 2011, Pronounced warmth during early Middle Pleistocene interglacials: Investigating the

Mid-Bruhnes Event in the British terrestrial sequence, *Earth-Science Reviews*, Vol. 103, pp. 183–196

Candy, I., Schreve, D.C., Sherriff, J. and Tye, G.J., 2014 , Marine Isotope Stage 11: Palaeoclimates, palaeoenvironments and its role as an analogue for the current interglacial, *Earth Science Reviews*, Vol. 128, pp. 18-51

Candy, I., Schreve, D.S., 2007. Land–sea correlation of Middle Pleistocene temperate sub-stages using high-precision uranium-series dating of tufa deposits from southern England. *Quaternary Science Reviews*, 26, 1223–1235.

Candy, I., Stephens, M., Hancock, J. and Waghorne, R., 2011, Palaeoenvironments of Ancient Humans in Britain: The Application of Oxygen and Carbon Isotopes to the Reconstruction of Pleistocene Environments, IN: Ashton, N., Lewis, S.G. and Stringer, C. (Eds), *The Ancient Human Occupation of Britain,* Amsterdam, pp. 23-37

Card, V.M., 1997, Varve-counting by the annual pattern of diatoms accumulated in the sediment of Big Watab Lake, Minnesota, AD 1837-1990, *Boreas*, Vol. 26, pp. 103-112

Carr, S.J. and Lee, J.A., 1998 Thin-section production of diamicts: problems and solutions. *Journal of Sedimentary Research, Research methods papers* 68, 217-220

Cerling, T., Quade, J., Wang, Y. and Bowman, J.R., 1989, Carbon isotopes in soils and paleosoils as ecology and paleoecology indicators, *Nature*, Vol. 341, pp.138–139

Cerling, T.E. and Quade, J., 1993, Stable carbon and oxygen isotopes in soil carbonates, IN: Swart, P.K. Lohmann, K.C. McKenzie, J. and Savin, S. (Eds.), *Climate change in continental isotopic records,* Geophysical Monograph 78, American Geophysical Union, Washington, pp.217-232

Chen, G., Dalton, C., Leira, M. and Taylor, D., 2008. Diatom-based total phosphorus (TP and pH transfer functions for the Irish Ecoregion. *Journal of Paleolimnology* 40, 143-163

Clark, I. and Fritz, P., 1997, *Environmental Isotopes in Hydrogeology*, Lewis publishers, New York, p. 328

Clark, C.D., Gibbard, P.L., Rose, J. 2004, Pleistocene glacial limits in England, Scotland and Wales. In: Ehlers, J., Gibbard, P.L. (eds.), *Quaternary Glaciations - Extent and Chronology, Part I: Europe*. Elsevier Publishers, Amsterdam, 47-82.

Clark, P.U., Marshall, S.J., Clarke, G.K.C., Hostetler, S.W., Licciardi, J.M., Teller, J.T., 2001. Freshwater forcing of abrupt climate change during the last glaciation. *Science* 293 (5528), 283–287.

Clarke, G.K.C., Leverington, D.W., Teller, J. and Dyke, A.S., 2004, Paleohydraulics of the last outburst flood from glacial Lake Agassiz and the 8200 BP cold event, *Quaternary Science Reviews,* Vol. 23, pp. 389-407

Cockburn, J.M.H. and Lamoureux, S.F., 2007 Century-scale variability in late-summer rainfall events recorded over seven centuries in subannually laminated lacustrine sediments, White Pass, British Columbia, *Quaternary Research*, Vol. 67, pp. 193-203

Colleta, P., Pentecost, A. and Spiro, B., 2001, Stable isotopes in charophyte incrustations: relationships with climate and water chemistry, *Palaeogeography, Palaeoclimatology, Palaeoecology*, Vol. 173, pp. 9-19

Coxon, P. 1993. The geomorphological history of the Waveney Valley and the interglacial deposits at Hoxne. In: Singer, R., Gladfelter, B.G. and Wymer, J.J. (eds), *The Lower Palaeolithic at Hoxne, England*. The University of Chicago Press, Chicago, 67-73.

Coxon, P., 1979. *Pleistocene environmental history in central East Anglia*. PhD thesis, Cambridge University.

Coxon, P., 1985. A Hoxnian interglacial site at Athelington, Suffolk, *New Phytologist*, Vol. 99,

Craig, H., 1961, Isotopic variations in meteoric waters, *Science*, Vol. 133, pp. 1702-1703

Craig, H., 1965, Measurement of oxygen isotope palaeotemperatures, IN: Tongiorgi, E. (Ed), *Stable isotopes in oceanographic studies and palaeotemperatures*, CNR lab, Pisa, pp. 161-182

Craig, H. and Gordon, L.I., 1965, Deuterium and oxygen 18 variations in the ocean and the marine atmosphere, IN: Tongiorgi, E. (Ed), *Stable Isotopes in Oceanographic Studies and palaeotemperatures*, Spoleto, pp. 9-130

Craig, H., 1953, The geochemistry of the stable carbon isotopes, *Geochimica et Cosmochimica Acta*, Vol. 3, pp. 53-92

Croudace, I.W. and Rothwell, R.G., 2010, Micro-XRF sediment core scanners: important new tools for the environmental and earth sciences, *Spectroscopy Europe*, Vol. 22, pp. 6-13.

Croudace, I.W., Rindby, A. and Rothwell, R.G., 2006, ITRAX: description and evaluation of a new multi-function X-ray core scanner, IN: Rothwell, R.G. 2006. *New Techniques in Sediment Core Analysis*. Geological Society, London, Special Publications, Vol. 267, pp. 51–63

Czymzik, M., Brauer, A., Dulski, P., Plessen, B., Naumann, R., von Grafenstein, U. and Scheffler, R., 2013. Orbital and solar forcing of shifts in Mid- to Late Holocene flood intensity from varved sediments of pre-alpine Lake Ammersee (southern Germany). *Quaternary Science Reviews* 61, 96-110.

D. Dahl-Jensen, M.R. Albert, A. Aldahan, N. Azuma, D. Balslev-Clausen, M. Baumgartner, A. Berggren, M. Bigler, T. Binder, T. Blunier, J.C. Bourgeois, E.J. Brook, S.L. Buchardt, C. Buizert, E. Capron, J. Chappellaz, J. Chung, H.B. Clausen, I. Cvijanovic, S.M. Davies, P. Ditlevsen, O. Eicher, H. Fischer, D.A. Fisher, L.G. Fleet, G. Gfeller, V. Gkinis, S. Gogineni, K. Goto-Azuma, A. Grinsted, H. Gudlaugsdottir, M. Guillevic, S.B. Hansen, M. Hansson, M. Hirabayashi, S. Hong, S.D. Hur, P. Huybrechts, C.S. Hvidberg, Y. Iizuka, T. Jenk, S.J. Johnsen, T.R. Jones, J. Jouzel, N.B. Karlsson, K. Kawamura, K. Keegan, E. Kettner, S. Kipfstuhl, H.A. Kjær, M. Koutnik, T. Kuramoto, P. Köhler, T. Laepple, A. Landais, P.L. Langen, L.B. Larsen, D. Leuenberger, M. Leuenberger, C. Leuschen, J. Li, V. Lipenkov, P. Martinerie, O.J. Maselli, V. Masson-Delmotte, J.R. McConnell, H. Miller, O. Mini, A. Miyamoto, M. Montagnat-Rentier, R. Mulvaney, R.

Muscheler, A.J. Orsi, J. Paden, C. Panton, F. Pattyn, J. Petit, K. Pol, T. Popp, G. Possnert, F. Prié, M. Prokopiou, A. Quiquet, S.O. Rasmussen, D. Raynaud, J. Ren, C. Reutenauer, C. Ritz, T. Röckmann, J.L. Rosen, M. Rubino, O. Rybak, D. Samyn, C.J. Sapart, A. Schilt, A.M.Z. Schmidt, J. Schwander, S. Schüpbach, I. Seierstad, J.P. Severinghaus, S. Sheldon, S.B. Simonsen, J. Sjolte, A.M. Solgaard, T. Sowers, P. Sperlich, H.C. Steen-Larsen, K. Steffen, J.P. Steffensen, D. Steinhage, T.F. Stocker, C. Stowasser, A.S. Sturevik, W.T. Sturges, A. Sveinbjörnsdottir, A. Svensson, J. Tison, J. Uetake, P. Vallelonga, R.S.W. van de Wal, G. van der Wel, B.H. Vaughn, B. Vinther, E. Waddington, A. Wegner, I. Weikusat, J.W.C. White, F. Wilhelms, M. Winstrup, E. Witrant, E.W. Wolff, C. Xiao, and J. Zheng, 2013, Eemian interglacial reconstructed from a Greenland folded ice core, *Nature,* vol. 493, pp. 489-494.

Daley, T.J., Thomas, E.R., Holmes, J.A., Street-Perrott, A., Chapman, M.R., Tindall, J.C., Valdes, P.J., Loader, N.J., Marshall, J.D., Wolff, E.R., Hopley, P.J., Atkinson, T., Barber, K.E., Fisher, E.H., Robertson, I., Hughes, P.D.M. and Roberts, N.C., 2011, The 8200 yr BP cold event in stable isotope records from the North Atlantic region, *Global and Planetary Change*, Vol. 79, pp. 288-302

Dansgaard, W., White, J.W.C. and Johnsen, S.J., 1989, The abrupt termination of the Younger Dryas climate event, *Nature*, Vol. 339, pp. 532-534

Dansgaard, W., 1964, Stable isotopes in precipitation, *Tellus*, Vol. 16, pp.436–468

Dansgaard, W., Johnsen, S.J., Clausen, H.B., Dahl-Jensen, D., Gundestrup, N.S., Hammer, C.U., Hvidberg, C.S., Steffensen, J.P., Sveinbjornsdottir, A.E., Jouzel, J., Bond, G., 1993, Evidence for general instability of past climate from a 250-kyr ice-core record. *Nature*, Vol. 364, pp. 218-220.

Darling , W.G., Bath, A.H. and Talbot, J.C., 2003, The O and H stable isotopic composition of fresh waters in the British Isles. 2. Surface waters and groundwater, *Hydrology and Earth System Sciences*, Vol. 7, pp. 183-195

Darling, W.G., Edmunds, W.M. and Smedley, P.L., 1997, Isotopic evidence for palaeowaters in the British Isles, *Applied Geochemistry*, Vol. 12, pp. 813-829

Darling, W.G. and Talbot, J.C., 2003, The O and H stable isotopic composition of fresh waters in the British Isles. 1. Rainfall, *Hydrology and Earth System Sciences*, Vol. 7, pp. 163-181

Darling, W.G., 2004, Hydrological factors in the interpretation of stable isotopic proxy data present and past: a European perspective, *Quaternary Science Reviews*, Vol. 23, pp. 743-770

de Abreu, L., Abrantes, F.F., Shackleton, N.J., Tzedakis, P.C., McManus, J.F., Oppo, D.W. and Hall, M.A., 2005, Ocean climate variability in the eastern North Atlantic during interglacial marine isotope stage 11: A partial analogue to the Holocene?, *Paleoceanography*, Vol. 20, PA3009

de Vernal, A., Hillaire-Marcel, C., 2008, Natural variability of Greenland climate, vegetation, and ice volume during the past million years, *Science*, Vol. 320, pp. 1622 1625.

Dean, W.E. and Fouch, T.D., 1983, Lacustrine carbonates, IN: Scholle, P.A., Bedout, D.G. and Moore, G.H. (Eds)., *Carbonate Depositional Environments*, Am. Assoc. Pet. Geol., Mem., 33, pp. 98–130

Dean, W., Pride, C. and Thunell, R., 2004. Geochemical cycles in sediments deposited on the slopes of the Guaymas and Carmen basins of the Gulf of California over the last 1980 years. *Quaternary Science Reviews* 23, 1817-1833

Dean, J.M., Kemp, A.E.S. and Pearce, R.B., 2001, Palaeo-flux records from electron microscope studies of Holocene laminated sediments, Saanich Inlet, British Columbia, *Marine Geology*, Vol. 174, pp. 139-158

Decampo, D.M., 2010, The geochemistry of continental carbonates, IN: Alonso-Zarza, A.M. and Tanner, L.H. (eds), *Carbonates in continental settings: Geochemistry, diagenesis and applications*, Developments in Sedimentology, Vol 62, Elsevier, pp.1-60

Denton, G.H., Alley, R.B., Comer, G.C. and Broecker, W.S., 2005, The role of seasonality in abrupt climate change, *Quaternary Science Reviews*, Vol. 24, pp. 1159-1182

Desprat, S., Sanchez Goni, M.F., Turon, J.L., McManus, J.F., Loutre, M.F., Duprat, J., Malaize, B., Peyron, O. and Peypouquet, J.P., 2005, Is vegetation responsible for glacial inception during periods of muted insolation changes? *Quaternary Science Reviews*, Vol. 24, pp. 1361-1374

Dickson, B., Yashayaev, I., Meincke, J., Turrell, B., Dye, S., Holfort, J., 2002. Rapid freshening of the deep North Atlantic Ocean over the past four decades. *Nature* 416, 832-837

Dickson, A.J., Beer, C.J., Dempsey, C., Maslin, M.A., Bendle, J.A., McClymont, E.L., Pancost, R.D., 2009. Oceanic forcing of the Marine Isotope Stage 11 interglacial, *Nature Geoscience*, Vol. 2, pp. 428–433.

Diefendorf, A.F., Patterson, W.P., Holden, C. and Mullins, H.T., 2008, Carbon isotopes of marl and lake sediment organic matter reflect terrestrial landscape change during the late Glacial and early Holocene (16,800 to 5,540 cal yr BP): a multiproxy study of lacustrine sediments at Lough Inchiquin, western Ireland, *Journal of Palaeolimnology*, Vol. 39, pp. 101-115

Diefendorf, A.F., Patterson, W.P., Mullins, H.T., Tibert, N. and Martini, A., 2006; Evidence for high-frequency late Glacial to mid-Holocene (16,800 to 5,500 cal yr BP) climate variability from oxygen isotope values of Lough Inchiquin, Ireland, *Quaternary Research*, Vol. 65, pp. 78-86

Diehl, M., Sirocko, F., 2007, A new Holsteinian record from the Dry Maar at Döttingen (Eifel). In: Sirocko, F., Claussen, M., Sánchez Goñi, M.F., Litt, T. (Eds.), *The Climate of Past Interglacials*, Developments in Quaternary Science. Elsevier, Amsterdam, pp. 397–416.

Dietzel, M., Tang, J., Leis, A. and Kohler, S.J., 2009, Oxygen isotopic fractionation during inorganic calcite precipitation – Effects of temperature, precipitation rate and pH, *Chemical Geology*, Vol. 286, pp. 107-115

Dong, X, Bennion, H., Battarbee, R.W. and Sayer, C.D., 2011. A multiproxy palaeolimnological study of climate and nutrient impacts on Esthwaite Water, England over the past 1200 years. *The Holocene* 22, 107-118.

Dorfler, W., Feeser, I., van den Bogaard, C., Dreibrodt, S., Erlenkeuser, H., Kleinmann, A., Merkt, J. and Wiethold, J., 2012, A high-quality annually laminated sequence from Lake Belau, Northern Germany: Revised chronology and its implications for palynological and tephrochronological studies, *The Holocene*, 1-14

Droxler, A.W., Alley, R.B., Howard, W.R., Poore, R.Z., Burckle, L.H., 2003. *Unique and exceptionally long interglacial Marine Isotope Stage 11: window into Earth warm future climate*. Geophysical Monograph Series 137, 1-14.

Droxler, A.W., Farrell, J.W., 2000, Marine Isotope Stage 11 (MIS 11): new insights for a warm future, *Global and Planetary Change*, Vol. 24, pp. 1–5.

Drummond, C.N., Patterson, W.P. and Walker, J.S.G., 1995, Climatic forcing of carbon-oxygen isotopic covariance in temperate-region marl lakes, *Geology*, Vol. 23, pp. 1031-1034

Duigan, S., 1956, Pollen analysis of the Nechells interglacial deposit, Quaternary Journal of the Geological Society, Vol. 112

Eastmond, W.J., Leng, M.J., Roberts, N. and Davies, B., 2007. Holocene climate change in the eastern Mediterranean region: a comparison of stable isotope and pollen data from Lake Golhisar, southwest Turkey. *Journal of Quaternary Science* 22, 327-341

Ebbeson, H., Kuijpers, A., Moros, M., Lloyd, J., Seidenkrantz, M.S. and Troelstra, S., 2008, The 8.2 ka cooling event related to extensive melting of the Greenland Ice Sheet, *Climate of the Past Discussions*, Vol. 4, pp. 1219-1235

Edwards, K.J., Whittington, G. and Tipping, R., 2000. The incidence of microscopic charcoal in late glacial deposits. *Palaeogeography Palaeoclimatology Palaeoecology* 164, 263–278.

Edwards, K.J., Langdon, P.G. and Sugden, H., 2007, Seperating climatic and possible human impacts in the early Holocene: biotic response around the time of the 8200 cal. Yr BP event, *Journal of Quaternary Science*, Vol. 22, pp. 77-84

Ehlers, J. and Gibbard, P.L. 2011. Quaternary glaciation. In: Singh, V.P. and Haritashya, U.K. (Eds.). *Encyclopedia of snow, ice and Glaciers*. Springer: Berlin, 659 pp.

Ellison, R.A., and Lake, R.D., 1986, Geology of the country around Braintree, *Memoir of the British Geological Survey,* Sheet 223 (England and Wales)

Ellison, C.R.W., Chapman, M.R. and Hall, I.R., 2006, Surface and deep ocean interactions during the cold climate event 8200 years ago, *Science*, Vol. 312, pp. 1929-1932

Emiliani*, C,.* 1955, Pleistocene temperatures, *Journal of Geology*, Vol. 63, pp. 538-557

EPICA community members, 2004, Eight glacial cycles from an Antarctic ice core, *Nature,* Vol. 429, pp. 623-628.

Epstein, S., Buchsbaum, R., Lowenstam, H.A. and Urey, H.C., 1953, Revised carbonate-water isotopic temperature scale, *Geological Society of America Bulletin*, Vol. 64, pp. 1315-1325

Erten, H.N., von Gunten, H.R., Rossler, E., Sturm, M., 1985, Dating of sediments from Lake Zurich (Switzerland) with ^{210}Pband ^{137}Cs, *Schwiz. Z. Hydrol*., Vol. 47 , pp. 5–11

Evans, D. J. A. & Benn, D. I., 2004, *A Practical Guide to the Study of Glacial Sediments*, Arnold.

Evans, G.H., 1972, The diatom flora of the Hoxnian deposits at Marks Tey, Essex, *New Phytologist*, Vol. 71, pp. 379-386

Firestone, R.B., West, A., Kennett, J.P., Becker, L., Bunch, T.E., Revay, Z.S., Schultz, P.H., Belyga, T., Kennett, D.J., Erlandson, J.M., Dickenson, O.J., Goodheay, A.C., Harris, R.S., Howard, G.A., Kloosterman, J.B., Lechler, P., Mayewski, P.A., Montgomery, J., Poreda, R., Darrah, T., Que Hee, S.S., Smith, A.R., Stich, A., Topping, W., Wittke, J.H., Wolbach, W.S., 2007, Evidence for an extraterrestrial impact 12,900 years ago that contributed to the megafaunal extinctions and the Younger Dryas cooling, *Proceedings of the National Academy of Sciences*, Vol. 4, pp. 16016-16021.

Fleitmann, D., Mudelsee, M., Burns, S.J., Bradley, R.S., Kramers, J. and Matter, A., 2008. Evidence for a widespread climatic anomaly at around 9.2 ke before present. *Paleoceanography* 23, PA1102.

Flower , R.J., Keatings, K., Hamdan, M., Hassan, F.A., Boyle, J.D., Yamada, K. and Yasuda, Y., 2012, The structure and significance of early Holocene laminated lake sediments in the Faiyum Depression (Egypt) with special reference to diatoms, *Diatom Research*, Vol. 27, pp. 127-140

Folk, R.L., 1974, *Petrology of sedimentary rocks*, The Walter Geology Library, Texas,

Francus, P., Ojala, A.E.K., Heinsalu, A., Behl, R., Grosjean, M. and Zolitschka, B., 2009. Advances in varved sediment studies during the last 10 years. *PAGES news* 18, 90-91

Fricke, H.C. and O'Neil, J.R., 1999, The correlation between $^{18}O/^{16}O$ ratios in meteoric water and surface temperature: its use in investigating terrestrial climate change over geologic time, *Earth Planetary Science Letters*, Vol. 170, pp. 181-196

Friedli, H. Lötscher, H., Oeschger, Siegenthaler, U., Stauffer, B., 1986, Ice core record of the $^{13}C/^{12}C$ ratio of atmospheric CO_2 in the past two centuries. *Nature,* Vol. 324, pp. 237–239

Freidman, O'Neil, J.R. and Cebula, G., 1982, Two new carbonate stable isotope standards. *Geostandard Newsletter* 6, 11-12

Fronval, T., Jensen, N.B. and Buchardt, B., 1995, Oxygen isotope disequilibrium precipitation of calcite in Lake Arreso, Denmark, *Geology*, Vol. 23, pp. 463-466

Gale, S. and Hoare, P., 1992, *Quaternary Sediments: Petrographic methods for the study of unlithified rocks,* John Wiley and Sons, London, 332 pp

Galloway, J.M., Lenny, A.M. and Cumming, B.F., 2011. Hydrological change in the central interior of British Columbia, Canada: diatom and pollen evidence of millennial-to-centennial scale changes over the Holocene. *Journal of Paleolimnology* 45, 183-197

Gat, I. and Gonfiantini, R., 1981, Stable isotope hydrology: deuterium and oxygen 18 in the water cycle, Int. Atom. Energy Agency, Vienna, Technical Report, p. 339

Gat, J.R., 1996, Oxygen and Hydrogen isotopes in the hydrological cycle, *Annual Review Earth Planetary Science*, Vol. 24, pp. 225-262

Gauthier, A. and Muñoz, A., 2009, Seasonal sedimentation in the Pliocene Villarroya Lake (N Spain) inferred from pollen analysis*, Sedimentary Geology*, Vol. 222, pp. 111-123

De Geer, G., 1912, Geochronologie der letzten 12,000 Jahre: Geologische Rundschau, *Zeitschrift fur allegemeine Geologie*, Vol. 3, pp. 457-47

Geyh, M.A. and Muller, H., 2005 Numerical 230^{Th}/U dating and a palynological review of the Holsteinian/Hoxnian Interglacial, *Quaternary Science Reviews,* Vol. 24, pp. 1861-1872

Geyh, M.A. and Muller, H., 2006, Missing evidence for two Holstein-like interglacials. Reply to the comments by J.D. Scourse on: Numerical ^{230}Th/U dating and a palynological review of the Holsteinian/Hoxnian interglacial, *Quaternary Science Reviews*, Vol. 25, pp. 3072-3073.

Ghilardi, B. and O'Connell, M., 2013, Early Holocene vegetation and climate dynamics with particular reference to the 8.2 ka event: pollen and macrofossil evidence from a small lake in western Ireland, *Vegetation history and Archaeobotany*, Vol. 22, pp. 99-114

Gibbard, P.L. and Clark, C.D., 2011, Pleistocene glaciation limits in Great Britain, IN: Ehlers, J., Gibbard, P.L. and Hughes, P.D. (eds), *Quaternary Glaciations – Extent and chronology, Developments in Quaternary Science*, Vol. 15, Elsevier, Amsterdam

Gibbard, P.L. and Head, M.J., 2010, The newly-ratified definition of the Quaternary System/Period and redefinition of the Pleistocene Series/Epoch, and comparison of proposals advanced prior to formal ratification. *Episodes* 33, pp. 52-158.

Gibson, C. E., Anderson, N. J., and Haworth, E. Y.:, 2003, *Aulacoseira subarctica* : taxonomy, physiology, ecology and palaeoecology, *European Journal of Phycol*ogy, Vol. 38, pp. 83–101.

Giesecke, T., Bennett, K.D., Birks, H.J.B., Bjune, A.E., Bozilova, E., Feurdean, A., Finsinger, W., Froyd, C., Pokorny, P., Rosch, M., Seppa, H., Tonkov, S., Valsecchi, V. and Wolters, S., 2011, The pace of Holocene vegetation change – testing for synchronous developments, *Quaternary Science Reviews,* Vol. 20, pp. 2805-2814

Giguet-Covex, C., Arnaud, F., Poulenard, J., Enters, D., Reyss, J.L., Millet, L., Lazzaroto, J. and Vidal, O., 2010, Sedimentological and geochemical records of past trophic state and hypolimnetic anoxia in large, hard-water Lake Bourget, French Alps, *Journal or Paleolimnology*, Vol. 43, pp. 171-190

Goslar, T., Arnold, M., Tisnerat-Laborde, N., Hattè, C., Paterne, M. and Ralska-Jasiewiczowa, M., 2000, Radiocarbon calibration by means of varves versus ^{14}C ages of terrestrial macrofossils from lake Gościaź and lake Peresplino, Poland, *Radiocarbon,* Vol. 42, pp. 335-349

Gruenert, U. and Raeder, U., 2014. Growth responses of the calcite-loricared freshwater phytoflagellate *Phacotus lenticularis* (Chlorophyta) to the$CaCO_3$ saturation state and meteorological changes. *Journal of Planktonic Research*, Vol. 36, pp. 630-640

Grün, R., Schwarcz, H.P. 2000, Revised open system U-series/ESR age calculations for teeth from Stratum C at the Hoxnian Interglacial type locality, England, *Quaternary Science Reviews*, Vol. 19, pp. 1151-1154.

Guyard, H., Chapron, E., St-Onge, G., Anselmetti, F.S., Arnaud, F., Magand, O., Francus, P. and Mélières, M.A., 2007, High-altitude varve records of abrupt environmental changes and mining activity over the last 4000 years in the Western French Alps (Lake Bramant, Grandes Rousses Massif), *Quaternary Science Reviews*, Vol. 26, pp. 2644-2660

Hajdas, I., Zolitschka, B., Ivy-Ochs, S.D., Beer, J., Bonani, G., Leroy, S.A.G., Negendank, J.W., Ramrath, M. and Suter, M., 1995, AMS Radiocarbon dating of annually laminated sediments from Lake Holzmaar, Germany, *Quaternary Science Reviews*, Vol. 14, pp. 137-143

Hakanson, L. and Jansson, M., 1983, *Principles of Lake Sedimentology*, Springer-Verlag, Berlin, p. 320

Haflidason, H., Sejrup, H.P., Kristensen, D.K., Johnsen, S., 1995. Coupled response of the late glacial climatic shifts of northwest Europe reflected in Greenland ice cores: Evidence from the northern North Sea. *Geology 23*, 1059-1062.

Hammarlund, D. and Lemdahl, G., 1994, A Late Weichselian stable isotope stratigraphy compared with biostratigraphical data: A case study from southern Sweden, *Journal of Quaternary Science,* Vol. 9, pp. 13-31

Hammarlund, D., 1993, A distinct $\delta^{13}C$ decline in organic lake sediments at the Pleistocene-Holocene transition in southern Sweden, *Boreas,* Vol. 22, pp. 236-243.

Hammarlund, D., Aravena, R., Barnekow, L., Buchardt, B. and Possnert, G., 1997, Multi-component carbon isotope evidence of early Holocene environmental change and carbon-flow pathways from a hard-water lake in northern Sweden, *Journal of Palaeolimnology*, Vol. 18, pp. 219-233

Hammarlund, D., Barnekow, L., Birks, H.J.B., Buchardt, B. and Edwards, T.W.D., 2002, Holocene changes in atmospheric circulation recorded in the oxygen-isotope stratigraphy of lacustrine carbonates from northern Sweden, *The Holocene*, Vol. 12, pp. 339-351

Hammarlund, D., Bjork, S., Buchardt, B. and Thomsen, C.T., 2005, Limnic responses to increased effective humidity during the 8200 cal. Yr BP cooling event in southern Sweden, *Journal of Palaeolimnology*, Vol. 34, pp. 471-480

Hardy, J.T., 2003. *Climate Change: Causes, Effetcs, and Solutions*. Wiley, 247pp.

Haug, G.H., Gunther, D., Peterson, L.C., Sigman, D.M., Hughen, K.A. and Aeschlimann, B. 2003. Climate and the collapse of Maya civilization. *Science* 299: 1731-1735.

Haug, G.H., Hughen, K.A., Sigman, D.M., Peterson, L.C. and Rohl, U. 2001. Southward migration of the intertropical convergence zone through the Holocene. *Science* 293: 1304-1308.

Hays, J.D., Imbrie, J., Shackleton, N.J., 1976, Variations in the earth's orbit: pacemaker of the Ice Ages, *Science*, Vol. 194, pp. 1121-1132.

Hays, P.D. and Grossman, E.L., 1991, Oxygen isotopes in meteoric calcite cements as indicators of continental palaeoclimate, *Geology*, Vol 19, pp. 441-444

Hede, M.F, Rasmussen, P., Noe-Nygaard, N., Clarke, A.L., Vinebrooke, R.D. and Olsen, J., 2010. Multiproxy evidence for terrestrial and aquatic ecosystem responses during the 8.2 ka cold event as recorded at Hojby So, Denmark. *Quaternary Research* 73, 485-496

Hede, M.U., Rasmussen, P., Noe-Nygaard, N., Clarke, A.L., Vinebrooke, R.D. and Olsen, J., 2010, Multiproxy evidence for terrestrial and aquatic ecosystem responses during the 8.2 ka cold event as recorded at Højby Sø, Denmark, *Quaternary Research*, Vol. 73, pp. 486-496

Heinrich, H., 1988. Origin and consequences of cyclic ice rafting in the northeast Atlantic Ocean during the past 130,000 years. *Quaternary Research* 29, 142-152

Hennekam, R. and de Lange, G., 2012, X-ray fluorescence core scanning of wet marine sediments: methods to improve quality and reproducibility of high-resolution palaeoenvironmental records, Limnology and Oceanography: Methods, Vol. 10, pp. 991, 1003

Hennekam, R. and Lange, G., 2012. X-ray fluorescence core scanning of wet marine sediments: methods to improve quality and reproducibility of high-resolution paleoenvironmental records. *Limnology and Oceanography: Methods* 10, 991-1003

Herczeg, A.L., 1988, Early diagenesis of organic matter in lake sediments: A stable carbon isotope study of pore waters, *Chemical Geology*, Vol. 72, pp. 199-209

Higgins, P. and MacFadden, B.J., 2004, ''Amount Effect'' recorded in oxygen isotopes of Late Glacial horse (*Equus*) and bison (*Bison*) teeth from the Sonoran and Chihuahuan deserts, southwestern United States, *Palaeogeography, Palaeoclimatology, Palaeoecology*, Vol. 206, pp. 337– 353

Hill, M.O. and Gauch, H.G., 1980. Detrended Correspondence Analysis: An Improved Ordination Technique. *Vegetation* 42, 47-58

Hillaire-Marcel, C., de Vernal, A. and Piper, D.J.W., 2007, Lake Agassiz final drainage event in the northwest North Atlantic, Geophysical Research Letters, Vol. 34, L15601

Hutchinson, G.E., 1967. *A Treatise on Limnology, Vol. II. Introduction to Lake Biology and the Limnoplankton*. John Wiley and Son's, 310pp

Hodell, D.A., Schelske, C.L., Fahnenstiel, G.L. and Robbins, L.L., 1998. Biologically induced calcite and it isotopic composition in Lake Ontario. *Limnology and Oceanography* 43, 187-199.

Hoefs, J., 1997, *Stable isotope geochemistry*, 6th Edition, Springer, Berlin, p.285

Hoffman, J.S., A.E. Carlson, K. Winsor, G.P. Klinkhammer, A.N. LeGrande, J.T. Andrews, and J.C. Strasser, 2012, Linking the 8.2 ka event and its freshwater forcing in the Labrador Sea, *Geophysical Research Letters*, Vol. 39, L18703

Hollander, D.J. and McKenzie, J.A., 1991, CO_2 control on carbon-isotope fractionation during aqueous photosynthesis: A paleo-pCO_2 barometer, *Geology*, Vol. 19, pp. 929-932

Holmes, J., Lowe, J., Wolff, E. and Srokosz, M., 2011, Rapid climate change: lessons from the recent geological past, *Global and Planetary Change*, Vol. 79, pp. 157-162

Horita, J. and Wesolowski, D.J., 1994, Liquid-vapor fractionation of oxygen and hydrogen isotopes of water from the freezing to the critical temperature, *Geochimica Cosmochimica Acta*, Vol. 58, pp. 3425-3437

Horne, A.J. and Goldman, C.R., 1983, *Limnology*, McGraw-Hill Book Co, New York, p. 464

Horton, A., 1974. The sequence of Pleistocene deposits proved during the construction of the Birmingham motorways. *Report of the Institute of Geological Sciences* 74/11, HMSO, London, 1-21

Horton, A., 1989. Quinton. In D.H. Keen (ed.) *The Pleistocene of the West Midlands. Field Guide*. Quaternary Research Association, Cambridge, 69-76.

Howard, W.R., 1997, A warm future in the past, *Nature*, Vol. 388, pp. 418-419.

Hu, F.S., Slawinski, D., Wright, H.E., Ito, E., Johnson, R.G., Kelts, K.R., McEwan, R.F. and Boedlghelmer, A., 1999, Abrupt changes in North American climate during early Holocene times, *Nature*, Vol. 400, pp. 437-440

Hughen, K.A., Overpeck, J.T., Peterson, L.C. and Anderson, R.F., 1996, The nature of varved sedimentation in the Cariaco Basin, Venezuela, and its palaeoclimatic significance, *Geological Society, London, Special Publications ,* Vol. 116, pp. 171-183

Hurrell, J.W., Kushnir, Y., Otterson, G. and Visbeck, M., 2003. An overview of the North Atlantic Oscillation. In Hurrell, J.W., Kushnir, Y., Otterson, G. and Visbeck, M., (eds.). *The North Atlantic Oscillation: Climatic Significance and Environmental Impact*. American Geophysical Union Geophysical Monograph Series 134, 279pp.

Huttunen, P., 1980, Early land use, especially the slash-and-burn cultivation in the commune of lammi, southern Finland, interpreted mainly from using pollen and charcoal analyses, *Acta Botanica Fennica*, Vol. 113, pp. 1-45.

Imbrie, J., 1985, A theoretical framework for the Pleistocene ice ages, *Geological Society of London Journal*, Vol. 142, pp. 417-432

Imbrie, J., Berger, A., Boyle, E.A., Clemens, S.C., Duffy, A., Howard, W.R., Kukla, G., Kutzbach, J., Martinson, D.G., McIntyre, A., Mix, A.C., Molfino, B., Morley, J.J., Peterson, L.C., Pisias, N.G., Prell, W.L., Raymo, M.E., Shackleton, N.J., Toggweiler, J.R., 1993, On the structure and origin of major glaciation cycles. Part 2: The 100,000-year cycle, *Paleoceanography*, Vol. 8, pp. 699-735.

Imbrie, J., Boyle, E.A., Clemens, S.C., Duffy, A., Howard, W.R., Kukla, G., Kutzbach, J., Martinson, D.G., MvIntyre, A., Mix, A.C., Molfino, B., Morley, J.J., Peterson, L.C., Pisias, N.G., Prell,W.L., Raymo, M.E., Shackleton, N.J., Toggweiler, J.R., 1992, On the structure and origin of major glaciation cycles 1. Linear responses to Milankovitch forcing, *Paleoceanography*, Vol. 7, pp. 701–738.

Imbrie, J., Shackleton, N.J., Pisias, N.G., Morley, J.J., Prell, W.L., Martinson, D.G., Hays, J.D., MacIntyre, A., Mix, A.C., 1984. The orbital theory of Pleistocene climate: support from a revised chronology of the marine $\delta^{18}O$ record. In: Berger, A. (ed.) *Milankovitch and climate*, Part 1. Reidel, Hingham, Massachusetts, 269-305.

IPCC, 2007. IPCC Fourth Assessment Report – Climate Change, The Scientific Basis, Cambridge University Press, Cambridge.

Ito, E., 2001, Application of stable isotope techniques to inorganic and biogenic carbonates, IN: Last, W.M. and Smol, J.P. (Eds), *Tracking environmental change using lake sediments, Vol. 2, Physical and Geochemical Methods,* Kluwer, Dordrecht, pp. 351-371

Johnsen, S., Clausen, H., Dansgaard, W., Fuhrer, K., Gundestrup, N., Hammer, C., Iversen, P., Jouzel, J., Stauffer, B., Steffensen, J., 1992, Irregular glacial interstadials recorded in a new Greenland ice core, *Nature*, Vol. 359, pp. 311 –313

Jones, A.P., Tucker, M.E. and Hart, J., 1999. *The Description & Analysis of Quaternary Stratigraphic Field Scetions. Technical Guide No. 7*. Quaternary Research Association, London, 295pp

Jones, M.D., Leng, M.J., Roberts, C.N. and Turkes, M. and Moyeed, R., 2005. A coupled calibration and modelling approach to the understanding of dry-land lake oxygen isotope records. *Journal of Paleolimnology* 34, 391-411

Jones, R.T., Marshall, J.D., Fisher, E., Hatton, J., Patrick, C., Anderson, K., Lang, B., Bedford, A. and Oldfield. Controls on lake level in the early to mid Holocene, Hawes Water, Lancashire, UK. *The Holocene,* 1-12

Jones, R.L. and Keen, D.H., 1993, *Pleistocene Environments in the British Isles*, Chapman and Hall, London, 346 pp.

Jouzel, J., V. Masson-Delmotte, O. Cattani, G. Dreyfus, S. Falourd, G. Hoffmann, B. Minster, J. Nouet, J. M. Barnola, J. Chappellaz, H. Fischer, J. C. Gallet, S. Johnsen, M. Leuenberger, L. Loulergue, D. Luethi, H. Oerter, F. Parrenin, G. Raisbeck, D. Raynaud, A. Schilt, J. Schwander, E. Selmo, R. Souchez, R. Spahni, B. Stauffer, J. P. Steffensen, B. Stenni, T.F. Stocker, J.-L. Tison, M. Werner, Wolff, E.W., 2007. Orbital and millennial Antarctic climate variability over the past 800,000 years, *Science,* pp. 793-796.

Karner, D.B. and Marra, F., 2003. $^{40}Ar/^{39}Ar$ Dating of Glacial Termination V and the Duration of Marine Isotope Stage 11. In: Droxler, A.W., Poore, R.Z. and Burkle, L.H. (eds.). *Earth's Climate and Orbital Eccentricity: The Marine Isotope Stage 11 Question. Geophysical Monograph Series* 137, 61-68

Kandiano, E.S., Bauch, H.A., Fahl, K., Helmke, J.P., Röhl, U., Pérez-Folgado, M., Cacho, I., 2012, The meridional temperature gradient in the eastern North Atlantic during MIS 11 and its link to the ocean–atmosphere system, *Palaeogeography, Palaeoclimatology, Palaeoecology*, Vol. 333–334, pp. 24–39.

Kandiano, E.S., Bauch, H.A., Fahl, K., Helmke, J.P., Röhl, U., Pérez-Folgado, M., Cacho, I.,

Keen, D.H., 2001, Towards a late Middle Pleistocene non-marine molluscan biostratigraphy for the British Isles, *Quaternary Science Reviews*, Vol. 20, pp. 1657-1665.

Kelly, M.R., 1964, The Middle Pleistocene of North Birmingham, *Philosophical Transactions of the Royal Society of London*, Vol. B247, pp. 533-592.

Kelts, K. and Hsu, K.J., 1978. Freshwater carbonate sedimentation. In: Lerman, A. (ed.), *Lakes: Chemistry, Geology, Physics*, 295-323

Kendall, C. and Caldwell, E.A., 1998. Fundamentals of Isotope Geochemistry. In: Kendall, C. and McDonnell, J.J. (eds.), *Isotope Tracers in Catchment Hydrology*, Elsevier, 839pp

Kent, M. and Coker, P., 1994. Vegetation description and analysis: A practical approach. Wiley, Chichester, 384pp

Kerwin, M.W., 1996. A regional stratigraphic isochron (ca 8000 C-14 yr BP) from final deglaciation of Hudson Strait. *Quaternary Research* 46, 89-98

Kienel, U., Schwab, M.J. and Schettler, G., 2005, Distinguishing climatic from direct anthropogenic influences during the past 400 years in varved sediments from Lake Holzmaar (Eifel, Germany), *Journal of Paleolimnology,* Vol. 33, pp. 327-347

Kilham, S., Theriot, E. and Fritz, S., 1996. Linking planktonic diatoms and climate change in the large lakes of the Yellowstone ecosystem using resourse theory. *Limnology and Oceanography* 41, 1052-1062

Kim, S.T. and O'Neil, J.R., 1997, Equilibrium and nonequilibrium oxygen isotope effects in synthetic carbonates, *Geochimica et Cosmochimica Acta*, Vol. 61, pp.3461-3475

Kirilova, E.P., van Hardenbroek, M., Heiri, O., Cremer, H. and Lotter, A.F., 2010. 500 years of trophic-state history of a hypertrophic Dutch dike-breach lake. *Journal of Paleolimnology* 43, 829-842

Kirilova, E.P., Bluszcz, P., Heiri, O., Cremer, H., Ohlendorf, C., Lotter, A.F. and Zolitschka, B., 2008, Seasonal and interannual dynamics of diatom assemblages in Sacrower See (NE Germany): a sediment trap study, *Hydrobiologia,* Vol. 614, pp. 159-170

Kleiven, H.F., Kissel, C., Laj, C., Ninnemann, U.S., Richter, T.O. and Cortijo, E., 2008. Reduced North Atlantic Dep Water coeval with the glacial Lake Agassiz freshwater outburst. *Science* 319, 60-64

Kobashi, T., Severunghaus, J.P. and Baronla, J.M., 2007, 4±1.5˚C abrupt warming 11,270 yr ago identified from trapped air in Greenland ice, *Earth and Planetary Science Letters*, Vol. 268, pp. 397-407

Korhola, A., Weckström, J., Holström, L. and Erästö, P., 2000, A quantitative Holocene Climatic record from diatoms in Northern Fennoscandia, *Quaternary Research*, Vol. 54, pp. 284-294

Koutsodendris, A., Brauer, A., Pälike, H., Müller, U.C., Dulski, P., Lotter, A.F., Pross, J., 2011, Sub-decadal- to decadal-scale climate cyclicity during the Holsteinian interglacial (MIS 11) evidenced in annually laminated sediments, *Climate of the Past*, Vol. 7, pp. 987–999.

Koutsodendris, A., Müller, U.C., Pross, J., Brauer, A., Kotthoff, U., Lotter, A.F., 2010, Vegetation dynamics and climate variability during the Holsteinian interglacial based on a pollen record from Dethlingen (northern Germany), *Quaternary Science Reviews*, Vol. 29, pp. 3298–3307.

Koutsodendris, A., Pross, J., Muller, U.C., Brauer, A., Fletcher, W.J., Kuhl, N., Kirilova, E., Verhagen, F.T.M., Lucke, A. and Lotter, A.F., 2012, A short-term climate oscillation during the Holsteinian interglacial (MIS 11c): An analogy to the 8.2ka climatic event?, *Global and Planetary Change*, Vol. 92-93, pp. 224-235

Krammer, K. and Lange-Bertalot, H., 1988. *Süßwasserflora von Mitteleuropa, 2/2 Bacillariophyceae, 2. Teil: Bacillariaceae, Epithemiaceae, Surirellaceae.* New York: Gustav Fischer Verlag, 596 pp.

Krammer, K. and Lange-Bertalot, H., 1991. *Süßwasserflora von Mitteleuropa, 2/3 Bacillariophyceae, 3. Teil: Centrales, Fragilariaceae, Eunotiaceae.* Berlin: Gustav Fischer Verlag, 576 pp.

Krammer, K. and Lange-Bertalot, H., 1991. *Süßwasserflora von Mitteleuropa, 2/4 Bacillariophyceae, 4. Teil: Achnanthaceae Kritische Ergansungen zu Achnanthes s.l, Navicula s.str., Gomphonema.* Berlin: Gustav Fischer Verlag, 437 pp.

Krammer, K. and Lange-Bertalot, H., 1999. *Süßwasserflora von Mitteleuropa, 2/1 Bacillariophyceae, 1. Teil: Naviculaceae*. New York: Gustav Fischer Verlag, 876 pp.

Kuenen, P.H., 1951. Properties of turbidity currents of high density. *Society of Economic Paleontologists and Mineralogists* Special Publication 2, 14-33

Kukla, G., 2003, Continental records of MIS 11. Earth's climate and orbital eccentricity: the Marine Isotope Stage 11 question, *Geophysical Monograph Series*, Vol. 137, pp. 207–211.

Lajeunesse, P. and St-Onge, G., 2008. The subglacial origin oft he Lake Agassiz-Ojibway final outburst flood. *Nature Geoscience* 1, 184-188

Lambert, A. and Hsu,K., 1979. Non-annual cycles of varve-like sedimentation in Walensee, Switzerland. *Sedimentology* 26, 453-461

Lamoureux, S., 2001. Varve chronology techniques. In: Last, W.M. and Smol, J.P. (eds.), *Tracking Environmental Change Using Lake Sediments: Physical and Geochemical Techniques, Developments in Paleoenvironmental Research* 1, 247-260.

Lamoureux, S. and Bradley, R.S., 1996, A late Holocene varved sediment record of environmental change from northern Ellesmere Island, Canada, *Journal of Palaeolimnology*, Vol. 16, pp. 239-255

Lamoureux, S., 1999, Spatial and interannual variations in sedimentation patterns recorded in nonglacial varved sediments from the Canadian High Arctic, *Journal of Palaeolimnology*, Vol. 21, pp. 73-84

Lampert, W., Fleckner, W., Rai, H. and Taylor, E., 1986. Phytoplankton control by grazing zooplankton: A study on the spring clear-water phase. *Limnology and Oceanography* 31, 478-490

Lang, B., Brooks, S.J., Bedford, A., Jones, R.T., Birks, H.J.B., Marshall, J.D., 2010, Regional consistency in Lateglacial chironomid-inferred temperatures from five sites in north-west England, *Quaternary Science Reviews*, Vol. 29, pp.1528-1538.

Larsen, C.P.S. and MacDonald, G.M., 1993, Lake morphometry, sediment mixing and the selection of sites for fine resolution palaeoecological studies, *Quaternary Science Reviews*, Vol. 12, pp. 781-792

Laskar, J., Robutel, P., Joutel, F., Gastineau, M., Correia, A.C.M., Levrard, B., 2004, A longterm numerical solution for the insolation quantities of the Earth, *Astronomy and Astrophysics*, Vol. 428, pp.261–285
(Data accessed through http://www.imcce.fr/Equipes/ASD/insola/earth/earth.html).

Lawrence, K.T., Herbert, T.D., Brown, C.M., Raymo, M.E. and Haywood, A.M., 2009, High-amplitude variations in North Atlantic sea surface temperature during the early Pliocene warm period, *Paleoceanography*, Vol. 24, PA001669

Leemann, A. and Niessen, F., 1994, Varve formation and the climatic record in an Alpine proglacial lake: calibrating annually- laminated sediments against hydrological and meteorological data, *The Holocene,* Vol. 4, pp. 1-8.

Lehman, J.T., 1975. Reconstructing the rate of accumulation of lake sediment: The effect of sediment focusing. *Quaternary Research* 4, 541-550.

Lehmann, M.F., Bernasconi, S.M. and McKenzie, J.A., 2004, Seasonal variation of the $\delta^{13}C$ and $\delta^{15}N$ of particulate and dissolved carbon and nitrogen in Lake Lugano: Constraints on biogeochemical cycling in a eutrophic lake, *Limnological Oceanography*, Vol. 49, pp. 415-429

Leng, M.J., Roberts, N., Reed, J.M. and Sloane, H.J., 1999. Late Quaternary palaeohydrology of the Konya Basin, Turkey, based on isotopes studies of modern hydrology and lacustrine carbonates. *Journal of Paleolimnology* 22, 187-204

Leng , M.J., Lamb, A.L., Heaton, T.H.E., Marshall., J.D., Wolfe, B.B., Jones, M.D., Holmes, J.A. and Arrowsmith, C., 2006. Isotopes in lake sediments. In: Leng, M.J. (ed). *Isotopes in Palaeoenvironmental Research*, Springer, 147-

Leng, M.J., 2003. Stable isotopes in lakes and lake sediment archives. In: Mackay, A., Battarbee, R., Birks, J. and Oldfield, F. (eds.). *Global Change during the Holocene*. Arnold Publishers, London, 124-139

Leng, M.J. and Marshall, J.D., 2004, Palaeoclimate interpretation of stable isotope data from lake sediment archives. *Quaternary Science Reviews*, Vol. 23, pp. 811–831

Leng, M.J., Jones, M.D., Frogley, M.R., Eastwood, W.J., Kendrick, C.P. and Roberts, N.C., 2010, Detrital carbonate influences on bulk oxygen and carbon isotope composition of lacustrine sediments from the Mediterranean, *Global and Planetary Change*, Vol. 71, pp. 175-182

Leonard, E.M., 1997, The relationship between glacial activity and sediment production: evidence from a 4450-year varve record of neoglacial sedimentation in Hector Lake, Alberta, Canada*, Journal of Paleolimnology*, Vol. 17, pp. 319-330

Leuenberger, M.C., Lang, C., Schwander, J., 1999. $\delta^{18}O$ measurements as a calibration tool for the paleothermometer and gas-ice differences: a case study for the 8200 BP event on GRIP ice. *Journal of Geophysical Research- Atmospheres* 104, 22163-22170

Lewis, J., 1983, Cysts and sediments: *Gonyaulax polyedra (Lingulodinium Machaerophorum)* in Loch Creran, *J. mar. biol. Ass. U.K.*, Vol. 68, pp. 701-714

Li, H.C. and Ku, T.L., 1997, $\delta^{13}C - \delta^{18}O$ covariance as a paleohydrological indicator for closed-basin lakes, *Palaeogeography, Palaeoclimatology, Palaeoecology*, Vol. 133, pp. 69-80

Lindell, T., 1980. Hydrographic characteristics. In: Welch, R. (ed). *Ecological Effect of Waste Water, 16-47*

Lisiecki, L.E. and Raymo, M.E., 2005, A Pliocene-Pleistocene stack of 57 globally distributed benthic $\delta^{18}O$ records, *Palaeoceanography*, Vol. 20, PA1003

Litt, T., Brauer, A., Goslar, T., Merkt, J., Balanga, K., Müller, H., Ralska-Jasiewiczowa, M., Stebich, M. and Negendank, J.F.W., 2001, Correlation and synchronisation of Lateglacial continental sequences in northern central Europe based on annually laminated lacustrine sediments, *Quaternary Science Reviews*, Vol. 20, pp. 1233-1249

Litt, T., Scholzel, C., Kuhl, N. and Brauer, A., 2009. Vegetation and climate history in the Westeifel Volcanic Field (Germany) during the past 11,000 years based on annually laminated lacustrine maar sediments. *Boreas* 38, 679-690

Lotter, A.F. and Lemcke, G., 1999, Methods for preparing and counting biochemical varves, *Boreas*, Vol. 28, pp. 243- 252

Lotter, A.F., 1989a, Evidence of annual layering in Holocene sediments of Soppensee, Switzerland, *Aquatic Sciences*, Vol. 51, pp. 19-30

Lotter, A.F., 1989b, Subfossil and modern diatom plankton and the paleolimnology of Rotsee (Switzerland) since 1850, *Aquatic Sciences,* Vol. 51, pp. 1015-1621.

Lotter, A.F., 1991, How long was the Younger Dryas? Preliminary evidence from annually laminated sediments of Soppensee (Switzerland), *Hydrobiologia*, Vol. 214, pp. 53-57

Lotter, A.F., Sturm, M., Teranes, J.L. and Wehrli, B., 1997, Varve formation since 1885 and high-resolution varve analyses in hypertrophic Baldeggersee (Switzerland), *Aquatic Sciences*, Vol. 59, pp. 304-325

Loutre, M.F. and Berger, A., 2000, Future climatic changes: Are we entering an exceptionally long interglacial? *Climatic change*, Vol. 46, pp. 61-90

Loutre, M.F., Berger, A., 2003, Marine Isotope Stage 11 as an analogue for the present interglacial, *Global and Planetary Change*, Vol. 762, pp. 1-9.

Lowe, J.J., Rasmussen, S.O., Bjork, S., Hoek, W.Z., Steffensen, J.P., Walker, M.J.C. and Yu, Z.C., the INTIMATE group, 2008. Synchronisation of palaeoenvironmental events in the North Atlantic region during the Last Terminatin: a revised protocol recommended by the INTIMATE group. *Quaternary Science Reviews* 27, 6-17

Lowemark, L., Chen, H.F., Yang, T.N., Kylander, M., Yu, E.F., Hsu, Y.W., Lee, T.Q., Song, S.R. and Jarvis, S., 2011, Normalising XRF-scanner data: A cautionary note on the interpretation of high-resolution records from organic-rich lakes, *Journal of Asian Earth Science*, Vol. 40, pp. 1250-1256

Lücke, A. and Brauer, A., 2004, Biogeochemical and micro-facial fingerprints of ecosystem response to rapid Late Glacial climatic changes in varved sediments of Meerfelder Maar (Germany), *Palaeogeography, Palaeoclimatology, Palaeoecology*, Vol. 211, pp. 139-155

Luder, B.G., Kirchner, G., Lucke, A. and Zolitschka, B., 2006. Palaeoenvironmental reconstructions based on geochemical parameters from annually laminated sediments of Sacrower See (northeast German) since the 17th century. *Journal of Paleolimnology* 35, 897-912

Ludlam, S.D., 1969, Fayetteville Green Lake, New York. III. The Laminated Sediments, *Limnology and Oceanography*, Vol. 14, pp. 848-857

Maberly, S.C., Hurley, M.A., Butterwick, C., Corry, J.E., Heaney, S.I., Irish, A.E., Jaworski, G.H.M., Lund, J.W.G., Reynolds, C.S. & Roscoe, J.V. (1994) The rise and fall of Asterionella formosa in the South Basin of Windermere: analysis of a 45-year series of data*. Freshwater Biology* 31, 19–34.

Mackay, A., 2007. The paleoclimatology of Lake Baikal: a diatom synthesis and prospectus. *Earth Science Reviews* 82, 181-215

Macleod, A., Palmer, A., Lowe, J., Rose, J., Bryant, C. and Merritt, J., 2010, Timing of glacier response to Younger Dryas climatic cooling in Scotland, *Global and Planetary Change*, Vol. 79, 264-274

Magney, M., Begeot, C., Guit, J. and Peyron, O., 2003. Contrasting patterns of hydrological changes in Europe in response to Holocene climate cooling phases. *Quaternary Science Reviews* 22, 1589-1596

Mangili, C., Brauer, A., Moscariello, A. and Naumann, R., 2005, Microfacies of detrital event layers deposited in Quaternary varved lake sediments of the Piánico-Sèllere Basin (northern Italy), *Sedimentology*, Vol. 52, pp. 927-943

Mangili, C., Brauer, A., Plessen, B. and Moscariello, A., 2007, Centennial-scale oscillation in oxygen and carbon isotopes of endogenic calcite from a 15,500 varve year record of the Pianico interglacial, *Quaternary Science Reviews*, Vol. 26, pp. 1725-1735

Mangili, C., Brauer, A., Dulski, P., Moscariello, A. and Plessen, B., 2009, A 1000 year mid-interglacial cold phase at about 400 ka BP in the Piánico lake record*, IOP conference series: Earth and Environmental Science 6*, doi:10.1088/1755-1307/6/7/072042

Mangili, C., Brauer, A., Plessen, B., Dulski, P., Moscariello, A. and Naumann, R., 2010a, Effects of detrital carbonate on stable oxygen and carbon isotope data from varved sediments of the interglacial Piánico palaeolake (Southern Alps, Italy), *Journal of Quaternary Science*, Vol. 25, pp. 135-145

Mangili, C., Plessen, B., Wolff, C. and Brauer, A., 2010b, Climatic implications of annual to decadal resolution stable isotope data from calcite varves of the Pianico interglacial lake record, southern Alps, *Global and Planetary Change*, 71, 168-174

Marshall, C.T. and Peters, R.H., 1989. General patterns in the seasonal development of chlorophyll *a* for temperate lakes. *Limnology and Oceanography* 34, 856-867

Marshall, J.D., Jones, R.T., Crowley, S.F., Oldfield, F., Nash, S. and Bedford, A., 2002, A high resolution Late-Glacial isotopic record from Hawes Water, Northwest England Climatic oscillations: calibration and comparison of palaeotemperature proxies, *Palaeogeography, Palaeoclimatology, Palaeoecology*, Vol. 185, pp. 25-40

Marshall, J.D., Lang, B., Crowley, S.F., Weedon, G.P., van Calsteren, P., Fisher, E.H., Holme, R., Holmes, J.A., Jones, R.T., Bedford, A., Brooks, S.J., Bloemendal, J., Kiriakoulakis, K. and Ball, J.D., 2007, Terrestrial impact of abrupt climate changes in the North Atlantic thermohaline circulation: Early Holocene, UK, *Geology*, Vol. 35, pp. 639-642

Marshall, M., Schlolaut, G., Nakagawa, T., Lamb, H., Brauer, A., Staff, R., Bronk Ramsey, C., Tarasov, P., Gotanda, K., Haraguchi, T., Yokoyama, Y., Yonenobu, H., Tada, R Suigestsu 2006 project members, 2012, A novel approach to varve counting using mXRF and X-radiography in combination with thin-section microscopy, applied to the Late Glacial chronology from Lake Suigetsu, Japan, *Quaternary Geochronology*, Vol. 13, pp. 70-80

Martín-Puertas, C., Brauer, A., Dulski, P. and Brademann, B., 2012, Testing climate-proxy stationarity throughout the Holocene: an example from the varved sediments of Lake Meerfelder Maar (Germany), *Quaternary Science Reviews*, Vol. 58, pp. 56-65

Martín-Puertas, C., Valero-Garcés, B.L., Brauer, A., Mata, M.P., Delgado-Huertas, A. and Dulski, P., 2008, The Iberian-Roman Humid Period (2600-1600 cal yr BP) in the Zoñar Lake varve record (Andalucía, Southern Spain), *Quaternary Research*, Vol. 71, 108-120

Martinson, D.G., Pisias, N.G., Hays, J.D., Imbrie, J., Moore jr, T.C., Shackleton, N.J., 1987, Age dating and the orbital theory of the ice ages: Development of a high-resolution 0 to 300,000-year chronostratigraphy, *Quaternary Research*, Vol. 27, pp. 1-29.

Martrat, B., Grimalt, J.O., Shackleton, N.J., de Abreu, L., Hutterli, M.A., Stocker, T.F., 2007, Four climate cycles of recurring deep and surfacewater destabilizations on the Iberian margin*, Science*, Vol. 317, pp. 502–507.

Maslin, M. and Tzedakis, C., 1996. Sultry last interglacial gets sudden chill. *EOS, Transactions American Geophysical Union* 77, 353-354

Maslin, M. Seidov, D. and Lowe, J., 2001, Synthesis of the nature and causes of rapid climate transitions during the Quaternary, IN: D. Seidov, B. J. Haupt, and M. Maslin (Eds.), *The oceans and rapid climate change: Past, present and future*, Geophysical Monograph 126, American Geophysical Union

Masson-Delmotte, V., Dreyfus, G., Braconnot, P., Johnsen, S., Jouzel, J., Kageyama, M., Landais, A., Loutre, M.-F., Nouet, J., Parrenin, F., Raynaud, D., Stenni, B., Tuenter, E., 2006, Past temperature reconstructions from deep ice cores: relevance for future climate change, *Climate of the Past*, Vol. 2, pp. 145–165

McConnaughey, T.A. and Whelan, J.F., 1997. Calcification generates protons for nutrient and bicarbonate uptake. *Earth Science Reviews* 42, 95-117

McCrea, J.M., 1950, On the isotopic chemistry of carbonates and a paleotemperature scale, *The Journal of Chemical Physics*, Vol. 18, pp. 849–857

McKenzie, J.A. and Hollander, D.J., 1993. Oxygen isotope record in recent carbonate sediments from Lake Griefen, Switzerland (1750-1986): Application of continental isotopic indicator for evaluation of changes in climate and atmospheric circulation patterns. In: Swart, P.K., Lohmann, K.C., McKenzie, J.A. and Savin, S. (eds.), *Climate Change in Continental Isotopic Records*. Geophysical Monographs 78, Washington, DC, American Geophysical Union, 101-112

McKenzie, J., 1982. Carbon-13 cycle in Lake Greifen: A model for restricted ocean basins. In: Schlanger, S.O. and Cita, M.B. (eds.), *Nature and origin of cretaceous carbon-rich facies*, Academic, 197-207.

McKenzie, J.A., 1985. Carbon isotopes and productivity in the lacustrine and marine environment. In: Stumm, W. (ed.) *Chemical Processes in Lakes*, Wiley-Interscience, 99-118

McKinney, C.R., McCrea, J.M., Epstein, S., Allen, H. and Urey, H.C., 1950, Improvements in mass spectrometers for the measurement of small differences in isotope abundance ratios, *Review of Scientific Instruments,* Vol. 21, pp. 724-730

Melles, M., Brigham-Grette, J., Minyuk, P.S., Nowaczyk, N.R., Wennrich, V., DeConto, R.M., Anderson, P.M., Andreev, A.A., Coletti, A., Cook, T.L., Haltia-Hovi, E., Kukkonen, M., Lozhkin, A.V., Rosén, P., Tarasov, P., Vogel, H. and Wagner, B., 2012, 2.8 Million years of Arctic climate change from Lake El'gygytgyn NE Russia, *Science*, Vol. 337, pp. 315-320

Merkt, J. and Müller, H., 1999, Varve chronology and palynology of the Lateglacial in Northwest Germany from lacustrine sediments of Hämelsee in Lower Saxony, *Quaternary International*, Vol. 61, pp. 41-59

Merlivat, L. and Jouzel, J., 1979. Global climatic interpretation of the deuterium-oxygen 18 relationship for precipitation. *Journal of Geophysical Research* 84, 5029-5033

Meyer, K.-J., 1974, Pollenanalytische Untersuchungen und Jahresschichtenzählungen an der Holstein-zeitlichen Kieselgu von Hetendorf, *Geologie Jahrbuch*, Vol. A 21, pp. 87–105.

Meyers, P.A. and Ishiwatari, R., 1993. Lacustrine organic geochemistry-an overview of indicators of organic matter sources and diagenesis in lake sediments. *Organic Geochemistry* 20, 867-900

Milankovitch, M.M., 1941, *Canon of insolation and the ice-age problem* (in German), Publication 132 Mathematical and Natural Sciences, 33, Royal Serbian Sciences, Belgrade (English translation, Israel Program for Scientific Translation, Jerusalem (1969)).

Mitchell, G.F., Penny, L.F., Shotton, F.W. ans West, R.G., 1973. *A correlation of Quaternary deposits in the British Isles*. Geological Society London Special Report 4

Mook, W.G., 2000. *Environmental isotopes in the hydrological cycle: principles and applications Volume I: Introduction*. UNESCO/IAEA, 291pp.

Mook, W.G., 2006. *Introduction to Isotope Hydrology. Stable and Radioactive Isotopes of Hydrogen, Oxygen and Carbon*. Taylor & Francis, London

Morrill, C., Anderson, D.M., Bauer, B.A., Buckner, R., Gille, E.P., Gross, W.S, Hartmann,M.and Shah, A., 2013. Proxy benchmarks for intercomparison of 8.2 ka simulations. *Climate of the Past* 9, 423-432

Mulder, T. and Alexander, J., 2001, The physical character of subaqueous sedimentary density flows and their deposits*, Sedimentology,* Vol. 48, pp. 269-299

Muller, H., 1974. Pollenanalytische Untersuchungen und Jahresschichtenzahlungen an der hosltein-zeitlichen Kieselgur von Munster-Breloh, *Geologie Jahrbuch*, Vol. A 21, pp. 107-140.

Myrdo, A. and Shapley, M.D., 2006, Seasonal water-column dynamics of dissolved inorganic carbon stable isotopic compositions ($\delta^{13}C$ DIC) in small hardwater lakes in Minnesota and Montana, *Geochimica et Cosmochimica Acta*, Vol. 70, pp. 2699-2714

Naeher, S., Gilli, A., North, R.P., Hamann, Y. and Schubert, C.J., 2013, Tracing bottom water oxygenation with sedimentary Mn/Fe ratios in Lake Zurich, Switzerland, *Chemical Geology*, Vol. 352, pp. 125-133

Nakagawa, T., Gotanda, K., Haraguchi, T., Danhara, T., Yonenobu, H., Brauer, A., Yokoyama, Y., Tada, R., Takemura, K., Staff, R.A., Payne, R., Bronk Ramsey, C., Bryant, C., Frock , C., Schlolaut, G., Marshall, M., Tarasovm, P., Lamb, H., Suigetsu 2006 Project Members, 2011, SG06, a fully continuous and varved sediment core from Lake Suigetsu, Japan: stratigraphy and potential for improving the radiocarbon calibration model and understanding of late Quaternary climate changes, *Quaternary Science Reviews*, 36, 164-176

Nesje, A., Bjune, A.E., Bakke, J., Dahl, S.O., Lie, O. and Birks, H.J.B., 2006. Holocene palaeoclimate reconstructions at Vanndalsvatnet, western Norway, with particular reference to the 8200 cal yr BP event. *The Holocene* 16, 717-729

Neugbauer, I., Brauer, A., Drägerm N., Dulski, P., Wulf, P., Plessen, B., Mingram, J., Herschuh, U. and Brande, A., 2012, A Younger Dryas varve chronology from the Rehweise palaeolake record in NE-Germany, *Quaternary Science Reviews*, Vol. 36, pp. 91-102

Nichols, G., 2009. *Sedimentology and Stratigraphy, 2nd edition*. Wiley, 432pp

Nier, A.O., 1936. A Mass-Spectrographic Study of the Isotopes of Argon, Potassium, Rubidium, Zinc and Cadmium. *Physical Review Letters* 49, 272

Nipkow, F., 1927. Uber das Verhalten der Skelette planktischer Keiselalgen im geschichteten Tiefenschlammdes Zurich- und Bladeggersees. *Z. Hydrobiol* 4, 71-120

Nitychoruk, J., Binka, K., Hoefs, J., Ruppert, H. and Schneider, J., 2005, Climate reconstruction for the Holsteinian Interglacial in eastern Poland and its comparison with isotopic data from Marine Isotope Stage 11, *Quaternary Science Reviews*, Vol. 24, pp. 631-644

Nitychoruk, J., Bińka, K., Ruppert, H., Schneider, J., 2006, Holsteinian Interglacial = Marine Isotope Stage 11, *Quaternary Science Reviews*, Vol. 25, pp. 2678-2681.

Nuhfer , E.B.,Anderson, R.Y., Bradbury, J.P. and Dean, W.E., 1993. Modern sedimentation in Elk Lake, Clearwater County, Minnesota. In: Bradbury, J.P. and Dean, W.E. (eds.), *Elk Lake, Minnesota: Evidence for Rapid Climate Change in the North-Central United States*. Geological Society of America, Boulder, Colorado, USA Special Paper 276, 75-96

O'Neil, J.R., 1986. Theoretical and experimental aspects of isotopic fractionation. *Reviews in Mineralogy and Geochemistry* 16, 1-40

O'Sullivan, P.E., 2004. Palaeolimnology. In: O'Sullivan, P.E. and Reynolds, C.S. (eds.). *The Lakes Handbook volume 1: Limnology and Limentic Ecology*, Blackwell Publishing, 609-666

O'Sullivan, P.E., 1983, Annually-laminated lake sediments and the study of Quaternary environmental changes – A review, *Quaternary Science Reviews*, Vol. 1, pp. 245-313.

O'Sullivan, P.E., 1995, Eutrophication, *International Journal of Environmental Studies*, Vol. 47, pp. 173-195

Ojala, A.E., Heinsalu, A., Kauppila, T., Alenius, T. and Saarnisto, M., 2008, Characterising changes in the sedimentary environment of a varved lake sediment record in southern central Finland around 8000 cal. Yr BP, *Journal of Quaternary Science*, Vol. 23, pp. 765-775

Ojala, A.E.K. and Saarnisto, M., 1999, Comparative varve counting and magnetic properties of the 8400-yr sequence of an annually laminated sediment in Lake Valkiajärvi, Central Finland, *Journal of Paleolimnology*, Vol. 22, pp. 335-348

Ojala, A.E.K. and Tiljander, M., 2003, Testing the fidelity of sediment chronology: comparison of varve and paleomagnetic results from Holocene lake sediments from central Finland, *Quaternary Science Reviews*, Vol. 22, pp. 1787-1803

Ojala, A.E.K., Francus, P., Zolitschka, B., Besonen, M. and Lamoureux, S.F., 2012, Characteristics of sedimentary varve chronologies – A review, *Quaternary Science Reviews*, Vol. 43, pp. 45-60

Ojala, A.E.K., Saarinen, T. and Salonen, V.P., 2000, Preconditions for the formation of annually laminated lake sediments in southern and central Finland, *Boreal Environment Research*, Vol. 5, pp. 243-255

Oppo, D.W., McManus, J.F. and Cullen, J.L., 1998. Abrupt climate events 500,000 to 340,000 years ago: evidence from subpolar North Atlantic sediments. *Science* 279, 1335-1338

Overpeck, J.T. and Cole, J.E., 2006. Abrupt Change in Earth's Climate System. *Annual Review of Environment and Resources* 31, 1-31

Padisak, J., Crossetti, L.O. and Naselli-Flores, L., 2004, Use and misuse in the application of the phytoplankton functional classification: a critical review within updates, *Hydrobiologia,* Vol. 621, pp. 1-19

Palmer, A.P., Rose, J. and Rasmussen, S.O., 2012, Evidence for phase-locked changes in climate between Scotland and Greenland during GS-1 (Younger Dryas) using micromorphology of glaciolacustrine varves from Glen Roy, *Quaternary Science Reviews*, Vol. 36, pp. 114-123

Palmer, A.P., Rose, J., Lowe, J.J. and MacLeod, A., 2010, Annually resolved events of Younger Dryas glaciation in Lochaber (Glen Roy and Glen Spean), Western Scottish Highlands, *Journal of Quaternary Science*, Vol. 25, pp. 581-596

Palmer, A.P., Rose, J., Lowe, J.J. and Walker, M.J.C., 2008, Annually laminated Late Pleistocene sediment from Llangorse Lake, South Wales, UK: a chronology for the pattern of ice wastage, *Proceedings of the Geologists' Association*, Vol. 119, pp. 245-258.

Parrenin, F., Barnola, J.-M., Beer, J., Blunier, T., Castellano, E., Chappellaz, J., Dreyfus, G., Fischer, H., Fujita, S., Jouzel, J., Kawamura, K., Lemieux-Dudon, B., Loulergue, L., Masson-Delmotte, V., Nareisi, B., Petit, J.-R., Raisbeck, G., Raynaud, D., Ruth, U., Schwander, J., Severi, M., Sphani, R., Steffensen, J.P., Svensson, A., Udisti, R., Waelbroeck, C. and Wolff, E., 2007, The EDC3 chronology for the EPICA Dome C ice core, *Climate of the Past,* Vol. 3, pp. 485-497.

Pawley, S.M., Bailey, R.M., Rose, J., Moorlock, B.S.P., Hamblin, R.J.O., Booth, S.J., Lee, J.R., 2008, Age limits on Middle Pleistocene glacial sediments from OSL dating, north Norfolk, UK, *Quaternary Science Reviews*, Vol. 27, pp. 1363–1377.

Pawley, S.M., Toms, P., Armitage, S.J., Rose, J., 2010, Quartz luminescence dating of Anglian Stage (MIS 12) fluvial sediments: Comparison of SAR age estimates to the terrace chronology of the Middle Thames valley, UK, *Quaternary Geochronology*, Vol. 5, pp. 569-582.

Pearson, F.J., Jr., and Coplen, T.B., 1978. Stable isotope studies of lakes. In: Lerman, A. (ed.), *Lakes: Chemistry, Geology, Physics*, New York, Springer Verlag, 325-336.

Peglar, S.M., Fritz, S.C., Alameti, T., Saarnisto, M. and Birks, J.B., 1984, Composition and formation of laminated sediments in Diss Mere, Norfolk, England, *Boreas*, Vol. 13, pp. 13-28

Penkman, K.E.H., Preece, R.C., Bridgland, D.R., Keen, D.H., Meijer, T., Parfitt, S.A., White, T.S., Collins, M.J., 2011, A chronological framework for the British Quaternary based on Bithynia opercula*, Nature*, Vol. 476, pp. 446–449.

Penkman, K.E.H., Preece, R.C., Keen, D.H., Maddy, D., Schreve, D.C. and Collins, M.J., 2007, Testing the aminostratigraphy of fluvial archives: the evidence from intra-crystalline proteins within freshwater shells, *Quaternary Science Reviews*, Vol. 26, pp. 2958-2969.

Perrin, R.M.S., Rose, J. and Davis, H., 1979. The distribution, variation and origin of pre-Devensian tills in eastern England. *Philosophical Transactions of the Royal Society of London* B287, 535-570

Petit, J.R., Jouzel, J., Raynaud, D., Barkov, N.I., Barnola, J.M., Basil, I., Bender, M., Chappellaz, J., Davis, J., Delaygue, G., Delmotte, M., Kotyakov, V.M., Legrand, M., Lipenkov, V.Y., Lorius, C., Pepin, L., Ritz, C., Saltzman, E., Stievenard, S., 1999, *Nature*, Vol. 399, pp. 429-436.

Petterson, G., Renberg, I., Geladi, P., Lindberg, A. and Lindgren, F. 1993, Spatial uniformity of sediment accumulation in varved lake sediments in northern Sweden, *Journal of Paleolimnology,* Vol. 9, pp. 195-208.

Phillips, L., 1976, Pleistocene vegetational history and geology in Norfolk, *Philosophical Transactions of the Royal Society of London B*, Vol. 275, pp. 215-286.

Pike, J. and Kemp, A.E.S., 1996, Preparation and analysis techniques for studies of laminated sediments, From Kemp, A. E. S. (ed.), 1996, *Palaeoclimatology and Palaeoceanography from Laminated Sediments*, Geological Society Special Publication No. 116, pp. 37--48

Pinti, D.L., Quidelleur, X., Chiesa, S., Ravazzi, C. and Gillot, P.-Y., 2001.K-Ar dating of an early Middle Pleistocene distal tephra in the interglacial varved succession of Pianico-Sellere (Southern Alps, Italy). *Earth and Planetary Science Letters 188, 1-7*

Pinti, D., Rouchon, V., Quidelleur, X., Gillto, P.Y., Chiesa, S. and Ravazzi, C., 2007, Comment: Tephrochronological dating of varved interglacial lake deposits from

Piánico-Séllere (Southern Alps, Italy) to around 400 ka, *Journal of Quaternary Science*, Vol. 22, pp. 411-414

Pinti, D.L., Quidelleur, X., Lahitte, P., Aznar, C., Chiesa, S. and Gillot, P.Y., 2003, The Piánico tephra: an early Middle Pleistocene record of intraplate volcanism in the Mediterranean, *Terra Nova*, Vol. 15, pp. 176-186

Pitkänen, A. and Huttunen, P., 1999, A 1300-year forest-fire history at a site in eastern Finland based on charcoal and pollen records in laminated lake sediment, *The Holocene*, Vol. 9, pp. 311-320

Poage, M.A. and Chamberlain, C.P., 2001, Empirical relationships between elevation and the stable isotope composition of precipitation and surface waters: considerations for studies of palaeoelevation change, *American Journal of Science*, Vol. 301, 1–15

Pol, K., Debret, M., Masson-Delmotte, V., Capron, E., Cattani, O., Dreyfus, G., Falourd, S., Johnsen, S., Jouzel, J., Landais, A., Minster, B. and Stenni, B., 2011, Links between MIS 11 millennial to sub-millennial climate variability and long term trends as revealed by new high resolution EPICA dome C deuterium data – A comparison with the Holocene, *Climate of the Past*, Vol. 7, pp. 437-450

Prasad, S., Brauer, A., Rein, B. and Negendank, J.F.W., 2006, Rapid climate change during the early Holocene in western Europe and Greenland, *The Holocene*, Vol. 16, pp. 153-158

Prasad, S., Witt, A., Kienel, U., Dulski, P., Bauer, E., Yancheva, G., 2009, The 8.2 ka event: Evidence for seasonal differences and the rate of climate change in western Europe, *Global and Planetary Change*, *Vol.* 67, pp. 218-226.

Preece, R.C., Parfitt, S.A., Bridgland, D.R., Lewis, S.G., Rowe, P.J., Atkinson, T.C., Candy, I., Debenham, N.C., Penkman, K.E.H., Rhodes, E.J., Schwenninger, J.L., Griffiths, H.I., Whittaker, J.E. and Gleed-Owen, C., 2007, Terrestrial environments during MIS 11: evidence from the Palaeolithic site at West Stow, Suffolk UK, *Quaternary Science Reviews*, Vol. 26, pp. 1236-1300

Prell, and N. J. Shackleton, 1984,The orbital theory of Pleistocene climate: Support from a revised chronology of the marine $\delta^{18}O$ record, IN: Berger, A.,Imbrie, J., Hays, J., Kukla, G. and Saltzman, B. (Eds), *Milankovitch and Climate, Part I*, Reidel, Dordrecht, pp. 269-305

Prokopenko, A.A., Karabanov, E.B., Williams, D.F., Kuzmin, M.I., Shackleton, N.J., Crowhurst, S.J., Peck, J.A., Gvozdkov, A.N. and King, J.W., 2001. Biogenic silica record of the Lake Baikal response to climate forcing during the Brunhes chron. *Quaternary Research* 55, 123-132

Prokopenko, A.A., Hinnov, L.A., Williams, D.F. and Kuzmin, M.I., 2006, Orbital forcing of continental climate during the Pleistocene: a complete astronomically tuned climatic record from Lake Baikal, SE Siberia, *Quaternary Science Reviews,* Vol. 25, pp. 3431-3457

Pyne, S.J., Andrews, P.L. and Laven, R.D., 1996. *Introduction to Wildland Fire.* J. Wiley and Sons, New York, 769pp.

Rach, O., Brauer, A., Wilkes, H. and Sachse, D., 2014. Deylayed hydrological response to Greenland cooling at the onset of the Younger Dryas in western Europe. *Nature Geoscience* 7, 109-112

Rahmstorf, S., 2008. Anthropogenic Climate Change: Revisiting the Facts. In: Zedillo, E. (ed.), *Global Warming: Looking Beyond Kyoto.* Brookings International Press, Washinton, 34-53

Raymo, M.E., Lisiecki, L.E., Nisancioglu, K.H., 2006, Plio-Pleistocene Ice Volume, Antarctic Climate and the Global δ^{18}O Record*, Science*, Vol. 28, pp. 492-495.

Raymo, M.E., Mitrovica, J.X., 2012, Collapse of polar ice sheets during the stage 11 interglacial, *Nature*, Vol. 483, pp. 453–456

Raynaud, D., Barnola, J.M., d'Souchet, R., Lorrian, R., Petit, J.R., Duval, P. and Lipenkov, V.Y., 2005, The record for marine isotopic stage 11, *Nature,* Vol. 436, pp. 39-40

Reille, M. and de Beaulieu, J.-L., 1995. Long Pleistocene pollen records from the Praclaux Crater, south-central France. *Quaternary Research* 44, 205-215

Reille, M., de Beaulieu, J.-L., Svobodova, H., Andrieu-Ponel, W., Goeury, C., 2000, Pollen analytical biostratigraphy of the last five climati cycles from a long continental sequence from the Velay region (Massif Central, France), *Journal of Quaternary Science*, Vol. 15, pp. 665-685.

Renberg, I. 1982. Varved lake sediments – geochronological records of the Holocene. *Geologiska Foreningens I Stockholm Forhandingar* 104, 275-279

Renberg, I., 1981, Improved methods for sampling, photographing and varve-counting of varved lake sediments, *Boreas*, Vol. 10, pp. 255-258.

Renberg, I., 1986. Photographic demonstration of the annual nature of a varve type common in N. Swedish lake sediments. *Hydrobiologia* 140, 93-95

Renberg, I., 1990, A procedure for preparing large sets of diatom slides from sediment cores*, Journal of Paleolimnology*, Vol. 4, pp. 87-90

Renssen, H., Goose, H., Fichefet, T., Campin, J.-M., 2001. The 8.2kyr BP event simulated by a global atmosphere-sea-ice-ocean model. *Geophysical Research Letters* 28, 1567-1570

Reyes, A.V., Carlson, A.E., Beard, B.L., Hatfield, R.G., Stoner, J.S., Winsor, K., Welke, B. and Ullman, D.J., 2014, South Greenland ice-sheet collapse during Marine Isotope Stage 11, *Nature*, Vol. 510, pp. 525-528

Reynolds, C.S., 1984 *The ecology of Freshwater Phytoplankton*. Cambridge University Press, 384pp

Ringberg, B. and Erlstrom, M., 1999. Micromorphology and petrography of Late Weichselian glaciolacustrine varves in southeastern Sweden. *Catena* 35, 147-177

Rioual, P., Andrieu-Ponel, V, de Beaulieu, J-L., Reille, M., Svobodova, H. and Battarbee, R.W., 2007, Diatom responses to limnological and climatic changes at Ribains Maar

(French Massif Central) during the Eemian and Early Würm, *Quaternary Science Reviews*, *Vol.* 26, pp. 1557-1609

Risebrobakken, B., Jansen, E., Andersson, C., Mjelde, E. and Hevrøy, K., 2003, A high-resolution study of Holocene paleoclimatic and paleoceanographic changes in the Nordic Seas, *Paleoceanography*, Vol. 18, PA000764

Rodrigues, T., Voelker, A.H.L., Grimalt, J.O., Abrantes, F., Naughton, F., 2011, Iberian Margin sea surface temperature during MIS 15 to 9 (580–300 ka): glacial suborbital variability versus interglacial stability, *Paleoceanography*, Vol. 26, PA1204

Rodwell, M.J., Rowell, D.P. and Folland, C.K., 1999. Oceanic forcing of the wintertime North Atlantic Oscillation and European climate. *Nature* 398, 320-323.

Rohling, E.J. and Palike, H., 2005, Centennial-scale climate cooling with a sudden cold event around 8,200 years ago, *Nature*, Vol. 434, pp. 975-979

Rohling, E.J., Braun, K., Grant, K., Kucera, M., Roberts, A.P., Siddall, M., Trommer, G., 2010, Comparison between Holcoene and Marine Isotope Stage-11 sea-level; histories, *Earth and Planetary Science Letters*, 291, 97-105.

Romanek, C.S., Grossman, E.L. and Morse, J.W., 1992, Carbon isotopic fractionation in synthetic aragonite and calcite: Effects of temperature and precipitation rate, *Geochemica et Cosmochemica Acta*, Vol. 56, pp. 419-430

Romero, L., Carmacho, A., Vicente, E. and Miracle, M.R., 2006. Sedimentation patterns of photosynthetic bacteria based on pigment markers in meromictic Lake La Cruz (Spain): Palaeolimnological implications. *Journal of Paleolimnology* 35, 167-177

Rose, J., 1987. Status of the Wolstonian glaciation in the British Quaternary. *Quaternary Newsletter* 53, 1-9

Rose, J., Lee, J.A., Candy, I. and Lewis, S.G., 1999, Early and Middle Pleistocene river systems in eastern England: evidence from Leet Hill, southern Norfolk, England*, Journal of Quaternary Science*, Vol. 14, pp. 347-360.

Rose, J., Moorlock, B.S.P. and Hamblin, R.J.O., 2001. Pre-Anglian fluvial and coastal deposits in Eastern England: lithostratigraphy and palaeoenvironments. *Quaternary International* 79, 5-22

Rothwell, R.G., Hoogakker, B., Thomson, J., Croudace, I.W. and Frenz, M., 2006, Turbidite emplacement on the southern Balearic Abyssal Plain (western Mediterranean Sea) during Marine Isotope Stages 1-3: an application of ITRAX XRF scanning of sediment cores to lithostratigraphic analysis, IN: Rothwell, R.G.(Ed), *New Techniques in Sediment Core Analysis*. Geological Society, London, Special Publications, Vol. 267, pp. 79–98

Rowe, P.J., Atkinson, T.C., Turner, C. 1999, U-series dating of Hoxnian interglacial deposits at Marks Tey, Essex, England, *Journal of Quaternary Science*, Vol. 14, pp. 693-702.

Rozanski, K., 1985, Deuterium and Oxygen-18 in European groundwaters- links to atmospheric circulation in the past, *Chemical Geology*, Vol. 52, pp. 349-363

Rozanski, K., Araguás-Araguás, L. and Gonfianti, R., 1992, Relation between long-term trends of Oxygen-18 isotope composition of precipitation and climate, *Science*, Vol. 258, pp. 981-985

Rozanski, K., Araguás-Araguás, L. and Gonfiantini, R., 1993, Isotopic patterns in modern global precipitation, IN: Swart, P.K. (Ed), *Climate change in Continental isotopic records,* Geophysical Monograph 78, pp.1-36, American Geophysical Union, Washington

Rozanski, K., Johnsen, S.J., Schotterer, U. and Thompson, I.G., 1997, Reconstruction of past climates from stable isotope records of palaeo-precipitation preserved in continental archives, *Hydrological sciences*, Vol. 45, pp. 725-745

Ruddiman, W.F., 2003. Orbital insolation, ice volume, and greenhouse gasses. *Quaternary Science Reviews* 22, 1597-1629

Ruddiman, W.F., 2007, The early anthropogenic hypothesis: challenges and responses, *Rev. Geophys*. 45, 1–37.

Ruddiman, W.F., Vavrus, S.J., Kutzbach, J.E., 2005, A test of the overdue-glaciation hypothesis, *Quaternary Science Reviews*, Vol. 24, pp. 1-10.

Saarinen, T., 1998, High-resolution palaeosecular variation in northern Europe during the last 3200 years, *Physics of the Earth and Planetary Interiors*, Vol. 106, pp. 299-309

Saarnisto, M., 1986, *Annually laminated lake sediments*. In: Berglund, B.E. (ed.), *Handbook of Holocene Palaeoecology and Palaeohydrology*, 343-370.

Sabater, S. and Haworth, E.Y., 1995. An assessment of recent trophic changes in Windermere South Basin (England) based on diatom remains and fossil pigments. *Journal of Paleolimnology* 14, 151-163

Sander, M., Bengtsson, L., Holmquist, B., Wohlfarth, B. and Cato, I., 2002, The relationship between annual varve thickness and maximum annual discharge (1909-1971), *Journal of Hydrology*, Vol. 263, pp. 23-35

Scardia, G. and Muttoni, G., 2009, Palaeomagnetic investigations of the Pleistocene lacustrine sequence of Piánico-Sèllere (northern Italy), *Quaternary International*, Vol. 204, pp. 44-53

Scott, A.C., 2010. Charcoal recognition, taphonomy and issues in palaeoenvironmental analysis. *Palaeogeography, Palaeoclimatology, Palaeoecology* 291, 11-39.

Scott, A.C., Bowman, D.M.J.S., Bond, W.J., Pyne, S.J. and Alexander, M.E., 2014. *Fire on Earth: An Introduction*. Wiley-Blackwell, 413pp.

Scheffler, W., Nicklisch, A. and Schonfelder, I., 2005. Beitrage zur Morphologies, Okologie und Ontogenie der plaktischen Diatomee *Cyclotella comensis* Grunow. Untersuchungenan historischem und rezentem Material. *Diatom Research*20, 171-200

Schlolaut, G., Brauer, A., Marshall, M.H., Nakagawa, T., Staff, R.A., Bronk Ramsey, C., Lamb, H.F., Bryant, C.L., Naumann, R., Dulski, P., Brock, F., Yokoyama, Y., Tada, R., Haraguchi, T. and Suigetsi 2006 project members., 2014, Event layers in the Japanese

Lake Suigetsu 'SG06' sediment core: description, interpretation and climatic implications, *Quaternary Science Reviews ,* Vol. 83, pp. 157-170.

Schreve, D.C. 2001a, Mammalian evidence from Middle Pleistocene fluvial sequences for complex environmental change at the oxygen isotope substage level, *Quaternary International*, Vol. 79, pp. 65-74.

Schreve, D.C. 2001b, Differentiation of the British late Middle Pleistocene interglacials: the evidence from mammalian biostratigraphy, *Quaternary Science Reviews*, Vol. 20, pp. 1693-1705.

Scourse, J., 2006, Comment on: Numerical ^{230}Th/U dating and a palynological review of the Holsteinian/Hoxnian Interglacial by Geyh and Müller, *Quaternary Science Reviews*, Vol. 25, pp. 3070-3071

Seppa, H., Birks, H.J., Giesecke,T., Hammarlund, D., Alenius, T., Antonsson, K., Bjune, A.E., Heikkila, M., MacDonald, G.M., Ojala,A.E.K., Telford, R.J. and Veski, S., 2007, Spatial structure of the 8200 cal yr BP event in northern Europe, *Climate of the Past,* Vol. 3, pp. 225-236.

Shackleton N.J., Turner, C. 1967, Correlation between marine and terrestrial Pleistocene successions, *Nature*, 216, 1079-1082.

Shackleton, N., 1975. The stratigraphic record of deep-sea cores and its implications for the assessment of glacials, interglacials, stadials and interstadials, in the Mid-Pleistocene. In: K.W. Butzer and G.L. Isaac, (eds) *After The Australopithecines*, 259–308. Mouton, The Hague.

Shackleton, N.J. and Opdyke, N.D., 1973, Oxygen isotope and palaeomagnetic stratigraphy of Equatorial Pacific core V28-238: Oxygen isotope temperatures and ice volumes on a 10^5 year and 10^6 year scale, *Quaternary Research*, Vol. 3, pp. 39-55

Shackleton, N.J. and Turner, C., 1968, Correlation between Marine and Terrestrial Pleistocene Successions, *Nature*, Vol. 216, pp. 1079-1082

Shackleton, N.J., 1987, Oxygen isotopes, ice volume and sea level, *Quaternary Science Reviews,* Vol. 6, pp. 183–190

Siddall, M., Rohling, E.J., Blunier, T. and Spahni, R., 2010. Patterns of millennial variability over the last 500 ka. *Climate of the Past* 6, 295-303

Simola, H., 1992. Structural elements in varved lake sediments. *Geological Survey of Finland Special Paper* 14, 5-9

Simola, H., 1979, Micro-Stratigraphy of Sediment Laminations Deposited in a Chemically Stratifying Eutrophic Lake during the years 1913-1976, *Holarctic Ecology*, Vol. 2, pp. 160-168

Skinner, L.C. and Shackleton, N.J., 2006. Deconstructing Terminations I and II: revisiting the glacioeustatic paradigm based on deep-water temperature estimates. *Quaternary Science Reviews* 25, 3312-3321

Smith, N.D. and Ashley, G.M., 1985. Proglacial lacustrine environments. In: Ashley, G.M. and Shaw, J. and Smith, N.D. (eds.). *Glacial sedimentary environments. SEPM Short Course* 16, 135-215

Smith, N.D., 1978. Sedimentation processes and patterns in a glacier-fed lake with low sediment input. *Canadian Journal of Earth Sciences* 15, 741-756

Smith, D.B., Downing, R.A., Monkhouse, R.A., Otlet, R.L. and Pearson, F.J., 1976, The age of groundwater in the Chalk of the London Basin, *Water Resources Research*, Vol. 12, pp. 392-403

Smol, J.P., 1988, Chrysophycean microfossils in paleolimnological studies, *Palaeogeography, Palaeoclimatology, Palaeoecology*, Vol. 62, pp. 287-297

Snowball, I., Muscheler, R., Zillèn, L., Sandgreen, P., Stanton, T. and Ijung, K., 2010, Radiocarbon wiggle matching of Swedish lake varves reveals asynchronous climate changes around the 8.2 kyr cold event, *Boreas*, Vol. 39, pp. 720-733

Snowball, I., Zillén, L., Ojala, A., Saarinen, T. and Sandgren, P., 2007, FENNOSTACK and FENNORPIS: Varve dated Holocene palaeomagnetic secular variation and relative palaeointensity stacks for Fennoscandia, *Earth and Planetary Science Letters*, Vol. 255, pp. 106-116

Soddy, F., 1913. The Radio-elements and the Periodic Law. *Chemical News* 107, 97-99

Sommer, U., Gliwicz, Z.M., Lampert, W. and Duncan, A., 1986. The PEG-model of seasonal succession of plankton in fresh waters. *Archiv Hydrobiol* 106, 433-471

Spahni, R., Chappellaz, J., Stocker, T.F., Loulergue, L., Hausammann, G., Kawamura, K., Flücklger, J., Schwander, J., Raynaud, D., Masson-Delmotte, V. and Jouzel, J., 2005, Atmospheric Methane and Nitrous Oxide of the Late Pleistocene from Antarctic Ice Cores, *Science*, Vol. 310, pp. 1317-1321

Sprowl, D.R., 1993. On the precision of the Elk Lake varve chronology. In: Bradbury, J.P. (ed.), *Elk Lake, Minnesota: evidence for radip climate change in the north-central United Staes,* Boulder CO: Geological Society of America: SpecialPaper 276, 69-74

Staff, R.A., Nakagawa, T., Schlolaut, G., Marshall, M.H., Brauer, A., Lamb, H.F., Bronk Ramsey, C., Bryant, C.L., Brock, F., Kiagawa, H., van der Plicht, J., Payne, R.L., Smith, V.C., Mark, D.F., Macleod, A., Blockley, S.P.E., Schwenninger, J.-L., Tarasov, P.E., Haraguchi, T., Gotanda, K., Youenobu, H., Yokoyama, Y. and Suigetsu 2006 Project Members., 2013. The multiple chronological techniques applied to the Lake Suigetsu SG06 sediment core, central Japan. *Boreas* 42, 259-266.

Stanton, T., Snowball, I., Zillén, L. and Wastegård, S., 2010, Validating a Swedish varve chronology using radiocarbon, palaeomagnetic secular variation, lead pollution history and statistical correlation, *Quaternary Geochronology*, Vol. 5, pp. 611-624

Stein, R., Hefter, J., Grützner, J., Voelker, A. and Naafs, B.D.A., 2009, Variability of surface water characteristics and Heinrich-like events in the Pleistocene midlatitude North Atlantic Ocean: Biomarker and XRD records from IODP site U1313 (MIS 16-9), *Paleoceanography,* Vol. 24, PA001639

Stockhecke, M., Anselmetti, F.S., Meydam, A.F., Odermatt, D. and Sturm, M., 2012, The annual partial cycle in Lake Van (Turkey), *Palaeogeography, Palaeoclimatology, Palaeoecology*, Vol. 333-334, pp. 148-159

Sturm, M. and Lotter, A.F., 1995. *Lake sediments as environmental archives*. EAWAG News 38E, 6-9

Sturm, M., 1979. Origin and composition of clastic varves. In: Schluchter, C. (ed.), *Moraines and varves*, A.A. Balkem, Rotterdam, 281-285

Stuiver, M., 1968. Oxygen-18 content of atmospheric precipitation during the last 11,000 years in the Great Lakes region. *Science* 162, 944-997

Stuiver, M., 1970, Oxygen and carbon isotope ratios of frash-water carbonates as climatic indicators, *Journal of Geophysical Research*, Vol. 75, pp. 5247-5257

Stuiver, M., Grootes, P.M. and Braziunas, T.F., 1995, The GISP2 $\delta^{18}O$ Climate Record of the Past 16,500 Years and the Role of the Sun, Ocean, and Volcanoes, *Quaternary Research,* Vol. 44, pp. 341–354

Talbot, M.R. and Kelts, K., 1990. Palaeolimnological signatures from carbon and oxygen isotopic ratios in carbonates from organic-rich lacustrine sediments. In: Katz, B.J. and Talbot, M.R. (eds.), *Lacustrine exploration: Case studies and Modern Analogues*. American Association for Petroleum Geology, 99-112

Talbot, M.R., 1990, A review of the palaeohydrological interpretation of carbon and oxygen isotopic ratios in primary lacustrine carbonates, *Chemical Geology*, Vol. 80, pp. 261-279

Taylor, K.C., Mayewski, P.A., Twickler, M.S. and Whitlow, S.I., 1996., Biomass burning recorded in the GISP2 ice core: A record from eastern Canada? *The Holocene* 6, 1-6

Teller , J.T. and Leverington, D.W., 2004, Glacial Lake Agassiz: A 5000 yr history of change and its relationship to the $\delta^{18}O$ record of Greenland, *Geological Society of America Bulletin*, May/June 2004, pp. 730-742

ter Braak, C. J. F., and P. Smilauer. 2002. *CANOCO reference manual and CanoDraw for Windows user's guide: software for canonical community ordination (version 4.5).* Microcomputer Power, Ithaca, New York, USA.

Teranes, J.L., McKenzie, J.A., Bernasconi, S.M., Lotter, A.F. and Sturm, M., 1999, A study of oxygen isotopic fractionation during bio-induced calcite precipitation in eutrophic Baldeggersee, Switzerland, *Geochemica et Cosmochimica Acta*, Vol. 63, pp. 1981-1989

Teranes, J.L., McKenzie, J.A., Lotter, A.F. and Sturm, M., 1999b; Stable isotope response to lake euthrophication: Calibration of a high-resolution lacustrine sequence from Baldeggersee, Switzerland, *Limnol. Oceanogr.* Vol. 44, pp. 320-333

Teranes, J.L. and McKenzie, J.A., 2001, Lacustrine oxygen isotope record of 20^{th} century climate change in central Europe: evaluation of climatic controls on oxygen isotopes in precipitation, *Journal of Palaeolimnology*, Vol. 26, pp. 131-146

Thomas, E.,Wolff, E.W., Mulvaney, R., Steffensen, J.P., Johnsen, S.J., Arrowsmith, C.,White, J.W.C., Vaughn, B., 2007, The 8.2 ka event from Greenland ice cores, *Quaternary Science Reviews*, Vol. 26, pp. 70–81.

Thomas, G.N. 2001, Late Middle Pleistocene pollen biostratigraphy in Britain: pitfalls and possibilities in the separation of interglacial sequences, *Quaternary Science Reviews*, Vol. 20, pp. 1621-1630.

Thomson, J.J., (1913), Rays of positive electricity, P*roceedings of the Royal Society*, A 89, 1–20

Tian, J., Brown, T.A. and Hul, F.S., 2005, Comparison of varve and 14C chronologies from Steel Lake, Minnesota, USA, *The Holocene*, Vol. 15, pp. 510-517

Tinner, W. and Lotter, A.F., 2001, Central European vegetation response to abrupt climate change at 8.2 ka, *Geology*, Vol. 29, pp. 551-554

Tippett, R., 1964. An investigation into the nature of the layering of deep-water sediments in two eastern Ontario lakes. *Canadian Journal of Botany* 42, 1693-1709

Tolonen, M., Palaeoecology of annually laminated sediments in Lake Ahvebainen, S. Finland. II. Comparison of dating methods. *Annale Botanici Fennici* 15, 209-222

Tuber, H., 1967. Investigations of the mode of pollen transfer in forested areas. *Review of Palaeobotany and Palynology* 3, 277-286.

Turner, C. and West, R.G. 1968. The subdivision and zonation of interglacial periods. *Eiszeitalter und Gegenwart,* Vol. 19, pp. 93-101

Turner, C., 1970, The Middle Pleistocene deposits at Marks Tey, Essex, Philosophical *Transactions of the Royal Society of London, Series B, Biological Sciences*, Vol. 257, pp. 373-437

Turner, C., 1975. The correlation and duration of Middle Pleistocene interglacial periods in northwest Europe. In: K.W. Butzer and G.L. Isaac, (eds) *After The Australopithecines*, 259–308. Mouton, The Hague.

Turner, C., 1998, Volcanic Maars, Long Quaternary sequences and the work of the INQUA subcommission on European Quaternary Stratigraphy, *Quaternary International*, Vol. 47, pp. 41-49

Turney, C.S.M., Baillie, M., Palmer, J. and Brown, D., 2006. Holocene climatic change and past Irish societal response. *Journal of Archaeological Science* 33, 34-38

Tylmann, W., Enters, D., Kinder, M., Moska, P., Ohlendorf, C., Poręba, G. and Zolitschka, B., 2013, Multiple dating of varved sediments from Lake Łazduny, northern Poland: Toward an improved chronology for the last 150 years, *Quaternary Geochronology,* Vol. 15, pp. 98-107

Tzedakis, P.C., 2010, The MIS 11 – MIS 1 anal;ogy, southern European vegetation, atmospheric methane and the “early anthropogenic hypothesis”, *Climates of the Past*, Vol. 6, pp. 131-144.

Tzedakis, P.C., Channell, J.E.T., Hodell, D.A., Kleiven, H.F., Skinner, L.C., 2012, Determining the natural length of the current interglacial, *Nature Geoscience*, Vol. 5, pp. 138–141.

Tzedakis, P.C., Raynouad, D., McManus, J.F., Berger, A., Brovkin, V., Kiefer, T., 2009, Interglacial diversity, *Nature Geoscience*, Vol. 2, pp. 751-755.

Tzedakis, P.C., Roucoux, K.H., de Abreu, L., Shackleton, N.J., 2004, The duration of forest stages in southern Europe and interglacial climate variability, *Science,* Vol. 306, pp. 2231–2235.

Urey, H.C., Lowenstam, H.A., Epstein, S. and McKinney, C.R., 1951. Measurements of palaeotemperatures and temperatures of the upper cretaceous of England, Denmark and southeastern United States. *Geological Society of America Bulletin* 62, 399-416

Urey, H.C., 1947. The thermodynamic properties of isotopic substances. *Journal of the Chemical Society,* 562-581

Urey, H.C., 1948, Oxygen isotopes in nature and in the laboratory, *Science,* Vol. 108, pp. 489-496.

Van Asch, N., Lutz, A.F., Duijkers, M.C.H., Heiri, O., Brookes, S.J. and Hoek, W.Z., 2012. Rapid climate change during the Weichselian Lateglacial in Ireland: Chironomid-inferred sumer temperatures from Fiddaun, Co. Galway. *Palaeogeography, Palaeoclimatology, Palaeoecology* 315-316, 1-11

Van der Hammen, T., 1951. *Late Glacial flora and periglacial phenomena in The Netherlands*, PhD thesis, Leiden, Leidse Geologische Mededelingen 17, 71-183.

Van der Hammen, T., 1957. The stratigraphy of the Late-Glacial. *Geologie en Mijnbouw* 19, 250-254.

Van der Hammen, T & Van Geel, B. (2008) Charcoal in soils of the Allerød-Younger Dryas transition were the result of natural fires and not necessarily the effect of an extra-terrestrial impact. *Netherlands Journal of Geosciences* 87, 359–361.

Vanni, M.J. and Temte, J., Seasonal patterns of grazing and nutrient limitation of phytoplankton in a eutrophic lake. *Limnology and Oceanography* 35, 697-709

Vellinga, M. and Wood, R.A., 2002. Global climatic impacts of a collapse of the thermohaline circulation. *Climatic Change* 54, 251-267

Vellinga, M. and Wood, R.A., 2008. Impacts of thermohaline circulation shutdown in the twenty-first century. *Climatic Change* 91, 43-63

Veski, S., Seppä, H. and Ojala, A.E.K., 2004, Cold event at 8200 yr B.P. recorded in annually laminated lake sediments in eastern Europe, *Geology*, Vol. 32, pp. 681-684

Vinther, Bo M; Clausen, Henrik B; Johnsen, Sigfus J; Rasmussen, Sune O; Andersen, Katrine K; Buchardt, SL; Dahl-Jensen, Dorthe; Seierstad, IK; Siggaard-Andersen, Marie-Louise; Steffensen, J¯rgen Peder; Svensson, Anders M; Olsen, GJ; Heinemeier, Jan, 2006. A synchronized dating of three Greenland ice cores throughout the Holocene. *Journal of Geophysical Research-Atmospheres* 111, D13102

Voelker, A.H.L., Rodrigues, T., Billups, K., Oppo, D.,McManus, J., Stein, R., Hefter, J., Grimalt, J.O., 2010, Variations in mid-latitude North Atlantic surface water properties during the mid-Brunhes (MIS 9–14) and their implications for the thermohaline circulation, *Climate of the Past*, Vol. 6, pp. 531–552.

Vogel, J.C., 1993. Variability of carbon isotope fractionation during photosynthesis. In: Ehleringer, J.R., Hall., A.E. and Farquhar, G.D. (eds.), *Stable Isotopes and Plant Carbon – Water Relations, Academic Press, 29-38*

von Grafenstein, U., Erlenkeuser, H., Müller, J., Jouzel, J. and Johnsen, S., 1998, The cold event 8200 years ago documented in oxygen isotope records of precipitation in Europe and Greenland, *Climate Dynamics*, Vol. 14, pp. 73-81

Wachniew, P. and Rozanski, K., 1997, Carbon budget of a mid-latitude, groundwater-controlled lake: Isotopic evidence for the importance of dissolved inorganic carbon recycling, *Geochimica et Cosmochimica Acta*, Vol. 61, pp. 2453-2465

Waghorne, R., Hancock, J.D.R. and Candy, I., 2012, Environmental controls on the $\delta^{18}O$ of freshwater calcite and aragonite in a temperate, lowland river system: significance for palaeoclimatic studies, *Proceedings of the Geologists' Association*, Vol. 123, pp. 576-583

Walker, M.J.C., Bjork, S., Lowe, J.J., Cwynar, L.C., Johnsen, S., Knudsen, K.-L., Wohlfarth, B., INTIMATE group., 1999. Isotopic 'events' in the GRIP ice core: a stratotype for the Late Pleistocene. *Quaternary Science Reviews* 18, 1143-1150

Walkley, A. and Black, I.A., 1934, An examination of the Degtjareff method for determining organic carbon in soils: Effect of variations in digestion conditions and of inorganic soil constituents. *Soil Science,* Vol. 63, pp. 251-263

Weltje, G.J. and Tjallingii, R., 2008, Calibration of XRF core scanners for quantitative geochemical logging of sediment cores: Theory and application, *Earth and Planetary Science Letters*, Vol. 274, pp. 423-438

Werner, P. and Smol, J.P. (2006) The distribution of the diatom *Cyclotella comensis* in Ontario (Canada) lakes. NOVA HEDWIGIA, 373- 391,

West, R.G., 1956, The Quaternary deposits at Hoxne, Suffolk, *Philosophical Transactions of The Royal Society of London,* Vol. B241, pp. 265-356.

West, R.G., 1961, The glacial and interglacial deposits of Norfolk, *Transactions of the Norfolk and Norwich Naturalists' Society*, Vol. 19, pp. 365–375.

Wetzel, R.G., 1975. *Limnology*. W.B. Saunders Co, 743pp

White, M.J., and Schreve, D.C., 2000, Island Britain – peninsula Britain: palaeogeography, colonisation and the Lower Palaeolithic settlement of the British Isles, *Proceedings of the Prehistoric Society*, Vol. 66, pp. 1-28.

White, R.M.P, Dennis, P.F. Atkinson, T.C., 1999. Experimental Calibration and Field Investigation of the Oxygen Isotopic Fractionation Between Biogenic Aragonite and Water. *Rapid Communications in Mass Spectrometry*, Vol. 13, pp. 1242–1247

Whiticar, M.J., Faber, E. and Schoell, M., 1986. Biogenic methane formation in marine and freshwater environments: CO_2 reduction vs acetate fermentation-isotope evidence. *Geochem Cosmochim Acta* 50, 693-709

Whitlock, C. and Larsen, C., 2001, Charcoal as a fire proxy, IN: J. P. Smol, H. J. B. Birks & W. M. Last (eds.), 2001, *Tracking Environmental Change Using Lake Sediments. Volume 3: Terrestrial, Algal, and Siliceous Indicators*, Kluwer Academic Publishers, Dordrecht, The Netherlands pp. 1-23

Whittington, G., Fallick, A.E. and Edwards, K.J., 1996, Stable oxygen isotope and pollen records from eastern Scotland and a consideration of Late-glacial and early Holocene climate change for Europe, *Journal of Quaternary Science,* Vol. 11, pp. 327-340

Whitlock, C. and Larsen, C., 2001. Charcoal as a fire proxy. In: Smol, J.P., Birks, H.J.B. and Last, W.M. (eds.), 2001. *Tracking Environmental Change Using Lake Sediments.*

Wiersma, A.P. and Renssen, H., 2006, Model-data comparison for the 8.2 ka BP event: confirmation of a forcing mechanism by catastrophic drainage of Laurentide Lakes, *Quaternary Science Reviews*, Vol. 25, pp. 63-88

Willen, E., 1991. Planktonic diatoms – An ecological review. *Archiv fur Hydrobiologie* 62, 69-108

Zhang, J., Quay, P.D. and Wilbur, D.O., 1995, Carbon isotope fractionation during gas-water exchange and dissolution of CO_2, *Geochimica et Cosmochimica Acta*, Vol. 59, pp. 107-114

Zillen, L. and Snowball, I., 2009, Complexity of the 8 ka climate event in Sweden recorded by varved lake sediments, *Boreas*, Vol. 38, pp. 493-503

Zillen, L.M., Wastegård, S. and Snowball, I.F., 2002, Calendar year ages of three mid-Holocene tephra layers identified in varved lake sediments in west central Sweden, *Quaternary Science Reviews*, Vol. 21, pp. 1583-1591

Zolitschka, B., 2003. Dating based on freshwater- and marine-laminated sediments. In:Mackay, A., Battarbee, R., Birks, J. and Oldfield, F. (eds.), *Global change in the Holocene*, Arnold, 92-106.

Zolitschka, B., 1996a. Recent sedimentation in a high arctic lake, northern Ellesmere Island, Canada. *Journal of Paleolimnology* 16, 169-186.

Zolitschka, B., 1996b, Image analysis and microscopic investigation of annually laminated lake sediments from Fayetteville Green Lake (NY, USA) Lake C2 (NWT, Canada) and Holmaar (Germany): a comparison, IN: Kemp, A. E. S. (ed.), 1996, *Palaeoclimatology and Palaeoceanography from Laminated Sediments*, Geological Society Special Publication No. 116, pp. 49-55.

Zolitschka, B. and Negendank, J.F.W., 1996, High-resolution records from European Lakes, *Quaternary Science Reviews*, Vol. 18, pp. 885-888

Zolitschka, B., 1991, Absolute dating of late Quaternary Lacustrine sediments by high resolution varve chronology, *Hydrobiologia*, Vol. 214, pp. 59-61

Zolitschka, B., 2007, Varved lake sediments, IN: Elias, S. (Ed), *Encyclopaedia of Quaternary Science*, Elsevier, Amsterdam, pp. 3105-3114